Dipl.-Ing. Andreas Johann Gutsche

# Robust Whiplash Protection

## Considering female occupants, variations in seated postures and seat adjustments

A thesis submitted in partial fulfilment of the requirements for the degree of
Doktor der Technik (Dr. techn.)
at
The Faculty for Mechanical Engineering
Vehicle Safety Institute
Graz University of Technology

Primary Supervisor
*Univ.-Prof. Dipl.-Ing. Dr.techn. Hermann Steffan*
*Graz University of Technology*
*Graz, Austria*

Secondary Supervisor
*Prof. Dr. Mats Svensson*
*Chalmers Tekniska Högskola*
*Gothenburg, Sweden*

Graz, December 2015

Dipl.-Ing. Andreas Johann Gutsche

# Umfassender Schleudertrauma Schutz

## Berücksichtigung von weiblichen Insassen, Variationen von Körperhaltung und Sitz Einstellungen

Dissertation zur Erlangung des akademischen Grades
Doktor der Technik (Dr. techn.)
eingereicht an der
Fakultät für Maschinenbau
Institut für Fahrzeugsicherheit
Technische Universität Graz

Erstbegutachter
*Univ.-Prof. Dipl.-Ing. Dr.techn. Hermann Steffan*
*Technische Universität Graz*
*Graz, Österreich*

Zweitbegutachter
*Prof. Dr. Mats Svensson*
*Chalmers Tekniska Högskola*
*Göteborg, Schweden*

Graz, Dezember 2015

# PREFACE

This thesis is the result of more than three years of research at *Graz University of Technology*. Investigations on the injury risk for different situations and occupants in rear end impacts have been analysed by and at the Vehicle Safety Institute. Additional twelve international partners contributed to this topic within the ADSEAT project.

The EU funded research project ADSEAT started in 2009. My Contribution to this project started in 2010 where I participated in three subtasks during the 42 months lasting venture. For me the project started being thrown in at the deep end, but immediately I found myself fond of the work. Especially enjoyable was the international cooperation and versatile field of research. During the project I was able to gain a broad overview and experience in managing work packages and sub tasks.

Within my tasks I participated in refinement of the developed numerical occupant model for female occupants which I later utilized in numerical studies. But among my challenges, there were also other interesting tasks, such as component testing and analysis along with the development of equipment especially assembled for the very special purposes within this project.

During these years of work on this project, I was able to gain knowledge in areas such as numerical simulation, but also real life component testing with all its weal and woes. Thanks to the very colourful working environment at the Vehicle Safety Institute I was also allowed to gain a broad knowledge on various topics concerning vehicle and occupant safety, far more than solely the protection during one particular accident scenario.

This thesis describes different tasks and thus is divided in several chapters to structure the content provided.

Chapter 1 introduces the term whiplash and describes what the aim of this thesis was.

In chapter 2, a brief overview of the current situation, based on an extensive literature review is presented. Besides some core numbers of why whiplash still needs to be addressed, emphasis is put on influencing factors of the occurrence of WAD and especially the diversification between male and female occupants. Furthermore current legal and consumer assessment, as well as typically implemented anti-whiplash systems are described.

The methods utilized to investigate the questions given in this project are described in chapter 3.

In chapter 4 and 5 results of the methods are presented and then compared in chapter 6.

Chapter 7 contains the conclusion and chapter 8 summarises the findings in these tasks, but also points out which aspects need further attention.

References of data and manuscripts quoted throughout the entire thesis are found in the bibliography and complementary data is presented in the appendix.

Detailed lists of graphics, tables, acronyms and symbols are provided.

# STATUTORY DECLARATION

I declare that I have authored this thesis independently, that I have not used other than the declared sources and resources, and that I have explicitly marked all material which has been quoted either literally or by content from the used sources. The text document uploaded to TUGRAZonline is identical to the present doctoral dissertation.

Andreas Johann Gutsche, Graz, December 12, 2015

# EIDESSTATTLICHE ERKLÄRUNG

Ich erkläre an Eides statt, dass ich die vorliegende Arbeit selbstständig verfasst, andere als die angegebenen Quellen und Hilfsmittel nicht benutzt, und die, den benutzten Quellen, wörtlich und inhaltlich entnommenen Stellen als solche kenntlich gemacht habe. Das in TUGRAZonline hochgeladene Textdokument ist mit der vorliegenden Dissertation identisch.

Andreas Johann Gutsche, Graz, am 12. Dezember 2015

# ACKNOWLEDGMENT

My gratitude goes to the colleagues and fellow workers at the Vehicle Safety Institute for a pleasant working atmosphere the support and valuable aid when needed. Also my acknowledgement goes to all participants who contributed to the successful performance of the ADSEAT project. In particular I owe thanks to Dr. Ernst Tomasch for his support and motivation in management issues during this project, for all the freedom to work autonomously but the support and guidance whenever needed. I am also much obliged to Prof. Hermann Steffan for facilitating the conduction of this project. Sincere thanks to Prof. Mats Svensson for the support and encouragement during all phases of the project.

Special thanks are owed to my parents, whose support throughout my years of education, both morally and financially, made it possible to achieve my personal goals and so much more. Further I would like to thank my girlfriend Melanie for her constant support, patience and encouragement, without which the completion of this work would not have been possible.

Also I would like to thank the following people whom I worked with and who supported me during the project:

Christian Ellersdorfer for sharing a workplace without any hassle,

Wolfgang Sinz for support and directions whenever on lost paths,

Thomas Pistotnig for all the dedication to a lot of work that had to be done,

Simon Heindl for answering so many questions no one ever really asked,

Florian Feist for assisting me with all usually self-created virtual issues and last but not least,

thanks to Alexander Hödl and Tim Fale for all the support and hands-on experience.

Parts of this thesis were performed within the FP7 project ADSEAT funded by the European Commission. Many thanks for the collaboration to the partners in the consortium (in alphabetic order):

Chalmers University of Technology (Gothenburg, Sweden), Cidaut Foundation (Valladolid, Spain), Faurecia (Etampes, France), Folksam (Stockholm, Sweden), Graz University of Technology (Graz, Austria), Humantics Euro (Heidelberg, Germany), Loughborough University (Leicestershire, Great Britain), Ludwig-Maximilian-Universität (Munich, Germany), The Swedish National Road and Transport Research Institute (Linköping, Sweden), University of Strasbourg (Strasbourg, France), Volvo Cars (Gothenburg, Sweden), Working Group on Accident Mechanics (Zurich, Switzerland).

# ABSTRACT

**Background:** Whiplash is the single most common and costly occupant injury. Within the European Union, an estimate of more than 800,000 victims (Linder, et al., 2013) suffer WAD resulting in insurance and other social costs of approximately € 10 billion annually (Norra K, 2005). Analysis of insurance data revealed, that whiplash is a larger threat to females than males. Statistics indicate an increased risk of up to three times for females compared to males (Jonsson, 2008). Furthermore it was found, that newer whiplash protection systems seem to bring less improvement for females than males (Kullgren, et al., 2010). Still, current regulations and consumer tests, which are passed by manufacturers with excellent scores, do not lead to a significant improvement and reduction of whiplash cases. These tests consider only 50$^{th}$ percentile male occupants, one seat configuration and up to three pulse intensities. Thus this thesis focused on investigations outside the strict boundaries of regulation- and consumer-tests.

**Methods:** Besides Finite Element Analysis, sled tests with PMHS and rear impact dummies were performed. For this purpose the state of the art Bio RID II dummy and virtual model were used. Furthermore the newly developed Eva RID virtual model and the Bio RID 50F prototype dummy, to represent female occupants, could be included. To consider different seated postures and seat adjustments, varying seat configurations were applied in sled tests and virtual investigations. In particular head restraint and backrest positions were configured, like they can be used in everyday traffic situations. For easier comparison of the individual configurations, the Neck Value (NV) was introduced as measure of the load on the occupant.

**Results:** Investigations showed, that small modifications to single components of the seat can vastly influence the actual load on the occupant. Compared to the male baseline configuration (Euro NCAP IIWPG 16 [km/h]) the female occupant has to withstand up to 100 % higher loads. Furthermore it was found that that different injury criteria are influenced diversely by certain changes. In particular, the two well established criteria Nkm and NIC were compared. Results showed an influence on Nkm by the head restraint height. For example, the values range from 0.50 [-], 0.38 [-] to 0.26 [-] for one configuration of the female occupant by just varying the head restraint height from a “high” to “low” position. The comparable male configurations however showed a different behaviour. Nkm values increased with a lower head restraint position (Nkm 0.22 [-], 0.28 [-], 0.39 [-]). The NIC criterion, on the other hand, seemed more sensitive to changes to the backrest. Values for three female configurations only differing in backrest position, show NIC values of 12.38 [m²/s²], 27.66 [m²/s²] and 36.74 [m²/s²] (from a forward to a backward backrest position). Male counterparts of these simulations show very comparable NIC values of 15.83 [m²/s²], 31.16 [m²/s²] and 36.84 [m²/s²]. Even if the absolute values for the male model are higher, the increase of the NIC value for further backward positioned backrests is very similar. Comparing the Euro NCAP “low” and “high” severity pulse for Bio RID II and Eva RID in the same seat configuration, the male showed a 45 % higher NV where the females’ increase was 59 % which seems to verify a higher sensitivity to higher pulse intensities for females (Temming, et al., 1997).

**Conclusion:** Vehicle seats can be designed perfectly to achieve a good score in rating tests (Euro NCAP, 2015). Real life accidents however show large variations in many different factors compared to test scenarios. Occupants differ from the 50$^{th}$ percentile male, seat adjustments usually differ from the test settings. Thus the aim in designing vehicle seats should be to develop seat designs which are capable to protect a large variety of occupants (male/female, tall/short, etc.…) in a wide range of different situations. For this purpose however, tools and methods must be made available, to quantify loads on different occupants (size, gender, seated posture, etc.…) in situations differing from one standardised test scenario.

# KURZFASSUNG

**Hintergrund:** Schleudertraumata sind die häufigsten und kostspieligsten Einzelverletzungen bei Verkehrsunfällen. Alleine innerhalb der Europäischen Union gibt es jährlich bis zu 800 000 Opfer (Linder, et al., 2013) mit einem wirtschaftlichen Schaden von bis zu 10 Milliarde € (Norra K, 2005). Untersuchungen von Versicherungsdaten und Statistiken zeigten, dass Frauen ein bis zu dreimal höheres Risiko für Schleudertraumata haben als Männer (Jonsson, 2008). Weiters wurde festgestellt, dass aktuelle Schleudertrauma Schutzsysteme wirkungsvoller für Männer als für Frauen funktionieren (Kullgren, et al., 2010). Obwohl aktuelle Zulassungs- und Verbrauchertests von Automobilherstellern mit ausgezeichneten Bewertungen durchgeführt werden, kann eine signifikante Verbesserung und Reduktion von Schleudertraumata nicht nachgewiesen werden. In diesen Tests wird derzeit nur der 50-perzentile männliche Insasse, eine einzelne Sitzkonfiguration sowie bis zu drei Pulsintensitäten berücksichtigt. Daher lag der Fokus der vorliegenden Arbeit auf der Untersuchung von Szenarien außerhalb dieser Grenzen der Zulassungs- und Verbrauchertests.

**Methoden:** Neben Finite Element Methoden, wurden Schlittentests mit PMHS und Heckaufprall-Dummys durchgeführt. Hierzu wurde der aktuelle Bio RID II Dummy sowie dessen virtuelles Modell verwendet. Zusätzlich konnte das neu entwickelte virtuelle Eva RID Modell sowie der Prototyp Dummy Bio RID 50F eingesetzt werden, welche einen weiblichen Insassen repräsentieren. In virtuellen Schlittenversuchen wurden verschiedene Parameter variiert. Insbesondere wurden verschiedene Rückenlehneneinstellungen und Kopfstützenpositionen untersucht, wie sie auch im täglichen Gebrauch angewendet werden. Zum einfacheren Vergleich der unterschiedlichen Konfigurationen wurde die Neck Value (NV) als Maß für die Belastung des Insassen eingeführt.

**Ergebnisse:** Bereits kleine Veränderungen an einzelnen Sitzkomponenten können die tatsächliche Last auf den Insassen stark beeinflussen. Im Vergleich zur männlichen Basiskonfiguration (Euro NCAP IIWPG 16 [km/h]) sind die Belastungen für das weibliche Insassenmodell um bis zu 100 % erhöht. Darüber hinaus konnte festgestellt werden, dass unterschiedliche Verletzungskriterien von bestimmten Faktoren stark beeinflusst werden können. Der Vergleich des Nkm Kriteriums beispielsweise zeigte großen Einfluss der Höhe der Kopfstütze auf das Ergebnis. Für das weibliche Insassenmodell einer Konfiguration, nur mit unterschiedlichen Kopfstützenhöhen (hoch, mittel, niedrig), reichten diese von 0,50 [-] über 0,38 [-] bis 0,26 [-]. Die vergleichbaren Konfigurationen mit männlichem Insassenmodell zeigten ein anderes Verhalten. Die Nkm Werte stiegen mit niedrigerer Position der Kopfstütze (0.22 [-] über 0.28 [-] auf 0.39 [-]). Das NIC Kriterium wiederum schien stärker von der Stellung der Rückenlehne beeinflusst zu sein. Die Werte der Konfigurationen mit weiblichem Insassenmodell stiegen, je weiter nach hinten die Rückenlehne geneigt wurde (nach vorne geneigt, mittig, nach hinten geneigt). Die Ergebnisse des NIC von 12,38 [$m^2/s^2$], 27,66 [$m^2/s^2$] und 36,74 [$m^2/s^2$] waren etwas niedriger als die der vergleichbaren Konfigurationen mit männlichem Insassenmodell (15,83 [$m^2/s^2$], 31,16 [$m^2/s^2$], 36.84 [$m^2/s^2$]). Die Zunahme mit weiter nach hinten geneigter Rückenlehne war jedoch vergleichbar. Bei Gegenüberstellung der Ergebnisse zweier identischer Konfigurationen mit unterschiedlichen Pulsintensitäten („low“ und „high“ Euro NCAP) für das männliche und weibliche (Bio RID, Eva RID) Insassenmodell, konnte einen Steigerung der NV um 45 % bzw. 59 % festgestellt werden. Dies scheint zu bestätigen, dass weibliche Insassen empfindlicher gegenüber höheren Pulsintensitäten reagieren (Temming, et al., 1997).

**Fazit:** Fahrzeugsitze lassen sich perfekt gestalten um eine gute Bewertung in Zulassungs- und Verbrauchertests (Euro NCAP, 2015) zu erreichen. Das reale Unfallgeschehen zeigt jedoch teilweise große Abweichungen von diesen Testkonfigurationen. Insassen entsprechen nur in den seltensten Fällen einem 50-perzentilen männlichen Modell und Sitzeinstellungen weichen in der Regel von jenen in Testvorschriften ab. Das Ziel bei der Gestaltung von Fahrzeugsitzen sollte es daher sein, eine Vielzahl von Insassen (Größe, Geschlecht, Sitzhaltung, etc…) in einer großen Bandbreite von verschiedenen Situationen bestmöglich zu schützen. Zu diesem Zweck müssen jedoch neue Methoden und Werkzeuge zur Verfügung gestellt werden um die unterschiedlichen Belastungen der unterschiedlichsten Insassen in Situationen die sich von standardisierten Testbedingungen unterscheiden zu quantifizieren.

# CONTENTS

# ACRONYMS

| Abbreviation | Explanation |
|---|---|
| ΔT | Duration |
| ΔT | Change of Velocity (delta v) |
| a | Acceleration |
| AAAM | American Association for Automotive Medicine |
| ACC, acc | Acceleration |
| ADSEAT | Adaptive Seat to Reduce Neck Injuries for Female and Male Occupants |
| AEB | Automatic Emergency Braking |
| AGU | Arbeitsgruppe für Unfallmechanik (The Working Group on Accident Mechanics) |
| AHR | Active Head Restraint |
| AIS (AIS 1 - AIS 9) | Abbreviated Injury Scale |
| AIS (AIS-101) | Automotive Industry Standards of India |
| $A_{max}$ | Maximum Acceleration |
| $A_{mean}$ | Mean Acceleration |
| ANCAP | Australian New Car Assessment Program |
| AOP | Adult Occupant Protection |
| ASEAN NCAP | Southeast Asian Nations New Car Assessment Programme |
| AT0 | Acceleration at t = 0 [ms] |
| ATD | Anthropomorphic Test Device |
| AZT | Allianz Center for Technology (Allianz Zentrum für Technik) |
| b | Setting of the Backrest |
| Bio RID | Biofidelic Rear Impact Dummy |
| Bio RID 50F | Biofidelic Rear Impact Dummy 50th Percentile Female |
| Bio RID II | Biofidelic Rear Impact Dummy Version 2 |
| Bio RID IIg | Biofidelic Rear Impact Dummy Version 2 Revision g |
| BMI | Body Mass Index |
| C (C1-C7) | Cervical Vertebra (Cervical Vertebrae 1 through 7) |
| C ($C_{moment}$, $C_{shear}$, $C_{tension}$) | Critical Moment, Shear Force or Tension Force, LNL Criterion |
| c.o.g. | Centre of Gravity |
| CAC | Channel Amplitude Class |
| CAK | Crash Active Head Restraint (Crash Aktive Kopfstütze) |
| CESVIMap | Research and Road Safety Centre of MAPFRE (centro de experimentación y seguridad vial Mapfre) |
| CFC | Channel Frequency Class |
| $c_i$ | Normalised Criterion of Index i |
| $C_i$ | Absolute Criterion of Index i |
| cm | Centimetre |
| CNCAP | Chinese New Car Assessment Programme |
| C-NCAP | Chinese New Car Assessment Programme |
| cos | Cosine, Trigonometric Function |
| CP | Contract Point |
| CT | Computer Tomography |
| D (D02, D24, …) | Distance between two Points, Number of Start point, Number of Endpoint |
| D.o.T. | British Department of Transport |
| daNm | Decanewtonmetre |
| DAU | Data Acquisition Unit |
| delta v | Change of Velocity |
| DSD | Dr. Steffan Datentechnik |
| EBS | Equivalent Barrier Speed |
| EC | European Commission |
| ECE | Economic Commission for Europe |
| ECE R17 (ECE R32, …) | Economic Commission for Europe Regulation, Number of Regulation |
| EES | Energy Equivalent Speed |
| EEVC | European Enhanced Vehicle Safety Committee |
| ESAR | Expert Symposium on Accident Research |

| | |
|---|---|
| EU | European Union |
| EU | European Union |
| Euro NCAP | European New Car Assessment Programme |
| Eva RID | Virtual Rear Impact Dummy Model 50th Percentile Female |
| FEA | Finite Element Analysis |
| FEM | Finite Element Methods |
| FIA | Federation Internationale de l'Automobile |
| $F_{int}$ | Critical Force, Nkm Criterion |
| FMVSS (FMVSS 202, FMVSS 303, …) | Federal Motor Vehicle Safety Standard, Number of Standard |
| FP7 | Seventh Framework Programme for Research |
| fps | Frames per Second |
| $Fx_{lower}$ | Force at the lower neck in x direction |
| $Fy_{lower}$ | Force at the lower neck in y direction |
| Fz | Tension / Compression Force at the Point of Transition from Head to Neck, Nij Criterion |
| Fzc | Critical Force, Nij Criterion |
| $Fz_{lower}$ | Force at the lower neck in z direction |
| g | Standard Gravity, 9.81 m/s² |
| GB (GB20072-2006) | Guobiao, Chinese National Standard |
| GDV | German Insurance Association (Gesamtverband der Deutschen Versicherungswirtschaft e.V.) |
| Global NCAP | Global New Car Assessment Program |
| GTR (GTR 7, …) | Global Technical Regulation, Number of Regulation |
| GUT | Graz University of Technology |
| h | Setting of the Head Restraint |
| H III | Hybrid III Dummy |
| H/R | Head Restraint |
| HBM | Human Body Model |
| $H_{eff}$ | Effective Height |
| HIC | Head Injury Criterion |
| HIC ($HIC_{15}$, …) | Head Injury Criterion (Head Injury Criterion of 15 Milliseconds Duration) |
| $H_{LE}$ | Height Lower Edge |
| HPM | H-Point Machine (H-Point-Machine, H-Point Mannequin) |
| H-Point | Hip-Point |
| H-Point Machine | Device to determine the H-point in a given Seat |
| H-Point Mannequin | Device to determine the H-point in a given Seat (H-Point Machine) |
| HR | Head Restraint |
| HRMD | Head Restraint Measuring Device |
| IAG | Insurance Australia Group Limited |
| ICBC | Insurance Corporation of British Columbia |
| IIHS | Insurance Institute for Highway Safety |
| IIWPG | International Insurance Whiplash Prevention Group (International Insurance Whiplash Protection Group) |
| IP | Intersect Point |
| IV-NIC | Intervertebral Neck Injury Criterion |
| JNCAP | Japanese New Car Assessment Program |
| kg | Kilogramme |
| kHz | Kilohertz |
| km/h | Kilometre |
| kN | Kilonewton |
| KNCAP | Korean New Car Assessment Program |
| LATIN NCAP | Latin American and the Caribbean New Car Assessment Programme |
| LNL | Lower Neck Load Index |
| m/s | Metre per Second |
| m/s² | Metre per Square Second |
| M1 | Vehicle Category, Vehicles used for the carriage of passengers and comprising not more than eight seats in addition to the driver's seat. |
| M2 | Vehicle Category, Vehicles used for the carriage of passengers, comprising more than eight seats in addition to the driver's seat, and having a maximum mass not exceeding 5 tonnes |

| | |
|---|---|
| MATD | Motorcyclist Anthropometric Test Dummy |
| mbar | Millibar |
| MD | Medical Doctor |
| $M_{int}$ | Critical Moment, Nkm Criterion |
| MIX | Combined Criterion |
| mm | Millimetre |
| Moc | Moment about the Occipital Condyle |
| $Moc_y$ | Total Moment, Nij Criterion |
| MRT | Magnetic Resonance Tomography |
| ms | Millisecond |
| $Mx_{lower}$ | Moment at the lower neck in x direction |
| Myc | Critical Moment, Nij Criterion |
| $My_{lower}$ | Moment at the lower neck in y direction |
| N | Newton |
| N1 | Vehicle category, Vehicles used for the carriage of goods and having a maximum mass not exceeding 3.5 tonnes |
| NASVA | National Agency for Automotive Safety and Victims' Aid |
| $N_{av}$ | Average Nkm Value, MIC Criterion |
| NCAP | New Car Assessment Programme / New Car Assessment Program |
| Nce | Normalized Neck Injury Criterion considering compression and extension |
| Ncf | Normalized Neck Injury Criterion considering compression and flexion |
| NDC | Neck Displacement Criterion |
| Nea | Neck Protection Criterion considering extension anterior |
| Nep | Neck Protection Criterion considering extension posterior |
| Nfa | Neck Protection Criterion considering flexion anterior |
| Nfp | Neck Protection Criterion considering flexion posterior |
| NHR | No Head Restraint |
| NHTSA | National Highway Traffic Safety Administration |
| NIC | Neck Injury Criterion |
| $NIC_{av}$ | Average NIC Value, MIC Criterion |
| $NIC_{max}$ | Maximum NIC value |
| NICprotraction | Neck Injury Criterion for low speed frontal impacts |
| NII | Neck Injury Index |
| Nij | Normalized Neck Injury Criterion |
| Nkm | Neck Protection Criterion |
| Nm | Newtonmetre |
| Nte | Normalized Neck Injury Criterion considering tension and extension |
| Ntf | Normalized Neck Injury Criterion considering tension and flexion |
| NV | Neck Value |
| O/B | Outboard Seats |
| OEM | Original Equipment Manufacturer |
| OOP | Out of Position |
| ORM | Objective Rating Method |
| p | Pulse |
| PMHS | Post Morten Human Surrogate (Post Mortem Human Subject, Post Mortem Human Specimen) |
| QTF | Quebec Task Force |
| RCAR | Research Council for Automobile Repair |
| RHR | Reactive Head Restraint |
| RID 2 | Rear Impact Dummy |
| R-Point | Reference Point |
| S | Thickness |
| s | Gender, Sex |
| SA | Safety Assist |
| SAAQ | Societe de l'assurance Automobile du Quebec |
| SAHR | Saab Active Head Restraint |
| SCS | Spinal Care System |
| sin | Sine, Trigonometric Function |
| SNRA | Swedish National Road Administration |

| | |
|---|---|
| SRA | Swedish Road Administration |
| sup | Supremum, Maximum Value |
| t (t1, t2, ... tn) | Instant of Time |
| T0 | Start time |
| T1 | First Thoracic Vertebra |
| TGT (TGT1, TGT2, …) | Tracking Target, Target Number |
| T-HRC | Duration of Head to Head Restraint Contact ($T\text{-}HRC_{end}$ - $T\text{-}HRC_{start}$) |
| $T\text{-}HRC_{end}$ | End Time of Head to Head Restraint Contact |
| $T\text{-}HRC_{start}$ | Start time of Heat to Head Restraint Contact |
| THUMS | Total Human Model for Safety |
| TRIAS | Test Requirements and Instructions for Automobile Standards |
| TRL | Transport Research Laboratory |
| U.S. D.o.T. | United States Department of Transportation |
| UK | United Kingdom |
| UN | United Nations |
| UN/ECA | United Nations Economic Commission for Africa |
| UN/ECE | United Nations / Economic Commission for Europe |
| UN/ECE R17 (UN/ECE R32, …) | United Nations / Economic Commission for Europe Regulation, Number of Regulation |
| UN/ECLAC | United Nations Economic Commission for Latin America and the Caribbean |
| UN/ESCAP | United Nations Economic and Social Commission for Asia and the Pacific |
| UN/ESCWA | United Nation Economic Commission for Western Asia |
| UNECE | United Nations Economic Commission for Europe |
| US NCAP | US New Car Assessment Program |
| USA | United States of America |
| v | Velocity |
| WAD | Whiplash Associated Disorders |
| WAD (WAD1, WAD2, WAD2+, …) | Whiplash Associated Disorders Severity according to the Quebec Task Force Classification of WAD |
| WHIPS | Whiplash Protection System, Volvo |
| $w_i$ | Weighting Factor of Index i |
| WIC | Bending Moment Criterion |
| WIL | Whiplash Injury Lessening |
| WP (WP 1 - WP 5) | Work Package, Work Package Number |

# 1. INTRODUCTION

In todays' fast moving world, personal mobility appears to be of capital importance for people living their lives. The ability to get to any place desired, at any time of the day, is a freedom modern people seem to not want to miss. Now with the great freedom and flexibility of this individual mobility, some downsides arise alongside. Besides the environmental impact, which for sure is not to be disregarded, individual mobility is a threat to peoples' health and lives. Annually approximately 1.3 million people die from road accidents and 20 to 50 million are injured (World Health Organisation, 2004).

Sadly road traffic injuries have become the leading cause of death for young people between 15 and 29 years of age. Within the European Union (EU), 28,000 people died on roads in 2012. Thus several organisations and programmes act jointly, to coordinate efforts being made to solve these problems. Among these partners are for instance the United Nations European Commission for Economics (UN/ECE), European Commission for Directives and Regulations, consumer information organisations like European New Car Assessment Programme (Euro NCAP), Global NCAP, and research frameworks such as Horizon 2020 or the Seventh Framework Programme FP7 (Lorenz, 2014).

Despite the tragedy of fatal accidents, the impact of non-fatal accidents must not be neglected, when considering traffic accidents. Thus the European Commission (EC) granted a co funded research project, called ADSEAT, initiated by a consortium of twelve European partners within the Seventh Framework Programme to investigate and reduce the harm caused by one very special "injury" very common in vehicle accidents.

## 1.1. Whiplash

> *Whiplash, injury to the cervical spine and its soft tissues caused by forceful flexion or extension of the neck, especially that occurring during an automobile accident. It may involve sprain, fracture, or dislocation and may vary greatly in location, extent, and degree. Sometimes it is accompanied by concussion. Whiplash is characterized by pain, muscle spasm, and limited motion. Treatment includes protective support for the neck and back and sometimes the attachment of weights to the head or legs to stretch the injured muscles and relieve pressure on nerves*. (Encyclopædia Britannica, 2014)

The injury described above was known before automobiles changed the mobility of people in the early 20th century. In times before the triumphal course of automobiles, it was called "railroad spine" resulting from the fact, that it was mostly reported in connection with train collisions. However, the number of

victims was rather low and the impact of this rare trauma not very significant. Things changed however, as automobiles became available to a large number of people for everyday traffic. The increasing number of motorised vehicles led to a sharp rise of injuries due to traffic accidents, including whiplash injuries frequently reported after rear end collisions. (Desapriya, 2010)

Generally the term whiplash is a non-medical term, describing a large variety of symptoms, thus, subsequently it was extended to "whiplash associated disorders" (WAD), a conglomeration of many different traumata and symptoms of the neck, cervical spine and surrounding tissue related to motor vehicle accidents. This development was mainly driven by the Québec Task Force on Whiplash Associated Disorders, who also defined a classification of severity for such disorders, which is still in use today.

Nowadays "whiplash associated disorders" or neck injuries are very likely to be the most frequently reported "injury" among all insurance claims, and therefor account for a very significant financial, but on the first hand painful modern world issue (IIHS, 2008) (IIHS, 2014).

## 1.2. Aims

Aim of this this work was to contribute to the development of improved whiplash protection with the main focus on improvements for female occupants.

In the course of this thesis, based on a thorough literature review, different approaches such as experimental testing, finite element analysis and assessment of possible injury relevant factors shall be used. The goal was to show, whether or not females need increased attention, and if so, what measures could be used to deliver the required improvements.

Thus within several tasks of this work, the following unsatisfactorily answered questions were analysed:

- What factors influence the occurrence of whiplash associated disorders?
- Is the current situation, with regard to legislation and consumer tests, sufficient to deliver an equal amount of protection for all (i.e. male and female) occupants in rear end accidents?
- Can differences between males and females be shown by any means of current accident research methodologies, such as component testing or FEA?
- What should be improved in future to increase protection? Which possible steps could be implemented to achieve better protection for females?

Target of this thesis was not to find a general solution for a very manifold issue, but to show points of actions which promise to improve the situation as it is today.

# 2. BACKGROUND

After more than forty years of research in the field of WAD, still no satisfactory explanation for the actual injury mechanism and solution for this issue could be presented. The suffering of victims and the financial burden caused gives reason to continuous research in this field. Generally there is a vast amount of publications and studies available on this topic. Thus in this overview a general understanding of the topic, current regulations, assessments and countermeasures shall be provided. Also a brief insight on influencing factors, in particular the difference between male and female occupants, shall be delivered.

## 2.1. ADSEAT

The European Commission (EC) granted a co-funded research project, called ADSEAT (adaptive seat to reduce neck injuries for female and male occupants), initiated by a consortium of twelve European partners within the Seventh Framework Programme (FP7) to investigate and reduce the harm and impact caused by this very special "disorder". Within this project real world data, such as insurance claims and accident statistics, were analysed and actual female injury risk was assessed, as well as the effect of recently introduced whiplash protection systems was evaluated. Furthermore a virtual female rear impact crash test dummy was defined based on biological data and developed. Based on current thresholds it was investigated whether female limits must be defined

The overall goal of ADSEAT was to highlight possibilities to improve future seat designs to benefit both, male and female occupants. Especially to target females, detailed objectives of ADSEAT were:

- To analyse real world data to (WP 1)
  - assess actual risk of female injury,
  - evaluate the effect of recently introduced whiplash systems for females and males,
  - define crash pulse characteristics representing high and low risks for females and males,
  - carry out statistical evaluation of the influence of anthropometric differences
- To establish female biological data, to provide (WP 2)
  - dynamic motion and acceleration data for model evaluation,
  - data on injury mechanisms, injury sites and risk assessment parameters
- To develop female computational models (WP 3)
  - as basis for a female dummy to serve as a design and test tool
- To establish injury criteria and thresholds for females (WP 4)
- To develop a seat demonstrator illustrating how whiplash protection can be achieved for a wider population using adaptive seat designs (WP 5)

This thesis was performed within several sub-tasks of ADSEAT, which further promoted the research on rear end collision accidents and injuries referred to as whiplash associated disorders.

## 2.2. Relevance of Whiplash Associated Disorders

Regardless of recent developments in active safety features of passenger vehicles, passive safety is and will also in the future be an important topic to be considered, when assessing and admitting vehicles for a broad public audience.
According to numerous studies WAD still are a major concern in todays' society. For instance within the European Union an estimated number of more than 800,000 citizens suffer neck problems after being involved in vehicle collisions each year. Among these up to 40,000 are expected to suffer from long term consequences. The associated cost of these injuries, according to insurance claim estimations is expected to range around ten billion Euro annually implying a major financial burden for the European society (Kullgren, et al., 2007). Other studies estimate the cost for WAD to rank around $9 billion per year for the United States of America (Whiplash Prevention Campaign, 2010).

Despite many approaches to reduce and prevent the occurrence of these injuries, WAD still are the most commonly reported trauma caused in vehicle accidents (Grant, 2012). Most of the victims experience symptoms for a few weeks or months after such incidents. Five to ten percent, however, are confronted with different levels of permanent disabilities. (Norra K, 2005) (Nygren Å, 1985) (Krafft, 1998)

WAD can occur, compared to other traumata, at rather low velocity changes, usually below 25 [km/h] (Eichberger A, 1996) (Kullgren A, 2003) Contrary to common understanding, WAD occur at impacts from all directions, even if rear impacts are certainly the most frequently featured accidents (Watanabe Y, 2000) (Linder, et al., 2013).

## 2.3. Whiplash Associated Disorders – Anatomy and Injury

Whiplash or Whiplash Associated Disorders are terms to describe a number of symptoms and injuries usually associated with rear end collisions in car accidents. Commonly they occur in the neck region, the cervical spine.

Symptoms can be:

- neck pain
- headache
- dizziness
- nausea
- vision disorder
- muscular tension
- reduced mobility of neck and head
- neurological deficit

Injuries include cases of:

- fractures
- displacements of vertebral bodies
- ligament rupture and tearing
- strains
- haematoma

These symptoms and injuries depend on the severity of such incidents as well as other influencing factors. Obviously certain symptoms and injuries are related to a high level of loading, which can also objectively be diagnosed medically, such as fractures or ligament ruptures. For other injuries, especially at low loading conditions, no objective medical evidence, such as tissue injuries can be found. However, symptoms as described, can still occur and also be objectively verified (Rashier, et al., 2008).

### 2.3.1. Spine – Backbone

The human spine consists of different anatomical structures such as bones, muscular tissue, ligaments, intervertebral discs etc. The osseous components of the vertebral column are 24 vertebral bodies, the sacrum and coccyx. A graphic of a human vertebral column can be found in Figure 1. The 24 vertebrae are grouped in three sections shown in Figure 1. These groups are namely cervical spine (seven cervical vertebrae), thoracic spine (twelve thoracic vertebrae) and lumbar spine (five lumbar vertebrae). WAD are commonly symptoms and injuries that occur in the most upper region of the human spine, the cervical spine. This part of the vertebral column can be found in Figure 2. In this picture, the vertebral column of the first seven vertebrae, known as cervical vertebrae C1 – C7, is shown. The first cervical vertebra (Atlas or C1) in interaction with the occipital bone, called atlanto-occipital joint, are responsible for the ability to flex the head anterior (nodding). Atlas and axis (C2) form the atlanto-axial joint. Indicated in Figure 2, they are a functional unit and allow for rotation of the head (shaking head motion). The occipital-atlanto-axial complex is usually referred to as “upper cervical spine”. C3 through C4 form the middle and C5 through C7 the lower cervical column. The vertebra prominens (C7) is highlighted, because its lateral form distinguishes from C3-C6. The extended processus spinosus of C7 can be felt through the skin when palpating the neck dorsal. (Gray, et al., 2008)

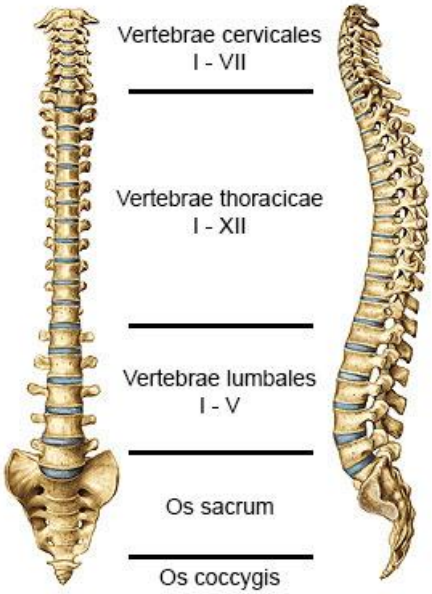


FIGURE 1 HUMAN SPINE, CERVICAL BODIES AND INTERVERTEBRAL DISCS (SOBOTTA, ET AL., 1993)

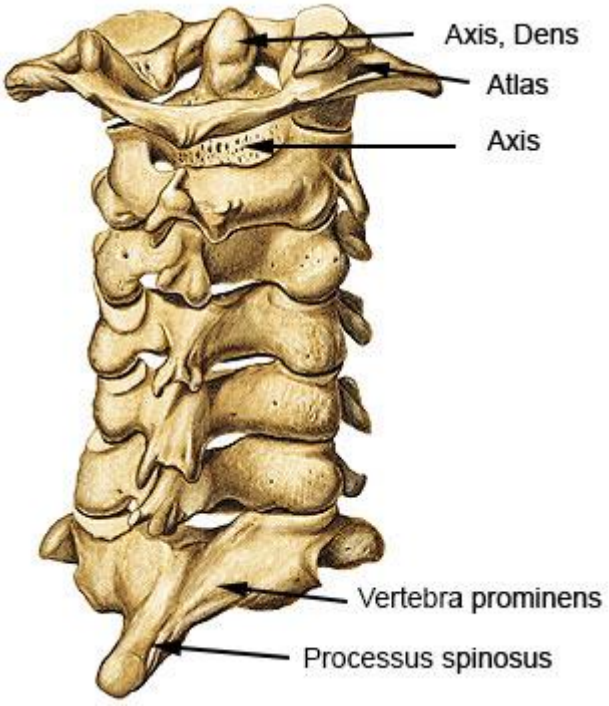


FIGURE 2 CERVICAL SPINE (SOBOTTA, ET AL., 1993)

### 2.3.2. Conventional Neck Injuries

Traumata to the (healthy) neck occur due to loading exceeding the normal limits for active movements by a human being. These loads can be tension, compression, bending, torsion, shear or a combination of two or several of them.
In (Pike, 2002) three different categories of injuries are described. Osseous injuries which describe cracking and breaking of bony structures, neurological injuries refer to damage to the spinal cord and spinal nerves' roots and thirdly soft tissue injuries such as ligamentous or muscular traumata. In accident trauma, these categories involved, overlap. A fractured vertebra for instance may involve or even cause damage to nerve structures.
No doubt, all these incidents are serious injuries and can cause severe consequences. Nerve damage in the upper cervical column can lead to paralysis that can include the inability to breath or even death. Nevertheless, these injuries can be diagnosed, evaluated and treated. Difficulties arise when no damage to tissue can be found but symptoms are present.

### 2.3.3. Whiplash Injury Hypotheses

Cases where examinations utilising computer tomography (CT) or magnetic resonance tomography (MRT) show no objective signs of injuries often cause disputes, especially in claims for compensation for pain and suffering. Disregarding the fact that deception certainly occurs, real suffering and pain is caused in many cases without objective evidence of injury. For these cases, a number of hypotheses exist to explain the symptoms.

All of the mechanisms and hypotheses assume, that a rapid deformation of the cervical spine, exceeding the physiologically normal ranges of movement, plays a decisive role. The injury mechanisms themselves are still not fully understood. Especially the s-shaped deformation of the cervical spine during rear end impacts, which consists of flexion in the upper and extension in the lower cervical column shows abnormal motions beyond normal physiological limits.

The following selected injury hypotheses or theories are examples and do not claim to be exhaustive.

Currently, among whiplash research, five or more basic pain causes are believed to have been identified. Five anatomical categories are classified by (Siegmund, et al., 2009). Categories are facet joint and capsular ligament, ligament and discs, vertebral artery, dorsal root ganglion and dorsal root as well as muscle. Similarly, (Curatolo, et al., 2011) define six different whiplash injury models and explain their development state and also effectiveness of treatment. The categories are zygapophysial joint (facet joint), dorsal root ganglion, muscle, vertebral artery, spinal ligaments and disc rim lesion.

According to (Curatolo, et al., 2011) a brief overview of the possible pain sources is given.

#### 2.3.3.1. Hyperextension

The most initial theory (Mertz, et al., 1971), but nowadays believed to be obsolete, takes into account the extension of the neck far beyond the normal scope of movement between head and neck. Today boundaries for this movement in rear end collisions are usually limited by head restraint systems.

#### 2.3.3.2. Zygapophysial Joints and Capsules

Numerous studies focus on the zygapophysial joint (facet joint) and its capsule (ligaments) (Lee, et al., 2004) (Lu, et al., 2005) (Kallakuri, et al., 2008) (Quinn, et al., 2010) (Dong, et al., 2010) (Quinn, et al.,

2007) (Dong, et al., 2008). Independent studies on animals (rats and goats) and human (cadavers and volunteers) show that strains of the facet capsular ligament between 15 % and 50 % can induce persistent pain. The same range of strain is associated with permanent modification of the neuronal signalling in the spinal cord due to swelling, altered morphology and collagen fibre damage. Interestingly, the induced pain occurred in the absence of observable rupture or tear of the affected ligaments. Furthermore farther tissue loading, causing capsular rupture results in no persistent pain. (Winkelstein, et al., 2008) All these findings support the theory, that even if no clinically detectable lesions can be found, symptoms can occur.

Studies (Lord, et al., 1996) (Barnsley, et al., 1995) (Lord, et al., 1994) furthermore prove, that anaesthesia of affected joints of patients with chronic neck pain from whiplash will lead to relieve these symptoms. Also (Lord, et al., 1996) (McDonald, et al., 1999) (Govind, et al., 2003) (Barnsley, 2005) show a treatment using radiofrequency neurotomy to be effective in eliminating chronic neck pain caused by zygapophysial joints.

Investigated by (Ono, et al., 1997) mechanisms concerning facet impingements and collision are described. During a whiplash load case, the lower cervical vertebrae C4 – C6 rotate backward in the early phase before the upper vertebrae. This leads to a flexion like shape in the early loading phase. Subsequently, due to the backward rotation of C6 and C5 the lower cervical column goes into an extension shape. The forward and upward motion of the torso in combination with the inertia of the head leads to an s-shape of the cervical column. Where the lower cervical spine now shows extension the upper cervical spine still remains in its initial flexion shape. This motion, as shown in Figure 3, leads to shear and (posterior) compression loading, but also tension of the anterior longitudinal ligaments at the lower cervical column. It could also be found, that the relative rotational movement is largest between C5 and C6. The backward rotation of the C5 vertebral body can occur to an extent, that the C5 inferior articular facet moves close enough to the C6 superior articular facet, so that impingements can occur

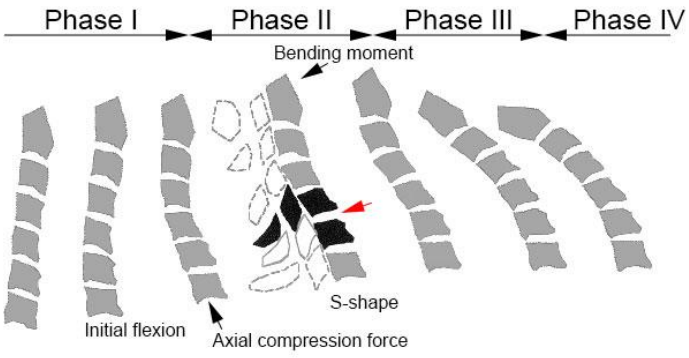


The cervical spine shows flexion in Phase I and S-shape formation in Phase II. At this phase, the motion segment at the apex of convex curvature (C5-C6) sufers from the stress of intervertebral articulation and strech of the anterior longitudinal ligament and forced to collide with each articulat facet (red arrow)

FIGURE 3 INJURY MECHANISM FACET IMPINGEMENT/COLLISION MECHANISM SCHEME ACCORDING TO (Ono, et al., 1997)

Due to the charge being applied from the seatback to the cervical spine, it is forced to move from the lower cervical vertebrae during rear-end collisions. This motion significantly differs from natural extension motions and is believed to be related to a relevant injury mechanism. (Kaneoka, et al., 1999)

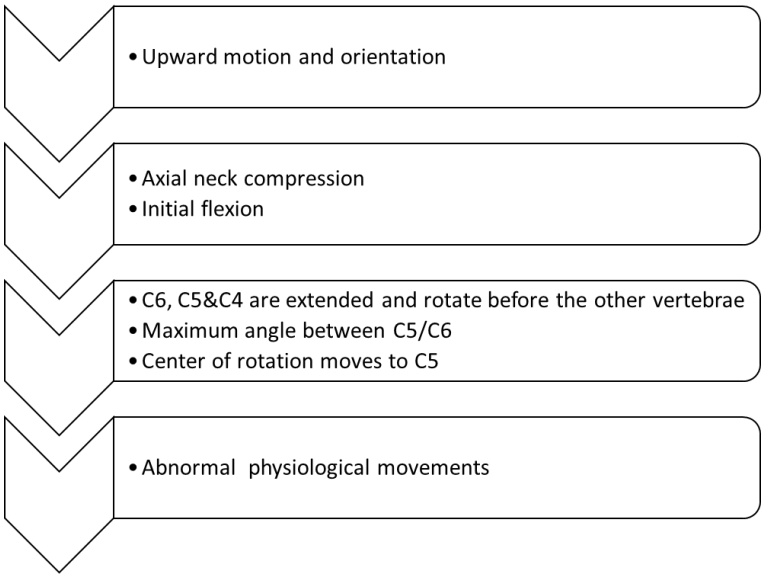


FIGURE 4 INJURY MECHANISM FACET IMPINGEMENT/PINCHING/COLLISION MECHANISM SEQUENCE

A study by (Yoganandan, et al., 2001) described a similar mechanism in the mid-lower part of the cervical column (C5/C6). A localized compression of the posterior region of the facet joint, in combination with the distraction of the anterior region leads to a pinching mechanism for rear impact induced motion.

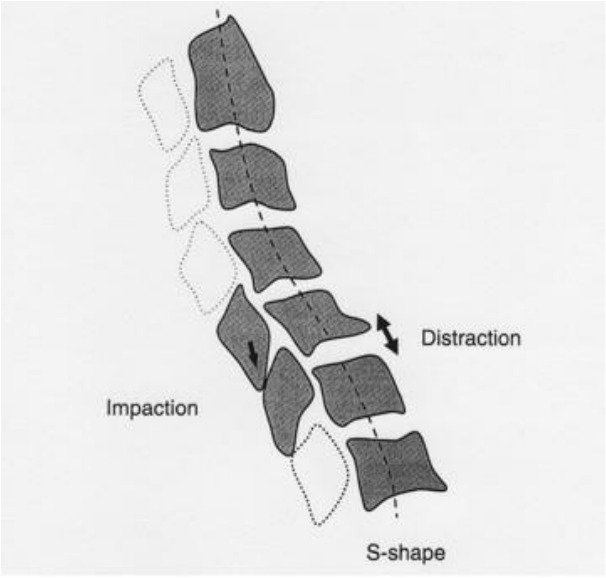


FIGURE 5 INJURY MECHANISM COMPRESSION OF THE POSTERIOR REGION OF THE FACET JOINT, IN COMBINATION WITH DISTRACTION OF THE ANTERIOR REGION (The Healthy Spine Ltd, 2011)

The posterior region of the facet joint may contact the subchondral bone via cartilage compression. Cartilage, being deprived of nerve endings, is an inadequate explanation for causing pain. However, considering cartilage degradation leading to osteoarthrosis inducing long term changes to joints and subchondral bone, painful phenomena can be explained.

#### 2.3.3.1. Lower neck capsular ligament tear

When observing vertebrae motion during whiplash loading, local relative motion between adjacent vertebrae is dependent on the observed location. Relative motion in joints differs from general observed motions of vertebrae. The local extension of the cervical column for instance leads to shear/sliding in the facet joints. Anterior and posterior regions respond with local stretch of the capsular ligaments, in some cases beyond physiological limits. Since pain fibres are present in these locations, this might be a source of pain. Outstanding is the local concentration of damage found in the lower region (C5-C7) of the cervical column by (Yoganandan, et al., 2001).

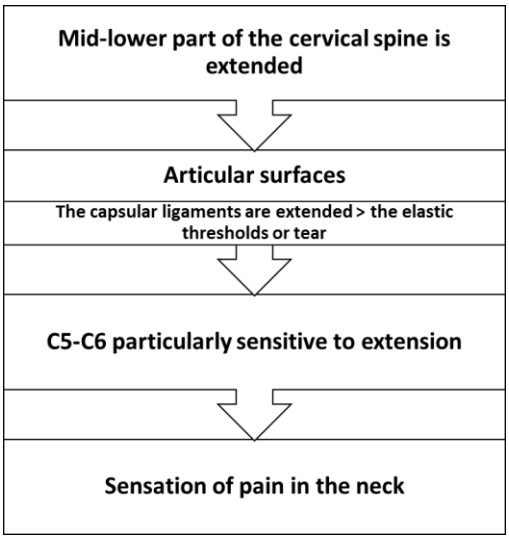


FIGURE 6 INJURY MECHANISM LOWER NECK CAPSULAR LIGAMENT TEAR SEQUENCE

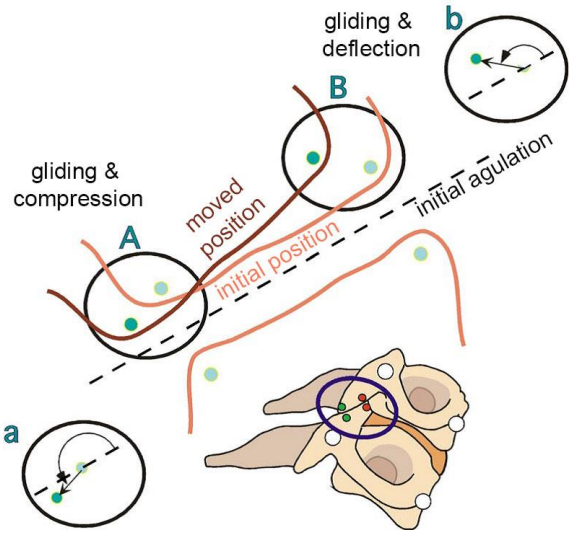


FIGURE 7 INJURY MECHANISM FACET JOINT MOTION ACCORDING TO (Yoganandan, et al., 2001).

Figure 7 illustrates the facet joint motion during a whiplash sled test. The lighter lines show the initial orientation of the facet joint where the darker line shows the movement of the superior surface of the facet joint with respect to the inferior surface. The dashed line shows initial angulation. Angulation of the facet joint is defined as the vectorial orientation between the initial and final positions of the target (shown in circles) at the anterior and posterior regions with respect to the initial joint line. An angle greater the initial angle (180 °) represents rearward motion of the particular region (e.g., anterior) of the joint. Inserts a (for A in the main figure) and b denote the vector directions of these motions at the posterior and anterior regions of the facet joint. Dashed lines in the inserts are drawn parallel to the initial facet joint line shown as a longer dashed line in the main figure. Thus gliding and deflection in the anterior region, gliding and compression in the posterior region is present. The local stretch increases with higher loads (delta-v) experienced during a whiplash incident. According to (Yoganandan, et al., 2001) a delta-v of 0.6 [m/s] can cause local facet joint stretch of up to 1 [mm] for the C5-C6 vertebrae pair. Increasing the load to 3.5 [m/s] the local stretch was determined to be as large as 5 [mm]. Thus displacements of adjacent vertebrae outside normal ranges occur during whiplash.

#### 2.3.3.2. Anterior Longitudinal Ligaments and Discs

The anterior longitudinal ligament and rims of the anterior annulus fibrosis could be found ruptured and torn in human cadavers studies loaded with whiplash (Yoganandan, et al., 2001). Since whiplash can cause strains exceeding physiological limits of the annulus fibrosus, especially in the lower region of the cervical spine, tears of the cervical discs and also the anterior longitudinal ligaments can be sources of symptoms (Panjabi, et al., 2004a) (Panjabi, et al., 2004b). For this hypothesis, the same mechanisms and causes as for the facet joint can be assumed, even if they were not investigated to

the same extent as the facet joint. In this regard it is generally believed, that if imaging techniques were to be improved further, these pain causing strains in the anterior regions of the discs could be demonstrated in patients.

#### 2.3.3.3. Vertebral Artery

Biomechanical research (Ivancic, et al., 2006) indicates, that coupled neck motions (cause by offset vehicle collisions and/or rotated head postures during collisions) can lead to injuries caused by elongations of the vertebral artery exceeding its normal range. The most common region for this kind of injury is the C1-C2 section of the vertebral column, where the most axial rotation of the head versus neck is present (Taneichi, et al., 2005) (Pollanen, et al., 1996) (Chung, et al., 2002). Additionally to overstretching, pinching to the artery can occur. Changes to the artery, as it recovers from excessive stretch, can thus influence the blood flow to the brain leading to common long term whiplash symptoms such as dizziness, head ache or nausea.

#### 2.3.3.4. Dorsal Root Ganglion

Damage to the dorsal root ganglion or directly to the nerve roots are believed to cause symptoms in this region. Two different mechanisms are described. Direct impingement of the dorsal root ganglion by rapid reduction of the space of the neural foramen can cause tissue damage (Nuckley, et al., 2002). Furthermore rapid motions of the neck can cause volumetric changes to the spinal canal or other fluid containing vessels. In this context, the pressure transient mechanism characterized by (Aldman, 1986) describes a volumetric change of the spinal canal during an extension-flexion motion of the cervical spine. Due to the rapid change of volume, a transient pressure gradient is induced in the spinal canal. This rapid pressure change, according to (Svensson, et al., 1993) and (Schmitt, 2001) is believed to cause damage to nerve cells, in the dorsal root ganglia leading to typical described symptoms. Pressure gradients result from blood flow resistance, acceleration and inertia of fluid mass. During normal motion, fluids inside and outside of the cervical canal can compensate. Rapid volumetric changes however can not be balanced fast enough leading to pressure differences. These differences can cause mechanical load on spinal ganglia and nerve roots leading to whiplash related symptoms. The presumed scheme is shown in Figure 8.

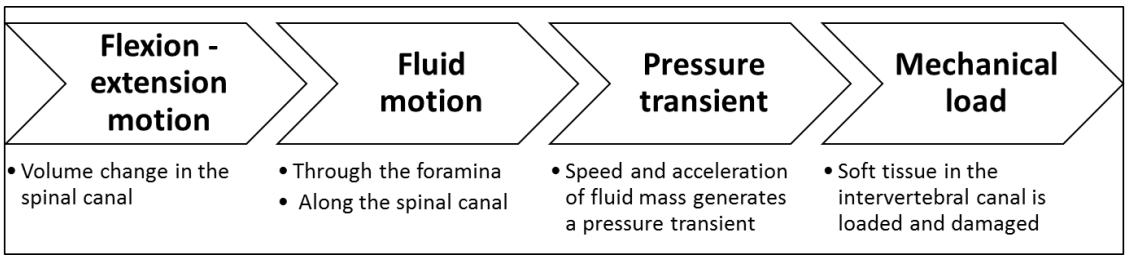


FIGURE 8 INJURY MECHANISM PRESSURE TRANSIENT MECHANISM

This mechanism, according to (Siegmund, et al., 2009) and (Curatolo, et al., 2011) is considered to cause damage to the dorsal root ganglion and dorsal root. The correlation of the relative motion between the head and neck is quantified by the NIC criterion, which relates to the horizontal relative acceleration and velocity of the head and T1 vertebra.

#### 2.3.3.5. Muscular Tissue

Muscular tissue takes up the largest volume of the human neck. Thus describing pain originating from regions corresponding to muscles is common for WADs. Symptoms from muscles can however have different sources.

Direct injury to muscle can occur from involuntarily lengthening of muscle during reflex activation. Strains exceeding the normal physiological range can be reached in crash scenarios leading to muscle injuries. Since clinical studies showed elevated serum creatine kinase (a marker for muscle injuries) 24 hours after the crash, but not after 48 hours, these muscle injuries appear to be responsible for acute pain rather than chronical issues. (Macpherson, et al., 1996) (McCully K, et al., 1985) (Scott, et al., 2002)

Long term issues may however origin from different causes involving muscular tissue. For instance repositioning errors (Heikkilä, et al., 1996) (Loudon, et al., 1997) and altered range of motion (Madeleine, et al., 2004) (Antonaci, et al., 2002) might origin from injuries to the facet joint, capsular ligament or annular fibres (Panjabi, 2006). Animal models have shown spinal ligaments to stimulate spinal muscle activities. Abnormal signals of injured capsules, ligaments and annular fibres may cause corrupted neck muscle response and the neuromuscular control systems might even stiffen the injured neck to prevent further injuries causing loss of range of motions or even painful muscle spasms. Furthermore the direct insertion of certain muscles (e.g. multifidus muscles) onto facet capsular ligaments may impair the lesion of already injured capsule, even during normal head motion. (Siegmund, et al., 2008) (Curatolo, et al., 2011)

#### 2.3.3.6. Shear between Vertebral Bodies

A study by (Yang, et al., 1997) describes a mechanism where anterior-posterior shearing of the vertebrae causes injuries to the soft tissue. In this study it is shown, that axial compression of the cervical column is responsible for a reduced shear stiffness of adjacent vertebrae , making it easier to cause soft tissue damage due to shear. The axial compression is initially caused by an upward acceleration of the spine caused by ramping or interaction with the seat back during a rear end impact. These rather low acceleration peaks in combination with the inertia of the head are capable to induce significant compressional forces in the cervical column. It was shown, that a preload of only 20 [kg] on the C5-C6 vertebrae couple reduced shear stiffness from 18.6 [N/mm²] to only 5 [N/mm]. Furthermore it is believed that the anatomy of the facet joint protects such shear injuries for frontal collisions. Frontal shear is believed to be prevented by facet joint contact, where rear end collisions lead to gapping of the facet joint and thus not preventing anterior shear. Thus this mechanism is believed to be more important for rear end collisions than front collisions.

#### 2.3.3.7. Upper Neck Tension Mechanism

Also explained by (Yoganandan, et al., 2001) was a tension mechanism found in the upper neck region. It describes morphological change to the ganglion of the greater occipital nerve due to increased flexion between the occiput and the C2 vertebra, which leads to an increased axial tension. It is believed, that this alteration causes headaches, which is frequently described as a symptom of WADs.

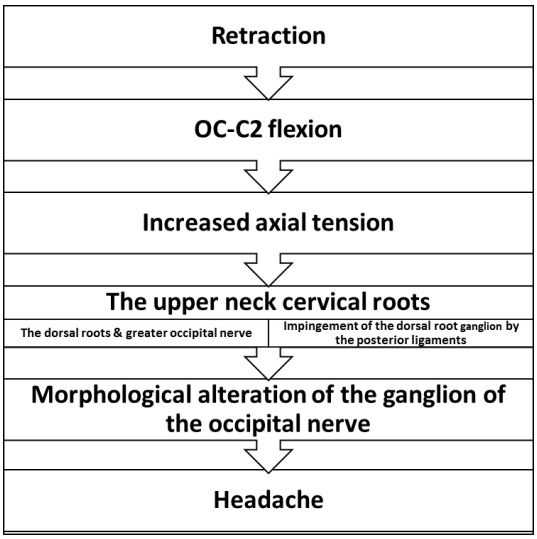


FIGURE 9 INJURY MECHANISM UPPER NECK TENSION MECHANISM

### 2.3.4. Whiplash Injury Severity Classification

#### 2.3.4.1. AIS

The Abbreviated Injury Scale (AIS) is a general purpose system to describe the severity of injuries throughout the entire body. Originally defined 1971 by the Committee of Injury Scaling of the Association for the Advancement of Automotive Medicine, formerly known as American Association for Automotive Medicine (AAAM), the current applicable version is the AIS2005 update 2008.
The AIS is intended to be a simple multipurpose scale to describe injuries from minor to lethal severity. Due to this broad spread, whiplash associated disorders are usually described as minor severe injuries (AIS1). The AIS coding allows very detailed description of injuries, injured regions and body parts and much more. The scheme however is intended to describe the lethality of injuries. This makes the system inadequate for describing whiplash associated disorders. (AAAM, 2008) Whiplash injuries, in principle, never lead to death. However, the impact of whiplash on life quality caused by possibly lifelong disabilities can be severe.

To meet these requirements, another method to describe these usually non-lethal injuries was necessary.

#### 2.3.4.2. Quebec Task Force

In January 1995 a consortium chaired by Walter O. Spitzer[A] published an article regarding whiplash associated disorders. The text addresses several issues such as prevention, examination diagnosis, treatment, rehabilitation and management of such conditions. The consortium having its origin in the Societe de l'assurance Automobile du Quebec (SAAQ), now known as Quebec Task Force (QTF), distinguishes five different grades of severity of whiplash associated disorders. This classification can be found in the subsequent Table 1 (Spitzer, et al., 1995).

| Grade | Clinical Presentation |
|---|---|
| 0 | Client does not complain of neck pain and no physical signs |
| 1 | Client complains of pain; normal range of motion, normal strength, no swelling suffer from small muscle lesions that are not significant enough to cause muscle spasm |
| 2 | Like grade 1 plus: musculoskeletal signs are found that could include: limited range of motion, spasm or swelling, point tenderness in neck or shoulders. Usually these clients have sprained ligaments in their neck and the muscle tears have caused bleeding and swelling |
| 3 | Like grade 1 plus: neurological signs are found (like decreased or absent reflexes, decreased or limited skin sensation, muscular weakness). Usually because of pressure on nerves. These clients will almost always have limited range of motion and other musculoskeletal signs as well |
| 4 | Like grade 1 plus: X-rays reveal fracture or dislocation |

TABLE 1 CLASSIFICATION ACCORDING TO THE QUEBEC TASK FORCE

[A] MD at the Department of Epidemiology and Biostatistics, McGill University, Montreal, Quebec, Canada

#### 2.3.4.3. Erdmann

Another classification of the severity of WAD was introduced by (Erdmann, 1983). The classification reaches from grades with no obvious symptoms to lethal injuries. An overview is given in the following Table 2.

| Criteria | Grade 0 (no trauma) | Grade I (light) | Grade II (medium) | Grade III (severe) | Grade IV (fatal) |
|---|---|---|---|---|---|
| Symptoms | None | Pain of neck muscular tissue and/or cervical spine with reduced range of motion (stiff neck) usually after symptom free period of time | Like Grade I but without symptom free period of time. Possible secondary insufficiencies of neck muscular tissue. Interscapular pain. Pain in the base of the mouth. Paraesthesia of arms. | Like Grade I and Grade II. Primary insufficiencies of neck muscular tissue. Brachialgia, arm paresis. Short initial loss of consciousness. | High paraplegia. Death due to failure of central nervous system regulatory functions, usually on site. Acute bulbar syndrome. |
| Symptom free period of time | NA | Common, usually > 1 h, max. 48 h, typically 12-16 h | Rarely, usually < 1 h, max. 8 h | usually not | inexistent |
| Duration of Symptoms | NA | Usually days to weeks, < 1 month | Weeks to months | Months, rarely > 1 year | Usually death on accident site |
| Confinement in bed | NA | Unusual | Common | Very likely | Permanently or death |
| Neurostatus | Normal, unchanged | no neurological deficits, possible reduced range of motion of the neck | no neurological deficit, painful reduced range of motion of the neck | Sensory and/or motoric neurological deficits | tetra paresis, possible damage to medulla-oblongata |
| Morphology | No lesions | Distortion, Strain and tear of cervical soft tissue | Like Grade I, Joint capsular tear (retropharyngeal hematoma, muscular strain and tear) | Like Grade II involving several segments, intervertebral disk rupture and/or bleeding, ligament rupture, vertebrae fracture/dislocation, medulla-, nerve-, root lesions | medulla contusion up to medulla transection, damage to the medulla oblongata and lower brainstem, fracture at the base of the skull, damage and fracture of the atlantoaxial joint |
| X-Ray | Unchanged | Unchanged, possible loss of cervical lordosis | possible loss of cervical lordosis, kyphotic bend, slight instabilities | Fractures, defective position, lift-off in function examination | Fractures and dislocations |
| Collision speed | 0-8 km/h | >8 to 30 km/h | >30 to 80 km/h | >50 to >100 km/h | >80 km/h |
| Head acceleration | <4g | 4-15g | 16-40g | >20-40g | >40g |
| Vehicle damage | Dents, Rear window shattered | Deformation of car body, several centimetres, depending on model | Like Grade I, Passenger compartment intrusions begin | More pronounced deformation of the passenger compartment | High deformation of the passenger compartment |

TABLE 2 CLASSIFICATION ACCORDING TO ERDMANN (ERDMANN, 2015)

Symptoms in Erdmann's classification appear similar to the QTF, which also shows four grades of severity. Table 2 however gives additional information about post-accident durations for symptoms and permanent disabilities, as well as typical medical issues.

## 2.4. Influencing factors for WADs

Influencing factors on the risk sustaining WADs during accidents were summarised by (Schick, et al., 2010). Their review points out that influencing factors can be divided into four major characteristics.

- Person characteristics
- Vehicle characteristics
- Crash characteristics
- Interaction and Situation characteristics.

These influencing factors are reviewed in more detail and point out what topics should be further thoroughly investigated.

### 2.4.1. Person characteristics

#### 2.4.1.1. Occupant Gender

Statistical reviews from the 1960's until very recent by (Linder, et al., 2013) indicate, that females appear to have a higher risk sustaining whiplash associated disorders than males. Numbers vary, but statistics indicate an increased risk up to three times higher than males. (Kihlberg, 1969); (O'Neil, et al., 1972); (Thomas, et al., 1982); (Otremski, et al., 1989); (Maag, et al., 1990); (Morris, et al., 1996); (Dolinis, 1997); (Temming, et al., 1998); (Richter, et al., 2000); (Chapline, et al., 2000); (Krafft, et al., 2003), (Jakobsson, et al., 2004b); (Storvik, et al., 2009).

One review found whiplash protection seats and concepts to be more effective for male than female occupants (Kullgren, et al., 2010). The reduction of injury risk concerning permanent medical impairment was approximated at 60 % for males and only 45 % for females. This suggests, that different seat concepts and whiplash protection systems show very different effectiveness when occupied by male or female passengers. It is important for future developments to understand the reason for such behaviour, in order to improve protection for any occupant regardless of gender. Anthropometry and mass distribution differ significantly for males and females (Carlsson, et al., 2012b). Thus an influence regarding the interaction of the upper body and head with the seatback and head restraint can be expected leading to a possible increase of injury risk. The differing lever about the seatback hinge due to the shorter upper body height, and the lower mass of female upper bodies (Carlsson, et al., 2014) are exemplary reasons for a smaller deflection of the seat frame, seat back padding and springs and so on. Reduced deformation of such components, leading to lower plastic deformations of these structures, goes along with reduced energy absorption. Thus the rebound of the torso and the dynamic head-to-head-restraint distance are influenced (Svensson, et al., 1993), (Croft, et al., 2002), (Viano, 2003). Also the dynamic response of the head relative to the head restrained appears to be influenced by the seated height. Females' dynamic responses in rear impact tests differ from males. Higher head x-acceleration and T1 x-acceleration was reported. The Neck Injury Criterion (NIC) is comparable or lower, but the rebound is more pronounced than for males. (Szabo, et al., 1994); (Siegmund, et al., 1997); (Hell, et al., 1999); (Welcher, et al., 2001), (Croft, et al., 2002); (Mordaka, et al., 2003); (Viano, 2003); (Ono, et al., 2006), (Linder, et al., 2008); (Schick, et al., 2008), (Carlsson, et al., 2012a); (Carlsson, et al., 2011). Self-explanatory females show anthropometric differences such as stature, weight, body part dimensions and mass distribution. (Pheasant, et al., 2006).

Recent reviews on WADs imply, that the increased risk for females is minor (Haldeman, et al., 2008) (Holm, et al., 2008) (Schick, et al., 2010). It is stated, that prevalence of neck pain is a risk factor for WAD. Females show a higher prevalence of episodes of neck pain. This might explain the increased risk for females found in many studies. The argument that females tend to seek for medical help more easily and more quickly cannot be confirmed when considering the study of (Brault, et al., 1998). Females show the same incidences and severity of neck symptoms compared to males, however the duration of the symptoms lasted longer compared to those of males.

Numerous recent as well as older studies show an increased risk for females (relative risk 1.2 to 2.2). ( (Krafft, et al., 2003), (Martin, et al., 2008), (Berglund, et al., 2003), (Chapline, et al., 2000), (Dolinis, 1997), (Hell, et al., 1998), (Temming, et al., 1998))

#### 2.4.1.2. Occupant Age

Age as a factor of risk was investigated in several studies. Among them a common conclusion can be found, that higher aged occupants appear to have lower risk sustaining WAD (Holm, et al., 2008). The risk – age relation appears to be of parabolic shape with its maximum around 20 to 30 years (age 18-27y: (Temming, et al., 1998), age 25-35y: (Jakobsson, et al., 2000), <40y: (Hell, et al., 1998) and the lowest for age classes greater 50 years (>65y: (Martin, et al., 2008), >54y: (Berglund, et al., 2003), >59y: (Hell, et al., 1998), >60y: (Jakobsson, et al., 2000)).

Since most of these data are based on insurance claims, it can be assumed, that elderly and more frequently retired people don't see a necessity to claim compensation. However the study by (Martin, et al., 2008) is based on clinical data and confirms the higher risk for the age group 34 to 49 with a relative risk of 0.6 where the group 65 and older shows a relative risk of 0.55.
These risk distributions by age can be found for both genders with a general higher absolute risk for females.

#### 2.4.1.3. Anthropometry

##### Body Height

(Lundell, et al., 1998), (Jakobsson, et al., 2000), (Temming, et al., 1998) state that, independent of gender, a higher body height increases the risk for WAD. These studies including samples of vehicle models from the 80s to the late 90s are contrary to one more recent study from 2004 (Jakobsson, et al., 2004a) where an increase of injury risk for WAD due to greater body height cannot be confirmed. Within this study it is however considered, that without the whiplash protection system WHIPS in place, taller females might be at higher risk sustaining WAD. However this study is limited on vehicle seats equipped with the WHIPS system and suggests that body height in very recent, well designed and assessed vehicle seats, is not an influencing factor on WAD risk anymore. A general conclusion for all very recent vehicle seats cannot be drawn.

##### Body Weight

Concluded in (Temming, et al., 1998), a relation between body weight and the risk sustaining WADs can be found. However some inconsistencies remain and these findings could not be confirmed with any other available studies.

### Body Mass Index (BMI)

The BMI is a number characterising the amount of soft tissue of an individual for classifying the stature of a person. It is derived as follows.

Equation 1 Body Mass Index calculation

$$BMI = \frac{(body\ weight)}{(body\ height)^2}$$

Where body weight is given in [kg] and body height in [m].

Two studies (Jakobsson, et al., 2004a), (Yang, et al., 2007) considering the relevance of the BMI regarding sustaining WAD or the recovery period from WAD do not show a significant correlation.

### Head to Neck Ratio

The head to neck ratio is described as head cross sectional area divided by neck cross sectional area. A study by (Brault, et al., 1998) focusing on short term WAD indicates, that no correlation between the head to neck ratio and the risk sustaining short term WAD can be found. Volunteer tests performed in this study at a change of velocity of 4 [km/h] lead to 29 % of the probands showing minor short term symptoms, tests at 8 [km/h] lead to a higher percentage of short term symptoms, namely 38 %. Due to the low severity of this study, long term symptoms could not be observed.

Studies based on reliable real life data, considering circumferences of neck, head, thorax, pelvis or other anthropometric characteristics influencing the risk sustaining WAD, could not be found.

### History of neck symptoms

Degenerations like disc bulging, protrusion, and herniation, spinal stenosis, and narrowing, vertebral spurring and osteophytes, degenerative disc disease, degenerative joint disease, radicular and myelopathic symptoms and abnormal structures like spondylolisthesis or spine curvature, according to (Bartsch, et al., 2008) do not show an influence on the risk of WAD. Results of (Holm, et al., 2008) brought up, that degenerative changes are primarily associated to age. However, since younger age groups show higher numbers for reporting and claiming WAD, it is assumed, that degenerative changes do not contribute to increasing WAD risk.

It appears, that all person related risk factors apply equally to male and female occupants.

## 2.4.2. Vehicle Characteristics

### 2.4.2.1. Vehicle Mass

Regarding vehicle mass, most studies, such as (Krafft, 1998), (Martin, et al., 2008), (Boström, et al., 1997), (Krafft, et al., 1996), (Temming, et al., 1997) find an increased risk sustaining WAD and long term WAD for light target vehicles struck by heavier vehicles. Thus a decreasing ratio between the mass of struck and striking vehicle leads to higher WAD risks irrespective of gender. One study (Dolinis, 1997) suggests, that no influence of the mass ratio between struck and striking vehicle can be found. The study however appears to show an overrepresentation of females and age class around 50 years, which might lead to this result.

#### 2.4.2.2. Vehicle Model

(Boström, et al., 1997), (Krafft, 1998) confirm, that car models built in the 1990 show a higher risk than vehicles from the 1980. Also (Eichberger A, 1996) found, that different car models show different risks, regardless of the mass ratio, using a “Neck Injury Factor”.

For Volvo cars, an 18 % relative higher risk was found for vehicles with more forward B-pillars, such as 4/5 door cars, compared with 2/3 door cars (Krafft, et al., 1996). Contrary (Temming, et al., 1997) states the exact opposite, where two door cars compared to four door cars were found to show higher risk. It is believed, that the anchor position of the seat belt influences the occupant kinematics, however the rebound phase is thought to be of low risk sustaining WAD. The influence of the seat belt during the initial acceleration is negligible. Also to be considered is the folding mechanism implemented in 2/3 door car seats (sometimes also in 4/5 door seats for storage room purpose). It can be assumed, that the folding mechanism has an influence on the stiffness of the seat back, or the recliner respectively. Whether the folding mechanism is softening or stiffening the seat back depends on the particular seat model. A statistical analysis on this topic however was not found.

A longitudinal position of the engine in the striking vehicle shows higher risk sustaining long term WAD compared to vehicles with transverse engine position. Also the presence of a trailer coupling on the struck vehicle increases the risk for long term WAD (22 %). These findings indicate, that an influence on long term WAD appears to be connected with the resulting crash pulse for the struck vehicle (Krafft, 1998).

Supplementary, and very astonishing, (Farmer, et al., 2008) found that higher vehicle prices seem to lead to lower WAD risk. Mass ratio did not lead to a more rational explanation in this study.

#### 2.4.2.3. Seat Characteristics

The seat with its components is the first structure to interact with the occupant. (Morris, et al., 1996), (Olsson, et al., 1990), (Parkin, et al., 1995) found, that a yielding seat, or more detailed a yielding seat back is in favour for occupants reducing resultant loads. This is implemented in the WHIPS system, where controlled yielding of the backrest is used to decrease load on occupants. However (Foret-Bruno, et al., 1991) state that a yielding backrest only benefits the occupant for seats with no head restraint in place. Seats with head restraints seem to not increase the protective performance if yielding, even a slight increase in cervical spine disorders could be found. These results based on seats from vehicle models from the 1980s are complemented by more recent studies such as (Farmer, et al., 2003). Here active head restraint systems are found to decrease the risk for WAD, and in particular females benefit from such systems. Furthermore, from a different point of view, anti-whiplash systems seem to decrease the number of neck injury claims (Avery, et al., 2008). But also simple geometrical redesigns of head restraints can benefit, especially females (Farmer, et al., 2003).

Other car model related factors such as stiffness and design of relevant front and rear structures are not investigated by any known real life data study. Vehicle related risk factors apply in the same way for males and females although sometimes with unequal severity.

### 2.4.3. Crash Characteristics

#### 2.4.3.1. Degree of Damage

A higher degree of damage of the struck car indicates an increased risk for WAD for male occupants. (Chapline, et al., 2000). This analogy could however not be found for females.
Considering all impact directions, an increased degree of damage is associated with an increased severity of injury symptoms (Ryan, et al., 1993). Considering, that the extent of damage is dependent on the energy absorbed during an impact, but also influenced by the stiffness of the deformed vehicle, different conclusions can be drawn. Large deformations can be interpreted as large amounts of energy absorbed, reducing the remaining force on the occupants. However comparing one vehicle (same vehicle model) with different extents of damage, certainly the larger deformation indicates larger overall loads and thus forces applied to the occupant.

Including developments of current vehicle fleets, younger car models, and especially small passenger cars are build more stiffly. This characteristic increases the acceleration on occupants, while the extent of damage will not display this behaviour. Thus a general association between the degree of damage and the load on occupants and thus on risk for WAD cannot be drawn. Studies on the explicit influence of the degree of damage on WAD risk could not be found, however (Jakobsson, et al., 2008) showed, that a higher impact severity, in this case based on repair extent, is an indicator increased reports of WAD also for more recent vehicles.

#### 2.4.3.2. Delta v

Delta v describes the change of velocity during a vehicle accident. Reviewing several studies (Krafft, et al., 2002a), (Kullgren, et al., 2003), (Kraft, et al., 2000), (Ryan, et al., 1993), it can be concluded, that increased delta v tends to increase the risk sustaining WAD, furthermore this goes for both genders, males and females.
At a certain change of velocity the risk sustaining WAD is believed to be 100 %. One suggestion by (Krafft, et al., 2002a) sets the threshold for 100 % injury risk at 25 [km/h], another (Kullgren, et al., 2003) at 30 [km/h]. A study by (Krafft, et al., 2002a) showed, that the risk for WAD lasting up to one month is highest at a delta v between 10 [km/h] and 15 [km/h] for both genders. Contrary (Temming, et al., 1997) found that the highest risk sustaining WAD occurs in the range of 13 to 17 [km/h] with risks around 53 % for females and 25 % for males.
The absolute risk for short duration WAD with low severity symptoms were investigated by (Brault, et al., 1998). The risks were found to be 29 % at delta v of 4 [km/h] and 38 % for 8 [km/h].

Other studies included different classifications such as Energy Equivalent Speed (EES) (Olsson, et al., 1990) and (Morris, et al., 1996) or Equivalent Barrier Speed (EBS) (Jakobsson, et al., 2000). Where (Olsson, et al., 1990) cannot find an influence of EES on WAD severity and duration, (Morris, et al., 1996) showed, that the risk for WAD is highest in a range of EES between 20 and 25 [km/h]. For the EBS no influence on the WAD risk could be found (Jakobsson, et al., 2000).

Females and males are only considered separately by (Temming, et al., 1997). The data, which is based on reconstruction calculations rather than real world measurements, shows, that the highest risk sustaining WAD occurs at a comparable range of delta v, around 13 to 17 [km/h]. However the absolute risks for males and females differ.

#### 2.4.3.3. Mean Acceleration

Acceleration has a vast influence on WAD. 1 [g] acceleration increase appears to raise the absolute injury risk by 20 % according to (Krafft, et al., 2002a). At 7 [g] the absolute risk is estimated to be 100 % for WAD with durations less than one month. Acceleration levels from 4 [g] to 7 [g] show an increase in risk for WADs lasting longer than one month. Different genders were not considered in this study.

#### 2.4.3.4. Direction of Impact

Rear end impacts are commonly known to bear high risk sustaining WAD. Several studies show, that the majority of WAD are related to rear impacts. All other impact directions are of minor importance but not to be ignored (Jakobsson, et al., 2004b). (Morris, et al., 1996), (Temming, et al., 1998), (Brault, et al., 1998), (Martin, et al., 2008), (Stürzenegger, et al., 1994), (Berglund, et al., 2003).
Considering the severity of injuries, e.g. lesions of transverse ligaments, or the membranes of the atlanto-occipital complex, frontal impacts are considered more serious. Frontal impacts also allow a larger range of motion. (Kaale, et al., 2005), (Brault, et al., 1998). Long term WAD however seem to be independent of impact direction. (Krafft, 1998). Also the vehicle motion in pre impact situations cannot be found to influence WAD outcomes (Dolinis, 1997).
Comparing relative risk for females and males in frontal and rear end impacts, females could be found to be at higher risk (Temming, et al., 1998).

Additional relevant factors, such as acceleration pulse shape, duration, vehicle overlap, impact angle were not found to be analysed by these real world data studies.

### 2.4.4. Interaction and Situation Characteristics

#### 2.4.4.1. Seating Position

Irrespective of gender, several studies (Jakobsson, et al., 2000), (Jakobsson, et al., 2008), (Krafft, et al., 2003), (Berglund, et al., 2003), (Temming, et al., 1997), (Krafft, et al., 2002b) showed an increased risk sustaining WAD for drivers compared to passengers in the front seats. Another study (Linder, et al., 2012) concludes, that males seated in the front passenger seat have a higher risk compared to males in driver seats sustaining long term neck pain, while the risk for females was similar for either front seat. A more significant difference could be found for short term neck pain symptoms, where the symptoms were more common for passenger seat occupants than driver seat, for males and females equally.

In an analysis about WHIPS (Jakobsson, et al., 2000) found that rear seat passengers have a lower risk compared to front seat passengers. A detailed analysis ( (Krafft, et al., 2003), (Krafft, et al., 2002b)), separately for rear seat passengers, front seat passengers and drivers for both genders independently showed, that female rear seat passengers have a higher risk compared to female front seat passengers, but female drivers remain being at highest risk. Contrary male rear seat passengers show a lower risk compared to male front seat passengers and male drivers.

Furthermore (Berglund, et al., 2003) showed the relative risk for drivers compared to passengers in rear seats to be at 1.78 (1.60-1.97, CI 0.95) and for drivers compared to front seat passengers to be at 1.26. A comparison looking at combinations of gender, seated position and whiplash outcome was

presented by (Jonsson, et al., 2013). It was concluded, that the driver position results in a double relative risk compared to front passenger position impairing whiplash (RR males: 1.4, females 2.5).

#### 2.4.4.2. Posture

In a number of studies, the influence of posture on the risk of WAD was investigated. The majority found, that postures differing from a straight forward facing, neutral position increase the risk for WAD (Jakobsson, et al., 2004a), (Jakobsson, et al., 2008). Also (Kaale, et al., 2005) found more severe lesions of the alar ligaments and (Stürzenegger, et al., 1994) evidently stated a higher frequency of multiple symptoms of WAD for patients with inclined head postures, compared to neutral positions. This information is however based on self-reported head posture description during the impact. Furthermore along with (Ryan, et al., 1993) it can be shown, that being unprepared for an impact leads to limitations in the range of motion (i.e. flexion) and an increased frequency of multiple WAD symptoms. Thus it is assumed, that rotation posture and awareness before a rear impact might severely influence the kind of symptoms and severity of WAD. Additional studies in this field would improve the understanding.

One study (Holm, et al., 2008) does not find an influence for head rotation, or for "being prepared at impact" on WAD risk.

Also the impact of wearing a seat belt was investigated by (Martin, et al., 2008). It is shown, that the WAD risk is reduced if a seat belt is worn, even though wearing a seat belt does not influence the loading phase with retraction, translation and extension of the occupants' neck, which is believed to bear the highest risk for WAD. The seatbelt does however influence the rebound phase, consequently additional studies should be of benefit for this understanding.

More factors influencing posture, such as seat back and head restraint positioning, relaxed or very upright posture, position of hands or even actions taken (e.g. adjusting radio, opening or closing the glove box,…) during the impact could not be found extensively in current real world data studies.

The findings towards posture seem to apply for both genders.

#### 2.4.4.3. Head to Head Restraint Distance

The distance between the back of the head and the head restraint is believed to have great influence on the risk sustaining WAD. A larger gap is described to bear a higher risk in several studies. ( (Jakobsson, et al., 2008), (Jakobsson, et al., 2004b), (Olsson, et al., 1990)). The risk is stated at 20 % for distances lower than 50 [mm] and 60 % for distances higher than 20 [cm]. However, (Brault, et al., 1998) showed, that distances between 0 mm and 80 mm do not differ largely in risk.
In general, poor positioning of the head restraint shows higher risks (Chapline, et al., 2000). Both, a large vertical gap (more than 100 [mm] from head centre of gravity (c.o.g.) to head restraint) between head and head restraint, but also a restraint set too low contribute to an increase of up to 88 % for females compared to all other configurations. This study showed these results for females, where afore mentioned analysis indicated a similar risk increase for males and females with increased head to head restraint distance.

#### 2.4.4.4. Driving Situation

In a study by (Temming, et al., 1997), absolute risk factors for males and females were investigated, in correspondence to driving situations.

Females show the following absolute risks: 44 % at intersections, 35 % at junctions, 30 % on straight roads and 25 % at roundabouts. Male risks look slightly different: 22% at intersections, 20 % at junctions, 13 % at straight roads and 27 % at roundabouts. The reason for these differences between males and females might be due to low case numbers in this study.

In a study by (Linder, et al., 2012), seven different collision sites are defined. These are traffic light, queue and zebra-crossing, give way, roundabout, give way roundabout, stop sign and others. The most common site for collisions in this study was at traffic lights (22 %), followed by queues (19 %), zebra crossings (17 %), give way signs (16 %), others (9 %), roundabouts (8 %) and give way roundabouts and stop signs (5 % each). The highest risk of those seven sites sustaining long term neck pain was found in the roundabout group (13 %). Interestingly, collisions at give way signs did not show any long term cases in this study.

### 2.4.5. Conclusion of Influencing Factors

The subsequent Table 3 gives an overview on how personal characteristics influence the risk for WAD.

| Person keyword | Factor/parameter value | Influence on females' risk | Influence on males' risk |
|---|---|---|---|
| Age group | Especially 20 to 40 years compared to older (>50y)[1] | + | + |
| anthropometry | Body height | +/0[2] | +/0[2] |
| anthropometry | Body weight | Not clear | Not clear |
| anthropometry | BMI | 0 | 0 |
| anthropometry | Head to neck ratio[3] | 0 | 0 |
| Neck history | History of neck pain | + | + |
| Neck history | Degenerative changes | 0 | 0 |

[1] different age classes used in studies
[2] in WHIPS seat no influence of body height found, in older seats higher body height = higher risk
[3] in low energy volunteer tests
+ higher risk for WAD when factor or higher value of parameter applies
- lower risk for WAD when factor or higher value of parameter applies
0 no influence on risk for WAD when factor or higher value of parameter applies

TABLE 3 SUMMARY OF INFLUENCING PERSONAL FACTORS ON WAD RISK FOR MALES AND FEMALES

The age group 20-40 years shows an increased risk for both, males and female.
Lowest risk was found for the age groups 50+.
Where male and female was differentiated, females show higher absolute risk in all studies.

Older studies show an increased risk for males and females with higher stature. A more recent study however, which focuses on seats equipped with anti-whiplash systems, could not identify this correlation. This might indicate that seat design can be developed to protect all kinds of person statures.

For body weight a weak association to higher WAD risk for males and females could be found. The study including only seats of 90s models however showed inconsistencies. Continuative, no influence of the BMI on WAD risk or recovery duration could be found.

The head to neck ratio (ratio of the cross sectional areas), which is assumed to be characteristic for separating female and male anthropometry in the head neck region was investigated. However, no influence on the occurrence of WAD in low speed impacts could be found.

Pre-existing neck pain (have experienced neck pain ever) seems to increase the risk for WAD, where degenerative changes did not show an influence on the risk for WAD in a real world data study. Degenerative changes are usually associated with higher age, where higher age groups seem to be at lower risk.

Seating height, thorax width, mass distribution, neck length and circumference, spinal curvature, proportions of length, width and other parameters are believed to influence the kinematic behaviour in case of rear end impact. The interaction with the seat back and head restraint, influenced by these parameters, affects the actual injury risk. These parameters could however not be found in literature.

Table 4 sums up the influence of vehicle parameters on WAD risk.

| Vehicle keyword | Factor/parameter value | Influence on females' risk | Influence on males' risk |
|---|---|---|---|
| vehicle | higher car mass (struck car) | - | - |
| vehicle | higher car mass (striking car) | + | + |
| vehicle | tow bar (struck car) | +/0 | +/0 |
| vehicle | 90s Car model | + | + |
| seat | Stiff seat back | + | + |
| seat | Good head restraint design | -- | - |
| seat | Good test result (IIWPG, IIHS)[1] | - | - |
| seat | WHIPS[2] | - | -- |
| seat | Anti-Whiplash Device[3] | - | - |

[1] "good" rated compared to "poor" rated seats, no statement on acceptable/marginal ratings
[2] two different study outcomes
[3] any seat system/design to reduce Whiplash except WHIPS
+ higher risk for WAD when factor or higher value of parameter applies
- lower risk for WAD when factor or higher value of parameter applies
-- even lower risk for females/males when good head restraint/WHIPS present
0 no influence on risk for WAD when factor or higher value of parameter applies

TABLE 4 SUMMARY OF INFLUENCING VEHICLE FACTORS ON WAD RISK FOR MALES AND FEMALES

With higher vehicle mass (target vehicle) when being struck, WAD protection is improved for males and females. Not to be ignored is the character of the crumple zones interacting. The more energy is absorbed during the impact, the lower the force level on occupants is. However, the extent of deformation can only be seen as indicator, if both interacting vehicles are of similar stiffness.
Interestingly, for higher degrees of damage, compared to "no visible damage" one study indicates an increased risk for males and females (m relative risk 2.2, f relative risk 1.4) where the increase is higher for males. Another study numbers the increased relative risk at 1.8 with higher degree of damage, regardless of gender.

A comparison of WAD risk for 2/3 and 4/5 door vehicles (two studies) lead to contradicting results. Two studies comparing the WAD risk for males and females from the 90s showed an increase for newer and lighter cars models.

A trailer coupling on a struck vehicle, and a stiffer front (longitudinal engine vs. transversal) of the bulleting vehicle appears to be increasing long term WAD risk. These factors influence the pulse and deformation behaviour in a crash.

Seats that deformed during rear impacts (seat or seat back) were found to be favourable for occupants in 80s and 90s vehicles models, which was later (1998) implemented in WHIPS as controlled yielding. The protective potential of WHIPS is however larger for males than females. Active head restraints in general were shown to decrease risk for WAD.

Seats rated good compared to poor (IIHS, IIWPG assessments) performed better in real world crashes for males and females. Seats rated marginal or acceptable did not correlate with real world data.

Geometric assessment criteria (head to head restraint distance vertical and horizontal) and dynamic parameters (Head-, T1x acceleration, upper neck tension and lower neck shear forces, T-HRC) used in these assessments seem to be practical parameters in risk assessment and should be further investigated.

Risk factors like e.g. stiffness of rear structures could not be found in studies based on real world data.

Table 5 shows a summary of relevant crash characteristics.

| Crash keyword | Factor/parameter value | Influence on females' risk | Influence on males' risk |
|---|---|---|---|
| Degree of damage | Degree of car damage | 0/+[1] | + |
| Delta v | Delta v | + | + |
| Delta v | EES | 0 | 0 |
| Delta v | Mean acceleration | + | + |
| Direction of impact | Rear end impact | ++ | + |

[1] in one study a higher degree of damage is only associated to males risk, other studies combine males and females risk
+ higher risk for WAD when factor or higher value of parameter applies
- lower risk for WAD when factor or higher value of parameter applies
++ even higher risk for females compared to males
0 no influence on risk for WAD when factor or higher value of parameter applies

TABLE 5 SUMMARY OF INFLUENCING CRASH FACTORS ON WAD RISK FOR MALES AND FEMALES

The degree of damage seems to be corresponding with the risk for WAD, being more pronounced for male occupants. Increased damage does not necessarily go along with increased crash severity. To quantify crash severity, the change of velocity (delta v), EES or mean acceleration should be assessed.

Some studies are based on real world measurements of actual crash recorders, so clear results are available. These showed the highest risk for WAD lasting at least one month at delta v of 10 [km/h] to 15 [km/h] for males and females similarly. At delta v of 25 [km/h] to 30 [km/h] the risk for WAD reaches 100 %. These studies however are limited to one vehicle manufacturer observing one car model and might vary for others. Another study based on reconstructions gives maximum risk for both males and females at delta v between 13 [km/h] and 17 [km/h] supporting the recorded data. One study of vehicles equipped with recorders suggests a 100 % WAD risk at a mean acceleration of 7 [g].

It is suspected, that females show lower resistance to external forces, thus lower pulses can induce WAD in females. A general difference in resistance to crash severity for males or females could not be proven in literature.

The main direction of impact at risk for WAD is the rear end impact with a relative risk of 2.0 or even higher in different studies. Females generally seem to be at higher risk than males. The impact direction is however not of importance when WAD occur considering long term conditions.
The pre-impact vehicle motion does not show an influence on WAD risk. Overlap or angular impacts could not be found as crash related factors for WAD risk in literature.

Table 6 summarizes interaction and situation factors and their influence on WAD risk.

| Situation and interaction keyword | Factor/parameter value | Influence on females' risk | Influence on males' risk |
|---|---|---|---|
| Seating position | Driver | + | + |
| posture | Turned head | + | + |
| posture | Inclined head[1] | (+)? | (+)? |
| posture | Seat belt | - | - |
| Head restraint distance | Horizontal distance | 0/+[2] | + |
| Head restraint distance | Vertical distance | + | 0 |
| Driving situation | Roundabout | + | ++ |
| Driving situation | Intersection | ++ | + |

[1] only the number of symptoms in case of WAD is increased, not the risk of WAD occurrence
[2] only one study shows no significant increased risk for females
+ higher risk for WAD when factor or higher value of parameter applies
++ even higher risk for females compared to males/ males compared to females
- lower risk for WAD when factor or higher value of parameter applies
0 no influence on risk for WAD when factor or higher value of parameter applies

TABLE 6 SUMMARY OF INFLUENCING INTERACTION AND SITUATION FACTORS ON WAD RISK FOR MALES AND FEMALES

A larger horizontal distance between head and head restraint system (backset) leads to an increase of WAD for gaps above 8 [cm] in low speed impacts. Other studies find an almost linear relation between backset and WAD risk. One specific study states that backset is more relevant for female than male occupants.
A turned head posture prior to impact seems to influence the WAD risk (Lenard, et al., 2015). Turned head postures are associated with higher risk for WAD than neutral straight forward positions. The rotated posture is connected to the severity of lesions of the alar ligaments and the severity of symptoms. An inclined posture of the head however only seems to influence the number of symptoms if WAD are sustained.

Usage of seat belts reduces the risk for WAD, even if seat belts can only influence the rebound phase. Thus this phase should probably not be ignored in future investigations, even if the first phases are believed to be of more importance.
Being unprepared at the moment of the rear end impact seems to be connected to limiting the range of motion, if WAD occur.

All studies investigating posture state a higher risk for drivers than all other passengers for males and females. Shoulder and arm positions, the curvature of the spine and muscle activities of neck and torso are influencing factors for the kinematics and thus WAD risk.

Real life driving situations with increased WAD risk for males seem to be roundabouts and intersections for females.
Other possible risk factors like arm positioning, feet and leg positioning or even tasks performed at the time of the impact were not examined in found real world studies focusing on WAD.

Summing up the findings of studies on risk for WAD it can be concluded:

personal attributes:
younger than 50 years of age
history of neck pain
➔ higher risk, irrespective of gender

posture:
head restraint distance (vertical and horizontal)
rotation and inclination posture
➔ higher risk

pulse:
higher mean acceleration and delta v
➔ higher risk

seat design:
yielding seat
active head restraints (or other whiplash protection systems)
➔ lower risk

### Male versus Female

Impact direction seems to be the only factor differing between male and female, but even there it is not direction but the extent that matters. Generally higher risks for females in rear impacts compared to males can be concluded from literature. Studies show however, that risk for males and females might be influenced differently by degree of damage of the struck car and horizontal and vertical head restraint distance.

No study reviewed could find the real cause for gender influence. Neither a different exposure profile, nor the anthropometric different characteristics could be found responsible for the increased risk. There are however indications that females suffer from chronic neck pain more often than males, which is a risk factor for suffering from WAD.

## 2.4.6. Acknowledgment

This summary about influencing factors was part of WP1 in the ADSEAT project and published at the 4th International ESAR Conference (Schick, et al., 2010).

## 2.5. Neck injury Criteria

There are a number of injury criteria available, some well-established, others rather unacquainted. Following, a short summary of selected criteria is given, to help understand the assessment of whiplash protection today. Some of the presented criteria were developed to meet the requirements for low speed rear impact crashes, other criteria origin from other load cases such as head on collisions. Their usability might be questionable in some cases. Currently none of the thresholds of these criteria differ between male and female occupants.

### 2.5.1. Head Injury Criterion HIC

The head injury criterion (HIC) is an acceleration based (linear head acceleration) criterion to characterise the load applied to the head. Based on the relation between the Wayne State Tolerance Curve (Gurdjian, et al., 1969-1970) and the Gadd Severity Index (Gadd, 1961) analysed by (Versace, 1971) the HIC was defined in 1972 by the National Highways Traffic Safety Administration (NHTSA). It is calculated as the standardised maximum integral value of the resultant head acceleration. The length of the corresponding time interval is, dependant on the requirements of the applied regulation or law, unlimited, 15 [ms], 36 [ms] or another specified time interval. The HIC value is calculated as follows:

Equation 2 HIC – calculation of head injury criterion

$$HIC = sup_{t_1,t_2}\left\{\left(\frac{1}{t_2 - t_1}\int_{t1}^{t2} a\, dt\right)^{2,5}(t_2 - t_1)\right\}$$

The acceleration $a$ is the resultant acceleration at the centre of gravity (c.o.g.) of the head calculated from the components in x, y, and z direction as follows:

Equation 3 calculation of resultant translational head acceleration

$$a = \sqrt{a_x + a_y + a_z}$$

The acceleration values are filtered, depending on the requirements of the corresponding regulation or law, with a channel frequency class (CFC) 1000 or CFC 600 filter and transformed to g values (1 [g] = 9.81 [m/s²]), the time interval $t_2 - t_1$ is calculated in seconds.

Although the HIC primarily describes the tolerance of the skull to fracture under translational anterior-posterior acceleration, this value is still used in current regulations, mainly due to compromise reasons caused by the use of the Hybrid III[B] (H III) dummy for whiplash risk assessment.

### 2.5.2. Normalized Neck Injury Criterion Nij

Based on a study by (Prasad, et al., 1984), the neck can withstand a certain value of tensile force or bending moment, or a linear combination of both, within borders for a maximum tensile force or bending moment. Extended later to include tension and compression, and differ between flexion and extension, Nij is an abbreviation for Normalized Neck Injury Criterion which is the aggregation of the four neck injury predictors Nte (tension and extension), Ntf (tension and flexion), Nce (compression and extension) and Ncf (compression and flexion).

The values for the criteria are determined using the axial force being compression or tension at the transition from the head to the neck expressed in [kN] as analysed and plotted over time. The neck

[B] Hybrid III, originally developed in 1976 by General Motors, is the most widely used crash test dummy for the evaluation of automotive safety systems in frontal crashes (Foster, et al., 1977).

bending moment is considered by the bending moment expressed in [Nm] about the lateral axis at the transition from the head to the neck.

Equation 4 Nij – calculation of Nij criterion

$$N_{ij} = \frac{F_z}{F_{zc}} + \frac{M_{OC_y}}{M_{yc}}$$

where

$F_z$ is the tension/compression force at the point of transition from head to neck
$F_{zc}$ is the critical force
$M_{OC_y}$ is the total moment and
$M_{YC}$ is the critical moment.

$M_{OC}$ generally is the moment about the occipital condyle. It is defined for different dummy models and incorporates the measured moments and forces. For more details refer to (Cichos, et al., 2006)

### 2.5.3. Neck Injury Criterion NIC

This criterion for neck injury with rear impacts is expressed by the relative acceleration between the upper and lower neck in [m/s²] and the relative velocity in [m/s].

The NIC value is calculated as the following formula shows:

Equation 5 calculation of NIC criterion

$$NIC = a_{relative} * 0{,}2 + v_{relative}^2$$

with:

$$a_{relative} = a_x^{T1} - a_x^{Head}$$

and

$$v_{relative} = \int a_{relative}$$

where $a_x^{T1}$ and $a_x^{T1Head}$ represents the acceleration in x-direction in [m/s²] of the first thoracic vertebral body and the head at c.o.g. respectively.

The criterion was initially proposed by (Boström, et al., 1996) based on a hypothesis of (Aldman, 1986) and (Svensson, et al., 1993) and is currently well established in numerous assessment programs.

### 2.5.4. Neck Protection Criterion Nkm

The Nkm similar to the Nij corresponds to four different criteria during a whiplash load case. They are Nfa (flexion anterior), Nea (extension anterior), Nfp (flexion posterior) and Nep (extension posterior). Anterior in this content describes the movement of the head backwards and torso forwards, where posterior describes the exact opposite movement. The criteria are calculated by adding the standardised shear force and the standardised corrected bending moment.

Equation 6 calculation of Nkm criterion

$$N_{km}(t) = \frac{F_x(t)}{F_{int}} + \frac{M_{OC_y}(t)}{M_{int}}$$

where
$F_x$ is the shear force at the point of transition from heat to neck
$F_{int}$ is the critical force
$M_{OC_y}$ is the total moment and (like already described in $N_{ij}$)
$M_{int}$ is the critical moment.

The criterion was developed by the working group for accident mechanics (AGU) in Zurich and proposed by (Schmitt, et al., 2001). It is currently included in the Euro NCAP whiplash protocol (Euro NCAP, 2014).

### 2.5.5. Forces and Moments – Spinal loads

Forces and moments are used in order to quantify the actual load on the neck. Commonly shear and tension forces as well as moments about the y-axis (nodding rotation) are used. (Euro NCAP, 2014)

In two regulations (UNECE, 2013) and (U.S. DoT, 1999) for the United States of America, thresholds for forces and moments are defined. However these thresholds are applicable for frontal impact situations.

### 2.5.6. Rebound Velocity

The rebound velocity is determined by methods of high speed video target tracking and describes the peak value of x-directional rebound velocity of the head relative to the vehicle occurring between T0 and 300 [ms]. The rebound velocity is characterising the amount of energy, the seat returns to the occupant after the initial impact. The lower the rebound velocity, the higher the amount of absorbed energy by the seat and this is rated to be favourable for occupants. (Euro NCAP, 2014) (Muser, et al., 2000)

### 2.5.7. Head to Head Restraint Distance - Backset

The head to head restraint distance, commonly known as backset, describes the horizontal gap between the back of the head of the occupant model and the head restraint system. It is a criterion used in static assessments of vehicle seats. A smaller distance is preferred for protective effectiveness (Euro NCAP, 2014) limiting relative movement between head and torso. Correlation with real life effectiveness was shown in several studies (Eichberger A, 1996), (Wilkund, et al., 1998), (Hofinger, et al., 1999).

### 2.5.8. Time to Head Restraint Contact

Time to head restraint contact (T-HRC) measured in milliseconds [ms] describes the duration until the head of the occupant model first contacts the head restraint after T0 during a rear impact crash. Values below 50 [ms] are usually considered favourable for the occupant where 90 [ms] or more are rated poor. It is an alternative method of describing the head to head restraint distance but dynamic effects can influence the T-HRC and head to head restraint contact time severely. However, active

systems can influence this duration by reducing the gap between head and restraint system during the impact. (Euro NCAP, 2014)

### 2.5.9. Lower Neck Load Index - LNL

The lower neck load index (LNL) is based on a hypotheses which claims, that the risk of damaging the lower neck vertebrae in rear end crashes is highest when forces and moments occur simultaneously. It was first proposed by (Heitplatz, et al., 2003). Due to its nature, the LNL is only valid for the RID 2 and Hybrid III dummy. It is calculated as follows:

Equation 7 calculation of LNL criterion

$$LNL(t) = \frac{\sqrt{[My_{lower}(t)]^2 + [Mx_{lower}(t)]^2}}{C_{moment}} + \frac{\sqrt{[Fx_{lower}(t)]^2 + [Fy_{lower}(t)]^2}}{C_{shear}} + \left|\frac{Fz_{lower}\,(t)}{C_{tension}}\right|$$

where:

$My_{lower}$ is the moment in y direction,
$Mx_{lower}$ is the moment in x direction,
$Fx_{lower}$ is the force in x direction,
$Fy_{lower}$ is the force in y direction,
$Fz_{lower}$ is the force in z direction,
$C_{moment}$ is the critical moment,
$C_{shear}$ is the critical shear force and
$C_{tension}$ is the critical tension force.

For the Hybrid III dummy, the $My_{lower}$ must be corrected as can be found in (Cichos, et al., 2006). Moments and forces are measured values filtered with the CFC 600 filter. The critical values for this evaluation are:

$$C_{moment} = 15\ [Nm]$$
$$C_{shear} = 250\ [N]$$
$$C_{tension} = 900\ [N]$$

Today the LNL has a minor significance.

### 2.5.10. Neck Displacement Criterion - NDC

NDC, an abbreviation for Neck Displacement Criterion is described in (Viano, et al., 2002). The criterion is evaluated for Hybrid III, Bio RID (P3 at that state) and volunteers. It is based on a hypotheses, that the displacement between head and torso should not exceed a certain measure. Further information on this not very commonly used criterion is to be found in (Viano, et al., 2002) and (Kullgren A, 2003).

### 2.5.11. MIX – Combined Criterion

MIX describes a combination of the NIC and Nkm criterion. It was suggested by (Kullgren A, 2003) and according to this study shows a stronger correlation to real world injury observations.

Equation 8 calculation of MIX criterion

$$MIX = \sqrt{\left(\frac{NIC_{max}}{NIC_{av}}\right)^2 + \left(\frac{N_{km}}{N_{av}}\right)^2}$$

Where $NIC_{av}$ and $N_{av}$ are the average NIC value and average Nkm value over time respectively.

### 2.5.12. WIC – Bending Moment Criterion

The WIC criterion is based on moment measurements within the Bio RID II dummy. It describes the difference between the moment about the y axis at the occipital condyle and the lower neck (Munoz, et al., 2005).

### 2.5.13. Head to torso rotation

The head to torso rotation describing the probability of whiplash injuries is based on the idea, that limited relative head to torso motion reduces the occurrence of whiplash injuries. It is applied in the FMVSS 202. (Kuppa, et al., 2005)

### 2.5.14. IV-NIC – Intervertebral Neck Injury Criterion

The IV-NIC is a criterion determined from cadaver tests. The hypotheses claims, that intervertebral motion exceeding the physiological range is injurious (Panjabi, et al., 1999). The criterion however cannot be applied to anthropomorphic test devices (ATD) and volunteers since its calculation is bound to the determination of relative rotations for each vertebral body. The Criterion is not limited to rear impact, it is also used for frontal impacts (Ivancic, et al., 2005).

### 2.5.15. NICprotraction

This criterion is a modified version of the NIC criterion adapted for low speed frontal impacts. The criterion is based on the NIC criterion like described above. (Boström, et al., 2000)

### 2.5.16. NII – Neck Injury Index

NII is an injury criterion based on forces and moments particularly developed for a motorcyclist anthropometric test dummy (MATD). The relevance in whiplash is to be neglected. Intercept values are given, for which, when exceeded, the load is rated as injurious. (Van Auken, et al., 2005)

## 2.6. Legislation and Consumer Testing

National legislations and larger organisations of affiliating nations (such as the European Union) do have different approaches regarding vehicle safety regulations and vehicle admission. Also the United States of America (USA), with the self-certification of vehicles represent a significantly different approach in vehicle safety regulations. This is why the United Nations (UN) currently[C] work on a global harmonization of Global Technical Regulations (GTR) in order to broaden the use of higher standards, regarding vehicle safety[D], also in development countries. The UN with its local sub organisations UN/ECE[E], UN/ECA[F], UN/ECLAC[G], UN/ESCAP[H], UN/ESCWA[I] counts 193 (UN, 2013) member states at the moment. 65 of these members and additionally, the "European Community" and the European Union signed the agreements of 1958 and 1998 regarding wheeled vehicles and their "technical requirements". The member states of agreements dated 1958 and 1998 can be found in Table 7 and Table 8. Both agreements show overlapping. The main goal of these organisations is a larger collaboration amongst all members. This however also refers to regulations and standardisations.

| Code | Country | Code | Country | Code | Country |
|---|---|---|---|---|---|
| 1 | Germany | 19 | Romania | 39 | Azerbaijan |
| 2 | France | 20 | Poland | 40 | Republic of Macedonia |
| 3 | Italy | 21 | Portugal | 42 | European Community |
| 4 | Netherlands | 22 | Russian Federation | 43 | Japan |
| 5 | Sweden | 23 | Greece | 45 | Australia |
| 6 | Belgium | 24 | Ireland | 46 | Ukraine |
| 7 | Hungary | 25 | Croatia | 47 | South Africa |
| 8 | Czech Republic | 26 | Slovenia | 48 | New Zealand |
| 9 | Spain | 27 | Slovakia | 49 | Cyprus |
| 10 | Serbia | 28 | Belarus | 50 | Malta |
| 11 | United Kingdom | 29 | Estonia | 51 | Republic of Korea |
| 12 | Austria | 31 | Bosnia and Herzegovina | 52 | Malaysia |
| 13 | Luxembourg | 32 | Latvia | 53 | Thailand |
| 14 | Switzerland | 34 | Bulgaria | 54 | Albania |
| 16 | Norway | 35 | Kazakhstan | 56 | Montenegro |
| 17 | Finland | 36 | Lithuania | 58 | Tunisia |
| 18 | Denmark | 37 | Turkey | 62 | Egypt |

TABLE 7 UN NATIONS OF THE 1958 AGREEMENT (AS OF FEBRUARY 2013)

[C] 1958, agreement concerning the adoption of uniform technical prescriptions for wheeled vehicles, equipment and parts which can be fitted and/or be used on wheeled vehicles and the conditions for reciprocal recognition of approvals granted on the basis of these prescriptions, signed by 51 nations, currently 131 UN-regulations

[D] 1998, agreement concerning the establishing of global technical regulations for wheeled vehicles, equipment and parts which can be fitted and/or be used on wheeled vehicles, signed by 33 nations, currently 12 GTRs

[E] Economic Commission for Europe

[F] Economic Commission for Africa

[G] Economic Commission for Latin-America and Caribbean

[H] Economic and Social Commission for Asia and Pacific

[I] Economic and Social Commission for West Asia

| Since | Country | Since | Country |
|---|---|---|---|
| Aug. 25th 2000 | Canada | Mar. 5th 2002 | Netherlands |
| Aug. 25th 2000 | United States of America | Jun. 14th 2002 | Azerbaijan |
| Aug. 25th 2000 | Japan | Jun. 22nd 2002 | Spain |
| Aug. 25th 2000 | France | Jun. 24th 2002 | Romania |
| Aug. 25th 2000 | United Kingdom | Mar. 1st 2003 | Sweden |
| Aug. 25th 2000 | Germany | Nov. 29th 2004 | Norway |
| Aug. 25th 2000 | Russian Federation | Jun. 11th 2005 | Cyprus |
| Aug. 25th 2000 | European Union | Nov. 15th 2005 | Luxembourg |
| Dec. 9th 2000 | P.R. China | Apr. 4th 2006 | Malaysia |
| Jan. 1st 2001 | Republic of Korea | Apr. 22nd 2006 | India |
| Jan. 30th 2001 | Italy | Jul. 25th 2006 | Lithuania |
| Jun. 17th 2001 | South Africa | Mar. 17th 2007 | Moldova |
| Aug. 7th 2001 | Finland | Jan. 1st 2008 | Tunisia |
| Aug. 21st 2001 | Hungary | Jun. 7th 2008 | Australia |
| Sep. 1st 2001 | Turkey | Aug. 27th 2011 | Kazakhstan |
| Jan. 6th 2002 | Slovakia | Feb. 26th 2012 | Tajikistan |
| Jan. 26th 2002 | New Zealand | | |

TABLE 8 UN NATIONS OF THE 1998 AGREEMENT (AS OF JUNE 2013)

The legislative requirements regarding head restraints in Europe are driven by two organisations, the European Enhanced Vehicle Safety Committee (EEVC) and the United Nations Economic Commission for Europe (UN/ECE). Within the United States of America, the Federal Motor Vehicle Safety Standard (FMVSS) serves as boundary for Vehicle Safety.

Furthermore consumer testing, such as the European New Car Assessment Protocol (Euro NCAP) or other NCAPs (Global NCAP) influence safety development in this direction. These legislative and consumer organisations also influence each other.

Additional to these organisations, the European Commission (EC) finances and co-finances regulation-related research projects (recently e.g. Thorax[J], Fimcar[K], Assess[L], Casper[M], Aspecss[N], Adseat[O] ...) to upkeep a steady development process in vehicle safety matters.

### Rules and Regulations on Occupant Protection:

The following table shall provide a short overview on which national and international rules and regulations exist throughout some nations worldwide, regarding rear end crash scenarios. This does not imply that all of those regulations also refer to whiplash associated disorders and their prevention.

| Region | Regulation | Reference |
|---|---|---|
| India | AIS-101 | (ARAI, 2012) |
| China | GB20072-2006 | (GB, 2006) |
| Japan | TRIAS 33 | (JASIC, 2013) |
| Europe | ECE R32 | (UNECE, 1993) |
| USA | FMVSS 202a | (U.S. DoT, 2000) |
| USA | FMVSS 301 | (U.S. DoT, 2004) |

TABLE 9 RULES AND REGULATIONS, NATIONAL AND INTERNATIONAL REGARDING REAR END COLLISIONS

[J] Thoracic injury assessment for improved vehicle safety
[K] Frontal impact and compatibility assessment research
[L] Assessment of Integrated Vehicle Safety Systems for improved vehicle safety
[M] Child advanced safety project for European roads
[N] Assessment methodologies for forward looking Integrated Pedestrian and further extension to Cyclists Safety Systems
[O] Adaptive seat to reduce neck injuries for female occupants

Also other regulations exist, that do not refer to occupant protection explicitly, but vehicle component development (e.g. UN /ECE R17), which will be discussed later on.

### Consumer Tests and Ratings:

Regardless of national and international rules and regulations a large amount of consumer tests have been established. Some of these tests and ratings are a major motivation for car manufacturers to improve their vehicle fleet. Consumer ratings nowadays can even be opinion leaders when decisions about purchasing a new vehicle are made. Thus a favourable rating is very essential to achieve acceptable sales numbers. The following table gives an overview of currently and in near future applicable consumer tests throughout the world. These tests are dedicated to the prevention and reduction of whiplash associated disorders.

| Euro NCAP | IIHS | JNCAP | C-NCAP | KNCAP[1)] | ANCAP |
|---|---|---|---|---|---|
| **front seat** | | | | | |
| static<br>dynamic<br>(3 pulses) | static<br>dynamic<br>(1pulse) | dynamic<br>(1 pulse) | dynamic (1 pulse) | static<br>dynamic<br>(1 pulse)<br>(3 pulse)[1)] | static<br>dynamic<br>(1 pulse) |
| **rear seat** | | | | | |
| static | | | | evaluation[1)] | |
| **other assessment** | | | | | |
| AEB city | | | | | |
| [1)] currently 1 pulse, 3 pulses in 2017, rear assessment 2017 | | | | | |

TABLE 10 CONSUMER TESTS AND RATINGS ACROSS THE WORLD REGARDING WHIPLASH PROTECTION

### 2.6.1. Legislative

Three legislative rules and regulations shall be looked at in more detail, due to their relevance, in this chapter.

- UN/ECE Regulation No. 17, Uniform provisions concerning the approval of vehicles with regard to the seats, their anchorages and any head restraints
- FMVSS 202a – Head restraints for passenger vehicles
- GTR 7 – Head restraint systems

Even though, different nations and regulations have developed a general consensus regarding the harmonisation, a global evolvement can be seen nowadays. Thus parallels between the FMVSS 202a, the ECE-R17 and naturally the GTR 7 can be found. Also the current development shows, that not only vehicle seats in the front row will be considered in future. Also second and third row seats will be assessed.

#### 2.6.1.1. UN/ECE Regulation No. 17 (UNECE, 1995)

As the title of the ECE-R17 already reveals, this regulations concern is the approval of seats and their anchorages according to their strength and also any sort of head restraint. Within the regulation several chapters refer to different aspects regarding head restraints. For example in section 5.3 of the regulation it is described, that a head restraints shall be mounted on every outboard front seat in every vehicle of category M1[P] or even M2[Q] with a maximum mass not exceeding 3500 kg, and category N1[R]. Furthermore in section 6 of the regulation measuring guidance is given how to determine height (ECE R17, section 6.5) width (ECE R17, section 6.6) and head restraint gaps (ECE R17, section 6.7). In section 6.4 of the ECE R17, a strength test for seats is described, where a force must be applied to the head restraint until a moment of 89 [daNm] about the R-point is reached, or the seat or seat-back breaks.

The ECE-R17 however does not consider low speed accident scenarios, with respect to whiplash associated disorders.

#### 2.6.1.2. FMVSS 202a (U.S. DoT, 2000)

The FMVSS 202a origins from the FMVSS 202 standard published January 1st 1969. Statistics and studies showed, that head restraint systems led to reductions in severity and prevention of whiplash injuries. Thus the FMVSS 202a was formed.
The FMVSS 202a, amongst others, for front outboard seats equipped with a head restraint describes both, a static and dynamic procedure in order to assess whiplash protection.

The static assessment procedures, as described in FMVSS 202a, Section 4.2, include geometric measuring of the head restraint with an H-point machine, such as backset and height, but also other criteria, such as gaps between head restraint and backrest. Furthermore energy absorption utilising a linear impactor propulsion system and a 6.8 [kg] 165 [mm] headform at 24.1 [km/h]. More detailed information can be found in Table 11 or in the FMVSS 202a (U.S. DoT, 2000).

---

[P] Passenger car: Vehicles used for the carriage of passengers and comprising not more than eight seats in addition to the driver's seat.
[Q] Bus: Vehicles used for the carriage of passengers, comprising more than eight seats in addition to the driver's seat, and having a maximum mass not exceeding 5 tonnes.
[R] Pick-up Truck: Vehicles used for the carriage of goods and having a maximum mass not exceeding 3.5 tonnes.

| Test Equipment | 202a Sec. 4.2 | Test Description | Test Criteria |
|---|---|---|---|
| H-Point machine and ICBC# head restraint measuring device (HRMD) | (1a) Minimum Height – Front outboard H/R | Uses the H-point machine with a design torso angle and highest achievable H-Point | Front: 800 mm at a minimum of one position |
| | (1b) Minimum height – All outboard H/R | | Front and Rear: 750 mm at all H/R positions |
| | (2) Width | | 170 mm – Bucket and Rear 254 mm – Front Seats with a Centre Occupant |
| | (3) Backset – Front O/B H/R only | | Less than 55 mm between 750 - 800 mm H/R height |
| 165 mm hemispherical headform or 25 mm cylinder | (4) Gaps – Within H/R and between H/R and Seat | Dimensional measurements only | No gap > 60 mm at full down H/R position and any backset<br>25 mm cylinder cannot pass through the bottom of the S/B and the top of the HR (adjustable type only) |
| 165 mm hemispherical headform using a linear impactor propulsion system | (5) Energy absorption | Impact the front surface of the head restraint at 24.1 km/h (within impact zone) | 3 ms clip < 80 g's |
| Vertical load test using 165 / 152 mm cylindrical headform | (6) Height retention | Apply 500 N in the vertical direction | Initial displacement < 25 mm to achieve 50 N.<br>Change in position at 50 N must be < 13 mm. must hold 500 N for 5 seconds. |
| Head restraint rearward moment test system | (7) Displacement | Simultaneous loads applied to seat back | Headform displacement <102 mm at 373 Nm about H-Point |
| | (7a)Backset retention | | Initial displacement < 25 mm to achieve 37 Nm.<br>Head form position change < 13 mm at 37 Nm |
| | (7b) Strength | | Reach and sustain 890 N for five seconds |
| # Insurance Company of British Columbia | | | |

TABLE 11 FMVSS 202A STATIC ASSESSMENT PROCEDURE

The dynamic testing is described in Section 4.3 of FMVSS 202a. Very briefly described the dynamic test according to FMVSS 202a looks as follows:

- Occupant sled test according to Section 5.3 (U.S. DoT, 2000)
- Half-sine acceleration pulse of 8-9.6 g's, duration 80-96 ms (17.3 [km/h] ± 0.6 [km/h])
- 50$^{th}$ percentile male ATD (H III) at any outboard seating position equipped with a head restraint
- Head restraint with vertical adjustment at mid up position
- Head restraint with horizontal adjustment to the backmost position

In order to comply with the specifications given, the $HIC_{15}$ must not exceed a value of 500 and the rearward relative angular rotation between the head and torso of the ATD must not exceed 12 °.

#### 2.6.1.3. GTR 7 (UNECE, 2010)

The global technical regulation 7 (GTR 7) describes the general requirements for head restraint systems and how they must be assessed. This regulation theoretically applies to countries described in Table 7 and Table 8. The formation of a GTR is a complex process where unanimity must be reached among all members. Also no time limit for the implementation in national legislations exists. All these

factors lead to a GTR 7, as it is at the moment, with a wide range of options. In Figure 10 the approved options of whiplash assessment according to GRT 7 are illustrated.

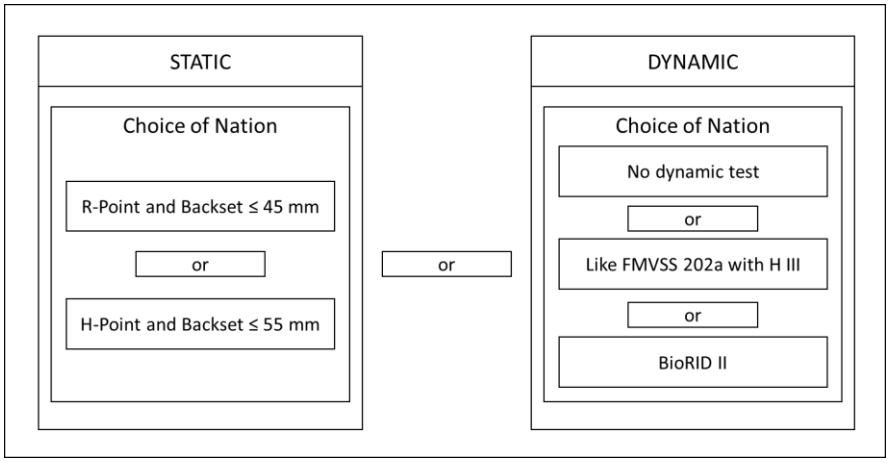


FIGURE 10 GTR7 CHOICES FOR ASSESSMENT OF VEHICLE SEATS DEPENDING ON NATION OF ADMISSION

In Accordance with the GTR 7 the vehicle manufacturer has the choice, dependant on the nation of vehicle admission, and dependant on the nations' implementation of the GTR 7 to assess the head restraint using:

- a static test evaluating the R-Point and backset or
- a static test evaluating the H-Point and backset or
- a dynamic test in accordance with the FMVSS 202a or
- a dynamic test using the Bio RID II dummy

A solely static assessment evaluating the position of H- or R-Point and the backset is also matter to a new approach in the Euro NCAP whiplash assessment for vehicle seats in the second and third row. The simple geometric assessment allows for a quick and easy test of the seat itself without a lot of effort and equipment. However, it shows a high sensitivity to production tolerance, especially to seat components made from soft materials, such as foam and fabric, which are very common in head restraint systems.
Regarding the Hybrid III dummy used in the FMVSS 202a it must be mentioned that this dummy was developed for frontal collisions at a rather high loading rate. The biofidelity and relevance in rear impact collision situations with a low change of velocity should be critically analysed. Also the HIC criterion (HIC ≤ 500) used to determine the severity of the impact seems rather odd and was never intended to be used for this purpose.

### 2.6.2. Insurances Efforts (GDV, 2010)

Naturally, since rear impact accidents cause a substantial financial burden on insurance companies, many insurance companies are interested in reducing their occurrence, or at least decrease the severity of injuries for which customers file claims.

Beginning in 2005 the International Insurance Whiplash Prevention Group (IIWPG) started to test and rate vehicle seats and head restraints leading to a significant improvement with regard to whiplash associated disorders (WAD).

#### 2.6.2.1. RCAR – IIWPG – IIHS (RCAR, 2008)

The Research Council for Automobile Repair (RCAR) in cooperation with the IIWPG developed a seat / head restraint evaluation protocol which describes a standard for evaluating and rating the ability of seats and head restraints to prevent neck injury in moderate and low-speed rear-end crashes. The procedures and criteria were developed by the IIWPG, which is comprised of various insurance industry supported research groups from around the world. These organizations are AZT (AZT Automotive GmbH, 2014), Centro Zaragoza (CENTRO ZARAGOZA, 2015), CESVIMap (MAPFRE, 2015), Folksam (Folksam, 2015), GDV (GDV, 2015), IAG (IAG, 2015), ICBC (ICBC, 2015), IIHS (IIHS, 2015), Thatcham (Thatcham, 2015), and Winterthur (AXA Winterthur, 2015).

The protocol itself describes why such an evaluation is of value, and very detailed how such an evaluation has to be conducted. The evaluation is divided in three steps.

- The initial evaluation – Measurement and rating of static head restraint geometry:
  This evaluation describes a geometric revision of the position of the head restraint relative to the head of a 50$^{th}$ percentile rear impact dummy (Bio RID II), using an H-point machine and a head restraint measuring device (HRMD). Depending on what distance above or below the highest point of the head restraint is compared to the top of the head, and on the backset (gap between the head and head restraint) the restraint is evaluated “good” (Zone 1), “acceptable” (Zone 2), “marginal” (Zone 3) or “poor” (Zone 4) as in Figure 11. This evaluation is used to qualify/disqualify a seat/head restraint for further investigation. Head restraints with “poor” or “marginal” rating in the static evaluation do not undergo dynamic testing and get overall rated “poor”.

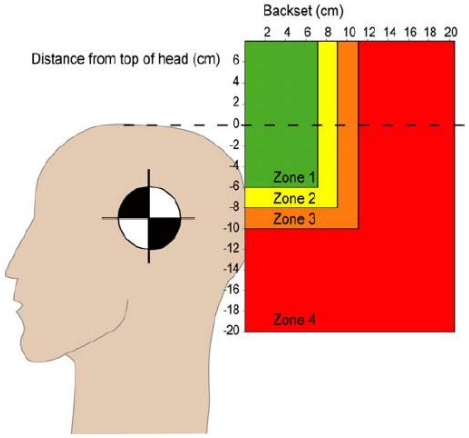


FIGURE 11 RCAR-IIWPG STATIC SEAT/HEAD RESTRAINT EVALUATION ZONES

- Dynamic testing – Dynamic rating:
  The dynamic test is a rear crash simulation with a Bio RID IIg dummy positioned in the seat to be tested. The seat is attached to a crash simulation sled system and accelerated to represent a rear crash. The acceleration pulse is roughly triangular shaped, with a peak of 10 [g] and a duration of 91 [ms] leading to a velocity change (delta v) of 16 [km/h]. The exemplary pulse from the RCAR-IIWPG Seat/Head Restraint Evaluation Protocol (RCAR, 2008) can be found in Figure 12 and the according restricting values in Table 12.
  The protocol also gives precise instructions on how to position all adjustable components of the seat, such as seat-rails, head restraint, backrest, seat cushion, etc.
  The dynamic rating considers T1 x-acceleration, time to head restraint contact and neck force classification.

| Acceleration Pulse Characteristic | Minimum | Maximum |
|---|---|---|
| Acceleration at time = 0 ms | -0,25 g | 0,50 g |
| Acceleration at time = 27 ms | 9,5 g | 10,5 g |
| Time that sled acceleration returns to 0 g | 88 ms | 94 ms |
| Velocity change (delta v) | 14,8 km/h | 16,2km/h |

TABLE 12 RCAR-IIWPG ACCELERATION PULSE DEFINITION

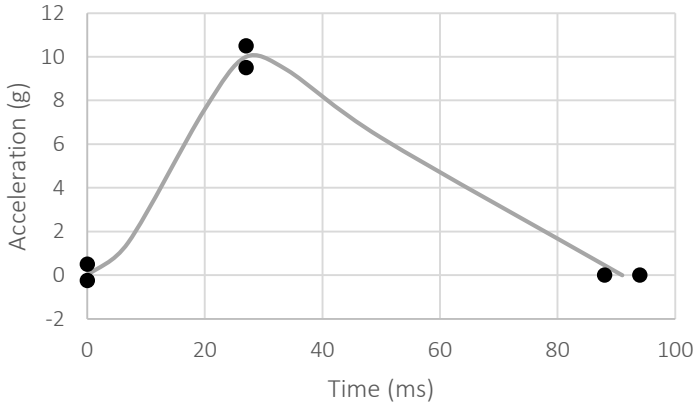


FIGURE 12 RCAR-IIWPG ACCELERATION PULSE

The evaluation of the dynamic test is based on three parameters.

1. Time to head restraint contact
   The time to head restraint contact must be lower or equal 70 [ms] to qualify for this criterion
2. T1 x-Acceleration
   The T1 x-Acceleration must be lower or equal to 9.5 [g] to qualify for this criterion
3. Neck Force Classification
   The Neck force classification takes into account vector sums of neck shear and tension forces and classifies the lower 30$^{th}$ percentile of originally 102 tested seats with good geometric rating as “low neck force” seats and all seats exceeding the 70$^{th}$ percentile as “high neck force” seats. All seats with the vector sum in between the 30$^{th}$ and 70$^{th}$ percentile are classified as “moderate neck force”.
   The vector sum is defined as:

Equation 9 RCAR-IIWPG combined shear and tension force „low“

$$F_x = 150 \; for \; F_z \leq 234$$

$$F_x = 150 * \sqrt{1 - \frac{(F_z - 234)^2}{516^2}} \; for \; 234 \; < F_z < 750$$

$$F_x = 0 \; for \; F_z \geq 750$$

for forces classified as “low” and:

Equation 10 RCAR-IIWPG combined shear and tension force „high“

$$F_x = 260 \; for \; F_z \leq 234$$

$$F_x = 260 * \sqrt{1 - \frac{(F_z - 234)^2}{936^2}} \; for \; 234 \; < F_z < 1170$$

$$F_x = 0 \; for \; F_z \geq 1170$$

for forces classified as “high”.

The Classification can be graphically determined from the following Figure 13.

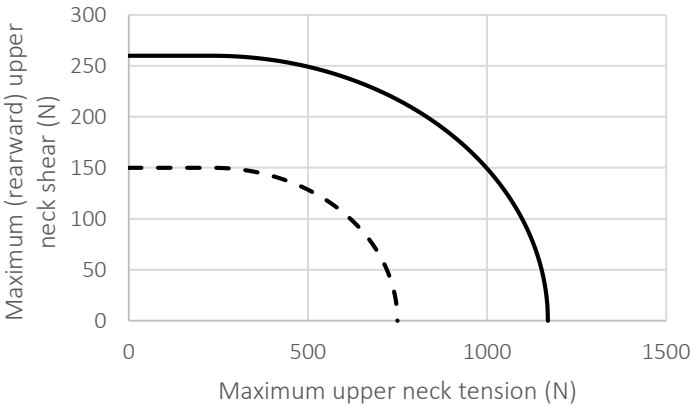


FIGURE 13 RCAR-IIWPG DYNAMIC COMBINED FORCE CLASSIFICATION GRAPH WITH BORDERS FOR LOWER NECK FORCES (DASHED) AND HIGHER NECK FORCES (SOLID)

If the combined force stays within (left and below) the borders of the dashed line in the graph the seats force classification is “low”. If the combined force reaches outside the solid line of the graph (right and above) the seats is classified “high” force level. All other force combinations are classified “moderate”.

The dynamic rating is derived as the following Table 13 shows.

| Seat Design Criteria | Neck Force Classification | Dynamic Rating |
|---|---|---|
| T1 X-acceleration ≤ 9.5 g<br>or<br>Time to head restraint contact ≤ 70 ms | Low | Good |
| | Moderate | Acceptable |
| | High | Marginal |
| T1 X-acceleration > 9.5 g<br>and<br>Time to head restraint contact > 70 ms | Low | Acceptable |
| | Moderate | Marginal |
| | High | Poor |

TABLE 13 RCAR-IIWPG DYNAMIC RATING SCHEME

- Overall rating:
  The overall rating is a combination of the static geometric evaluation and the dynamic evaluation according to Table 14.

| Geometric Rating | + | Dynamic Rating | = | Overall Rating |
|---|---|---|---|---|
| Good | + | Good | = | Good |
| | + | Acceptable | = | Acceptable |
| | + | Marginal | = | Marginal |
| | + | Poor | = | Poor |
| Acceptable (Good height, but too large Backset) | + | Good | = | Good |
| Acceptable | + | Good | = | Acceptable |
| | + | Acceptable | = | Acceptable |
| | + | Marginal | = | Marginal |
| | + | Poor | = | Poor |
| Marginal | + | No dynamic test | = | Poor |
| Poor | + | No dynamic test | = | Poor |

TABLE 14 RCAR-IIWPG OVERALL RATING SCHEME

Seats geometrically rated as good or acceptable undergo a dynamic rating. Geometrically good rated seats achieve an overall rating dependant on the dynamic result (geometric good + dynamic good = overall good, geometric good + dynamic acceptable = acceptable and so on, see Table 14 ).

The rating for geometric acceptable seats is similar, but the maximum achievable overall rating is acceptable (geometric acceptable + dynamic good = overall acceptable.). An exception was made to give credit to seats with geometry that is tall enough to support a 50$^{th}$ percentile male and when dynamic performance can make up for the too large backset. These seats can also reach an overall "good" rating if performing "good" in the dynamic test.

If the geometrical rating of a seat leads to a result marginal or poor, no dynamic test is performed and the overall rating is poor.

### 2.6.3. Consumer Testing

The New Car Assessment Programs all over the world are consumer information programs. Their major mission is to reduce motor vehicle crash related deaths and injuries. In general these programs include a broad spectrum of testing of vehicles. For simplicity reasons, since consumers are the main target audience, the results are usually described by a "star" rating, where e.g. a maximum of five stars can be reached. Testing, depending on the NCAP program, can include frontal crashworthiness, side crashes (vehicle and/or pole), rollover resistance, vulnerable road user protection (pedestrian, cyclists...), rear impacts (whiplash), child protection and lately, crash avoidance technologies.
Currently there are NCAPs for Australia (ANCAP), Southeast Asian Nations (ASEAN NCAP), Latin America and the Caribbean (LATIN NCAP), Korea (KNCAP), Japan (JNCAP), China (CNCAP), Europe (Euro NCAP) and the USA (US NCAP). Additional the Global New Car Assessment Program (Global NCAP) serves as financial and technical support for the development and cooperation between all associated NCAPs around the world (Global NCAP, 2014).
Five NCAPs shall be looked at closer, since their programs include evaluations with regard to preventing whiplash associated disorders.

#### 2.6.3.1. Euro NCAP

A national NCAP was proposed for the United Kingdom (UK) in 1994 by the Transport Research Laboratory (TRL) for the British Department of Transport (D.o.T.) which should be expanded across Europe later on. The development in this area were discussed at and with the European Commission (EC) in July 1995 and steps to take this program forward were discussed. As a result, Euro NCAP was

formed in December 1996 together with the Swedish National Road Administration (SNRA), the Federation Internationale de l'Automobile (FIA) and International Testing. Early 1997 the first ratings of the Euro NCAP were published. With the continuous development of Euro NCAP, in 2008 Thatcham in the UK published the first round of rear impact or so called whiplash tests. 25 front seats of passenger cars were tested and the results revealed, that a lot of development work was necessary to reach an acceptable level of protection for whiplash. The consequence in February 2009 was, that the whiplash test became part of the Euro NCAP rating scheme. Since January 2014 additional to front seats, also all outboard seats from the second and other rows are being tested, and their results are incorporated in a new rating scheme (Euro NCAP, 2014).

The Euro NCAP Adult Occupant Protection (AOP) Protocol v6.0 (Euro NCAP, 2013) describes the Whiplash Seat Assessment as follows:

> *Whiplash is assessed for both the front seats and the rear outboard seats. Front seats are tested statically and dynamically according to Euro NCAP Whiplash Test Protocol* (Euro NCAP, 2014). *Rear seats are assessed according to the Euro NCAP Rear Whiplash Test Protocol* (Euro NCAP, 2013).

Additional to the Euro NCAP Protocol two different testing protocols exist for the complete whiplash assessment at the moment.

- Whiplash Test Protocol V3.2 (Euro NCAP, 2014)
  This document describes the static and dynamic testing procedure for vehicle seats in passenger vehicles in the first row.

- Rear Whiplash Test Protocol V1.0 (Euro NCAP, 2013)
  This document describes the static geometric assessment procedure for all outboard vehicle seats in passenger vehicles' second and further backward rows. If Inboard seats exist, they must comply with the UN/ECE R17-08 (UNECE, 1995).

The static evaluation of front row passenger seats is done with the Head Restraint Measuring Device (HRMD). After adjusting the seats components (e.g. backrest, seat cushion...) and positioning the H-point mannequin, the HRMD is attached. For the evaluation, the head restraint must be placed in a defined position, whether it is adjustable or not and if the adjustable head restraints has locking positions. If not adjustable, no further adaption but the before done seat adjustment are necessary. If the head restraint is non-locking, it is to be positioned in its most downward and rearward (worst case) position. A locking adjustable head restraint must be positioned in its midrange of its locking adjustments. All non-locking adjustments must be set to worst case settings (e.g. most downward, most rearward, etc.). Height and backset are measured using the height and backset measuring probes attached to the HRMD as Figure 14 illustrates.

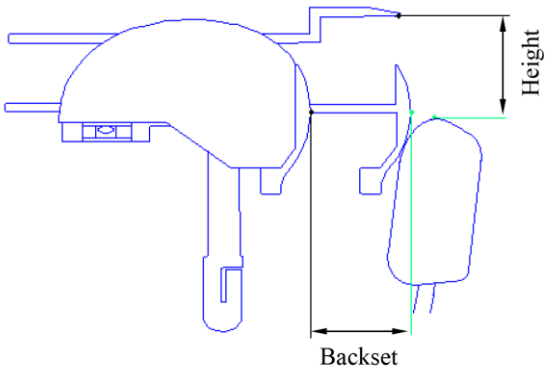


FIGURE 14 EURO NCAP STATIC EVALUATION - MEASURING OF THE BACKSET AND HEIGHT

Backset and height are evaluated separately. The worse value is used for the whiplash score. The geometric rating has a range from plus one (1) to minus one (-1) depending on the values measured.

The limits for higher and lower performance are defined as follows:

Higher performance limit:
Height: 0mm below top height of HPM & HRMD
Backset: 40mm

Lower performance limit:
Height: 80mm below top height of HPM & HRMD
Backset: 100mm

The limiting borders are shown in Figure 15. In between the two limits, no score (0) is added to the whiplash score. Below and behind the lower performance borders minus one (-1) is added.

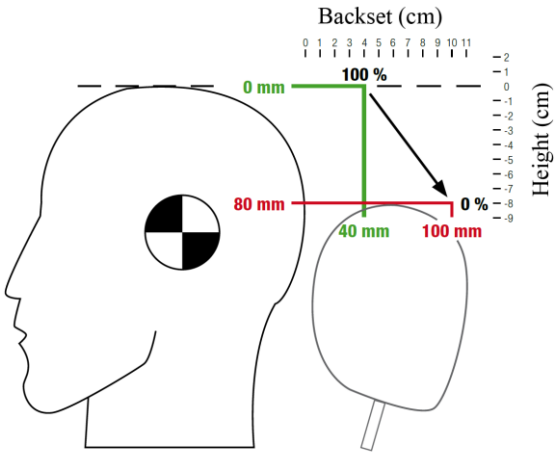


FIGURE 15 EURO NCAP STATIC EVALUATION – HIGHER AND LOWER PERFORMANCE LIMITS

Only seats with head restraints closer to the head and higher than the higher performance criterion gain one (1) point in score.

The dynamic evaluation and testing of front row passenger seats for the Euro NCAP rating consists of three dynamic sled tests for each different seat. The three sled tests are conducted with three different acceleration levels:

- Low severity pulse – Swedish Road Administration 16 [km/h] (SRA 16)
- Medium severity pulse – International Insurance Whiplash Prevention Group 16 [km/h] (IIWPG 16)
- High severity pulse – Swedish Road Administration 24 [km/h] (SRA 24)

The acceleration pulses are defined within the Euro NCAP Whiplash test protocol and are described in the following Table 15 - Table 21 and Figure 16 - Figure 18.

The main data about the low severity pulse can be found in the following Table 15.

| Parameter | | Requirement | Limits +/- | Unit |
|---|---|---|---|---|
| Velocity change | delta v | 16.10 | 0.80 | km/h |
| Mean acceleration | $A_{mean}$ | 42.35 | 4.50 | m/s² |
| Maximum acceleration | $A_{max}$ | 5 | 0.50 | g |

TABLE 15 EURO NCAP LOW SEVERITY ACCELERATION PULSE PARAMETERS

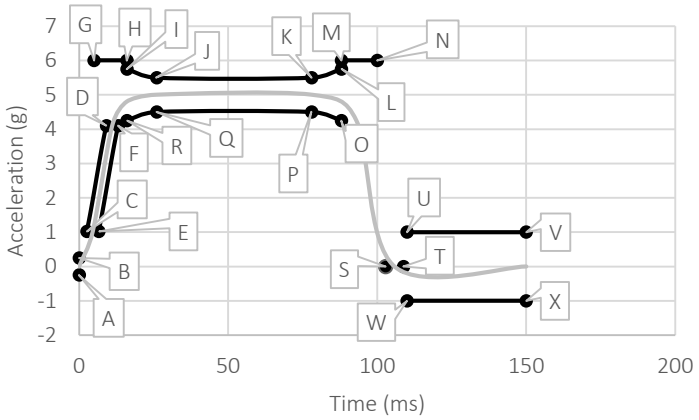


FIGURE 16 EURO NCAP LOW SEVERITY ACCELERATION PULSE ACCORDING TO SRA, 16 KM/H CHANGE OF VELOCITY

The corridor of the low severity pulse is defined by borders which are displayed in Figure 16. The values of the boundaries can be found in Table 16.

| | Time (ms) | Acceleration (g) | | Time (ms) | Acceleration (g) |
|---|---|---|---|---|---|
| A | 0 | 0,25 | M | 88 | 6 |
| B | 0 | -0,25 | N | 100 | 6 |
| C | 2,6 | 1,0222 | O | 88 | 4,25 |
| D | 9,14 | 4,0982 | P | 78 | 4,5 |
| E | 6,6 | 1,0222 | Q | 26 | 4,5 |
| F | 13,1 | 4,0982 | R | 16 | 4,25 |
| G | 5 | 6 | S | 102,8 | 0 |
| H | 16 | 6 | T | 108,8 | 0 |
| I | 16 | 5,75 | U | 110 | 1 |
| J | 26 | 5,5 | V | 150 | 1 |
| K | 78 | 5,5 | W | 110 | -1 |
| L | 88 | 5,75 | X | 150 | -1 |

TABLE 16 EURO NCAP LOW SEVERITY ACCELERATION PULSE CORRIDOR BORDERS

The rising acceleration pulse is calculated according to the following formula, Equation 11.

Equation 11 Euro NCAP low severity acceleration pulse rising pulse

$$acc_{(t)} = \frac{a_{max}}{2} * \left\{1 - \cos\frac{t * \pi}{15.4}\right\} \; for \; 4.6\,ms \; \leq t \; \leq 11.1\,ms$$

For the borders of the rising corridor, the result for formula must be shifted – 2 [ms] for the lower border and + 2 [ms] for the upper border.

The main data about the medium severity pulse can be found in Table 17.

| Parameter | | Requirement | Limits +/- | Unit |
|---|---|---|---|---|
| Velocity change | delta v | 15.65 | 0.80 | km/h |
| Mean Acceleration | $A_{mean}$ | 47.85 | 4.00 | m/s² |

TABLE 17 EURO NCAP MEDIUM SEVERITY ACCELERATION PULSE PARAMETERS

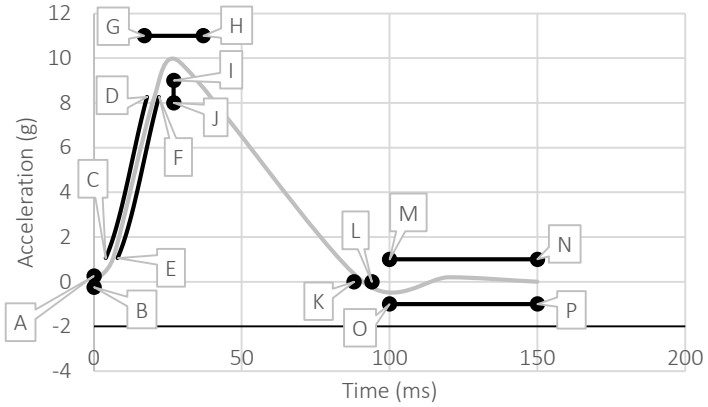


FIGURE 17 EURO NCAP MEDIUM SEVERITY ACCELERATION PULSE ACCORDING TO IIWPG, 16 KM/H CHANGE OF VELOCITY

The corridor of the medium severity pulse is also defined by borders which are displayed in Figure 17. The values of the boundaries can be found in Table 18. Even if the pulse is often referred to as IIWPG 16, the definition in the Euro NCAP protocol is more detailed than in the RCAR – IIWPG protocol.

| | Time (ms) | Acceleration (g) | | Time (ms) | Acceleration (g) |
|---|---|---|---|---|---|
| A | 0 | 0.25 | I | 27 | 8 |
| B | 0 | -0.25 | J | 27 | 9 |
| C | 4 | 1.0531 | K | 88 | 0 |
| D | 18 | 8.2705 | L | 94 | 0 |
| E | 8 | 1.0531 | M | 100 | 1 |
| F | 22 | 8.2705 | N | 150 | 1 |
| G | 17 | 11 | O | 100 | -1 |
| H | 37 | 11 | P | 150 | -1 |

TABLE 18 EURO NCAP MEDIUM SEVERITY ACCELERATION PULSE CORRIDOR BORDERS

The rising upper and lower limits are defined by values shown in Table 19.

| Upper limit of rising margin | | Lower limit of rising margin | |
|---|---|---|---|
| Time (ms) | Acceleration (g) | Time (ms) | Acceleration (g) |
| 4 | 1.0531 | 8 | 1.0531 |
| 5 | 1.3751 | 9 | 1.3751 |
| 6 | 1.7443 | 10 | 1.7443 |
| 7 | 2.1608 | 11 | 2.1608 |
| 8 | 2.623 | 12 | 2.623 |
| 9 | 3.1267 | 13 | 3.1267 |
| 10 | 3.6691 | 14 | 3.6691 |
| 11 | 4.2406 | 15 | 4.2406 |
| 12 | 4.8336 | 16 | 4.8336 |
| 13 | 5.4384 | 17 | 5.4384 |
| 14 | 6.0446 | 18 | 6.0446 |
| 15 | 6.6414 | 19 | 6.6414 |
| 16 | 7.2181 | 20 | 7.2181 |
| 17 | 7.7645 | 21 | 7.7645 |
| 18 | 8.2705 | 22 | 8.2705 |

TABLE 19 EURO NCAP MEDIUM SEVERITY ACCELERATION PULSE RISING CORRIDOR BORDERS

The high severity pulse is similarly shaped as the low severity pulse. The peak value however is 2.5 [g] higher and thus the velocity change approximately 24 [km/h]. The main pulse parameters can be found in Table 20.

| Parameter | | Requirement | Limits +/- | Units |
|---|---|---|---|---|
| Velocity change | delta v | 24.45 | 1.20 | km/h |
| Mean acceleration | $A_{mean}$ | 63.15 | 4.85 | m/s² |
| Maximum acceleration | $A_{max}$ | 7.50 | 0.75 | g |

TABLE 20 EURO NCAP HIGH SEVERITY ACCELERATION PULSE PARAMETERS

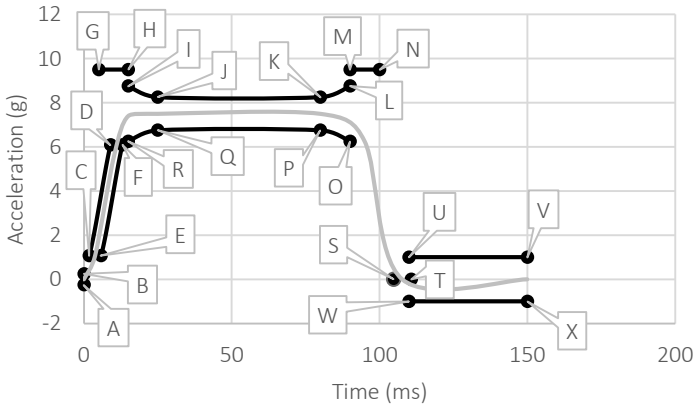


FIGURE 18 EURO NCAP HIGH SEVERITY ACCELERATION PULSE ACCORDING TO SRA, 24 KM/H CHANGE OF VELOCITY

Again the shape is defined by corridors for which again all values can be found in Table 21. A graph of the corridors and pulse can be found in Figure 18. The rising pulse is defined by a formula which can be found in Equation 12.

Equation 12 Euro NCAP high severity acceleration pulse rising pulse

$$acc_{(t)} = \frac{a_{max}}{2} * \left\{1 - \cos\frac{t * \pi}{15.4}\right\} \; for \; 3.7\; ms \; \leq t \; \leq 11.0\; ms$$

| | Time (ms) | Acceleration (g) | | Time (ms) | Acceleration (g) |
|---|---|---|---|---|---|
| A | 0 | 0.25 | M | 90 | 9.5 |
| B | 0 | -0.25 | N | 100 | 9.5 |
| C | 1.8 | 1.0714 | O | 90 | 6.25 |
| D | 9 | 6.088 | P | 80 | 6.75 |
| E | 5.8 | 1.0714 | Q | 25 | 6.75 |
| F | 13 | 6.088 | R | 15 | 6.25 |
| G | 5 | 9.5 | S | 104,7 | 0 |
| H | 15 | 9.5 | T | 110,7 | 0 |
| I | 15 | 8.75 | U | 110 | 1 |
| J | 25 | 8.25 | V | 150 | 1 |
| K | 80 | 8.25 | W | 110 | -1 |
| L | 90 | 8.75 | X | 150 | -1 |

TABLE 21 EURO NCAP HIGH SEVERITY ACCELERATION PULSE CORRIDOR BORDERS

For the upper and lower borders of the rising pulse, the values computed in Equation 12 must be shifted plus 2 [ms] and minus 2 [ms].

After adjusting the seat according to the Whiplash test protocol (Euro NCAP, 2014) and positioning the rear impact dummy (Bio RID II) as described in the same protocol, these three acceleration pulses are applied to the seat by a sled test system. For each pulse a different, usually new seat is used. The test is recorded with high speed video cameras with a number of video motion targets attached to the seat, sled and dummy. Still photographs of pre- and post-situations are recorded and the following measurements (Table 22) are recorded during the test.

| Position | Function | Measurement | CFC | CAC |
|---|---|---|---|---|
| Sled X | Pulse acceptance | Acceleration (g) | 60 | 100 |
| | Pulse acceptance | Velocity (m/s) | 30 | NA |
| | Rebound velocity | Displacement (m) | NA | NA |
| Head X | NIC | Acceleration (g) | 60 | 100 |
| | | Acceleration (g) | 1000 | 100 |
| Head c.o.g. X | Rebound velocity | Velocity (m/s) | 30 | NA |
| Neck T1 X (LH and RH) | NIC | Acceleration (g) | 60 | 100 |
| Neck Force X | | Force (N) | 1000 | 1400 |
| Neck Force X | My OC and Nkm | Force (N) | 600 | 1400 |
| Neck Force Z | | Force (N) | 1000 | 4500 |
| Neck Moment Y | My OC | Moment (Nm) | 600 | 115 |
| Head Restraint Contact Time (T-HRC) | $T\text{-}HRC_{start}$ $T\text{-}HRC_{end}$ | Time (ms) | NA | NA |
| Neck T1 X | | Force (N) | 1000 | 5000 |
| Neck T1 Z | | Force (N) | 1000 | 5000 |
| Neck T1 Moment Y | | Moment (Nm) | 600 | 200 |
| 1st Lumbar X | | Acceleration (g) | 60 | 200 |
| 1st Lumbar Z | | Acceleration (g) | 60 | 100 |
| Seat Belt Force (lap section) | | Force (kN) | 60 | 16 |

TABLE 22 EURO NCAP REQUIRED INSTRUMENTATION FOR THE DYNAMIC TEST

From the high speed footage and data acquired during each sled test the following whiplash assessment criteria are derived.

- Head Restraint Contact Time
  - $T\text{-}HRC_{start}$
  - $T\text{-}HRC_{end}$
  - $T\text{-}HRC = (T\text{-}HRC_{end}) - (T\text{-}HRC_{start})$
- T1 x-acceleration (until $T\text{-}HRC_{end}$)
- Upper Neck Forces (until $T\text{-}HRC_{end}$)
  - Upper Neck Shear Force
  - Upper Neck Tension Force
- Head Rebound Velocity (max 300 ms)
  - Magnitude
  - Timing
- NIC (until $T\text{-}HRC_{end}$)
  - Magnitude
  - Timing
- Nkm (until $T\text{-}HRC_{end}$)
  - Neck Extension Posterior - $N_{ep}$
  - Neck Extension Anterior - $N_{ea}$
  - Neck Flexion Posterior - $N_{fp}$
  - Neck Flexion Anterior - $N_{fa}$
- Seatback Dynamic Opening (until $T\text{-}HRC_{end}$)

The assessment of the dynamic test results is defined with three performance ranges for each different acceleration pulse. The performance ranges are called “higher performance”, “lower performance” and “capping limit” If the value determined for the assessed criterion exceeds the capping limit, the score for this criterion is set to zero (0). If the values lies between “higher” and “lower” performance criterion the score is scaled between zero (0) and 0.5. If the criterion performs better than the “higher performance” limit, 0.5 points are scored. The criterion T1 acceleration and T-HRC are exclusive, only the better performing criterion contributes to the score. The limits for each test can be found in Table 23.

| | Lower Severity Pulse | | | Medium Severity Pulse | | | High Severity Pulse | | |
|---|---|---|---|---|---|---|---|---|---|
| | Higher Performance | Lower Performance | Capping Limit | Higher Performance | Lower Performance | Capping Limit | Higher Performance | Lower Performance | Capping Limit |
| NIC ($m^2/s^2$) | 9 | 15 | 18.3 | 11 | 24 | 27 | 13 | 23 | 25.5 |
| Nkm (-) | 0.12 | 0.35 | 0.5 | 0.15 | 0.55 | 0.69 | 0.22 | 0.47 | 0.78 |
| Rebound Velocity (m/s) | 3 | 4.4 | 4.7 | 3.2 | 4.8 | 5.2 | 4.1 | 5.5 | 6 |
| Upper Neck Shear Fx (N) | 30 | 110 | 187 | 30 | 190 | 290 | 30 | 210 | 364 |
| Upper Neck Tension Fz (N) | 270 | 610 | 734 | 360 | 750 | 900 | 470 | 770 | 1024 |
| T1 acceleration (g) | 9.4 | 12 | 14.1 | 9.3 | 13.1 | 15.55 | 12.5 | 15.9 | 17.8 |
| T-HRC (ms) | 61 | 83 | 95 | 57 | 82 | 92 | 53 | 80 | 92 |

TABLE 23 EURO NCAP WHIPLASH ASSESSMENT CRITERIA FOR ALL PULSES

Additional to the static and dynamic rating there are three modifiers that can vastly influence the rating.

- Worst case geometry (Euro NCAP, 2013)
  1/n points (where n is the number of front seats) are added to the score, if the raw score of the dynamic tests is greater than 4.5 points after capping and modifiers have been applied and a geometry assessment of the "worst case" adjustment of the head restraint (i.e. most downward and backward position) leads to more than zero (0) points.
- Seat stability modifier (Euro NCAP, 2013)
  If the seatback rotates backward more than 32 ° during the dynamic test with the high severity pulse (SRA 24 [km/h]) three (3) points are subtracted in the whiplash rating.
- Dummy artefact modifier (Euro NCAP, 2013)
  If the design of the seat exploits dummy artefacts or leads to unfavourable loading of other body regions a penalty of minus two (-2) points will be applied.

The rear whiplash assessment is a rather simple evaluation of geometric correlations between a 50$^{th}$ percentile male occupant, in this case represented by the HRMD, and the vehicles' seat. The evaluation is a three step process.

1. Evaluation of the effective height of the head restraint in its highest and lowest position.
   The effective height $H_{eff}$ is relevant to support the head in case of a rear end collision and must be $H_{eff} \geq 770$ mm in the head restraints highest position and $H_{eff} \leq 720$ mm in its worst case (lowest and most rearward) in-use position. The effective height $H_{eff}$ is determined as follows:

Equation 13 Euro NCAP rear whiplash, determination of the effective height for head restraints

$$H_{eff} = \Delta IP\ X * \ sin(Torso\ angle) + \ \Delta IP\ Z * \ cos(Torso\ angle)$$

   Where IP is the intersection point as described in the rear whiplash test protocol (Euro NCAP, 2013). This value is determined for the highest locking in-use and lowest and most rearward in-use locking position. If this condition is not fulfilled, the evaluation of the backset and non-use position must be skipped and no score is gained.

2. Evaluation of the backset with the head restraint in the
   a. Middle position and
   b. In the lowest position

   The backset ΔCP score for both scenarios (middle and low position of the head restraint) can only be gained, if the effective height is reached.

3. Evaluation of the non-use position
   Also this point can only be acquired if the score for the effective height was made.
   The non-use position has three characteristics that are checked.

   a. 60 ° rotation evaluation
      This factor is concluded positive, if the angle, rotating the head restraint from in-use to non-use position exceeds 60 °. This applies for head restraints that fold away for non-use.

b. 10 ° Torso line change
In this evaluation, the H-point mannequin is used to determine the torso angle with the head restraint in its non-use position and in-use position. If the difference of the torso angle is larger than 10 ° this factor is concluded positive.

c. Discomfort metric
In this evaluation, the lower edge of the head restraint in its non-use position must be at a height ($H_{LE}$) between 250 mm and 460 mm. Also the thickness (S) of the lower edge of the head restraint must be larger than 40 mm. Both measurements are illustrated in Figure 21.

The evaluation of the rear seat parameters is displayed in Figure 19, Figure 20 and Figure 21. Table 24 holds the corresponding limits for the evaluation according to the rear whiplash protocol (Euro NCAP, 2013).

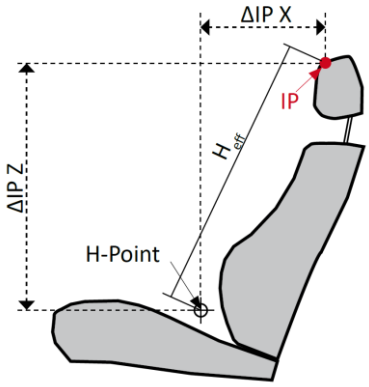


FIGURE 19 EURO NCAP $H_{EFF}$ IN REAR WHIPLASH EVALUATION

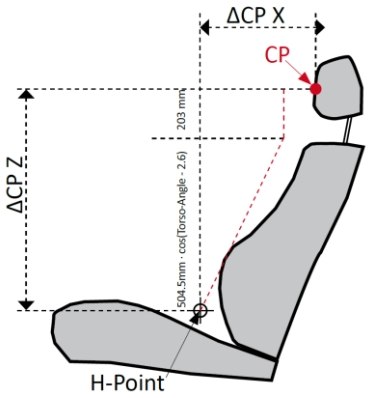


FIGURE 20 EURO NCAP BACKSET IN REAR WHIPLASH EVALUATION

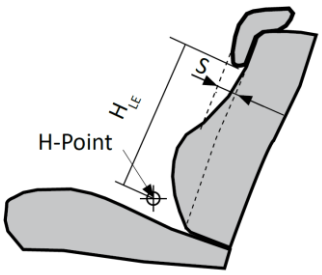


FIGURE 21 EURO NCAP NON-USE POSITION IN REAR WHIPLASH EVALUATION

| Parameter | Value | Score per seat |
|---|---|---|
| $H_{eff}$ (high) | ≥ 770 mm | 1.5 |
| $H_{eff}$(worst case) | ≤ 720 mm | |
| ΔCP $X_{mid}$ | ≤ 7.128 * torso-angle +153 | 1[1)] |
| ΔCP $X_{worstcase}$ | | 0.5[1)] |
| Non-use | | 1[1)] |
| [1)] applies only if $H_{eff}$ scored. Otherwise no score for backset and non-use position. | | |

TABLE 24 EURO NCAP REAR WHIPLASH SCORING SCHEME

All outboard vehicle seats of all seat rows except the first are to be assessed like this. The score shall be scaled as follows:

**Equation 14 Euro NCAP scaling of rear whiplash score**

$$Score_{\ scaled} = Score_{each\ seat} \frac{1}{4 * n}$$

Where the scaled score is the effective score adding to the Euro NCAP overall score, n is the number of seats in second of further backward outboard seats.

The whiplash scoring for the 2014 Euro NCAP protocol, for the front and rear whiplash assessment (Euro NCAP, 2013) is explained in the following Figure 22 and Figure 23. Front seats whiplash assessment and rear seats whiplash assessment are visualised independently:

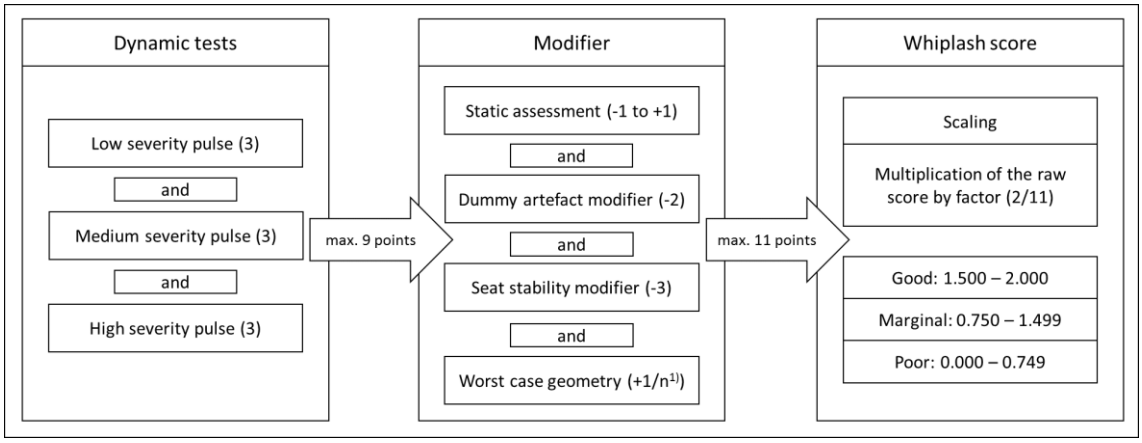


1) n is the number of seats in the front row

FIGURE 22 EURO NCAP FRONT WHIPLASH SCORING SCHEME AND RATING VISUALIZATION

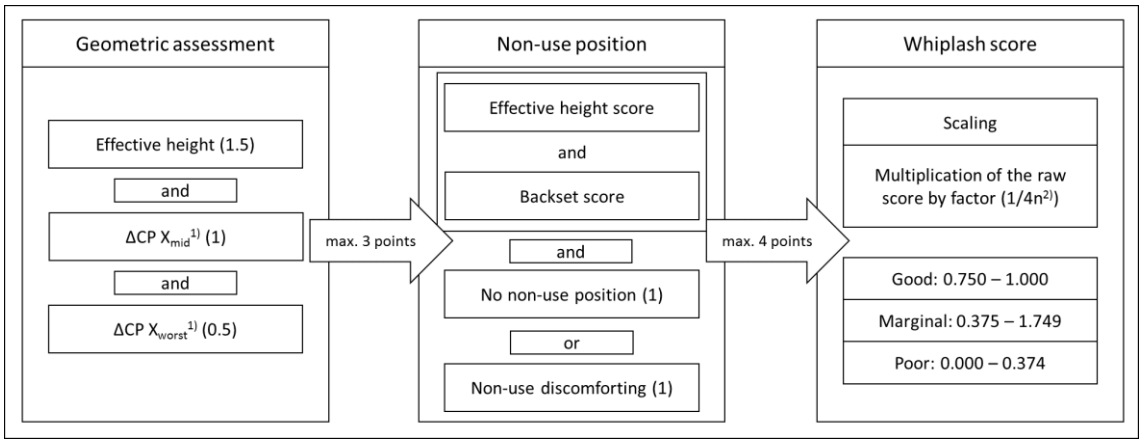


1) applies only if $H_{eff}$ scored. Otherwise no score for backset and non-use position.
2) n is the number of outboard seats in all rows except the front row

FIGURE 23 EURO NCAP REAR WHIPLASH SCORING SCHEME AND RATING VISUALIZATION

This leads to a total of three points for the overall rating in whiplash since 2014. Two can be gained in the front whiplash assessment, and one in the rear whiplash assessment. It should be mentioned, that automatic emergency braking (AEB) systems for city traffic are assessed as part of the AOP assessment, not the Euro NCAP Safety Assist (SA) assessment, as might be assumed. The assessment of AEB can score only if the dynamic whiplash assessment lead to a score greater than 1.5. However the score for a positive AEB assessment can be as high as three point. This almost inevitably requires an AEB city system to be able to get a five star rating from 2014 on. A more detailed review of the assessment of AEB systems is however not part of this manuscript. More information can be found in the Euro NCAP AOP protocol (Euro NCAP, 2013).

#### 2.6.3.2. China NCAP (C-NCAP, 2012)

China NCAP was established 2006 based on developments of other NCAPs including head injury, thorax compression and thigh axial force, as well as neck and leg damage parameters.

Regarding the Whiplash assessment the China NCAP Protocol states:

*"The driver seat and its restrain system of the test vehicle shall be such fitted on the sled as they originally on the test vehicle. The sled shall be launched at a speed of 15.65 ± 0.81 [km/h] with a specified acceleration pulse to simulate the rear-end impact. A Bio RID II dummy is placed in the seat to measure the injuries to occupant neck during the rear-end impact and to evaluate the protective performance of headrest to occupant neck."*

Within the protocol, no static test is described. The full score for a whiplash test is four out of 62 points in total. For evaluation a higher performance limit and a lower performance limit is defined leading to the maximum or minimum possible score within this category. Seatback dynamic opening, head interference space of head restraint and seat track dynamic displacement are absolute criteria which can only reduce the score if a certain state is reached. Details of limits and associated scores can be found in Table 25 or in the C-NCAP protocol (C-NCAP, 2012).

| Criteria | Higher performance limit | Lower performance limit | score | Score of whiplash test | Bonus score converted for C-NCAP |
|---|---|---|---|---|---|
| NIC | 8 m²/s² | 30 m²/s² | 0 ~ 2 | 0 ~ 8 | 0 ~ 4 |
| Upper neck Fx+ | 340 N | 730 N | 0 ~ 6 | | |
| Upper neck Fz+ | 475 N | 1,130 N | | | |
| Upper neck My | 12 Nm | 40 Nm | | | |
| Lower neck Fx+ | 340 N | 730 N | | | |
| Lower neck Fz+ | 257 N | 1,480 N | | | |
| Lower neck My | 12 Nm | 40 Nm | | | |
| Seatback dynamic opening | 32 ° | | -2 or 0 | | |
| Head interference space of head restraint | Yes/No | | -2 or 0 | | |
| Seat track dynamic displacement | 20 mm | | -4 or 0 | | |

TABLE 25 C-NCAP SCORING SCHEME

The whiplash test, depending on its results allows for a raw score from zero (0) to eight (8) points. For the integration in the overall C-NCAP score it is transformed as described in the graph in the subsequent Figure 24.


FIGURE 24 C-NCAP RAW WHIPLASH SCORE TRANSFORMATION FUNCTION

The test procedure itself is very much like the IIHS, IIWPG or Euro NCAP mid severity dynamic test. The dummy used is, as well, the Bio RID II and the acceleration pulse is the same triangular pulse as used in the Euro NCAP mid severity test, with a peak of 10 g and a duration of 91 ms like in Figure 25.

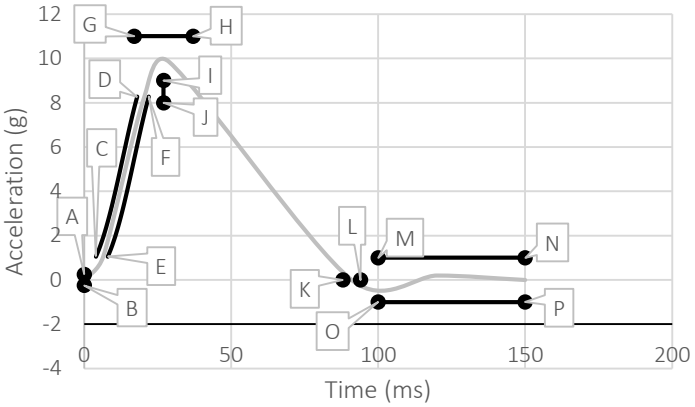


FIGURE 25 C-NCAP DYNAMIC TEST ACCELERATION PULSE

A more detailed discussion about the China NCAP whiplash assessment shall not be made within this manuscript, since the before described Euro NCAP appears to be more sophisticated already.

#### 2.6.3.3. Japan NCAP

JNCAP was started and operated by the Japanese National Agency for Automotive Safety and Victims' Aid (NASVA). JNCAP publishes consumer test results since 1995. Assessment for neck injury protection in rear-end collisions has been started in 2009. (NASVA, 2013)

The neck injury assessment, was developed for 4 year beginning in the year 2005. JNCAP also uses the Bio RID II dummy and a very similar protocol for the dynamic assessment, dummy positioning and so on like the IIHS or Euro NCAP. (JNCAP, 2011) Japanese research revealed, since JNCAP wanted to protect and prevent occupants from WAD2+ (according to the Quebec Task Force Classification of WAD) injuries, that the IIWPG pulse was not sufficient for their assessment. It was decided to use a triangular pulse with a change of velocity of 20 [km/h]. However, most vehicle seats at that time could not withstand this dynamic test, thus it was decided to use a triangular pulse with a change of velocity of 17.6 [km/h] for three (3) years. After this period of time, the initially proposed 20 [km/h] change of velocity pulse should be used again, which reflects the current situation. (TAKAHIRO , et al., 2009) The two pulses are displayed in Figure 26 and Figure 27. The general data about the pulses' parameters are listed in Table 26 and Table 28 as well as more detailed data about the corridor parameters in Table 27 and Table 29 (JNCAP, 2011).

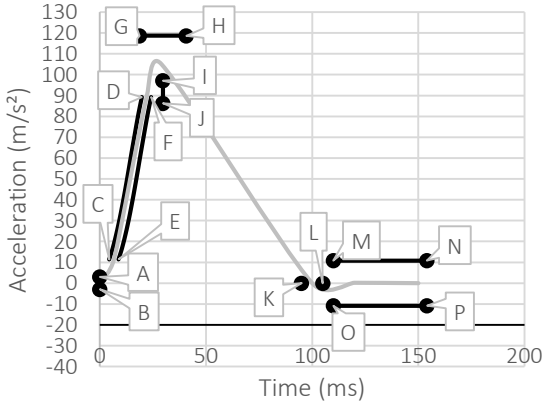


FIGURE 26 JNCAP DYNAMIC TEST ACCELERATION PULSE 20 KM/H

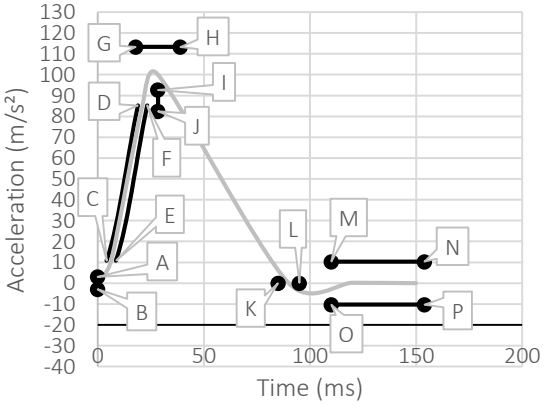


FIGURE 27 JNCAP DYNAMIC TEST ACCELERATION PULSE 17 KM/H

| | | Value | Limit | Unit |
|---|---|---|---|---|
| Change of velocity | ΔV | 20 | ± 1.0 | km/h |
| Duration | ΔT | 100 | ± 5.0 | ms |
| Acceleration | Mean Acceleration | 55.5 | ± 5.0 | m/s² |
| Acceleration at T=0 | AT0 | 0.0 | ± 3.0 | m/s² |

TABLE 26 JNCAP ACCELERATION PULSE PARAMETERS 20 KM/H

| | Time (ms) | Acceleration (m/s²) | | Time (ms) | Acceleration (m/s²) |
|---|---|---|---|---|---|
| A | 0 | 3 | K | 95 | 0 |
| B | 0 | -3 | L | 105 | 0 |
| C | 4.4 | 11.4 | E | 8.8 | 11.4 |
| C-D | 5.5 | 14.8 | E-F | 9.9 | 14.8 |
| C-D | 6.6 | 18.8 | E-F | 11 | 18.8 |
| C-D | 7.7 | 23.3 | E-F | 12.1 | 23.3 |
| C-D | 8.8 | 28.3 | E-F | 13.2 | 28.3 |
| C-D | 9.9 | 33.7 | E-F | 14.3 | 33.7 |
| C-D | 11 | 39.6 | E-F | 15.4 | 39.6 |
| C-D | 12.1 | 45.7 | E-F | 16.5 | 45.7 |
| C-D | 13.2 | 52.1 | E-F | 17.6 | 52.1 |
| C-D | 14.3 | 58.7 | E-F | 18.7 | 58.7 |
| C-D | 15.4 | 65.2 | E-F | 19.8 | 65.2 |
| C-D | 16.5 | 71.6 | E-F | 20.9 | 71.6 |
| C-D | 17.6 | 77.9 | E-F | 22.0 | 77.9 |
| C-D | 18.7 | 83.8 | E-F | 23.1 | 83.8 |
| D | 19.8 | 89.2 | F | 24.2 | 89.2 |
| G | 18.7 | 118.7 | M | 110 | 10.8 |
| H | 40.7 | 118.8 | N | 154 | 10.8 |
| I | 29.7 | 97.1 | O | 110 | -10.8 |
| J | 29.7 | 86.3 | P | 154 | -10.8 |

TABLE 27 JNCAP ACCELERATION PULSE CORRIDOR BORDERS 20 KM/H

| | | Value | Limit | Unit |
|---|---|---|---|---|
| Change of velocity | ΔV | 17.6 | ± 0.9 | km/h |
| Duration | ΔT | 90.0 | ± 5.0 | ms |
| Acceleration | Mean Acceleration | 54.3 | ± 5.0 | m/s² |
| Acceleration at T=0 | AT0 | 0.0 | ± 3.0 | m/s² |

TABLE 28 JNCAP ACCELERATION PULSE PARAMETERS 17 KM/H

| | Time (ms) | Acceleration (m/s²) | | Time (ms) | Acceleration (m/s²) |
|---|---|---|---|---|---|
| A | 0 | 3 | K | 90 | 0 |
| B | 0 | -3 | L | 100 | 0 |
| C | 4.2 | 10.8 | E | 8.8 | 10.8 |
| C-D | 5.3 | 14.2 | E-F | 9.9 | 14.2 |
| C-D | 6.3 | 18.0 | E-F | 11 | 18.0 |
| C-D | 7.4 | 22.3 | E-F | 12.1 | 22.3 |
| C-D | 8.4 | 27.0 | E-F | 13.2 | 27.0 |
| C-D | 9.5 | 32.2 | E-F | 14.3 | 32.2 |
| C-D | 10.5 | 37.8 | E-F | 15.4 | 37.8 |
| C-D | 11.6 | 43.7 | E-F | 16.5 | 43.7 |
| C-D | 12.6 | 49.8 | E-F | 17.6 | 49.8 |
| C-D | 13.7 | 56.0 | E-F | 18.7 | 56.0 |
| C-D | 14.7 | 62.2 | E-F | 19.8 | 62.2 |
| C-D | 15.8 | 68.4 | E-F | 20.9 | 68.4 |
| C-D | 16.8 | 74.3 | E-F | 22.0 | 74.3 |
| C-D | 17.9 | 80.0 | E-F | 23.1 | 80.0 |
| D | 18.9 | 85.2 | F | 24.2 | 85.2 |
| G | 17.9 | 113.3 | M | 105 | 10.3 |
| H | 38.9 | 113.3 | N | 147 | 10.3 |
| I | 28.4 | 92.7 | O | 105 | -10.3 |
| J | 28.4 | 82.4 | P | 147 | -10.3 |

TABLE 29 JNCAP ACCELERATION PULSE CORRIDOR BORDERS 17 KM/H

The assessed dynamic criteria can be found in Table 30. Within the already mentioned study (TAKAHIRO , et al., 2009) JNCAP found that the correlation between the severity of WAD and the criteria NIC and forces and moments was not equal. Thus a weighting was implemented, prioritising the force and moment criteria by the factor two (2). From all force and moment criteria, only the worst criterion contributes to the scoring.

| Criterion | Weighting | Score | Limits |
|---|---|---|---|
| NIC | 1 | 4 | < 8 m²/s² |
| | | 0 | > 30 m²/s² |
| Upper Neck Fx+[1)] | 2 | 4 | < 340 N |
| | | 0 | > 730 N |
| Upper Neck Fz+[1)] | | 4 | < 475 N |
| | | 0 | > 1130 N |
| Upper Neck My[1)] | | 4 | < 12 Nm |
| | | 0 | > 40 Nm |
| Lower Neck Fx+[1)] | | 4 | < 340 N |
| | | 0 | > 730 N |
| Lower Neck Fz+[1)] | | 4 | < 257 N |
| | | 0 | > 1480 N |
| Lower Neck My[1)] | | 4 | < 12 Nm |
| | | 0 | > 40 Nm |
| | max. sum after weighting: | 12 | |
| [1)] only the worst rating contributes to the rating | | | |

TABLE 30 JNCAP WHIPLASH ASSESSMENT CRITERIA

For all values of the corresponding criteria which are between the upper and lower limit of the criterion, a sliding scale scoring (zero to four) is calculated. For a criterion below the lower limit all four (4) points are applied, for criteria exceeding the higher limit, no score is applied. After the assessment a maximum of twelve (12) points can be scored for each, the driver and passenger seat. The whiplash rating is based on four (4) score levels as shown in the following Table 31.

| Level | Score |
|---|---|
| 1 – dark green | > 10 |
| 2 – light green | > 8 |
| 3 – yellow | > 5 |
| 4 – orange | ≤ 5 |

TABLE 31 JNCAP WHIPLASH PROTECTION LEVEL RATING

After weighting for the overall rating, multiplying both values by 0.625, a maximum total whiplash score of 7.5 for each seat (15 in total) can be gained. The total occupant protection score is one hundred (100) points.

#### 2.6.3.4. Australia NCAP

The Australian New Cars Assessment Program (ANCAP) (ANCAP, 2015), according to own statements provides consumer test ratings since 1993. Vehicles are rated in a star rating similar to the Euro NCAP. However currently ANCAP uses a static evaluation and one dynamic test to assess car seats with regard to whiplash. The whiplash assessment (ANCAP, 2012) is conducted in accordance with the RCAR-IIWPG Seat/Head Restraint Evaluation Protocol (RCAR, 2008). The Euro NCAP medium severity dynamic tests matches the RCAR criteria quite well and so data from that Euro NCAP test may be used by ANCAP to derive a whiplash rating according to the RCAR protocol.

#### 2.6.3.5. Korea NCAP

The Korea New Car Assessment Program (KNCAP, 2012) started publishing consumer crash test results in 1999. Since 2008 (KNCAP, 2012) KNCAP publishes ratings of seat assessments. The assessment is at the moment, one static evaluation in accordance with the RCAR-IIWPG Seat/Head Restraint Evaluation Protocol (RCAR, 2008) and one dynamic test very much like the Euro NCAP medium severity test. The assessment criteria for the dynamic sled test can be found in the following Table 32. (KNCAP, 1999)

| Criteria | Lower border | Higher border | Score |
|---|---|---|---|
| T-HRC (ms) | 57 | 82 | 0.0-1.5 |
| T1 acceleration (g) | 9.3 | 13.1 | |
| Upper neck Shear Fx (N) | 30 | 190 | 0.0-1.5 |
| Upper Neck Tension Fz (N) | 260 | 750 | 0.0-1.5 |
| Head rebound velocity (m/s) | 3.2 | 4.8 | 0.0-1.5 |
| NIC ($m^2/s^2$) | 11 | 24 | 0.0-1.5 |
| Nkm | 0.15 | 0.55 | 0.0-1.5 |
| | | Total sum | 0.0-9.0 |

TABLE 32 KNCAP DYNAMIC WHIPLASH ASSESSMENT CRITERIA AND SCORE

The static assessment contributes, depending on its result minus one (-1) to plus one (1) point to the whiplash score. Modifiers for unwanted behaviour can be applied to reduce another two points (-2). The dynamic evaluation scores up to nine (9) points. This leads to an overall maximum whiplash raw score of ten (10). The total passenger protection score is one hundred (100).

Future ambitions of the Korean NCAP include the extension of the whiplash assessment. By the year 2017 three dynamic tests, as well as an evaluation of rear seat rows.

## 2.7. Current Protection Systems

The first “active” head restraint systems were introduced in series-production vehicles around 1996. Ever since, all different kinds of vehicle manufacturers and component suppliers developed systems and concepts for the protection and reduction of whiplash associated disorders.

However, reviewing the results of head restraint and seat assessments, for example the Euro NCAP Assessment, it appears to be rather inconclusive, whether passive, active, reactive, proactive or whatever other system is to be favoured. The ratings clearly show, that passive systems, if designed well, can provide a decent, even very good level of protection. But they also show, that having an active system does not mean protection is improved simultaneously. (Euro NCAP, 2015)

In this chapter a few systems shall be described. There is a number of different systems and not all of them can be covered within this summary. The selected systems are examples to give a brief overview.

### 2.7.1. Saab – Saab Active Head Restraint (SAHR)

Saab introduced in 1997, probably as the first car manufacturer, a completely mechanical active head restraint system in serial production cars. IIHS found in a study, that with SAHR a reduction of 43 % in injury claims was reached. In case of a rear end collision, the head restraint is moved upwards and towards the passengers head by a mechanical system as displayed in Figure 28. The system is reversible, without resetting or replacing any components, as long as no structural damage is caused to the seat itself. According to Saab, the system is activated by the inertia of the torso of the occupant, as soon as a change of velocity of more than 8 [km/h] is reached, independent of the weight or stature of the passenger. The movement of the first SAHR system was rather limited (~15 [mm]) but was improved in later implementations. Also since the first system was developed with the HIII dummy, the activation of the mechanism was developed with a very stiff back and spine. The rather flexible human body however caused a different response, especially in low change of velocity cases. All these factors were adapted and in 2003 a second generation of SAHR was introduced. (Gizmag, 2013) (Wilkund, et al., 1998)

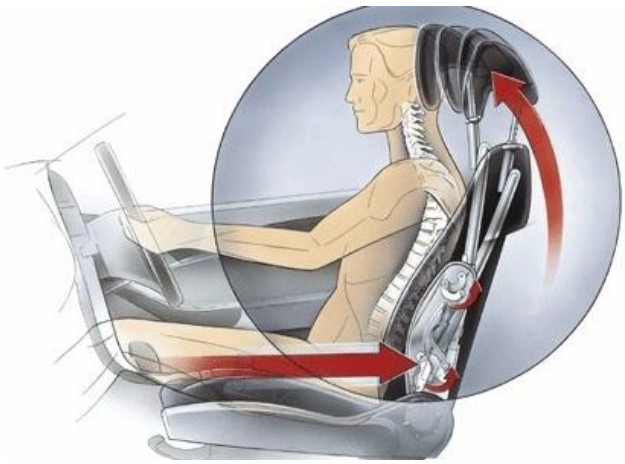

FIGURE 28 SAAB SAHR ACTIVE REVERSIBLE HEAD RESTRAINT CONCEPT.

### 2.7.2. Daimler – Neck-Pro (Daimler AG, 2012)

FIGURE 29 DAIMLER NECK PRO - ACTIVE REUSABLE ANTI-WHIPLASH HEAD RESTRAINT SYSTEM (DAIMLER AG, 2012)

Daimler provides its passenger vehicles with a "crash active" head Restraint System called NECK-PRO-Head Restraint. According to Daimler this device is available in driver and passenger car seat and is standard equipment in many Mercedes Benz models. The mechanism is triggered by an electronic control unit, which activates the head restraint in the case of a rear end crash. The head restraint is moved approximately 40 [mm] to the front and 30 [mm] upwards by preloaded springs, thus to support the occupants heads earlier during a rear end crash scenario.

After release usage of the head restraint, it can, with a supplied tool, be put back in its initial position and is ready for the next use.

### 2.7.3. Volvo - Whiplash Protection System (WHIPS) (Jakobsson, et al., 2000)

Volvo developed an anti-whiplash system based on the inertia of the occupants' body. The so called WHIPS seat was developed during a study and research project lasting approximately ten (10) years. By the year 2000 Volvo equipped all new vehicle models with this system.

WHIPS allows the seatback to move in a controlled way after a rear-end impact. The behaviour and motion is defined within the recliners, which are present at both sides of the backrest in Volvo seats. The motion is defined in two phases. First a translational rearward motion of the entire backrest in the first phase. This allows the occupant to sink into the backrest thus reducing the distance between head and head restraint. It also reduces the occupants' acceleration level. Secondly a reclining motion of the backrest with its rotational centre in the recliner. This allows absorbing the energy of the occupants mass at a controlled level of acceleration. The force and therewith acceleration level is limited by a metallic energy absorption component in the recliner, which deforms plastically. The motion phases are illustrated in Figure 30 and Figure 31. During real rear end collisions, phase one and phase two overlap, depending on different parameters (e.g. occupant weight, posture, acceleration level …). After a rear end collision, the seats recliner is permanently damaged. Resetting of the system is not implemented, thus the seats must be replaced.

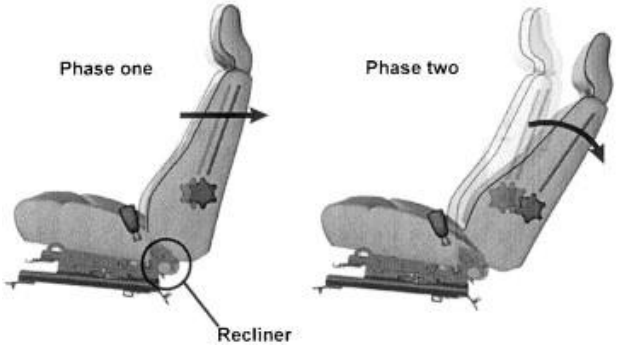


FIGURE 30 VOLVO WHIPS SEAT BACK MOTION PHASES (JAKOBSSON, ET AL., 2000)

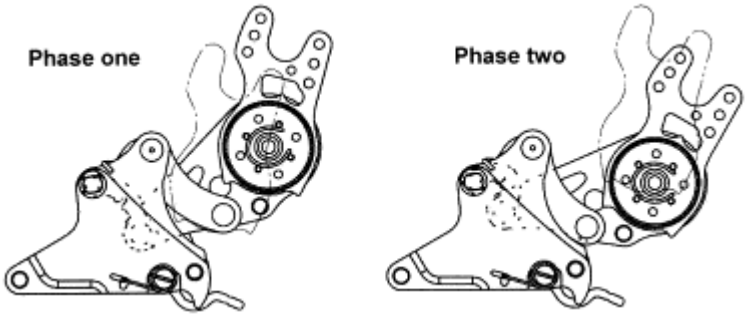


FIGURE 31 VOLVO WHIPS RECLINER SCHEME (JAKOBSSON, ET AL., 2000)

Today WHIPS is implemented in several Volvo and Jaguar vehicles.

### 2.7.4. Toyota - Whiplash Injury Lessening (WIL)

The WIL concept was implemented in Toyotas passenger car seats in 1997. An improved version was introduced in 2005. This system is designed to cushion the passengers head and chest simultaneously in case of rear end collision, thus helping to minimize injuries in such, usually lower speed collisions. The concept is based on a redesign of the rigidity and layout of the seatback, seat frame and head restraint, allowing for a reduction of the relative opposite movement between head and torso. The system is based on the inertia of the occupants' torso and is reusable without any resetting. (Toyota Motor Corporation, 1995-2015)

Figure 32 explains the principle concept of the WIL system.

1) When driver (vehicle) is hit, the (passengers) back sinks into the seat.
2) The seat and head restraint support the head and body simultaneously to help minimize whiplash.


FIGURE 32 TOYOTA WIL CONCEPT PRINCIPLE FUNCTIONALITY (TOYOTA MOTOR CORPORATION, 1995-2015)

### 2.7.5. Lear – ProTec

FIGURE 33 LEAR PROTEC ACTIVE HEAD RESTRAINT (LEAR CORPORATION, 2015)

FIGURE 34 LEAR VISIONTEC HEAD RESTRAINT FOR REAR SEATS (LEAR CORPORATION, 2015)

Lear, in contrast to all system developers before, is component supplier for a wide range of industry. Among other components, Lear produces passenger car seating. The corporation supplies an active head restraint (AHR) system called ProTec since 1998, displayed in Figure 33. This head restraint, according to IIHS reports, is capable of reducing whiplash associated disorders by up to 43 percent. The ProTec head restraint passes the FMVSS202a dynamic test and the IIWPG dynamic test with a "GOOD" rating according to Lear. The system itself is activated by pressure applied against the upper cross member of the backrest moving forward the head restraint by a lever system. Recently, developments regarding the rear seat rows have been leading to another system provided by Lear. The VisionTec head restraint is shown in Figure 34. This development shows that a European demand can drive developments not only in Europe, but on a global market. (Lear Corporation, 2015)

### 2.7.6. AHR – RHR, General Comments

Today in several vehicles from numerous manufacturers all different kinds of active head restraints (AHR) and reactive head restraints (RHR) exist. The first implemented RHR was the SAHR by Saab. Similar concepts are widely implemented today in several vehicles fleets such as Audi, Ford, Mercedes, Nissan, Opel, Skoda, Seat, Volkswagen and others. (Kullgren, et al., 2007)

Other systems were developed and implemented in different vehicles and vehicle fleets such as:

- Spinal Care System (SCS) developed by Faurecia, very similar to other systems, pressure against the upper cross member moves a lever system to position the head restraint closer to the head
- Lear Spring System, a system with a pre engaged spring system that is triggered either mechanically or electronically to move the head restraint closer to the occupants head
- Crash aktive Kopfstütze CAK by Keiper is a spring powered system to move the head restraint closer to the head (50 [mm] backset and 27 [mm] height) released either electronically or mechanically
- Controlled Yield systems, similar to the WHIPS, brackets, absorbers or other devices implemented in the anchorage of vehicle seats absorb energy in case of a rear end collision and reduce the energy released to the occupant

### 2.7.7. Comparison of Major Protection Systems

Comparison between different protective systems shows good results for the WHIPS system. Additionally the system also appears to also be more protective for female occupants than others. The performance of WHIPS is followed by SAHR and WIL before other systems. (Viano, et al., 2001), (Kullgren, et al., 2007), (Jakobsson, et al., 2008), (Jakobsson, et al., 2004a), (Kullgren, et al., 2008).

The overall risk reduction (for all available grades of crash severity) was estimated at 29 % for females and 10 % for males with an implemented WHIPS system (Jakobsson, et al., 2004a). The initial WAD risk reduction for minor impacts is numbered at 21 % irrespective of gender and the risk reduction for persistent WAD at moderate impacts up to 47 % (Jakobsson, et al., 2008). Furthermore (Kullgren, et al., 2008) found, that WHIPS reduced the relative risk for long term WAD (longer than one month) by up to 60 % in two car crashes (paired comparison – victim, opponent, passenger cars).

A reduction of relative risk by up to 30 % for long term WAD (lasting longer than one month) in two car crashes by the WIL system was found by (Kullgren, et al., 2008). In this study also the SAHR was investigated. A decrease of the relative risk sustaining long term WAD lasting longer than one month of 55 % could be found for two car crashes.
A decrease of 18 % to 4 % of the absolute risk for WAD lasting longer than a week for SAHR could be found by (Viano, et al., 2001).

| Factor | change of WAD Risk | Reference |
|---|---|---|
| geometric head restraint redesign | 37 % lower risk for Ford Taunus and Mercury Sable for females, not for males (models with "standard" and "improved" seat/head restraint design) | (Farmer, et al., 2003) |
| active head restraints | 55 % lower risk for active head restraints (except WIL and WHIPS) for females (sig.), 43 % overall (sig.) (males reduction not significant.) (models with "standard" and "improved" seat/head restraint design) | (Farmer, et al., 2003) |
| WHIPS | absolute risk reduction for females 29 %, for males 10 %; at moderate impact severity 45 % reduction for females, (all sig.) and not significant. 24 % reduction for males | (Jakobsson, et al., 2004a) |
| WHIPS | reduction of 22 % for initial risk and 34 % reduction of long term risk | (Jakobsson, et al., 2008) |
| WHIPS | 60 % relative risk reduction for long term (>1 month) WAD in two car crashes | (Kullgren, et al., 2008) |
| WHIPS | reduction of 25 % for initial risk and 40 % reduction of long term risk, absolute risk reduction for initial symptoms by 18 % for males, and 17 % for females | (Jakobsson 2010 for ADSEAT) |
| WHIPS | 35 % relative risk reduction for long term (>1 month) WAD in two car crashes compared to cars with standard seats | (Kullgren, et al., 2010) |
| SAHR | absolute Risk Reduction of 14 % (from 18 % to 4 %) risk of WAD >1 week | (Viano, et al., 2001) |
| SAHR | 55 % relative risk reduction for long term (>1 month) WAD in two car crashes | (Kullgren, et al., 2008) |
| SAHR | 5 0% relative risk reduction for long term (>1 month) WAD in two car crashes compared to cars with standard seats | (Kullgren, et al., 2010) |
| WIL | 30 % relative risk reduction for long term (>1 month) WAD in two car crashes | (Kullgren, et al., 2008) |
| WIL | 40 % relative risk reduction for more than 1 month and more than 6 months at 20 km/h | (Kullgren et al. 2010 for ADSEAT) |
| WIL | 20 % relative risk reduction for long term (>1 month) WAD in two car crashes compared to cars with standard seats | (Kullgren, et al., 2010) |
| WHIPS, RHR, WIL | Relative risk for long-term (> 1 month) neck injury in seats with a system is about 50 % of the risk in seats without a system, absolute Risk Reduction of 7 % (from around 14 % to 7 %) | (Kullgren, et al., 2007) |
| other than WHIPS, SAHR, WIL | 25 % relative risk reduction by whiplash protection systems for long term (>1 month) WAD in two car crashes | (Kullgren, et al., 2008) |
| All Whiplash Protection concepts | (seat labelled by manufacturer) 45 % risk reduction for females, 60 % risk reduction for males (for WAD > 6months) | (Kullgren, et al., 2010) |

TABLE 33 OVERVIEW OF INVESTIGATIONS REGARDING PROTECTIVE POTENTIAL OF CAR SEATS WITH SYSTEMS/DESIGNS TO REDUCE WHIPLASH INJURY

It can be concluded, that all whiplash protection and prevention systems implemented (WHIPS, RHR, WIL) appear to benefit vehicle occupants in case of a rear end impact (Kullgren, et al., 2007), becoming long term WAD patients. Relative long term neck injury risk of seats equipped with a WAD protection system is about 50 % of one without any systems. The absolute risk reduction ranges between 7 % and 14 %.

Comparing real world data with the IIWPG rating, which combines geometric and dynamic testing of seats, a reduction of 50 % to 90 % for seats rated "good" compared to seats geometrically assessed as "poor" could be found (Avery, et al., 2008). Comparing the risk based on the static assessment of IIHS (Farmer, et al., 2008):

- "good" rated seats show a 15 % reduction in real world risk, compared to
- "poor" rated seats (not significant).
- For "marginal" and "acceptable" rated seats, no relation to real world injury risk could be found.

Active head restraint systems and energy absorbing, yielding backrests are found to decrease the risk for WAD, and in particular females benefit from such systems, even if development was based on the male occupant model Bio RID II. But also simple geometrical redesigns of head restraints can benefit, especially females (Farmer, et al., 2003).

## 2.8. Summary of the current situation

Development of WAD protection nowadays is focused on consumer tests. No matter which test, the occupant model of choice in all these assessments is the Bio RID II dummy (Davidsson, et al., 1998). Only one regulation (U.S. DoT, 2000) includes only the Hybrid III dummy (which for the whiplash load case is not the better choice). There is no doubt, that the Bio RID II, at the moment, is the most reasonable choice, however even this dummy does bring some uncertainties to the tests (Depinet, 2013) when it comes to reproducibility. According to (Eriksson, et al., 2007) applying the Objective Rating Method (ORM), the Bio RID II shows higher repeatability (ORM value 83 % to 90 %) than the widely used and accepted Hybrid III. For the Hybrid III in (Hovenga, et al., 2005) a repeatability of 65 % (ORM) is considered high.
One of the main issues is however, that the Bio RID II is a $50^{th}$ percentile male dummy. This means that all efforts put into seat developments with this ATD, improve conditions for occupants meeting the anthropometry and characteristics of this device. A seat protecting the Bio RID II dummy can be developed very well. This can be reviewed if the whiplash score of recent vehicle seats are observed (Euro NCAP, 2015). No matter if active, reactive, pro-active or passive, a good whiplash score in consumer tests can be reached with knowledge about the assessment. The assessment however does not reflect all real world incidents. Not all vehicle occupants are $50^{th}$ percentile males, or at least meet this anthropometry. Neither do all of those adjust their vehicle seats to their needs, or protection for that matter. Furthermore pre-impact posture appears to influence the risk for WAD (Jakobsson, et al., 2008). Contrary, many occupants do not meet this anthropometry, just looking at the share of females driving passenger cars (Tavris, et al., 2001). Also the seat adjustment of vehicle occupants being smaller than the $50^{th}$ percentile male differ very much from what is being tested in consumer tests at the moment (Gutsche, et al., 2013).

Another major factor is that people traveling in cars are not aware of their responsibility to adjust their protective devices, such as head restraints in case of WAD to their needs. But then vehicle seats

must also be capable of meeting those requirements. There are still vehicle seats available that do not allow for adjustments of head restraints to meet the height a 50$^{th}$ percentile females needs, let alone 5$^{th}$ percentile females.

All these factors point out, that there is still a large potential for development in this field. Some of the possible factors were thus investigated and looked at further.

# 3. METHODS

Within this thesis, based on the literature reviewed, different approaches were used to investigate questions pointed out:

- Experimental testing with the Bio RID II dummy
- Experimental testing with the Bio RID 50F dummy
- Experimental testing with Post Mortem Human Surrogates (PMHS)
- Numerical simulations with the Bio RID II numerical dummy model
- Numerical simulations with the Eva RID numerical dummy model
- Numerical simulations with the Hybrid III numerical dummy model

This wide approach enabled the comparison of results based on different methods. This was for instance comparisons of numerical simulations with experimental sled testing with dummies and human subjects.

## 3.1. Experimental Testing

Within this study, different types of sled tests were conducted. The testing included the state of the art Bio RID II dummy and a prototype female rear impact dummy named Bio RID 50F. For these tests setups in accordance with the Euro NCAP protocol, and tests differing from the protocol, were conducted. This was done to highlight the influence of occupant behaviour, occupant posture, and seat component settings on the risk sustaining WAD in real life situations. PMHS tests included two male and two female subjects to determine if differences in gender lead to different behaviour in rear end collision accidents. These tests provided information to identify possible gender specific behaviour.

### 3.1.1. Bio RID II Tests accordant and not accordant to Euro NCAP

A series of six sled tests (out of position tests, OOP1 – OOP6) was conducted, complementary to the ADSEAT project. For these tests, seats of the type Seat A were used. Seat A is a middle class vehicle production seat of a European make. The seat was used in new European vehicles until 2012. The seat is not equipped with any whiplash protection system. It has head restraints heights conform to legislational regulations (law), but not as high as requested by the Euro NCAP protocol (consumer test). As a consequence the mid-height position of the head restraint is lower than the top of the head of the Bio RID. Purpose of this test series was to highlight the influence of seat adjustment configurations and seated posture such as backrest angle and head restraint to head distance on the whiplash injury risk. For all six tests, the Bio RID II dummy and the IIWPG 16 [km/h] (medium severity) pulse were used. Selection of this seat was made, due to its similarity to the later utilised generic FEA seat.

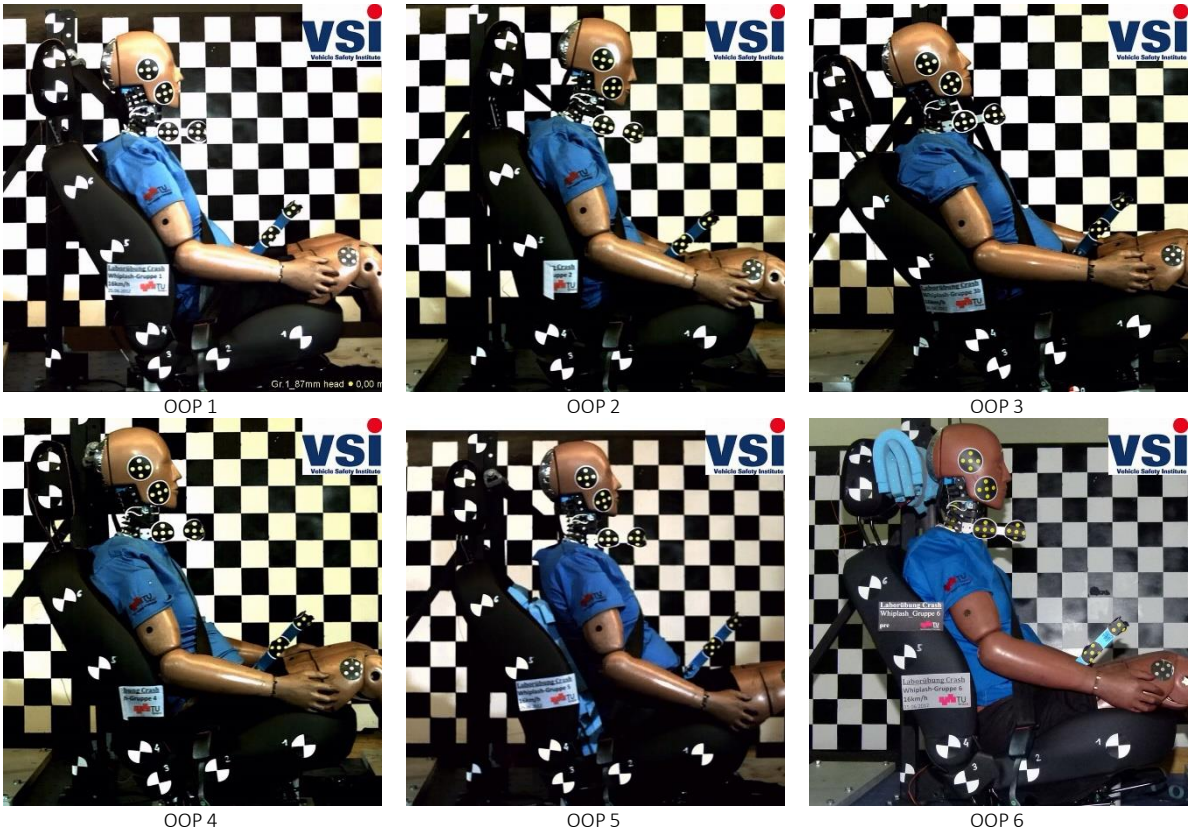


FIGURE 35 SETUP OF THE DIFFERENT OUT OF POSITION SCENARIO SLED TESTS.

This series was conducted to show, that different seat adjustment and different seated posture has a vast influence on neck loading for the occupant, and thus influences the risk sustaining WAD. Apparently some of these tests do not comply with the Euro NCAP assessment protocol or any other regulation or consumer test. Nevertheless, the seat adjustments and seated postures do reflect situations that can occur in everyday use of vehicles. These tests certainly are not of quantitative interest, but show which scenario can lead to what kind of extended loading.

- OOP 1 and OOP 4 were conducted as a basis for comparison. They represent the Euro NCAP medium severity pulse setup. Other Euro NCAP pulses were not used.
- OOP 2 represents a configuration with a steep backrest 10 ° forward from the Euro NCAP configuration, where the backrest is tilted forward about the recliner by 10 ° from the configuration required in the Euro NCAP protocol.
- OOP 3 represents just the opposite, 10 ° backward from the Euro NCAP configuration.
- OOP 5 represents a configuration where the occupant takes a seated posture with a large backset. In this case the increased backset was achieved by adding foam between the torso and backrest of the occupant model leading to a backset of approximately 170 [mm].
- OOP 6 on the other hand represents just the opposite of OOP 5, a seated posture, where the head of the occupant almost contacts the head restraint. The reduced backset was maintained by adding foam between the head restraint and the occupants back of the head.

All configurations are displayed in Figure 35. For this test instrumentation according to Table 22 was used. Additionally two high speed videos were recorded, one lateral overview and one lateral detail of the upper body.

### 3.1.2. Bio RID 50F Tests

Complementary to the sled tests described in chapter 3.1.1, additional tests, which do not comply with the Euro NCAP whiplash protocol were conducted within the ADSEAT project. The major difference here is, that the Bio RID II dummy was replaced with a modified version of this dummy. For these tests the same seat model (Seat A) as for the tests in chapter 3.1.1 was used.

FIGURE 36 OVERVIEW OF THE MODIFIED BIO RID 50F IN SEAT A

This so called Bio RID 50F (Carlsson, 2012c) was adapted to roughly meet the anthropometry, weight and weight distribution of a 50$^{th}$ percentile female occupant model (Figure 36). For this purpose, among other modifications, the spine was shortened, mass from arms, legs and head were removed and so on. Since no protocol for a female occupant exists, best practise was applied, and the posture of the female occupant model in the seat sought to comply in angles and positions of the Bio RID II if positioned for Euro NCAP tests.

Two lateral pictures of the test setups TUG11007 and TUG11008 can be found in Figure 37 and Figure 38.

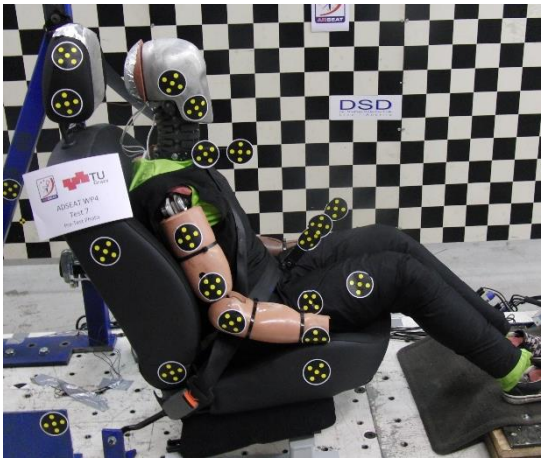


FIGURE 37 SETUP OF TEST NO. TUG11007 BIO RID 50F IN SEAT A


FIGURE 38 SETUP OF TEST NO. TUG11008 BIO RID 50F IN SEAT A

Additional tests with different seat models (Seat B through Seat D) were conducted in the course of the ADSEAT project (Schmitt, et al., 2012). For comparison reason, only Seat A is looked into further in this manuscript.

### 3.1.3. Tests with Post Mortem Human Subjects

The main objective of PMHS testing was to compare behaviour during rear-end collisions of male and female occupants at a change of velocity level, comparable to current rating tests. Since volunteer sled tests are limited due to the risk of injury, PMHS tests are a valuable tool for such investigations. Staged rear impact sled tests were performed using acceleration input corresponding to two different levels of injury risk. The acceleration level is considered important for the occurrence of whiplash injury. Head and neck vertebrae kinematics were monitored with high speed cineradiography. Pressure measurements in the spinal canal, head-neck accelerations, and vertebral displacements were determined for comparison.

A total of sixteen tests with four different subjects were conducted at the anatomy institute in Ljubljana. Two male and two female PMHS matching a 50$^{th}$ percentile male, respectively female, were tested.
Two different levels of acceleration, according to literature, were identified and used for cadaver testing. It was concluded that following parameters in the PMHS tests should be met:

- Mean acceleration 5 [g] and delta v of 16 [km/h] (comparable to IIWPG 16 triangular pulse)
- Mean acceleration 5.5 to 6 [g] and at least a delta v of 19 [km/h] (up to 25 [km/h])

For the medium level the triangular shaped IIWPG pulse (Figure 17) with a change of velocity of 16 [km/h] was used. For the high level the Euro NCAP trapezoid shaped SRA high severity pulse (Figure 18) with a delta v of 24 [km/h] was used. For each pulse and PMHS one test with and one test without a head restraint were performed. Hence, each PMHS was tested in four different configurations as listed in Table 34. After each test, forensic doctors examined the PMHS for traumata such as fractures or dislocations. Tests without head restraints were conducted in order to gather longer kinematic trajectories. The PMHS were maintained in their seated posture prior to T0 with supportive objects such as low density foams. Furthermore, the head and neck posture was secured with a belt system attached to an electromagnetic release, which was triggered 5 [ms] prior to T0.

| PMHS | Seat | Sex | Test no. | | Pulse | Comment |
|---|---|---|---|---|---|---|
| 1 | ECE-R16 | Female | 1 | 11 | Medium | w headrest |
| | | | 2 | 12 | Medium | w/o headrest |
| | | | 3 | 13 | High | w headrest |
| | | | 4 | 14 | High | w/o headrest |
| 2 | ECE-R16 | Male | 5 | 21 | Medium | w headrest |
| | | | 6 | 22 | Medium | w/o headrest |
| | | | 7 | 23 | High | w headrest |
| | | | 8 | 24 | High | w/o headrest |
| 3 | ECE-R16 | Male | 9 | 31 | Medium | w headrest |
| | | | 10 | 32 | High | w headrest |
| | | | 11 | 33 | Medium | w/o headrest |
| | | | 12 | 34 | High | w/o headrest |
| 4 | ECE-R16 | Female | 13 | 41 | Medium | w headrest |
| | | | 14 | 42 | High | w headrest |
| | | | 15 | 43 | Medium | w/o headrest |
| | | | 16 | 44 | High | w/o headrest |

TABLE 34 PMHS TEST CONDITIONS AND PARAMETERS

Two of the PMHS were chosen to be close to an average 50th percentile male occupant, the other two were approximately average 50th percentile female occupants. Data of the PMHS can be found in Table 35 and photographs can be found in Figure 39.

PMHS 1 PMHS 2 PMHS 3 PMHS 4

FIGURE 39 PMHS OVERVIEW PHOTOGRAPHS OF ALL SUBJECTS WITH HEAD RESTRAINT

| | | | | Subject ID | | | |
|---|---|---|---|---|---|---|---|
| | | | | 1 | 2 | 3 | 4 |
| | Gender | | | Female | Male | Male | Female |
| | Age | | [years] | 64 | 38 | 57 | 83 |
| | Body weight | | [kg] | 54 | 75 | 69 | 70 |
| | Body size | | [m] | 1.57 | 1.74 | 1.71 | 1.61 |
| 1 | Hat size | | [m] | 0.520 | 0.540 | 0.555 | 0.52 |
| 2 | Chin-occiput circumference | | [m] | 0.064 | 0.660 | 0.69 | 0.63 |
| 2a | Head height | | [m] | 0.205 | 0.235 | 0.215 | 0.22 |
| 2b | Head length | | [m] | 0.180 | 0.160 | 0.18 | 0.18 |
| 2c | Head breadth | | [m] | 0.153 | 0.190 | 0.17 | 0.16 |
| 3 | Neck circumference | | [m] | 0.380 | 0.325 | 0.405 | 0.44 |
| 4 | Upper arm | | [m] | NOVALUE | NOVALUE | 0.28 | 0.31 |
| 5 | Chest circumference | | [m] | 0.870 | 0.860 | 0.91.5 | 1.03 |
| 6 | Chest height | | [m] | NOVALUE | NOVALUE | 0.22 | 0.22 |
| 7 | Chest width | | [m] | 0.300 | 0.280 | 0.29 | 0.31 |
| 8 | Abdomen circumference | | [m] | 0.770 | 0.780 | 0.83 | 1.00 |
| 9 | Buttocks – Shoulder | | [m] | 0.580 | 0.710 | 0.64 | 0.58 |
| 10 | Seat height | | [m] | NOVALUE | NOVALUE | 0.87 | 0.84 |
| 11a | Pelvis – Knee | Right | [m] | 0.450 | 0.590 | 0.56 | 0.53 |
| 11b | Pelvis – Knee | Left | [m] | 0.450 | 0.590 | 0.57 | 0.53 |
| 12a | Sole of foot – Knee | Right | [m] | 0.475 | 0.520 | 0.52 | 0.44 |
| 12b | Sole of foot – Knee | Left | [m] | 0.475 | 0.520 | 0.52 | 0.44 |
| 13a | Pelvis – Heel | Right | [m] | 0.780 | 0.930 | 0.96 | 0.92 |
| 13b | Pelvis – Heel | Left | [m] | 0.780 | 0.930 | 0.96 | 0.92 |
| 14 | Sternum to Chin | | [m] | NOVALUE | NOVALUE | 0.105 | 0.08 |
| 15a | T1 to Inion (0°) | | [m] | NOVALUE | NOVALUE | 0.105 | 0.08 |
| 15b | T1 to Inion (flexion) | | [m] | NOVALUE | NOVALUE | NOVALUE | NOVALUE |
| 15c | T1 to Inion (extension) | | [m] | NOVALUE | NOVALUE | NOVALUE | NOVALUE |
| 16 | Hip circumference | | [m] | 0.870 | 0.970 | NOVALUE | NOVALUE |
| 17 | Shoulder width | | [m] | NOVALUE | NOVALUE | 40 | 36 |

TABLE 35 PMHS ANTHROPOMETRIC DATA OF THE TESTED PMHS

Anthropometry measures are taken according to Figure 40 and given in Table 35.

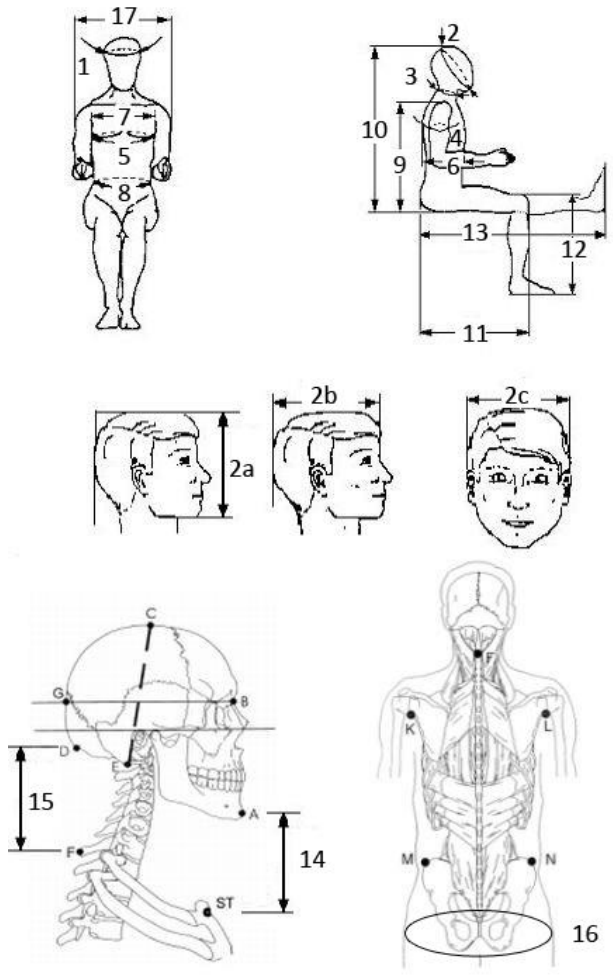


| | |
|---|---|
| 1 | Hat size |
| 2 | Chin-occiput circumference |
| 2a | Head height |
| 2b | Head length |
| 2c | Head breadth |
| 3 | Neck circumference |
| 4 | Upper arm |
| 5 | Chest circumference |
| 6 | Chest height |
| 7 | Chest width |
| 8 | Abdomen circumference |
| 9 | Buttocks - shoulder |
| 10 | Seated height |
| 11a | Pelvis - knee right |
| 11b | Pelvis - knee left |
| 12a | Sole of foot - knee right |
| 12b | Sole of foot - knee left |
| 13a | Pelvis - heel right |
| 13b | Pelvis - heel left |
| 14 | Sternum to chin (0°) (STA) |
| 15a | T1 to inion (0°) (DF) |
| 15b | T1 to inion (flexion) (DF) |
| 15c | T1 to inion (extension) (DF) |
| 16 | Hip circumference (MN) |
| 17 | Shoulder width |

FIGURE 40 PMHS ANTHROPOMETRIC MEASURES DEFINITION

The suggested anthropometry of a 50$^{th}$ percentile male and 50$^{th}$ percentile female can be found in Table 36.

| | Stature [cm] | Tolerance [cm] | Percent [%] | Min [cm] | Max [cm] |
|---|---|---|---|---|---|
| **Female** | 161.8 | ±4.0 | ±2.5 | 157.8 | 165.8 |
| **Male** | 175.3 | ±4.3 | ±2.5 | 171.0 | 179.6 |
| | **Weight** [kg] | **Tolerance** [kg] | **Percent** [%] | **Min** [kg] | **Max** [kg] |
| **Female** | 62.3 | ±5.0 | ±8.0 | 57.3 | 67.3 |
| **Male** | 77.3 | ±6.2 | ±8.0 | 71.1 | 83.5 |
| | **Sitting Height** [cm] | **Tolerance** [cm] | **Percent** [%] | **Min** [cm] | **Max** [cm] |
| **Female** | 84.4 | ±2.5 | ±3.0 | 81.9 | 86.9 |
| **Male** | 90.1 | ±2.7 | ±3.0 | 87.4 | 92.8 |

TABLE 36 PMHS SUGGESTED ANTHROPOMETRY FOR 50TH PERCENTILE MALE AND FEMALE SUBJECTS (YOUNG, ET AL., 1983)

For the projects purpose a high pressure air powered sled system was used capable to run ordinary whiplash pulses such as SRA 16 [km/h] (low severity pulse), SRA 24 [km/h] (high severity pulse) or

IIWPG 16 [km/h] (medium severity pulse). However, the system is also able to run real world rear-end accident pulses of arbitrary shape if necessary. The sled system uses an active online (closed loop) control of the acceleration pulse. Thus each pulse can be reproduced without calibration tests of predefined acceleration pulses. A quick change between different test pulses is possible even if they are completely different in acceleration or velocity. Furthermore no additional parts need to be replaced. The system can be completely controlled by a computer system. For the calculation of the required parameters, the payload needs to be estimated to run the test accurately. The testing device with its components is shown in Figure 44.

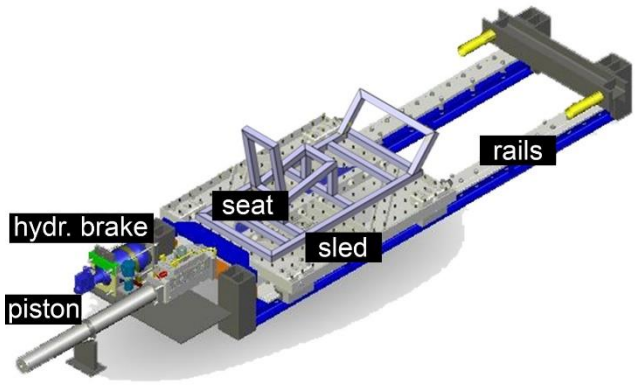


FIGURE 41 PMHS SLED TEST DEVICE CAD

The sled device was equipped with a rigid ECE-R16 seat (UNECE, 1995) to eliminate the influence of seat foam characteristics and maintain repeatable conditions. It was slightly modified so it could hold a head restraint in the corresponding tests. The head restraint used was a simple standard foam only height adjustable device. The head restraint, when present, was positioned, so that the top of the head restraint aligned with the top of the head of each PMHS. The distance between head and head restraint was set to 80 [mm] to 100 [mm]. A simple three-point safety belt system was added to secure the PMHS on the seat during the rebound phase.

Seat acceleration was measured with one uniaxial acceleration sensor (Vibration Sensor - Model 1201 Accelerometer, Measurement Specialties, USA) attached to the sled system.
The time interval and the moment of time of contact between head and head restraint were recorded for several tests. This was done by a special contact transducer that was attached to the surface of the head restraint and the back of the head.
Furthermore each vertebral body was marked with a screw. The screws were positioned directly into the bony material of the vertebral bodies on the front side of the neck in the mid sagittal plane. The positions for the markers were chosen, so that the screws describe the same motion as the vertebral bodies they were placed in. The ligamentum longitudinale anterius was punctured in this process. Damage to the ligaments was prevented as far as possible. These markers for vertebral bodies could be used as targets for a slightly modified target tracking.

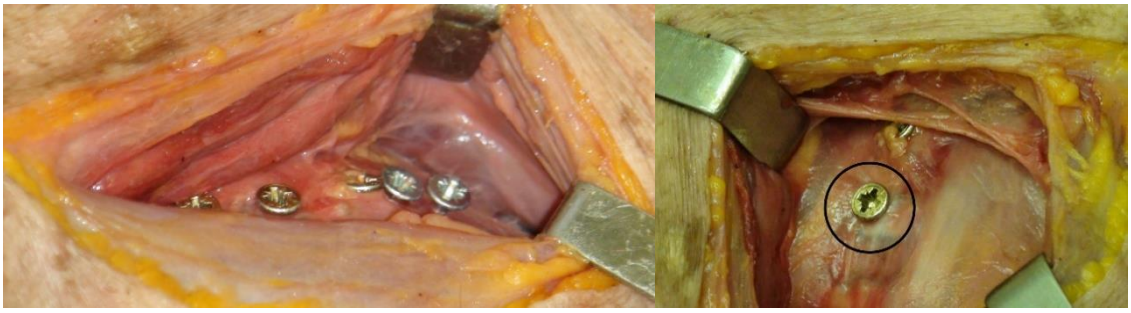

FIGURE 42 PMHS SCREWS MARKING SINGLE VERTEBRAL BODIES FOR CONTRAST ON X-RAY RADIOGRAPHY

PRESSURE TRANSDUCER AND HEAD ACCELERATION SENSOR

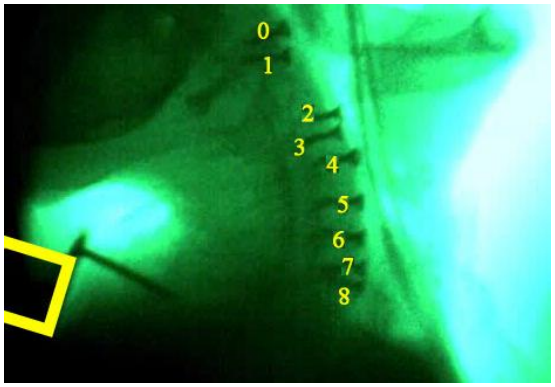


LATERAL X-RAY OF THE HEAD AND CERVICAL SPINE WITH ACCELERATION SENSOR AND PRESSURE TRANSDUCER

FIGURE 43 PMHS INSTRUMENTATION OF THE HEAD

Instrumentation furthermore included a tri-axial DSD 200 accelerometer mounted at the approximated x- and z-position of the centre of gravity of the head at the left side of the subject. The accelerometer was attached with screws directly into the skull to deliver accurate acceleration-measurements. Another tri-axial DSD 200 linear accelerometer was attached directly into the sternum. On the height of the first thoracic vertebra (T1), on the mid sagittal plane, one tri-axial DSD 200 accelerometer was attached directly to the vertebral body by inserting two screws into the arcus vertebrae.

For PMHS 1 and PMHS 2 three small pressure transducers were placed in the liquor space of the spinal canal. These measured pressure effects in the spinal canal during the typical whiplash motion. For PMHS 3 and PMHS 4 one combined pressure transducer (Sentron, OEM-625, Netherlands) for three measuring-positions (C2, C5 and C7) was used to gain this data.
The application of all measuring devices was performed by a forensic doctor.

Data was recorded using a data acquisition unit (DAU - Mini DAU K3700, KT Automotive, Germany) at a rate of 20 [kHz]. All acceleration sensors were [g] sensitive. Pressure was recorded in mbar.

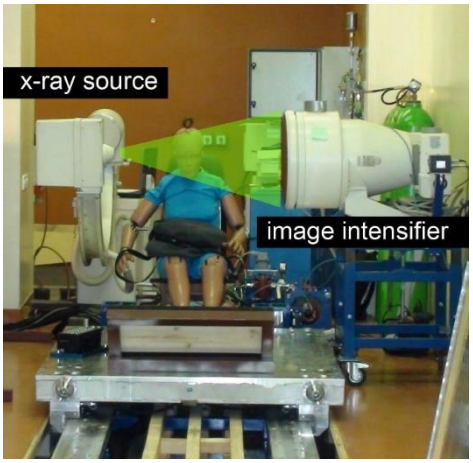


FIGURE 44 PMHS SETUP OF THE WHIPLASH SLED SYSTEM WITH X-RAY SOURCE AND IMAGE INTENSIFIER

High speed video footage was recorded at a frame rate of 1.000 [fps] recording a lateral overview and x-ray kinematics of the cervical vertebrae. The approximate setup and picture area of the x-ray system is exemplary demonstrated in Figure 44. T0 of sensor and film data was synchronized by a trigger via the sled system.

FIGURE 45 PMHS C-ARM X-RAY SYSTEM WITH IMAGE INTENSIFIER.

To record the bony kinematics of the cervical vertebrae, a commonly used, slightly modified, C-arch x-ray system (BV 25 Family-N/HR Philips, The Netherlands) was used. Additionally an alternative image-intensifier (SIRECON, Siemens, Germany) was adapted to receive the image produced by the x-ray-beam, in order to increase the picture-area to a reasonable size. The intensifiers diameter of approximately 400 [mm] allowed for a larger picture-area and displayed the entire neck-region during its whiplash motion.

The real time motion of the x-ray picture was recorded using a high speed camera system (SpeedCam MiniVis, Weinberger, Germany) at a frame rate of up to 1.000 frames per second. These devices are displayed in Figure 45
In Figure 46 pictures at different time steps of the high speed cineradiography show the motion of the PMHSs head and neck. The markers placed in each vertebra body of the spine from C1 to C7 allow motion and rotation tracking of each single vertebral body.

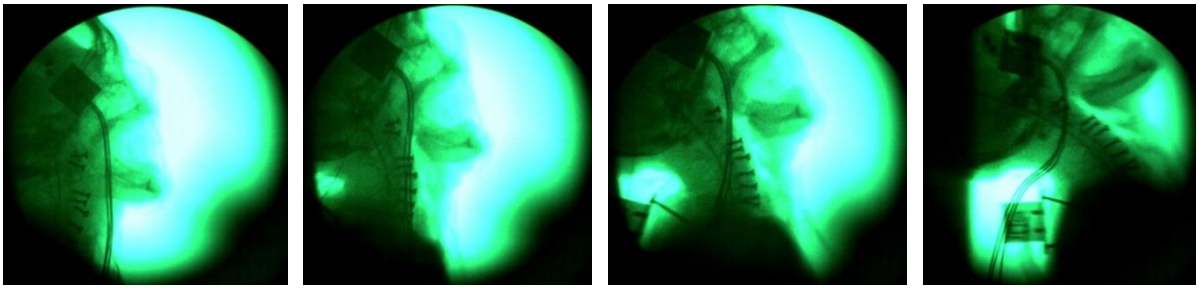

FIGURE 46 PMHS HIGH SPEED X-RAY VIDEO SEQUENCES DURING WHIPLASH

In addition to the high speed x-ray video, a high-speed overview video was recorded of each sled test. These videos deliver information about the motion of the head and body of the PMHS thus different phenomena, such as rotation and tilting of the head can be identified. Also incidents, like interference of accelerometers with the seat structure or seat belt components can be found in this footage. For kinematic analysis video-tracking targets were attached to the right side of the head, near the approximated c.o.g. as well as on the head restraint and the shoulder of the subject. A high speed video system (SpeedCam MacroVis, Weinberger, Germany) was used for this purpose. The frame rate was set to 1.000 [fps]. T0 for the data acquisition, the cineradiography and the high speed overview video were synchronized. All tests were conducted under approval of the responsible ethic committee of the republic of Slovenia (Reference Number 47 10.3.10).

## 3.2. Finite Element Analysis

Finite element analysis (FEA) was used for a broad study to show the influence of various factors on the whiplash injury risk. For Finite Element Methods (FEM) the proprietary FEM code LS-Dyna (Version 971 R5.1.1) was used. In these virtual investigations, a number of different simulation models were utilized. The occupant was represented by the:

- Bio RID II v2.5 dummy model (Schuster, et al., 2005),
  representing the 50$^{th}$ percentile male and the
- Eva RID development dummy model (ADSEAT-Eva RID Model LS-Dyna Release Version 1.0 August 2010 (Carlsson, et al., 2012b)
  Representing the 50$^{th}$ percentile female occupant.
- Hybrid III (LSTC H3 50$^{TH}$ FAST 111130 V2.0 (Guha, et al., 2011))
  Representing an alternative 50th percentile male.

Within the ADSEAT (Linder, 2011) project a female virtual occupant model named Eva RID was developed. Based on findings in ADSEAT (Linder, 2011), females meeting the 50$^{th}$ percentile anthropometry were identified to show the highest whiplash injury frequency. Thus the existing Bio RID II virtual dummy model was scaled and adapted to meet the characteristics of an average female occupant (Carlsson, et al., 2012b) (Carlsson, 2012c) (Chang, et al., 2010). This model could thus be utilized in this thesis to investigate the behaviour of female occupants in whiplash load cases for the first time.

The different seat models were represented by the

- Generic Car Seat provided by Faurecia[S]
- GUT Parametric Car Seat (Leimgruber, et al., 2014)[T]

Within all these simulations occupant comfort and feasibility of the geometric modification were not considered. This investigation is solely numerical and physical feasibility was not targeted.

As part of a sensitivity analysis the Faurecia Generic Car Seat Model (Figure 47, left) was used to demonstrate the influence of seat adjustments on the whiplash loading on occupants. The seat model was provided by Faurecia to selected partners of the ADSEAT consortium. According to the supplier material models and mechanical behaviour of this generic seat model are validated based on production seat models which are well comparable (Seat A).

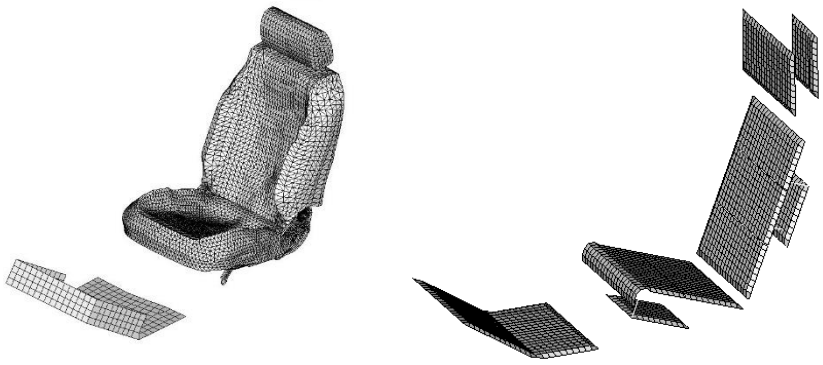

FAURECIA GENERIC SEAT MODEL GUT PARAMETRIC CAR SEAT

FIGURE 47 GENERIC FINITE ELEMENT SEAT MODELS

The GUT parametric car seat (Figure 47, right) was used for fast computable comparison simulations. All three dummy models, as in Figure 48 were analysed for comparison with this seat.

Also the influence of the anthropometric difference between an average male and an average female occupant was investigated by using two different virtual occupant models Bio RID II and Eva RID (Figure 48).

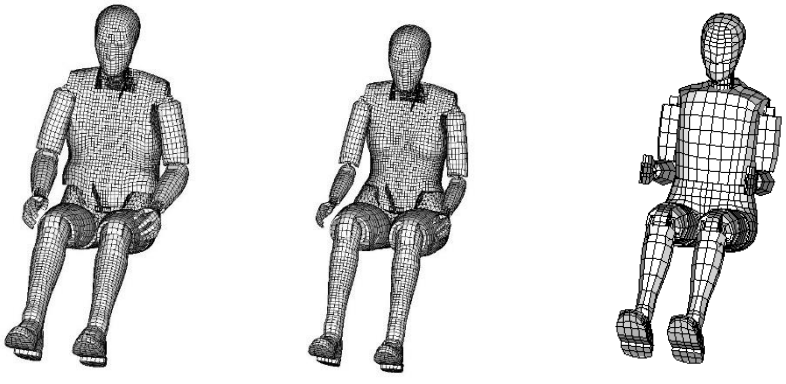

BIO RID II EVA RID HYBRID III

FIGURE 48 BIO RID II, EVA RID AND HYBRID III VIRTUAL OCCUPANT MODEL

[S] Faurecia Sièges D' Automobile SA, Route de Brières-les-Scellés, 91150 Étampes, France

[T] Graz University of Technology Parametric Car Seat

Regarding validation of the female occupant model Eva RID some restrictions have to be made. No physical dummy model representing this anthropometry is currently available. The kinematics of the Eva RID were compared with simulations of the Bio RID dummy model and volunteer tests. Eva RID was compared to low speed (delta v ~ 5 [km/h]) volunteer tests (Carlsson, et al., 2011), but no test at 16 [km/h] or even higher. The model responds plausible and kinematics seem realistic, however a state of the art validation against a physical dummy model was not possible. Data was logged and injury criteria were computed.

### 3.2.1. Euro NCAP Configurations

Since this generic seat model is not a production seat model no physical seat model of this design is available. This also leads to the absence of real test results for this specific seat. The model is however very similar to the seat model used in 3.1.1, which was selected due to this similarity. Nevertheless a series of three FEA baseline simulations was computed and analysed. In these simulations, the seat was configured as described in the Euro NCAP whiplash protocol. Also the three different loading pulses (SRA 16 [km/h], IIWPG 16 [km/h] and SRA 24 [km/h]) were applied. These simulations, particularly the simulation applying the IIWPG 16 [km/h] pulse, were used as baseline for further comparisons within the Finite Element Analyses.

| | | | Pulse | | |
|---|---|---|---|---|---|
| Occupant model | Backrest | Head Restraint | SRA 16 km/h | IIWPG 16 km/h | SRA 24 km/h |
| Bio RID II | Euro NCAP | Euro NCAP | L122 | M122 | H122 |

TABLE 37 NUMERICAL EURO NCAP COMPLIANT CONFIGURATIONS

### 3.2.2. Non Euro NCAP Configurations

To investigate the influence of different seat adjustments the generic seat model itself was modified. Adjustments were limited to the main adjustable components, which the majority of recent production car seats feature. Modifications where applied to the seat models backrest and head restraint as depicted in Figure 49. These modifications lead to initial situations differing from any regulation or consumer assessment (chapter 2.6) but reflect what was described as different postures in chapter 2.4.5.

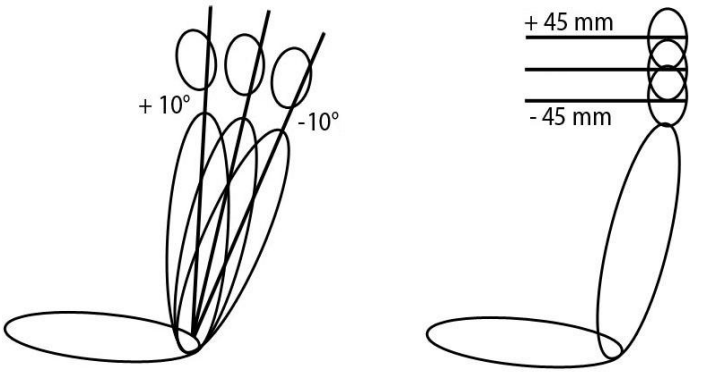


BACKREST ADJUSTMENT HEAD RESTRAINT ADJUSTMENTS

FIGURE 49 ADJUSTABLE COMPONENTS OF THE GENERIC SEAT MODEL AND CONFIGURATION

The different adjustments as shown in Figure 49 are numbered according to Table 38 to identify all different simulation setups as shown in Table 39.

| Digit | Parameter | Value | |
|---|---|---|---|
| 1 | Acceleration severity (Pulse) | L (low, SRA 16 km/h)<br>M (medium, IIWPG 16 km/h)<br>H (high, SRA 24 km/h) | |
| 2 | Gender (Occupant Model) | 1 (male, Bio RID)<br>2 (female, Eva RID) | |
| 3 | Backrest Position | 1 Forward<br>2 Centred<br>3 Backward | backrest +10° in Figure 49<br>backrest centred in Figure 49<br>backrest -10° in Figure 49 |
| 4 | Head Restraint Position | 1 High<br>2 Middle<br>3 Low | head restraint +45mm in Figure 49<br>head restrain middle in Figure 49<br>head restraint -45mm in Figure 49 |

TABLE 38 FEA SIMULATION NUMBERING SCHEME

The difference based on the fact that average male and average female occupants do have different anthropometric properties was considered by the use of two occupant models. The male occupant was represented by the Bio RID II occupant model where the female occupant was represented by the Eva RID development occupant model. The dummy models are displayed in Figure 48. For a broad base of data, all three acceleration pulses used in the Euro NCAP were considered. In Table 39 all configurations that were computed in this analysis with the before described adaptions and occupant models are explained.

| Occupant Model | Backrest Position | Head Restraint Position | Pulse | | |
|---|---|---|---|---|---|
| | | | SRA 16 km/h | IIWPG 16 km/h | SRA 24km/h |
| | | | Simulation ID | | |
| *Bio RID II* | Forward | High | L111 | M111 | H111 |
| | | Middle | L112 | M112 | H112 |
| | | Low | L113 | M113 | H113 |
| | Centred | High | L121 | M121 | H121 |
| | | Middle | L122 | M122 | H122 |
| | | Low | L123 | M123 | H123 |
| | Backward | High | L131 | M131 | H131 |
| | | Middle | L132 | M132 | H132 |
| | | Low | L133 | M133 | H133 |
| *Eva RID* | Forward | High | L211 | M211 | H211 |
| | | Middle | L212 | M212 | H212 |
| | | Low | L213 | M213 | H213 |
| | Centred | High | L221 | M221 | H221 |
| | | Middle | L222 | M222 | H222 |
| | | Low | L223 | M223 | H223 |
| | Backward | High | L231 | M231 | H231 |
| | | Middle | L232 | M232 | H232 |
| | | Low | L233 | M233 | H233 |

TABLE 39 NUMERICAL CONFIGURATIONS FOR SEAT COMPONENT SENSITIVITY ANALYSIS

### 3.2.3. Potential Analysis

Supplementary to the analysis within the range of the adjustable components of the generic seat model additional simulations with geometric modifications of the seat models were conducted. The purpose of these simulations was to show possibilities to improve future seat designs. Following, one configuration, as shown in Figure 50, will be looked at closer.

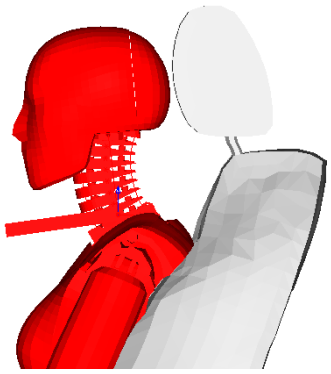

FIGURE 50 ADDITIONAL SIMULATION CONFIGURATION WITH A MODIFIED SEAT MODEL

The simulation was numbered M22X, referring to the same scheme as for all other FEA, the number represents a female occupant model (Eva RID) with a centred backrest and a “forward” positioned head restraint. For this configuration as shown in Figure 50, only the IIWG 16 [km/h] pulse was computed. Same data as in simulations described before were recorded and injury criteria computed.

### 3.2.4. Hybrid III

Supplementary, a small series of simulations utilising the virtual Hybrid III (H III) dummy model (LSTC.H3_50TH_FAST.111130_V2.0 (Guha, et al., 2011)) was conducted (Figure 51). The H III (Figure 48, right) is a frontal crash test dummy and thus was not intentionally developed for low speed rear impact crash tests. For simplicity reasons a reduced seat model (Figure 47, right) was used. For comparison additional simulations with the Bio RID II and Eva RID dummy models (Figure 48, left & middle) in the simplified seat model (Leimgruber, et al., 2014) were conducted.

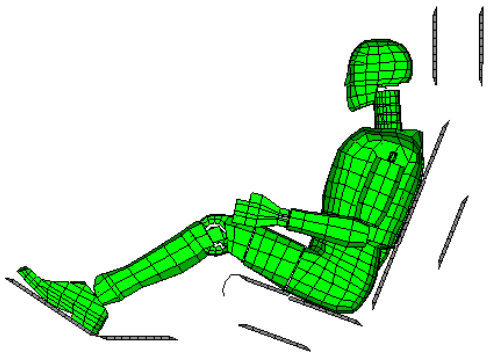

FIGURE 51 HYBRID III 50TH PERCENTILE CRASH TEST DUMMY IN GUT PARAMETRIC CAR SEAT MODEL

The simulations were performed under the load of the IIWPG 16 [km/h] pulse as described in Figure 17. For comparison head and T1 acceleration were analysed and the NIC criterion calculated. Comparisons between the Bio RID II and H III (Kim, et al., 2005) in real seat tests show deviations for the different dummy models. The availability of the Eva RID dummy model allows the introduction and comparison of another additional occupant model.

## 3.3. Assessment – Neck Value

To compare different configurations of one seat the Neck Value (NV) method was developed.

The NV was introduced to compare whiplash assessments of one seat at different loading scenarios. Different loading scenarios are explained as different occupant models, different configurations of adjustable components of a seat as well as different initial loading pulses as already described. Baseline for comparison in any case, is the Euro NCAP accordant configuration, applied with the medium severity pulse (IIWPG 16 [km/h]). Thus, when comparing the NV of different test setups, the robustness of one particular seat can be evaluated, for different loading scenarios. The NV takes into account well established Injury criteria which are used for whiplash assessment in current regulations and consumer ratings (Gutsche, et al., 2013).

This approach was used, and is intended, mainly for virtual investigations, due to the lack of test data for configurations other than consumer test like configurations. It can however be applied to real test data if available.

### 3.3.1. Included Values

Based on the available data from previously described FEA, several injury criteria, as listed in Table 40, were computed and used for comparison. Since the goal of this task was to compare different configurations of one seat, not rate this seat according to the Euro NCAP protocol, all criteria mentioned in Table 40 were summarised and normalised.

INJURY CRITERIA

| *Abbreviation* | Description | Criterion Number | Normalised Criterion. | Weighting | Unit |
|---|---|---|---|---|---|
| *NIC* | Neck Injury Criterion | $C_1$ | $c_1$ | $w_1$ | (-) |
| *Nkm* | Neck criteria $N_{fa}$, $N_{ea}$, $N_{fp}$, $N_{ep}$ | $C_2$ | $c_2$ | $w_2$ | (-) |
| *Fx upper neck* | Tension Force upper neck | $C_3$ | $c_3$ | $w_3$ | (N) |
| *Fz upper neck* | Shear Force upper neck | $C_4$ | $c_4$ | $w_4$ | (N) |
| *T1 acc* | Acceleration of T1 vertebral body | $C_5$ | $c_5$ | $w_5$ | (g) |
| *T-HRC* | Time until head to head restraint contact | $C_6$ | $c_6$ | $w_6$ | (ms) |
| *My OC Flex* | Flexion bending moment at occiput | $C_7$ | $c_7$ | $w_7$ | (Nm) |
| *My OC Ext* | Extension bending moment at occiput | $C_8$ | $c_8$ | $w_8$ | (Nm) |
| *Nij* | Normalised neck injury criterion | $C_9$ | $c_9$ | $w_9$ | (-) |

$N_{fa}$ flexion anterior, $N_{ea}$ extension anterior

$N_{fp}$ flexion posterior, $N_{ep}$ extension posterior

TABLE 40 NV RELEVANT INJURY CRITERIA

### 3.3.2. Normalisation

The baseline for normalisation is the result gathered from the configuration according to the Euro NCAP Whiplash testing protocol (Euro NCAP, 2014) using the IIWPG 16 [km/h] pulse. The normalised criterion was compared with the corresponding criterion of the simulation according to Euro NCAP (centred backrest, middle head restraint height) under the load of the IIWPG 16 [km/h] pulse equipped with the male occupant model as in the following equation:

**Equation 15 NV – calculation of normalized injury criterion**

$$c_{i(p,s,b,h)} = \frac{C_{i(p,s,b,h)}}{C_{i(M,1,2,2)}}$$

| *Variable* | Explanation |
|---|---|
| $c_{i(p,s,b,h)}$ | normalised neck injury criterion listed in Table 40 dependent on |
| $p$ | pulse used which can be L (SRA 16km/h), M (IIWPG 16km/h) or H (SRA 24 km/h) |
| $s$ | the gender of the occupant model which can be 1 (male) or 2 (female) |
| $b$ | the setting of the backrest which can be 1 (forward),2 (centred) or 3 (backward) |
| $h$ | the setting of the head restraint which can be 1 (High), 2 (Middle) or 3 (Low) |
| $C_{i(p,s,b,h)}$ | the corresponding neck injury criterion dependent on the above parameters and |
| $C_{i(M,1,2,2)}$ | the corresponding neck injury criterion from the simulation according to Table 40 with the IIWPG 16 km/h pulse and the male occupant model (Bio RID II) |

TABLE 41 NV ELEMENTS USED IN NORMALISATION

For example, the normalised NIC of the load case low severity pulse (SRA16 [km/h]), the female occupant model, with the backrest in its backward position and the head restraint at the highest possible setting (L231) is $c_{1(L231)} = \frac{C_{1(L,2,3,1)}}{C_{1(M,1,2,2)}}$ (-).

The weighting and summarisation of the normalised neck injury criteria $c_i$ leading to the normalised and weighted value (*NV*) were conducted in accordance with the following equation:

**Equation 16 NV – calculation of NV**

$$NV = \frac{\sum_{i=1}^{n} c_i \cdot w_i}{\sum_{i=1}^{n} w_i}$$

| *Variable* | Explanation |
|---|---|
| $NV$ | the normalised and weighted value (-) |
| $C_i$ | each of the normalised neck injury criteria listed in Table 40 |
| $W_i$ | the corresponding weighting factor (-) listed in Table 40 |

TABLE 42 NV ELEMENTS USED IN CALCULATION OF NECK VALUE NV

The weighting factors w1 through w9 were set to one (unity) for this first investigation. Future weighting can be adapted to represent the relevance of the included injury criteria with respect to their relevance regarding injury risk.

In this rating a value of $NV_{(p,s,b,h)} = 1$ represents the corresponding seat configuration with its occupant model and pulse performing equally well compared to the configuration with the head restraint in its middle position, the backrest centred, the IIWPG 16 [km/h] pulse and the male occupant model (Bio RID II). A value lower than one (unity) indicates that the occupant has to cope with lower loads, and a value higher than one that the occupant has to sustain higher loads than in the configuration according to (Euro NCAP, 2013) and the IIWPG 16 [km/h] pulse.

### 3.3.3. Graphical Interpretation

Figure 52 shows a graph in which all possible seat adjustment configurations are displayed. These notional results were chosen in order to explain the graph. For each pulse and occupant model, every configuration result can be displayed in this graph.

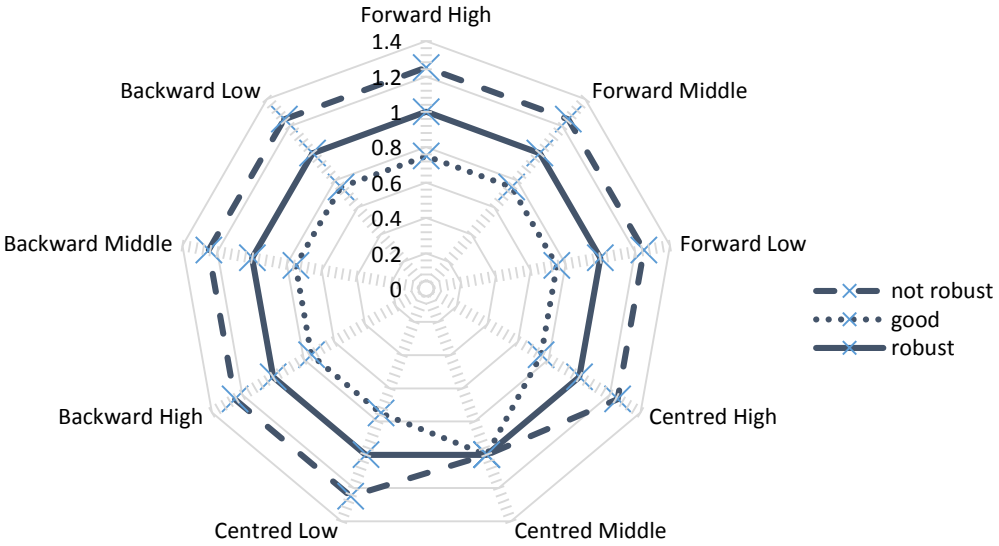


FIGURE 52 NECK VALUE GRAPHICAL INTERPRETATION OF LARGE NUMBERS OF SEAT CONFIGURATIONS

Since the *NV* values are normalised the configurations according to the Euro NCAP protocol (centred, middle) show a value of one (unity). The three lines in Figure 52 are examples of the possible outcome of such an investigation. One line represents one occupant model under the loading of one specific

pulse. The solid line, for example, represents a car seat which for one occupant delivers the same loading level in all possible seat adjustment configurations when exposed to the same pulse (robust).

The dashed line (not robust) shows that the performance is about 25 % worse in all configurations than in the Euro NCAP configuration (centred, middle). The dotted line (good) shows the result for a seat performing 25 % better in all configurations than the Euro NCAP configuration (centred, middle). The ultimate aim is to develop a seat for which all *NV* values are lower than one (unity) whereby the graph would be surrounded by the solid line (robust) in Figure 52. This graph is limited to two adjustable components in a maximum of three adjustment positions. For more adjustable components and adjustment positions, additional axis can be added to the graph.

# 4. Results Experimental Testing

## 4.1. Bio RID II Tests accordant and not accordant to Euro NCAP

A series of six dynamic whiplash tests was conducted. These tests, not according to any consumer rating or regulation, had the aim to highlight the major influence of seat component adjustment, which can be influenced by the occupant, on the loading and risk on the occupant seated. For this purpose two tests were set up according to the Euro NCAP protocol. Backrest and head restraint were adjusted to the protocol. The dummy was positioned using an H-point mannequin. These tests (OOP 1 and OOP 4) were supposed to serve as reference. All other tests were set up significantly different from the protocols requested adjustments as already described in chapter 3.1.1. The general results are presented in the following chapter.

Figure 53 OOP Setup of the OOP 1 test configuration, reference according to the Euro NCAP protocol

Figure 54 OOP Setup of the OOP 2 test configuration, 10 ° forward tilted backrest.

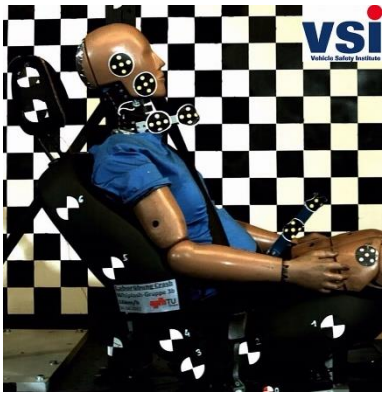

Figure 55 OOP Setup of the OOP 3 test configuration, 10 ° backward tilted backrest

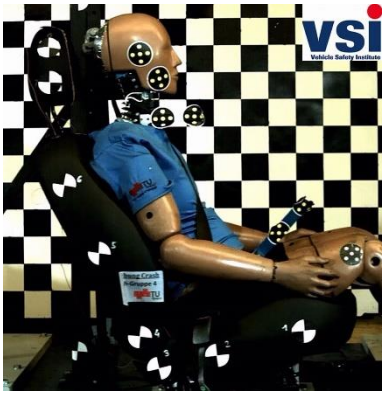

Figure 56 OOP Setup of the OOP 4 test configuration, reference according to the Euro NCAP protocol

Figure 57 OOP Setup of the OOP 5 test configuration, extended backset of 170 mm

Figure 58 OOP Setup of the OOP 6 test configuration, reduced backset of 0 mm

Data acquisition during test OOP1 was faulty. Data seems to be from a wrong period of time (trigger problem). A High speed video was recorded. According to the high speed video, head contact start time THRC start was at approximately 69 [ms]. The end of the head to head restraint contact at approximately 152 [ms]. The maximum deflection of the backrest was recorded at around 106 [ms]. Obvious in this test is the tendency of the Bio RID dummy to slip up on the backrest like on a ramp.

The initial position of test OOP2 appears “unnatural”. The dummy seems to be in a forward bent position, also the head is not oriented at 0 ° at T=0 [ms]. The backset in this scenario, unlike the forward tilted backrest might suggest, is not reduced compared to OOP 1 or OOP 4. In contrary it is of equal distance, or even slightly larger, since the dummy is bent forward. Naturally due to the steeper backrest, the upward sliding of the dummy is not as distinct as in OOP 1 or OOP 4. The torso transfers a lot of energy to the backrest maintaining a certain distance between head and head restraint for approximately 90 [ms] where a steep rise of the head acceleration can be found (Appendix 7 ). The torso comes to a rest in rearward translation at around 80 [ms] with a gap of about 50 [mm] between head and head restraint remaining. The closing of this gap is achieved by bending (extension) of the neck only. The seat in this configuration appears to behave rather stiff.

In configuration OOP3, the occupant at T=0 [ms] is positioned in a leaning backward sort of position. The head at this time is not levelled with the horizon, just like in OOP 2, but in the opposite direction. This leads to a gap between head restraint and head which is not significantly different to the scenarios of OOP 1 and OOP 4. The slope like backrest however leads to a significant amount of sliding upwards of the dummy. Furthermore, the torso bends back the backrest even further leading to a rather late head to head restraint contact at around 92 [ms]. The seat back and head restraint furthermore shows a significant amount of oscillation which is very nicely reflected in the graph of the T1 acceleration in Appendix 13 . The rebound of this test shows a significantly longer duration, due to the large angle which the dummy can move before being caught by the belt. However, the loading during the rebound is rather low.

The OOP4 scenario, representing the same situation as OOP1 shows a T-HRC start of 65 [ms], which is similar in OOP1. The end of the head to head restraint contact is at 174 [ms]. The dummy slides up the backrest at the beginning of the pulse, before head to head restraint contact is reached.

Comparisons with the Euro NCAP setup are thus made with configuration OOP4.

Data acquisition was faulty during test OOP5 but limited data is available. The setup obviously leads to a very large backset. At T=0 [ms] the backset is about 170 [mm]. The dummy starts to push the foam support of the torso at the beginning of the pulse until about 80 [ms] without any significant relative motion between the torso and the head. At 80 [ms] the head to head restraint distance is reduced to approximately 40 [mm]. Head to head restraint contact is made at 91 [ms], which is almost capping limit in the Euro NCAP medium severity dynamic assessment.

The setup OOP6 with reduced backset would cause comfort issues in production vehicles. However the THRC start of 40 [ms] is believed to be of benefit for the occupant. The end of the head to head restraint contact is not much different from other scenarios at 177 [ms]. Also the dynamic response and maximum deflection of the backrest do not differ much.

The series of sled tests conducted to distinguish the differences between several seat component adjustments is concluded in the following. The main data to compare the different configurations can be found in Table 43. The configuration OOP1 must be excluded due to malfunctioning data acquisition.

| | Setting | 0 | Head ACC X | Upper Neck Fx | Upper Neck Fz | Upper Neck My | Sled ACC | T1 ACC | Torso ACC (L1) | NIC |
|---|---|---|---|---|---|---|---|---|---|---|
| | | unit | (g) | (N) | (N) | (Nm) | (g) | (g) | (g) | ($m^2/s^2$) |
| OOP1 | 25° | max | 0.06 | 2.13 | 14.85 | 0.48 | 0.00 | 0.00 | 0.18 | 0.33 |
| | | min | -0.17 | -6.17 | -10.84 | -0.46 | 0.00 | 0.00 | -0.35 | -0.11 |
| OOP2 | 15° | max | 27.21 | 189.74 | 437.23 | 6.15 | 9.58 | 10.94 | 12.52 | 14.54 |
| | | min | -5.42 | -101.42 | -114.05 | -11.20 | -0.49 | -1.67 | -3.23 | -44.24 |
| OOP3 | 35° | max | 21.79 | 131.06 | 768.84 | 10.52 | 9.42 | 9.41 | 10.47 | 14.96 |
| | | min | -1.22 | -57.89 | -17.58 | -5.34 | -0.44 | -1.25 | -2.78 | -37.19 |
| OOP4 | 25° | max | 20.05 | 140.42 | 477.76 | 5.50 | 9.46 | 9.61 | 12.43 | 15.63 |
| | | min | -0.96 | -39.05 | -65.64 | -6.86 | -0.51 | -0.20 | -2.28 | -32.75 |
| OOP5 | 170 mm | max | 21.42 | 42.09 | 485.12 | 13.94 | 9.39 | 15.52 | 0.00 | 13.56 |
| | | min | -1.13 | -61.47 | -49.98 | -6.26 | -0.56 | -2.02 | 0.00 | -20.33 |
| OOP6 | 0 mm | max | 16.24 | 16.66 | 349.12 | 4.32 | 9.39 | 12.16 | 13.05 | 18.19 |
| | | min | -2.01 | -86.48 | -13.50 | -3.05 | -0.56 | -1.05 | -1.97 | -19.35 |

TABLE 43 NON EURO NCAP TEST RESULTS OVERVIEW

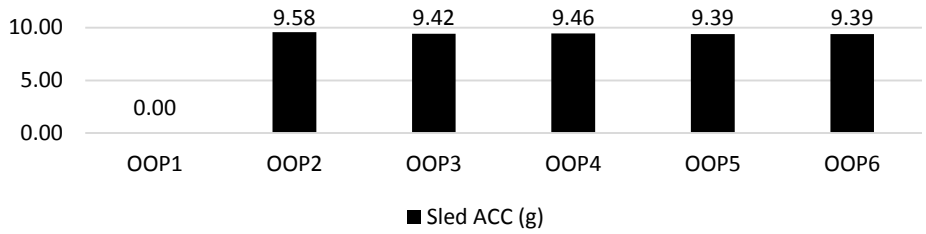


FIGURE 59 OOP COMPARISON OF SLED ACCELERATION MAXIMA

Even though, a simple multi-level bending brake sled system was used for this series of tests, the sled acceleration comparison shows little deviation. The loading level on the sled was very uniformly. Maximum acceleration of the pulse was from 9.39 [g] to 9.58 [g], thus comparable tests were conducted.

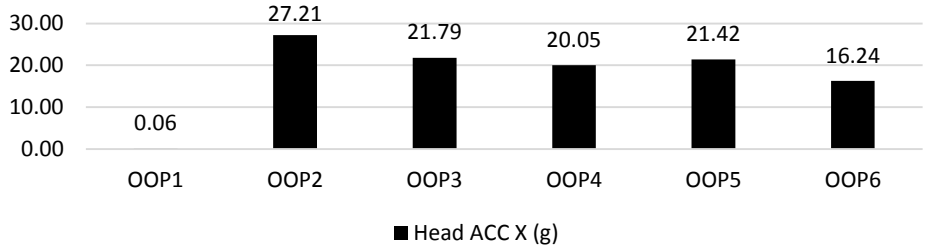


FIGURE 60 OOP COMPARISON OF HEAD X ACCELERATION MAXIMA

Maximum head acceleration displayed in Figure 60 of configuration OOP2, despite other expectations, with a steeper backrest is the highest occurring value. Where in OOP6, with a significantly reduced backset, head acceleration is the minimum in this series of test. Also surprisingly, the extended backset of OOP5 with more than two times the distance between head restraint and head does not lead to a significant increase of the head acceleration.

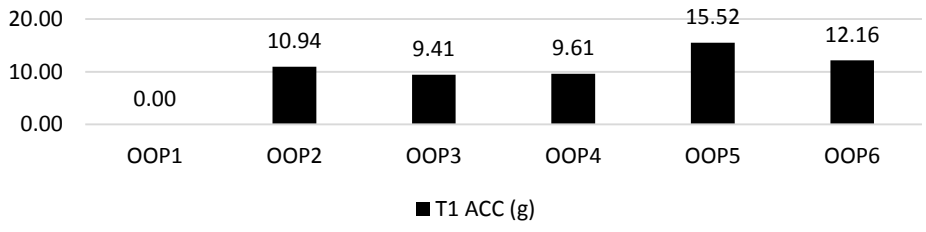


FIGURE 61 OOP COMPARISON OF T1 X ACCELERATION MAXIMA

T1 acceleration was highest in the OOP5 configuration which is the configuration with extended backset. This value is just below the current capping limit of the Euro NCAP. Surprisingly the T1 acceleration of the OOP3 configuration is the lowest measured value almost reaching the higher performance limit of the Euro NCAP assessment.

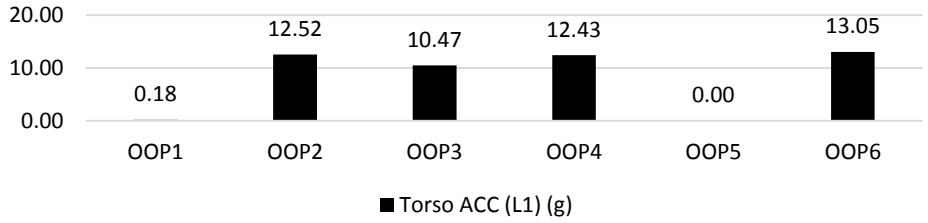


FIGURE 62 OOP COMPARISON OF L1 X ACCELERATION MAXIMA

L1 X acceleration was chosen to represent the thoracic acceleration level of the dummy. The acceleration is not assessed in any protocol or regulation. The values draw a similar picture as the T1 acceleration. They also indicate, that this particular seat does have a soft centre of the backrest, which leads to an increase of acceleration compared to the sled acceleration level. The L1 acceleration is, even if not utilised in any assessment, a valuable set of data for comparison with virtual simulations to validate simulation models of virtual seat models. For OOP5 this value was not recorded.

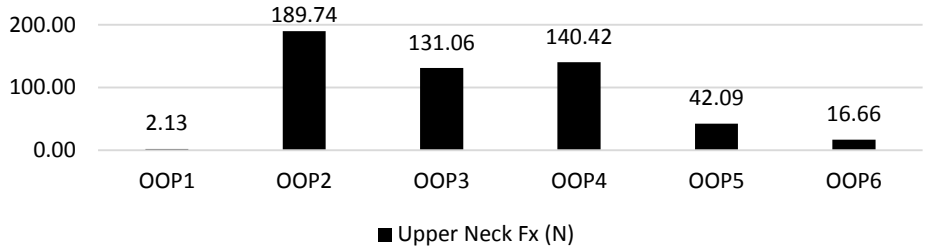


FIGURE 63 OOP COMPARISON OF UPPER NECK SHEAR FORCE (FX) MAXIMA

The upper neck shear force shows a minimum value for OOP6 and a maximum for OOP2. All values are between upper and lower performance limits of the Euro NCAP except for 16.66 [N] for OOP6. This value is extraordinarily low and was not expected in this configuration.

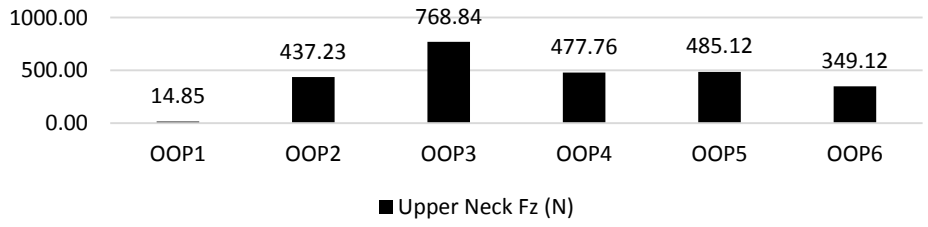


FIGURE 64 OOP COMPARISON OF UPPER NECK TENSION FORCE (FZ) MAXIMA

Tension in the upper neck shows again the lowest value for the OOP6 scenario. The difference to the other configurations is not as significant as for shear, but still was not expected. Compared to the higher performance limit of 360 [N] this is again a very good result. OOP3 with the highest value measured is just outside the border of lower performance.

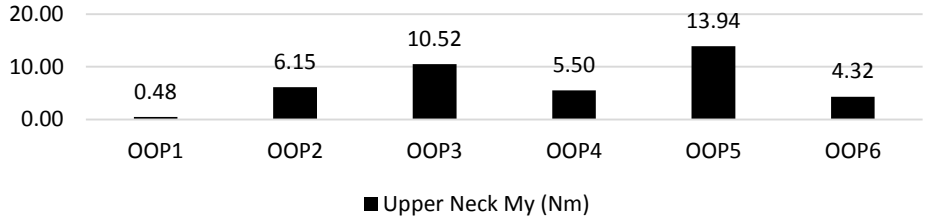


FIGURE 65 OOP COMPARISON OF UPPER NECK MOMENT ABOUT Y (MY) MAXIMA

The configuration OOP6 also shows the lowest value for My. The difference to OOP4 and OOP2 are not that significant, and these three configurations are better than required for higher performance in the Euro NCAP assessment (9.3 Nm).

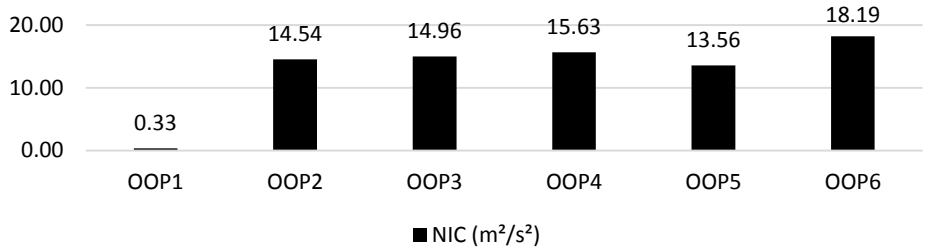


FIGURE 66 OOP COMPARISON OF NORMALISED NECK INJURY CRITERION (NIC) MAXIMA

Surprisingly, the NIC value for the OOP6 configuration is the highest value calculated. OOP5 which showed the highest moment My and T1 x-acceleration scores best in this assessment. Neither of the configurations however reaches higher performance values (11.00 [m²/s²]) but are all safe within the lower performance limit (24 [m²/s²]) of the Euro NCAP assessment.

In this comparison, the configuration OOP6 shows lowest values for forces, moment and head acceleration, and is not out of scope regarding T1 acceleration. Still the result for the NIC criterion is the highest among this series of tests. The configuration OOP5 with an enormous backset which would disqualify this configuration for dynamic testing in the Euro NCAP assessment, scores best for the NIC criterion.

OOP2, OOP3 and OOP4 show, that adjustability which can be influenced by consumers can have quite a large influence on the protection capability of a vehicle seat. The steeper seatback in configuration OOP2 causes a higher head acceleration and higher shear force than all other configurations. Also T1 acceleration is higher than in OOP3 and OOP4. Contrary, this configuration shows the lowest NIC value and the lowest tension force among the consumer influenceable configurations OOP2, OOP3 and OOP4. These results show, that improvement for one criterion does not imply general improvement for all criteria.

This is best shown when analysing OOP6. No doubt, this configuration is unlikely, but it achieves the lowest tension and shear force and moreover the lowest bending moment and lowest head acceleration. Nevertheless, its NIC value is the highest among all configurations. The head acceleration of OOP6 sticks out in all these tests. It shows a very early (40 [ms]) steep rise to about 4 [g], residing there for about 35 [ms] followed by a gentle rise to its maximum value. All other tests show a steeper acceleration increase at later times (80 [ms] – 100 [ms]).

The question at stake here is, which criterion should be addressed? Is it important to keep forces and moments low, or is relative acceleration and motion (head to torso) more critical? Limiting to this series of tests is the application of the Bio RID II dummy for scenarios it is not intended for. Furthermore, the configuration OOP5 is not achievable with a standard vehicle seat. It represents a worst case scenario which should not be sought in vehicle seat designs. Surprisingly the loads on the occupant model do not reflect the expected unfavourable performance. OOP6 with literally no backset was expected to outperform all other configurations. This is also confirmed for all criteria except the NIC value, which indicates just the opposite. The head restraint configuration in OOP6 however is considered to be not acceptable due to comfort reasons. Configurations such as OOP2 and OOP3 with altered backrest angles are very likely to be used by many consumers.

The influence of different backrest angles can be explained using different measurements. First of all, the steeper backrest in OOP2 reduces the ramping effect. This leads to a reduced upward motion of the Bio RID II dummy on the seat. Reduction of this ramping is believed to reduce the axial forces applied to the neck, which OOP2 shows compared to OOP3. On the other hand, this behaviour leads to an increase of the shear force for OOP2. Due to the earlier force transmitting contact between the torso and backrest, the T1 acceleration rises about 10 [ms] earlier for OOP2 than OOP4. OOP3 shows a later increase of T1 acceleration. This also has a direct influence on the NIC curve progression.

## 4.2. Bio RID 50F Tests

The two independent Bio RID 50F test showed very good repeatability. The Bio RID 50F female dummy prototype appeared to work very well. All mechanical components and also data acquisition performed as expected.

| | Setting | 0 | Head ACC X | Upper Neck Fx | Upper Neck Fz | Upper Neck My | Sled ACC | T1 ACC | Torso ACC (L1) | NIC |
|---|---|---|---|---|---|---|---|---|---|---|
| | | unit | (g) | (N) | (N) | (Nm) | (g) | (g) | (g) | ($m^2/s^2$) |
| TUG11007 | Euro NCAP | max | 24.52 | 0.33 | 0.28 | 13.77 | 10.30 | 16.83 | NV | 12.68 |
| | | min | -0.97 | -0.09 | -0.15 | -4.80 | -6.05 | -1.30 | NV | -22.04 |
| TUG11008 | Euro NCAP | max | 21.49 | 0.35 | 0.31 | 11.97 | 10.69 | 17.96 | NV | 12.35 |
| | | min | -1.02 | -0.07 | -0.14 | -3.71 | -6.93 | -1.29 | NV | -18.00 |

TABLE 44 BIO RID 50F EURO NCAP LIKE TEST RESULTS OVERVIEW

Besides the overview of maximum and minimum values for the two tests utilizing the Seat A model, complementary graphs for the main values of interest ( T1 x-acceleration, head x- acceleration, upper neck tension and shear force, upper neck extension and flexion moment, NIC injury criterion) can be found in chapter A.2.

## 4.3. Tests with Post Mortem Human Subject

Subsequently a resume of the results found during the PMHS tests is given.
In the following Table 45 the maxima and minima of the different loadings measured and criteria computed can be found. Values with grey background are faulty measurements which are not considered in the comparison. Furthermore the basic results of all PMHS are concentrated for a general overview.

In addition, for each test, three detailed diagrams and a data overview table can be found in Appendix A.3. The first diagram gives an impression about the acceleration levels on characteristic positions, which are also recorded in consumer tests. It must be mentioned, that due to the acceleration sensor application on the PMHS, for head, T1 vertebral body and sternum acceleration, the resultant acceleration is representative.
The second diagram shows the pressure gradients in the spinal canal at the approximate height of the C2, C5 and C7 vertebral body respectively.
The third diagram displays the neck injury criterion NIC, which analyses the relative movement between Head and T1 based on their acceleration.
For each test, a table with minimum and maximum of all these values within 200 [ms] is prepared. This does not comply with the general requirements for some of the criteria in consumer tests, such as the Euro NCAP, but still gives an overview of the limits within which these criteria reside.

| | | | | | mbar | mbar | mbar | g | g | g | g | m²/s² |
|---|---|---|---|---|---|---|---|---|---|---|---|---|
| | | | | | C2_CFC60 | C5_CFC60 | C7_CFC60 | SLED_CFC60 | HEAD_RES_CFC180 | T1_RES_CFC180 | STR_RES_CFC180 | NIC |
| FEMALE 1 | HR# | IIWPG | 1_1 | max | 55.88 | -10268 | 376.94 | 10.11 | 21.39 | 12.71 | 15.94 | 11.69 |
| | | | | min | -34.69 | -10268 | -55.99 | -7.57 | 0.59 | 0.56 | 0.20 | -25.17 |
| | NHR+ | IIWPG | 1_2 | max | 115.24 | -9244 | 480.53 | 10.06 | 9.09 | 18.52 | 16.49 | 24.91 |
| | | | | min | -48.04 | -10291 | -128.75 | -8.94 | 0.16 | 0.07 | 0.21 | -9.48 |
| | HR | SRA | 1_3 | max | 180.66 | -9258 | 533.95 | 8.24 | 24.03 | 20.51 | 18.52 | 16.77 |
| | | | | min | -121.11 | -10282 | -533.57 | -9.32 | 0.04 | 0.06 | 0.14 | -27.99 |
| | NHR | SRA | 1_4 | max | 158.07 | 489.23 | 483.07 | 10.20 | 12.81 | 26.41 | 28.11 | 36.12 |
| | | | | min | -43.55 | -521.14 | -200.64 | -10.08 | 0.41 | 0.06 | 0.16 | -13.80 |
| MALE 1 | HR | IIWPG | 2_1 | max | 6.67 | 559.14 | 329.45 | 10.45 | 16.97 | 9.40 | 12.12 | 16.33 |
| | | | | min | -2.57 | -507.18 | -514.75 | -7.33 | 0.06 | 0.15 | 0.08 | -27.69 |
| | NHR | IIWPG | 2_2 | max | 10.19 | 506.60 | 487.01 | 10.06 | 20.21 | 48.02 | 13.18 | 85.17 |
| | | | | min | -1.42 | 506.60 | -271.32 | -9.46 | 0.04 | 0.09 | 0.09 | -36.22 |
| | HR | SRA | 2_3 | max | 10.02 | -9267 | 71.16 | 9.91 | 26.47 | 17.26 | 14.14 | 21.32 |
| | | | | min | -4.32 | -9267 | -517.27 | -10.39 | 0.06 | 0.10 | 0.06 | -39.62 |
| | NHR | SRA | 2_4 | max | 14.12 | 514.19 | 505.64 | 8.02 | 23.47 | 64.34 | 13.30 | 109.35 |
| | | | | min | -4.89 | -339.40 | -147.64 | -10.64 | 0.31 | 0.24 | 0.16 | -36.70 |
| MALE 2 | HR | IIWPG | 3_1 | max | 97.14 | 104.92 | 187.32 | 9.59 | 25.41 | 27.69 | 10.99 | 50.45 |
| | | | | min | -92.73 | -123.70 | -113.03 | -8.90 | 0.19 | 0.05 | 0.04 | -30.98 |
| | HR | SRA | 3_2 | max | 146.53 | 149.85 | 200.66 | 8.04 | 31.64 | 33.35 | 20.01 | 61.96 |
| | | | | min | -122.36 | -122.16 | -150.25 | -9.91 | 0.22 | 0.06 | 0.07 | -28.54 |
| | NHR | IIWPG | 3_3 | max | 100.28 | 401.95 | 402.77 | 9.85 | 12.19 | 14.59 | 11.82 | 14.09 |
| | | | | min | -135.87 | -157.41 | -161.49 | -9.83 | 0.30 | 0.07 | 0.09 | -15.54 |
| | NHR | SRA | 3_4 | max | 160.69 | 401.57 | 403.33 | 8.16 | 25.31 | 27.05 | 14.62 | 22.14 |
| | | | | min | -102.27 | -159.32 | -86.80 | -10.75 | 0.13 | 0.10 | 0.11 | -29.38 |
| FEMALE 2 | HR | IIWPG | 4_1 | max | 49.15 | 98.43 | 79.61 | 9.90 | 16.26 | 15.28 | 29.78 | 20.91 |
| | | | | min | -24.81 | -9.19 | -105.60 | -8.61 | 0.37 | 0.17 | 0.25 | -25.88 |
| | HR | SRA | 4_2 | max | 0.49 | 0.76 | 143.96 | -0.09 | 0.12 | 0.13 | 0.11 | 0.15 |
| | | | | min | 0.11 | 0.32 | 126.53 | -0.11 | 0.04 | 0.05 | 0.04 | -0.08 |
| | NHR | IIWPG | 4_3 | max | 69.00 | 93.67 | 382.43 | 9.82 | 8.49 | 15.30 | 12.74 | 17.98 |
| | | | | min | -55.25 | -73.57 | -416.81 | -9.33 | 0.13 | 0.14 | 0.15 | -11.31 |
| | NHR | SRA | 4_4 | max | 393.69 | 394.59 | 400.39 | 8.07 | 23.04 | 53.22 | 61.85 | 88.95 |
| | | | | min | -85.54 | -102.57 | -305.14 | -11.46 | 0.06 | 0.29 | 0.12 | -37.29 |

# Head restraint present
+ No head restraint present

TABLE 45 PMHS TEST RESULTS OVERVIEW, MAXIMUM AND MINIMUM CHARACTERISTIC VALUES

All measurements of test no 4_2 were faulty thus the data will not be considered in the comparison. In the following bar charts, maxima for all tests are displayed. The different blocks are separated for the distinction of tests with the IIWPG 16 [km/h] pulse or the SRA 24 [km/h] pulse. Furthermore the different setups such as with head restraint (HR) and without head restraint (NHR) are separated. The four (4) different occupants are indicated by different bar shading.

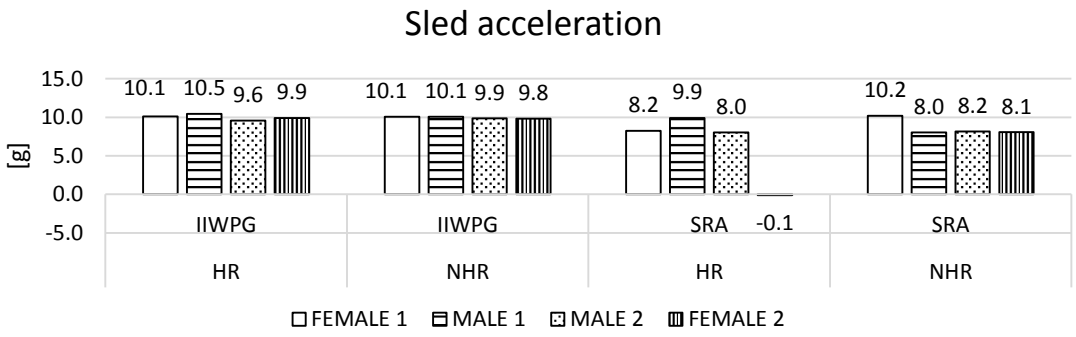


FIGURE 67 PMHS SLED ACCELERATION MAXIMA

The comparison of the maximum sled acceleration shows a steady repeatability of the sled system.

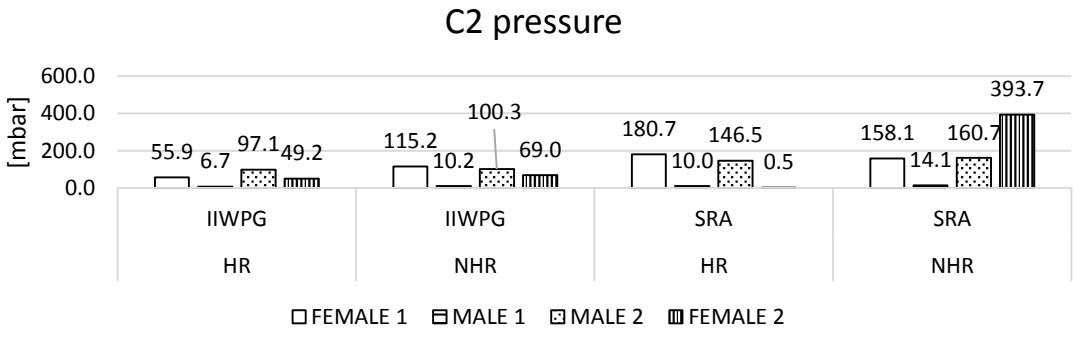


FIGURE 68 PMHS C2 SPINAL CANAL PRESSURE MAXIMA

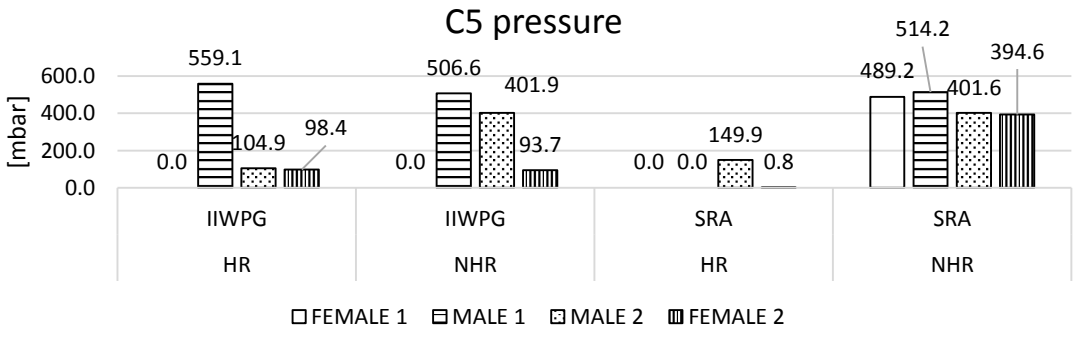


FIGURE 69 PMHS C5 SPINAL CANAL PRESSURE MAXIMA

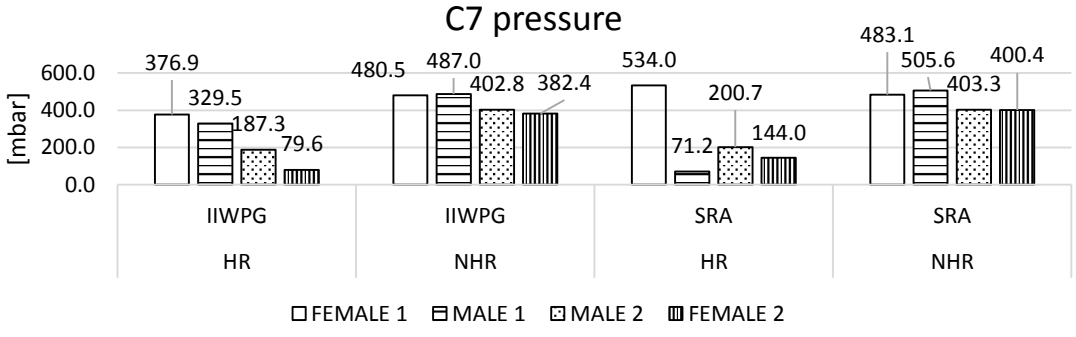


FIGURE 70 PMHS C7 SPINAL CANAL PRESSURE MAXIMA

Comparing pressure change in the spinal canal, like displayed in the above figures indicates, that pressure rise without head restraint is more significant than with head restraint. This also confirms the findings of (Aldman, 1986). However, comparing the different occupants, it cannot be concluded, that female pressure maxima are higher compared to male pressure values.

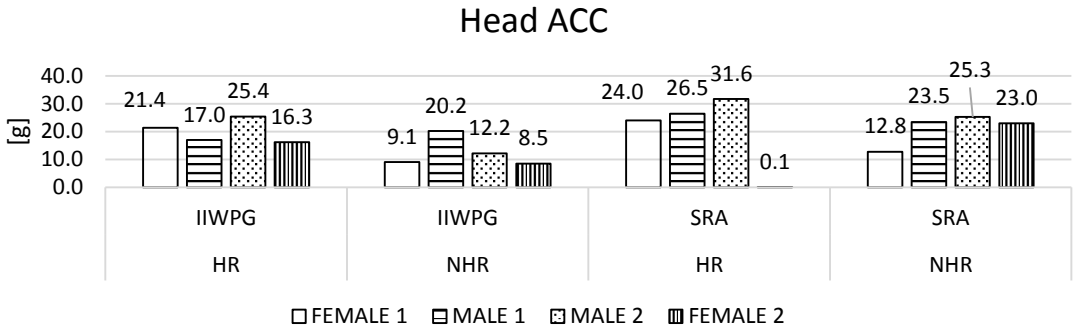


FIGURE 71 PMHS HEAD ACCELERATION MAXIMA

Looking at the maximal head acceleration, in this case resultant acceleration, it can be confirmed, that acceleration levels differ between the two different loaded pulses. Head accelerations under the SRA 24 [km/h] loading are higher compared to the IIWPG 16 [km/h] loads. Neither test configuration does however indicate, that head acceleration levels for female occupants are higher than for male occupants. As an example, the IIWPG 16 [km/h] configuration with a head restraint in place shows the highest head acceleration for the occupant MALE 2 and the lowest for the FEMALE 2 occupant.

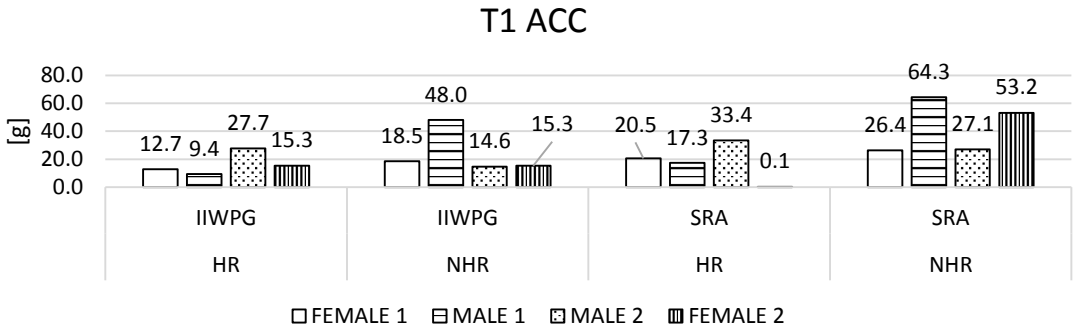


FIGURE 72 PMHS T1 ACCELERATION MAXIMA

The three peak T1 acceleration values are spike signals of a duration less than 10 ms. Other than that those three signals show a level of approximately 10 [g] to 15 [g]. All these configurations are setups without head restraints, where a contact of the T1 accelerometer with the seat structure cannot be ruled out. High speed video footage also confirms these events. Certainly such acceleration peaks are very unlikely in real accident scenarios, since no sensor structure can interfere with seat components. Thus these peak values are considered irrelevant. Other than that, for example the IIWPG 16 [km/h] configuration, no significant difference between male and female occupants can be made out. In particular, a higher level of T1 acceleration for females cannot be confirmed.

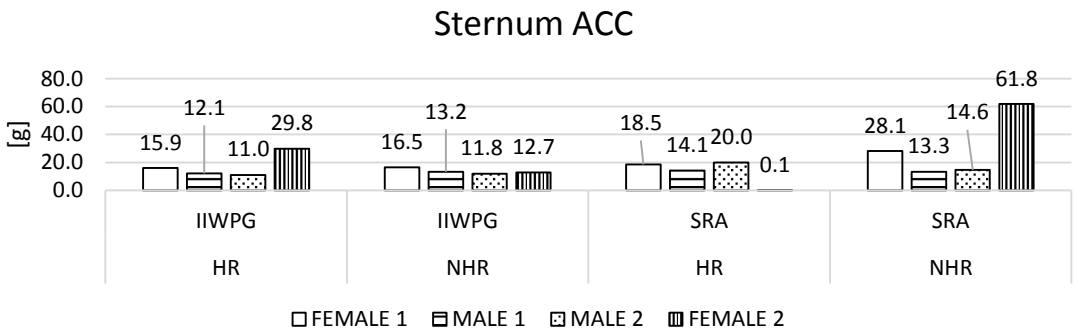


FIGURE 73 PMHS STERNUM ACCELERATION MAXIMA

The one value sticking out here (Female 2, NHR, SRA 24 [km/h]) is a late peak at about 200 [ms]. This peak value refers to a single event where the sternum accelerometer contacts the seat belt. Other than this the acceleration level for this test is around 10 [g] to 15 [g] very uniformly, thus leading to the conclusion, that sternum acceleration is not dependant on the occupant gender in this series of tests, when comparing all other configurations.

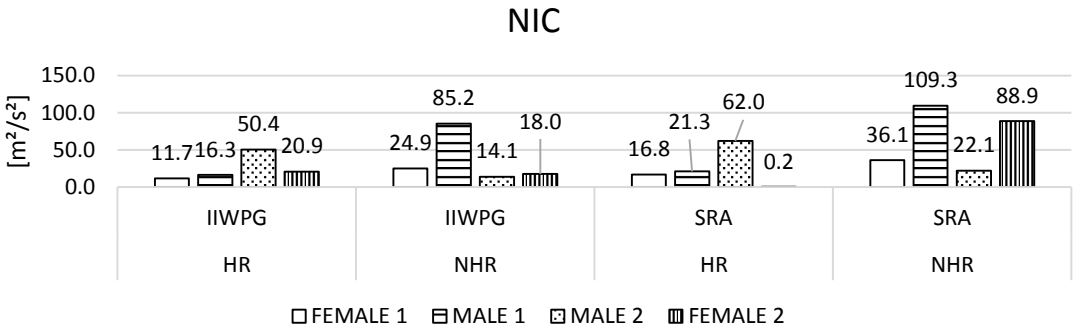


FIGURE 74 PMHS NIC MAXIMA

The maximum NIC values result from T1 acceleration peaks as described before. Excluding these peaks, the NIC for the FEMALE 2 SRA 24 [km/h] configuration without a head restraint shows a maximum of approximately 12 [m²/s²] looking at Figure 74. Same goes for the configuration with a peak NIC of 109 [m²/s²]. This peak is very late at about 150 [ms] past T0 and also results from a T1 acceleration peak at this time. The maximum value if this value is excluded would be approximately 15 [m²/s²]. Keeping those two in mind and comparing NIC values for the SRA 24 [km/h] configuration without a head restraint, the same conclusion as with all other values before can be drawn. A significant difference between male and female occupant loading is not immanent.
Negative NIC values like shown in Table 45 are relevant for low speed frontal collisions (2.5.15) or during the rebound phase. For this series of tests, no further discussion of negative NIC values shall be made.

Since in Figure 74 and Table 45 the absolute maxima of NIC values are shown, in the following Figure 75 relevant NIC values are presented. The selection of these values is based on exclusion of single acceleration peaks and reduction of the selected time period to a maximum of 150 [ms] or the first time point within 150 [ms] where the head changes the direction of relative movement regarding T1 (Cichos, et al., 2006). Late values of tests without a head restraint were thus excluded. The period for tests without a head restraint in place was furthermore limited to the stages retraction and extension. Hyperextension was not included. Head to backrest contact was not considered. Furthermore T1

acceleration peaks resulting from T1 accelerometer contact with structural parts of the restraint system or the seat were removed.

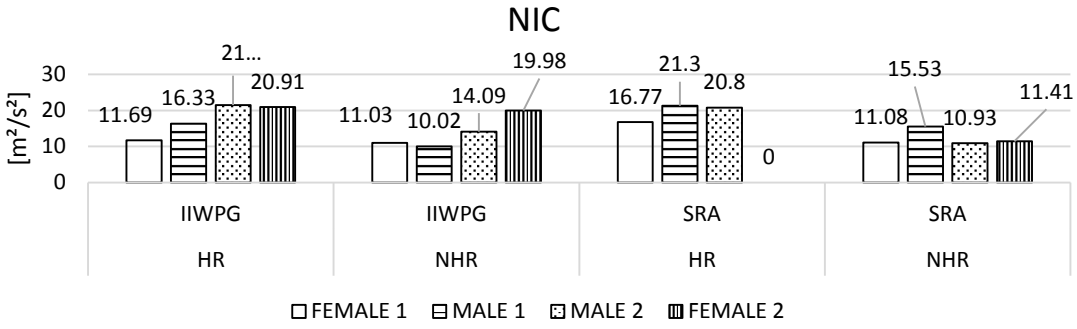


FIGURE 75 PMHS RELEVANT NIC VALUES

Comparing the values in Figure 75 shows a more uniform picture than the absolute maxima in Figure 74. Ignoring the zero value of test 4_2 the average NIC is 15.56 [m²/s²] with a standard deviation of 4.27 [m²/s²]. Comparing the average NIC for females 12.86 [m²/s²] with the average NIC of males 16.31 [m²/s²] an increased load on the female neck can not be confirmed.

Taking a closer look at the time history of pressure in the spinal canal and comparing it with the NIC plot over time, some sort of relation can be found. For example looking at the graph Figure 76, a distinct pressure drop in the spinal canal between 60 and 80 [ms] can be found. At the same time, Figure 77 shows the peak value for NIC in the relevant time range for this criterion. Similar behaviour can be found for other PMHS tests which can be seen in Appendix A.3.10, A.3.12, A.3.13 and A.3.16. These findings correlate with the results found in (Svensson, et al., 1993) for animal tests and the analytical approach of (Boström, et al., 1996).

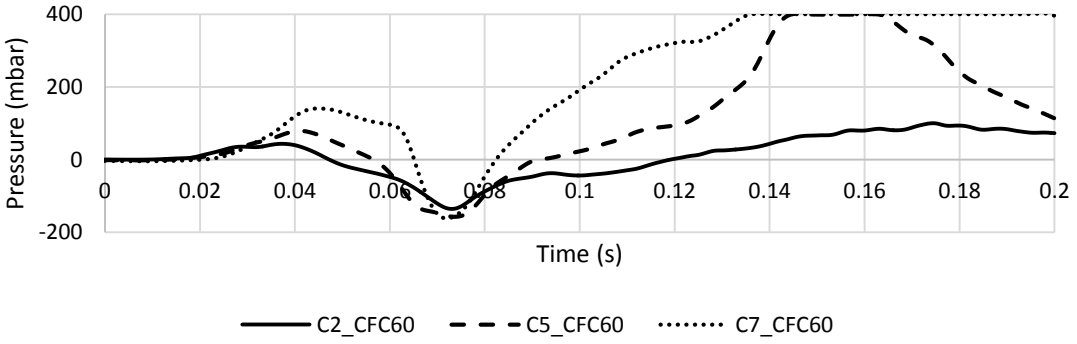


FIGURE 76 PMHS 3 TEST 3 SPINAL CANAL PRESSURE AT C2, C5 AND C7 OVER TIME

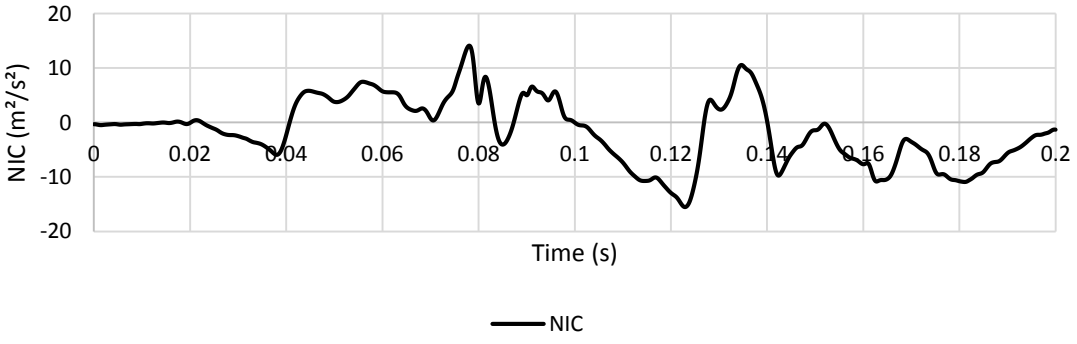


FIGURE 77 PMHS 3 TEST 3 NIC OVER TIME

# 5. Results Finite Element Analysis

For each occupant model (Bio RID II and Eva RID) nine different geometrical configurations were set up and simulated where for each geometrical setup, all three relevant acceleration pulses assessed in the Euro NCAP protocol were used. The results from these simulations are presented in brief in the following diagrams and descriptions.

For each setup and every applied pulse, five graphs can be found in Appendix A.6 and A.7.

- The first graph displays the sled x-acceleration, the head x-acceleration and the T1 x-acceleration.
- The second graph shows the upper neck tension/compression (Fz) and shear (Fx) force. Positive values of Fz are considered tension, negative values compression.
- In the third graph, moments about the Y axis (My) at the occipital are displayed. Positive values of My are considered flexion, negative values are considered extension.
- The fourth diagram shows the NIC value. Only positive values are of interest, since negative values describe a relative displacement of head and T1 in the opposite direction already and are not considered in current regulation or consumer test.
- In the last diagram, the Nkm criteria Ntf, Ncf, Nte and Nce are displayed.

A comparison of the head and neck kinematics of the male (upper row) and the female (lower row) occupant model can be seen in Figure 78. It shows, that the kinematics are similar, although timing and deflection differ. Also the anthropometric differences lead to a significant difference in loading on the neck for the Bio RID II and Eva RID model as shown in Figure 78. Where for the Bio RID II the axial load is predominantly tension, the Eva RID shows large amounts of compression forces in the neck. The associated graphs of force versus time can be found in A.6.5 and A.7.5 respectively.

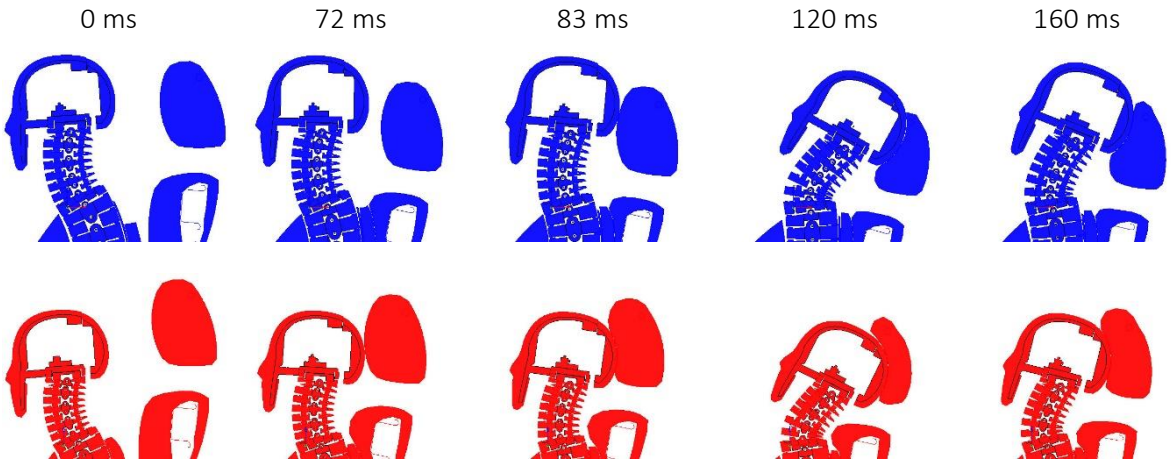


Figure 78 FEA Comparison of head - neck kinematics of the Bio RID II (upper row) and Eva RID (lower row) dummy model

In the following Table 46, Table 47 and Table 48 the maxima for all criteria taken into account in the comparison of all virtual generic seat simulations are presented. For criteria, where Euro NCAP sets borders (Table 23), the cells were coloured depending on the value. Green represents values

achieving full score (higher performance criterion). Yellow represents values between the higher and lower performance criteria. Orange values represent values between the lower performance and capping limits and red indicates values above the capping limits. For each acceleration pulse, different limits exist (Euro NCAP, 2013). Self-evidently, no limits for the female occupant model Eva RID exist. Even though (Linder, et al., 2013) suggest the application of reduced thresholds for female occupants, the comparison in this study was based on thresholds defined in the Euro NCAP. A reduction of the thresholds for female occupants would only lead to an even more pronounced result for female occupants.

| | | [m²/s²] | [-] | [kN] | [kN] | [g] | [ms] | [Nm] | [Nm] | [-] |
|---|---|---|---|---|---|---|---|---|---|---|
| Gender | Simulation | NIC | Nkm | UpNeckSh | UpNeckT | T1Acc | T-HRC | OcMyFlex | OcMyExt | Nij |
| Male | L111 | 12.05 | 0.19 | 0.12 | 0.22 | 8.70 | 55.72 | 16.58 | -2.03 | 0.06 |
| | L112 | 10.84 | 0.15 | 0.07 | 0.22 | 9.44 | 48.82 | 13.30 | -1.95 | 0.06 |
| | L113 | 10.64 | 0.11 | 0.08 | 0.22 | 9.66 | 50.32 | 9.46 | -3.65 | 0.05 |
| | L121 | 22.05 | 0.23 | 0.17 | 0.32 | 11.47 | 90.62 | 20.29 | -4.15 | 0.07 |
| | L122 | 21.94 | 0.25 | 0.06 | 0.33 | 11.23 | 90.12 | 7.89 | -11.78 | 0.10 |
| | L123 | 24.41 | 0.37 | 0.07 | 0.38 | 11.55 | 91.62 | 7.88 | -17.75 | 0.15 |
| | L131 | 27.82 | 0.23 | 0.17 | 0.40 | 13.92 | 97.52 | 20.66 | -5.77 | 0.08 |
| | L132 | 27.96 | 0.28 | 0.06 | 0.38 | 14.16 | 96.22 | 12.18 | -13.33 | 0.11 |
| | L133 | 29.37 | 0.36 | 0.05 | 0.42 | 13.74 | 97.82 | 12.26 | -17.10 | 0.15 |
| Female | L211 | 13.50 | 0.17 | 0.12 | 0.07 | 8.97 | 68.72 | 15.18 | -1.60 | 0.06 |
| | L212 | 9.57 | 0.16 | 0.08 | 0.07 | 8.70 | 58.72 | 14.16 | -1.56 | 0.06 |
| | L213 | 8.55 | 0.04 | 0.05 | 0.07 | 8.77 | 54.92 | 9.05 | -1.70 | 0.03 |
| | L221 | 17.83 | 0.37 | 0.25 | 0.21 | 10.36 | 87.02 | 32.71 | -1.09 | 0.13 |
| | L222 | 14.89 | 0.28 | 0.17 | 0.11 | 9.75 | 82.22 | 24.48 | -0.96 | 0.10 |
| | L223 | 11.29 | 0.18 | 0.10 | 0.09 | 10.24 | 78.72 | 15.63 | -6.20 | 0.07 |
| | L231 | 28.63 | 0.34 | 0.24 | 0.27 | 12.80 | 99.72 | 29.96 | -5.09 | 0.11 |
| | L232 | 21.97 | 0.24 | 0.14 | 0.23 | 12.65 | 95.62 | 21.07 | -5.93 | 0.08 |
| | L233 | 19.90 | 0.14 | 0.07 | 0.22 | 11.80 | 93.92 | 11.67 | -10.33 | 0.10 |

TABLE 46 FEA SRA 16 KM/H GENERIC SEAT SIMULATIONS RESULT OVERVIEW INJURY CRITERIA

In Table 46 results do not emphasise the general opinion that the female occupant model is exposed to significantly higher loads than the male occupant model. Except from some high shear force values in configurations with a high head restraint position loading values are comparable with those of the Bio RID II model. Tension forces are even lower than those for the male occupant model.

| | | [m²/s²] | [-] | [kN] | [kN] | [g] | [ms] | [Nm] | [Nm] | [-] |
|---|---|---|---|---|---|---|---|---|---|---|
| Gender | Simulation | NIC | Nkm | UpNeckSh | UpNeckT | T1Acc | T-HRC | OcMyFlex | OcMyExt | Nij |
| Male | M111 | 16.37 | 0.23 | 0.14 | 0.28 | 14.15 | 50.62 | 20.09 | -2.00 | 0.08 |
| | M112 | 15.83 | 0.14 | 0.07 | 0.26 | 12.43 | 45.82 | 12.41 | -1.95 | 0.08 |
| | M113 | 14.94 | 0.11 | 0.01 | 0.27 | 12.73 | 45.82 | 8.87 | -5.11 | 0.07 |
| | M121 | 30.55 | 0.22 | 0.18 | 0.41 | 14.04 | 82.52 | 19.15 | -7.55 | 0.08 |
| | M122 | 31.16 | 0.28 | 0.07 | 0.41 | 15.08 | 81.42 | 11.17 | -13.50 | 0.11 |
| | M123 | 32.57 | 0.39 | 0.09 | 0.47 | 13.61 | 83.42 | 11.36 | -18.71 | 0.17 |
| | M131 | 39.39 | 0.29 | 0.20 | 0.44 | 17.06 | 86.52 | 25.94 | -6.52 | 0.10 |
| | M132 | 36.84 | 0.28 | 0.11 | 0.44 | 17.47 | 85.32 | 16.59 | -13.46 | 0.11 |
| | M133 | 38.77 | 0.19 | 0.09 | 0.47 | 16.07 | 87.42 | 16.56 | -19.70 | 0.17 |
| Female | M211 | 17.45 | 0.26 | 0.16 | 0.13 | 10.14 | 60.22 | 22.97 | -1.60 | 0.09 |
| | M212 | 12.38 | 0.23 | 0.13 | 0.10 | 9.31 | 51.62 | 20.63 | -1.56 | 0.08 |
| | M213 | 11.69 | 0.17 | 0.09 | 0.11 | 9.23 | 48.52 | 14.60 | -1.70 | 0.06 |
| | M221 | 33.08 | 0.50 | 0.34 | 0.33 | 17.37 | 76.42 | 44.18 | -1.37 | 0.19 |
| | M222 | 27.66 | 0.38 | 0.24 | 0.19 | 16.56 | 72.92 | 33.74 | -4.30 | 0.14 |
| | M223 | 26.68 | 0.26 | 0.17 | 0.20 | 16.54 | 70.62 | 23.09 | -9.31 | 0.09 |
| | M231 | 41.10 | 0.41 | 0.18 | 0.31 | 17.68 | 87.42 | 10.34 | -6.26 | 0.08 |
| | M232 | 36.74 | 0.31 | 0.20 | 0.23 | 18.93 | 84.22 | 36.23 | -4.86 | 0.13 |
| | M233 | 37.98 | 0.23 | 0.13 | 0.22 | 18.02 | 82.82 | 26.87 | -4.87 | 0.10 |

TABLE 47 FEA IIWPG 16 KM/H GENERIC SEAT SIMULATIONS RESULT OVERVIEW INJURY CRITERIA

Table 47 similar to Table 46 does not indicate a significant higher loading on the female occupant. Also looking at tensile forces, again the female is on a lower level than the male occupant model. Nevertheless, comparing the configurations with centred backrests, especially with the high and medium head restraint, the female has disadvantages.

| | | [m²/s²] | [-] | [kN] | [kN] | [g] | [ms] | [Nm] | [Nm] | [-] |
|---|---|---|---|---|---|---|---|---|---|---|
| Gender | Simulation | NIC | Nkm | UpNeckSh | UpNeckT | T1Acc | T-HRC | OcMyFlex | OcMyExt | Nij |
| Male | H111 | 16.06 | 0.20 | 0.14 | 0.33 | 12.43 | 48.82 | 17.16 | -2.025 | 0.06511 |
| | H112 | 15.99 | 0.14 | 0.08 | 0.33 | 13.18 | 43.12 | 12.01 | -1.949 | 0.06297 |
| | H113 | 15.18 | 0.18 | 0.05 | 0.35 | 11.67 | 43.12 | 8.737 | -8.424 | 0.07551 |
| | H121 | 28.01 | 0.48 | 0.09 | 0.41 | 13.34 | 81.22 | 11.94 | -22.88 | 0.19757 |
| | H122 | 19.75 | 0.46 | 0.08 | 0.43 | 12.91 | 79.82 | 11.82 | -22.6 | 0.21496 |
| | H123 | 31.23 | 0.43 | 0.16 | 0.70 | 13.79 | 86.52 | 12.18 | -28.54 | 0.28815 |
| | H131 | 42.63 | 0.41 | 0.20 | 0.56 | 18.59 | 86.22 | 18.97 | -19.49 | 0.16821 |
| | H132 | 42.67 | 0.46 | 0.11 | 0.56 | 18.99 | 85.12 | 17.42 | -24.61 | 0.22395 |
| | H133 | 44.32 | 0.62 | 0.15 | 0.65 | 18.76 | 87.62 | 17.42 | -29.32 | 0.28566 |
| Female | H211 | 17.23 | 0.25 | 0.16 | 0.13 | 12.21 | 59.42 | 22.25 | -18.7411 | 0.0828 |
| | H212 | 13.26 | 0.21 | 0.14 | 0.09 | 12.78 | 50.22 | 18.85 | -1.5634 | 0.0719 |
| | H213 | 12.09 | 0.14 | 0.08 | 0.10 | 13.96 | 47.02 | 12.27 | -1.6982 | 0.06144 |
| | H221 | 49.02 | 0.49 | 0.35 | 0.35 | 23.96 | 75.72 | 42.25 | -11.45 | 0.17452 |
| | H222 | 36.42 | 0.39 | 0.25 | 0.22 | 20.76 | 70.10 | 34.24 | -12.75 | 0.15302 |
| | H223 | 34.04 | 0.38 | 0.18 | 0.21 | 19.63 | 69.22 | 24.57 | -17.98 | 0.1608 |
| | H231 | 55.39 | 0.49 | 0.34 | 0.51 | 24.12 | 85.72 | 43.21 | -16.66 | 0.16491 |
| | H232 | 51.37 | 0.44 | 0.24 | 0.33 | 26.73 | 82.92 | 32.33 | -20.79 | 0.20779 |
| | H233 | 52.36 | 0.44 | 0.21 | 0.29 | 25.65 | 81.52 | 24.63 | -20.96 | 0.17082 |

TABLE 48 FEA SRA 24 KM/H GENERIC SEAT SIMULATIONS RESULT OVERVIEW INJURY CRITERIA

For the high severity pulse results in Table 48 NIC values for the female are significantly higher than for the male occupant model. Again a disadvantage in configurations with high and medium positioned head restraints can be found. Only in configurations with a forward backrest no significant influence of the head restraint position can be seen.

A closer look is taken at three selected female FEA with only a minor difference in setup. The compared simulations are M221, M222 and M223 (Figure 79) which only differ in their head restraint height.

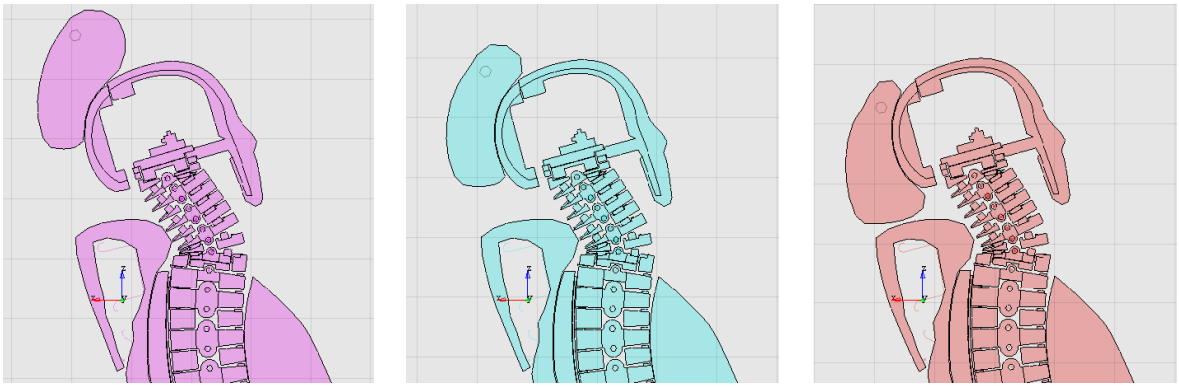

M221 M222 M223

FIGURE 79 EVA RID FEA KINEMATIC COMPARISON AT 90 MS

The kinematics[U] of the three models' necks are very similar. Comparing the displacements of the c.o.g. of the head, a difference between the three configurations of less than 8.2 [mm] (resultant distance between c.o.g.) can be found for the first 120 [ms]. At 188 [ms] the maximum resultant difference between the c.o.g. of the different setups occurs between M221 and M222 at as much as 15 [mm], which is approximately 60 [ms] to 90 [ms] after the peak forces and moments are measured.

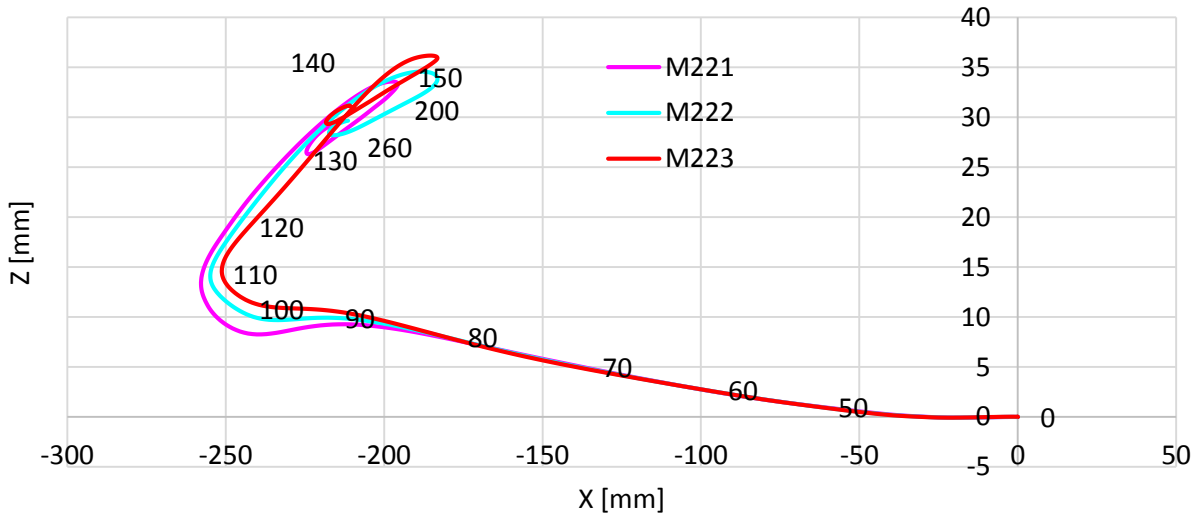


FIGURE 80 EVA RID FEA HEAD C.O.G. KINEMATICS COMPARISON

Looking at the shear force over time (Figure 81) the difference is significant. Peak values occur at approximately the same time (shortly before 100 [ms]). The trend of the different curves are similar, but the magnitude differs significantly. M221 with its highest shear force at 0.3418 [kN] is more than

[U] Relative kinematics of the c.o.g. of the head of the occupant model in a coordinate system fixed to the sled.

twice as high as the maximum shear force of M223 at 0.1658 [kN]. M222 lies in-between with 0.2385 [kN]

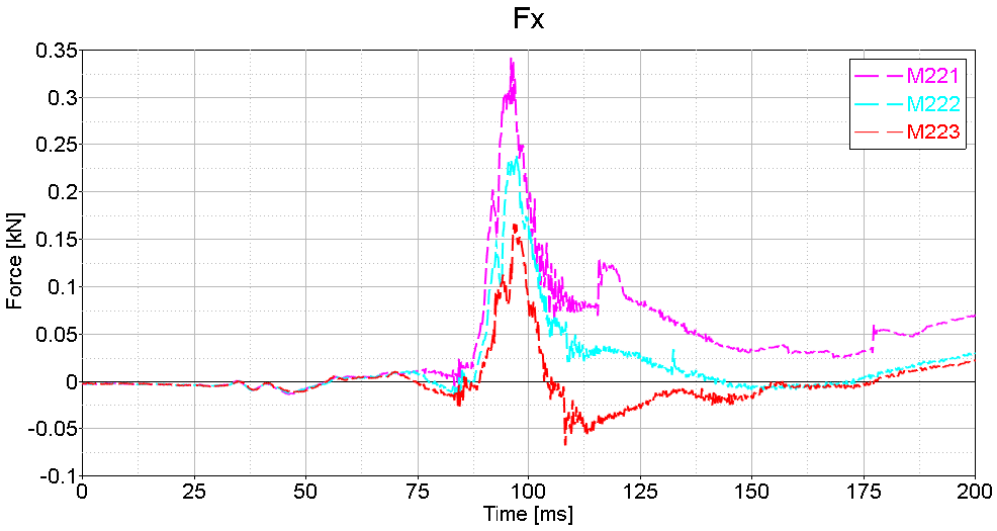


FIGURE 81 EVA RID FEA SHEAR FORCE COMPARISON

Tension force graphs (Figure 82) show similar timing for peaks, but with differences in their magnitudes. The first peak, which is very alike for all three configurations between 80 [ms] and 90 [ms] is the absolute peak value M222 and M223. Also the following negative peak (compression) occurs for all three configurations, but with different magnitudes and slightly different timing. Interestingly, the peak value for M221 occurs slightly later, approximately between 100 [ms] and 110 [ms] where M222 shows tension as well, but for M223 compression is to be found. This behaviour can only be explained by the resultant contact force of the head and head restraint. Where for M221 and M222 the resultant contact force seems to induce a tension, M223 results in compression. Maximum values for tension are M221 with 0.3256 [kN], M222 with 0.1877 [kN] and M223 at 0.1969 [kN]. Compression values are -0.2706, -0.2109 and -0.1595 for M221, M222 and M223 respectively.

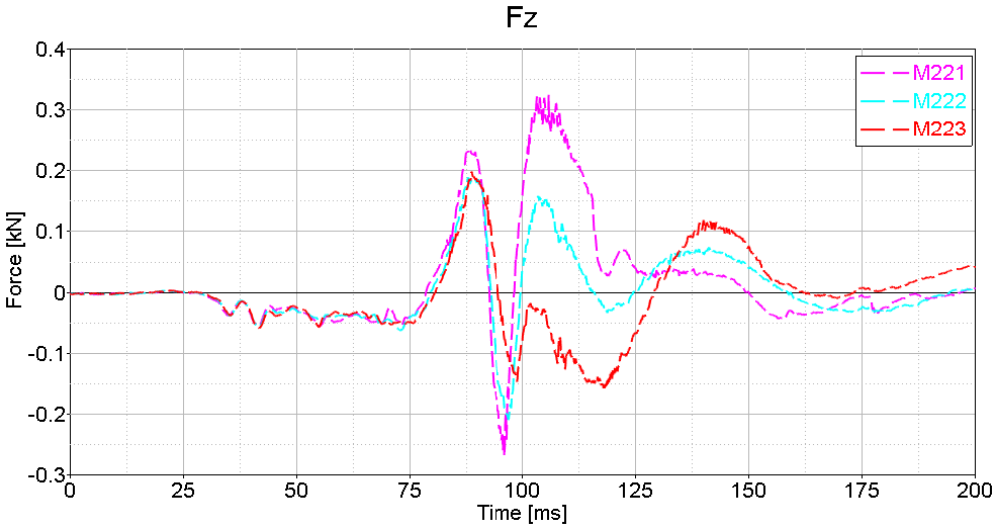


FIGURE 82 EVA RID FEA TENSION FORCE COMPARISON

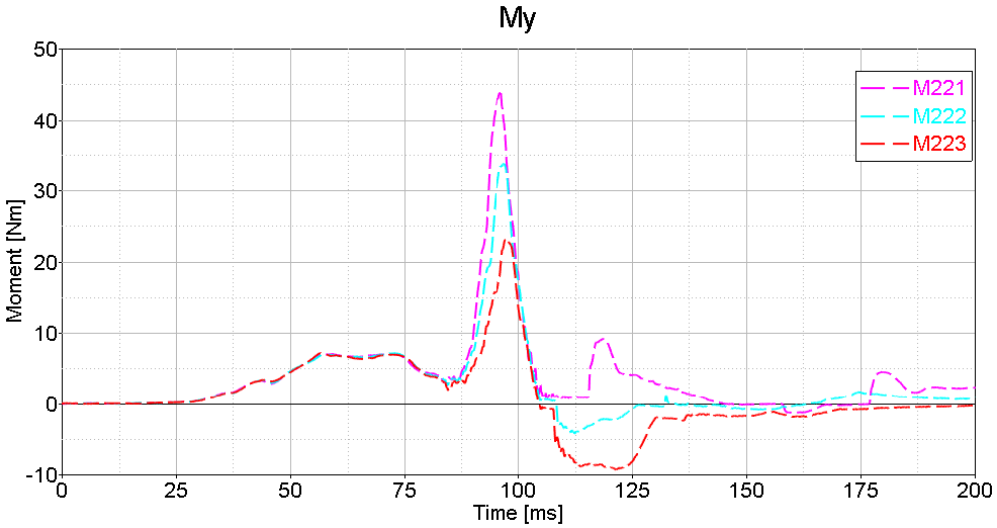


FIGURE 83 EVA RID FEA BENDING MOMENT COMPARISON

Very similar to shear, the timing and trends for My are very similar for all three configurations, however magnitudes differ again. M221 maximum flexion moment is again almost twice as high as the one present for M223 at the same time. M222 again lies between the two other configurations. In the later period of approximately 105 [ms] until 130 [ms], where the magnitudes are much lower than for the initial peak at around 95 [ms], M221 still shows flexion where M222 and M223 show extension. Maximum flexion and extension moments can be found in Table 47.

It appears, that the height configuration of the head restraint, especially for this investigated seat model, is very relevant for the formation of shear, tension and compression force as well as bending moment. It can also be seen, that "high" is not necessarily of benefit for every occupant model. In this comparison, the lowest possible head restraint configuration appears to deliver the highest level of protection for the female occupant model w.r.t. force and moment. It seems, like the important aspect in this comparison is, that the head of the occupant model is supported by a structural part of the head restraint at the height level of the c.o.g. of the occupants head. This reduces flexion and extension to a minimum and thus keeps levels of tension and bending moment low.

All recorded peak values for shear, tension and compression force as well as flexion and extension moment occur in the range between 90 [ms] and 125 [ms] for these three configurations. This is the time, when the occupants' head reaches its farthest translation backwards (relative to the sled). The reversal point in this investigation is thus the interesting period of time to consider, when trying to reduce loads on the occupants' neck.

# 6. COMPARISON

The subsequent comparisons of results from experimental testing and FEA attempts to show associations and diversities between the methods. Where for some comparisons good compliance could be found, others make it difficult to find analogies.

## 6.1. Comparison of Sled Tests and FEA with the Bio RID II dummy

Data in the following Table 49 gives an overview of the maxima of relevant criteria available for both, the OOP tests and corresponding FEA analysis. In this contrasting juxtaposition OOP2 and M112 represent an equal configuration. Furthermore comparable couples are OOP3 and M132 and also OOP4 and M122. OOP6 and M22X are comparable only regarding setup. The occupant model used in M22X was the female Eva RID but in OOP6 the Bio RID II, due to the lack of a physical female dummy. Comparable configurations were coloured accordingly.

| | Upper Neck Fx | Upper Neck Fz | Upper Neck My | T1 ACC | NIC |
|---|---|---|---|---|---|
| | (N) | (N) | (Nm) | (g) | ($m^2/s^2$) |
| OOP2 | 189.74 | 437.23 | 6.15 | 10.94 | 14.54 |
| OOP3 | 131.06 | 768.84 | 10.52 | 9.41 | 14.96 |
| OOP4 | 140.42 | 477.76 | 5.5 | 9.61 | 15.63 |
| OOP6 | 16.66 | 349.12 | 4.32 | 12.16 | 18.19 |
| M112 | 69.62 | 263.6 | 12.41 | 12.425 | 15.8279 |
| M132 | 106.9 | 443.5 | 16.59 | 17.473 | 36.8431 |
| M122 | 69.75 | 406.3 | 11.17 | 15.0792 | 31.1587 |
| M22X | 8.625 | 70.53 | 17.6 | 15.0647 | 6.88 |

TABLE 49 FEA COMPARISON OF INJURY CRITERIA MAXIMA IN FEA AND OOP

In Figure 84 the NIC criterion for experimental tests and corresponding FEA analysis were compared. Where for the configuration with a forward positioned backrest (OOP2 and M112) a similar result could be found, all other configurations diverge significantly. Also for the configuration according to the Euro NCAP protocol (OOP4 and M122) (Euro NCAP, 2013) results diverge severely.

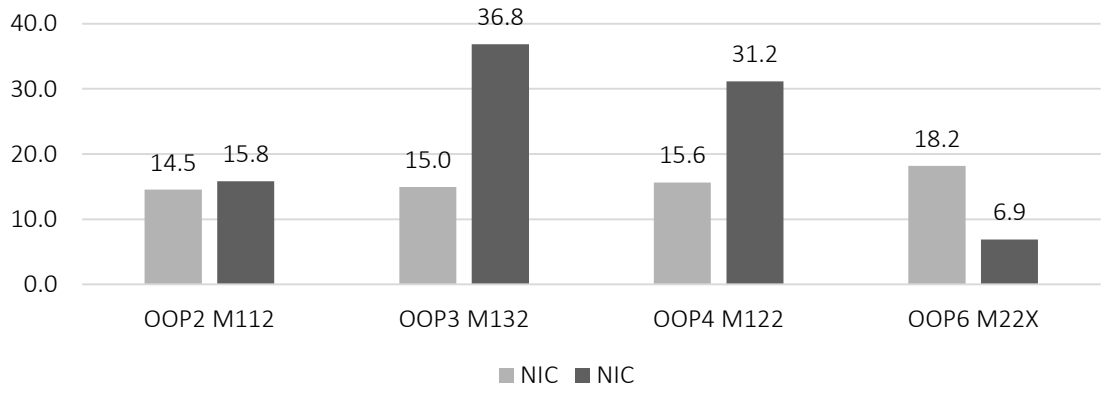


FIGURE 84 FEA & OOP COMPARISON OF NIC CRITERION

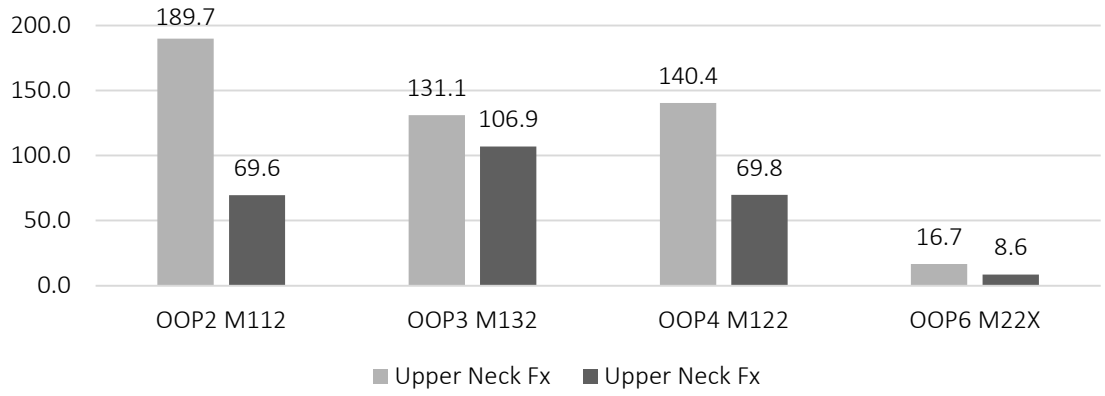


FIGURE 85 FEA & OOP COMPARISON OF UPPER NECK SHEAR FORCE

Even if Figure 85 reflects a significant reduction of shear force in both configurations OOP6 and M22X, the similarity for other criteria is not that well. The tension force in Figure 86 is the lowest for both categories (FEA and experimental) but the upper neck bending moment (Figure 87) diverges. Certainly also the fact, that in M22X the female occupant model and in OOP6 only the available Bio RID II were used, reduces direct comparability.

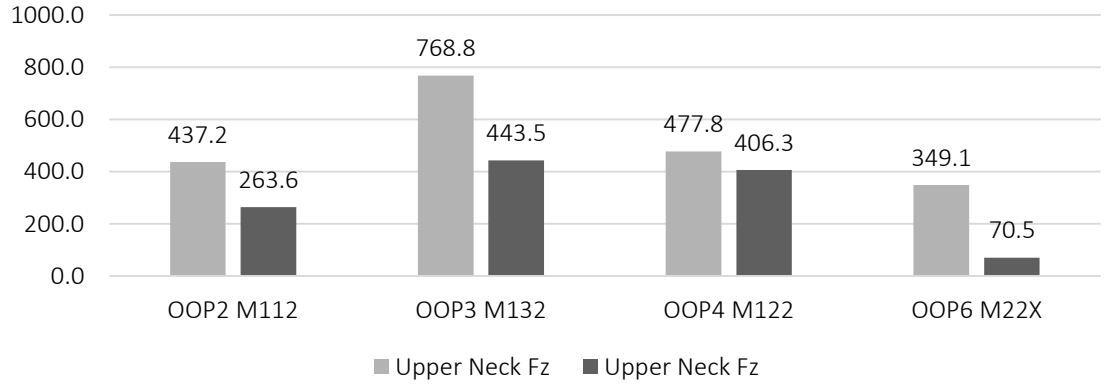


FIGURE 86 FEA & OOP COMPARISON OF UPPER NECK TENSION FORCE

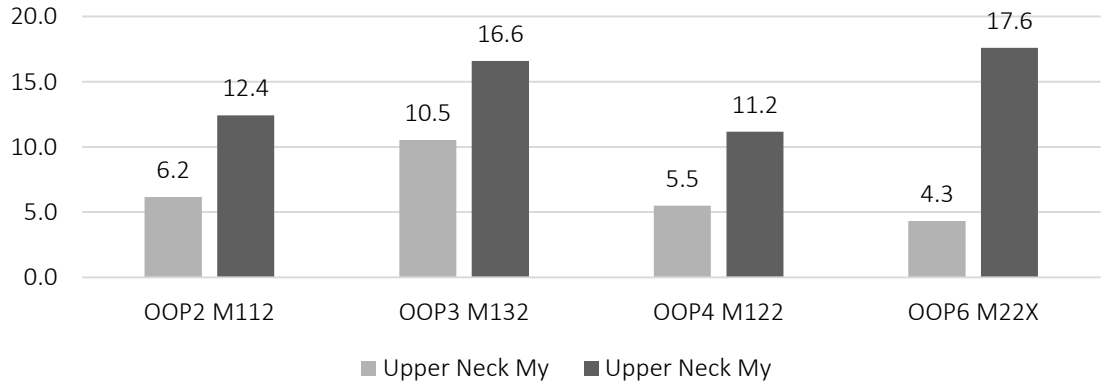


FIGURE 87 FEA & OOP COMPARISON OF UPPER NECK FLEXION / EXTENSION MOMENT

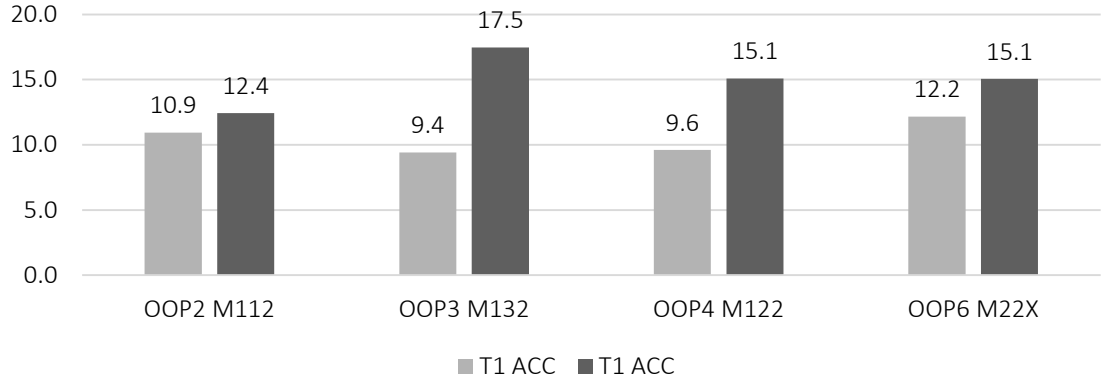


FIGURE 88 FEA & OOP COMPARISON OF T1 X-ACCELERATION

T1 acceleration, like the NIC criterion, shows some similarity for the configuration with a forward positioned backrest. Also the modified configuration with a significantly reduced backset shows similar results for T1. Just the results for NIC in configurations M22X and OOP6 distinguish significantly.

The FEA and experimental tests show, that different configurations of the vehicle seat influence the results, in some cases significantly, with up to 200 % difference. However unfortunately the comparison between FEA and experimental testing does not allow a general conclusion that FEA and experimental always show results in agreement. Some criteria, like e.g. shear force with an eliminated backset demonstrate a very promising behaviour, other data such as NIC diverge for the same configuration.

## 6.2. Comparison of Bio RID 50F Sled Tests and Eva RID FEA

The following Table 50 shows a number of injury criteria computed for the Bio RID 50F tests and comparable FEA. The correlating FEA in this table is the M222 setup. It represents a female occupant model (Eva RID) in a seat configured according to the Euro NCAP protocol applying the IIWPG 16 [km/h] pulse. For comparison M221 and M223 are presented complementary, with a head restraint positioned in its “highest” and “lowest” position.

| | | Sled Acc X | Head Acc X | T1 Acc X | Fx | Fz | My | NIC |
|---|---|---|---|---|---|---|---|---|
| | | (g) | (g) | (g) | (kN) | (kN) | (Nm) | (m²/s²) |
| TUG11007 | max | 10.30 | 24.52 | 16.83 | 0.33 | 0.28 | 13.77 | 12.68 |
| | min | -6.05 | -0.97 | -1.30 | -0.09 | -0.15 | -4.80 | -22.04 |
| TUG11008 | max | 10.69 | 21.49 | 17.96 | 0.35 | 0.31 | 11.97 | 12.35 |
| | min | -6.93 | -1.02 | -1.29 | -0.07 | -0.14 | -3.71 | -18.00 |
| M221 | max | 9.45 | 26.24 | 17.37 | 0.34 | 0.33 | 44.18 | 33.08 |
| | min | -0.56 | -6.54 | -3.83 | -0.02 | -0.27 | -1.37 | -49.34 |
| M222 | max | 9.34 | 19.94 | 16.56 | 0.24 | 0.19 | 33.74 | 27.66 |
| | min | -0.48 | -5.82 | -2.81 | -0.03 | -0.21 | -4.30 | -36.42 |
| M223 | max | 9.36 | 22.12 | 16.54 | 0.17 | 0.20 | 23.09 | 26.68 |
| | min | -0.44 | -5.76 | -4.03 | -0.07 | -0.16 | -9.31 | -34.65 |

TABLE 50 COMPARISON OF INJURY CRITERIA MAXIMA IN FEA AND BIO RID 50F TESTS

Repeatability of sled tests was very good. In the following diagram Figure 89 the correlation of the real sled tests and the FEA are compared. The acceleration peaks range from 9.34 to 10.69 [g]. The

difference in deceleration must be explained as braking of the sled system in real sled tests, which is not necessary in the FEA.

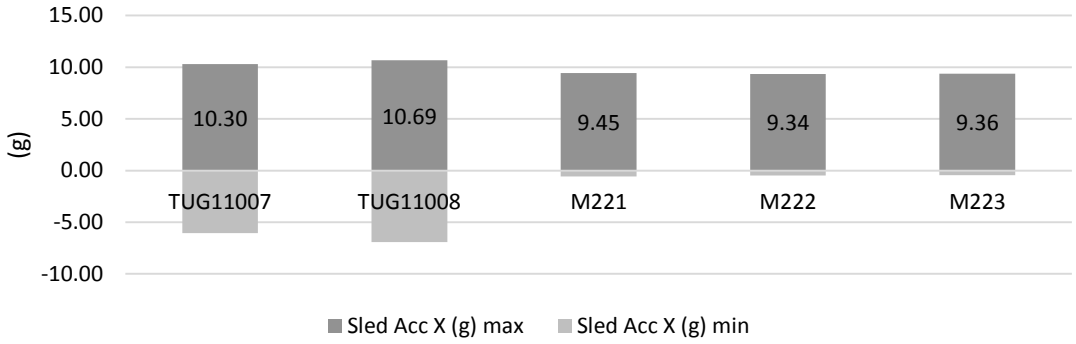


FIGURE 89 FEA & BIO RID 50F COMPARISON OF SLED X-ACCELERATION

Also the peak values of the head acceleration as shown in Figure 90 and T1 acceleration Figure 91 show very good correlation for the FEA and prototype dummy tests. However, the negative peak values for all FEAs (head and T1 deceleration) shows larger values. The maximal acceleration values range between 19.93 and 26.24 [g] for the FEA head acceleration and 21.49 and 24.52 [g] for the Bio RID 50F tests.

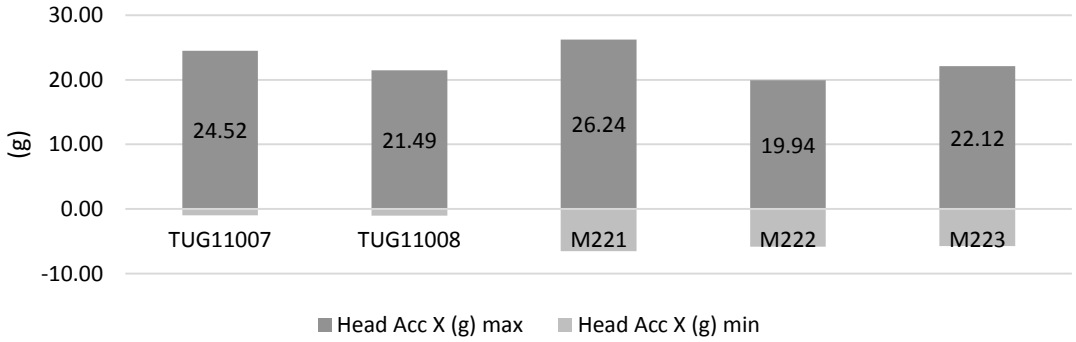


FIGURE 90 FEA & BIO RID 50F COMPARISON OF HEAD X-ACCELERATION

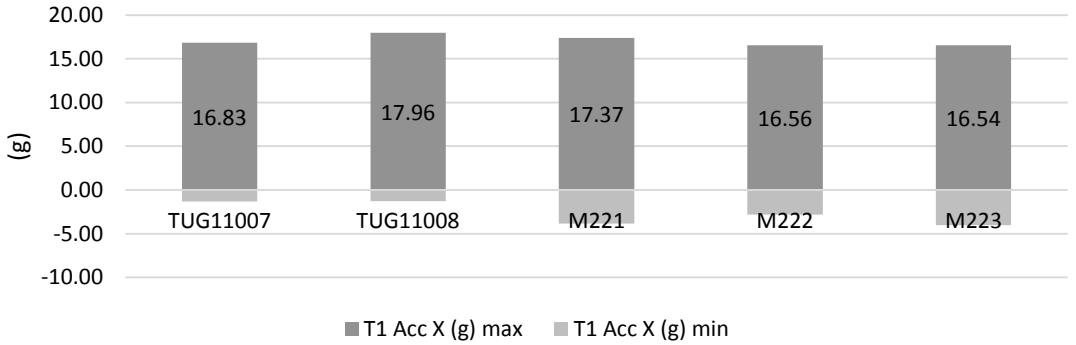


FIGURE 91 FEA & BIO RID 50F COMPARISON OF T1 X-ACCELERATION

Looking at Forces, the following graph Figure 92 shows a good repeatability for the Bio RID 50F sled tests. Comparing the peak value of the sled tests with the FEA, it seems, that the head restraint position has a large influence on the shear force. For the FEA configuration with a high head restraint the maximum shear force is very much at the same level as the sled tests, where the configuration

with the head restraint in the middle and lowest position shows lower shear loading on the Eva RID models neck.

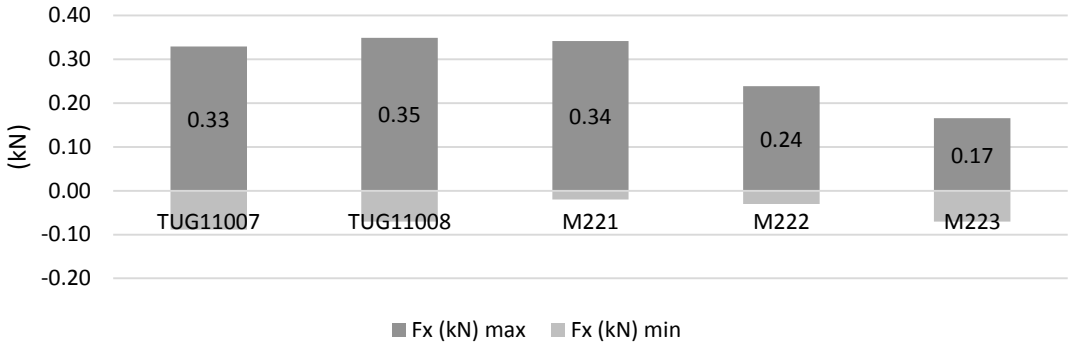


FIGURE 92 FEA & BIO RID 50F COMPARISON OF FX

A very similar picture is drawn when looking into tension forces. Figure 93 again shows good repeatability for the Bio RID 50F tests with 0.31 and 0.28 [kN] tension force. Again the FEA setup with the head restraint in its highest position delivers a similar picture for tension at 0.33 [kN]. However if the compression on the neck is considered, all FEAs show higher values for the Eva RID model compared to the Bio RID 50F.

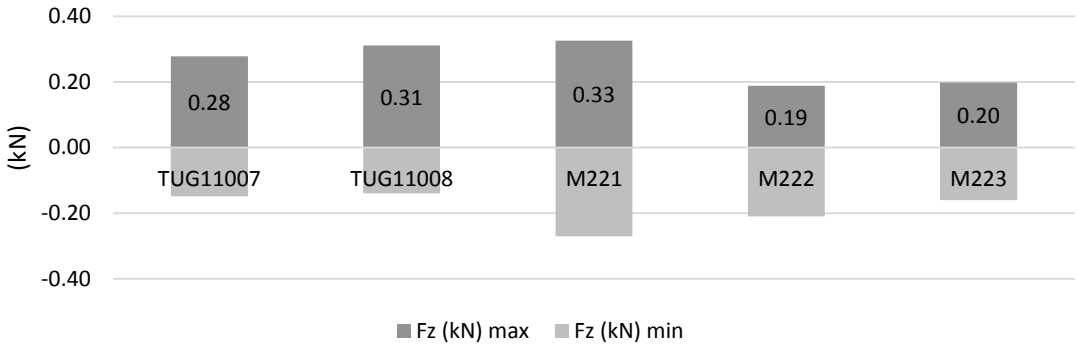


FIGURE 93 FEA & BIO RID 50F COMPARISON OF FZ

Even larger differences between FEA and real sled testing can be found in the results for the upper neck bending moment. All FEAs show higher peak values for flexion (positive values). Again a large influence of the head restraint position on the outcome of bending moment values can be found. The graph in Figure 94 shows the tendency to higher flexion moments for higher head restraint positions, and higher extension moments (negative values) for lower head restraint positions.

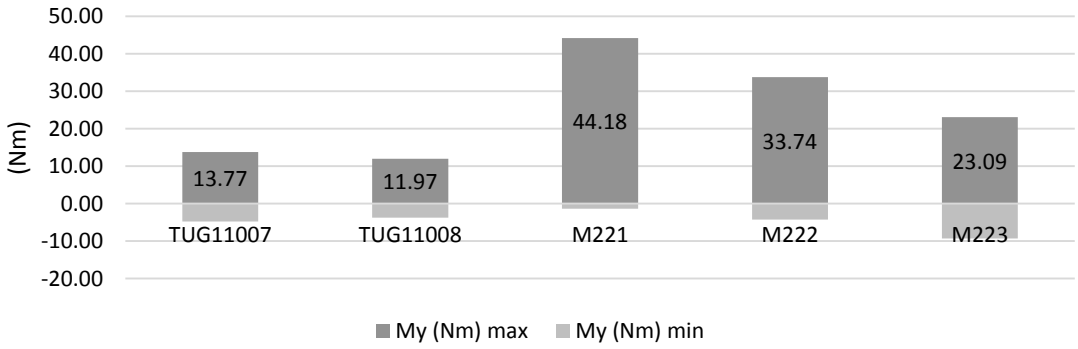


FIGURE 94 FEA & BIO RID 50F COMPARISON OF MY

Figure 95 again shows very good repeatability for both Bio RID 50F tests. This can especially be seen in the graph Figure 96 where the solid and dashes lines correlate very well. The dotted line, representing the Eva RID FEA result of the M222 configuration shows some deviation in peak values as well as timing.

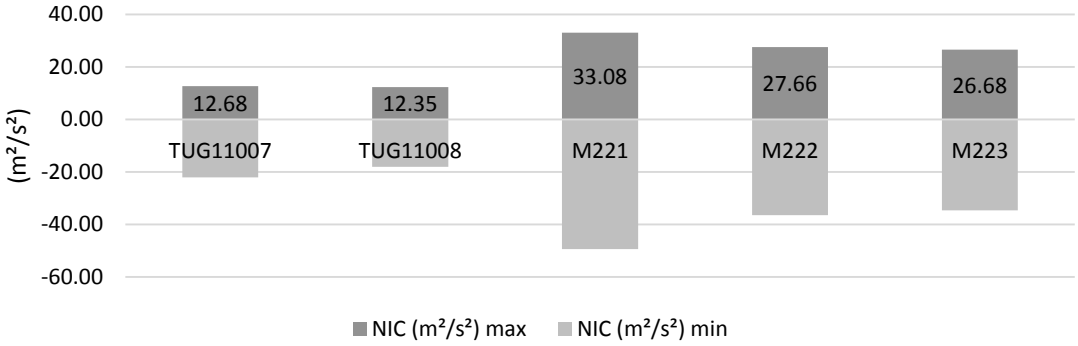


FIGURE 95 FEA & BIO RID 50F COMPARISON OF NIC CRITERION

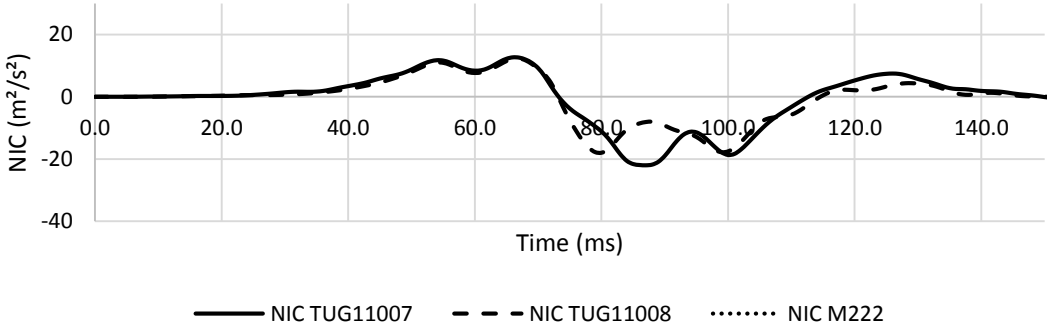


FIGURE 96 FEA & BIO RID 50F COMPARISON OF NIC CRITERION

Overall the Bio RID 50F performed very well for a simple mass reduced prototype. Repeatability and mechanical performance were good. It must however be kept in mind, that major components such as spinal components were not modified to meet the anthropometry of a 50th percentile female. Size and stiffnesses of the vertebral components were unchanged in the Bio RID 50F while the Eva RID was adapted in size and stiffness characteristics in this region as well. Considering these limitations correlation between the Bio RID 50F and Eva RID was acceptable for a first physical female 50$^{th}$ percentile rear impact dummy prototype.

## 6.3. Comparison of Numerical Eva RID simulations and female PMHS tests

Of special interest was the kinematic behaviour of the vertebrae of the virtual Eva RID model for the comparison with bony kinematics gathered from PMHS high-speed x-ray videos (Gutsche, et al., 2014). Therefore two nodes, aligned on the mid sagittal plane on the mid horizontal plane of each vertebral body were tracked and analysed, like exemplary in Figure 97.

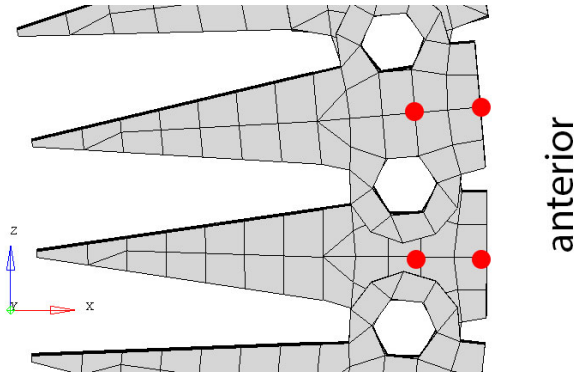


FIGURE 97 EXAMPLE OF NODES TRACKED FOR TRAJECTORY

From the high speed x-ray videos, trajectories of vertebral bodies were generated using target tracking. This data from PMHS testing was compared with trajectories extracted from the FEA. The comparison gives a general overview of the kinematic behaviour of PMHS and the FEA dummy, i.e. of their cervical vertebral bodies.

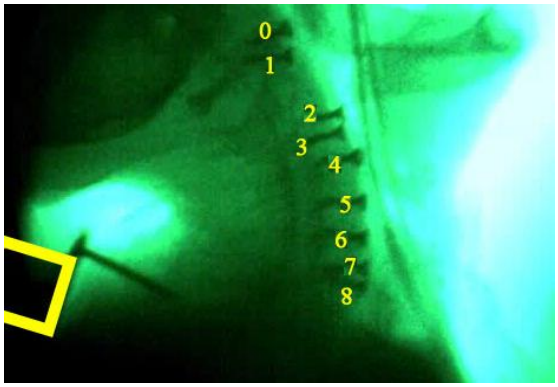


FIGURE 98 EXAMPLE OF RADIOGRAPHIC PICTURE OF A HIGH SPEED VIDEO WITH NUMBERED MARKERS FOR TARGET TRACKING AND T1 ACCELEROMETER

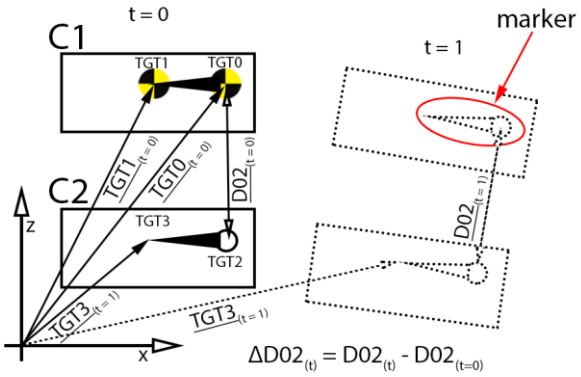


FIGURE 99 DETERMINATION OF POSITIONS OF TRACED TARGETS AND DISTANCES BETWEEN THEM

In Figure 98 an example picture with the numbered markers for the trajectory tracking is given. In some x-ray videos, the tip and the head of the marker could be tracked, in some only the head was clearly visible for tracking. Also the T1 accelerometer can be found in the lower left corner of the picture (indicated with a yellow frame). Radiographic pictures for all PMHS tests can be found in Appendix 127 through Appendix 134. The picture area of all high speed x-ray videos is limited by the diameter of the image intensifier. In this picture all mounted screws to identify vertebrae are visible. Depending on the test configuration and PMHS, up to twelve targets (TGT) were used, since head and tip of each marker were tracked where possible as indicated in Figure 99. Not in all tests all markers are visible for a sufficient period of time, thus not all trajectories are available in some configurations. For each captured picture the positions of each available target in the picture was measured as shown in Figure 99. A coordinate system which is fixed to the picture area (origin at pixel x = 0 and y = 0) was used as global

system. Markers as described were placed in each vertebral body. Each Marker was assigned with two targets, one the leading head and one the following tip of the screws used as traceable targets. Where possible, all targets were tracked by vectors as shown in Figure 99, e.g. TGT3 (t=0 [ms]). Due to restrictions in picture quality not for all PMHS the tips of the markers could be tracked. The dimensions of the markers are known thus the coordinates could be determined and transformed to mm.

The tracking of the vertebral bodies during the rear impact was analysed for comparison. In the following Figure 100 and Figure 101 examples are given for one PMHS test and one FEA simulation respectively. The graphs show the trajectory of the targets (vertebral bodies) during the whiplash motion in a coordinate system fixed to the picture intensifier. The extent of available data for all PMHS tests is limited by the size of the picture intensifier. The values on the abscissas represent the forward movement of the targets in x-direction, values on the ordinate the corresponding z-oriented upward movement. The lines in these graphs represent the curves of the tips of the vectors described as TGT0(t) through TGT11(t) as displayed in Figure 99 during the whiplash loading.

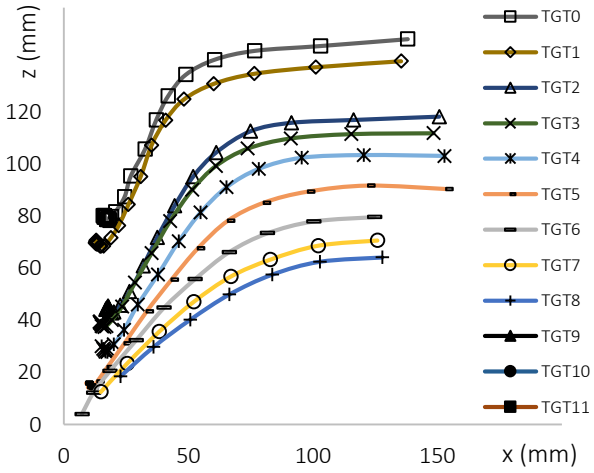


FIGURE 100 TRAJECTORIES OF VERTEBRAL BODIES OF PMHS 1 DURING IIWPG PULSE WITH A HEAD RESTRAINT IN PLACE

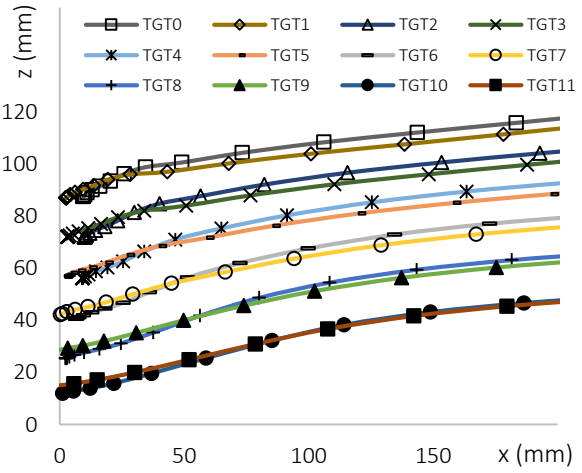


FIGURE 101 TRAJECTORIES OF VERTEBRAL BODIES OF FEA SIMULATION CORRESPONDING THE TEST IN FIGURE 100

The rise of the trajectories of the vertebral bodies of the FEA in Figure 101 is significantly less steep than that of the PMHS' in Figure 100. This is explained by an obvious ramping effect of the PMHS during the forward acceleration, which does not occur in the FEA. This upward motion is an accumulation of two factors. The first component is an upward motion of the PMHS on the seat itself caused by the angle of the backrest. The second component is caused by straightening of the spine. The pressure applied to back of the PMHS straightens the curvature of the thoracic spine. A similar behaviour of the thoracic spine in the FEA can not be seen. This leads to a resultant upward motion of the upper end of the thoracic spine and thus pushing the cervical spine and head upwards. The vertical motion of the FEAs cervical bodies thus is smaller than that of the PMHS, very likely to be caused by a too stiff thoracic spine of the Bio RID and its FEA models.

In the graph of the FEA (Figure 101), a point of intersection between two adjacent trajectories can be found (e.g. TGT8 and TGT9). This is explained by the rotation of the vertebral body, where the leading node rises up more than the following node of each vertebral body. In Figure 100 this effect is not visible, since for this specific PMHS only the leading head of the marker could be tracked. Also it can be observed, that e.g. the C2 vertebral body in FEA (represented by TGT0 and TGT1 in Figure 101) shows the intersection at an earlier state than e.g. the C6 (represented by TGT9 and TGT10 in Figure 101). This behaviour can also be found in the graph for the PMHS 4 test configuration 3, where for example TGT0

and TGT1 intersect (Appendix 141). In this case TGT0 and TGT1 represent the tip and head of one marker tracked and the rotation of the vertebral body causes the same effect. Trajectories of all tests and relevant simulations can be found in Appendix 135 through Appendix 144. Unfortunately, the radiography of PMHS1 under the IIWPG loading without a head restraint, configuration 2, was not usable. Therefor no trajectories could be extracted for this test.

For easier comparison, the trajectories were transformed to relative movement graphs. In these graphs, only the relative movement of each tracked vertebral body (or target, where more than one target were tracked for each vertebral body), compared to the corresponding TGT0, is shown. In addition to the subsequent motion graphs, a theoretical circular trajectory with a radius of approximately 64 [mm] and 45 [mm] respectively, is given as reference.

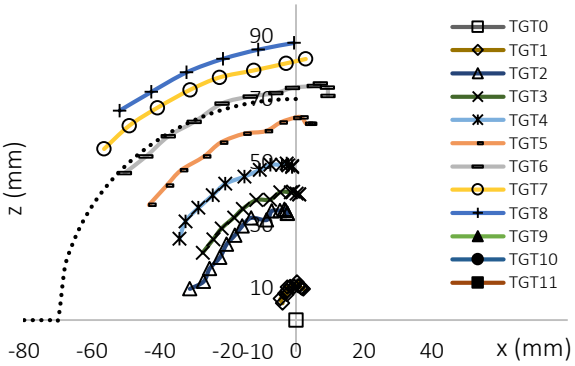


FIGURE 102 MOVEMENT OF VERTEBRAL BODIES OF PMHS 1 DURING SRA 24 KM/H PULSE WITHOUT A HEAD RESTRAINT

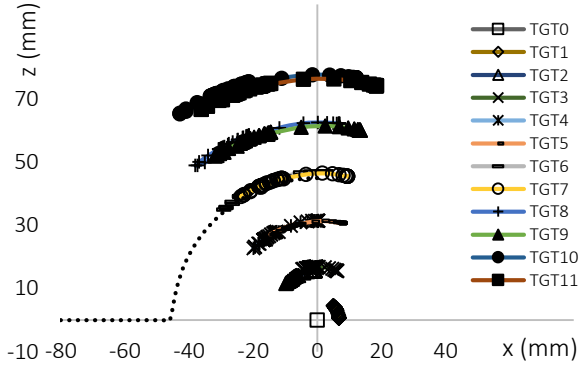


FIGURE 103 MOVEMENT OF VERTEBRAL BODIES OF FEA SIMULATION CORRESPONDING THE TEST IN FIGURE 102

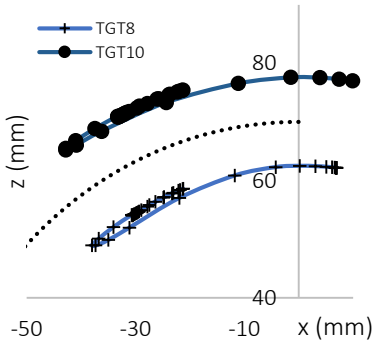


FIGURE 104 DETAIL OF THE "HOOK LIKE" REBOUND MOTION OF THE NODES TRACKED IN THE FEA ANALYSIS.

The movement of the vertebral bodies shows a circular like motion about the referenced target TGT0 for Figure 102 and Figure 103. In Figure 104 also parts of the rebound movement are displayed which causes a hook like shape of the single lines on the left hand side. This motion is not captured in Figure 102 since the PMHS' neck runs out of the picture area of the image intensifier before the rebound motion occurs. In addition, the absence of the head restraint for this test causes a very late rebound. However, the lines in graph Figure 102 and Figure 103 appear to follow a strict circular trajectory about the TGT0 in the C1 ($x = 0 | z = 0$) vertebral body, like the dotted circle of radius 70 [mm] indicated. All available motion graphs, for all PMHS and FEA analysed, are to be found in Appendix 145 through Appendix 154.

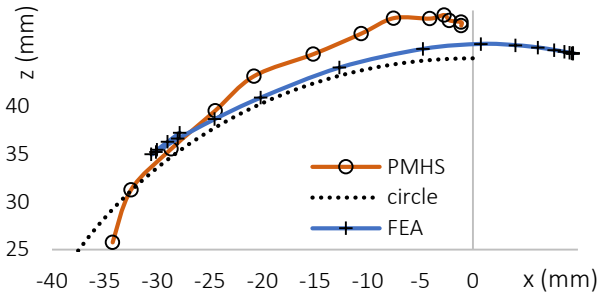


FIGURE 105 MOVEMENT OF ONE TARGET IN REFERENCE TO TGT0 FOR PMHS1 DURING SRA 24 KM/H PULSE WITHOUT A HEAD RESTRAINT COMPARED TO THE CORRESPONDING FEA.

Comparing the trajectory of one vertebral body in detail, e.g. one target at C4 like in Figure 105, little differences in the motion can be found. The trajectory of the FEA follows a motion very similar to the circle indicated as reference (dotted line radius 45 [mm]). The line of the PMHS on the other hand shows some deviations. Especially on the left end of the line, a variation form a circular trajectory can be found.

This deviation from the circular trajectory is caused by the changing neck curvature during the different phases of whiplash. In the first phase, the neck is in its natural posture ($r_0$) and shows its initial length. During the retraction, where the neck forms the typical s-shaped curvature, the radius ($r_1$) appears to "shorten." This continues into the extension phase ($r_2$) where the neck length also appears shorter than in its initial shape (Figure 106). This might explain the curve progression in Figure 105 for the PMHS graph. For the FEA this characteristic can not be seen to that extent.

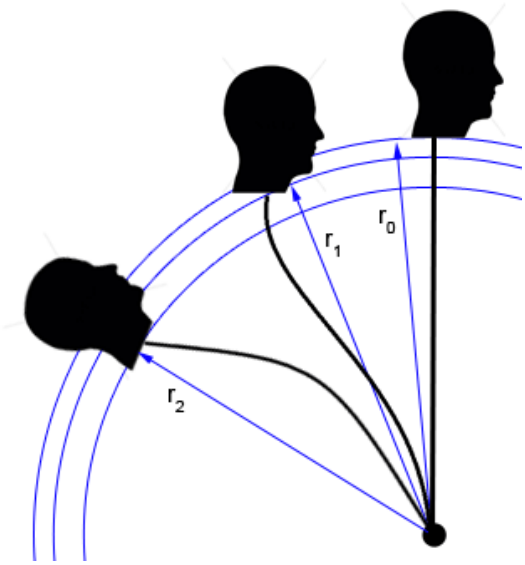


FIGURE 106 SCHEME OF CHANGING RADIUS DURING WHIPLASH IN DIFFERENT PHASES

This behaviour can also be observed in the following Figure 107 and Figure 108.

For these graphs, the distances between all targets of one PMHS test or FEA respectively were computed in reference to the TGT0. The distance of all targets in reference to TGT0 over time were calculated where D02 represents the distance between TGT0 and TGT2, D03 between TGT0 and TGT3 and so on, like illustrated in Figure 99. Furthermore the initial length at t = 0 [ms] (e.g. $\underline{D02}_{(t=0)}$ for TGT2 in Figure 99) of each distance vector was subtracted leading to a graph of relative length change over time.

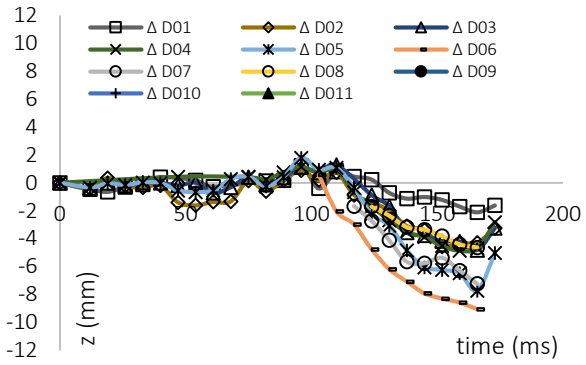


FIGURE 107 RELATIVE ELONGATION OF DISTANCE BETWEEN EACH TARGET AND TGT0 OF PMHS1 DURING IIWPG PULSE WITH A HEAD RESTRAINT IN PLACE

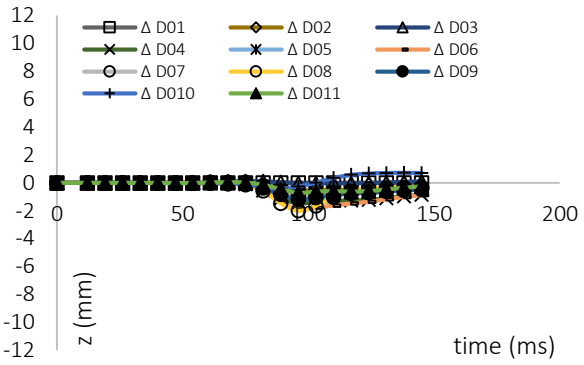


FIGURE 108 RELATIVE ELONGATION OF DISTANCE BETWEEN EACH TARGET AND TGT0 OF AN FEA DURING IIWPG PULSE WITH A HEAD RESTRAINT

Figure 107 shows some shortening around 50 [ms] and little elongation around 100 [ms]. Between 120 [ms] and 150 [ms] reduction of the distances for each target in reference to TGT0 can be found. Figure 108 shows hardly any elongation or shortening for the first 80 [ms]. After that ΔD02 through ΔD07 show length reduction. However, ΔD010 and ΔD011 after little shortening between 80 [ms] and 100 [ms] show a minor amount of elongation after 100 [ms]. This behaviour results from the rotational motion of the vertebral bodies of the virtual modelled cervical spine of the Eva RID model.

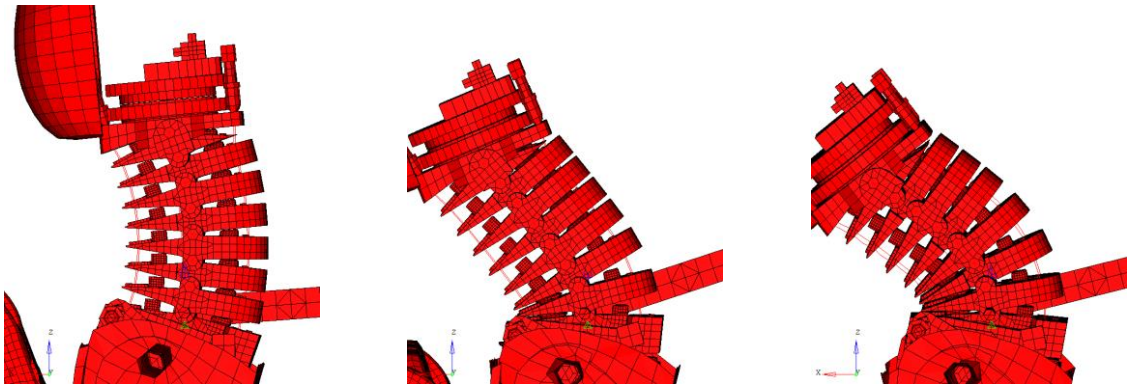

T = 75 MS T = 100 MS T = 125 MS

FIGURE 109 EVA RID NECK MODEL DETAIL UNDER WHIPLASH LOADING FOR THREE DIFFERENT TIME STEPS

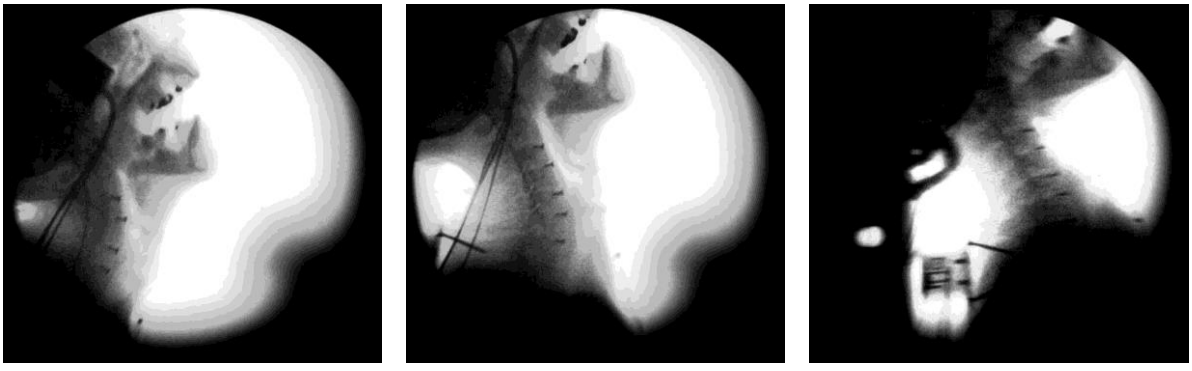

T = 75 MS T = 100 MS T = 125 MS

FIGURE 110 PMHS NECK DETAIL UNDER WHIPLASH LOADING FOR THREE DIFFERENT TIME STEPS

Looking at the above Figure 109 for t = 75 [ms] the Eva RID neck model appears to be in a shape very much like the initial position with hardly any deformation. The human neck in Figure 110 for t = 75 [ms] already shows a relatively large amount of extension. Comparing the two pictures for t = 100 [ms] a similar overall shape of the neck for the Eva RID and the human neck can be found. For t = 125 [ms] the shape of the cervical spine of the Eva RID model and human neck differ. Where the neck of the PMHS looks almost straight again, the neck of the Eva RID shows an s-shape. The Eva RID model shows large rotational displacements between C5 to C7. This amount of bending of the neck cannot be found for the PMHS in Figure 110.

Supplementary an FEA conducted with the Bio RID II model was compared. Interestingly but not unexpected, the virtual Bio RID II model, commonly used in vehicle seat development, shows a very similar behaviour in bony kinematics compared to the Eva RID model, as can be found in Figure 111.

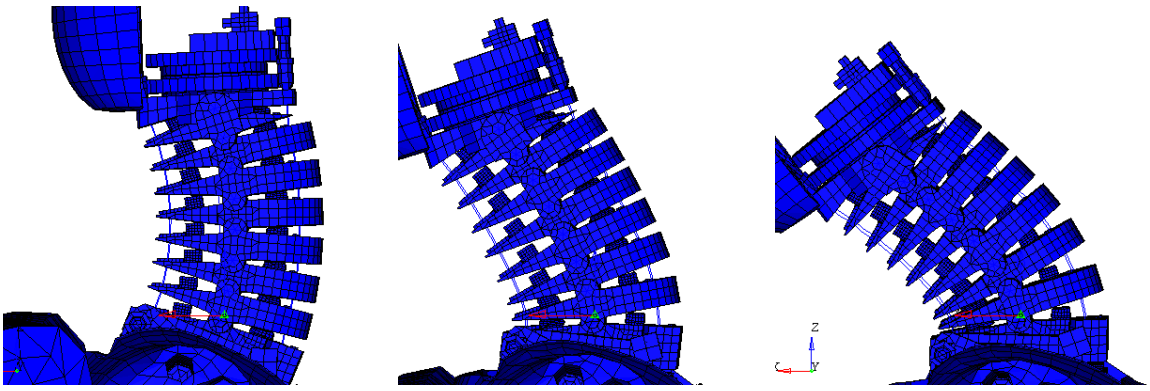

T = 75 MS T = 100 MS T = 125 MS

FIGURE 111 BIO RID NECK MODEL DETAIL UNDER WHIPLASH LOADING FOR THREE DIFFERENT TIME STEPS

The deformation and shape of the Bio RID II models' neck looks very much like the behaviour of the Eva RID model. In the following Figure 112 an overlay of the two virtual dummies is displayed. The pictures were scaled to the size of the Bio RID to be comparable. Shape and curvature of the cervical spine look similar. The neck of the Bio RID II seems bent back further, which might be explained by the larger inertia of the head and larger length of the neck. Nevertheless, especially at t =125 [ms] the rotational motions of the cervical bodies or the Bio RID model seems more homogeneous than those of the Eva RID neck. These deviations between male and female FEA may be caused by the differences in the rotational stiffness of the connections of the vertebrae, as well as the different rubber pad characteristics. Unfortunately a physical Eva RID dummy for validation is not available at the moment. Differences between the male and female virtual dummy model can be seen in Figure 112.

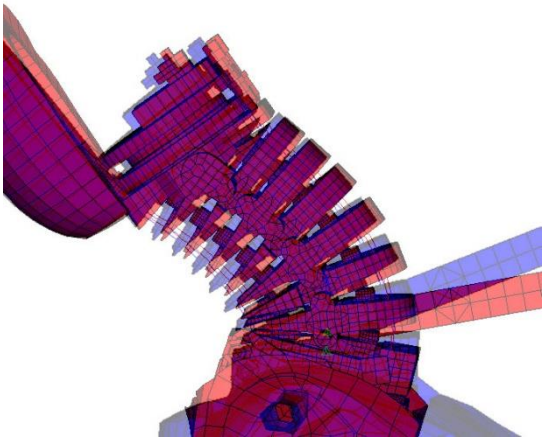

T = 125 MS
FIGURE 112 OVERLAY OF EVA RID AND BIO RID CERVICAL SPINE DEFORMATION

T = 125 MS
FIGURE 113 X-RAY PICTURE OF MALE PMHS UNDER THE SAME LOADING AS THE FEAS IN FIGURE 112

Looking at Figure 113 the shape of the neck differs for the PMHS tests and FEAs analysed in this study at t = 125 [ms]. It is believed, that the overly stiff characteristics of the Bio RID II thoracic spine (physical and virtual, and thereby Eva RID as well) may cause differences in the interaction with the seat back and thus generate such discrepancies.

## 6.4. Comparison of Hybrid III, Bio RID and Eva RID Simulations

The comparison of the simulations utilising the parametric simplified seat model and the three different occupant models H III, Bio RID II and Eva RID is shown in the following diagrams Figure 114 through Figure 117 and the kinematic comparison in Figure 118. For these simulations, the parametric seat was configured to correlate with the Euro NCAP test protocol (Euro NCAP, 2014). However, positioning and seating for the two dummy models H III and Eva RID, for which no protocols exist, was done to the best of knowledge.

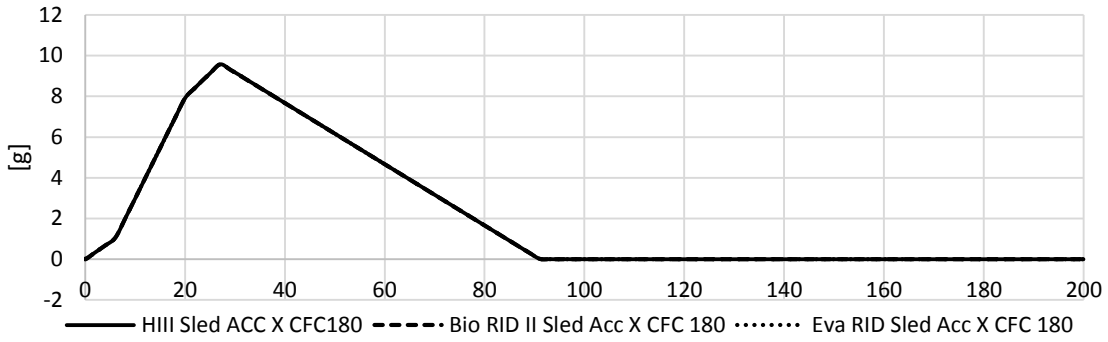


FIGURE 114 FEA HIII, BIO RID AND EVA RID SIMULATION, IIWPG 16 KM/H SLED X-ACCELERATION PULSE COMPARISON

The sled acceleration (Figure 114) shows perfect repeatability for all three load cases. Due to the generic simplified seat model and the fact that acceleration was prescribed, no deviation can be found.

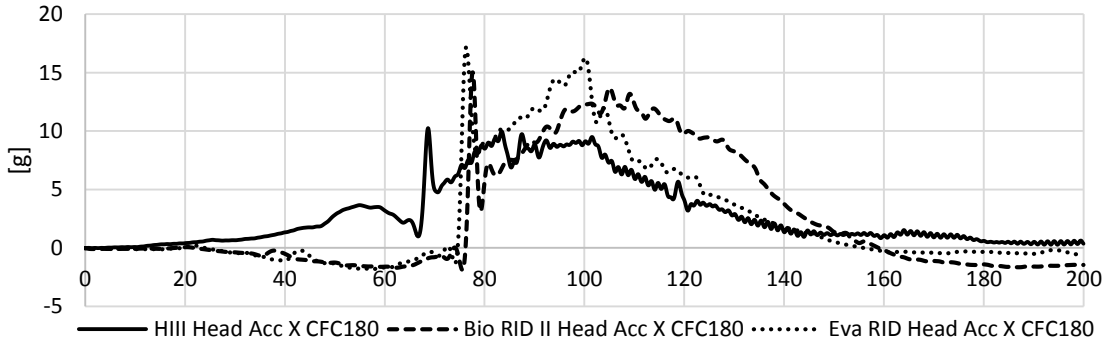


FIGURE 115 FEA HIII, BIO RID AND EVA RID SIMULATION, HEAD X-ACCELERATION COMPARISON

Figure 115 shows the head acceleration of the three different occupant models. Due to the higher stiffness of the neck of the H III, head acceleration starts to rise long before the head actually contacts (indicated by the peak of the solid line at around 65 [ms]) the head restraint at around 30 [ms]. This early head acceleration could also be found in (Matsuoka, et al., 2001). This behaviour is believed to be caused by the different structure of the neck. Almost at the same moment, head acceleration sets in for the Bio RID II and the Eva RID dummy models at approximately 75 [ms] after a minor negative head acceleration caused by rearward rotation of the upper torso (straightening of the thoracic spine due to the seatback contact). Even the initial peak is very comparable. The Eva RID however shows a higher peak for the initial spike, as also higher values for the period between 80 [ms] and 105 [ms]. The decrease starts earlier but lasts almost as long as for the Bio RID II dummy model.

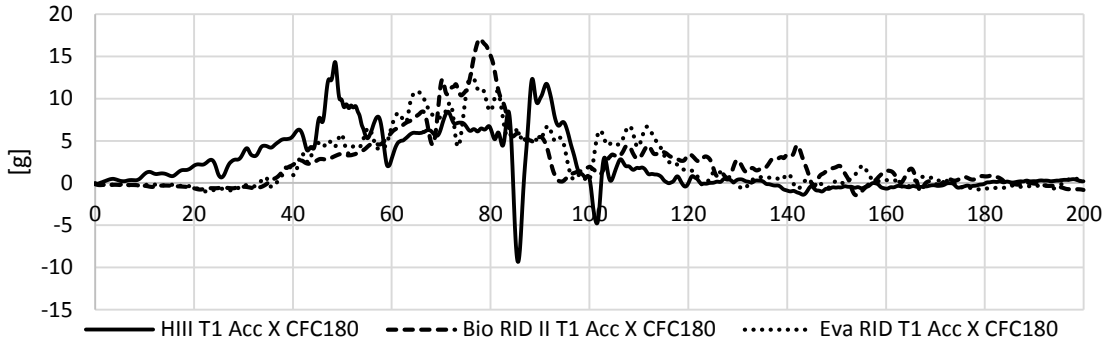


FIGURE 116 FEA HIII, BIO RID AND EVA RID SIMULATION, T1 X-ACCELERATION COMPARISON

In Figure 116 the graphs for T1 acceleration are shown. Bio RID II and Eva RID show a very comparable result for a long period of time. The maximum acceleration of the Bio RID II however is higher than for the Eva RID model. The H III again starts off earlier with the acceleration. The overall level for all three occupant models is however comparable. The stiff upper body of the H III however seems to cause a more noisy acceleration, even with an interruption of torso to backrest contact at around 85 [ms].

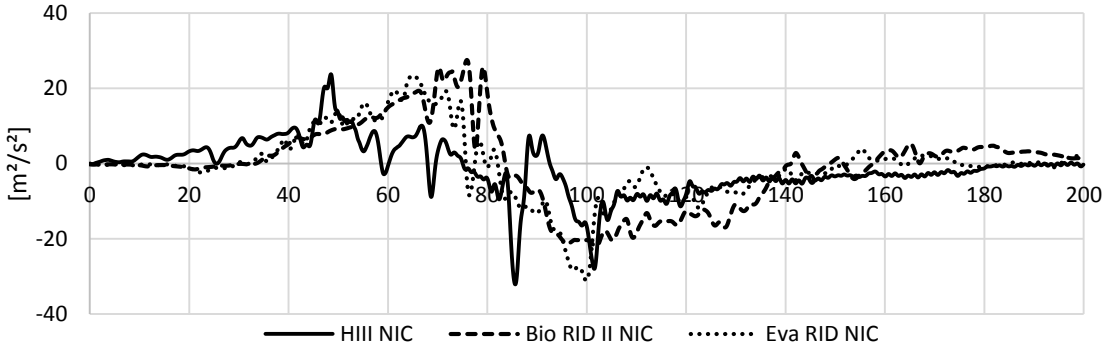


FIGURE 117 FEA HIII, BIO RID AND EVA RID SIMULATION, NIC CRITERION COMPARISON

Dependant on the already discussed T1 and head acceleration, Figure 117 depicts the computed NIC criterion for all three occupant models. Peak values for all three occupants are at a very comparable level. The timing of the NIC value however shows a very early maximum for the H III (~ 50 [ms]) where Bio RID II and Eva RID show this peak later. All NIC maxima seem to correlate with the T1 acceleration maxima very well.

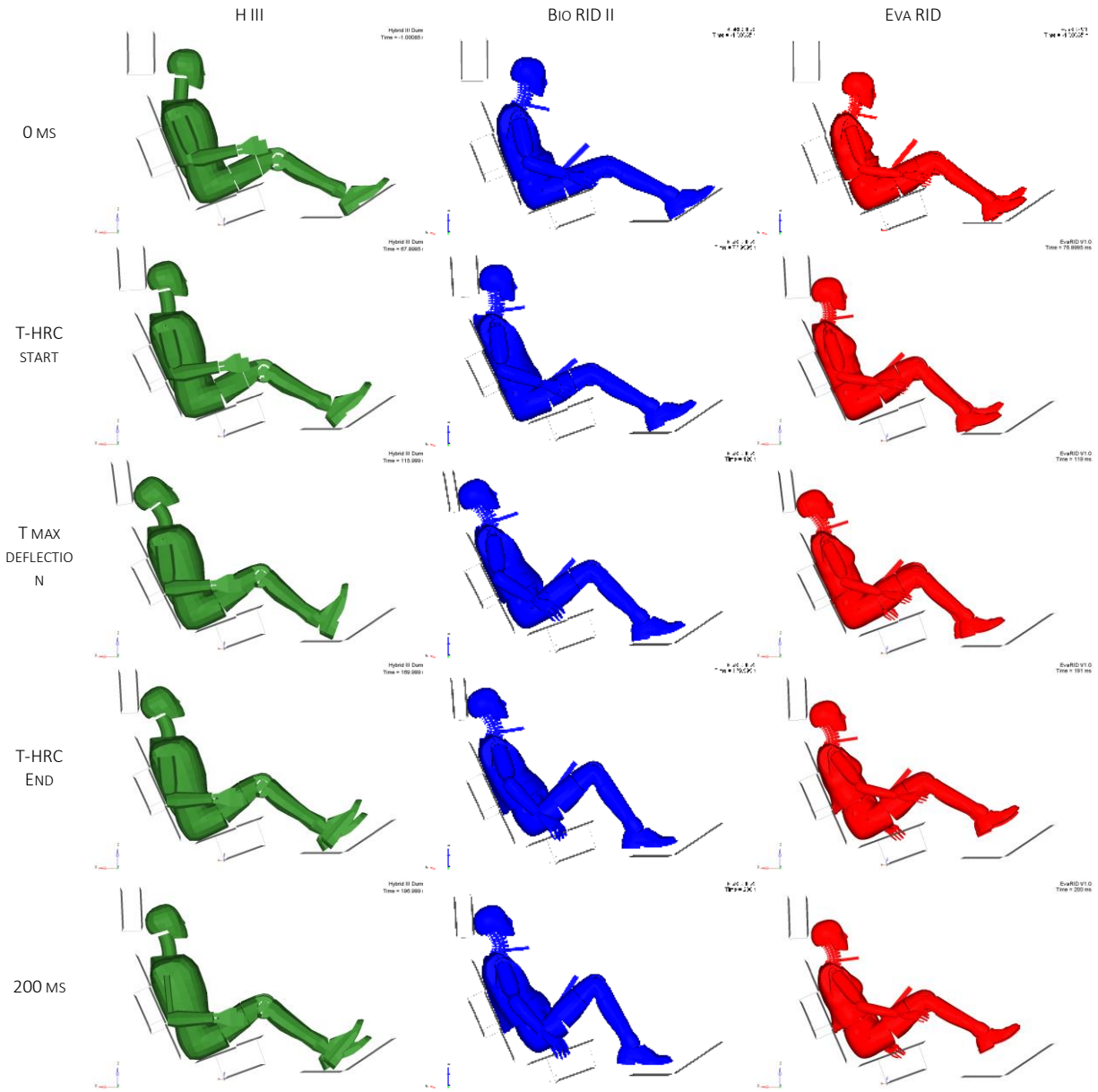


FIGURE 118 FEA HIII, BIO RID AND EVA RID SIMULATION, KINEMATIC COMPARISON

Figure 118 compares the three different occupant models at different time steps. The initial posture already reveals the difference between the H III and RID dummy models. Interestingly, the backset for the H III is smaller than for the two RID models. Comparing the neck and upper body of the three occupants, it becomes obvious, that the H III closes the gap between head and head restraint mainly by pushing back the backrest cushions and bending of the rubber neck. In contrast, the two RID models, additionally to backrest cushion and neck bending also deform their upper body regions. This is caused by the structured setup of the vertebral column which also causes a more natural behaviour during the neck and upper body bending.

## 6.5. Comparison of Eva RID and Bio RID Simulations

Several factors such as gender, age, acceleration level, seated posture, seat geometry, seat stiffness, configuration of adjustable seat components and so on influence the risk of WAD sustained during rear impact crash loadings. However these factors are not yet assessed in any current regulation or consumer test. All current tests represent a very narrow scenario with very little deviation for such adjustments.

In this comparison the influence of four parameters that could be represented with the available virtual model were investigated. Based on a basic comparison of (Gutsche, et al., 2012), these parameters are gender, acceleration pulse, backrest configuration and head restraint configuration. Simulations were set up using the two available occupant models (Eva RID and Bio RID II), three different acceleration levels (according to Euro NCAP), three different head restraint positions and three different backrest adjustments. Head restraint and backrest configurations were chosen to be in the range every vehicle occupant can adjust and influence. This led to 54 different configurations of one seat model (Table 39).

The results of these 54 simulations conducted utilizing the generic seat model, as shown in Table 46, Table 47 and Table 48, are difficult to interpret. Thus in the following Figure 119 through Figure 127 results are put into graphs for the medium severity pulse (Figure 17). For each Injury criterion computed, a distinct bar chart was generated. On the ordinate the particular injury criterion is plotted, where the abscissa distinguishes the different configurations of the seats' adjustable components. The abscissa classifies the three different settings of the backrest (forward, middle and backward). Furthermore each backset position is subdivided by one of the three possible head restraint position (high, medium and low). For each seat configuration, the value for the male (Bio RID II, blue) and female (Eva RID, red) occupant model is shown. Additional graphs for the low and high severity pulse can be found in Appendix A.4.

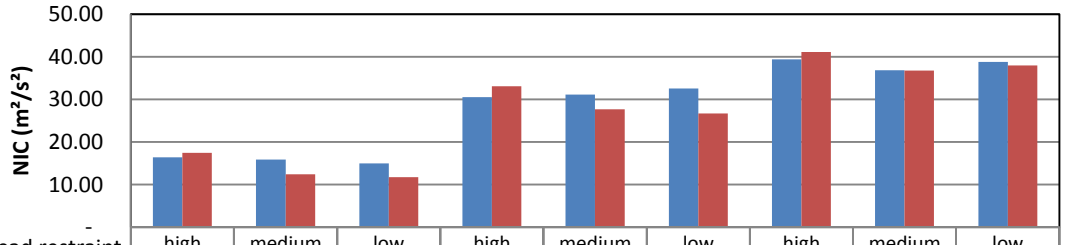


| head restraint | high | medium | low | high | medium | low | high | medium | low |
|---|---|---|---|---|---|---|---|---|---|
| backrest | forward | | | middle | | | backward | | |
| NIC male | 16.37 | 15.83 | 14.94 | 30.55 | 31.16 | 32.57 | 39.39 | 36.84 | 38.77 |
| NIC female | 17.45 | 12.38 | 11.69 | 33.08 | 27.66 | 26.68 | 41.10 | 36.74 | 37.98 |

FIGURE 119 GENERIC SEAT MODEL SIMULATIONS NIC MAXIMA FOR THE IIWPG 16 KM/H PULSE

Taking a closer look at Figure 119, a significant difference between the female and male occupants' models loading is hard to make out. Six of the configurations show a higher NIC value for the male model. The highest setting of the head restraint delivers the highest NIC value for each backrest setting for the female occupant model. Except for the backward backrest, a lower head restraint setting seems to benefit the outcome of the NIC criterion for the Eva RID. For the Bio RID II model, the position of the head restraint seems to be of lower effect. The main difference appears to origin from the positioning of the backrest, where obviously a forward backrest seems to be preferable. Nevertheless, the lowest NIC value could be found for the female occupant model in a configuration with a low head restraint and forward backrest position. This is also valid for all three acceleration pulses (Figure 16, Figure 17, Figure 18) like can be seen in Appendix A.4.

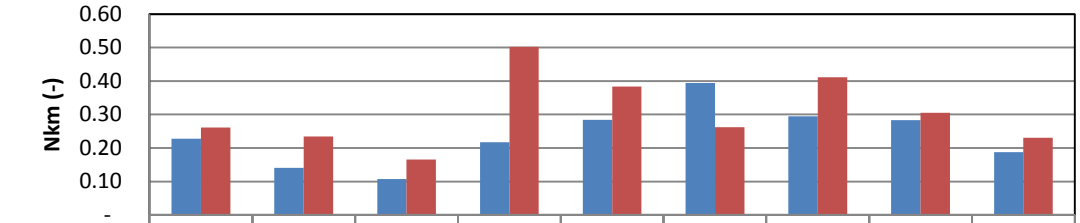


| head restraint | high | medium | low | high | medium | low | high | medium | low |
|---|---|---|---|---|---|---|---|---|---|
| backrest | forward | | | middle | | | backward | | |
| Nkm male | 0.23 | 0.14 | 0.11 | 0.22 | 0.28 | 0.39 | 0.29 | 0.28 | 0.19 |
| Nkm female | 0.26 | 0.23 | 0.17 | 0.50 | 0.38 | 0.26 | 0.41 | 0.31 | 0.23 |

FIGURE 120 GENERIC SEAT MODEL SIMULATIONS NKM MAXIMA FOR THE IIWPG 16 KM/H PULSE

Comparing results for the Nkm criterion in Figure 120, a greater sensitivity for different head restraint positions can be seen. For each backrest position of the female occupant, the Nkm value is highest for the high, and lowest for the low head restraint position. This behaviour could not be found for the male occupant model. Contrary, in the middle position configuration of the backrest, the lowest Nkm was found for the high head restraint position, where in the forward backrest situation, the lowest (and overall lowest Nkm) was found at the low head restraint configuration. Overall, the Nkm criterion is higher for the female than the male in eight out of nine configurations for the IIWPG 16 [km/h] pulse.

Looking at Figure 119 and Figure 120 it can be seen, that the NIC criterion appears to be more sensitive to the setting of the backrest, where the Nkm criterion is more influenced by the height of the head restraint.

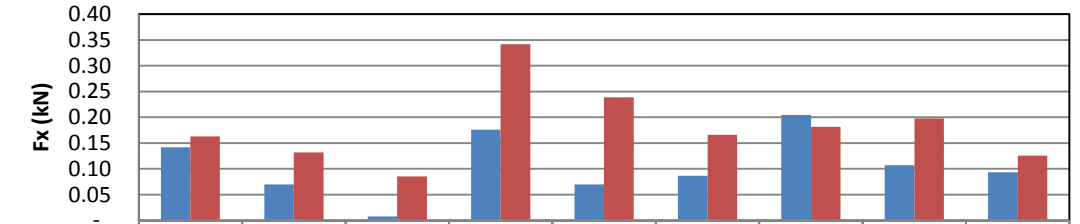


| head restraint | high | medium | low | high | medium | low | high | medium | low |
|---|---|---|---|---|---|---|---|---|---|
| backrest | forward | | | middle | | | backward | | |
| Fx male | 0.14 | 0.07 | 0.01 | 0.18 | 0.07 | 0.09 | 0.20 | 0.11 | 0.09 |
| Fx female | 0.16 | 0.13 | 0.09 | 0.34 | 0.24 | 0.17 | 0.18 | 0.20 | 0.13 |

FIGURE 121 GENERIC SEAT MODEL SIMULATIONS FX MAXIMA FOR THE IIWPG 16 KM/H PULSE

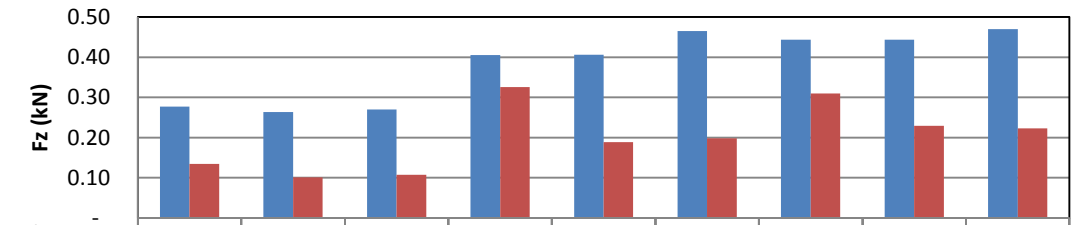


| head restraint | high | medium | low | high | medium | low | high | medium | low |
|---|---|---|---|---|---|---|---|---|---|
| backrest | forward | | | middle | | | backward | | |
| Fz male | 0.28 | 0.26 | 0.27 | 0.41 | 0.41 | 0.47 | 0.44 | 0.44 | 0.47 |
| Fz female | 0.13 | 0.10 | 0.11 | 0.33 | 0.19 | 0.20 | 0.31 | 0.23 | 0.22 |

FIGURE 122 GENERIC SEAT MODEL SIMULATIONS FZ MAXIMA FOR THE IIWPG 16 KM/H PULSE

Comparing shear (Figure 121) and tension (Figure 122) forces for the IIWPG 16 [km/h] pulse, opposing results can be found. Where shear is higher for the majority of the configurations for females (eight out

of nine), tension is higher in all nine configurations for the male occupant model. Again, the lowest values considering shear forces for both occupants can be found in the configuration with a forward backrest and the lowest possible head restraint position. The minimum tensile forces for both occupant models, like before mentioned criteria, can be found with a forward backrest. Just the minimum for the female occurs with the medium positioned head restraint, not the lowest which best benefits the male occupant again.

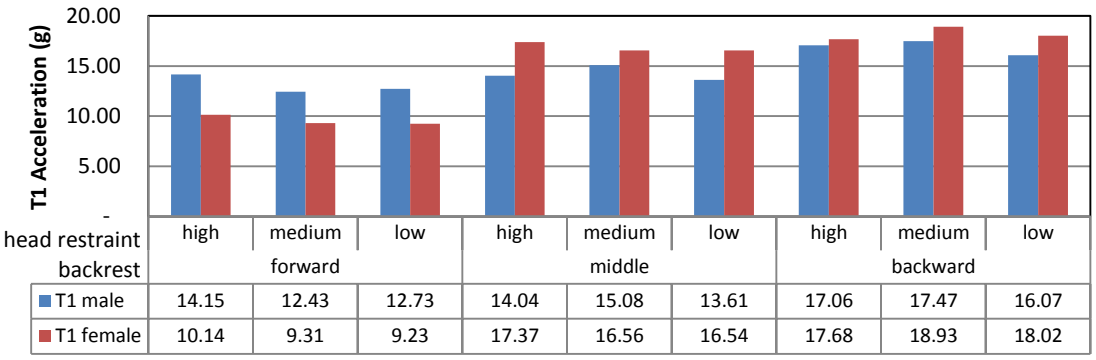


| head restraint | high | medium | low | high | medium | low | high | medium | low |
|---|---|---|---|---|---|---|---|---|---|
| backrest | forward | | | middle | | | backward | | |
| T1 male | 14.15 | 12.43 | 12.73 | 14.04 | 15.08 | 13.61 | 17.06 | 17.47 | 16.07 |
| T1 female | 10.14 | 9.31 | 9.23 | 17.37 | 16.56 | 16.54 | 17.68 | 18.93 | 18.02 |

FIGURE 123 GENERIC SEAT MODEL SIMULATIONS T1 ACCELERATION MAXIMA FOR THE IIWPG 16 KM/H PULSE

The T1 x-acceleration shows very little deviation for all configurations regarding the male occupant Bio RID II. Nevertheless, lowest values can again be found for a forward positioned backrest. More distinctly, the female Eva RID shows significantly reduced T1 accelerations for the forward backrest compared to all other configurations. The lowest value overall, like the NIC in Figure 119, is found for the female with a forward backrest and lowest possible head restraint configuration.

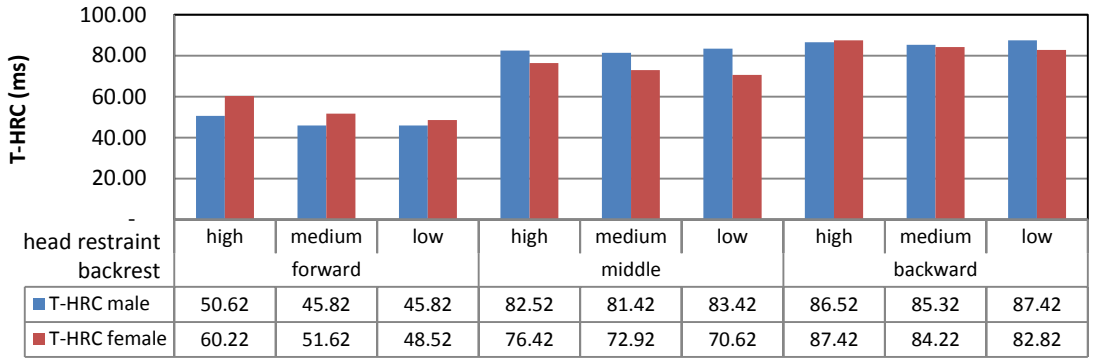


| head restraint | high | medium | low | high | medium | low | high | medium | low |
|---|---|---|---|---|---|---|---|---|---|
| backrest | forward | | | middle | | | backward | | |
| T-HRC male | 50.62 | 45.82 | 45.82 | 82.52 | 81.42 | 83.42 | 86.52 | 85.32 | 87.42 |
| T-HRC female | 60.22 | 51.62 | 48.52 | 76.42 | 72.92 | 70.62 | 87.42 | 84.22 | 82.82 |

FIGURE 124 GENERIC SEAT MODEL SIMULATIONS T-HRC MAXIMA FOR THE IIWPG 16 KM/H PULSE

T-HRC duration is longer for five out of nine cases for the male occupant model Bio RID II in the comparison in Figure 124. It can be found, that the forward backrest in general delivers the shortest T-HRC values. The overall minimum value is to be found for Bio RID II in a forward backrest with medium head restraint position. For the Eva RID model in any backrest configuration, the T-HRC improves the lower the head restraint is positioned. This behaviour cannot be found for the male Bio RID II model.

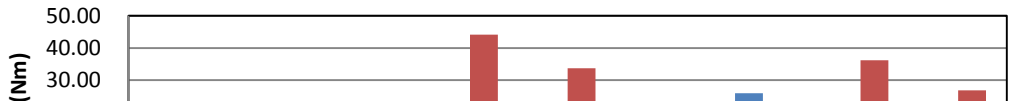


| head restraint | high | medium | low | high | medium | low | high | medium | low |
|---|---|---|---|---|---|---|---|---|---|
| backrest | forward | | | middle | | | backward | | |
| My-flex male | 20.09 | 12.41 | 8.87 | 19.15 | 11.17 | 11.36 | 25.94 | 16.59 | 16.56 |
| My-flex female | 22.97 | 20.63 | 14.60 | 44.18 | 33.74 | 23.09 | 10.34 | 36.23 | 26.87 |

FIGURE 125 GENERIC SEAT MODEL SIMULATIONS MY FLEXION MAXIMA FOR THE IIWPG 16 KM/H PULSE

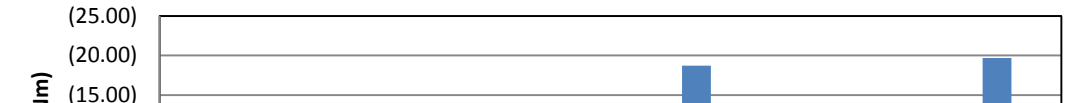


| head restraint | high | medium | low | high | medium | low | high | medium | low |
|---|---|---|---|---|---|---|---|---|---|
| backrest | forward | | | middle | | | backward | | |
| My-ext male | (2.00) | (1.95) | (5.11) | (7.55) | (13.50) | (18.71) | (6.52) | (13.46) | (19.70) |
| My-ext female | (1.60) | (1.56) | (1.70) | (1.37) | (4.30) | (9.31) | (6.26) | (4.86) | (4.87) |

FIGURE 126 GENERIC SEAT MODEL SIMULATIONS MY EXTENSION MAXIMA FOR THE IIWPG 16 KM/H PULSE

The neck flexion and extension moment are plotted in Figure 125 and Figure 126. For the two occupant models, flexion and extension show an opposite behaviour. Where flexion is larger in eight of nine cases for the Eva RID, extension is larger for all nine configurations for the Bio RID II. The minimum flexion moment again was found for the Bio RID II in the configuration with a forward backrest and most downward head restraint. The minimum extension in contrast was found for the Eva RID in middle backrest and high head restraint configuration. This interestingly is the configuration in which the flexion moment for the Eva RID reaches its maximum.


| head restraint | high | medium | low | high | medium | low | high | medium | low |
|---|---|---|---|---|---|---|---|---|---|
| backrest | forward | | | middle | | | backward | | |
| Nij male | 0.08 | 0.08 | 0.07 | 0.08 | 0.11 | 0.17 | 0.10 | 0.11 | 0.17 |
| Nij female | 0.09 | 0.08 | 0.06 | 0.19 | 0.14 | 0.09 | 0.08 | 0.13 | 0.10 |

FIGURE 127 GENERIC SEAT MODEL SIMULATIONS NIJ MAXIMA FOR THE IIWPG 16 KM/H PULSE

The Nij criterion is not a commonly used criterion to classify WAD. Nevertheless it is an established neck injury criterion and thus was included in this analysis. Again, for both occupant models, the minimum value can be found for the forward backrest and most downward head restraint configuration. For both

other backrest settings, the Nij for the male occupant reaches its maximum value. The overall maximum however is to be found for the Eva RID in the middle backrest and highest head restraint configuration.

The results of this comparison reveal, that the configuration of the backrest (forward, middle, backward) shows a significant influence on the loading of the occupant. This certainly is partially caused by the fact, that both, Bio RID II and Eva RID were solely designed for one specific backrest configuration. They are simply unable to accommodate to different seat back angles. However, the differing results for the three different seat back configurations indicate, that this factor influences the loading on the dummy significantly. Since the dummy models represent human occupants, this behaviour can be assumed to be equal in real word accidents.

Furthermore, the three different head restraint positions (high, medium, low) also show large influence on the different neck criteria measured for the occupant. The different heights can influence single criteria by factors of a few percent or even a hundred percent (e.g. Figure 125, My female). The following Figure 128 shows, how the head restraint position can affect the forces applied to the head.

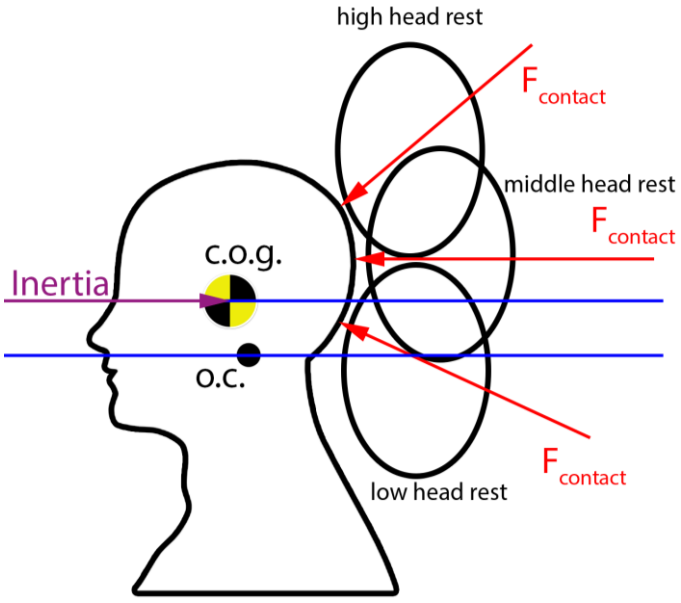


FIGURE 128 HEAD TO HEAD RESTRAINT CONTACT FORCE DIRECTION DUE TO HEAD RESTRAINT ADJUSTMENT

Due to the different contact points, not only the lever for moments, but also the direction of the force is changed. This can lead to different internal forces and moments at the occiput. Shear forces for example should be reduced, if the contact force reacts at the level of the c.o.g. and in line with the inertia force of the head. Results of these changes can also be seen in different graphs such as A.6.5.2 compared to A.7.5.2. The Bio RID II simulation shows only tension between 80 [ms] and 110 [ms] where the Eva RID is loaded with a significant amount of compression. Furthermore the different head restraint height can cause different contact conditions. Simulations with the Eva RID model and a high head restraint show, that the head can slip under structural components of the restraint und thus block the upward slipping of the dummy. Thereby a significant amount of force is generated due to the inertia of the upward movement of the torso which is blocked by a stuck head. This behaviour could not be identified in Bio RID II simulations, which suggests that the head restraint (height) is optimised for assessment scenarios. The comparison also shows, that various injury criteria show a different sensitivity to altered head restraint height positions. For example, the NIC criterion (acceleration based criterion) appears to be rather robust for different positions. Fx and also the Nkm criterion (force and moment based criteria) however are affected noticeable.

Complementary bar charts for the SRA 16 [km/h] and the SRA 24 [km/h] pulse results can be found in Appendix A.4. Similar tendencies can be made out for the additional loading situations, even though the female occupant model appears to react more pronounced to an increased level of acceleration pulse.

## 6.6. Neck Value – Seat Robustness Analysis

Comparing the large number of injury criteria for all available configurations for every occupant model and each acceleration pulse proved to be very challenging, thus a method was sought to achieve a comparison of different scenarios. Since the Euro NCAP configuration utilizing the IIWPG 16 [km/h] pulse is the test most widely used in consumer testing today, this was the scenario chosen to be the baseline for further assessment of alternative configurations. Results of the virtual investigations were thus compared using the NV. All criteria were equally weighted. (Gutsche, et al., 2013)

### 6.6.1. NV Results

Table 51 shows all available NV values for all 54 virtual sled tests performed. Additionally an indicator for better advantageous (+), disadvantageous performance (-) and similar performance (0) compared to the Euro NCAP IIWPG 16 [km/h] configuration are noted. Similar (0) is defined between 0.85 and 1.15. A NV equal or higher than 1.15 is considered disadvantageous (-) and a NV equal and lower than 0.85, advantageous (+).

| Occupant Model | Backrest Position | Head Restraint Position | Pulse | | |
|---|---|---|---|---|---|
| | | | SRA 16 km/h | IIWPG 16 km/h | SRA 24km/h |
| | | | | NV \| Perf. | |
| *Bio RID II* | Forward | High | 0.75\|(+) | 0.92\|(0) | 0.86\|(0) |
| | | Middle | 0.61\|(+) | 0.67\|(+) | 0.68\|(+) |
| | | Low | 0.58\|(+) | 0.54\|(+) | 0.67\|(+) |
| | Centred | High | 1.04\|(0) | 1.13\|(0) | 1.26\|(-) |
| | | Middle | 0.84\|(+) | 1.00\|(0) | 1.22\|(-) |
| | | Low | 1.03\|(0) | 1.19\|(-) | 1.59\|(-) |
| | Backward | High | 1.14\|(0) | 1.36\|(-) | 1.55\|(-) |
| | | Middle | 0.98\|(0) | 1.16\|(-) | 1.52\|(-) |
| | | Low | 1.08\|(0) | 1.22\|(-) | 1.77\|(-) |
| *Eva RID* | Forward | High | 0.72\|(+) | 0.95\|(0) | 1.08\|(0) |
| | | Middle | 0.61\|(+) | 0.81\|(+) | 0.81\|(+) |
| | | Low | 0.41\|(+) | 0.66\|(+) | 0.61\|(+) |
| | Centred | High | 1.32\|(-) | 1.82\|(-) | 1.98\|(-) |
| | | Middle | 0.99\|(0) | 1.41\|(-) | 1.59\|(-) |
| | | Low | 0.75\|(+) | 1.13\|(0) | 1.40\|(-) |
| | Backward | High | 1.37\|(-) | 1.46\|(-) | 2.09\|(-) |
| | | Middle | 1.02\|(0) | 1.28\|(-) | 1.83\|(-) |
| | | Low | 0.81\|(+) | 1.07\|(0) | 1.65\|(-) |

TABLE 51 NV COMPARISON OF NECK VALUES FOR ALL FEA ANALYSIS

The minimum NV for this particular seat with the male occupant model was found to be under the loading of the IIWPG 16 [km/h] pulse (male, forward backrest, low head restraint), not as may have been expected at the lower SRA 16 [km/h] pulse. The lowest loading for the female occupant model, however, could be determined under loading with what is referred to as the low severity pulse (SRA 16 [km/h]) at the configuration of forward backrest, low head restraint. This is also the overall minimum value causing a load of only 41 % of the basis value from the male Euro NCAP configuration with the IIWPG 16 [km/h] pulse to the (female) occupant model. Nevertheless, the maximum value was also found to be applied to the female occupant model at the configuration high severity pulse (SRA 24 [km/h]), backward backrest and high head restraint with a NV of 2.09, meaning that more than double the loading was applied to the neck of the occupant.

These results were plotted in a radar diagram Figure 129. Each axis of this plot represents one seat configuration. Thus in the case of additional adjustable components, more configurations could be added by adding extra axis. Of the different curves each one represents one occupant model exposed to one specific acceleration scenario.

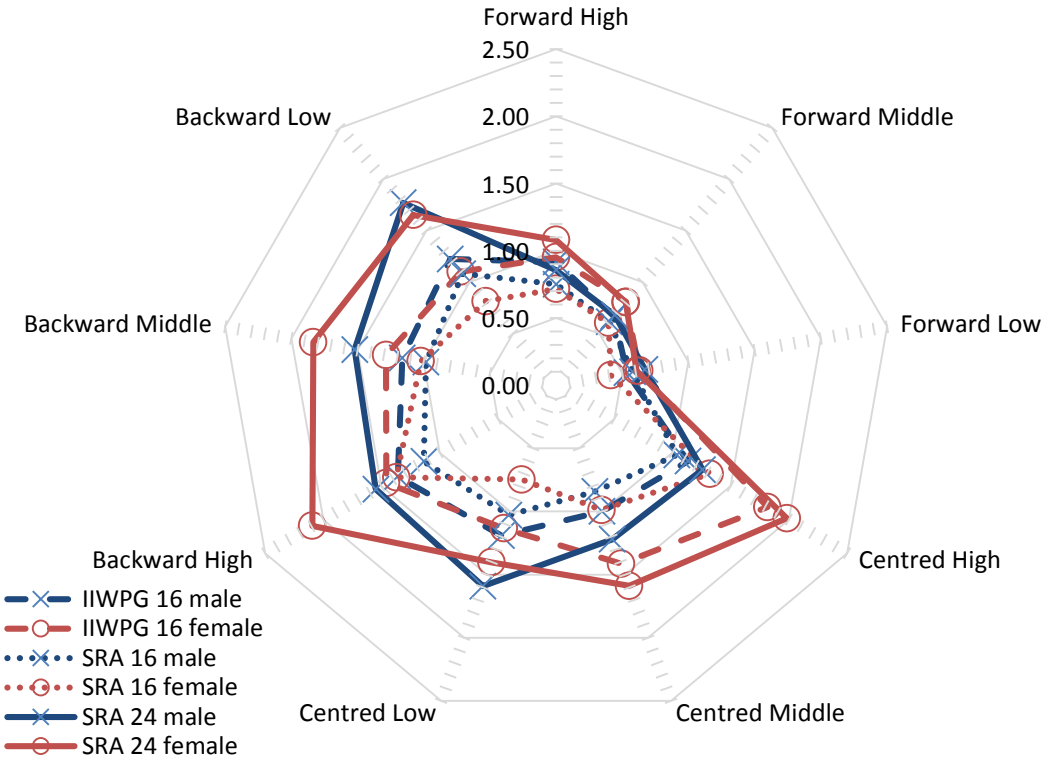


FIGURE 129 NV RADAR PLOT OF ALL CONFIGURATIONS ANALYSED

From this plot, it was assumed, that this particular seat appeared to be favourable in configurations with a forward adjusted backrest. Also it could be seen that the female occupant model is disadvantaged for high severity loading in almost any case. The less severe the acceleration pulse, the less distinct the gender dependency seemed to be for this particular seat.

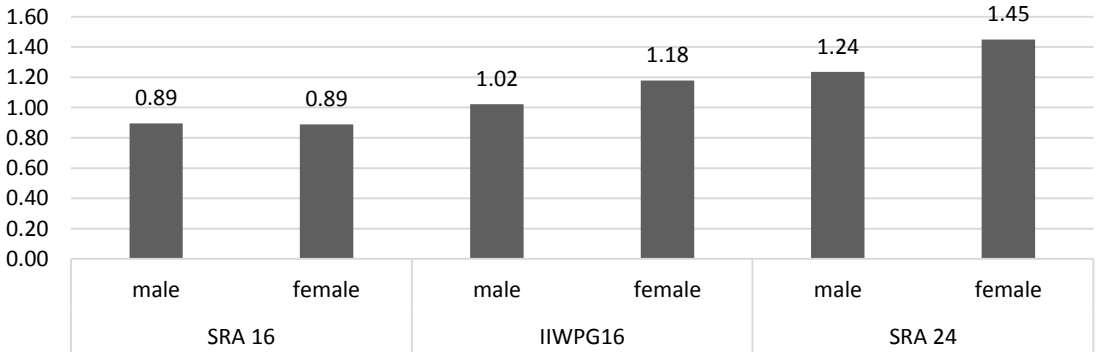


FIGURE 130 NV AVERAGE NV GROUPED BY PULSE SEVERITY AND GENDER

Figure 130 shows the average NV grouped by acceleration loading and gender. This chart also indicates, that the gender dependency of this investigated seat increases with severity of the acceleration pulse. Where the SRA 16 [km/h] pulse delivered an average NV of 0.89 for both occupant models, the

IIWPG 16 [km/h] and the SRA 24 [km/h] pulse showed a distinct increase for the female occupant models loading.

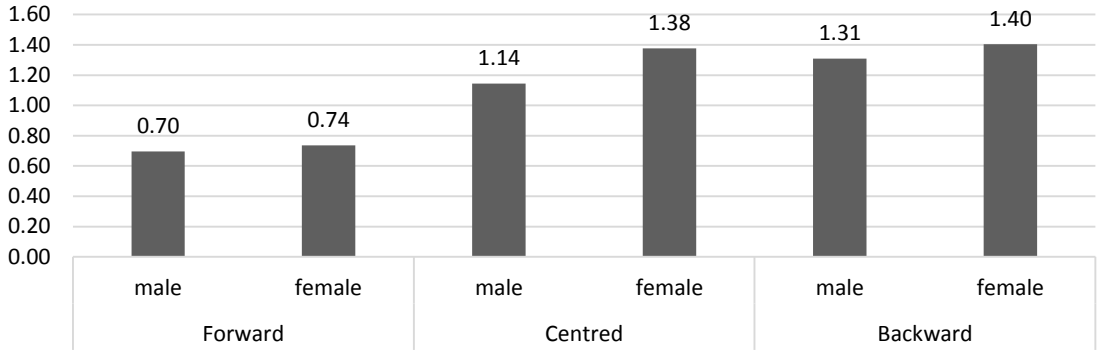


FIGURE 131 NV AVERAGE NV GROUPED BY BACKREST POSITION AND GENDER

Furthermore, grouping the results of the average NV by backrest position and gender (Figure 131) indicates, that the female occupant model is also sensitive to this parameter. For the forward backrest, both occupant models (Eva RID and Bio RID II) showed an NV on comparable level. The centred backrest indicated, that the females' response increased more with the more backward backrest, but the backward positioned scenario showed, that also the male occupant model is affected in a disadvantageous way by further backward backrests.

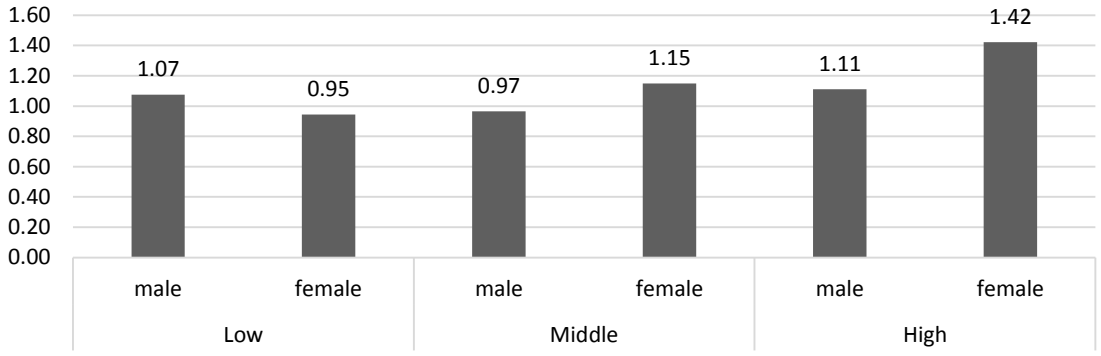


FIGURE 132 NV AVERAGE NV GROUPED BY HEAD RESTRAINT POSITION AND GENDER

In Figure 132 the average NV grouped by head rest position and gender can be found. It clearly pointed out, that for this particular seat, it does not make a large difference whether the head restraint is in a low middle or high position to the male Bio RID II occupant model. However, the female Eva RID does show a very significant increase of the average NV with an increasing head restraint height.

It must be kept in mind, that this is only a relative comparison of the actual seat and its performance in different adjustment scenarios (robustness), not a qualitative rating. The NV only describes the performance of a seat compared to the performance it delivers in the Euro NCAP IIWPG 16 [km/h] test.

Overall, the average NV for the male occupant model (1.05) and female occupant model (1.17), for all configurations considered in this task contributed to the opinion, that the female occupant is underprivileged in this present seat.

### 6.6.2. Including in Rating

Provided that the seat assessed delivered a “good” rating in a consumer test such as Euro NCAP, the following should be the goal for seat development.

A well designed, robust vehicle seat for rear impact crashes, with an equal protection level for all possible occupants (male, female, young, old, tall, short, light and heavy), for any available seat adjustment (backrest, head restraint, lumbar support, adjustable seat cushion and so on) under the loading of all acceleration levels and pulse shapes (consumer test pulses and real pulses) would achieve a NV for all scenarios of 1.0. The quality of protection would then be equal for all scenarios.

Certainly restrictions must be made with respect to available occupant models, currently used acceleration pulses and adjustable components of the seat. Extending the currently conducted testing to cover this entire range of possibilities would very likely outrun the available capacities (financially and technically). Thus an integration of virtual methods into current consumer testing should be considered. With the application of FEA a large range of possibilities would be available, such as virtually any acceleration level and pulse shape, all adjustable seat components, or even human body models as occupants like in Figure 133.

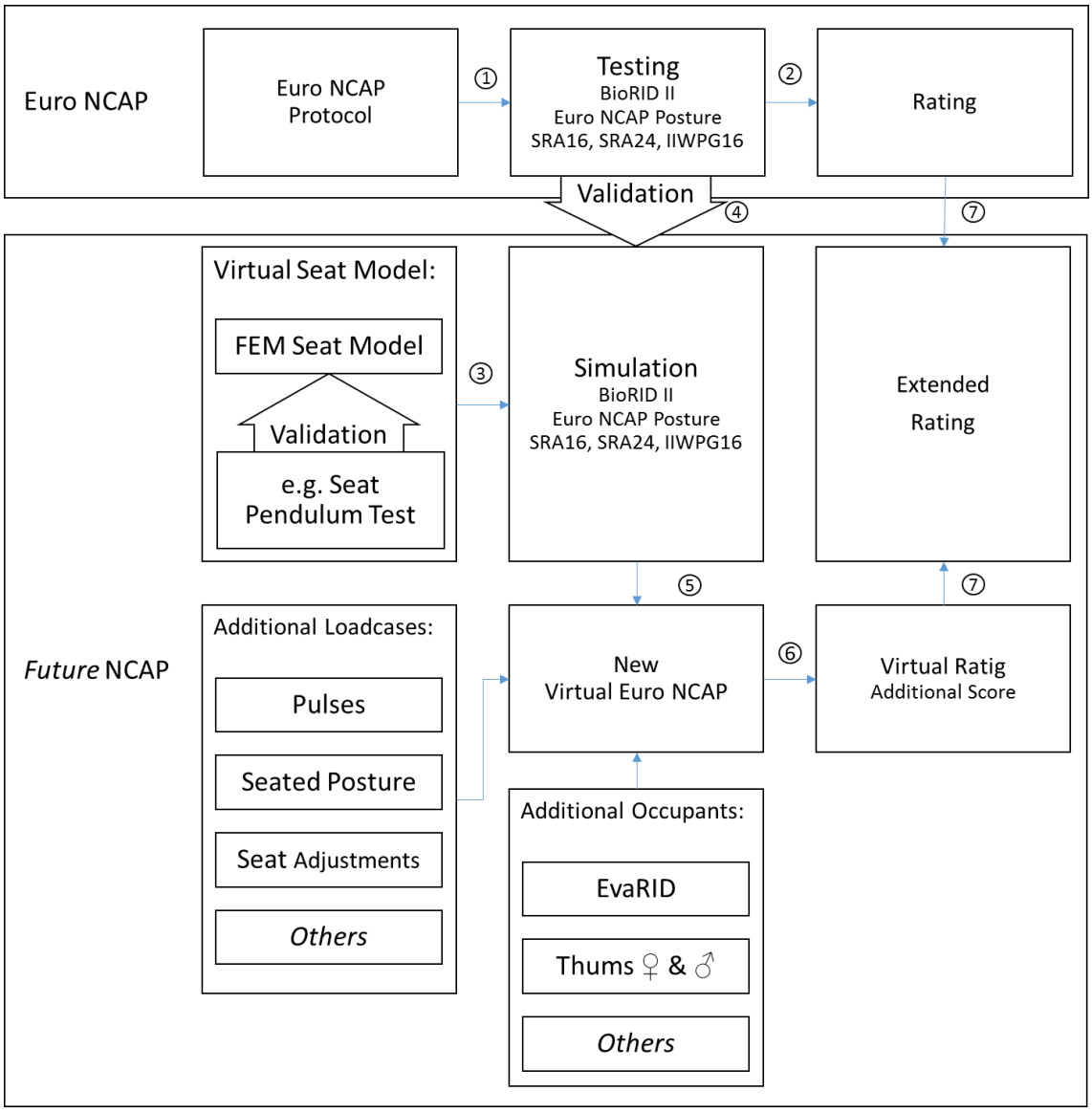


FIGURE 133 NV POSSIBLE INTEGRATION OF NV EVALUATION IN CURRENT EURO NCAP

## 6.6.3. Potential in Seat Development

Already mentioned in 3.2.3 one additional scenario, a simulation with the female occupant model Eva RID, in a seat with centred backrest and the IIWPG 16 [km/h] pulse was computed. Only geometrical changes to the head restraint were applied. The head restraint was put to the lowest possible position and further pushed forward translational to close the gap between head and head restraint.

| | [m²/s²] | [-] | [kN] | [kN] | [g] | [ms] | [Nm] | [Nm] | [-] |
|---|---|---|---|---|---|---|---|---|---|
| Simulation | NIC | Nkm | UpNeckSh | UpNeckT | T1Acc | T-HRC | OcMyFlex | OcMyExt | Nij |
| M122 | 31.16 | 0.28 | 0.07 | 0.41 | 15.08 | 81.42 | 11.17 | -13.50 | 0.11 |
| M222 | 26.68 | 0.26 | 0.17 | 0.20 | 16.54 | 70.62 | 23.09 | -9.31 | 0.09 |
| M22X | 6.88 | 0.13 | 0.01 | 0.07 | 15.06 | 30.00 | 17.60 | -10.95 | 0.10 |

TABLE 52 FEA IIWPG 16 KM/H GENERIC SEAT SIMULATIONS RESULT POTENTIAL IN SEAT DEVELOPMENT

Like in Table 52, which is coloured according to the description in Chapter 5, can be seen, the slightly modified setup (M22X) decreased loading on the female occupant model significantly. The setup M22X (Figure 50) represents a configuration with significantly reduced backset not achievable by normal adjustability of the used seat model. For comparison the female simulation result of the configuration with a centred backrest and middle positioned head restraint (M222) is additionally shown in Table 52. As can be found in Appendix A.7.10, the acceleration loading on head and T1 for the modified seat are very similar, thus a very low NIC value is generated. Also the force levels were low, just like the moments.

Calculating the NV (0.5) for this particular case shows a reduction of loading of 50 %. This is the lowest NV for all IIWPG 16 [km/h] simulations (male and female occupant model, forward, centred and backward backrest, high, medium and low head restraint position) performed.

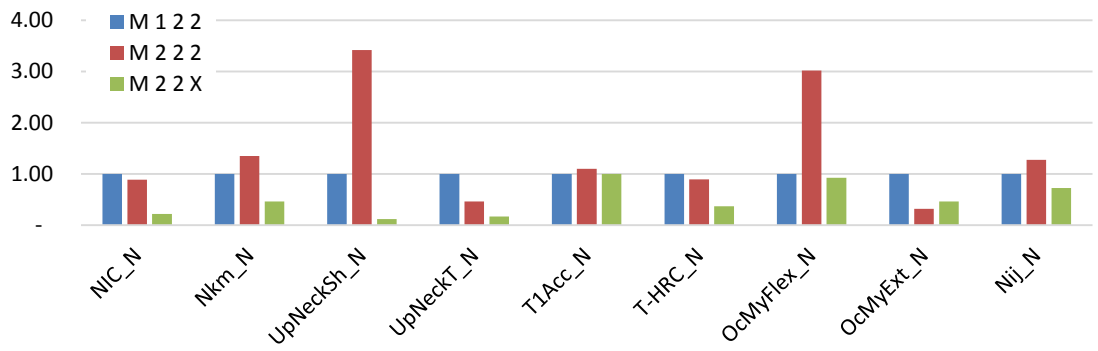


FIGURE 134 POTENTIAL OF FAVOURABLE SEAT CONFIGURATION FOR THE EVA RID MODEL; NORMALISED NECK INJURY CRITERIA FOR M122, M222 AND M22X CONFIGURATION

Figure 134 shows a comparison of all criteria investigated in the virtual sled test study relative to the normalised results for the Bio RID II model results in the Euro NCAP configuration under the IIWPG 16 km/h pulse loading. The bar-chart shows Neck Values for the Bio RID II (all unity) in its Euro NCAP configuration (blue), the Eva RID in the same configuration (red) and the Eva RID in a modified configuration (M22X) like described in Figure 50 (green) under the IIWPG 16 [km/h] pulse. It clearly points out, that the Eva RID in an unmodified or even only not properly adjusted vehicle seat bears with substantial larger shear forces and flexion moments. A significant increase for the NIC value and the T1 x-acceleration cannot be found, just like for the extension moment and tension force.

Considering the adapted seat (green), a reduction for all values can be achieved.

# 7. DISCUSSION

## General Factors

Rear-end collisions are one of the most common accidents in today's traffic. These crashes occur at relatively low velocity changes (typically < 25 [km/h]). The fatality rate in these kinds of accidents is very low, however, rear-end collisions can result in Whiplash Associated Disorders. The majority of those experiencing initial neck symptoms as a result of a low severity impacts recover within a few weeks or months after the crash. However, 5–10 % of individuals experience different levels of permanent disabilities. About 5 % of all WAD victims sustain a permanent degree of disability of at least 10 % while 1.7 % are signed off work permanently due to WAD. Such permanent cases of WAD are an immense burden on victims and their surroundings. Within the European Union (EU 27), according to (Linder, et al., 2013), an estimate of more than 800,000 victims suffer WAD resulting in insurance and other social costs of approximately €10 billion annually (e.g. Italy € 2.4 billion, Germany € 0.5 billion, Sweden € 0.46 billion, UK € 3.5 billion, US $ 29 billion (Norra K, 2005)).

Real world accidents and analysis of insurance data have shown, that whiplash associated disorders appear to be a larger threat to female occupants than males. Numbers vary, but statistics indicate an increased risk up to three times higher than for males. (Kihlberg, 1969); (O'Neil, et al., 1972); (Thomas, et al., 1982); (Otremski, et al., 1989); (Maag, et al., 1990); (Morris, et al., 1996); (Dolinis, 1997); (Temming, et al., 1998); (Richter, et al., 2000); (Chapline, et al., 2000); (Krafft, et al., 2003), (Jakobsson, et al., 2004b); (Jonsson, 2008); (Storvik, et al., 2009).

## Previous Findings

Literature concerning this topic indicates that vehicle seat designs nowadays are capable of delivering a reasonable level of protection, if designed well. This certainly also includes all different kinds of active, and passive whiplash protection systems which are available today. Nevertheless, comparing the current test results of assessments (e.g. Euro NCAP), where most seats reach high scores, and the protective improvements in real accident scenarios (accident statistics) of newer improved seats, the risk reduction for WAD is not as high as would be expected. Considering that whiplash is the single most common and costly occupant injury, other results would be desirable.
Kullgren et al. (Kullgren, et al., 2010) found that newer whiplash protection systems seem to bring less improvement for females than for males. It appears, that the protective properties of vehicle seats are focused on a small number of load case scenarios, which not surprisingly, all consider a very narrow scope of adjustments for seat components and furthermore only one occupant model and size. Complementary to legislation and regulations with regard to collision safety, vehicle safety is assessed in consumer tests such as the New Car Assessment Programme (NCAP). For Europe, the Euro NCAP conducts consumer tests, where the whiplash score is part of the overall rating. Currently whiplash tests are performed with the 50th percentile male occupant model Bio RID II (Euro NCAP, 2013). At present, Euro NCAP rates the performance of car seats during rear-end collisions by conducting one static and three dynamic tests for the front row seats. Second and third row seats are assessed by static measurements only (Euro NCAP, 2013). In addition, car and car component manufacturers today also develop and evaluate new designs of seats by performing finite element methods. For this purpose, the Bio RID II dummy model and virtual seat models are used. All these investigations however are currently focused on the $50^{th}$ percentile male occupant model. Since high rating scores in current assessments (e.g. Euro NCAP) appear to not be a guarantee for adequate improvements in real world accident whiplash injury risk, this thesis' focus was put on deviations from such assessments. Investigations were carried out to show deviations from the Euro NCAP test cases

affect the loads and injury criterion outputs for available and new occupant models. Besides the gender aspects (female and male occupant) modifications to seatback, head restraint and seated posture were looked into. The configurations were chosen to be within the range of variations that occur when drivers and passenger move in the vehicle during typical normal every day driving conditions. These comparisons were carried out by means of testing and computational modelling, involving sled testing with dummies and PMHS as well as FE-simulations using female and male size rear impact dummy models.

## New Developments

With the availability of the Eva RID dummy model, it was possible to include a second occupant model, representing the 50$^{th}$ percentile female (Carlsson, et al., 2012b). The lack of regulations or assessments demanding other occupants than the Bio RID II currently prevents or at least reduces its use to a minimum. The Eva RID and Bio RID II virtual model simulations showed a similar behaviour of the two models. This was not unexpected because the Eva RID model is a downscaled virtual model of the Bio RID II. Looking at the outcome of these simulations, it can be concluded, that the female virtual occupant model Eva RID has to bear with higher loads. The NV value for the female was found to be more than 100 % higher than for the male model (comparison of all Eva RID simulations with the male baseline simulation M122 applying the IIWPG 16 [km/h] pulse). Looking at the comparison of all male and all female configurations, increased loading for the female model in the majority of all configurations can be found. For example, comparing the male baseline configuration M122 with the female counterpart M222, the NV values are 1.00 (baseline) for the male and 1.41 for the female simulation respectively. Also investigating the different influencing factors such as pulse intensity, backrest position or head restraint position, a higher sensitivity of the female compared to the male occupant model could be found. Comparing two pulse sensitivities, the “low” and “high” severity pulse for both gender occupant models in the same seat configuration, the male shows an increased NV value of 45 % (L122/H122) where the females’ loads are 59 % (L222/H222) higher. This seems to verify, that females show a higher sensitivity to higher pulse intensities (Temming, et al., 1997).
Comparing two configurations utilising the Euro NCAP high severity pulse (e.g. H131 male vs. H231 female) the NV values show higher loads for the female (2.09) than the male (1.55). It can be found, that the high positioned head restraint shows a more distinct influence for the loads on the female neck than the male. By lowering the head restraint to its lowest possible position (H133 male and H233 female), the NV value for the male increases from 1.55 (H131) to 1.77 (H133) where for the female it decreases from 2.09 (H231) to 1.65 (H233). Using both male and female dummy models and the adjustable components of a seat (in this case head restraint and backrest), a significant influence on the loads on occupants’ necks could be shown. All parameters included (occupant model, pulse intensity, head restraint and backrest configuration) influence the load on the particular occupant. However, it appears, that in general a more forward backrest position benefits the protective capabilities in this series of simulations (Figure 129), regardless of the occupant model (gender). Furthermore, a generally “high” positioned head restrained is not always preferred. Especially the female occupant model showed higher loads with higher head restraint positions (H231 vs. H233). It must however be kept in mind, that “low” in this case means lowest possible configuration of the seat. The head restrain is still in a position with the top of the head restraint above the top of the head of the female occupant model. Thus it can be concluded, that this seat is not designed to meet the height requirements of a 50$^{th}$ percentile female or smaller occupant. Rather to a “high”, a well-positioned head restraint should be preferred. This means the restraint should be able to support the head at the level of its c.o.g.
Supplementary in one additional seat configuration (M22X) utilizing the female occupant model, it could be proven, that with a suiting configured seat (Figure 50), loading for the female occupant model can be reduced far below what was immanent during any other seat configuration.

## Seat Robustness

Simulations in this study were limited to one available virtual seat model and the two occupant models Bio RID II and Eva RID. In order to be able to draw a more general conclusion on this topic, more seat models should be investigated. Dependent on the seat models, further adjustability options should be considered in simulations and seat testing, including more detailed and smaller increment adjustments (i.e. tilting of head restraint, lumbar support, etc.). Furthermore, no general seating procedure for female occupant models, such as the virtual Eva RID dummy model is currently available. Thus presumptions had to be made.

This leads to the hypothesis that the introduction of additional occupant sizes, and different seat adjustment configurations would be beneficial if considered in protection development of vehicle seats. It would offer a better coverage of the range of variation that is present in real world accidents and result in more robust seat designs.

In a series of experimental sled tests with the state of the art Bio RID II dummy, everyday situations with varying seat adjustments were investigated. This series of tests revealed, that small adjustment modifications to components that occupants are able to influence by just using the available comfort adjustments in modern seats, result in large variation of protective capabilities of seats. These results confirm what could be shown in the FEA already. Current seats are well designed to provide a certain amount of protection for one occupant model in one seat adjustment configuration.

Unfortunately the lack of dummies representing other occupant sizes than a $50^{th}$ percentile male currently brings restrictions to the experimental testing. A physical counterpart of the virtual Eva RID does not exist at the moment thus a comparison of the virtual Eva RID (Linder, 2011) model with a physical Eva RID dummy (Carlsson, 2012c) (Chang, et al., 2010) is impossible. Only the roughly adapted Bio RID 50F could be utilised in a first step for comparison. This comparison showed a surprisingly good correlation between the virtual Eva RID and the roughly adapted Bio RID 50F. Results of the physical sled tests showed a very good repeatability of the prototype dummy tests.

## Current Limitations

The currently established Bio RID II is limited to straight forward facing positions. Numerous studies on WAD, such as (Jakobsson, et al., 2004a), (Jakobsson, et al., 2008) or (Kaale, et al., 2005) state, that head rotation, inclined head positions and other situations differing from straight forward positions increase WAD risk. Even if additional dummy sizes (e.g. $50^{th}$ percentile female) were implemented, these issues could not be addressed. Such cases cannot be investigated with either, the currently available male or female rear impact dummies or virtual models. Additionally all these scenarios do not consider, that whiplash is not only an issue caused by rear end impacts. Other impact directions do not get much attention when assessing whiplash, even with studies such as (Cappon, et al., 2003) that proved WAD to also be a problem in frontal impacts. For a more profound investigation of such scenarios, different methods and tools must be implemented. HBM (e.g. THUMS) might have the potential to predict loads and risk in such cases. Even if human body models were to be implemented to cover scenarios with rotated or inclined head positions, comparison between results for dummy models and HBMs might prove to be difficult.

## Criteria Sensitivity

Without knowing the cause for single WAD symptoms, it might be difficult to identify which criterion to further investigate. In this thesis, it could be shown, that different injury criteria show different

sensitivities to certain factors (chapter 6.5). For example, the female occupant model shows a large sensitivity for forces (Fx) and moments (My) dependent on the height of the head restraint. The virtual investigations M221, M222 and M223 (only differing in head restraint height) show a range for Fx from 0.34 [kN], 0.24 [kN] to 0.17 [kN] from a "high" to a "low" head restraint position. The comparable male simulations (M121, M122, M123) result in Fx values 0.18 [kN], 0.07 [kN] to 0.09 [kN]. The absolute values are lower than for the female, but also the change with an altered head restraint position is not as significant (Figure 121). Resulting from these values, the Nkm and Nij criteria are influenced to a similar extent. Nkm for the female occupant model for instance ranges from 0.50 [-], 0.38 [-] to 0.26 [-] for M221, M222 and M223. The male counterparts (M121, M122, M123) contrary show an increase with lower head restraint height (Nkm 0.22 [-], 0.28 [-], 0.39 [-]) (Figure 120). The Nij behaves very similarly.
My also shows a dependency on head restraint height. Male and female occupant model both show an increase in flexion moment with a higher head restraint position but a reduction of the extension moment (e.g. M121, M122, M123 male and M221, M222, M223 female in Figure 125, flexion and Figure 126 extension). Absolute values are higher for the female than for the male in flexion. Extension moment values on the other hand are higher for the male occupant model.

Looking at the NIC criterion, the height of the head restraint seems to be of minor importance. The change in backrest positioning however does show a significant influence. For both occupant models (Eva RID and Bio RID II) the forward backrest configuration leads to lower NIC values than a more backward backrest position. Values for the female configurations M212, M222 and M232, only differing in backrest position, show NIC values 12.38 [$m^2/s^2$], 27.66 [$m^2/s^2$] and 36.74 [$m^2/s^2$]. The comparable male configurations M112, M122 and M132 result in very comparable NIC values 15.83 [$m^2/s^2$], 31.16 [$m^2/s^2$] and 36.84 [$m^2/s^2$]. Surprisingly the absolute values for the male occupant model are higher for all these configurations. However the increased NIC value with a further backward positioned backrest is very similar (Figure 119).

The NIC criterion, based on (Boström, et al., 1996) is computed using acceleration values only. It is dependent on relative acceleration between the head and upper torso. In several PMHS tests, relevant pressure drops can be found before the head contacts the head restraint. Furthermore, tests without head restraints also show these negative pressure peaks. In some cases they occurred as early as 20 [ms] to 40 [ms] after T0 (e.g. Appendix A.3.3 or A.3.4) and show a similar timing with a peak value in NIC. The early occurrence of these peaks indicates, that the NIC is more sensitive to acceleration levels than to e.g. delta-v. It also indicates that before head rest contact, a significant pressure drop may occur in the cervical spinal canal. Furthermore results in animal testing (Svensson, et al., 1993) it could be shown, that a higher acceleration, regardless of delta-v resulted in higher pressure drops and in principle also a higher NIC.

Results show, that different criteria (e.g. NIC and Nkm) are influenced by different factors. This behaviour is understandable when considering, that NIC is based on acceleration where Nkm is based on forces and moments. Studies like Curatolo et al. (Curatolo, et al., 2011) suggest different possible causes for WAD. Different injury criteria may be able to predict different causes and mechanisms that potentially cause WAD. The NIC criterion for instance is believed to be an indicator for disorders caused by damage to the dorsal root ganglia caused by loading from liquid-inertia induced pressure-gradients. The Nkm contrary could be more relevant when considering facet joint related issues, as well as shear or tension induced injuries. It is however not in all cases identified which injury criterion correlates with which injury mechanism. With this insight, the question at stake is whether or not improvements should be made to reduce either of the two injury criteria, especially since they do show divergent results. A reduced NIC can potentially lead to an increased Nkm and vice versa. Also both criteria are included in assessments such as the Euro NCAP. Thus development to increase

performance for both, the NIC and Nkm for a variety of occupant sizes and seat adjustments are challenging.

## Female Aspects

The Eva RID model, represents a 50th percentile female and was developed within the ADSEAT project. Its performance was compared with volunteer tests with females. Validation at higher speed levels, i.e. Euro NCAP whiplash testing, was not available as they were judged to be too risky for the volunteers. Thus PMHS tests under the IIWPG 16 [km/h] and SRA 24 [km/h] were conducted and compared with the Eva RID model. The kinematics of the vertebral bodies compared showed good correlation, even if the lower neck bending response of the virtual model (Eva RID) appears to be excessive. The comparison of male and female PMHS versus their virtual dummy models indicates that these differences in kinematics occur more pronounced for the female dummy model. This behaviour might be caused by adaptions in rotational stiffness of the vertebral joints and rubber bumpers. Deviations could be further reduced by refinement and development efforts i.e. joint stiffness properties and geometry. In addition to the absolute higher loads, which occur in female simulations, Schmitt et al. (Schmitt, et al., 2012) suggested applying reduced injury thresholds when assessing female occupant protection. However, no broadly accepted thresholds are currently established.

In the comparison of PMHS and FEA, a large amount of upward motion of the head (and cervical spine) of all PMHS could be found. This effect is the sum of ramping of the PMHS on the test seat, and straightening of the thoracic spine. A similar behaviour of the thoracic spine in the FEA, and even in sled tests with the Bio RID II dummy can not be seen. It is likely caused by a too stiff thoracic spine of the Bio RID II and its derived FEA models.

The limited number of PMHS tests performed is certainly limiting the representativeness. Effects of the repeated application of each single PMHS in several sled tests are also difficult to estimate. For more accurate conclusions, additional testing and improvement in this field is inevitable.

## Recommendations

The additional application of a female occupant model, virtual or physical, would be of great benefit for the versatility of seat development. Currently further development of the physical female rear impact dummy Bio RID 50F is ongoing (Carlsson, et al., 2014). Developments in this area should be promoted.

Vehicle seats can be perfectly designed to achieve a good score in rating tests. As can be seen when reviewing current rating scores (Euro NCAP, 2015). However it should be considered, that current tests focus on a very narrowly defined scenario. Real life accidents on the other hand show large variations in many different factors. Many, if not all occupants differ from the $50^{th}$ percentile male. Seat adjustments frequently differ from the setting defined in current test protocols. Thus the aim in designing vehicle seats should not be to find a cheap and quick solution to gain the highest possible score in one single load case (rating test scenario). In fact, the aim should be to develop seat designs which are capable to protect a large variety of occupants (male/female, tall/short, etc.…) in a wide range of different situations. For this purpose however, tools and methods must be made available, to quantify loads on different occupants (size, gender, seated posture, etc.…) in situations differing from one standardised scenario.

## Limitations to this Study

Due to the fact that the finite element car seat model and the car seat used in physical sled tests behaved slightly differently, a comparison was possible but it was not possible to draw detailed conclusions from the results.
Investigations of configurations not accordant to the Euro NCAP protocol do not comply with any current test protocol. Best efforts were made to base the configurations on the protocols of Euro NCAP, but obvious differences were volitional. The validity of results of both, the physical and virtual Bio RID II dummy in such situations, is not proven. This restriction also goes for the virtual Eva RID, for which no preconditions are defined at all. Positioning procedure and thresholds for this dummy model are not generally available at the moment but should be established.

# 8. CONCLUSIONS

Rear-end collisions are one of the most common accidents in today's traffic. Whiplash is the single most common and costly occupant injury. Within the European Union, an estimate of more than 800,000 victims (Linder, et al., 2013) suffer WAD resulting in insurance and other social costs of approximately € 10 billion annually (Norra K, 2005)

Analysis of insurance data and numerous studies dating back to the 1960 revealed, that whiplash is a larger threat to females than males. Statistics indicate an increased risk of up to three times for females compared to males (Jonsson, 2008); (Kihlberg, 1969).

It was found, that newer whiplash protection systems seem to bring less improvement for females than for males (Kullgren, et al., 2010). It appears, that the protective properties of vehicle seats are focused on a small number of load case scenarios, which not surprisingly, all consider a very narrow scope of adjustments for seat components and furthermore only one occupant model and size. State of the art for development and assessment of vehicle seats is the Bio RID II dummy. Development is based on the current regulations and consumer test. Possible real life seat adjustments and seated postures are not considered in such tests.

The availability of the Eva RID dummy model made it possible to include a second occupant model, representing the 50$^{th}$ percentile female (Carlsson, et al., 2012b). The lack of regulations or assessments demanding other occupants than the Bio RID II currently prevents or at least reduces its use to a minimum. For comparison with the Eva RID virtual model, only the roughly adapted Bio RID 50F could be utilised in a first step (Carlsson, et al., 2014).

Analysis of Finite Element Analysis showed, that compared to the male baseline, the female Eva RID had to withstand loads up to 100 % higher than the male. Simulations also showed that loads on occupants are greatly influenced by different seat adjustments, such as different head restraint and backrest positions. This could also be confirmed in real sled tests utilising the Bio RID II dummy.

Sensitivities of different Injury criteria to variations in seat adjustments could be found. The Nkm criterion showed great deviations with different head restraint heights (high to low head restraint positions) The NIC criterion was more influenced by changing backrest positions (forward – backward) than by head restraint height.

Differences between male and female occupants could be found. Females seem to be more sensitive to higher pulse intensities. Also a higher head restraint increased the Nkm for the female, where it decreases for males. A more backward backrest however increased the NIC for both occupant models similarly.

Head rotation, inclined head positions and other situations differing from straight forward positions increase WAD risk (Jakobsson, et al., 2004a), (Jakobsson, et al., 2008) or (Kaale, et al., 2005). Current dummies are not capable of assessing such scenarios. Different methods and tools must be implemented such as HBM (e.g. THUMS) which might have the potential to predict loads and risk in such cases.

Currently seats are developed and optimised for the 50$^{th}$ percentile male occupant as demanded by the current regulation and consumer test environment. The aim in designing vehicle seats should not be to find a cheap and quick solution to gain the highest possible score in one single load case (rating test scenario). It should be to develop seat designs which are capable to protect a large variety of occupants (male/female, tall/short, etc.…) in a wide range of different situations. For this purpose however, tools and methods must be made available, to quantify loads on different occupants (size, gender, seated posture, etc.…) in situations differing from one standardised scenario.

# 9. REFERENCES

**AAAM** ABBREVIATED INJURY SCALE © 2005 UPDATE 2008 [Book] / ed. Gennarelli Thomas A. and Wodzin Elaine. - Barrington, IL, USA : Association for the Advancement of Automotive Medicine, 2008.

**Aldman B.** An analytical approach to the impact biomechanics of head and neck injury [Report]. - Canada, Montreal : Proceedings, 30th annual AAAM conference, 1986. - pp. 439-454. - TRID: Accession Number: 01419307.

**ANCAP** About ANCAP [Online]. - Australasian New Car Assessment Program, 2015. - 18 03 2015. - http://www.ancap.com.au/about-ancap.

**ANCAP** ANCAP Notes on the Assessment Protocol [Book]. - Manuka, Australia : Australian New Car Assessment Program, 2012. - v5.1.

**Antonaci F [et al.]** 3D kinematic analysis and clinical evaluation of neck movements in patients with whiplash injury [Article] // Cephalalgia : an international journal of headache.. - September 2002. - 7 : Vol. 22. - pp. 533-542.

**ARAI** AIS-101 Automotive Industry Standard No 101 - Requirements for the Protection of Fuel System in the Event of Rear Impact of a Motor Vehicle [Book]. - [s.l.] : Automotive Research Association of India - Research Institute of the Automotive Industry with the Ministry of Heavy Industries & Public Enterprises, Govt. of India, 2012.

**Avery M. and Weekes A.** Real World Injury Claims Database: A New Approach in Gathering Infurance Personal Injury Claims Data [Conference] // Program Book World Congress on Neck Pain. - Los Angeles, CA, USA : [s.n.], 2008. - pp. 84-85.

**AXA Winterthur** Home | AXA Winterthur [Online]. - AXA Schweiz, 2015. - 01 03 2015. - https://www.axa-winterthur.ch/de.

**AZT Automotive GmbH** Allianz Zentrum für Technik [Online] // AZT Automotive. - AZT Automotive GmbH, 9 2014. - 12 12 2014. - http://azt-automotive.com/de/.

**Barnsley Les** Percutaneous Radiofrequency Neurotomy for Chronic Neck Pain: Outcomes in a Series of Consecutive Patients [Article] // Pain Medicine. - July 2005. - 4 : Vol. 6. - pp. 282-286.

**Barnsley Leslie [et al.]** The Prevalence of Chronic Cervical Zygapophysial Joint Pain After Whiplash [Article] // Spine. - [s.l.] : Lippincott-Raven Publishers, January 1995. - 1 : Vol. 20. - pp. 20-25.

**Bartsch Adam J. [et al.]** Minor Crashes and 'Whiplash' in the United States [Article] // Annals of Advances in Automotive Medicine / Annual Scientific Conference. - 2008. - Vol. 52. - pp. 117-130. - PMCID: PMC3256773.

**Berglund Anita [et al.]** Occupant- and Crash-Related Factors Associated with the Risk of Whiplash Injury [Article] // Annals of Epidemiology / ed. Elsevier. - January 2003. - 1 : Vol. 13. - pp. 66-72.

**Boström O. [et al.]** A new nech injury criterion candidate based on injury findings in the cervical spinal ganglia after experimental neck extension trauma [Report]. - Dublin, Ireland : Proceedings of the IRCOBI conference 1996, 1996.

**Boström Ola [et al.]** New AIS1 Long-Term Nech Injury Criteria Candidated Based on real Frontal Crash Analysis [Report]. - Montpellier, France : Proceedings of the IRCOBI conference 2000, 2000. - pp. 249 - 264.

**Boström Ola [et al.]** Prediction of Neck Injuries in Rear Impacts Based on Accident Data and Simulation [Conference] // Proc. of IRCOBI conference 1997. - Hannover Germany : [s.n.], 1997.

**Brault John R. [et al.]** Clinical response of human subjects to rear-end automobile collisions [Article] // Archives of Physical Medicine and Rehabilitation. - [s.l.] : Elsevier, Jannuary 1998. - 1 : Vol. 79. - pp. 72-80.

**Cappon Hans [et al.]** Whiplash injuries, not only a problem in rear end impact [Conference] // Proceedings 18th International Technical Conference on The Enhanced Safety of Vehicles. - Nagoya, Japan : NHTSA, 2003. - Vol. 18.

**Carlsson Anna [et al.]** Anthropometric Specifications, Development, and Evaluation of EvaRID—A 50th Percentile Female Rear Impact Finite Element Dummy Model [Article] // Traffic Injury Prevention. - [s.l.] : Taylor & Francis Online, 15 Jul 2014. - 8 : Vol. 15. - pp. 855-865.
**Carlsson Anna [et al.]** Dynamic Kinematic Responses of Female Volunteers in Rear Impacts and Comparison to Previous Male Volunteer Tests [Article] // Traffic Injury Prevention. - [s.l.] : Taylor & Francis Online, 08 August 2011. - 4 : Vol. 12. - pp. 347-357.
**Carlsson Anna [et al.]** EvaRID - A 50th Percentile Female Rear Impact Finite Element Dummy Model [Conference]. - Dublin, Ireland : Elsevier, 2012b.
**Carlsson Anna [et al.]** Motion of the Head and Neck of Female and Male Volunteers in Rear Impact Car-to-Car Impacts [Article] // Traffic Injury Prevention. - [s.l.] : Taylor & Francis Online, 20 July 2012a. - 4 : Vol. 13. - pp. 378-387.
**Carlsson Anna** Adressing Female Whiplash Injury Protection - A Step Towards 50th Percentile Female Rear Impact Occupant Models [Book]. - Gothenburg, Sweden : Chalmers University of Technology, 2012c. - ISBN/ISSN 978-91-7385-671-3.
**Carlsson Anna and Svensson Mats** SLUTRAPPORT – SKYLTFONDEN, Krockdocka som testar whiplashskyddet för kvinnor [Report]. - Göteborg : Chalmers, 2014.
**CENTRO ZARAGOZA** CENTRO ZARAGOZA [Online]. - The Instituto de Investigación sobre Reparación de Vehículos, S.A., 2015. - 13 03 2015. - http://www.centro-zaragoza.com:8080/web/.
**Chang Fred [et al.]** EVARID: A DUMMY MODEL REPRESENTING FEMALES IN REAR END IMPACTS [Conference] // 3rd International Conference on Neck Pain in Car Crashes. - Munich, Germany : Proceedings of the "Whiplash 2010, 3rd International Conference on Neck Pain in Car Crashes", 2010.
**Chapline Janella F. [et al.]** Neck pain and head restraint position relative to the driver's head in rear-end collisions [Article] // Accident Analysis & Prevention / ed. Elsevier. - March 2000. - pp. 287-297.
**Chung Young-Seob and Han Dae-Hee** Vertebrobasilar dissection: A possible role of whiplash injury in its pathogenesis [Article] // Neurological Research. - [s.l.] : Maneyonline, 1 March 2002. - 2 : Vol. 24. - pp. 129-128.
**Cichos D. [et al.]** Crash Analysis Criteria Description [Book]. - Bergisch Gladbach, Germany : Workgroup Data Processing Vehicle Safety, 2006.
**C-NCAP** C-NCAP Management Regulation [Report]. - Tianjin, China : China Automotive Technology and Research Center, 2012.
**Croft A. C., Haneline M. T. and Freeman M. D.** Differential Occupant Kinematics and Forces between Frontal and Rear Automobile Impacts at Low Speed: Evidence for a Differential Injury Risk [Conference] // Proc. of IRCOBI Conference 2002. - Munich, Germany : [s.n.], 2002. - pp. 365-366.
**Curatolo Michele [et al.]** The role of tissue damage in whiplash associated disorders [Article] // Spine. - Philadelphia, US : [s.n.], 2011. - 25 Suppl : Vol. 25. - pp. 309-315.
**Daimler AG** NECK-PRO-Kopfstützen - aktiv bei Heckaufprall [Online]. - 2012. - https://www.daimler.com/dccom/0-5-1210222-49-1210366-1-0-0-1210342-0-0-135-0-0-0-0-0-0-0-0.html.
**Davidsson Johan [et al.]** Biorid I - A new biofidelic rear impact dummy [Report]. - Gothenburg, Sweden : Proceedings of the IRCOBI conference 1998, 1998.
**Depinet Paul** BioRID TEG - Transport - Vehicle Regulations - UNECE Wiki [Online]. - UNECE, 21 04 2013. - 15 03 2014. - https://www2.unece.org/wiki/download/attachments/4064167/TEGID-14-03e.pdf?api=v2.
**Desapriya Ediriweera** Head Restraints and Whiplash, The Past, Present and Future [Book]. - New York : Nova Science Publisher, 2010. - ISBN10: 978-1-61668-150-0.
**Dolinis J.** Risk factors for 'whiplash' in drivers: a cohort study of rear-end traffic crashes [Article] // Injury - International Journal of the Care of the Injured. - [s.l.] : Elsevier, April 1997. - 28 : Vol. 3. - pp. 173-179.
**Dong Ling [et al.]** Painful facet joint injury induces neuronal stress activation in the DRG: Implications for cellular mechanisms of pain [Article] // Neuroscience Letters. - [s.l.] : Elsevier, 3 October 2008. - 2 : Vol. 443. - pp. 90-94.
**Dong Ling and Winkelstein Beth A.** Simulated Whiplash Modulates Expression of the Glutamatergic System in the Spinal Cord Suggesting Spinal Plasticity Is Associated with Painful

Dynamic Cervical Facet Loading [Article] // Journal of Neurotrauma. - New Rochelle, NY, USA : [s.n.], January 2010. - 1 : Vol. 27. - pp. 163-174.

**Eichberger A Geigl BC, Moser A, Fachbach B, Steffan H** Comparison of Different Car Seats Regarding Head-Neck Kinematics of Volunteers During Rear End Impact [Article] // IRCOBI. - 1996. - pp. 153–164.

**Encyclopædia Britannica** Encyclopædia Britannica Online [Online] // Encyclopædia Britannica. - Encyclopædia Britannica, 09 09 2014. - 08 01 2015. - http://www.britannica.com/EBchecked/topic/641849/whiplash.

**Erdmann H.** Halswirbelsäulenerkrankungen mit Beteiligung des Nervensystems [Article] // Neuroorthopädie / ed. Hohmann D. [et al.]. - Berlin, Germany : Springer, 1983. - Vol. 1. - 978-3-642-68922-2.

**Erdmann** Klassifikation von Störungen bei HWS-Beschleunigungsverletzung nach Erdmann [Online] // Traumascores. - traumascores.com, 2015. - 03 03 2015. - http://www.traumascores.com/index.php/kl2-2/43-wirbelsaeule8/123-122.

**Eriksson Linda and Zellmer Harald** Assessing the BioRID II Repeatability and Reproducibility by Applying the Objective Rating Method (ORM) on Rear-End Sled Tests [Conference] // The 20th ESV Conference Proceedings. - Lyon, France : NHTSA, 2007.

**Euro NCAP** ASSESSMENT PROTOCOL – ADULT OCCUPANT PROTECTION [Report]. - Brussels, Belgium : EUROPEAN NEW CAR ASSESSMENT PROGRAMME, 2013.

**Euro NCAP** History | Euro NCAP - For safer cars crash test safety rating [Online] // History | Euro NCAP - For safer cars crash test safety rating. - 04 February 2014. - http://www.euroncap.com/Content-Web-Page/ee0e0c41-f8e8-4cdc-90fe-414ae5883db6/history.aspx.

**Euro NCAP** NEUESTE SICHERHEITSBEWERTUNGEN [Online]. - Euro NCAP, 2015. - 02 03 2015. - http://www.euroncap.com/de/bewertungen-u-auszeichnungen/neueste-sicherheitsbewertungen/.

**Euro NCAP** REAR WHIPLASH TEST PROTOCOL [Report]. - Brussels, Belgium : EUROPEAN NEW CAR ASSESSMENT PROGRAMME, 2013.

**Euro NCAP** The dynamic assessment of car seats for neck injury protection testing protocol [Book]. - Brussels, Belgium : European New Car Assessment Programme, 2014. - V3.2.

**Farmer Charles M. [et al.]** Relationship of Dynamic Seat Ratings to Real-World Neck Injury Rates [Article] // Traffic Injury Prevention. - [s.l.] : Taylor & Francis Online, 04 December 2008. - 6 : Vol. 9. - pp. 561-567.

**Farmer Charles M., Wells Joann K. and Lund Adrian K.** Effects of Head Restraint and Seat Redesign on Neck Injury Risk in Rear-End Crashes [Article] // Traffic Injury Prevention. - 15 September 2003. - 2 : Vol. 4. - pp. 83-90.

**Folksam** About Folksam [Online]. - Folksam, 2015. - 01 03 2015. - http://omoss.folksam.se/inenglish/aboutfolksam.

**Foret-Bruno J. Y. [et al.]** Influence of the Seat and Head Rest Stiffness on the Risk of Cervical Injuries in Rear Impact [Conference] // Procs. of the 13th Int. Conf. on Experimental Safety Vehicles (ESV). - Paris, France : [s.n.], 1991. - pp. 968-973. - No 91-S8-W-19.

**Foster J., Kortge J. and Wolanin M.** Hybrid III-A Biomechanically-Based Crash Test Dummy [Report]. - Warrendale, PA, USA : SAE International, 1977. - 770938.

**Gadd C.W.** Criteria for injury potential [Report]. - Washington, D.C., USA : National Academy of Science, 1961. - pp. pp 141-144. - National Research Council publication n. 977.

**GB** GB 20072-2006 - THE REQUIREMENTS OF FUEL SYSTEM IN THE EVENT OF REAR-END COLLISION FOR PASSENGER CAR [Report]. - China : GB Standard press of china, 2006.

**GDV** GDV [Online] // GDV. - GDV Gesamtverband der Deutschen Versicherungswirtschaft e.V., 2015. - 01 03 2015. - http://www.gdv.de/.

**GDV** Sitze und Kopfstützen werden immer besser – Defizite bei Kleinwagen und Minivans [Online]. - 28 07 2010. - 15 02 2014. - http://www.gdv.de/2010/07/unfallforschung-der-versicherer-sitze-und-kopfstuetzen-werden-immer-besser-defizite-bei-kleinwagen-und-minivans/.

**Gizmag** Saab pro-active restraint system [Online]. - Gizmag 2003 - 2015, 2013. - 01 03 2015. - http://www.gizmag.com/go/1615/.

**Global NCAP** Global NCAP | Promoting Safer Cars in the UN Decade of Action [Online]. - Global NCAP, 2014. - 01 01 2015. - http://www.globalncap.org/.

**Govind J [et al.]** Radiofrequency neurotomy for the treatment of third occipital headache [Article] // Journal of Neurology, Neurosurgery and Psychiatry. - [s.l.] : BMJ Publishing Group Ltd, 2003. - 1 : Vol. 74.

**Grant Helen** Reducing the number and costs of whiplash claims - A consultation on arrangements concerning whiplash injuries in England and Wales [Report] = Consultation Paper CP17/2012. - London, UK : The Stationery Office Limited on behalf of the Controller of Her Majesty's Stationery Office, 2012. - p. 11. - ISBN: 9780101842525.

**Gray Henry and Carter H. V.** Gray's Anatomy [Book]. - London, UK : Churchill Livingstone Elsevier, 2008. - 40th edition. - First edition JW Parker & Son 1858, Editor: Susan Standring, PhD, DSc, FKC. - ISBN: 978-0-8089-2371-8.

**Guha Sarba, Bhalsod Dilip and Krebs Jacob** LSTC Hybrid III 50th Fast Dummy, Positioning & Post-Processing // Dummy Version: LSTC.H3_50TH_FAST.111130_V2.0. - [s.l.] : LSTC Michigan, 2011.

**Gurdjian Elisha S. [et al.]** IMPACT INJURY AND CRASH PROTECTION [Report]. - Springfiels, IL : [s.n.], 1969-1970. - p. 556.

**Gutsche Andreas J. [et al.]** Basic comparison of the injury risk of a male and female dummy model in rear impact collisions [Conference] // Proc. of the IRCOBI Conference 2012. - Dublin, Ireland : [s.n.], 2012.

**Gutsche Andreas J. [et al.]** Comparison of the cervical spine bony kinematics for female PMHS with the virtual EvaRID dummy under whiplash loading [Conference] // Proc. of the IRCOBI Conference 2014. - Berlin : [s.n.], 2014.

**Gutsche Andreas J. [et al.]** Improve Assessment and Enhance Safety for the Evaluation of Whiplash Protection Systems Addressing Male and Female Occupants in Different Seat Configurations by Introducing Virtual Methods in Consumer Tests [Report]. - Gothenburg, Sweden : Proceedings of the IRCOBI conference 2013, 2013. - pp. 77 - 90. - IRC-13-16.

**Haldeman Scott [et al.]** The Bone and Joint Decade 2000–2010 Task Force on Neck Pain and Its Associated Disorders [Article] // European Spine journal. - [s.l.] : PMC, 2008. - Suppl 1 : Vol. 17. - pp. 5-7.

**Heikkilä H and Aström PG.** Cervicocephalic kinesthetic sensibility in patients with whiplash injury. [Article] // Scandinavian journal of rehabilitation medicine.. - Stockholm : Scandinavian University Press, September 1996. - 3 : Vol. 28. - pp. 133-138.

**Heitplatz Frank [et al.]** An evaluation of existing and proposed injury criteria with various dummies to determine their ability to predict the levels of soft tissue neck injury seen in real world accidents [Report]. - Nagoya, Japan : Proceedings of the 18th International Technical Conference on the Enhanced Safety of Vehicles (ESV), 2003.

**Hell Wolfram [et al.]** CONSEQUENCES FOR SEAT DESIGN DUE TO REAR-END ACCIDENT ANALYSIS, SLED TESTS AND POSSIBLE TEST CRITERIA FOR REDUCING CERVICAL SPINE INJURIES AFTER REAR-END COLLISION [Conference] // Proc. of IRCOBI Conference 1999. - Sitges, Spain : [s.n.], 1999. - pp. 234-259.

**Hell Wolfram, Langwieder Klaus and Walz Felix** Reported Soft Tissue Neck Injuries after Rear End Car Collision [Conference] // Proc. of IRCOBI Conference 1998. - Gothenburg, Sweden : [s.n.], 1998. - pp. 261-274.

**Hofinger M. [et al.]** REDUCTION OF NECK INJURIES BY IMPROVING THE OCCUPANT INTERACTION WITH THE SEAT BACK CUSHION [Conference] // Proceedings of the IRCOBI Conference. - Sitges, Spain : [s.n.], 1999.

**Holm Lena W. [et al.]** The Burden and Determinants of Neck Pain in Whiplash-Associated Disorders After Traffic Collisions: Results of the Bone and Joint Decade 2000–2010 Task Force on Neck Pain and Its Associated Disorders [Article] // Spine. - [s.l.] : Wolters Kluwer Health, 15 February 2008. - 4S : Vol. 33. - pp. 52-59.

**Hovenga P., E. [et al.]** Improved Prediction of Hybrid-III Injury Values Using Advanced Multibody Techniques and Objective Rating [Conference] // 2005 SAE World Congress. - Detroit Michigan, USA : SAE International, 2005.

**IAG** IAG Limited [Online]. - Insurance Australia Group Limited (IAG) , 2015. - 12 03 2015. - http://www.iag.com.au/.
**ICBC** ICBC Home [Online]. - Insurance Corporation of British Columbia (ICBC), 2015. - 01 03 2015. - http://www.icbc.com/Pages/default.aspx.
**IIHS** IIHS - HLDI [Online]. - IIHS - HLDI Insurance Institute for Highway Safety , Highway Loss Data Institute, 2015. - 12 02 2015. - http://www.iihs.org/.
**IIHS** IIHS Neck Injury [Online]. - Highway Safety/Highway Loss Data Institute, 3 2014. - 20 12 2014. - http://www.iihs.org/iihs/topics/t/neck-injury/qanda.
**IIHS** NHTSA's Activities Under the United Nations Economic Commission for Europe 1998 Global Agreement: Head Restraints; Request for Comments; Docket No. NHTSA-2008-0016, Notice 1 [Report]. - Arlington, VA : IIHS, 2008.
**Ivancic Paul, C. [et al.]** Effect of rotated head posture on dynamic vertebral artery elongation during simulated rear impact [Article] // Clinical Biomechanics. - State of New York, USA : Elsevier Inc., 2006. - 3 : Vol. 21. - pp. 213-220.
**Ivancic Paul, C. [et al.]** INTERVERTEBRAL NECK INJURY CRITERION FOR SIMULATED FRONTAL IMPACTS [Conference] // 2005 Annual Meeting (Combined with the ISB) of the American Society of Biomechanics. - Cleveland, OH, USA : American Society of Biomechanics, 2005.
**Jakobsson Lotta [et al.]** WHIPS – Volvo's whiplash protection study [Article] // Accident Analysis & Prevention. - [s.l.] : Elsevier, March 2000. - 2 : Vol. 32. - pp. 307-319.
**Jakobsson Lotta [et al.]** WHIPS – Volvo's whiplash protection study [Article] // Accident Analysis and Prevention 32. - 2000. - pp. 307-319.
**Jakobsson Lotta and Norin Hans** AIS1 Neck injury reducing effect of WHIPS (Whiplash Protection System) [Conference] // Proc. of IRCOBI Conference 2004. - Graz, Austria : [s.n.], 2004a. - pp. 297-305.
**Jakobsson Lotta, Isaksson-hellman Irene and Lindman Magdalena** WHIPS (Volvo Cars' Whiplash Protection System)—The Development and Real-World Performance [Article] // Traffic Injury Prevention. - 04 Dec 2008. - 6 : Vol. 9. - pp. 600-605.
**Jakobsson Lotta, Norin Hans and Svensson Mats Y.** Parameters Influencing AIS 1 Neck Injury Outcome in Frontal Impacts [Article] // Traffic Injury Prevention. - [s.l.] : Taylor & Francis Online, 2004b. - pp. 156-163.
**JASIC** TRIAS 33 - Test Requirements and Instructions for Automobile Standard No. 33 [Book]. - Tokyo, Japan : Japan Automobile Standards Internationalization Center, 2013.
**JNCAP** Heckaufprall Nackenschutz 平成23年度 後面衝突頚部保護性能試験方法 [Report]. - Tokyo, Japan : JNCAP New Car Assessment Japan Safety Information Group, 2011.
**Jonsson Bertil [et al.]** The risk of whiplash-induced medical impairment in rear-end impacts for males and females in driver seat compared to front passenger seat [Article] // IATSS Research. - July 2013. - 1 : Vol. 37. - pp. 8-11.
**Jonsson Bertil** Interaction between humans and car seats : studies of occupant seat adjustment, posture, position, and real world neck injuries in rear-end impacts [Book Section] // Interaction between humans and car seats : studies of occupant seat adjustment, posture, position, and real world neck injuries in rear-end impacts. - Umeå, Sweden : Department of Surgical and Perioperative Sciences, UMEA Univeritet, 2008. - ISSN 0346-6612-1163 ISBN 978-91-7264-525-7.
**Jonsson Bertil** Interaction between humans and car seats : studies of occupant seat adjustment, posture, position, and real world neck injuries in rear-end impacts [Book Section] // Interaction between humans and car seats : studies of occupant seat adjustment, posture, position, and real world neck injuries in rear-end impacts. - Umeå, Sweden : Department of Surgical and Perioperative Sciences, UMEA Univeritet, 2008. - ISSN 0346-6612-1163 ISBN 978-91-7264-525-7 .
**Kaale Bertel, Rune [et al.]** Head Position and Impact Direction in Whiplash Injuries: Associations with MRI-Verified Lesions of Ligaments and Membranes in the Upper Cervical Spine [Article] // Journal of Neurotrauma. - [s.l.] : Mary Ann Liebert, Inc., 23 November 2005. - 11 : Vol. 22. - pp. 1294-1302.

**Kallakuri Srinivasu [et al.]** Tensile stretching of cervical facet joint capsule and related axonal changes [Article] // European Spine Journal. - Switzerland : Springer, April 2008. - 4 : Vol. 17. - pp. 556-563.
**Kaneoka Koji [et al.]** Motion analysis of cervical vertebrae during whiplash loading. [Report]. - Philadelphia, PA : Spine Conference / PubMed - indexed for MEDLINE, 1999. - PMID: 10222526.
**Kihlberg J. K.** Flexion-Torsion Nech Injury in Rear Impacts [Conference]. - Des Plaines, IL, USA : Proc. of the 13th AAAM, 1969. - pp. 1-16.
**Kim A. [et al.]** A COMPARISON OF THE BIORID II, HYBRID III, AND RID2 IN LOW-SEVERITY REAR IMPACTS [Conference] // Proc. of the 19th International Technical Conference on the Enhanced Safety of Vehicles (ESV). - Washington, D.C., USA : US D.o.T., 2005.
**KNCAP** Assessment for Whiplash [Online]. - Korean New Car Assessment Program, 1999. - 04 02 2014. - http://www.car.go.kr/jsp/kncap/waySeat.jsp.
**KNCAP** Korean New Car Assessment Program [Online]. - Korean New Car Assessment Program, 2012. - 03 02 2014. - http://www.car.go.kr/jsp/kncap_eng/introduction.jsp.
**KNCAP** Safety Korea 1999 - 2012 [Online]. - Korean New Car Assessment Program, 2012. - 02 02 2014. - http://www.car.go.kr/jsp/kncap/result.jsp.
**Krafft M** A Comparison of Short- and Long-Term Consequences of AIS1 Neck Injuries, in Rear Impacts [Article] // IRCOBI. - 1998. - pp. 235-248.
**Krafft M. [et al.]** Whiplash Associated Disorders - Factors Influencing the Incidence on Rear-end Collisions [Conference]. - Melbourne, Australia : [s.n.], 1996. - pp. 1426-1432. - ESV 96S9O09.
**Krafft Maria [et al.]** Influence of Crash Pulse Characteristics on Whiplash Associated Disorders in Rear Impacts--Crash Recording in Real Life Crashes [Article] // Traffic Injury Prevention. - [s.l.] : Taylor & Francis Online, 15 September 2002a. - 2 : Vol. 3. - pp. 141-149.
**Krafft Maria [et al.]** The Risk of Whiplash Injury in the Rear Seat Compared to the Front Seat in Rear Impacts [Article] // Traffic Injury Prevention. - [s.l.] : Taylor & Francis, 2003. - pp. 136-140.
**Krafft Maria [et al.]** THE RISK OF WHIPLASH INJURY IN THE REAR SEAT COMPARED TO THE FRONT SEAT IN REAR IMPACTS [Conference] // Proc. of the IRCOBI conference 2002. - Munich, Germany : [s.n.], 2002b. - pp. 203-209.
**Kraft Maria [et al.]** Injury as a function of change of velocity, an alternative method to derive risk functions [Conference] // Vehicle Safety 2000 - IMechE. - London, GB : [s.n.], 2000. - pp. 263-273. - ISBN 1356-1448.
**Kullgren A [et al.]** The effect of whiplash protection systems in real-life crashes and their correlation to consumer crash test programmes [Article] // Enhanced Safety of Vehicles. - 2007. - pp. Paper number: 07-0468.
**Kullgren A Eriksson L, Boström O, Krafft M** Validation of neck injury criteria using reconstructed real-life rear-end crashes with recorded crash pulses [Article] // ESV. - Nagoya, Japan : [s.n.], 19-22 May 2003. - pp. 1–13.
**Kullgren A, Boström O and Avery M** Correlation Between Whiplash Injury Outcome in Real-Life Crashes and Results ins Consumer Crash Test Programmes [Conference] // Program Book of the World Congress on Neck Pain 2008. - Los Angeles, CA, USA : [s.n.], 2008.
**Kullgren Anders [et al.]** COMBINING CRASH RECORDER AND PAIRED COMPARISON TECHNIQUE: INJURY RISK FUNCTIONS IN FRONTAL AND REAR IMPACTSWITH SPECIAL REFERENCE TO NECK INJURIES [Conference] // The 18th International Technical Conference on the Enhanced Safety of Vehicles (ESV) Proceedings. - Nagoya, Japan : [s.n.], 2003.
**Kullgren Anders and Krafft Maria** Gender analysis on whiplash seat effectiveness: results Rrom real-world crashes [Conference] // Proc. of IRCOBI Conference 2010. - Hanover, Germany : [s.n.], 2010. - pp. 17-28.
**Kuppa Shashi, Saunders James and Stammen Jason** KINEMATICALLY BASED WHIPLASH INJURY CRITERION [Report]. - Washington D.C. : ESV, 2005. - ESV Paper 05-0211.
**Lear Corporation** Automotive Seating Head Restraint Systems, ProTec, ComfortRest, VisionTec | Lear Corporation [Online]. - 2015. - http://lear.com/en/seating/head-restraints.aspx.
**Lee Kathryn ,E [et al.]** A novel rodent neck pain model of facet-mediated behavioral hypersensitivity: implications for persistent pain and whiplash injury [Article]. - [s.l.] : Elsevier, 30 August 2004. - 2 : Vol. 137. - pp. 151-159.

**Leimgruber Benjamin, Steffan Hermann and Gutsche Andreas J.** Validierung eines generischen numerischen Parametersitzes für Whiplash - Lastfälle anhand von statischen und dynamischen Versuchsdaten [Book]. - Graz : [s.n.], 2014.

**Lenard James, Ekambaram Karthikeyan and Morris Andrew** Position And Rotation of Driver's Head as Risk Factor for Whiplash in Rear Impacts [Article] // Journal of Ergonimics. - [s.l.] : Open Access, 2015. - 12 : Vol. 3.

**Linder Astrid [et al.]** ADSEAT – Adaptive seat to reduce neck injuries for female and male occupants [Article] // Accident Analysis & Prevention. - [s.l.] : Elsevier, November 2013. - Vol. 60. - pp. 334-343.

**Linder Astrid [et al.]** Dynamic Responses of Female and Male Volunteers in Rear Impacts [Article] // Traffic Injury Prevention. - [s.l.] : Taylor & Francis Online, 04 December 2008. - 6 : Vol. 9. - pp. 592-599.

**Linder Astrid [et al.]** Influence of Gender, Height, Weight, Age, Seated Position and Collision Site related to Neck Pain Symptoms in Rear End Impacts [Conference] // 2012 IRCOBI Conference Proceedings. - Dublin, Ireland : [s.n.], 2012.

**Linder Astrid** Adaptive Seat to reduce Neck Injuries for Female and Male Occupants [Online]. - 2011. - 12 March 2014. - http://www.adseat.eu.

**Lord Susan, M. [et al.]** Chronic Cervical Zygapophysial Joint Pain After Whiplash: A Placebo-Controlled Prevalence Study [Article] // Spine. - [s.l.] : Lippincott-Raven Publishers., 1996. - 15 : Vol. 21.

**Lord Susan, M. [et al.]** Percutaneous Radio-Frequency Neurotomy for Chronic Cervical Zygapophyseal-Joint Pain [Article] // The New England Journal of Medicine. - 5 December 1996. - 23 : Vol. 335. - pp. 1721-1726.

**Lord Susan, M. [et al.]** Third occipital nerve headache: a prevalence study. [Article] // J Neurol Neurosurg Psychiatry / ed. 1190. - [s.l.] : group.bmj.com, October 1994. - 10 : Vol. 57. - p. 1187.

**Lorenz Bernd** Interaction of Research, Legislation and Consumer Information [Report] = Keynote Lecture IRCOBI 2014. - Berlin : [s.n.], 2014. - pp. 15-17.

**Loudon Janice, K., Ruhl Mary and Field Edelle** Ability to Reproduce Head Position After Whiplash Injury [Article] // Spine. - [s.l.] : Lippincott-Raven Publishers., 15 April 1997. - 8 : Vol. 22. - pp. 865-868.

**Lövsund P., Nygren A and Tingvall C** Nech Injuries in Rear End Collissions Among Front and Rear Seat Occupants [Conference] // Proc. of the IRCOBI Conference 1988. - Bergisch Gladbach, Germany : IRCOBI, 1988.

**Lu Ying [et al.]** Neural response of cervical facet joint capsule to stretch: a study of whiplash pain mechanism [Article] // Stapp Car Crash Journal. - Washington D.C., USA : [s.n.], November 2005. - 49. - pp. 49-65. - PMID: 17096268.

**Lundell Björn [et al.]** Guidelines for and the Design of a Car Seat Concept for Improved Protection against Neck Injuries in Rear End Car Impacts [Conference] // International Congress & Exposition. - 1998. - SAE 980301.

**Maag Urs [et al.]** Seat Belts and Neck Injuries [Conference] // Proc. of IRCOBI Conference 1990. - Bron-Lyon, France : [s.n.], 1990. - pp. 1-13.

**Macpherson P,C, Schork M,A and Faulkner J,A** Contraction-induced injury to single fiber segments from fast and slow muscles of rats by single stretches. [Article] // The American journal of physiology.. - November 1996. - 5 Part 1 : Vol. 271. - pp. 1438-1446.

**Madeleine P [et al.]** Quantitative posturography in altered sensory conditions: a way to assess balance instability in patients with chronic whiplash injury [Article] // Archives of physical medicine and rehabilitation. - March 2004. - 3 : Vol. 85. - pp. 432-438.

**MAPFRE** CESVIMAP [Online] // Research and Road Safety Centre of MAPFRE. - MAPFRE TECH, S.A., 2015. - 13 03 2015. - http://www.mapfre.es/wcesvimap/en/general/inicio.shtml.

**Martin Jean-Louis, Marí-Dell'Olmo M and Chiron M** Whiplash risk estimation based on linked hospital–police road crash data from France and Spain [Article] // Injury Prevention. - 12 March 2008. - 3 : Vol. 14. - pp. 75-80.

**Matsuoka Fumio [et al.]** A Comparison Between BioRId And Hybrid III Head/Neck/Torso Response In Middle Speed Sled Rear Impact Tests [Conference] // Proceedings of the International Technical Conference on the Enhanced Safety of Vehicles (ESV). - Amsterdam : [s.n.], 2001. - Vol. 17.

**McCully K K and Faulkner J A** Injury to skeletal muscle fibers of mice following lengthening contractions. [Article] // Journal of applied physiology. - [s.l.] : American Physiological Society,, 1985. - 1 : Vol. 59. - pp. 119-126.

**McDonald Greg, J., Lord Susan, M. and Bogduk Nikolai** Long-term Follow-up of Patients Treated with Cervical Radiofrequency Neurotomy for Chronic Neck Pain [Article] // Neurosurgery. - [s.l.] : Congress of Neurological Surgeons, 1999. - 1 : Vol. 45. - pp. 61-68.

**Mertz H. J. and Patrick L. M.** Strength and response of the human [Report]. - Coronado, CA : Society of Automotive Engineers, 1971. - SAE: 710855.

**Mordaka J. and Gentle R.** The Biomechanics of Gender Difference and Whiplash Injury: Designing Safer Car Seats for Women [Article] // Acta Polytechnica. - 2003. - 3 : Vol. 43. - pp. 47-54.

**Morris Andrew P. and Thomas Pete** Neck Injuries in the UK Co-operative Crash Injury Study [Conference] // Proc. of 40th Stapp Car Crash Conference. - Albuquerque, NM, USA : Society of Automotive Engineers, 1996. - pp. 317-329. - SAE962433.

**Munoz D. [et al.]** A STUDY OF CURRENT NECK INJURY CRITERIA USED FOR WHIPLASH ANALYSIS. PROPOSAL OF A NEW CRITERION INVOLVING UPPER AND LOWER LOAD CELLS. [Report]. - Washington D.C. : ESV, 2005. - Paper Number 05-0313 .

**Muser Markus H., Walz Felix H. and Zellmer Harrald** Biomechanical significance of the rebound phase in low speed rear end impacts [Report]. - Montpellier, France : Proc. of the IRCOBI 2000, 2000. - pp. 411-424.

**NASVA** Car Safety Performance Guidebook [Report]. - Sumida-ku, Tokyo, Japan : National Agency fpr Automotive Safety & Victims' Aid, 2013.

**Norra K Vowles B** The Whiplash Commission Final Report [Book]. - Sandviken : Sandvikens tryckeri, 2005.

**Nuckley David, J. [et al.]** Neural space integrity of the lower cervical spine: effect of normal range of motion [Article] // Spine / ed. Wolters Kluwer Health Inc.. - Philadelphia, PA, USA : [s.n.], 2002. - 6 : Vol. 27. - pp. 587-95. - PMID:.

**Nygren Å Gustafsson H, Tingvall C** Effects of Different Types of Headrests in Rear-End Collisions [Article] // ESV. - 1985. - pp. 85–90.

**Olsson I. [et al.]** AN IN-DEPTH STUDY OF NECK INJURIES IN REAR END COLLISIONS [Conference] // Proc. of the IRCOBI conference 1990. - Bron - Lyon, France : [s.n.], 1990. - pp. 270-280.

**O'Neil Brian [et al.]** Automobile Head Restraints—Frequency of Neck Injury Claims in Relation to the Presence of Head Restraints [Article] // American Journal of Public Health / ed. National Center for Biotechnology Information U.S. National Library of Medicine. - March 1972. - 3 : Vol. 63. - pp. 399-406. - PMC1530082.

**Ono Koshiro [et al.]** PREDICTION OF NECK INJURY RISK BASED ON THE ANALYSIS OF LOCALIZED CERVICAL VERTEBRAL MOTION OF HUMAN VOLUNTEERS DURING LOW-SPEED REAR IMPACTS [Conference] // Proc. of IRCOBI Conference 2006. - Madrid, Spain : [s.n.], 2006. - pp. 103-113.

**Ono Koshiro and Kaneoka Koji** MOTION ANALYSIS OF HUMAN CERVICAL VERTEBRAE DURING LOW SPEED REAR IMPACTS BY THE SIMULATED SLED [Report]. - Germany, Hannover : Proceedings of IRCOBI conference 1997, pp 223-237, 1997.

**Otremski I. [et al.]** Soft tissue cervical spinal injuries in motor vehicle accidents. [Article] // Injury - International Journal of the Care of the Injured. - Nov 1989. - 6 : Vol. 20. - pp. 349-351. - PMID: 2628332.

**Panjabi Manohar M., Wang Jaw-Lin and Delson Nathan** Neck Injury Criterion Based on Intervertebral Motions and its Evaluation using an Instrumented Neck Dummy [Report]. - Sitges, Spain : Proceedings of IRCOBI, 1999. - pp. 179-190.

**Panjabi Manohar, M. [et al.]** Cervical spine curvature during simulated whiplash [Article] // Clinical Biomechanics. - January 2004a. - 1 : Vol. 19. - pp. 1-9.

**Panjabi Manohar, M. [et al.]** Injury Mechanisms of the Cervical Intervertebral Disc During Simulated Whiplash [Article] // Spine. - [s.l.] : Lippincott Williams & Wilkins, Inc., 1 June 2004b. - pp. 1217-14225.

**Panjabi MM** A hypothesis of chronic back pain: ligament subfailure injuries lead to muscle control dysfunction [Article] // European spine journal. - 2006. - 5 : Vol. 15. - pp. 668-676.

**Parkin S. [et al.]** Rear end collisions and seat performance: to yield or not to yield [Conference] // 39th Annual Proceedings, Association for the Advancement of Automotive Medicine (AAAM). - Chicago, IL, USA : [s.n.], 1995.

**Pheasant Stephen and Haslegrave Christine** Bodyspace : Anthropometry, Ergonomics and the Design of Work [Book]. - Boca Raton : Taylor & Francis Group, 2006. - ISBN 0-415-28520-8.

**Pike Jeffrey A.** Neck Injury: the use of x-rays, CTs and MRIs to study crash related injury mechanisms [Book]. - PA, USA : Society of Automotive Engineers, Inc., 2002. - ISBN 0-7680-0905-7.

**Pollanen Michae,l S., Deck John, H.N. and Blenkinsop Barry** Injury of the Tunica Media in Fatal Rupture of the Vertebral Artery [Article] // American Journal of Forensic Medicine and Pathology. - [s.l.] : Lippincott-Raven Publishers, September 1996. - pp. 197-201.

**Prasad Priya and Daniel Roger D.** A biomechanical analysis of head, neck and torso injuries to childr surrogates due to sudden torso acceleration [Report]. - San Diego, California : Proc. of the 28th Stapp Car Crash Conference, 1984. - SAE Technical Paper 841656.

**Quinn Kyle,P. [et al.]** Neuronal hyperexcitability in the dorsal horn after painful facet joint injury [Article] // Pain. - November 2010. - 2 : Vol. 151. - pp. 414-421.

**Quinn Kyle,P. [et al.]** Structural Changes in the Cervical Facet Capsular Ligament: Potential Contributions to Pain Following Subfailure Loading [Article] // Stapp Car Crash Journal. - San Diego, California, USA : [s.n.], October 2007. - Vol. 51. - pp. 169-187. - PMID 18278597.

**Rashier Amanda and Monk Jonathan** Whiplash - Synopsis of Causation [Report]. - Queen's Medical Centre Nottingham : UK Ministry of Defen, 2008.

**RCAR** RCAR-IIWPG Seat/Head Restraint Evaluation Protocol (Version 3) [Report]. - Arlington, VA, USA : Insurance Institute for Highway Safety, 2008.

**Richter M. [et al.]** Whiplash-type neck distortion in restrained car drivers: frequency, causes and long-term results [Article] // European Spine Journal. - [s.l.] : Springer-Verlag, April 2000. - 2 : Vol. 9. - pp. 109-117. - PMCID: PMC3611361.

**Ryan G. A. [et al.]** Neck strain in car occupants - The influence of Crash-related Factors on Initial Severity [Article] // The Medical Journal of Australia. - November 1993. - 10 : Vol. 159. - pp. 651-656.

**Schick S. [et al.]** Differences and commons in kinetic parameters of male and female volunteers in low speed rear end impacts [Conference] // Whiplash Neck Pain in Car Crashes, 2nd International Conference. - Erding, Germany : TÜV SÜD, 2008.

**Schick Sylvia [et al.]** BASICS FOR DEVELOPING A FEMALE OCCUPANT MODEL FOR INVESTIGATING CERVICAL SPINE DISTORTION INJURY (CSD) [Conference] // Proceedings of the 4th International ESAR Conference. - Hanover, Germany : [s.n.], 2010.

**Schmitt Kai-Uwe [et al.]** A New Neck Injury Criterion Candidate For Rear-End Collisions Taking Into Account Shear Forces And Bending Moments [Report]. - Amsterdam, Netherlands : Enhanced Safety of Vehicles ESV, 2001.

**Schmitt Kai-Uwe [et al.]** Seat testing to investigate the female neck injury risk – preliminary results using a new female dummy prototype [Conference] // IRCOBI conference 2012. - Dublin, Ireland : [s.n.], 2012. - Vol. Proc. of the IRCOBI conference 2012.

**Schmitt Kai-Uwe** A CONTRIBUTION TO THE TRAUMA-BIOMECHANICS OF THE CERVICAL SPINE - PRESSURE PHENOMENA OBSERVED UNDER CONDITIONS OF LOW SPEED REAR-END COLLISIONS [Book]. - Switzerland, Zürich : Diss., Technische Wissenschaften ETH Zürich, Nr. 14197, 2001, 2001. - Diss. ETH No. 14197.

**Schuster Peter , Stahlschmidt Sebastian and Franz Uli** Development of BioRID-II Dummy Model In Cooperation with German Automotive Industry [Report]. - Stuttgart, Germany : Dynamore, 2005.

**Scott S. and Sanderson P.** Whiplash: a biochemical study of muscle injury [Article] // European Spine Journal. - [s.l.] : Springer, 2002. - 4 : Vol. 11. - pp. 389-392.

**Siegmund Gunter P. [et al.]** Head/Neck Kinematic Response of Human Subjects in Low-Speed Rear-End Collisions [Conference] // Proc. of the 41st Stapp Car Crash Conference. - [s.l.] : Society of Automotive Engineers, 1997. - pp. 357-385. - SAE 973341.

**Siegmund Gunter, P [et al.]** Are cervical multifidus muscles active during whiplash and startle? An initial experimental study. [Article] // BMC Musculoskelet Disord. - June 2008. - Vol. 9. - p. 80.

**Siegmund Gunter, P. [et al.]** The anatomy and biomechanics of acute and chronic whiplash injury. [Article] // Traffic Injury Prevention. - [s.l.] : Taylor and Francis, 2009. - 2 : Vol. 10. - pp. 101-112.

**Sobotta J., Putz R. and Papst R.** Atlas of the Human Anatomy [Book]. - München : Urban & Schwarzenberg, 1993.

**Spitzer Walter O. [et al.]** Scientific monograph of the Quebec Task Force on Whiplash-Associated Disorders: redefining "whiplash" and its management. [Article] // Spine. - 15 April 1995. - 20. - pp. 1-73.

**Storvik S. G. [et al.]** Population-based estimates of whiplash injury using nass cds data - biomed 2009 [Article] // Biomedical Sciences Instrumentation. - 2009. - 45. - pp. 244-249. - PMID: 19369770.

**Stürzenegger Matthias [et al.]** Presenting symptoms and signs after whiplash injury: The influence of accident mechanisms [Article] // Nyrology. - [s.l.] : AAN Enterprises, Inc., April 1994. - 4 : Vol. 44. - pp. 668-693.

**Svensson Mats [et al.]** ADSEAT - D2a Biological Test [Report]. - Brussels, Belgium : [s.n.], 2012.

**Svensson Mats Y. [et al.]** Pressure Effects in the Spinal Canal during Whiplash Extension Motion: A Possible Cause of Injury to the Cervical Spinal Ganglia [Report]. - The Netherlands, Eindhoven : Proceedings of IRCOBI conference, 1993.

**Svensson Mats Y. [et al.]** Rear-End Collisions - A Study of the Influence of Backrest Properties on Head-Neck Motion using a New Dummy Neck [Conference] // SAE International Congress and Exposition. - 1993. - pp. 129-142.

**Szabo Thomas J. [et al.]** Human Occupant Kinematic Response to Low Speed Rear-End Impacts [Conference] // International Congress & Exposition. - [s.l.] : Society of Automotive Engineers, 1994. - SAE 940532.

**TAKAHIRO IKARI [et al.]** JAPAN NEW CAR ASSESSMENT PROGRAM FOR MINOR NECK INJURY PROTECTION IN REAR END COLLISIONS [Report]. - Stuttgart, Germany : Proceedings of the 21st International Technical Conference on the Enhanced Safety of Vehicles, 2009. - Paper Number 09-0364.

**Taneichi Hiroshi [et al.]** Traumatically Induced Vertebral Artery Occlusion Associated with Cervical Spine Injuries: Prospective Study Using Magnetic Resonance Angiography [Article] // Spine. - [s.l.] : Lippincott Williams & Wilkins, Inc., 1 September 2005. - 17 : Vol. 30. - pp. 1955-1962.

**Tavris Dale R, Kuhn Evelyn M and Layde Peter M** Age and gender patterns in motor vehicle crash injuries: importance of type of crash and occupant role [Report]. - Milwaukee, Wisconsin, USA : Accident Analysis and Prevention 33, 2001.

**Temming J. and Zobel R.** Frequency and Risk of Cervical Spine Distortion Injuries in Passenger Car Accidents: Significance of Human Factors Data [Conference] // Proc. of IRCOBI Conference 1998. - Gothenburg, Sweden : [s.n.], 1998. - pp. 219-234.

**Temming J. and Zobel R.** -Whiplash- HWS-Distorsionen angegurteter PKW-Insassen bei Heck-Kollisionen [Report]. - [s.l.] : BRITE-EURAM Whiplash1 Project, 1997.

**Thatcham** Thatcham Research Centre [Online]. - Thatcham, 2015. - 11 03 2015. - http://www.thatcham.org/.

**The Healthy Spine Ltd** Clinical Whiplash [Online]. - The Healthy Spine Ltd, 2011. - 11 11 2014. - http://clinicalwhiplash.com/resources/what-happens-in-whiplash-injury/.

**Thomas C. [et al.]** Protection against rear-end accidents [Conference]. - Cologne, Germany : Proc. of IRCOBI Conference 1982, 1982. - pp. 17-29.

**Toyota Motor Corporation** Restraint Device : Whiplash Injury Lessening (WIL) Concept Seat [Online]. - 1995-2015. - http://www.toyota-global.com/innovation/safety_technology/safety_technology/technology_file/passive/wil.html.

**U.S. DoT** FMVSS 202a HEAD RESTRAINTS FOR PASSENGER VEHICLES // Federal Motor Vehicle Safety Standards and Regulatoins 202a. - Washington, DC : NATIONAL HIGHWAY

TRAFFIC SAFETY ADMINISTRATION, OFFICE OF VEHICLE SAFETY COMPLIANCE, 2000. - FMVSS NO. 202a.

**U.S. DoT** FMVSS 208 Occupant Crash Protection // Federal Motor Vehicle Safety Standards and Regulatoins 208. - Washington, DC : NATIONAL HIGHWAY TRAFFIC SAFETY ADMINISTRATION, OFFICE OF VEHICLE SAFETY COMPLIANCE, 1999. - FMVSS NO. 208.

**U.S. DoT** FMVSS 301 FUEL SYSTEM INTEGRITY // Federal Motor Vehicle Safety Standards and Regulatoins 301. - Washington, DC : NATIONAL HIGHWAY TRAFFIC SAFETY ADMINISTRATION, OFFICE OF VEHICLE SAFETY COMPLIANCE, 2004.

**UN** United Nations Member Statues [Online]. - July 2013. - 7 July 2013. - http://www.un.org/en/members/index.shtml.

**UNECE** Concerning the Adoption of Uniform Technical Prescriptions for Wheeled Vehicles, Equipment and Parts which can be Fitted and/or be Used on Wheeled Vehicles and the Conditions for Reciprocal Recognition of Approvals Granted on the Basis of these Prescripti. - Geneva, Switzerland : United Nations Economic Commission for Europe , 2013. - E/ECE/324/Rev.1/Add.93/Rev.2−E/ECE/TRANS/505/Rev.1/Add.93/Rev.2.

**UNECE** GTR 7 - Head Restraints [Report]. - [s.l.] : UNECE Transport Division, 2010. - GTR7-06-10. Rev.1.

**UNECE** Regulation No. 16 - Uniform provisions concerning the approval of Safety-belts, restraint systems, child restraint systems and ISOFIX child restraint systems for occupants of power-driven vehicles [Report]. - Geneva, Switzerland : United Nations, 1995. - E/ECE/324/Rev.1/Add.15/Rev.7−E/ECE/TRANS/505/Rev.1/Add.15/Rev.7.

**UNECE** Regulation No. 17 - Uniform provisions concerning the approval of vehicles with regard to the seats, their anchorages and any head restraints [Report]. - Geneva, Switzerland : United Nations, 1995. - E/ECE/324/Rev.1/Add.16/Rev.5 - E/ECE/TRANS/505/Rev.1/Add.16/Rev.5.

**UNECE** Regulation No. 32 - Uniform provisions concerning the approval of vehicles with regard to the behaviour of the structure of the impacted vehicle in a rear-end collision [Report]. - [s.l.] : United Nations, 1993.

**Van Auken R. Michael [et al.]** DEVELOPMENT OF AN IMPROVED NECK INJURY ASSESSMENT CRITERIA FOR THE ISO 13232 MOTORCYCLIST ANTHROPOMETRIC TEST DUMMY [Report]. - Washington D.C. : Proceedings of the 19th International Technical Conference on the Enhanced Safety of Vehicles (ESV), 2005. - ESV Paper No. 05-0227.

**Versace John** A review of the severity index [Report] / Ford Motor Co.. - Coronado, CA : Proceedings of the 15th Stapp Car Crash Conference, 1971. - pp. 771-796. - SAE: 710881.

**Viano David C. and Davidsson Johan** Neck Displacements of Volunteers, BioRID P3 and Hybrid III in Rear Impacts: Implications to Whiplash Assessment by a Neck Displacement Criterion (NDC) [Article] // Traffic Injury Prevention. - 2002. - Issue 2 : Vol. Volume 3. - pp. pages 105-116.

**Viano David C. and Olsen Stefan** The Effectiveness of Active Head Restraint in Preventing Whiplash [Article] // Journal of Trauma-Injury Infection & Critical Care. - [s.l.] : Lippincott Williams & Wilkins, Inc., November 2001. - 5 : Vol. 51. - pp. 959-969.

**Viano David C.** Seat Influences on Female Neck Responses in Rear Crashes: A Reason Why Women Have Higher Whiplash Rates [Article] // Traffic Injury Prevention / ed. Online Taylor & Francis. - 17 September 2003. - 3 : Vol. 4. - pp. 228-239.

**Watanabe Y Ichikawa H, Kayama O, Ono, K, Kaneoka K, Inami S** Influence of Seat Characteristics on Occupant Motion in Low-Velocity Rear-End Impacts [Article] // AAP. - 2000. - pp. 243–250.

**Welcher Judson B. and Szabo Thomas J.** Relationships between seat properties and human subject kinematics in rear impact tests [Article] // Accident Analysis & Prevention. - [s.l.] : Elsevier, May 2001. - 3 : Vol. 33. - pp. 289-304.

**Whiplash Prevention Campaign** Whiplash Prevention Campaign [Online] // www.whiplashprevention.org. - Whiplash Prvention Campaign, 2010. - 25 12 2014. - http://www.whiplashprevention.org/JoinUs/Pages/ProjectStaff.aspx.

**Wilkund Kristian and Larsson Hakan** Saab Active Head Restraint (SAHR) - Seat Design to Reduce the Risk of Neck Injuries in Rear Impacts [Report]. - Detroit Michigan : International Congress and Exposition, 1998. - SAE 980297.

**Winkelstein Beth A. and Santos Diana G.** An Intact Facet Capsular Ligament Modulates Behavioral Sensitivity and Spinal Glial Activation Produced by Cervical Facet Joint Tension [Article] // Spine. - [s.l.] : Lippincott Williams & Wilkins, Inc., 15 April 2008. - 8 : Vol. 33. - pp. 856-862.

**World Health Organisation** World report on road traffic injury prevention [Book]. - Geneva, Switzerland : WHO Library Cataloguing-in-Publication Data, 2004. - Margie Peden, Richard Scurfield,David Sleet, Dinesh Mohan, Adnan A. Hyder, Eva Jarawan, Colin Mathers. - ISBN 92 4 156260 9.

**Yang King H. [et al.]** On the Role of Cervical Facet Joints in Rear End Impact Neck Injury Mechanisms [Report]. - 1997. - SAE 970497.

**Yang Xiaoqing [et al.]** Association between Body Mass Index and Recovery from Whiplash Injuries: A Cohort Study [Article] // American Journal of Epidemiology. - [s.l.] : Oxford Journals, 01 May 2007. - pp. 1063-1069.

**Yoganandan Narayan [et al.]** SINGLE REAR IMPACT PRODUCES LOWER CERVICAL SPINE SOFT TISSUE INJURIES [Report]. - Isle of man, UK : IRCOBI, 2001.

**Yoganandan Narayan [et al.]** Whiplash Injury Determination With Conventional Spine Imaging and Cryomicrotomy [Article] // Spine. - [s.l.] : Lippincott Williams & Wilkins, Inc., 15 November 2001. - pp. 2443-2448.

**Young Joseph W. [et al.]** Anthropometric and Mass Distribution Characteristics of the Adult Female [Report]. - Oklahoma City, Oklahoma, USA : FAA Civil Aeromedical Institute, 1983. - FAA-AM-83-16.

# 10. Figures

# 11. TABLES

# 12. EQUATIONS

# A. APPENDIX

## A.1. Bio RID II tests accordant and not accordant to Euro NCAP whiplash protocol

### A.1.1. OOP 1

Faulty data acquisition during OOP1.

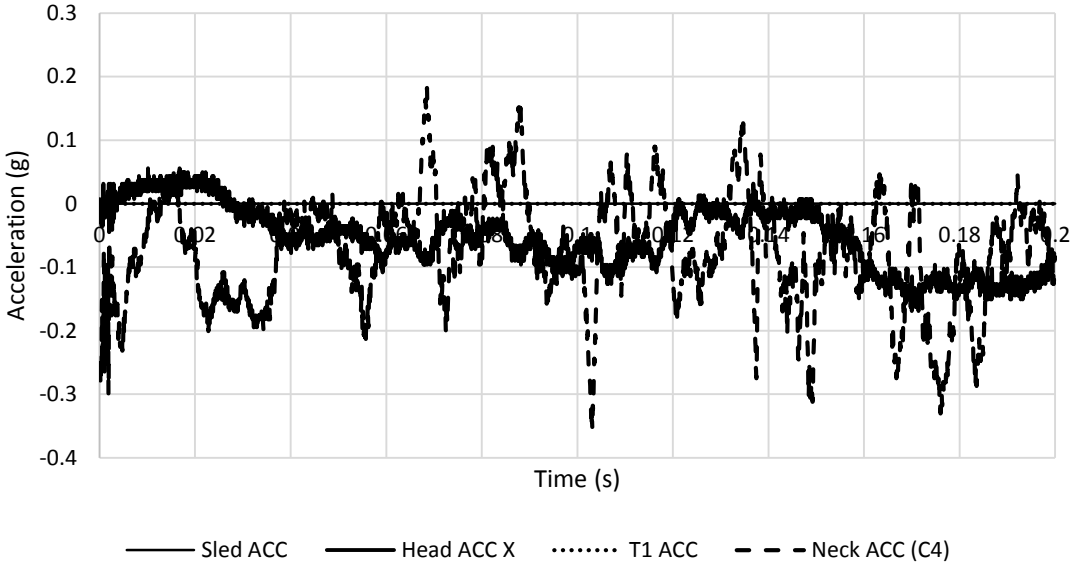


APPENDIX 1 OOP 1 SLED-, HEAD-, T1- AND TORSO- (L1) X ACCELERATION

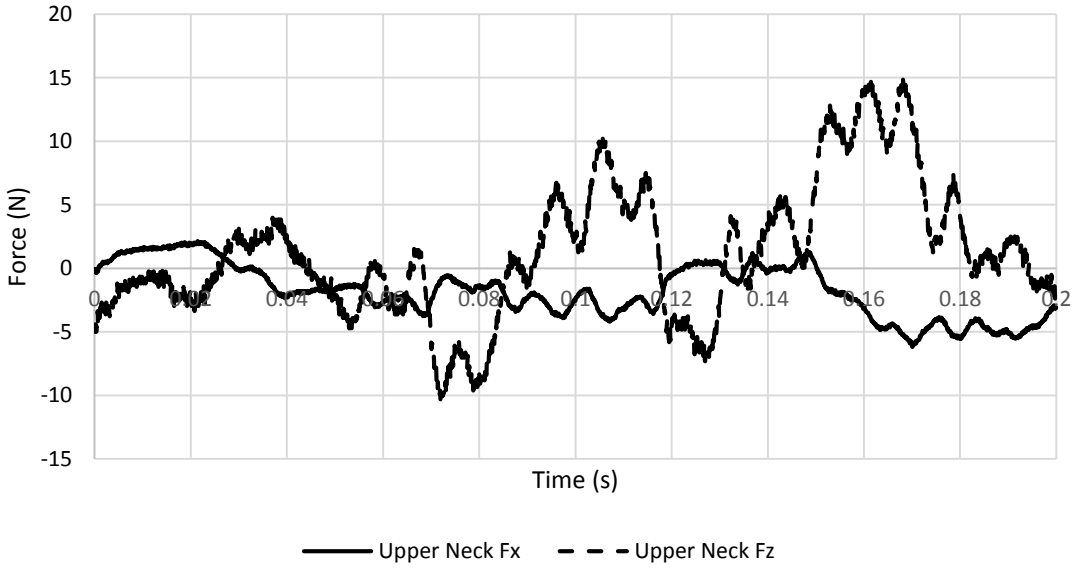


APPENDIX 2 OOP 1 UPPER NECK SHEAR (FX) AND TENSION (FZ) FORCE

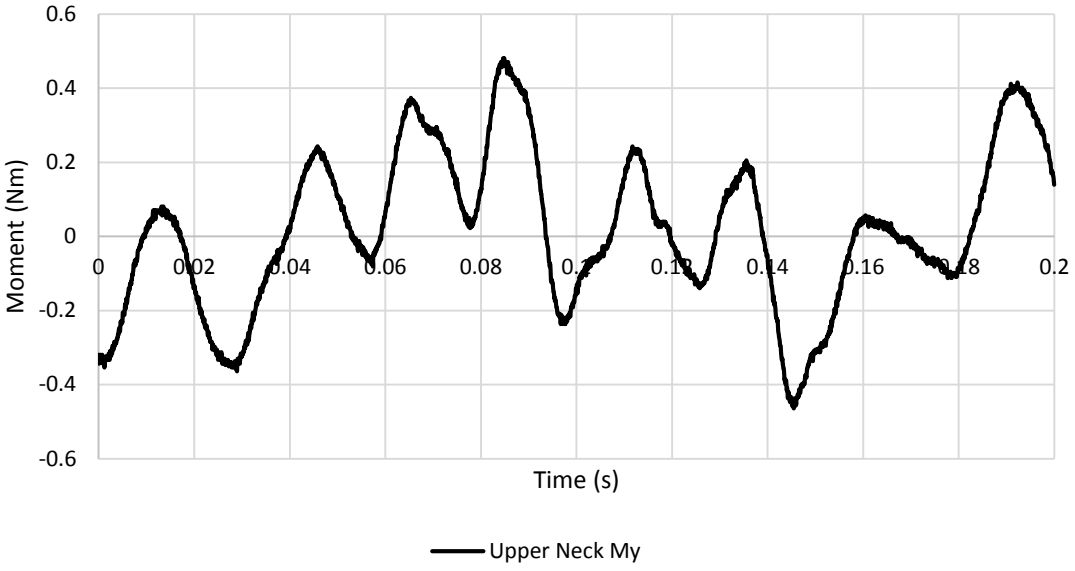


APPENDIX 3 OOP 1 UPPER NECK BENDING MOMENT ABOUT THE Y-AXIS (MY)

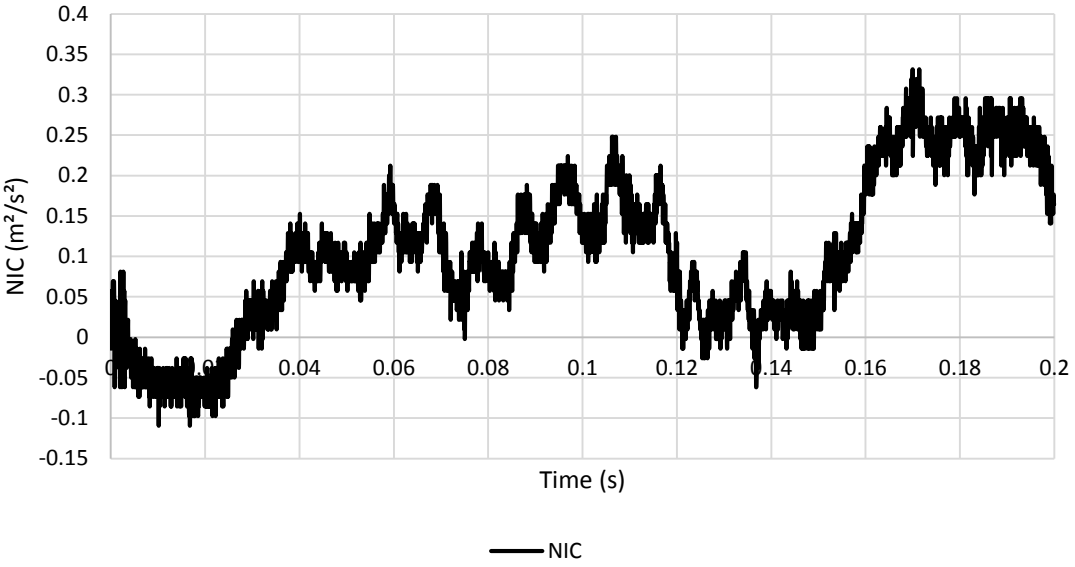


APPENDIX 4 OOP 1 NORMALISED NECK INJURY CRITERION (NIC)

| | Head ACC X | Upper Neck Fx | Upper Neck Fz | Upper Neck My | Sled ACC | T1 ACC | NECK ACC (C4) | NIC |
|---|---|---|---|---|---|---|---|---|
| unit | g | N | N | Nm | g | g | g | m²/s² |
| max | 0.06 | 2.13 | 14.85 | 0.48 | 0.00 | 0.00 | 0.18 | 0.33 |
| min | -0.17 | -6.17 | -10.84 | -0.46 | 0.00 | 0.00 | -0.35 | -0.11 |

APPENDIX 5 TEST RESULTS OOP1 OVERVIEW, MINIMA AND MAXIMA

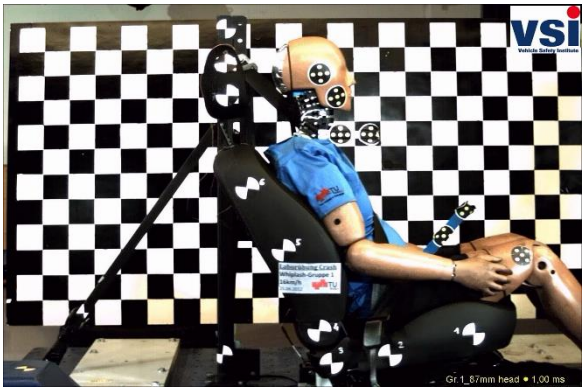


T = 0 MS

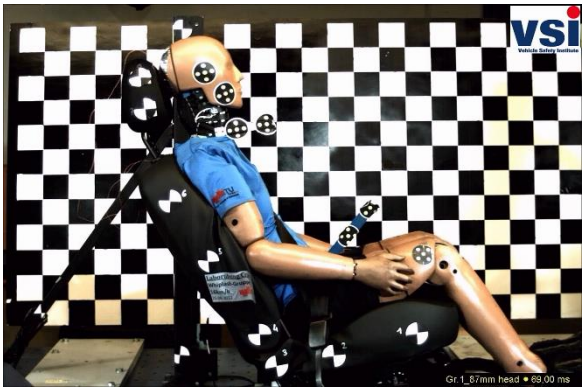


THRC START


MAX BACKREST DEFLECTION


THRC END

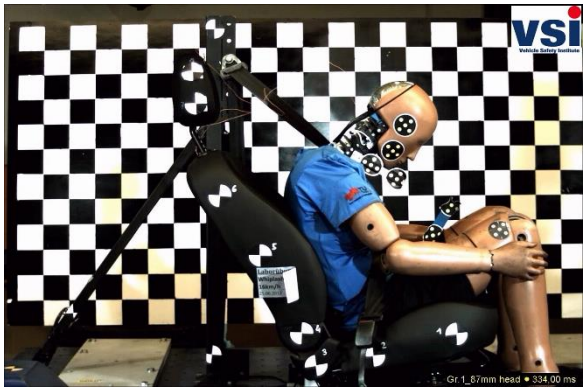


MAX REBOUND

APPENDIX 6 OOP 1 CINEMATIC OF OCCUPANT IN EURO NCAP CONFIGURED SEAT

## A.1.2. OOP 2

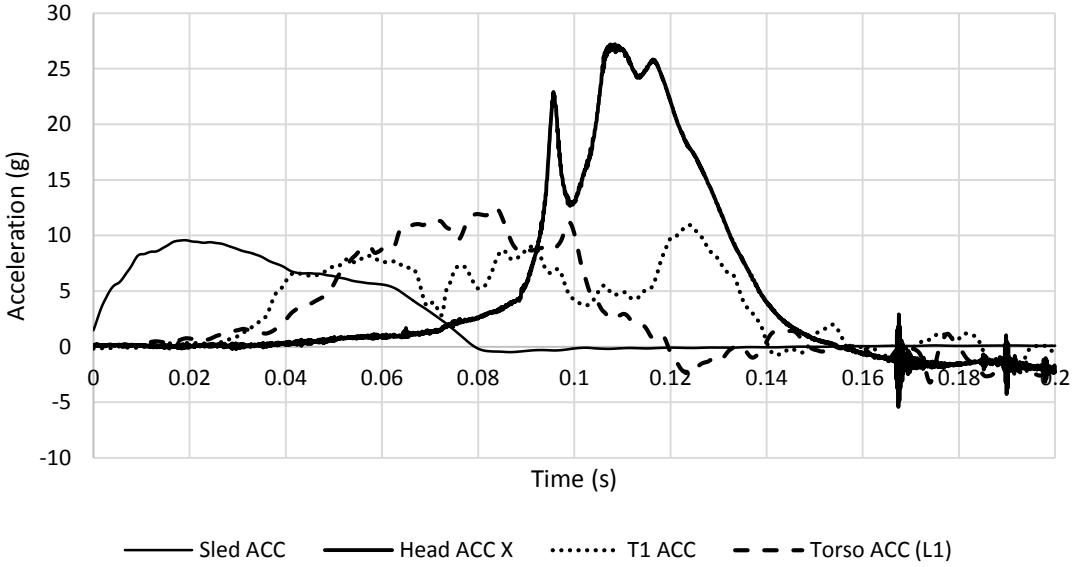


APPENDIX 7 OOP 2 SLED-, HEAD-, T1- AND TORSO- (L1) X ACCELERATION

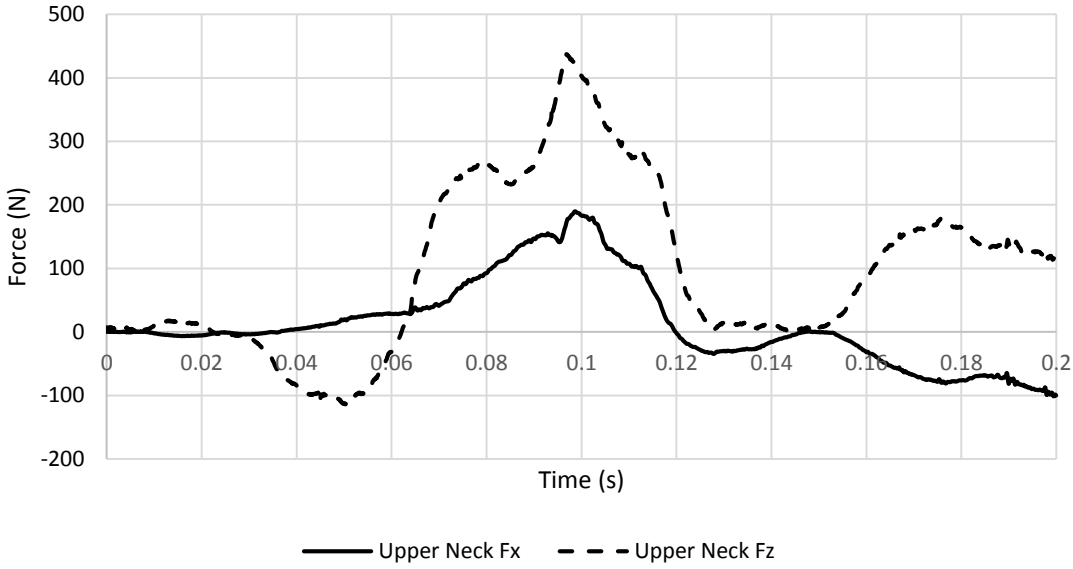


APPENDIX 8 OOP 2 UPPER NECK SHEAR (FX) AND TENSION (FZ) FORCE

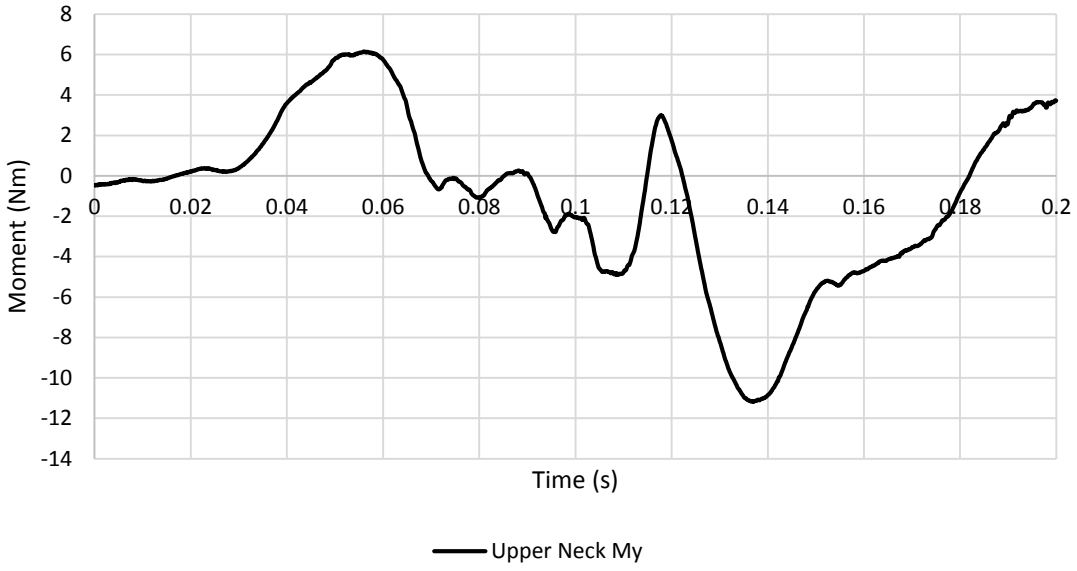


APPENDIX 9 OOP 2 UPPER NECK BENDING MOMENT ABOUT THE Y-AXIS (MY)

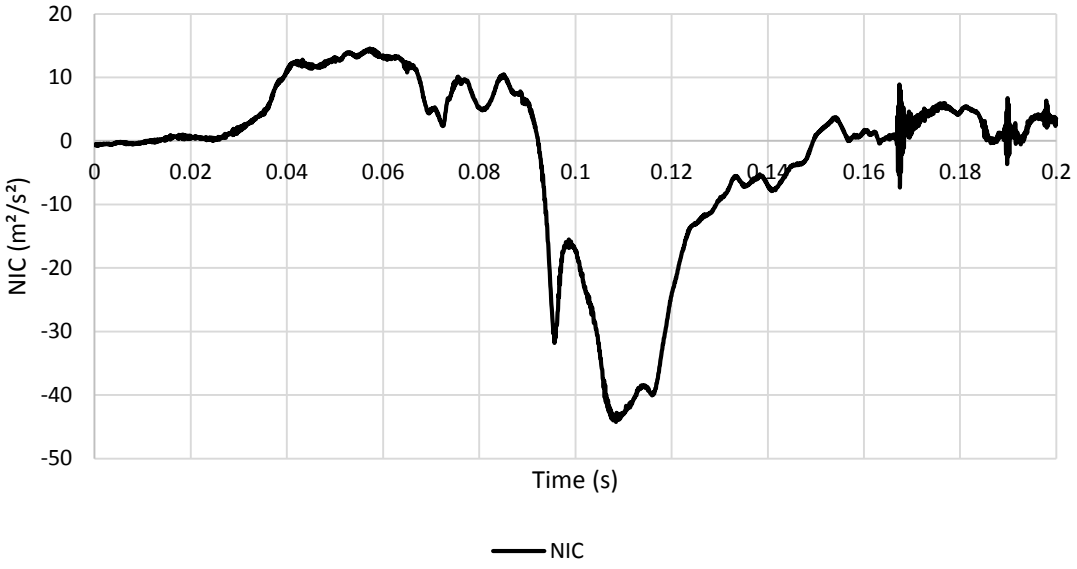


APPENDIX 10 OOP 2 NORMALISED NECK INJURY CRITERION (NIC)

| | Head ACC X | Upper Neck Fx | Upper Neck Fz | Upper Neck My | Sled ACC | T1 ACC | Torso ACC (L1) | NIC |
|---|---|---|---|---|---|---|---|---|
| unit | g | N | N | Nm | g | g | g | m²/s² |
| max | 27.21 | 189.74 | 437.23 | 6.15 | 9.58 | 10.94 | 12.52 | 14.54 |
| min | -5.42 | -101.42 | -114.05 | -11.20 | -0.49 | -1.67 | -3.23 | -44.24 |

APPENDIX 11 TEST RESULTS OOP2 OVERVIEW, MINIMA AND MAXIMA


T = 0 MS

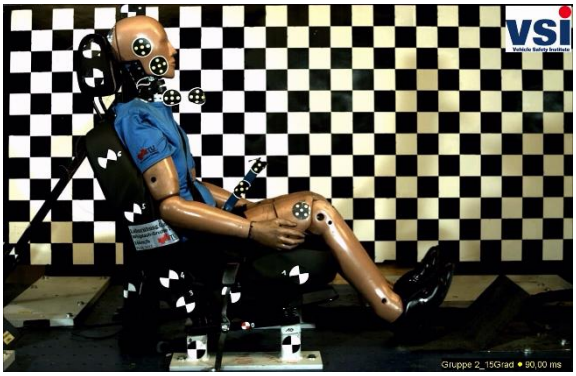


THRC START


MAX BACKREST DEFLECTION

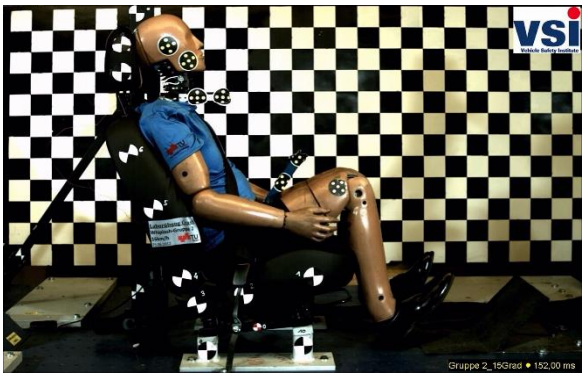


THRC END


MAX REBOUND

APPENDIX 12 OOP 2 CINEMATIC OF OCCUPANT IN A SEAT CONFIGURATION WITH THE BACKREST TILTED 10 ° FORWARD

## A.1.3. OOP 3

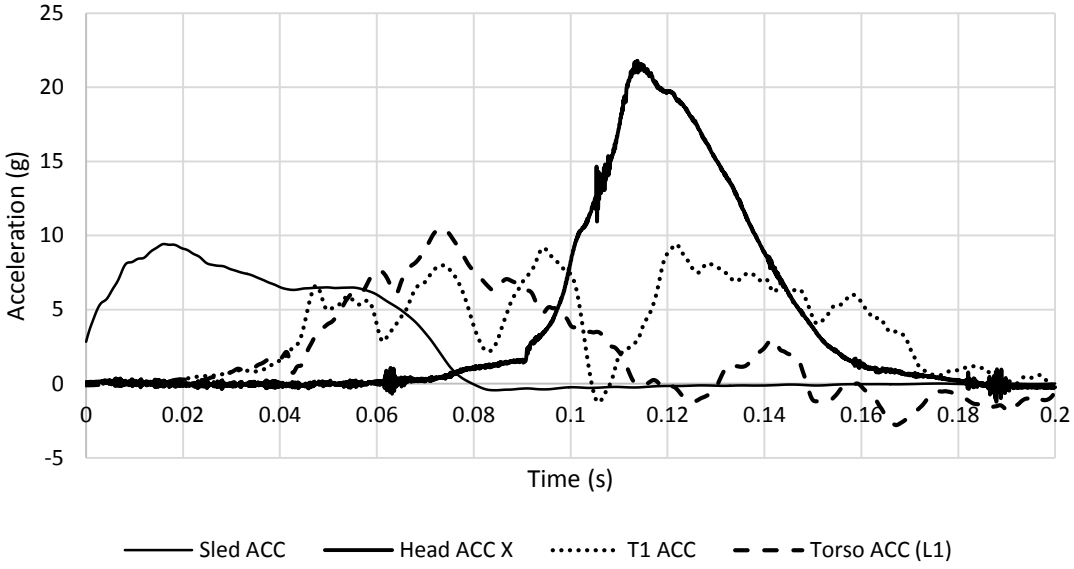


APPENDIX 13 OOP 3 SLED-, HEAD-, T1- AND TORSO- (L1) X ACCELERATION

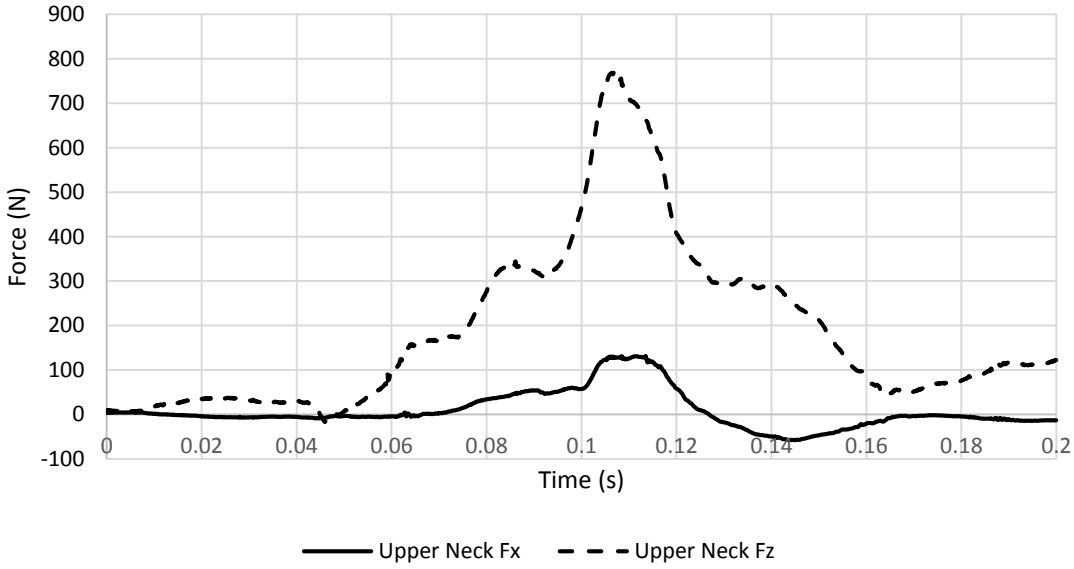


APPENDIX 14 OOP 3 UPPER NECK SHEAR (FX) AND TENSION (FZ) FORCE

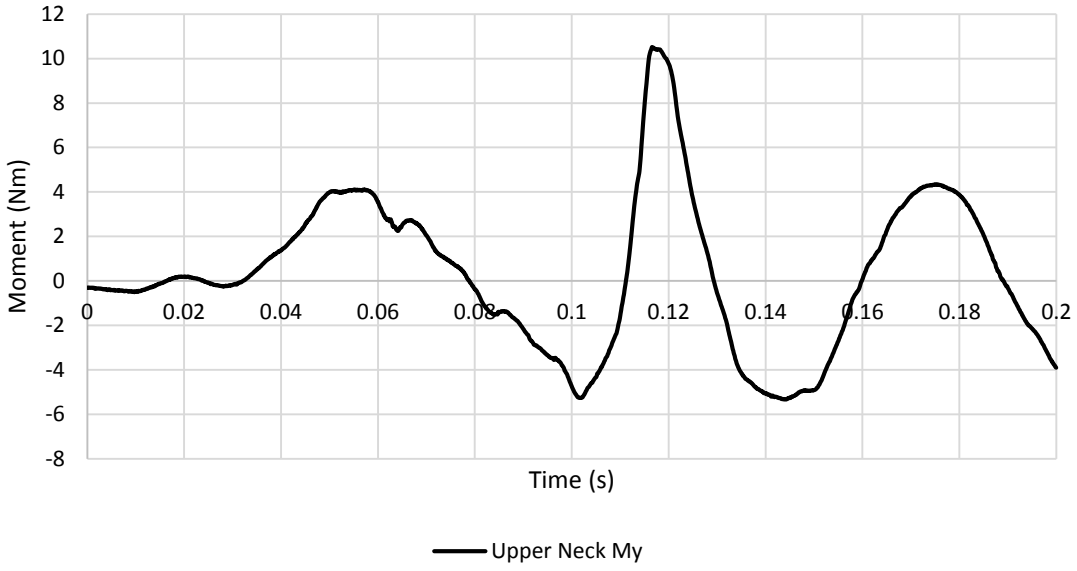


APPENDIX 15 OOP 3 UPPER NECK BENDING MOMENT ABOUT THE Y-AXIS (MY)

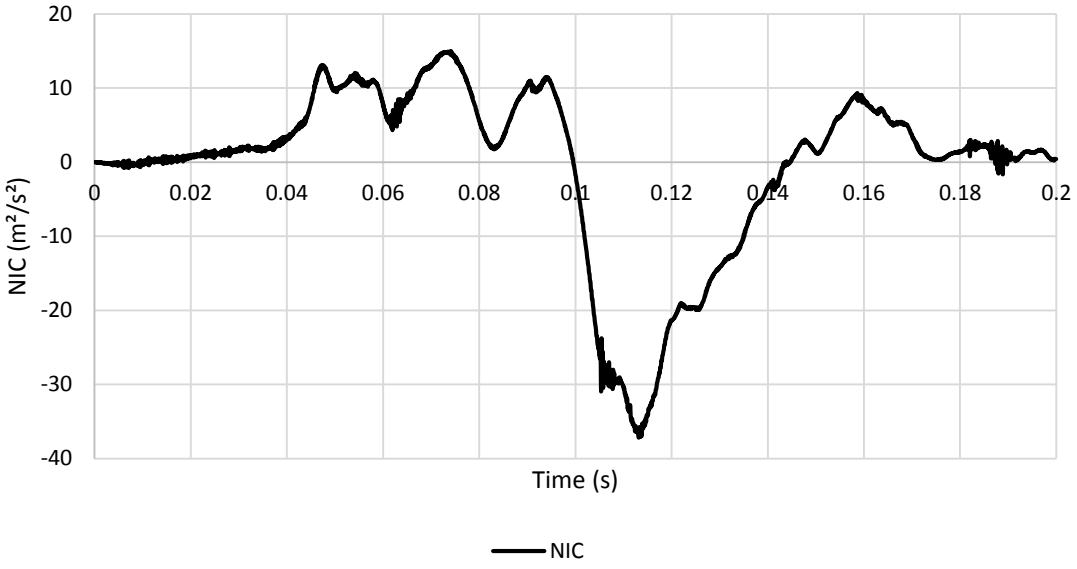


APPENDIX 16 OOP 3 NORMALISED NECK INJURY CRITERION (NIC)

| | Head ACC X | Upper Neck Fx | Upper Neck Fz | Upper Neck My | Sled ACC | T1 ACC | Torso ACC (L1) | NIC |
|---|---|---|---|---|---|---|---|---|
| unit | g | N | N | Nm | g | g | g | m²/s² |
| max | 21.79 | 131.06 | 768.84 | 10.52 | 9.42 | 9.41 | 10.47 | 14.96 |
| min | -1.22 | -57.89 | -17.58 | -5.34 | -0.44 | -1.25 | -2.78 | -37.19 |

APPENDIX 17 TEST RESULTS OOP3 OVERVIEW, MINIMA AND MAXIMA

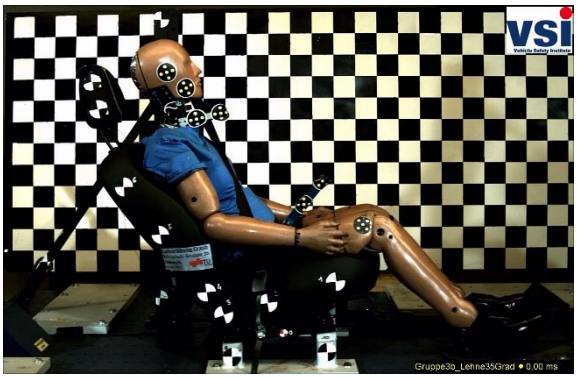


T = 0 MS


THRC START


MAX BACKREST DEFLECTION


THRC END

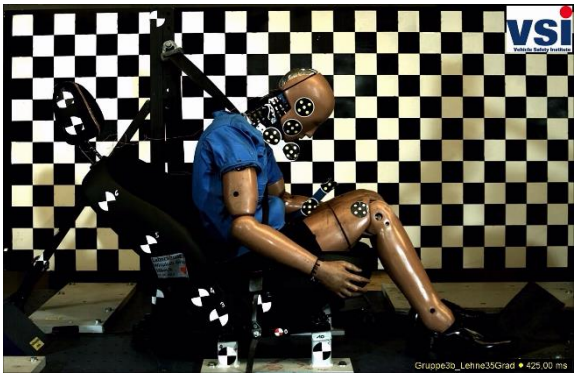


MAX REBOUND

APPENDIX 18 OOP 3 CINEMATIC OF OCCUPANT IN A SEAT CONFIGURATION WITH THE BACKREST TILTED 10 ° BACKWARD

## A.1.4. OOP 4

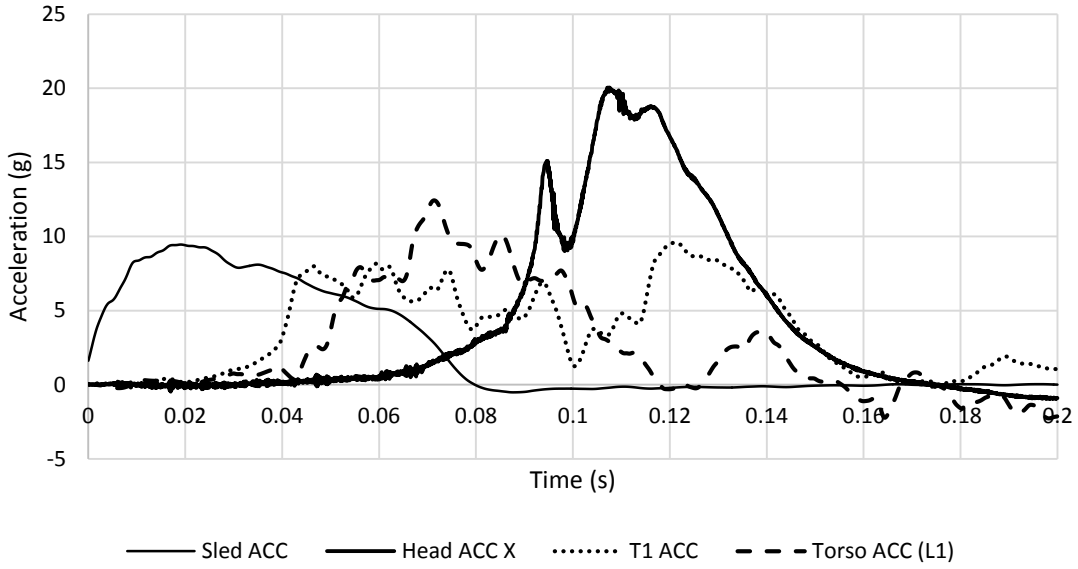


APPENDIX 19 OOP 4 SLED-, HEAD-, T1- AND TORSO- (L1) X ACCELERATION

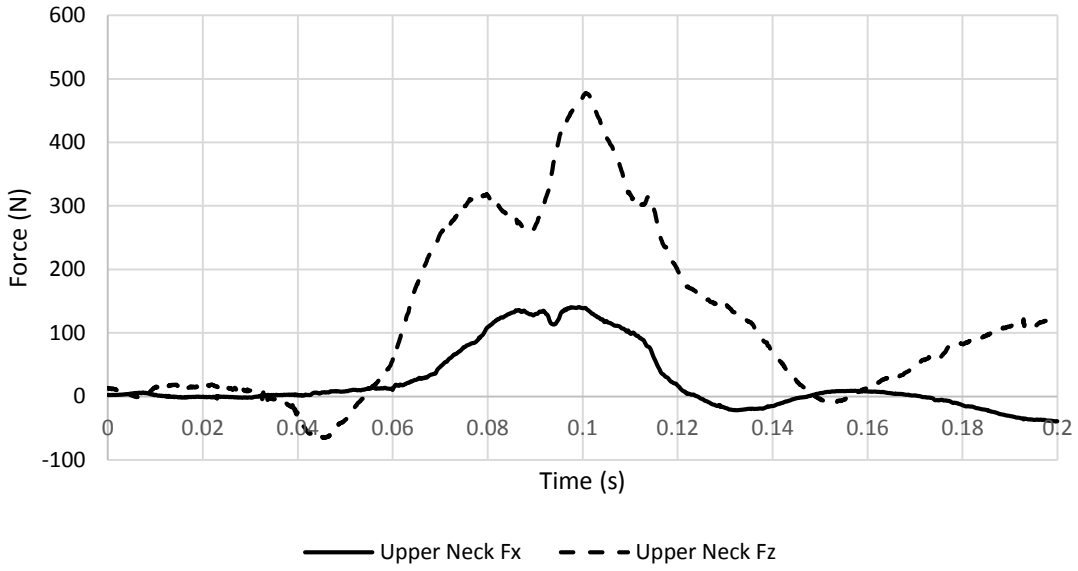


APPENDIX 20 OOP 4 UPPER NECK SHEAR (FX) AND TENSION (FZ) FORCE

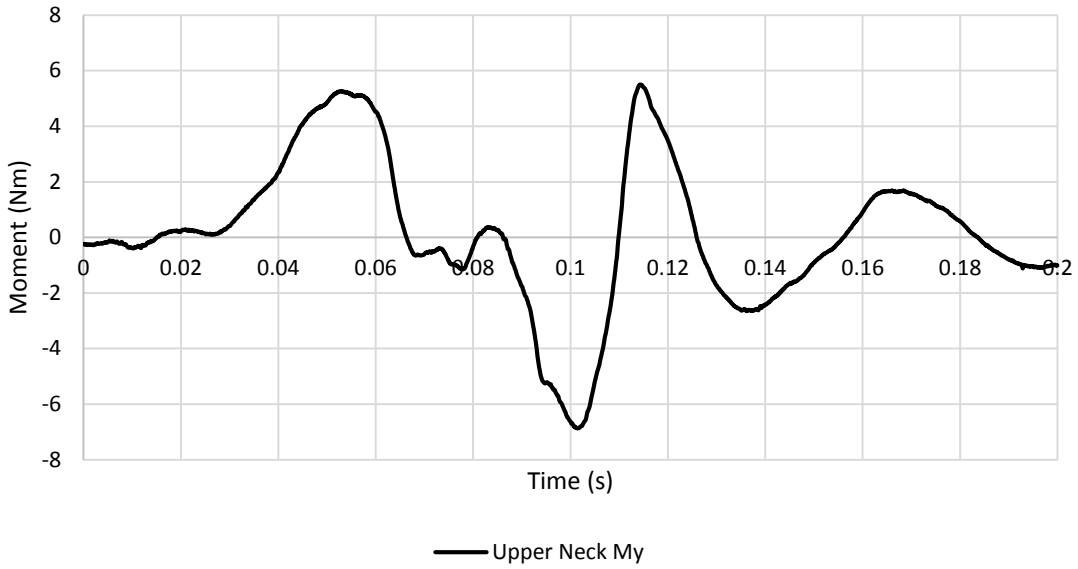


APPENDIX 21 OOP 4 UPPER NECK BENDING MOMENT ABOUT THE Y-AXIS (MY)

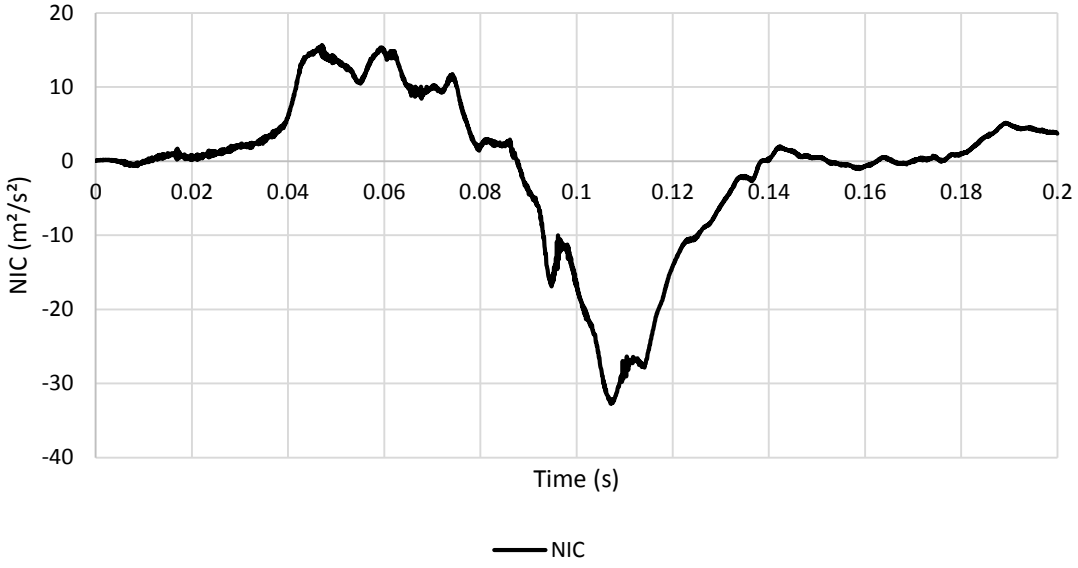


APPENDIX 22 OOP 4 NORMALISED NECK INJURY CRITERION (NIC)

| | Head ACC X | Upper Neck Fx | Upper Neck Fz | Upper Neck My | Sled ACC | T1 ACC | Torso ACC (L1) | NIC |
|---|---|---|---|---|---|---|---|---|
| unit | g | N | N | Nm | g | g | g | (m²/s²) |
| max | 20.05 | 39.05 | 65.64 | 6.86 | 9.46 | 9.61 | 12.43 | 15.63 |
| min | -0.96 | -140.42 | -477.76 | -5.50 | -0.51 | -0.20 | -2.28 | -32.75 |

APPENDIX 23 TEST RESULTS OOP1 OVERVIEW, MINIMA AND MAXIMA

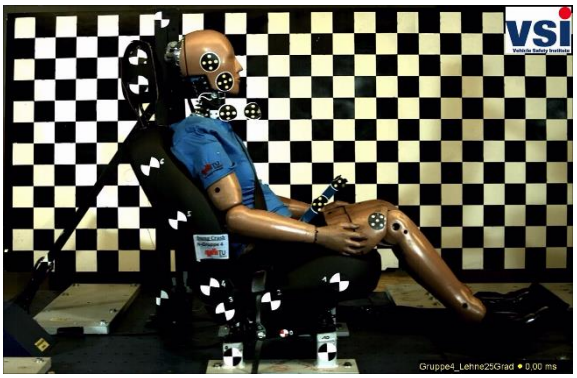


T = 0 MS

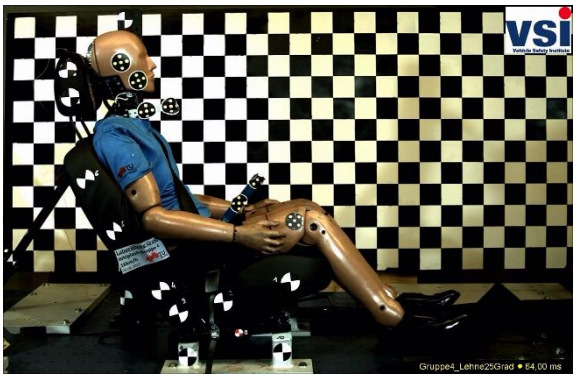


THRC START


MAX BACKREST DEFLECTION

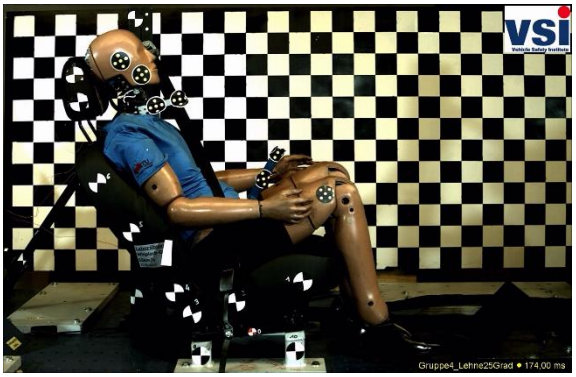


THRC END


MAX REBOUND

APPENDIX 24 OOP 4 CINEMATIC OF OCCUPANT IN EURO NCAP CONFIGURED SEAT

## A.1.5. OOP 5

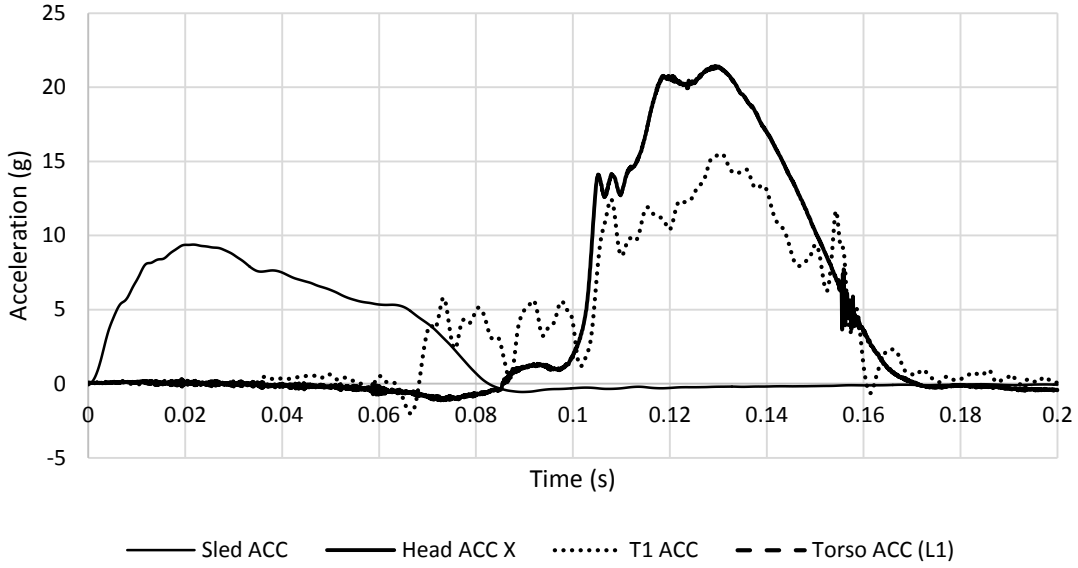


APPENDIX 25 OOP 5 SLED-, HEAD-, T1- AND TORSO- (L1) X ACCELERATION

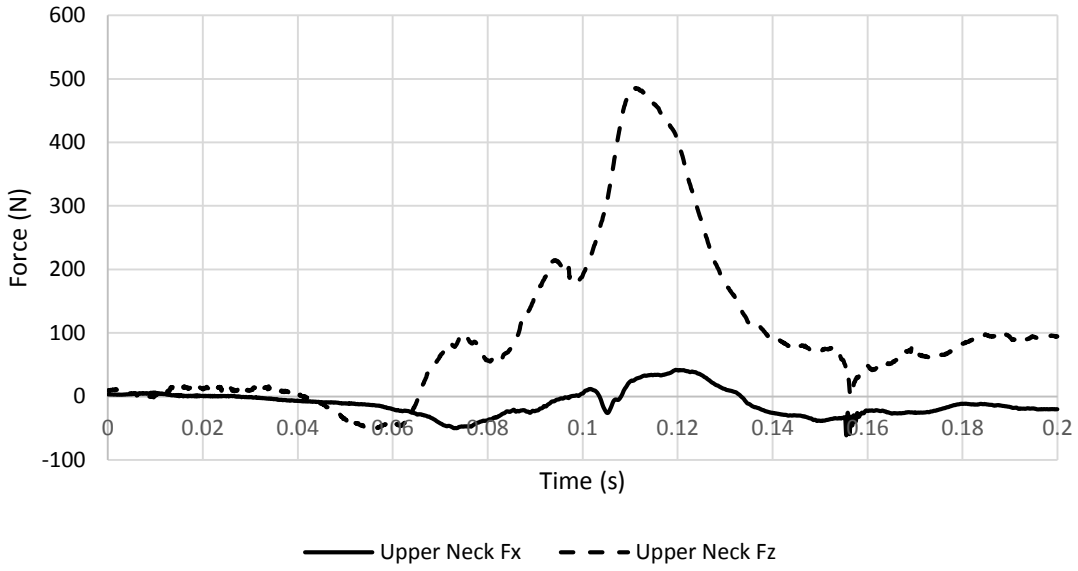


APPENDIX 26 OOP 5 UPPER NECK SHEAR (FX) AND TENSION (FZ) FORCE

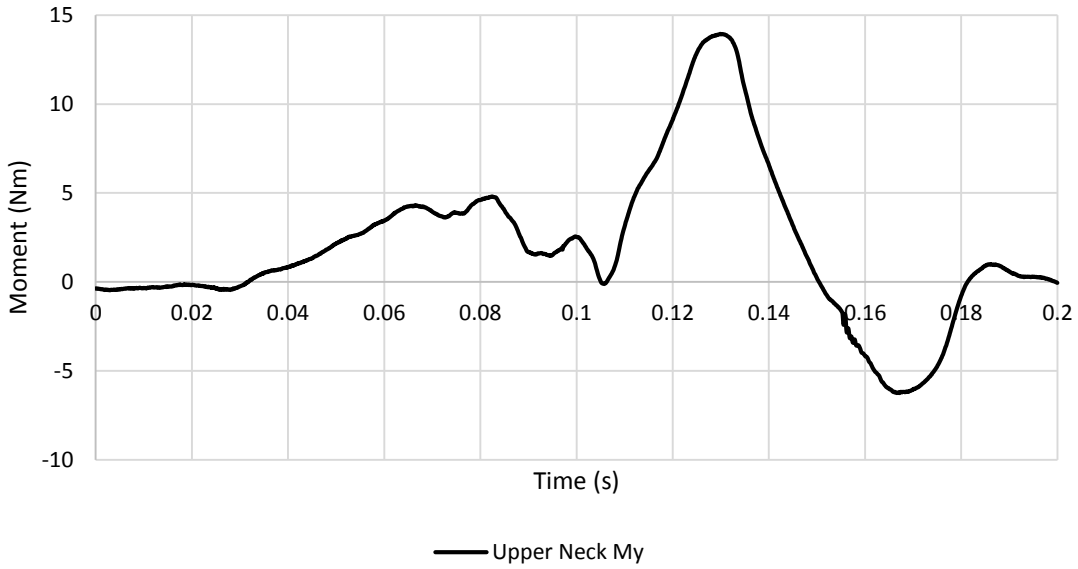


APPENDIX 27 OOP 5 UPPER NECK BENDING MOMENT ABOUT THE Y-AXIS (MY)

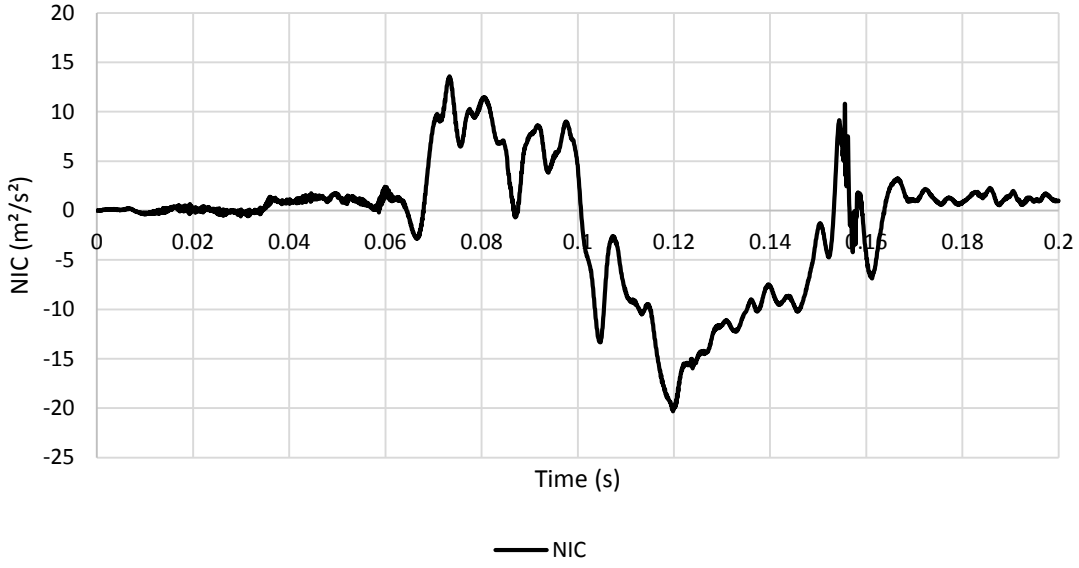


APPENDIX 28 OOP 5 NORMALISED NECK INJURY CRITERION (NIC)

| | Head ACC X | Upper Neck Fx | Upper Neck Fz | Upper Neck My | Sled ACC | T1 ACC | Torso ACC (L1) | NIC |
|---|---|---|---|---|---|---|---|---|
| unit | g | N | N | Nm | g | g | g | $m^2/s^2$ |
| max | 21.42 | 42.09 | 485.12 | 13.94 | 9.39 | 15.52 | - | 13.56 |
| min | -1.13 | -61.47 | -49.98 | -6.26 | -0.56 | -2.02 | - | -20.33 |

APPENDIX 29 TEST RESULTS OOP5 OVERVIEW, MINIMA AND MAXIMA

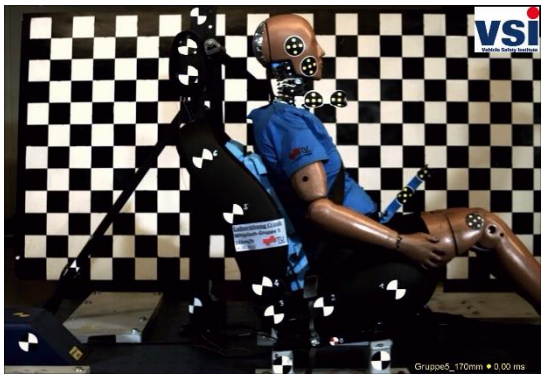


T = 0 ms

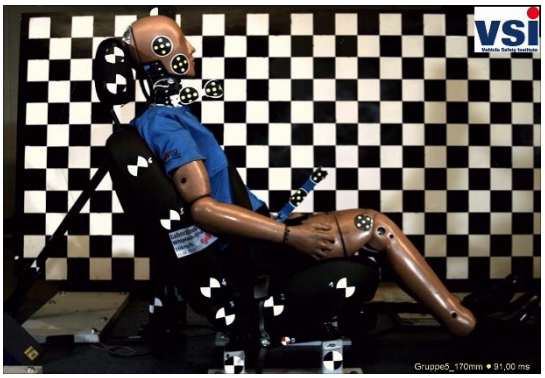


THRC start

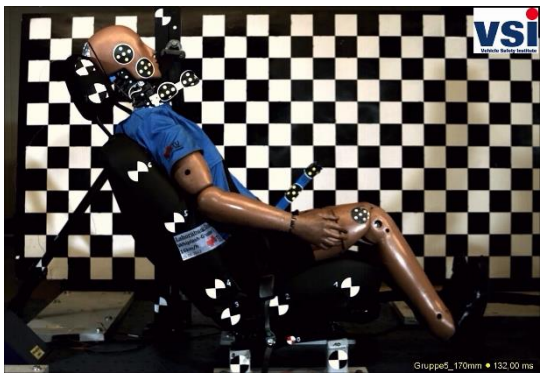


max backrest deflection

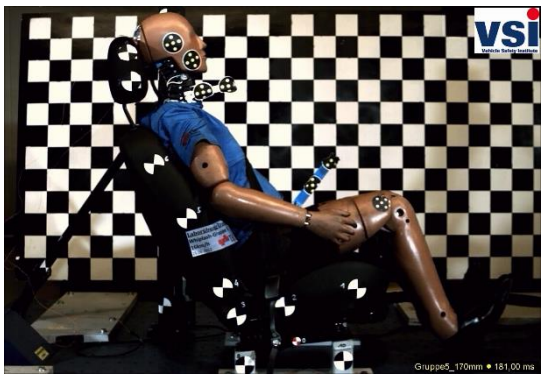


THRC end


max rebound

APPENDIX 30 OOP 5 CINEMATIC OF OCCUPANT IN SEAT WITH EXTENDED BACKSET OF 170 MM

## A.1.6. OOP 6

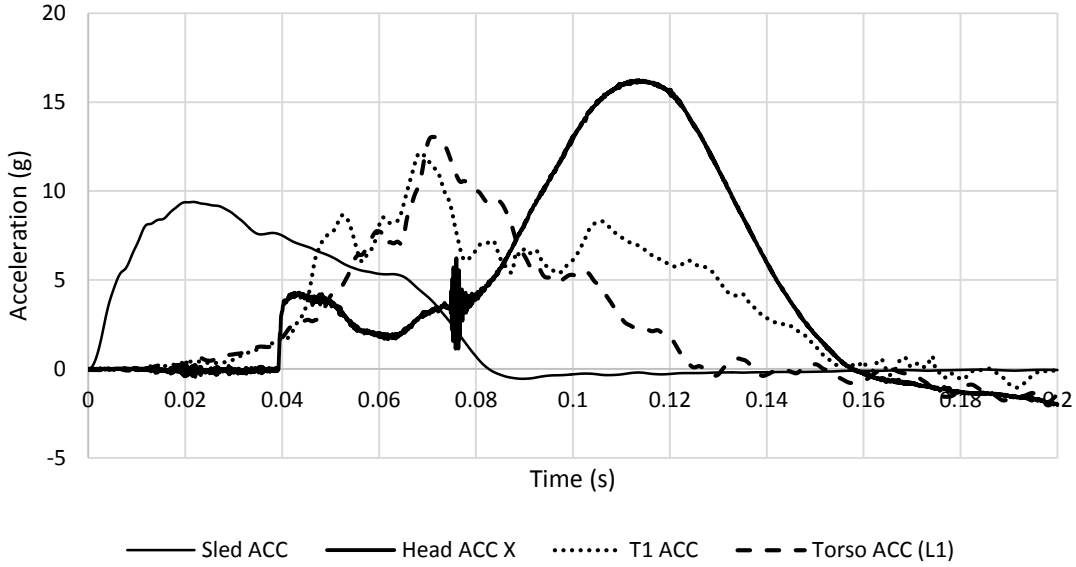


APPENDIX 31 OOP 6 SLED-, HEAD-, T1- AND TORSO- (L1) X ACCELERATION

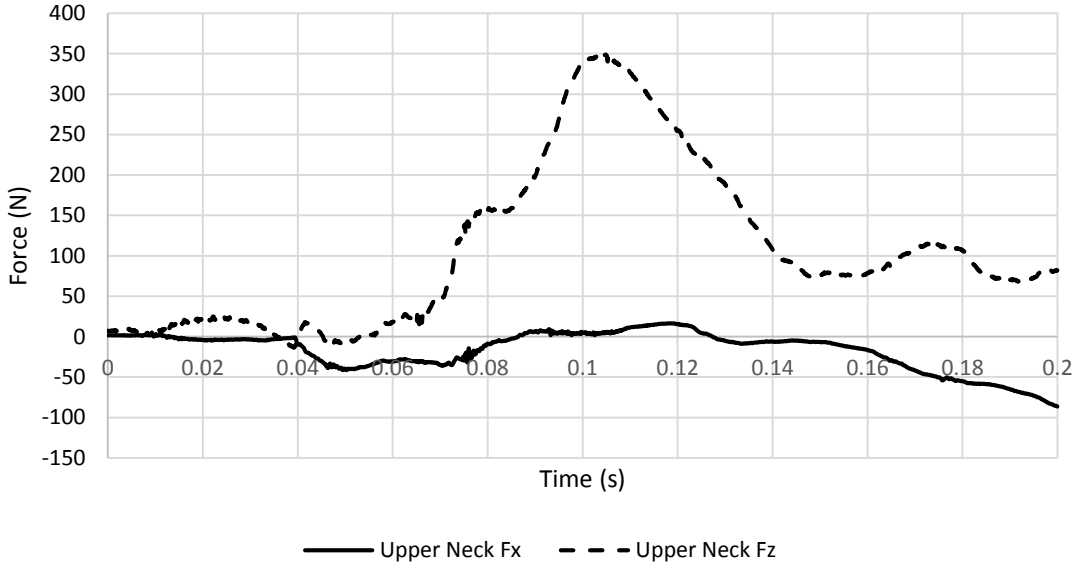


APPENDIX 32 OOP 6 UPPER NECK SHEAR (FX) AND TENSION (FZ) FORCE

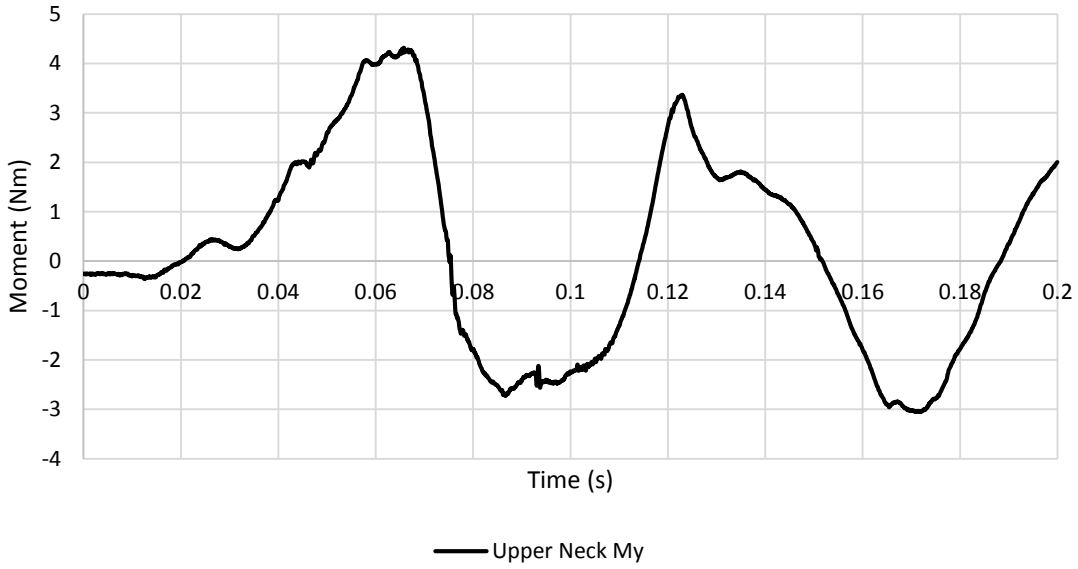


APPENDIX 33 OOP 6 UPPER NECK BENDING MOMENT ABOUT THE Y-AXIS (MY)

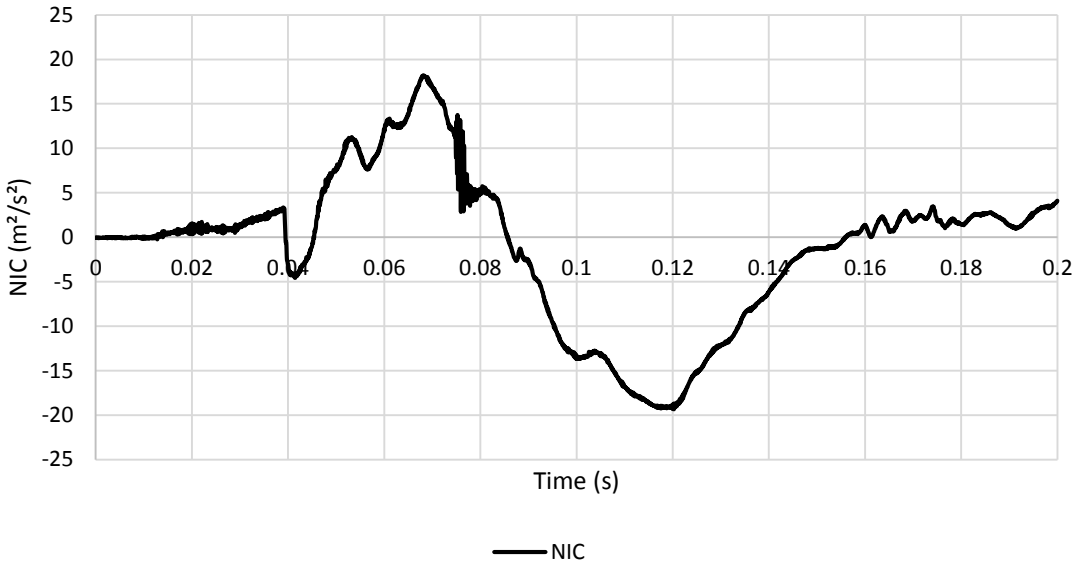


APPENDIX 34 OOP 6 NORMALISED NECK INJURY CRITERION (NIC)

| | Head ACC X | Upper Neck Fx | Upper Neck Fz | Upper Neck My | Sled ACC | T1 ACC | Torso ACC (L1) | NIC |
|---|---|---|---|---|---|---|---|---|
| unit | g | N | N | Nm | g | g | g | $m^2/s^2$ |
| max | 16.24 | 16.66 | 349.12 | 4.32 | 9.39 | 12.16 | 13.05 | 18.19 |
| min | -2.01 | -86.48 | -13.50 | -3.05 | -0.56 | -1.05 | -1.97 | -19.35 |

APPENDIX 35 TEST RESULTS OOP6 OVERVIEW, MINIMA AND MAXIMA


T = 0 MS

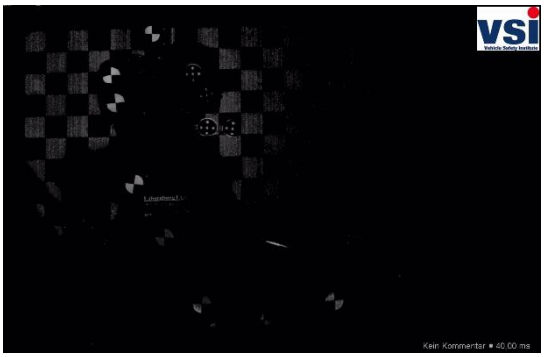


THRC START


MAX BACKREST DEFLECTION

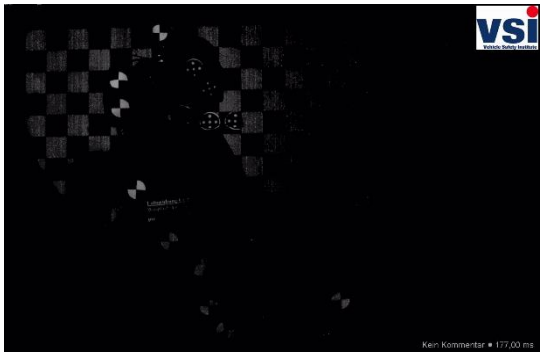


THRC END

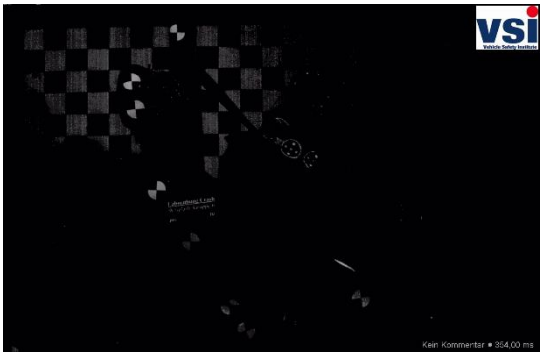


MAX REBOUND

APPENDIX 36 OOP 6 CINEMATIC OF OCCUPANT IN SEAT WITH REDUCED BACKSET OF CLOSE TO 0 MM

## A.2. Bio RID 50F Test Details

### A.2.1. TUG11007

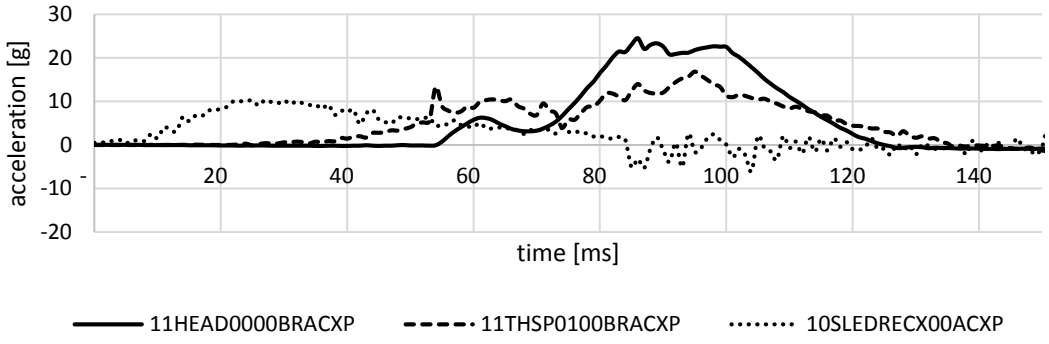


APPENDIX 37 BIO RID 50F TUG11007 SLED, HEAD, T1 ACCELERATION OVER TIME

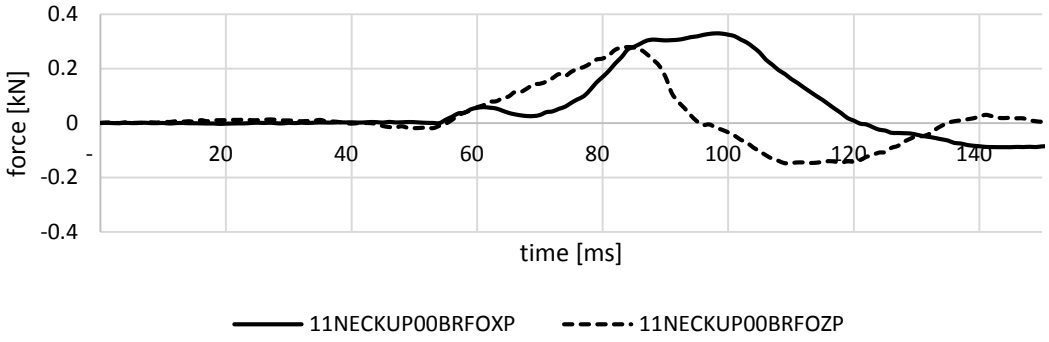


APPENDIX 38 BIO RID 50F TUG11007 UPPER NECK TENSION (FZ) AND SHEAR (FZ) FORCE OVER TIME

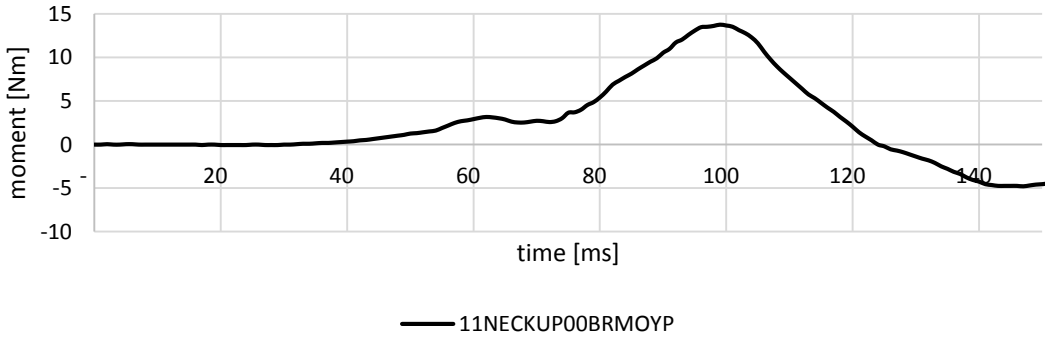


APPENDIX 39 BIO RID 50F TUG11007 UPPER NECK EXTENSION AND FLEXION (MY) MOMENT OVER TIME

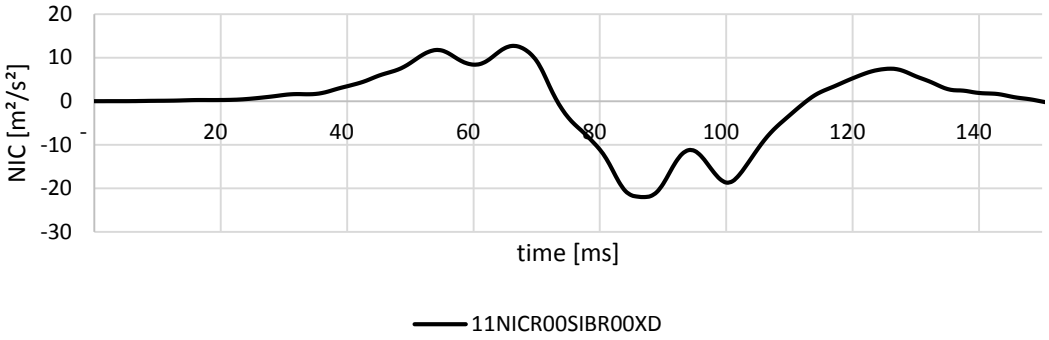


APPENDIX 40 BIO RID 50F TUG11007 NIC CRITERION OVER TIME

## A.2.2. TUG11008

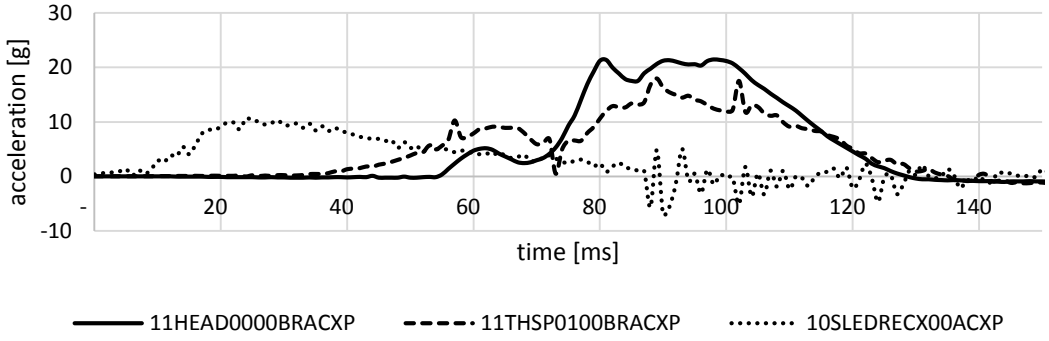


APPENDIX 41 BIO RID 50F TUG11008 SLED, HEAD, T1 ACCELERATION OVER TIME

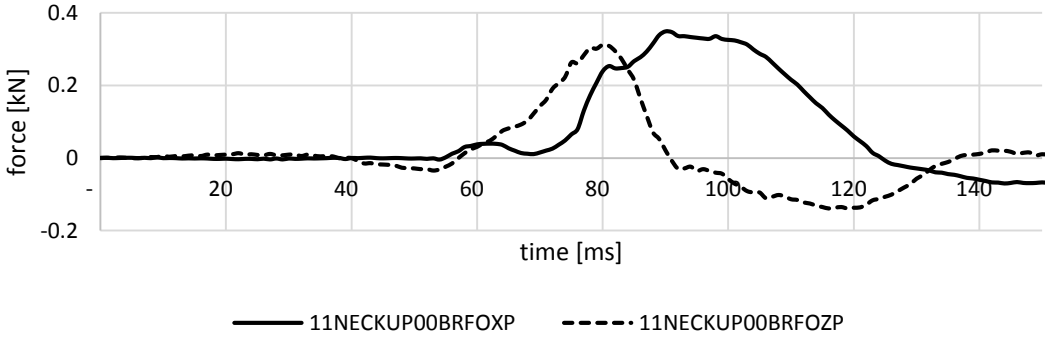


APPENDIX 42 BIO RID 50F TUG11008 UPPER NECK TENSION (FZ) AND SHEAR (FZ) FORCE OVER TIME

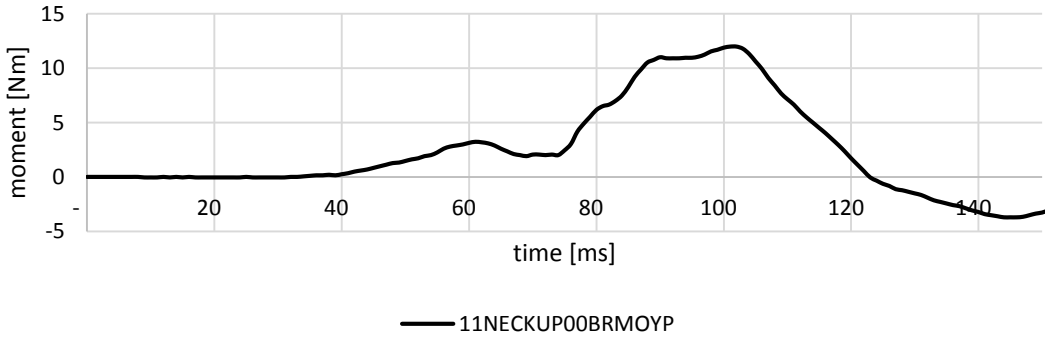


APPENDIX 43 BIO RID 50F TUG11008 UPPER NECK EXTENSION AND FLEXION (MY) MOMENT OVER TIME

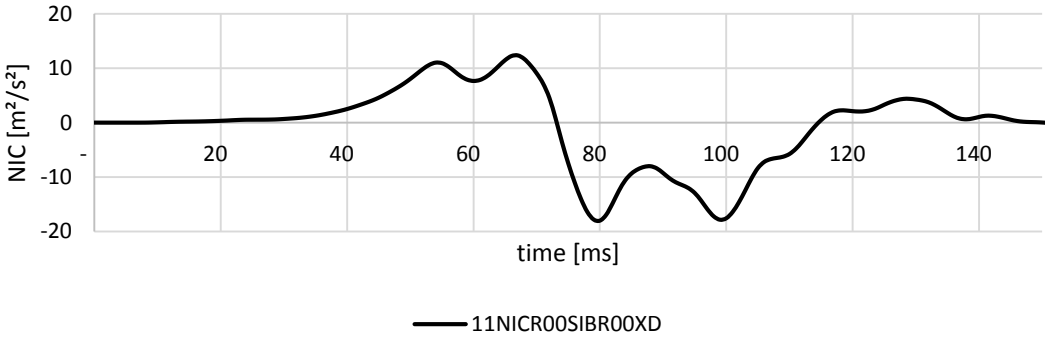


APPENDIX 44 BIO RID 50F TUG11008 NIC CRITERION OVER TIME

## A.3. PMHS Test Result Details

### A.3.1. PMHS 1 Test 1

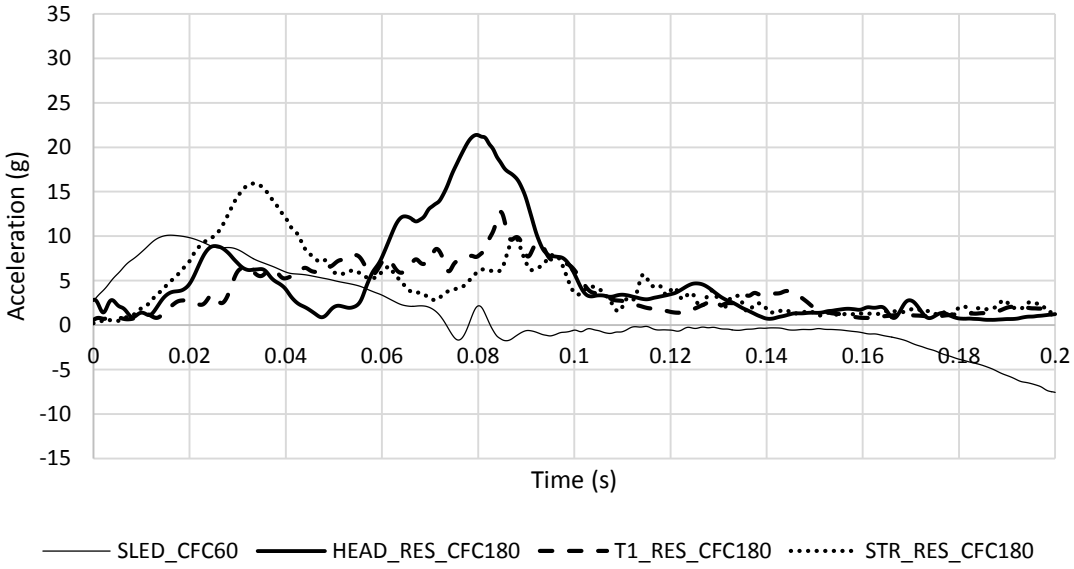


APPENDIX 45 PMHS 1 TEST 1 SLED, HEAD, T1, STERNUM ACCELERATION OVER TIME

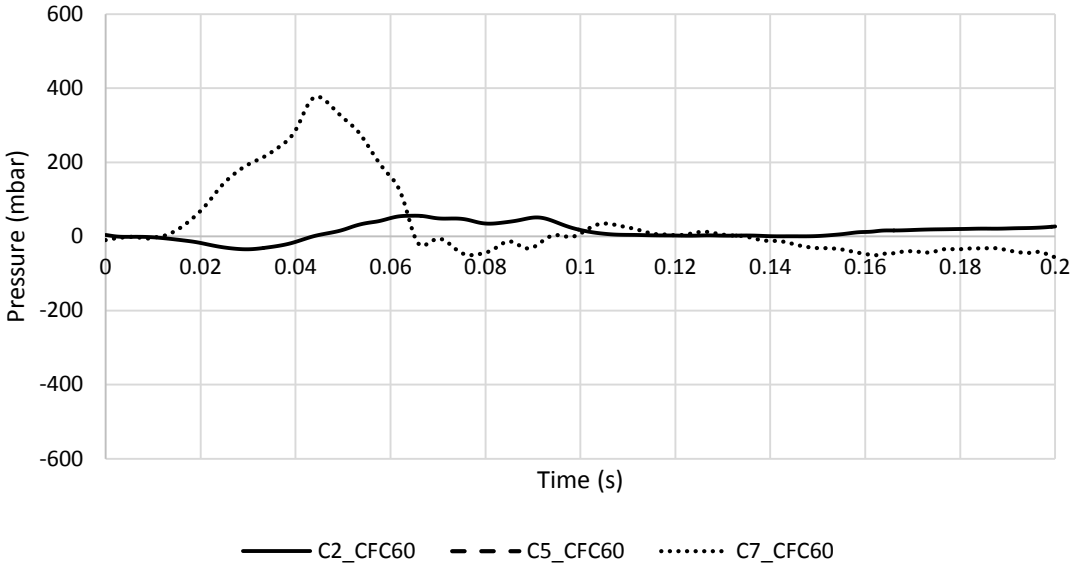


APPENDIX 46 PMHS 1 TEST 1 SPINAL CANAL PRESSURE AT C2, C5 AND C7 OVER TIME

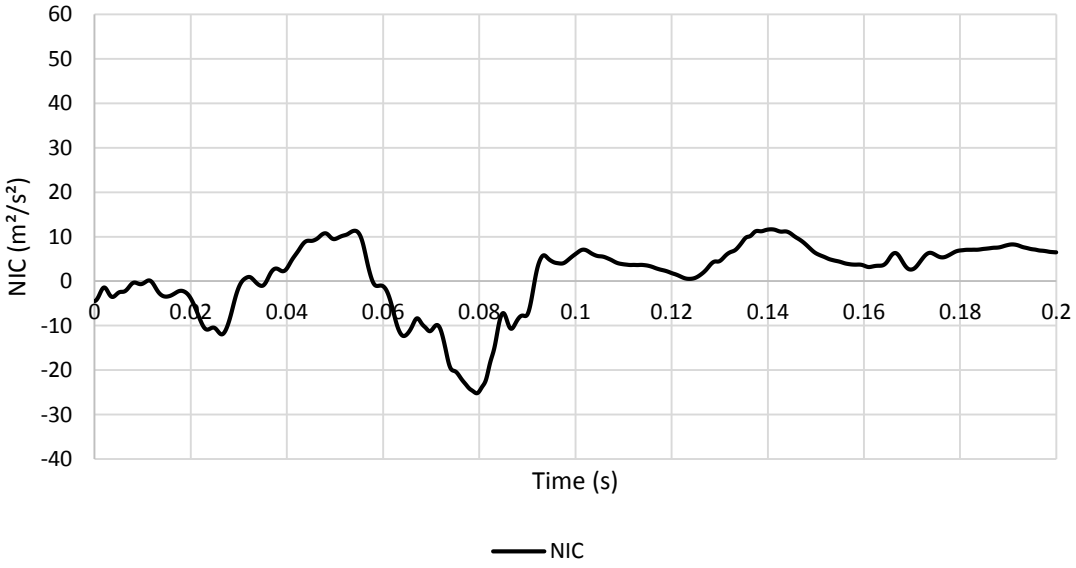


APPENDIX 47 PMHS 1 TEST 1 NIC OVER TIME

| 11 | C2_CFC60 | C5_CFC60 | C7_CFC60 | SLED_CFC60 | HEAD_RES_CFC180 | T1_RES_CFC180 | STR_RES_CFC180 | NIC |
|---|---|---|---|---|---|---|---|---|
| unit | mbar | mbar | mbar | g | g | g | g | m²/s² |
| max | 56 | -10268 | 377 | 10 | 21 | 13 | 16 | 12 |
| min | -35 | -10268 | -56 | -7.6 | 0.6 | 0.6 | 0.2 | -25 |

APPENDIX 48 PMHS 1 TEST 1 MAXIMUM AND MINIMUM CHARACTERISTIC VALUES

## A.3.2. PMHS 1 Test 2

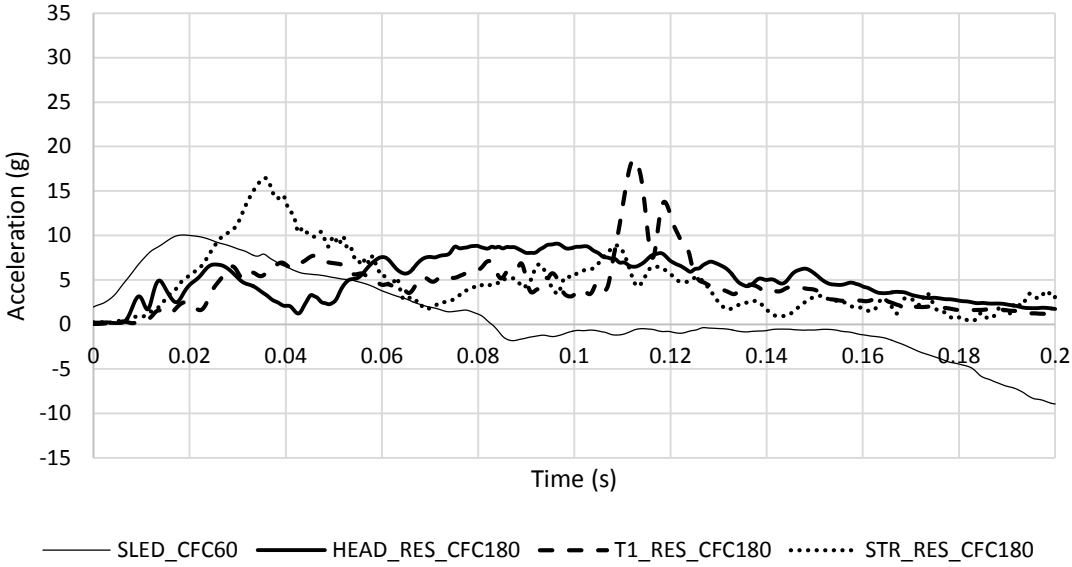


APPENDIX 49 PMHS 1 TEST 2 SLED, HEAD, T1, STERNUM ACCELERATION OVER TIME

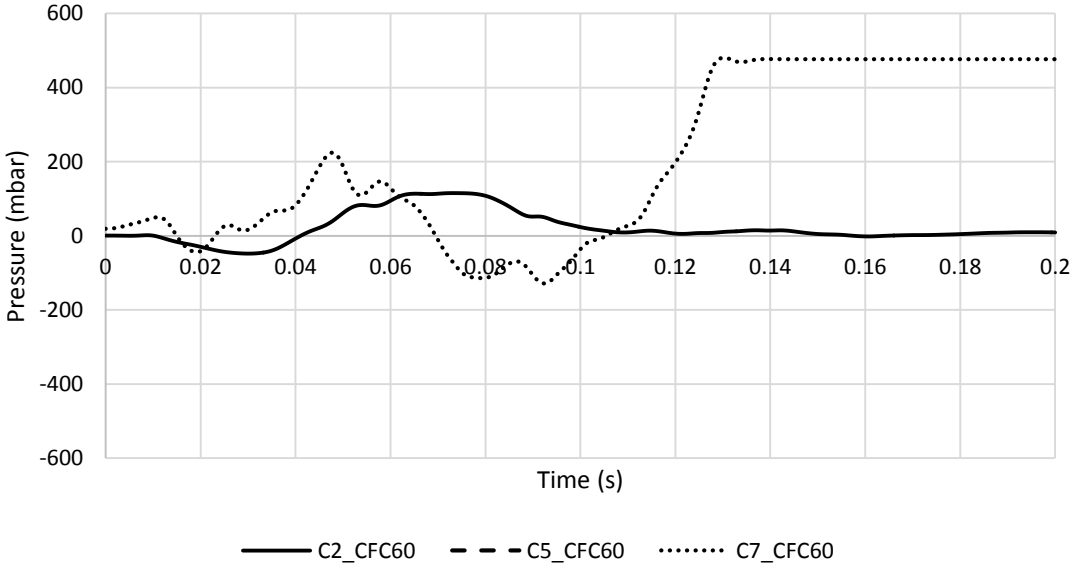


APPENDIX 50 PMHS 1 TEST 2 SPINAL CANAL PRESSURE AT C2, C5 AND C7 OVER TIME

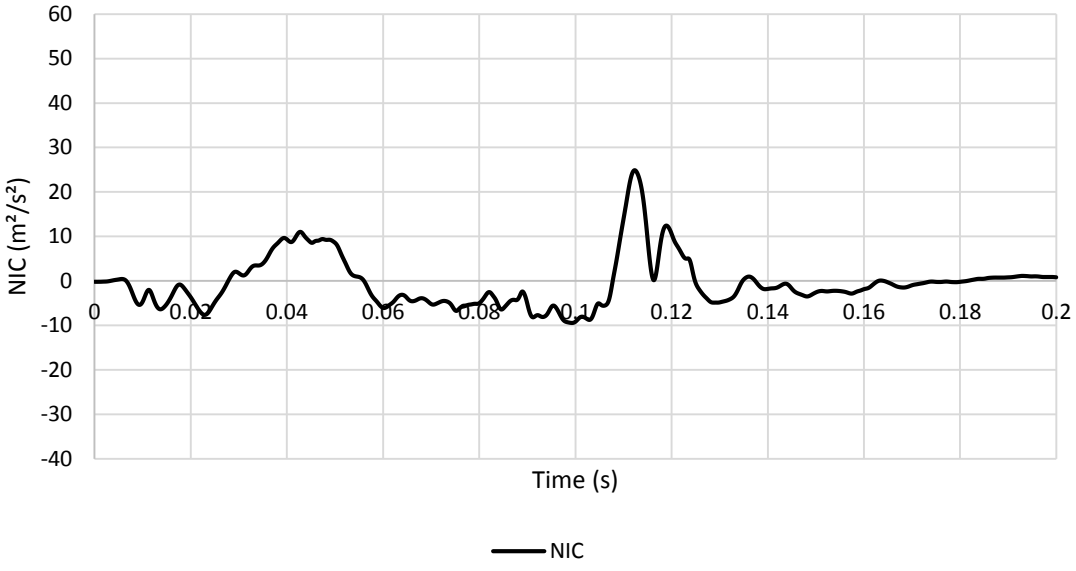


APPENDIX 51 PMHS 1 TEST 2 NIC OVER TIME

| 12 | C2_CFC60 | C5_CFC60 | C7_CFC60 | SLED_CFC60 | HEAD_RES_CFC180 | T1_RES_CFC180 | STR_RES_CFC180 | NIC |
|---|---|---|---|---|---|---|---|---|
| unit | mbar | mbar | mbar | g | g | g | g | m²/s² |
| max | 115 | -9245 | 481 | 10 | 9.1 | 19 | 16 | 25 |
| min | -48 | -10291 | -129 | -8.9 | 0.2 | 0.1 | 0.2 | -9.5 |

APPENDIX 52 PMHS 1 TEST 2 MAXIMUM AND MINIMUM CHARACTERISTIC VALUES

### A.3.3. PMHS 1 Test 3

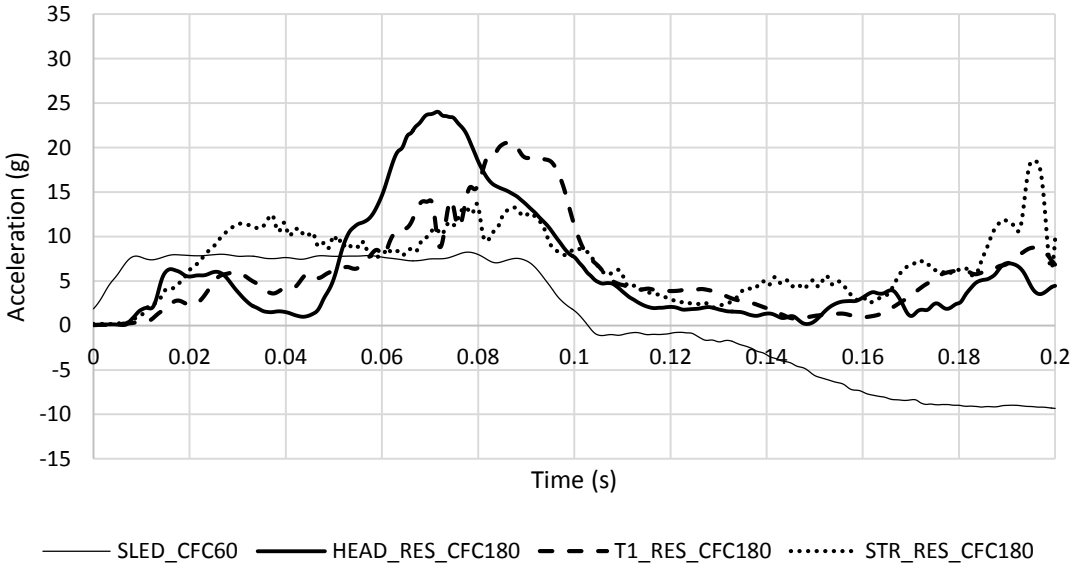


APPENDIX 53 PMHS 1 TEST 3 SLED, HEAD, T1, STERNUM ACCELERATION OVER TIME

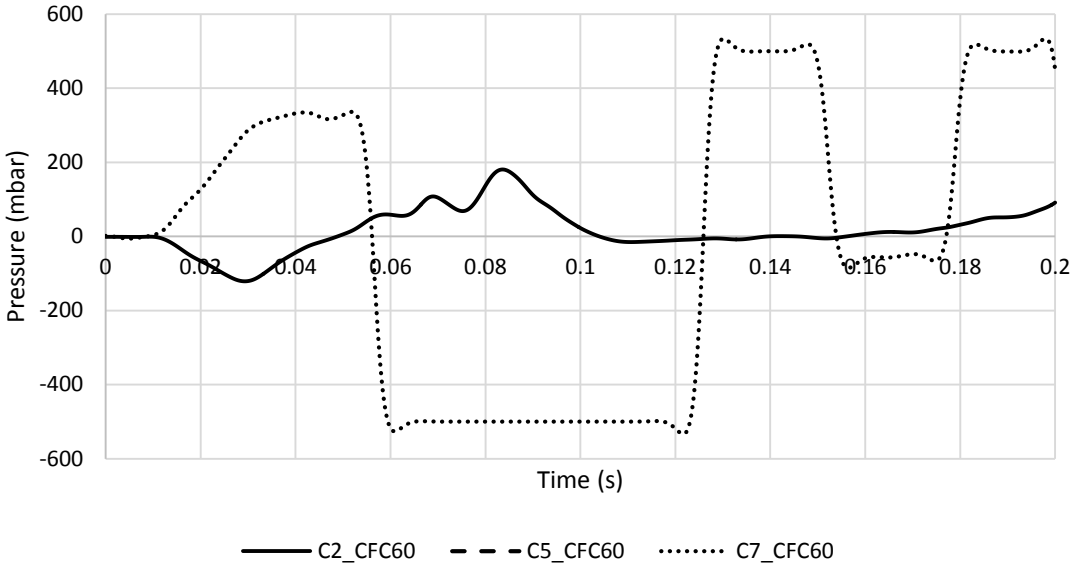


APPENDIX 54 PMHS 1 TEST 3 SPINAL CANAL PRESSURE AT C2, C5 AND C7 OVER TIME

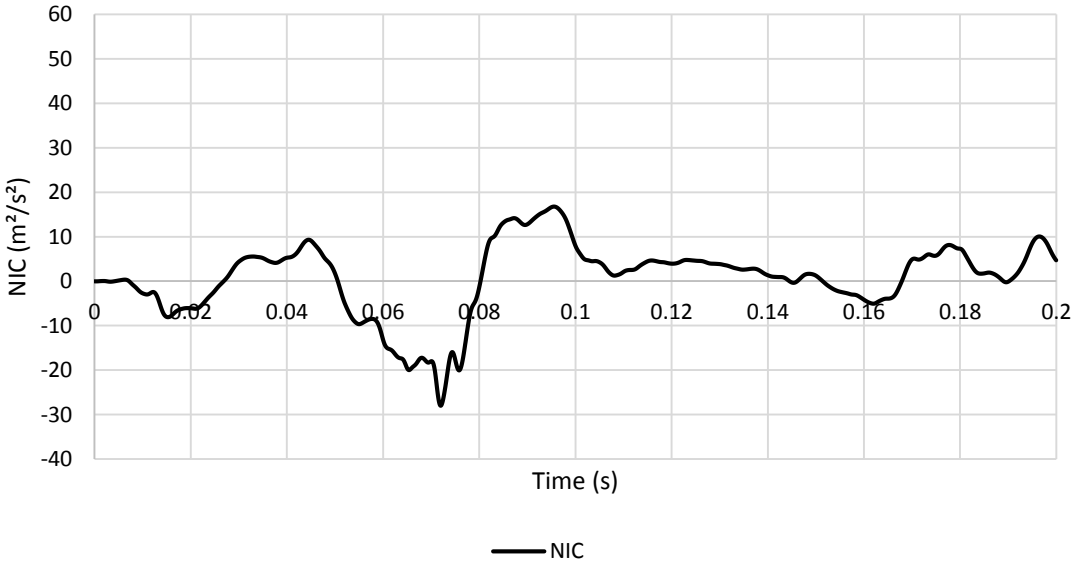


APPENDIX 55 PMHS 1 TEST 3 NIC OVER TIME

| 13 | C2_CFC60 | C5_CFC60 | C7_CFC60 | SLED_CFC60 | HEAD_RES_CFC180 | T1_RES_CFC180 | STR_RES_CFC180 | NIC |
|---|---|---|---|---|---|---|---|---|
| unit | mbar | mbar | mbar | g | g | g | g | m²/s² |
| max | 181 | -9258 | 534 | 8.2 | 24 | 21 | 19 | 17 |
| min | -121 | -10283 | -534 | -9.3 | 0 | 0.1 | 0.1 | -28 |

APPENDIX 56 PMHS 1 TEST 3 MAXIMUM AND MINIMUM CHARACTERISTIC VALUES

## A.3.4. PMHS 1 Test 4

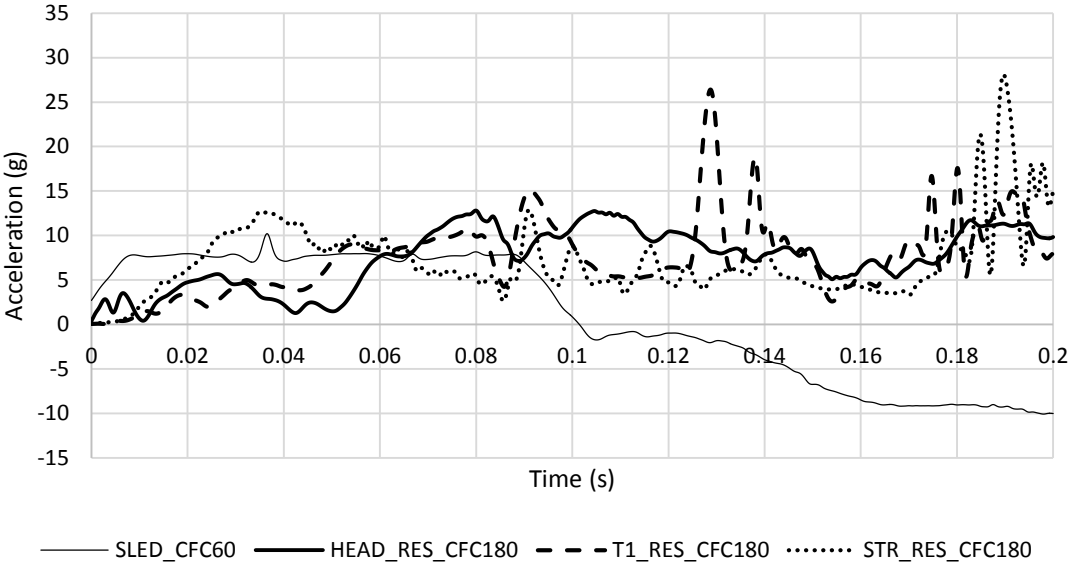


APPENDIX 57 PMHS 1 TEST 4 SLED, HEAD, T1, STERNUM ACCELERATION OVER TIME

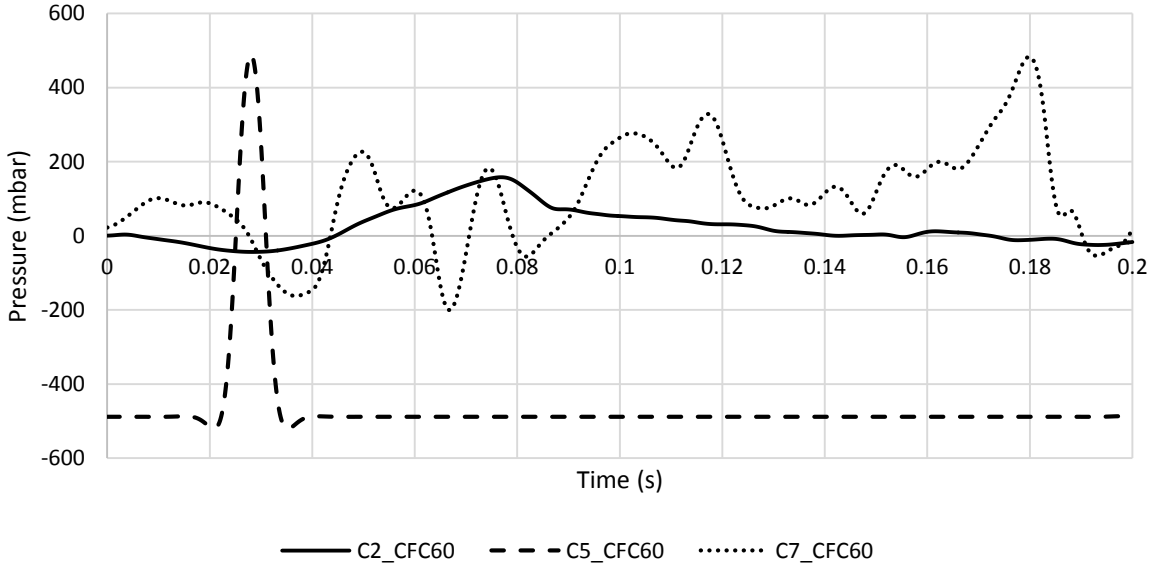


APPENDIX 58 PMHS 1 TEST 4 SPINAL CANAL PRESSURE AT C2, C5 AND C7 OVER TIME

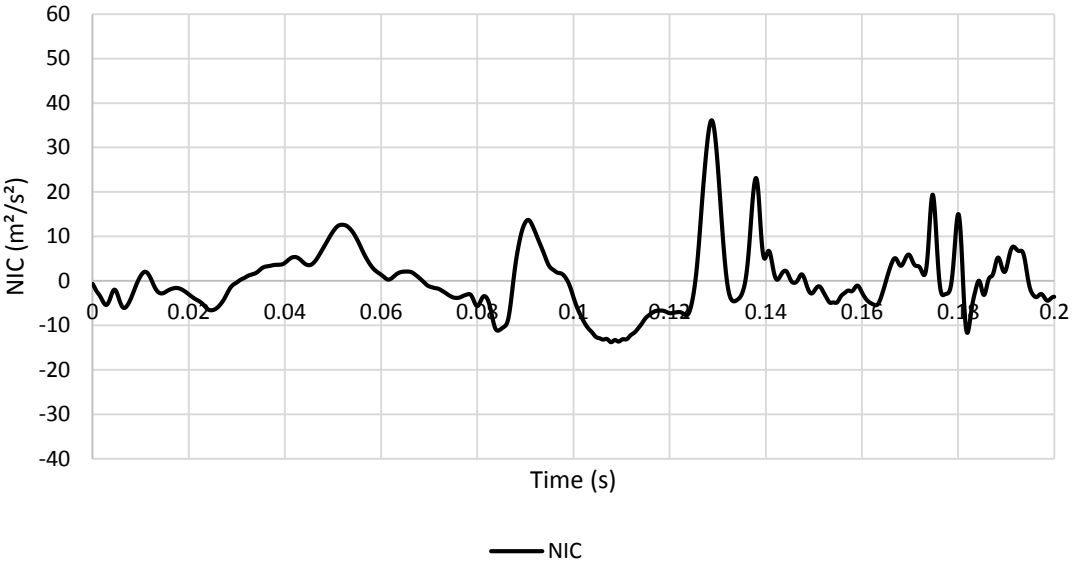


APPENDIX 59 PMHS 1 TEST 4 NIC OVER TIME

| 14 | C2_CFC60 | C5_CFC60 | C7_CFC60 | SLED_CFC60 | HEAD_RES_CFC180 | T1_RES_CFC180 | STR_RES_CFC180 | NIC |
|---|---|---|---|---|---|---|---|---|
| unit | mbar | mbar | mbar | g | g | g | g | m²/s² |
| max | 158 | 489.23 | 483 | 10 | 13 | 26 | 28 | 36 |
| min | -44 | -521.1 | -201 | -10 | 0.4 | 0.1 | 0.2 | -14 |

APPENDIX 60 PMHS 1 TEST 4 MAXIMUM AND MINIMUM CHARACTERISTIC VALUES

### A.3.5. PMHS 2 Test 1

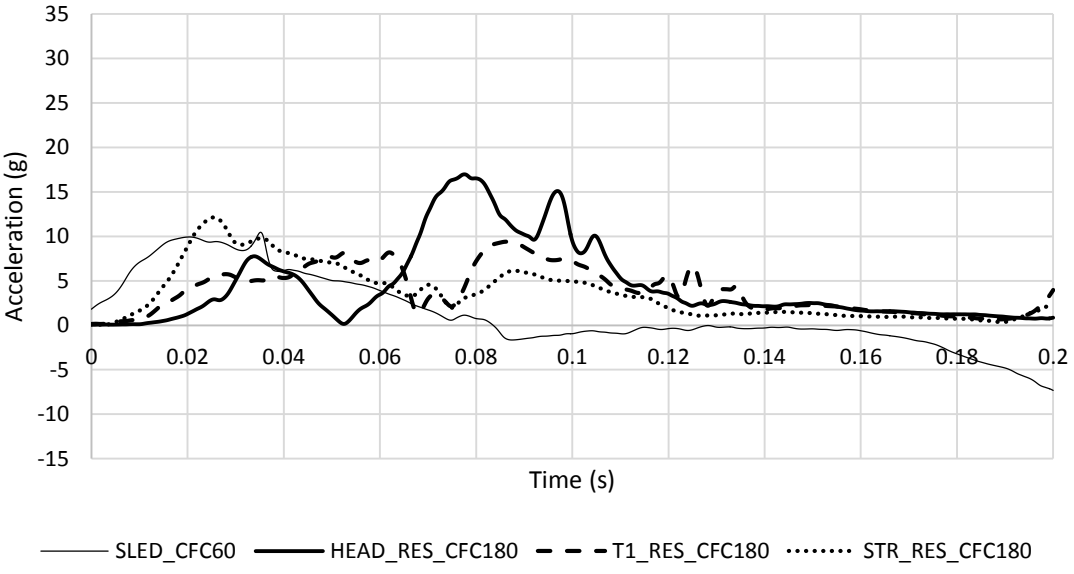


APPENDIX 61 PMHS 2 TEST 1 SLED, HEAD, T1, STERNUM ACCELERATION OVER TIME

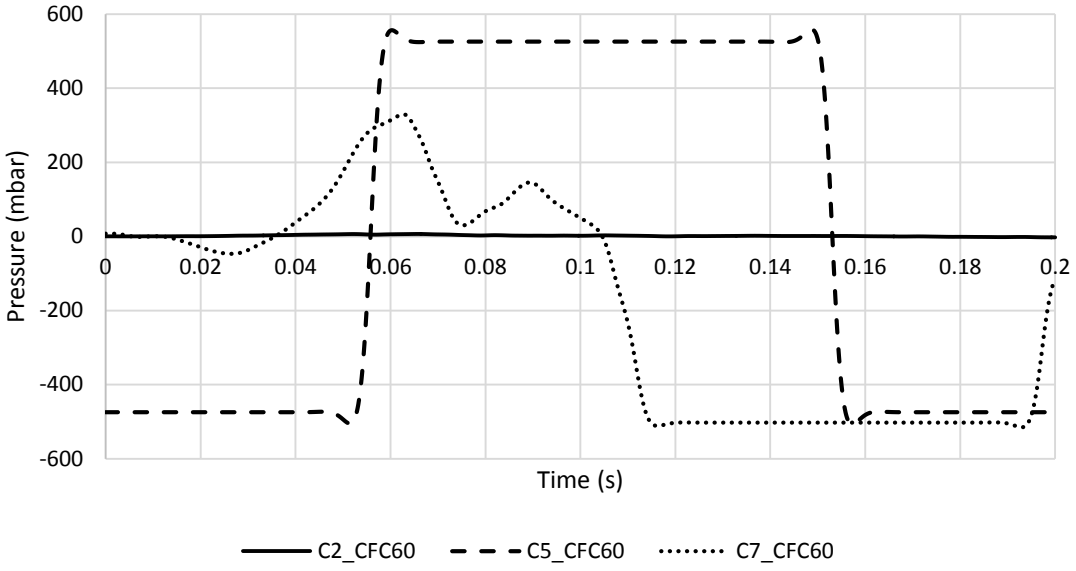


APPENDIX 62 PMHS 2 TEST 1 SPINAL CANAL PRESSURE AT C2, C5 AND C7 OVER TIME

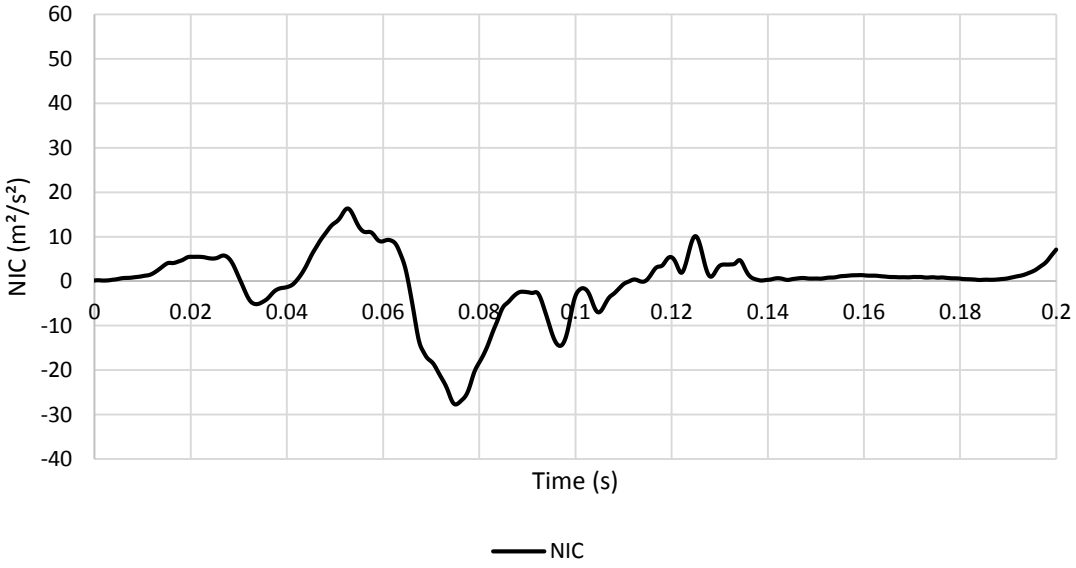


APPENDIX 63 PMHS 2 TEST 1 NIC OVER TIME

| 21 | C2_CFC60 | C5_CFC60 | C7_CFC60 | SLED_CFC60 | HEAD_RES_CFC180 | T1_RES_CFC180 | STR_RES_CFC180 | NIC |
|---|---|---|---|---|---|---|---|---|
| unit | mbar | mbar | mbar | g | g | g | g | m²/s² |
| max | 6.7 | 559.14 | 329 | 10 | 17 | 9.4 | 12 | 16 |
| min | -2.6 | -507.2 | -515 | -7.3 | 0.1 | 0.1 | 0.1 | -28 |

APPENDIX 64 PMHS 2 TEST 1 MAXIMUM AND MINIMUM CHARACTERISTIC VALUES

## A.3.6. PMHS 2 Test 2

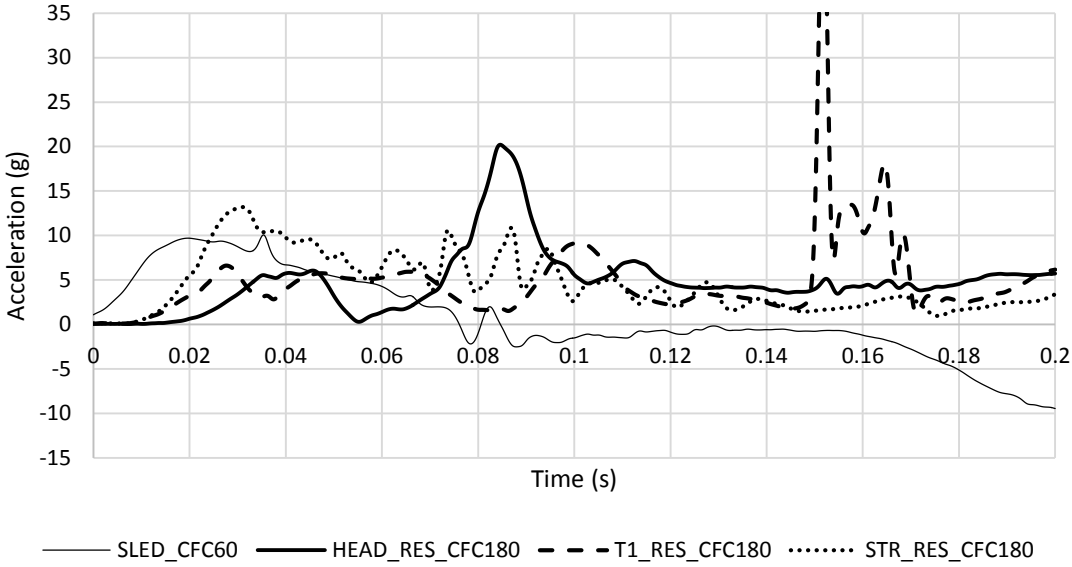


APPENDIX 65 PMHS 2 TEST 1 SLED, HEAD, T1, STERNUM ACCELERATION OVER TIME

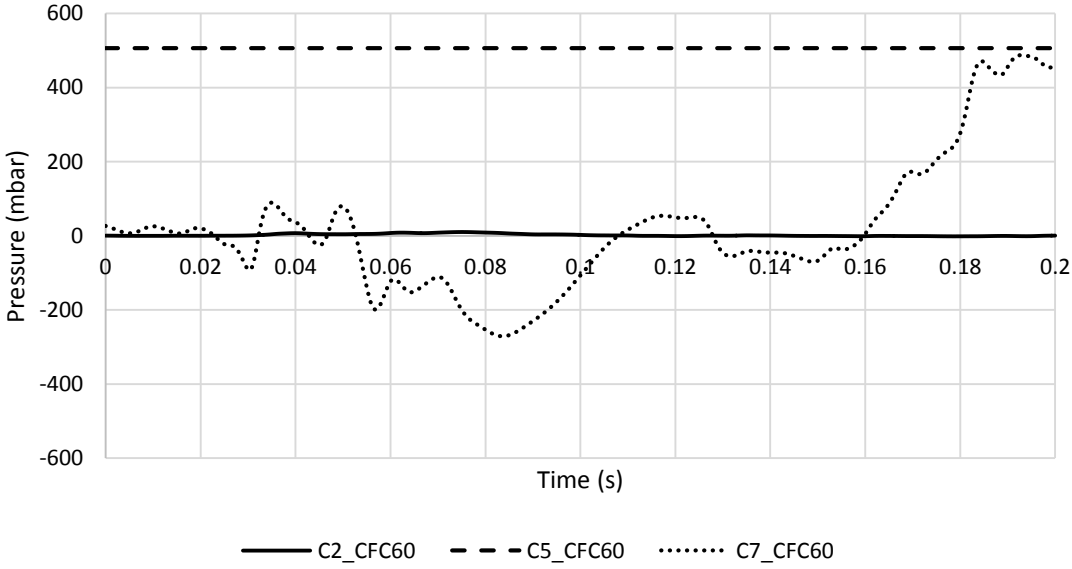


APPENDIX 66 PMHS 2 TEST 2 SPINAL CANAL PRESSURE AT C2, C5 AND C7 OVER TIME

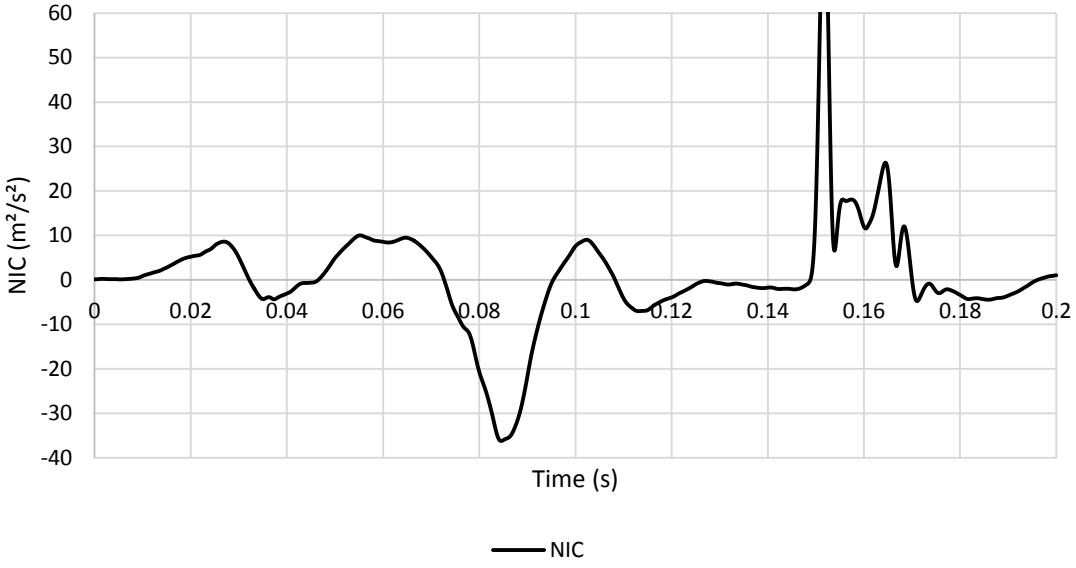


APPENDIX 67 PMHS 2 TEST 2 NIC OVER TIME

| 22 | C2_CFC60 | C5_CFC60 | C7_CFC60 | SLED_CFC60 | HEAD_RES_CFC180 | T1_RES_CFC180 | STR_RES_CFC180 | NIC |
|---|---|---|---|---|---|---|---|---|
| unit | mbar | mbar | mbar | g | g | g | g | m²/s² |
| max | 10 | 506.6 | 487 | 10 | 20 | 48 | 13 | 85 |
| min | -1.4 | 506.6 | -271 | -9.5 | 0 | 0.1 | 0.1 | -36 |

APPENDIX 68 PMHS 2 TEST 2 MAXIMUM AND MINIMUM CHARACTERISTIC VALUES

## A.3.7. PMHS 2 Test 3

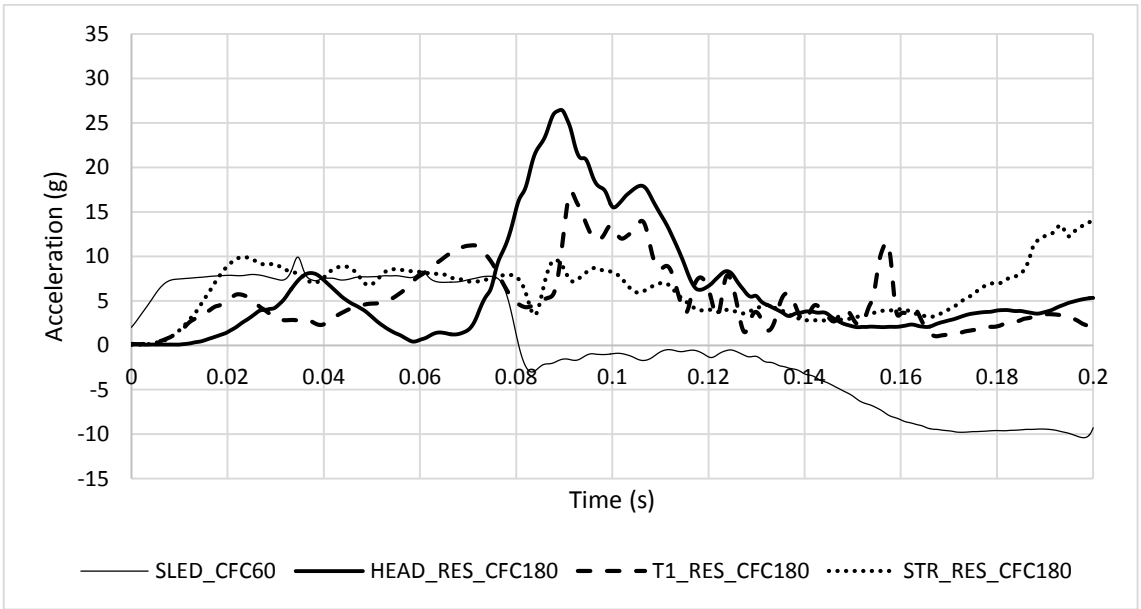


APPENDIX 69 PMHS 2 TEST 3 SLED, HEAD, T1, STERNUM ACCELERATION OVER TIME

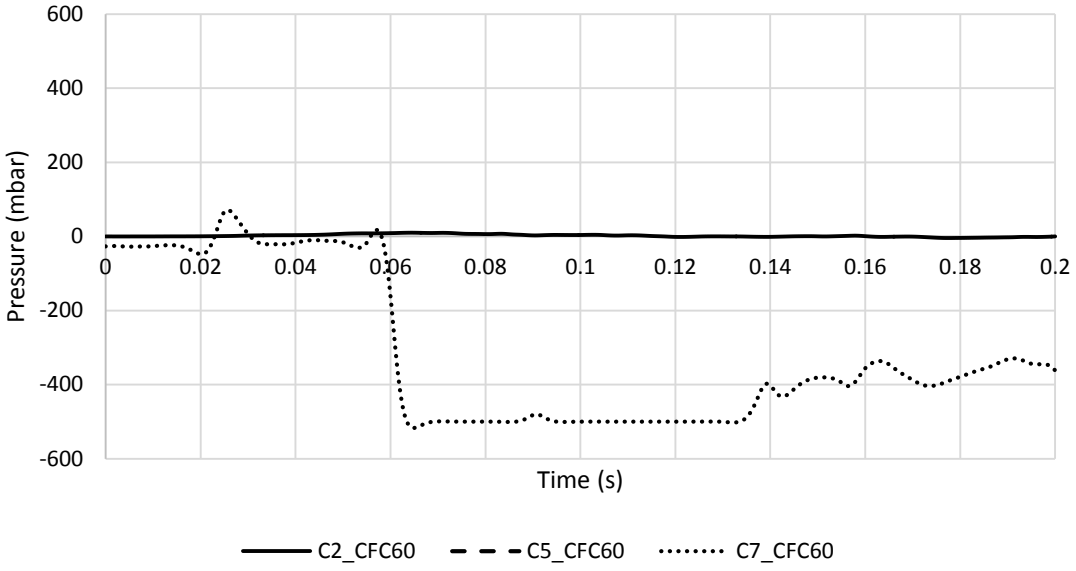


APPENDIX 70 PMHS 2 TEST 3 SPINAL CANAL PRESSURE AT C2, C5 AND C7 OVER TIME

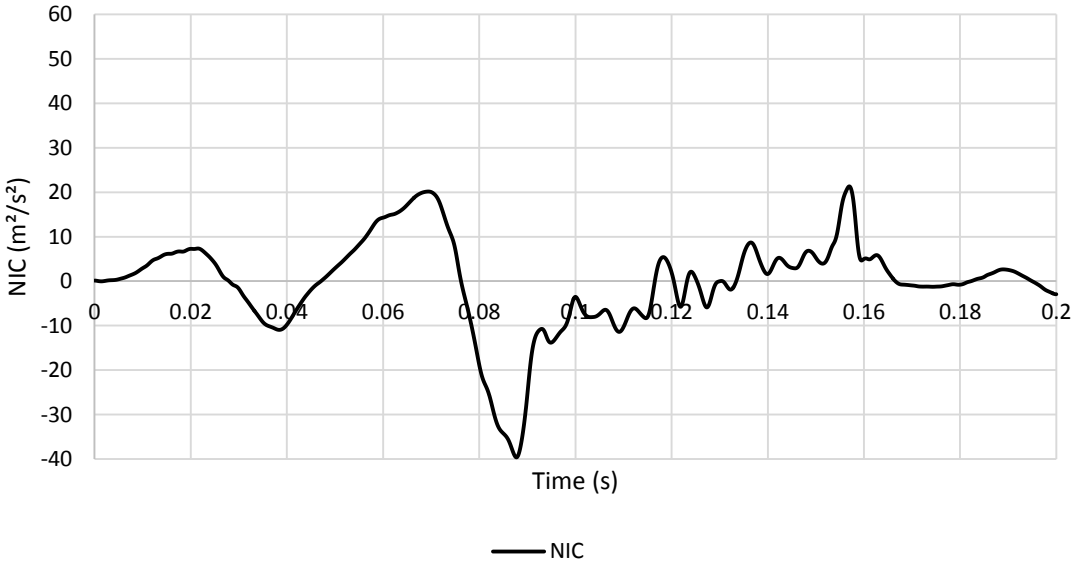


APPENDIX 71 PMHS 2 TEST 3 NIC OVER TIME

| 23 | C2_CFC60 | C5_CFC60 | C7_CFC60 | SLED_CFC60 | HEAD_RES_CFC180 | T1_RES_CFC180 | STR_RES_CFC180 | NIC |
|---|---|---|---|---|---|---|---|---|
| unit | mbar | mbar | mbar | g | g | g | g | m²/s² |
| max | 10 | -9268 | 71 | 9.9 | 26 | 17 | 14 | 21 |
| min | -4.3 | -9268 | -517 | -10 | 0.1 | 0.1 | 0.1 | -40 |

APPENDIX 72 PMHS 2 TEST 3 MAXIMUM AND MINIMUM CHARACTERISTIC VALUES

## A.3.8. PMHS 2 Test 4

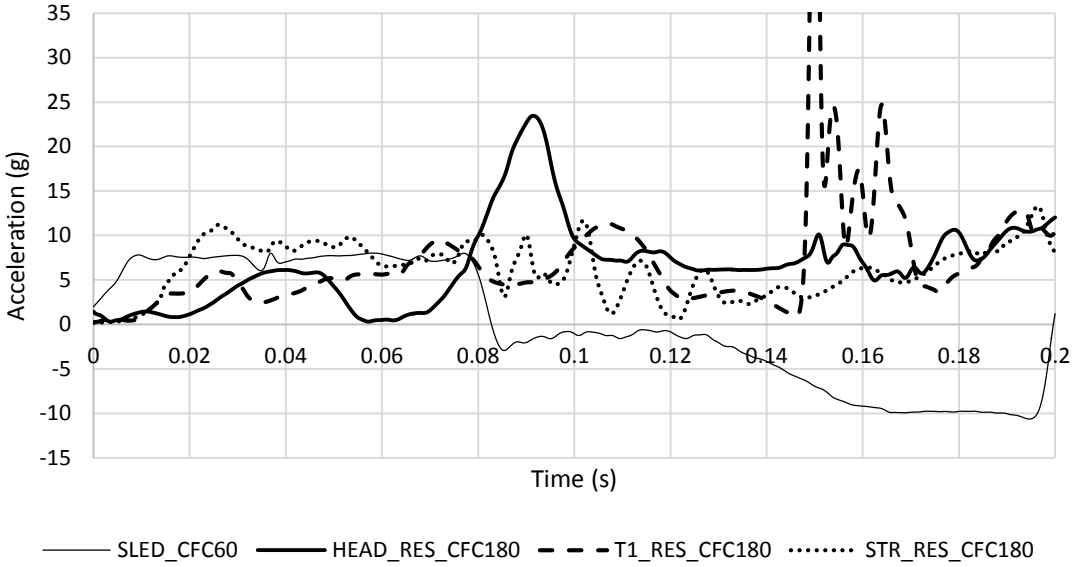


APPENDIX 73 PMHS 2 TEST 4 SLED, HEAD, T1, STERNUM ACCELERATION OVER TIME

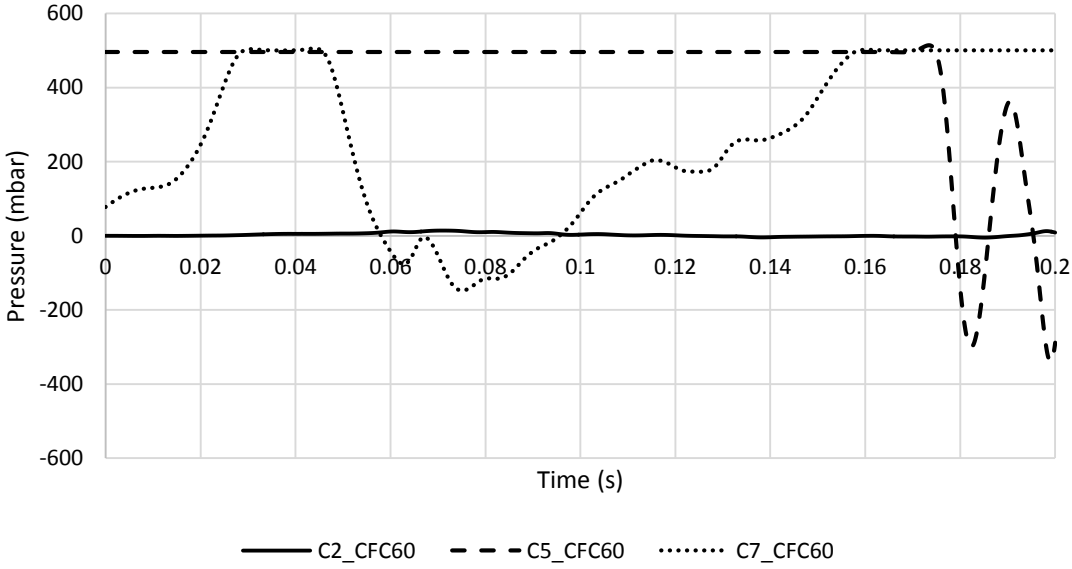


APPENDIX 74 PMHS 2 TEST 4 SPINAL CANAL PRESSURE AT C2, C5 AND C7 OVER TIME

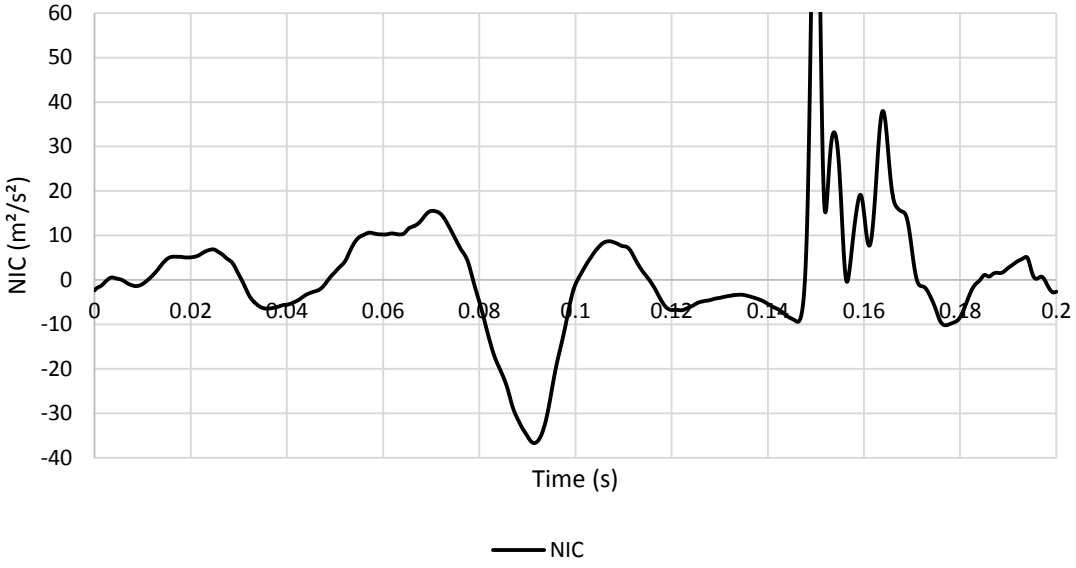


APPENDIX 75 PMHS 2 TEST 4 NIC OVER TIME

| 24 | C2_CFC60 | C5_CFC60 | C7_CFC60 | SLED_CFC60 | HEAD_RES_ CFC180 | T1_RES_CFC 180 | STR_RES_CF C180 | NIC |
|---|---|---|---|---|---|---|---|---|
| unit | mbar | mbar | mbar | g | g | g | g | m²/s² |
| max | 14 | 514.19 | 506 | 8 | 23 | 64 | 13 | 109 |
| min | -4.9 | -339.4 | -148 | -11 | 0.3 | 0.2 | 0.2 | -37 |

APPENDIX 76 PMHS 2 TEST 4 MAXIMUM AND MINIMUM CHARACTERISTIC VALUES

## A.3.9. PMHS 3 Test 1

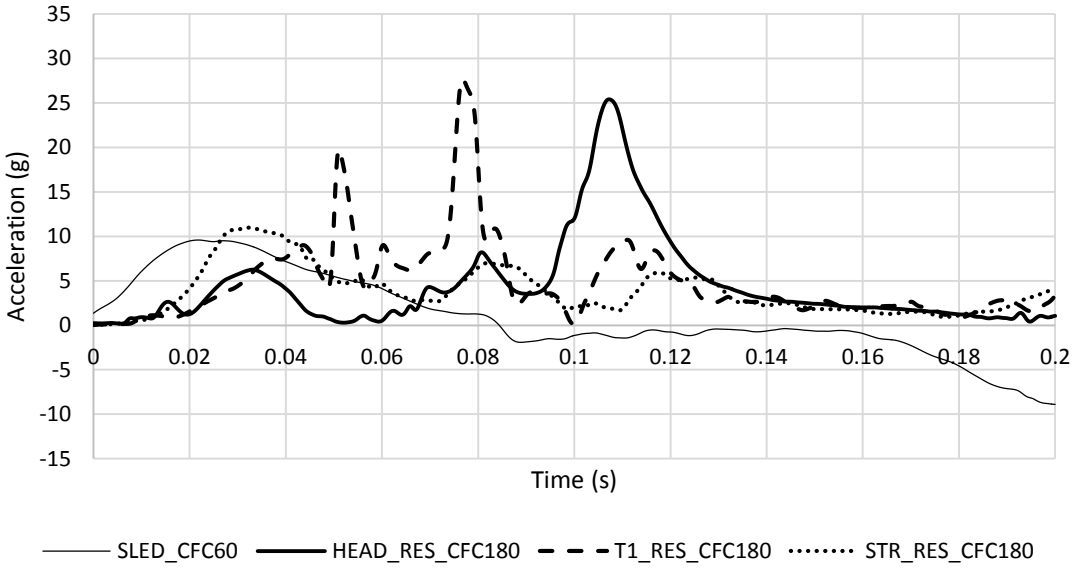


APPENDIX 77 PMHS 3 TEST 1 SLED, HEAD, T1, STERNUM ACCELERATION OVER TIME

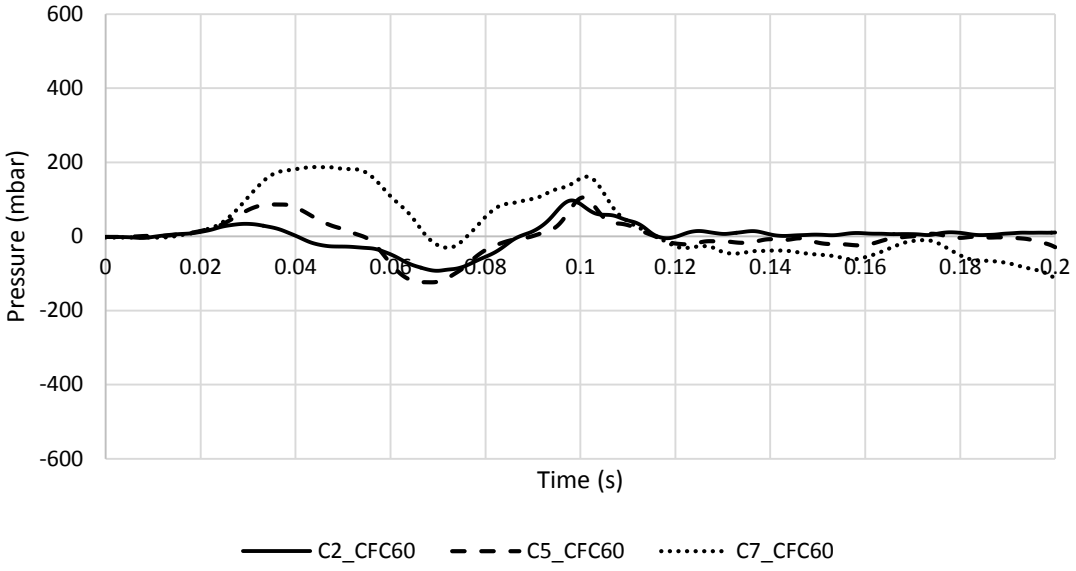


APPENDIX 78 PMHS 3 TEST 2 SPINAL CANAL PRESSURE AT C2, C5 AND C7 OVER TIME

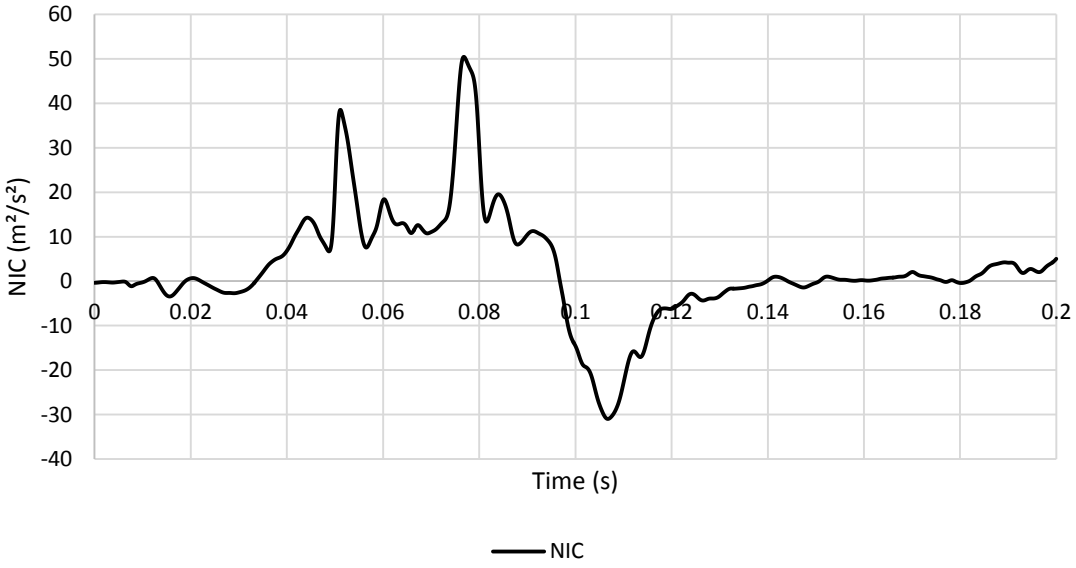


APPENDIX 79 PMHS 3 TEST 1 NIC OVER TIME

| 31 | C2_CFC60 | C5_CFC60 | C7_CFC60 | SLED_CFC60 | HEAD_RES_CFC180 | T1_RES_CFC180 | STR_RES_CFC180 | NIC |
|---|---|---|---|---|---|---|---|---|
| unit | mbar | mbar | mbar | g | g | g | g | m²/s² |
| max | 97 | 104.92 | 187 | 9.6 | 25 | 28 | 11 | 50 |
| min | -93 | -123.7 | -113 | -8.9 | 0.2 | 0 | 0 | -31 |

APPENDIX 80 PMHS 3 TEST 1 MAXIMUM AND MINIMUM CHARACTERISTIC VALUES

## A.3.10. PMHS 3 Test 2

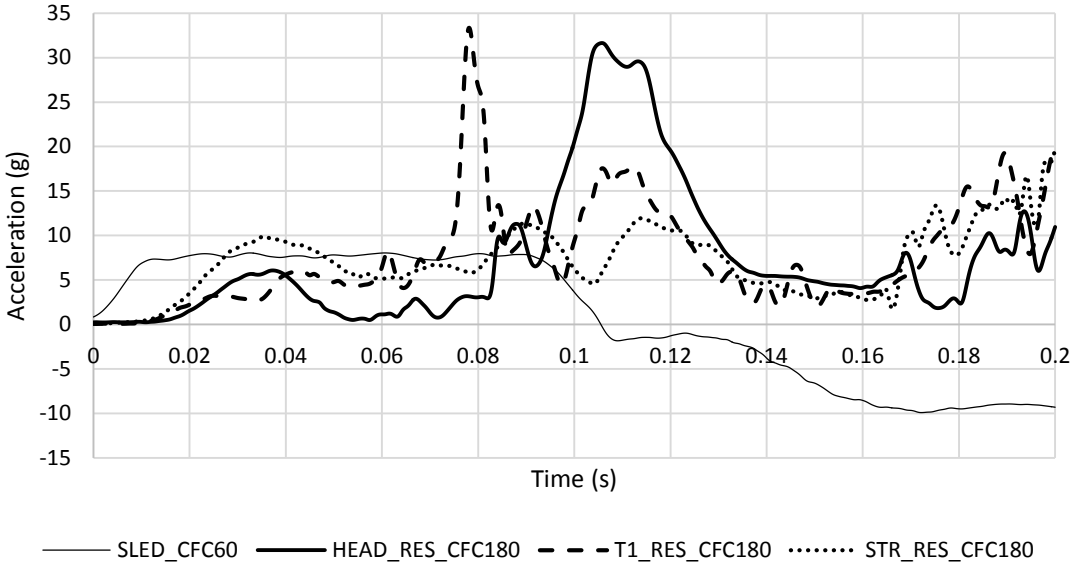


APPENDIX 81 PMHS 3 TEST 2 SLED, HEAD, T1, STERNUM ACCELERATION OVER TIME

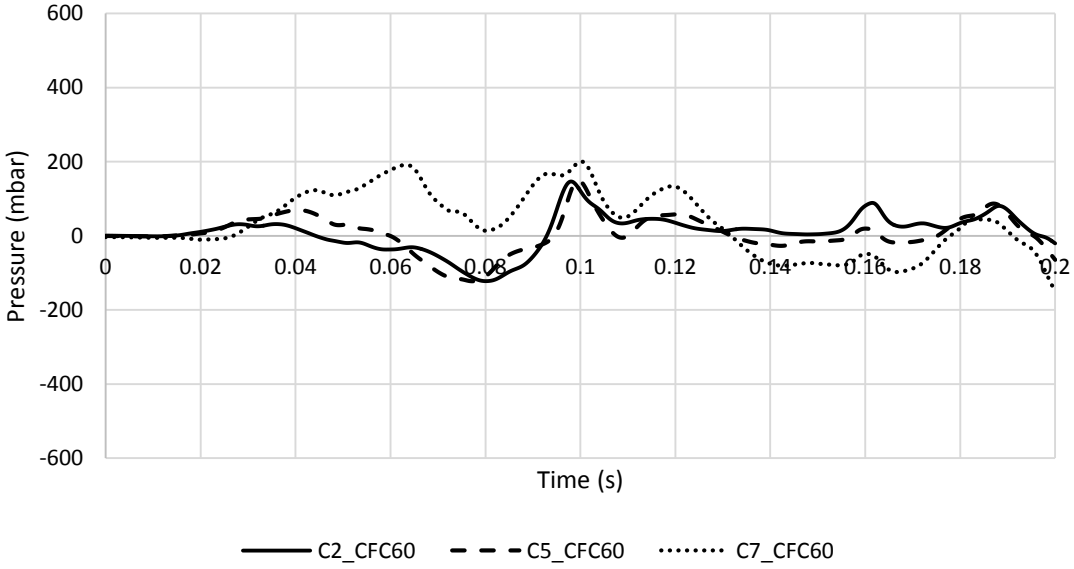


APPENDIX 82 PMHS 3 TEST 2 SPINAL CANAL PRESSURE AT C2, C5 AND C7 OVER TIME

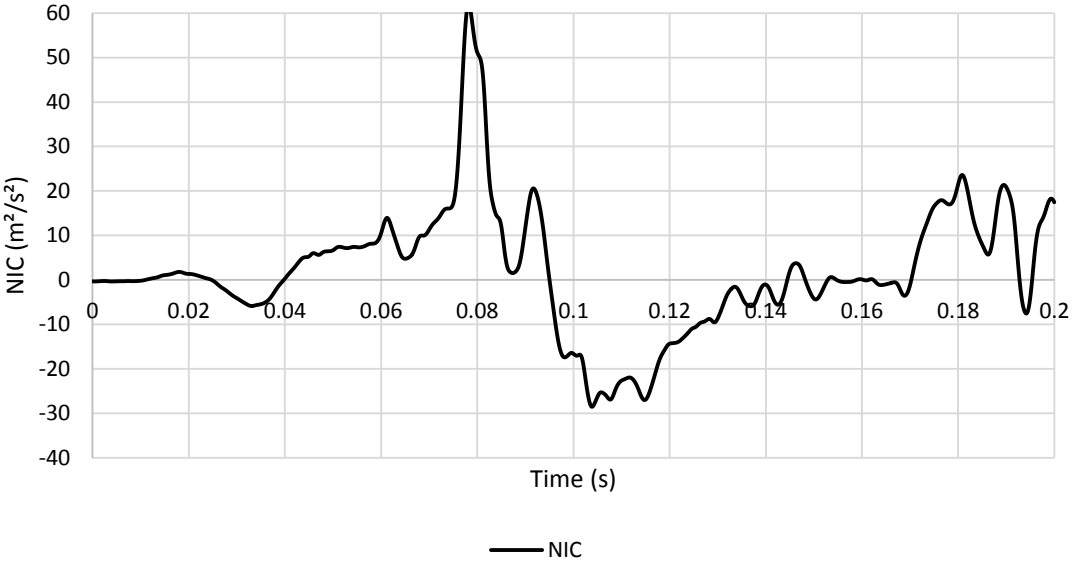


APPENDIX 83 PMHS 3 TEST 2 NIC OVER TIME

| 32 | C2_CFC60 | C5_CFC60 | C7_CFC60 | SLED_CFC60 | HEAD_RES_CFC180 | T1_RES_CFC180 | STR_RES_CFC180 | NIC |
|---|---|---|---|---|---|---|---|---|
| unit | mbar | mbar | mbar | g | g | g | g | m²/s² |
| max | 147 | 149.85 | 201 | 8 | 32 | 33 | 20 | 62 |
| min | -122 | -122.2 | -150 | -9.9 | 0.2 | 0.1 | 0.1 | -29 |

APPENDIX 84 PMHS 3 TEST 2 MAXIMUM AND MINIMUM CHARACTERISTIC VALUES

## A.3.11. PMHS 3 Test 3

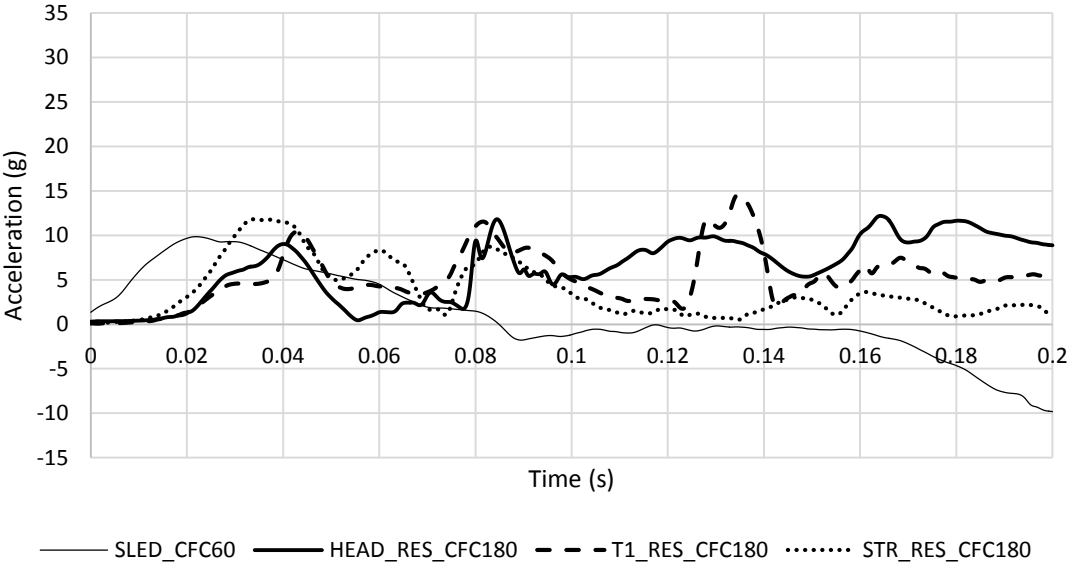


APPENDIX 85 PMHS 3 TEST 3 SLED, HEAD, T1, STERNUM ACCELERATION OVER TIME

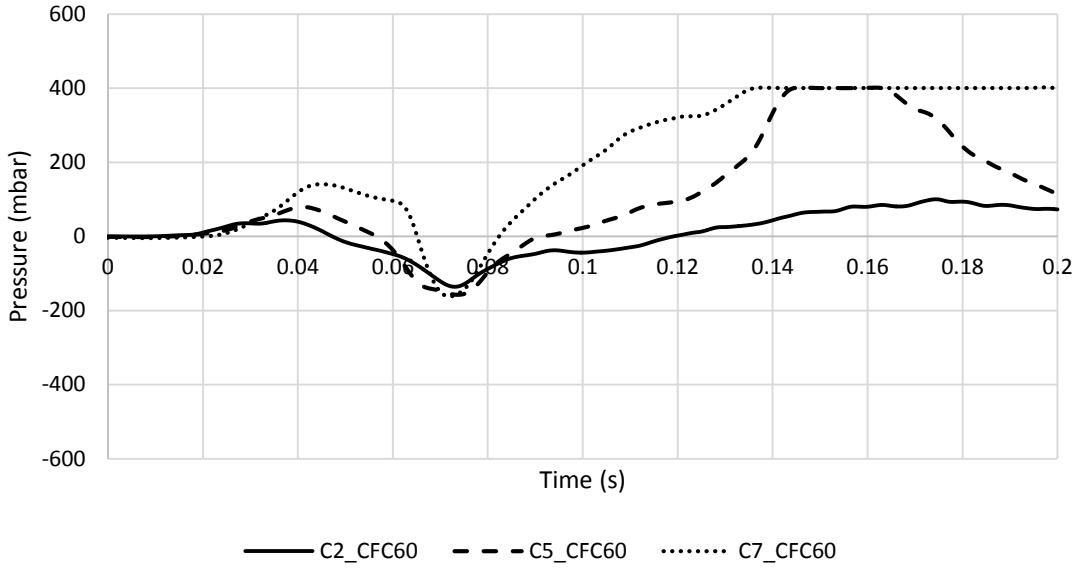


APPENDIX 86 PMHS 3 TEST 3 SPINAL CANAL PRESSURE AT C2, C5 AND C7 OVER TIME

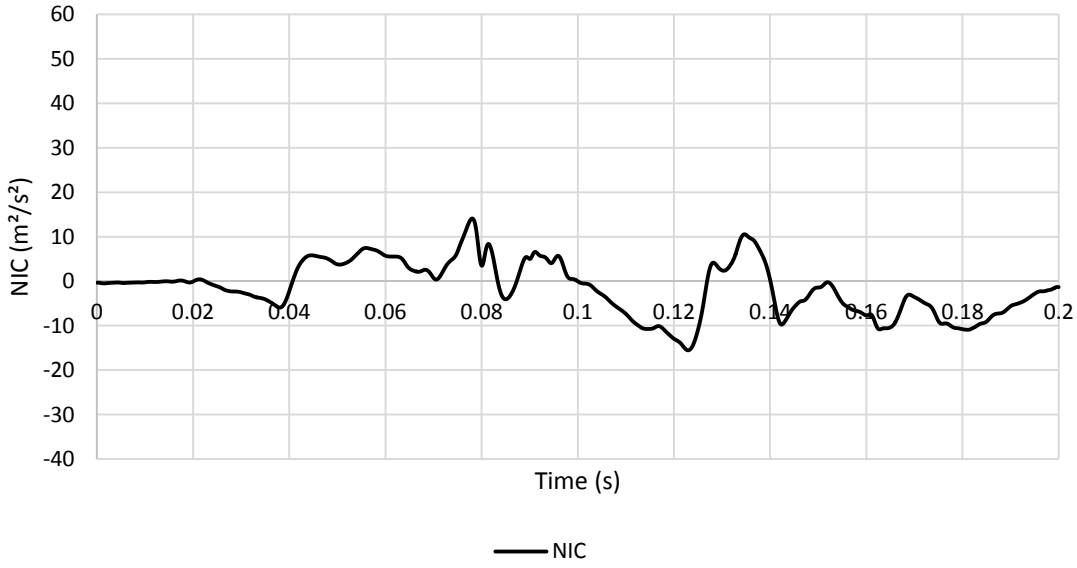


APPENDIX 87 PMHS 3 TEST 3 NIC OVER TIME

| 33 | C2_CFC60 | C5_CFC60 | C7_CFC60 | SLED_CFC60 | HEAD_RES_CFC180 | T1_RES_CFC180 | STR_RES_CFC180 | NIC |
|---|---|---|---|---|---|---|---|---|
| unit | mbar | mbar | mbar | g | g | g | g | m²/s² |
| max | 100 | 401.95 | 403 | 9.9 | 12 | 15 | 12 | 14 |
| min | -136 | -157.4 | -161 | -9.8 | 0.3 | 0.1 | 0.1 | -16 |

APPENDIX 88 PMHS 3 TEST 3 MAXIMUM AND MINIMUM CHARACTERISTIC VALUES

## A.3.12. PMHS 3 Test 4

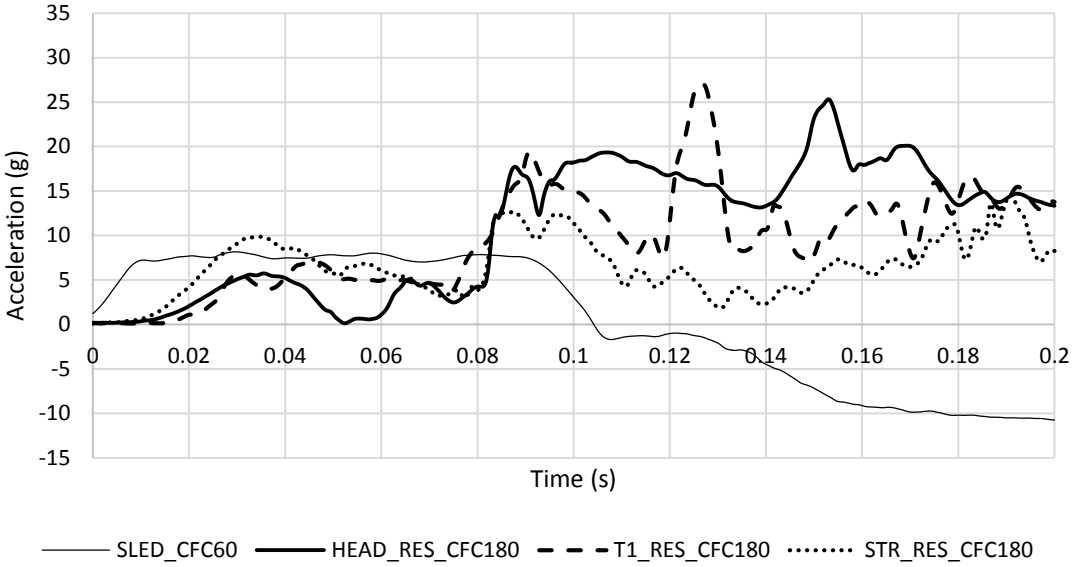


APPENDIX 89 PMHS 3 TEST 4 SLED, HEAD, T1, STERNUM ACCELERATION OVER TIME

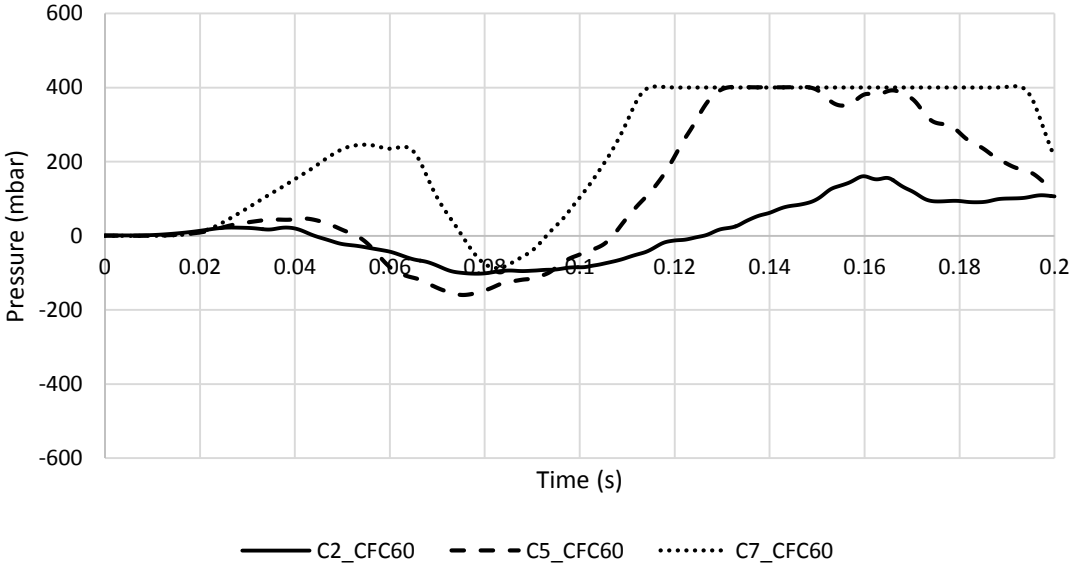


APPENDIX 90 PMHS 3 TEST 4 SPINAL CANAL PRESSURE AT C2, C5 AND C7 OVER TIME

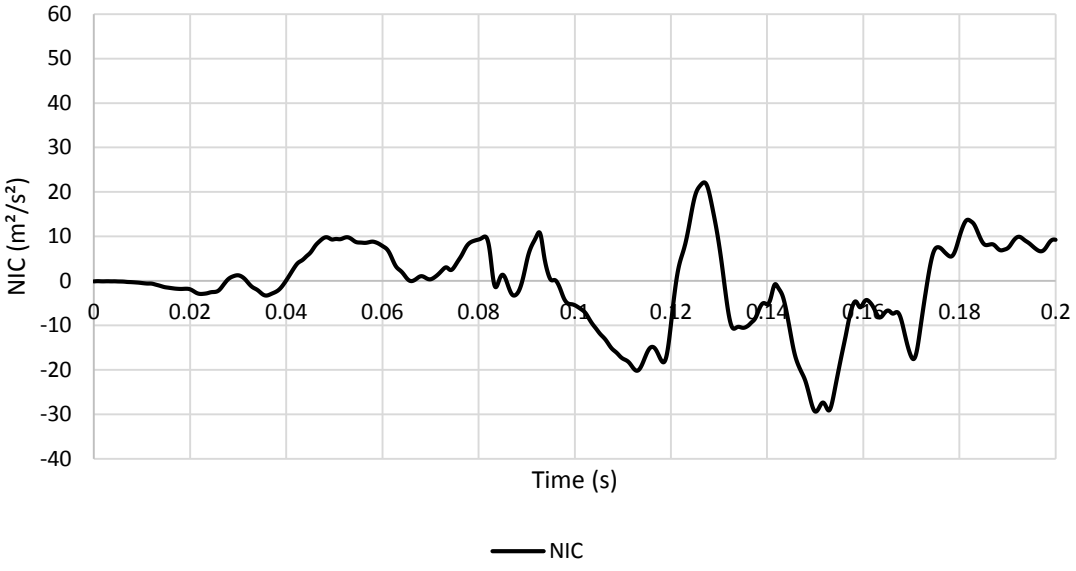


APPENDIX 91 PMHS 3 TEST 4 NIC OVER TIME

| 34 | C2_CFC60 | C5_CFC60 | C7_CFC60 | SLED_CFC60 | HEAD_RES_CFC180 | T1_RES_CFC180 | STR_RES_CFC180 | NIC |
|---|---|---|---|---|---|---|---|---|
| unit | mbar | mbar | mbar | g | g | g | g | m²/s² |
| max | 161 | 401.57 | 403 | 8.2 | 25 | 27 | 15 | 22 |
| min | -102 | -159.3 | -87 | -11 | 0.1 | 0.1 | 0.1 | -29 |

APPENDIX 92 PMHS 3 TEST 4 MAXIMUM AND MINIMUM CHARACTERISTIC VALUES

## A.3.13. PMHS 4 Test 1

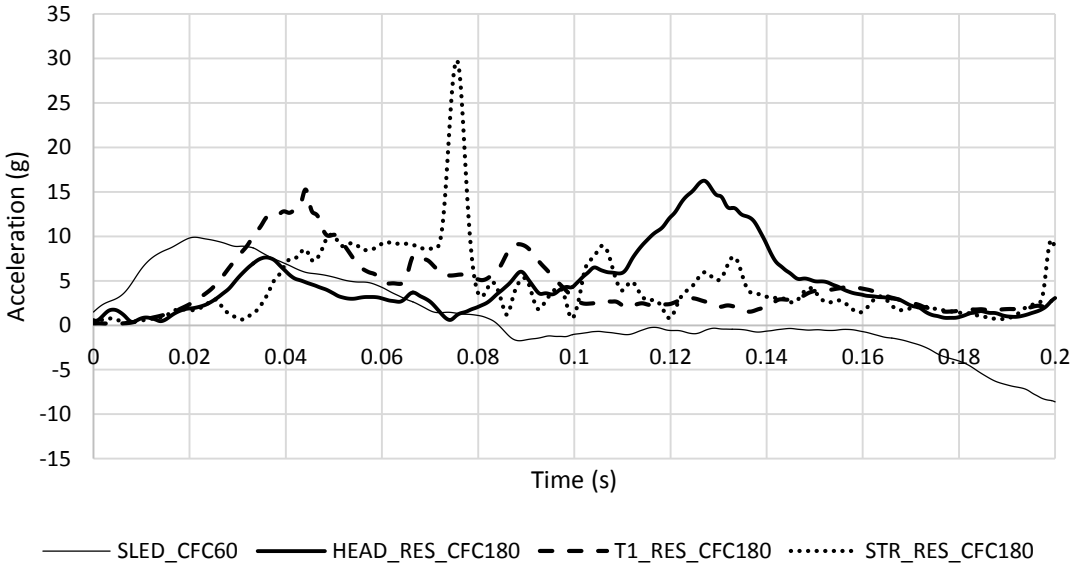


APPENDIX 93 PMHS 4 TEST 1 SLED, HEAD, T1, STERNUM ACCELERATION OVER TIME

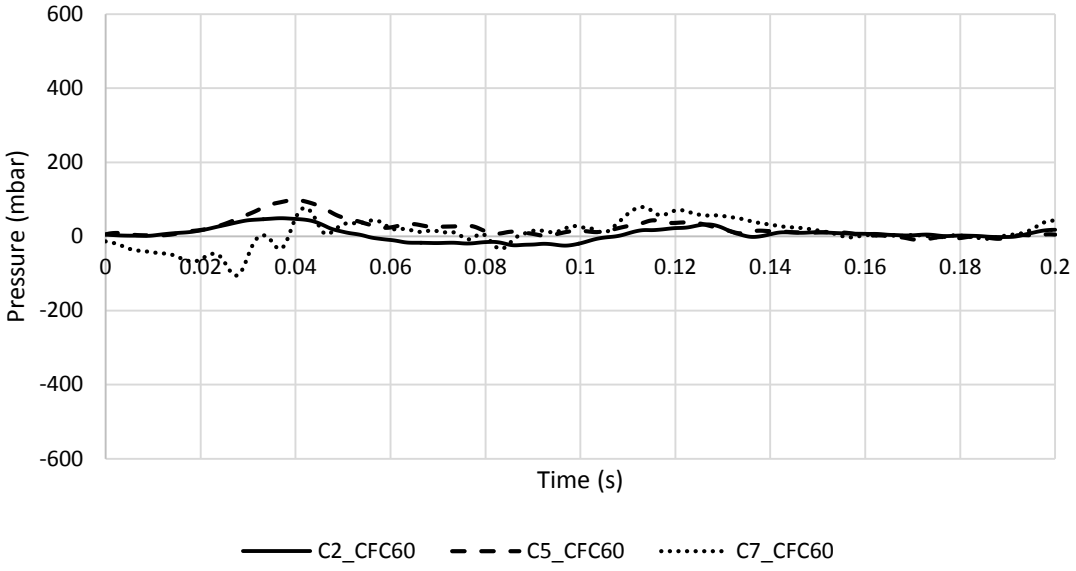


APPENDIX 94 PMHS 4 TEST 1 SPINAL CANAL PRESSURE AT C2, C5 AND C7 OVER TIME

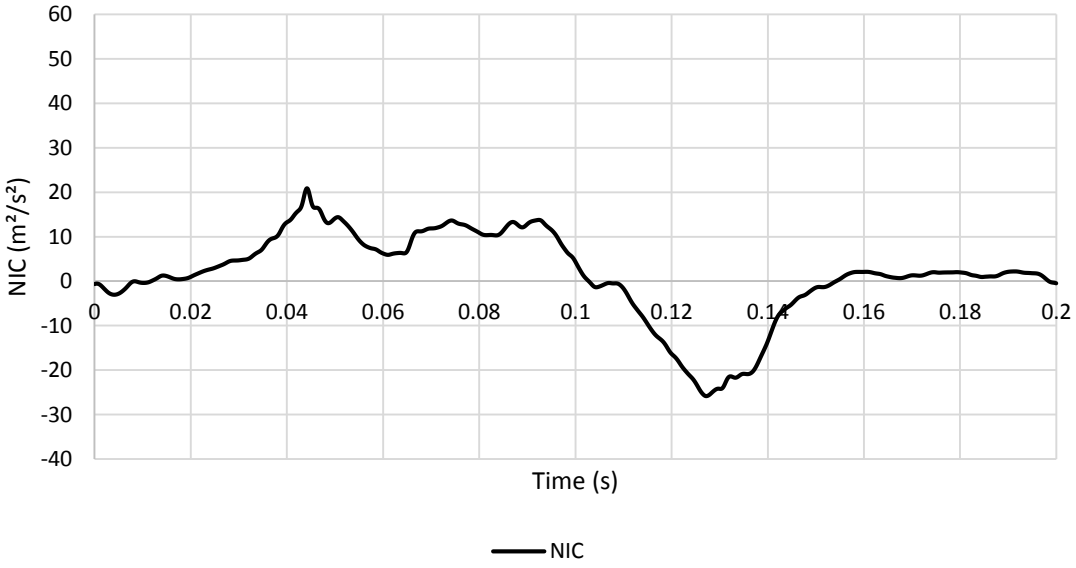


APPENDIX 95 PMHS 4 TEST 1 NIC OVER TIME

| 41 | C2_CFC60 | C5_CFC60 | C7_CFC60 | SLED_CFC60 | HEAD_RES_CFC180 | T1_RES_CFC180 | STR_RES_CFC180 | NIC |
|---|---|---|---|---|---|---|---|---|
| unit | mbar | mbar | mbar | g | g | g | g | m²/s² |
| max | 49 | 98.431 | 80 | 9.9 | 16 | 15 | 30 | 21 |
| min | -25 | -9.186 | -106 | -8.6 | 0.4 | 0.2 | 0.2 | -26 |

APPENDIX 96 PMHS 4 TEST 1 MAXIMUM AND MINIMUM CHARACTERISTIC VALUES

## A.3.14. PMHS 4 Test 2

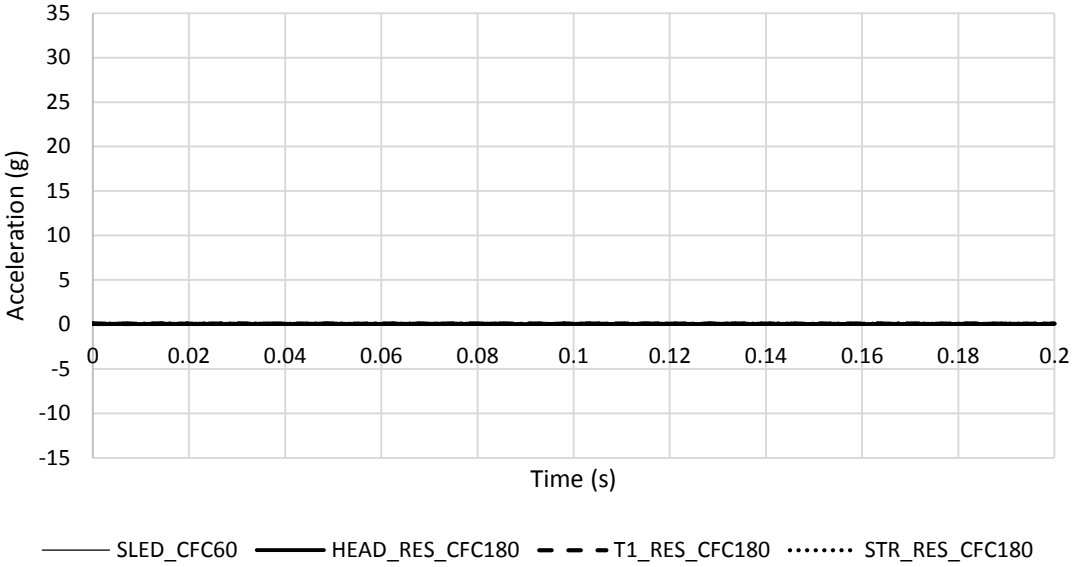


APPENDIX 97 PMHS 4 TEST 2 SLED, HEAD, T1, STERNUM ACCELERATION OVER TIME

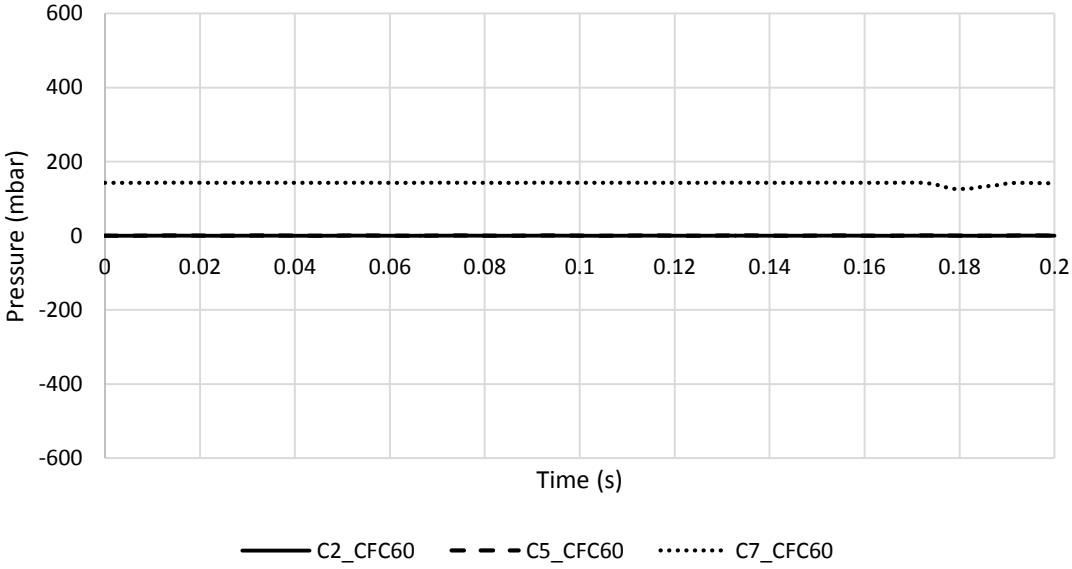


APPENDIX 98 PMHS 4 TEST 2 SPINAL CANAL PRESSURE AT C2, C5 AND C7 OVER TIME

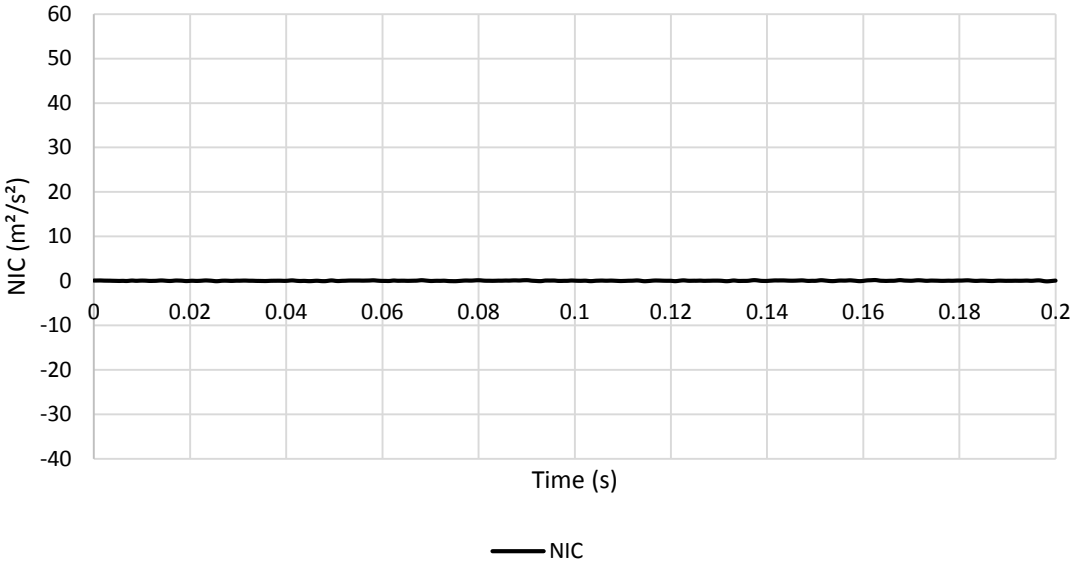


APPENDIX 99 PMHS 4 TEST 2 NIC OVER TIME

| 42 | C2_CFC60 | C5_CFC60 | C7_CFC60 | SLED_CFC60 | HEAD_RES_CFC180 | T1_RES_CFC180 | STR_RES_CFC180 | NIC |
|---|---|---|---|---|---|---|---|---|
| unit | mbar | mbar | mbar | g | g | g | g | m²/s² |
| max | 0.5 | 0.7579 | 144 | -0.1 | 0.1 | 0.1 | 0.1 | 0.2 |
| min | 0.1 | 0.3207 | 127 | -0.1 | 0 | 0.1 | 0 | -0.1 |

APPENDIX 100 PMHS 4 TEST 2 MAXIMUM AND MINIMUM CHARACTERISTIC VALUES

### A.3.15. PMHS 4 Test 3

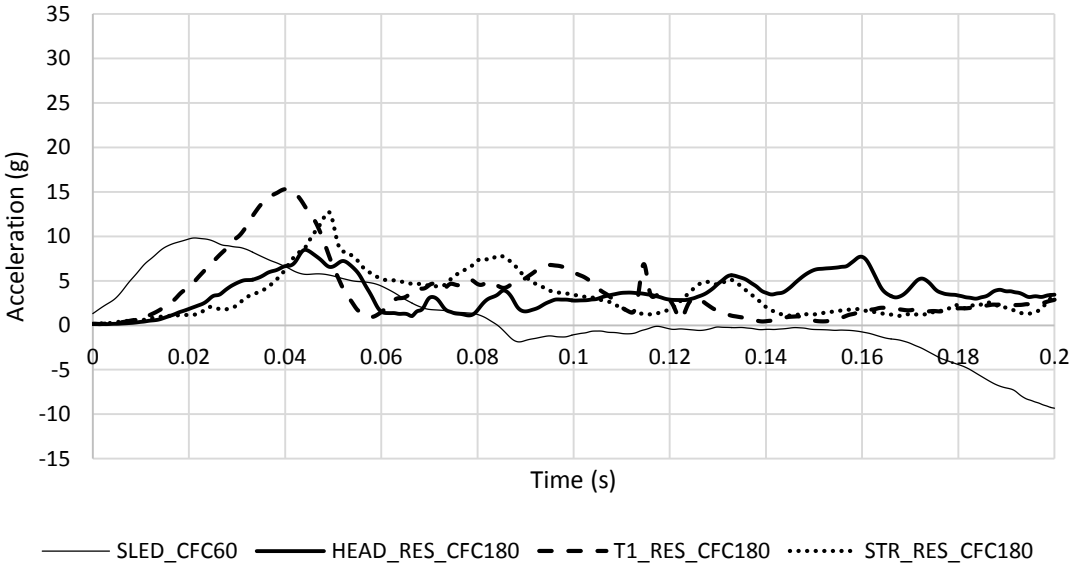


APPENDIX 101 PMHS 4 TEST 3 SLED, HEAD, T1, STERNUM ACCELERATION OVER TIME

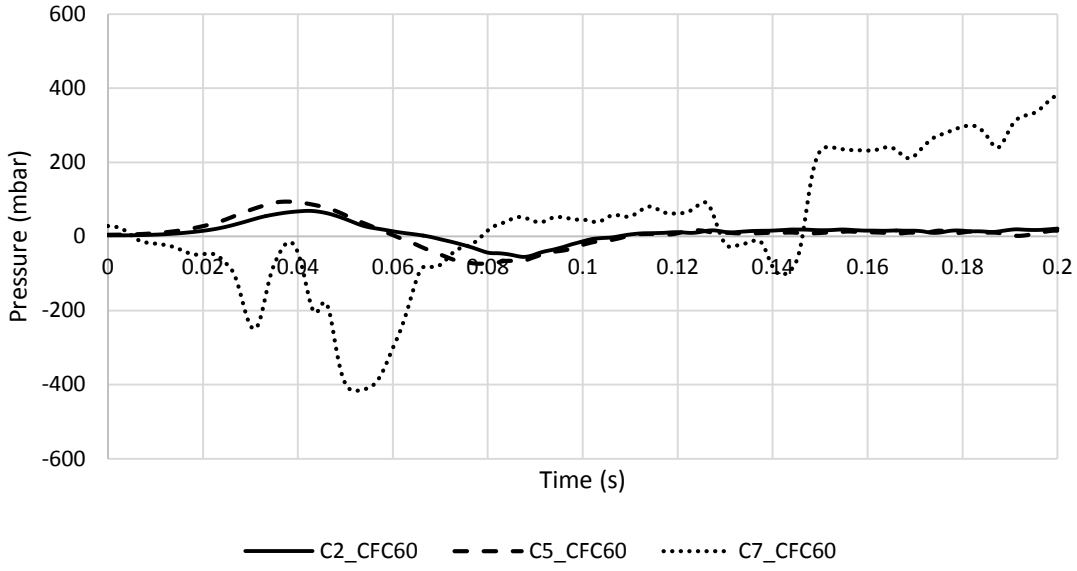


APPENDIX 102 PMHS 4 TEST 3 SPINAL CANAL PRESSURE AT C2, C5 AND C7 OVER TIME

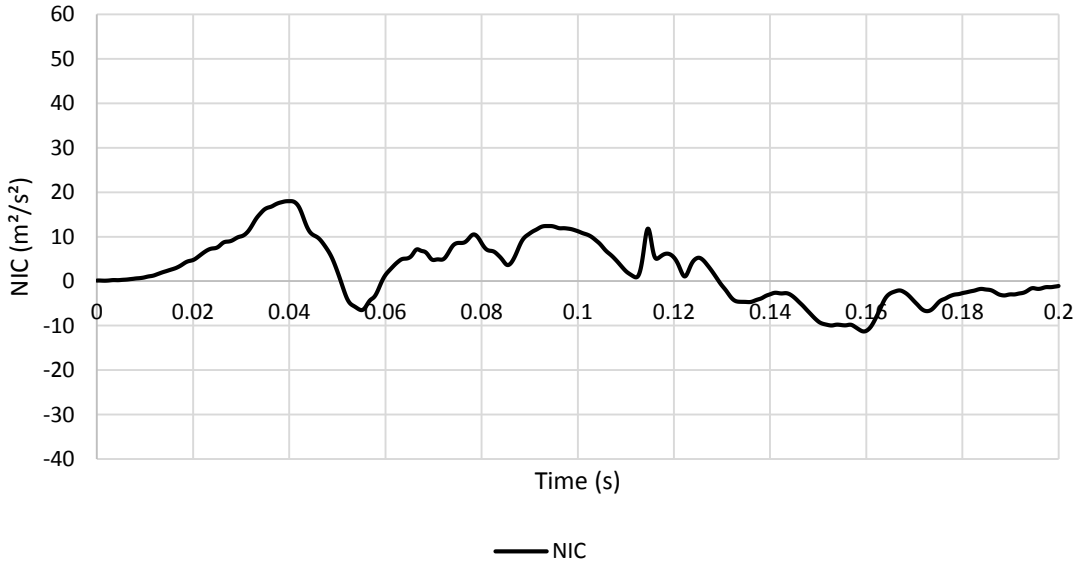


APPENDIX 103 PMHS 4 TEST 3 NIC OVER TIME

| 43 | C2_CFC60 | C5_CFC60 | C7_CFC60 | SLED_CFC60 | HEAD_RES_CFC180 | T1_RES_CFC180 | STR_RES_CFC180 | NIC |
|---|---|---|---|---|---|---|---|---|
| unit | mbar | mbar | mbar | g | g | g | g | m²/s² |
| max | 69 | 93.666 | 382 | 9.8 | 8.5 | 15 | 13 | 18 |
| min | -55 | -73.57 | -417 | -9.3 | 0.1 | 0.1 | 0.2 | -11 |

APPENDIX 104 PMHS 4 TEST 3 MAXIMUM AND MINIMUM CHARACTERISTIC VALUES

## A.3.16. PMHS 4 Test 4

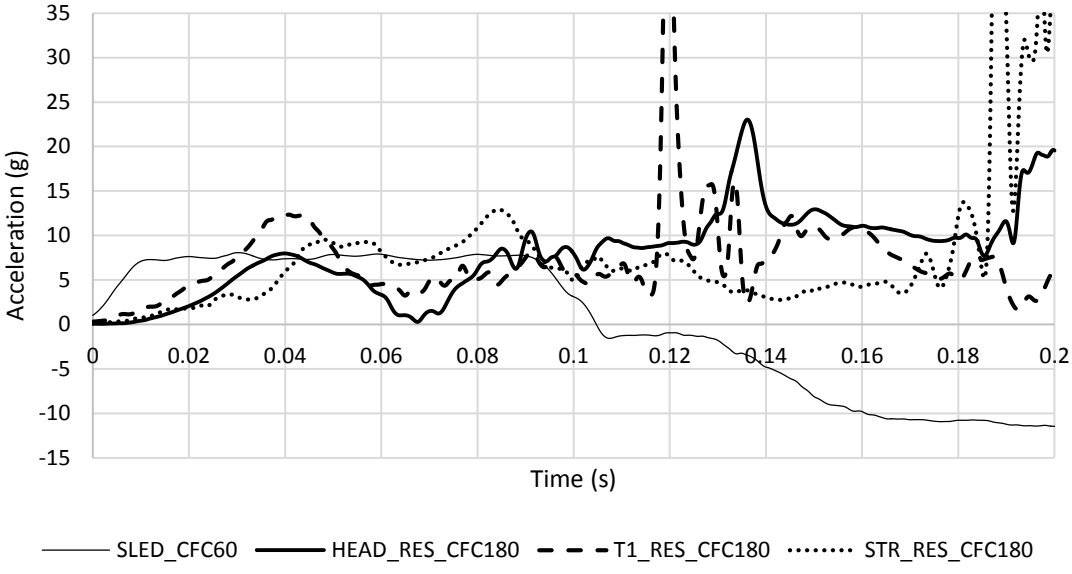


APPENDIX 105 PMHS 4 TEST 4 SLED, HEAD, T1, STERNUM ACCELERATION OVER TIME

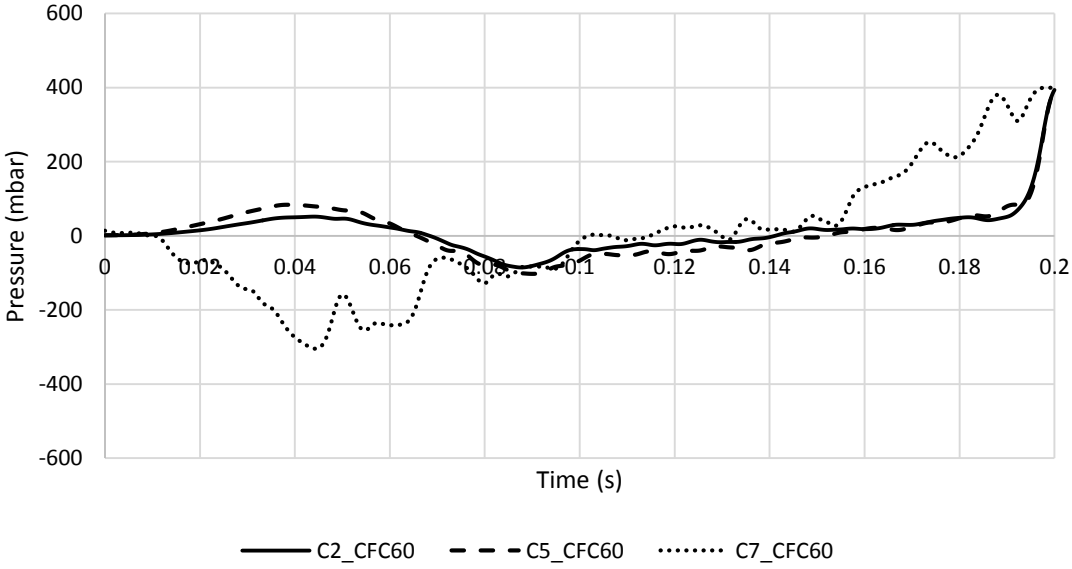


APPENDIX 106 PMHS 4 TEST 4 SPINAL CANAL PRESSURE AT C2, C5 AND C7 OVER TIME

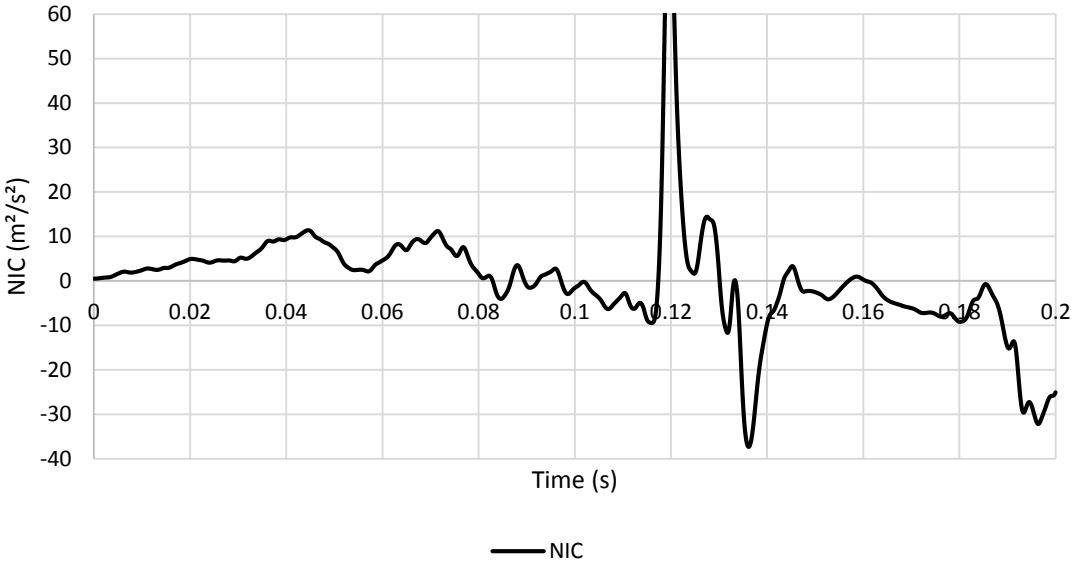


APPENDIX 107 PMHS 4 TEST 4 NIC OVER TIME

| 44 | C2_CFC60 | C5_CFC60 | C7_CFC60 | SLED_CFC60 | HEAD_RES_CFC180 | T1_RES_CFC180 | STR_RES_CFC180 | NIC |
|---|---|---|---|---|---|---|---|---|
| unit | mbar | mbar | mbar | g | g | g | g | m²/s² |
| max | 394 | 394.59 | 400 | 8.1 | 23 | 53 | 62 | 89 |
| min | -86 | -102.6 | -305 | -11 | 0.1 | 0.3 | 0.1 | -37 |

APPENDIX 108 PMHS 4 TEST 4 MAXIMUM AND MINIMUM CHARACTERISTIC VALUES

## A.4. Comparison Eva RID and Bio RID Simulations

### A.4.1. SRA 16 km/h Eva RID and Bio RID Simulations

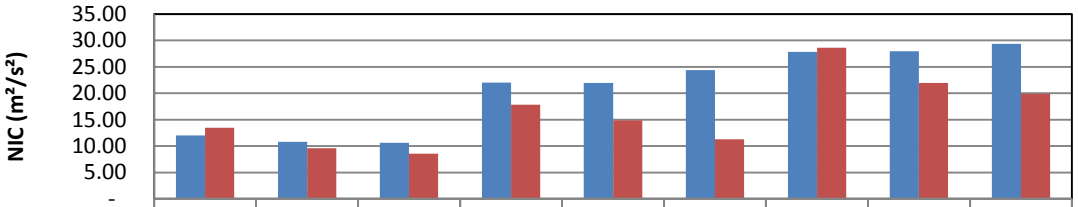


| | high | medium | low | high | medium | low | high | medium | low |
|---|---|---|---|---|---|---|---|---|---|
| | forward | | | middle | | | backward | | |
| NIC male | 12.05 | 10.84 | 10.64 | 22.05 | 21.94 | 24.41 | 27.82 | 27.96 | 29.37 |
| NIC female | 13.50 | 9.57 | 8.55 | 17.83 | 14.89 | 11.29 | 28.63 | 21.97 | 19.90 |

APPENDIX 109 GENERIC SEAT MODEL SIMULATIONS NIC MAXIMA FOR THE SAR 16 KM/H PULSE

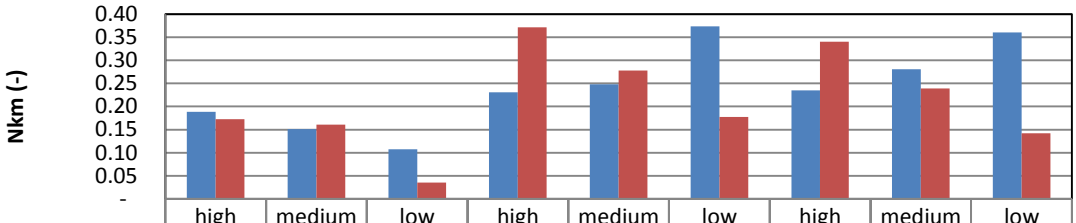


| | high | medium | low | high | medium | low | high | medium | low |
|---|---|---|---|---|---|---|---|---|---|
| | forward | | | middle | | | backward | | |
| Nkm male | 0.19 | 0.15 | 0.11 | 0.23 | 0.25 | 0.37 | 0.23 | 0.28 | 0.36 |
| Nkm female | 0.17 | 0.16 | 0.04 | 0.37 | 0.28 | 0.18 | 0.34 | 0.24 | 0.14 |

APPENDIX 110 GENERIC SEAT MODEL SIMULATIONS NKM MAXIMA FOR THE SAR 16 KM/H PULSE

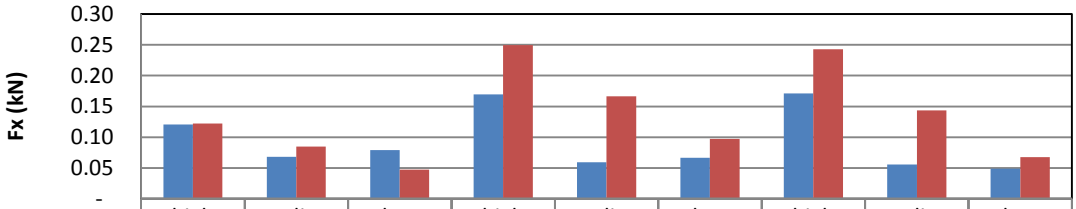


| | high | medium | low | high | medium | low | high | medium | low |
|---|---|---|---|---|---|---|---|---|---|
| | forward | | | middle | | | backward | | |
| Fx male | 0.12 | 0.07 | 0.08 | 0.17 | 0.06 | 0.07 | 0.17 | 0.06 | 0.05 |
| Fx female | 0.12 | 0.08 | 0.05 | 0.25 | 0.17 | 0.10 | 0.24 | 0.14 | 0.07 |

APPENDIX 111 GENERIC SEAT MODEL SIMULATIONS FX MAXIMA FOR THE SAR 16 KM/H PULSE

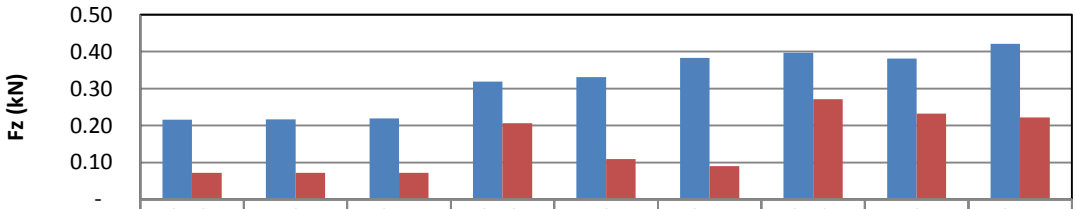


| | high | medium | low | high | medium | low | high | medium | low |
|---|---|---|---|---|---|---|---|---|---|
| | forward | | | middle | | | backward | | |
| Fz male | 0.22 | 0.22 | 0.22 | 0.32 | 0.33 | 0.38 | 0.40 | 0.38 | 0.42 |
| Fz female | 0.07 | 0.07 | 0.07 | 0.21 | 0.11 | 0.09 | 0.27 | 0.23 | 0.22 |

APPENDIX 112 GENERIC SEAT MODEL SIMULATIONS FZ MAXIMA FOR THE SAR 16 KM/H PULSE

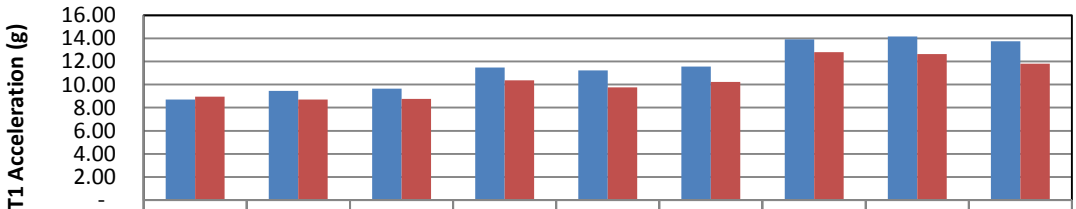


| | high | medium | low | high | medium | low | high | medium | low |
|---|---|---|---|---|---|---|---|---|---|
| | forward | | | middle | | | backward | | |
| T1 male | 8.70 | 9.44 | 9.66 | 11.47 | 11.23 | 11.55 | 13.92 | 14.16 | 13.74 |
| T1 female | 8.97 | 8.70 | 8.77 | 10.36 | 9.75 | 10.24 | 12.80 | 12.65 | 11.80 |

APPENDIX 113 GENERIC SEAT MODEL SIMULATIONS T1 X-ACCELERATION MAXIMA FOR THE SAR 16 KM/H PULSE

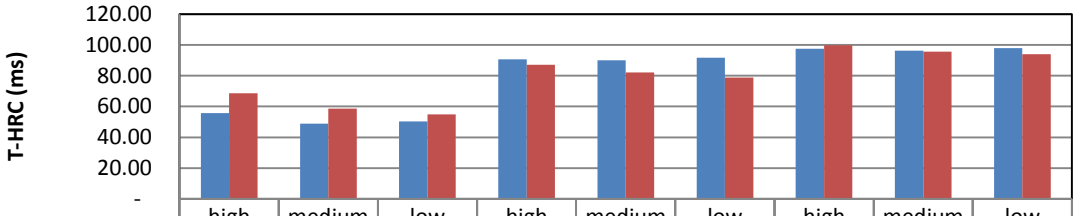


| | high | medium | low | high | medium | low | high | medium | low |
|---|---|---|---|---|---|---|---|---|---|
| | forward | | | middle | | | backward | | |
| T-HRC male | 55.72 | 48.82 | 50.32 | 90.62 | 90.12 | 91.62 | 97.52 | 96.22 | 97.82 |
| T-HRC female | 68.72 | 58.72 | 54.92 | 87.02 | 82.22 | 78.72 | 99.72 | 95.62 | 93.92 |

APPENDIX 114 GENERIC SEAT MODEL SIMULATIONS T-HRC MAXIMA FOR THE SAR 16 KM/H PULSE

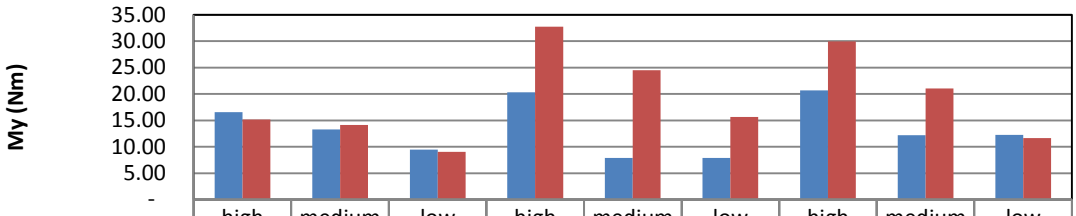


| | high | medium | low | high | medium | low | high | medium | low |
|---|---|---|---|---|---|---|---|---|---|
| | forward | | | middle | | | backward | | |
| My-flex male | 16.58 | 13.30 | 9.46 | 20.29 | 7.89 | 7.88 | 20.66 | 12.18 | 12.26 |
| My-flex female | 15.18 | 14.16 | 9.05 | 32.71 | 24.48 | 15.63 | 29.96 | 21.07 | 11.67 |

APPENDIX 115 GENERIC SEAT MODEL SIMULATIONS MY FLEXION MAXIMA FOR THE SAR 16 KM/H PULSE

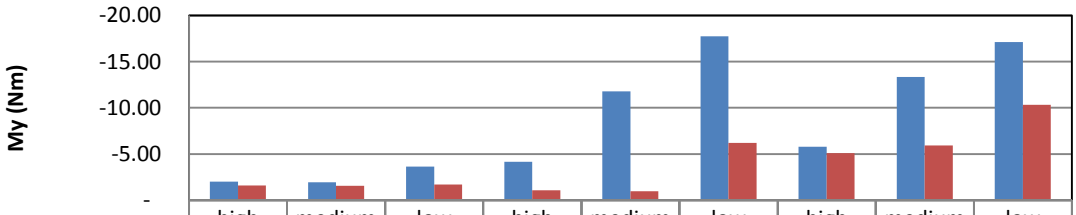


| | high | medium | low | high | medium | low | high | medium | low |
|---|---|---|---|---|---|---|---|---|---|
| | forward | | | middle | | | backward | | |
| My-ext male | -2.03 | -1.95 | -3.65 | -4.15 | -11.78 | -17.75 | -5.77 | -13.33 | -17.10 |
| My-ext female | -1.60 | -1.56 | -1.70 | -1.09 | -0.96 | -6.20 | -5.09 | -5.93 | -10.33 |

APPENDIX 116 GENERIC SEAT MODEL SIMULATIONS MY EXTENSION MAXIMA FOR THE SAR 16 KM/H PULSE

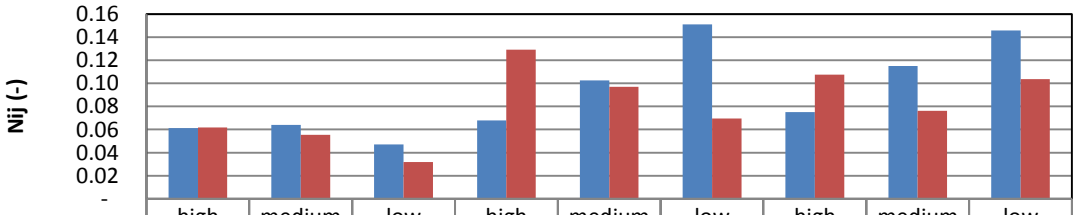


| | high | medium | low | high | medium | low | high | medium | low |
|---|---|---|---|---|---|---|---|---|---|
| | forward | | | middle | | | backward | | |
| Nij male | 0.06 | 0.06 | 0.05 | 0.07 | 0.10 | 0.15 | 0.08 | 0.11 | 0.15 |
| Nij female | 0.06 | 0.06 | 0.03 | 0.13 | 0.10 | 0.07 | 0.11 | 0.08 | 0.10 |

APPENDIX 117 GENERIC SEAT MODEL SIMULATIONS NIJ MAXIMA FOR THE SAR 16 KM/H PULSE

## A.4.2. SRA 24 km/h Eva RID and Bio RID Simulations

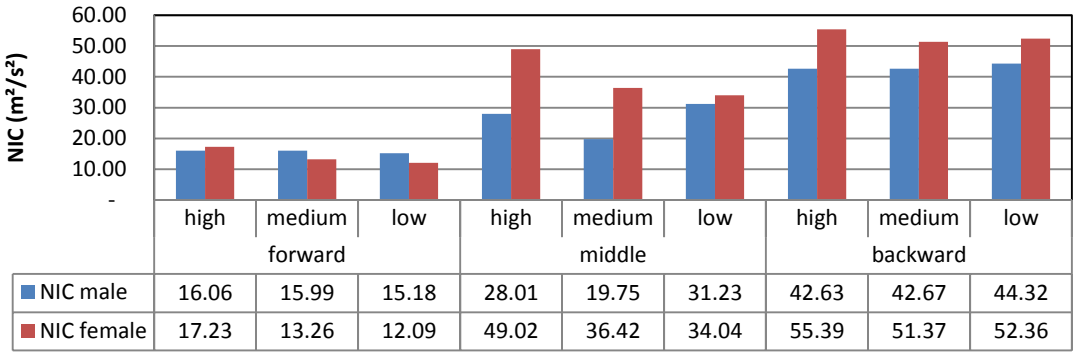


| | high | medium | low | high | medium | low | high | medium | low |
|---|---|---|---|---|---|---|---|---|---|
| | forward | | | middle | | | backward | | |
| NIC male | 16.06 | 15.99 | 15.18 | 28.01 | 19.75 | 31.23 | 42.63 | 42.67 | 44.32 |
| NIC female | 17.23 | 13.26 | 12.09 | 49.02 | 36.42 | 34.04 | 55.39 | 51.37 | 52.36 |

APPENDIX 118 GENERIC SEAT MODEL SIMULATIONS NIC MAXIMA FOR THE SAR 24 KM/H PULSE

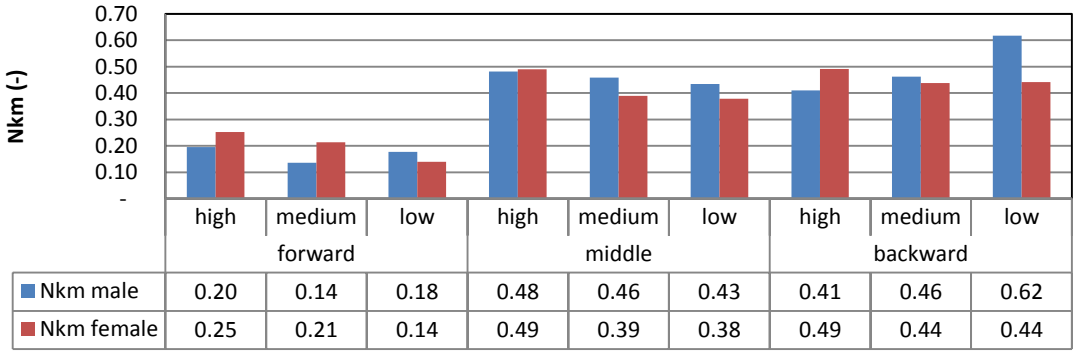


| | high | medium | low | high | medium | low | high | medium | low |
|---|---|---|---|---|---|---|---|---|---|
| | forward | | | middle | | | backward | | |
| Nkm male | 0.20 | 0.14 | 0.18 | 0.48 | 0.46 | 0.43 | 0.41 | 0.46 | 0.62 |
| Nkm female | 0.25 | 0.21 | 0.14 | 0.49 | 0.39 | 0.38 | 0.49 | 0.44 | 0.44 |

APPENDIX 119 GENERIC SEAT MODEL SIMULATIONS NKM MAXIMA FOR THE SAR 24 KM/H PULSE

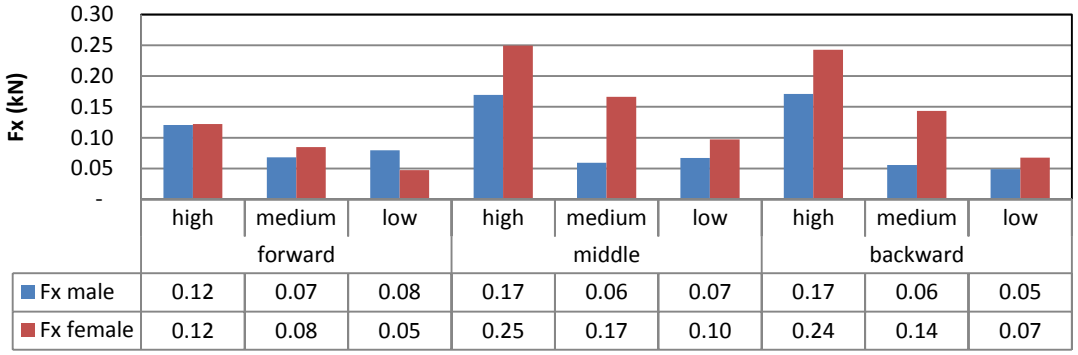


| | high | medium | low | high | medium | low | high | medium | low |
|---|---|---|---|---|---|---|---|---|---|
| | forward | | | middle | | | backward | | |
| Fx male | 0.12 | 0.07 | 0.08 | 0.17 | 0.06 | 0.07 | 0.17 | 0.06 | 0.05 |
| Fx female | 0.12 | 0.08 | 0.05 | 0.25 | 0.17 | 0.10 | 0.24 | 0.14 | 0.07 |

APPENDIX 120 GENERIC SEAT MODEL SIMULATIONS FX MAXIMA FOR THE SAR 24 KM/H PULSE

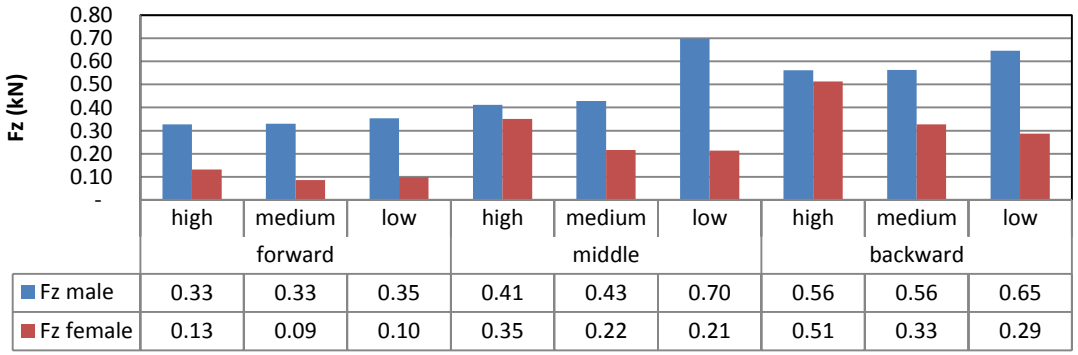


| | high | medium | low | high | medium | low | high | medium | low |
|---|---|---|---|---|---|---|---|---|---|
| | forward | | | middle | | | backward | | |
| Fz male | 0.33 | 0.33 | 0.35 | 0.41 | 0.43 | 0.70 | 0.56 | 0.56 | 0.65 |
| Fz female | 0.13 | 0.09 | 0.10 | 0.35 | 0.22 | 0.21 | 0.51 | 0.33 | 0.29 |

APPENDIX 121 GENERIC SEAT MODEL SIMULATIONS FZ MAXIMA FOR THE SAR 24 KM/H PULSE

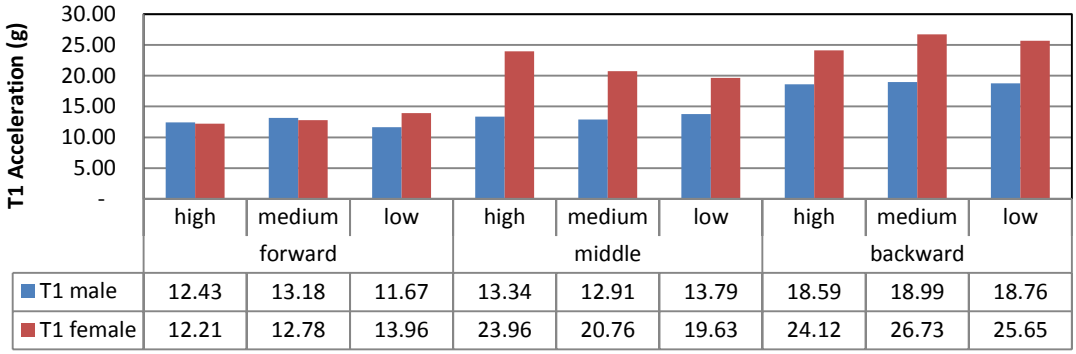


| | high | medium | low | high | medium | low | high | medium | low |
|---|---|---|---|---|---|---|---|---|---|
| | forward | | | middle | | | backward | | |
| T1 male | 12.43 | 13.18 | 11.67 | 13.34 | 12.91 | 13.79 | 18.59 | 18.99 | 18.76 |
| T1 female | 12.21 | 12.78 | 13.96 | 23.96 | 20.76 | 19.63 | 24.12 | 26.73 | 25.65 |

APPENDIX 122 GENERIC SEAT MODEL SIMULATIONS T1 X-ACCELERATION MAXIMA FOR THE SAR 24 KM/H PULSE

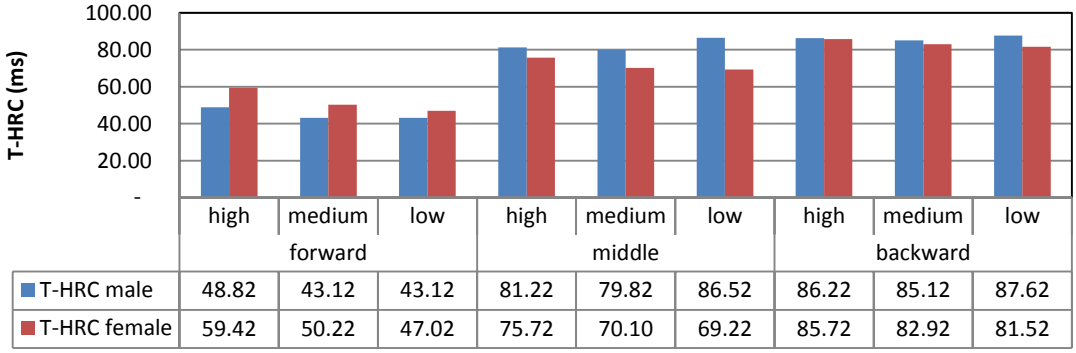


| | high | medium | low | high | medium | low | high | medium | low |
|---|---|---|---|---|---|---|---|---|---|
| | forward | | | middle | | | backward | | |
| T-HRC male | 48.82 | 43.12 | 43.12 | 81.22 | 79.82 | 86.52 | 86.22 | 85.12 | 87.62 |
| T-HRC female | 59.42 | 50.22 | 47.02 | 75.72 | 70.10 | 69.22 | 85.72 | 82.92 | 81.52 |

APPENDIX 123 GENERIC SEAT MODEL SIMULATIONS T-HRC MAXIMA FOR THE SAR 24 KM/H PULSE

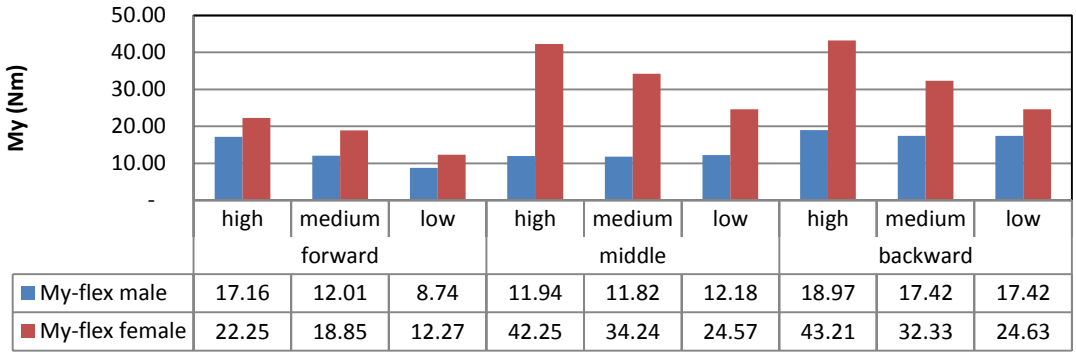


| | high | medium | low | high | medium | low | high | medium | low |
|---|---|---|---|---|---|---|---|---|---|
| | forward | | | middle | | | backward | | |
| My-flex male | 17.16 | 12.01 | 8.74 | 11.94 | 11.82 | 12.18 | 18.97 | 17.42 | 17.42 |
| My-flex female | 22.25 | 18.85 | 12.27 | 42.25 | 34.24 | 24.57 | 43.21 | 32.33 | 24.63 |

APPENDIX 124 GENERIC SEAT MODEL SIMULATIONS MY FLEXION MAXIMA FOR THE SAR 24 KM/H PULSE

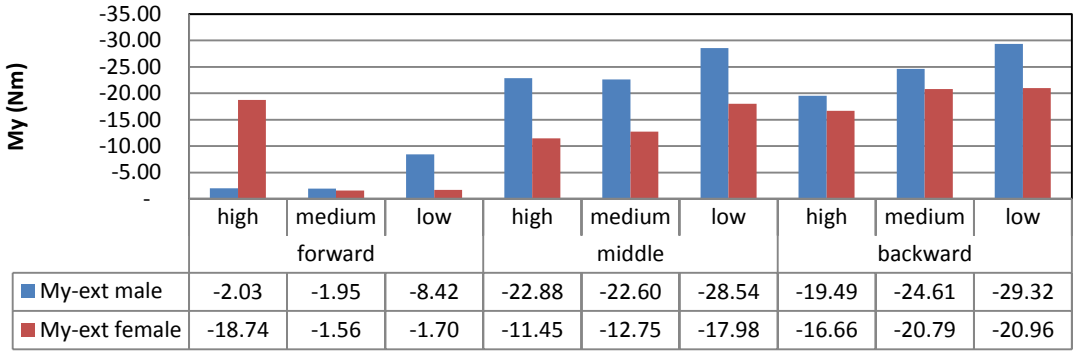


| | high | medium | low | high | medium | low | high | medium | low |
|---|---|---|---|---|---|---|---|---|---|
| | forward | | | middle | | | backward | | |
| My-ext male | -2.03 | -1.95 | -8.42 | -22.88 | -22.60 | -28.54 | -19.49 | -24.61 | -29.32 |
| My-ext female | -18.74 | -1.56 | -1.70 | -11.45 | -12.75 | -17.98 | -16.66 | -20.79 | -20.96 |

APPENDIX 125 GENERIC SEAT MODEL SIMULATIONS MY EXTENSION MAXIMA FOR THE SAR 24 KM/H PULSE

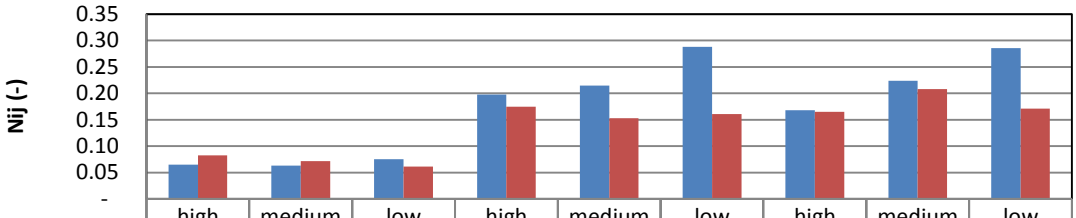


| | high | medium | low | high | medium | low | high | medium | low |
|---|---|---|---|---|---|---|---|---|---|
| | forward | | | middle | | | backward | | |
| Nij male | 0.07 | 0.06 | 0.08 | 0.20 | 0.21 | 0.29 | 0.17 | 0.22 | 0.29 |
| Nij female | 0.08 | 0.07 | 0.06 | 0.17 | 0.15 | 0.16 | 0.16 | 0.21 | 0.17 |

APPENDIX 126 GENERIC SEAT MODEL SIMULATIONS NIJ MAXIMA FOR THE SAR 24 KM/H PULSE

## A.5. Comparison of Numerical Eva RID simulations and female PMHS tests

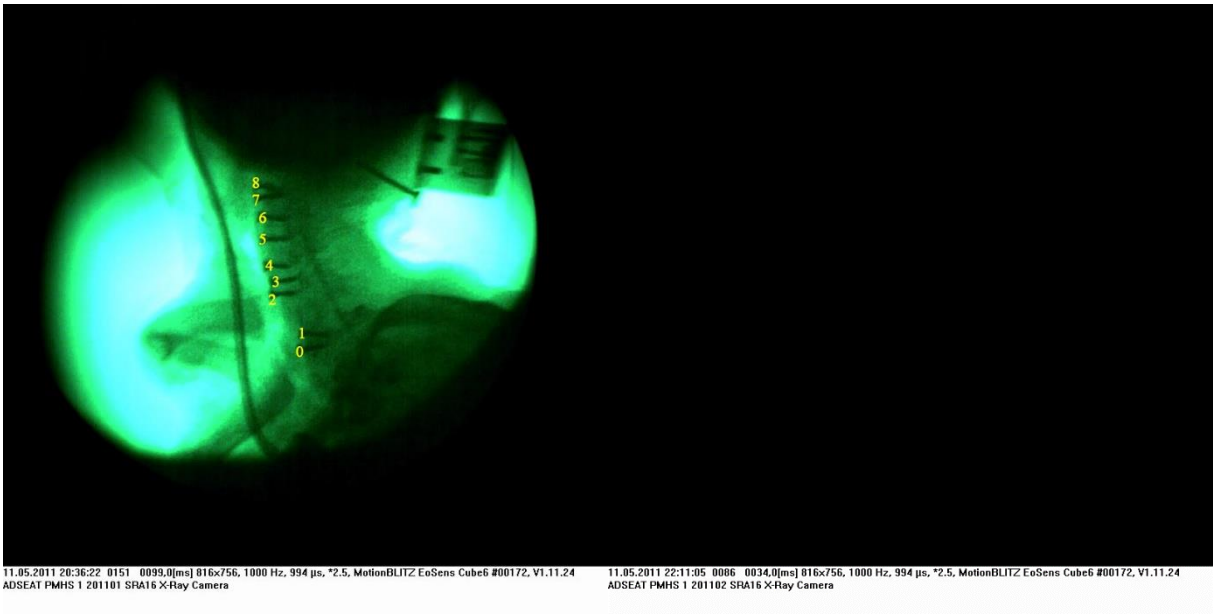


APPENDIX 127 PMHS1_1 X-RAY PICTURE WITH TGT NUMBERS




APPENDIX 128 PMHS1_2 X-RAY PICTURE WITH TGT NUMBERS

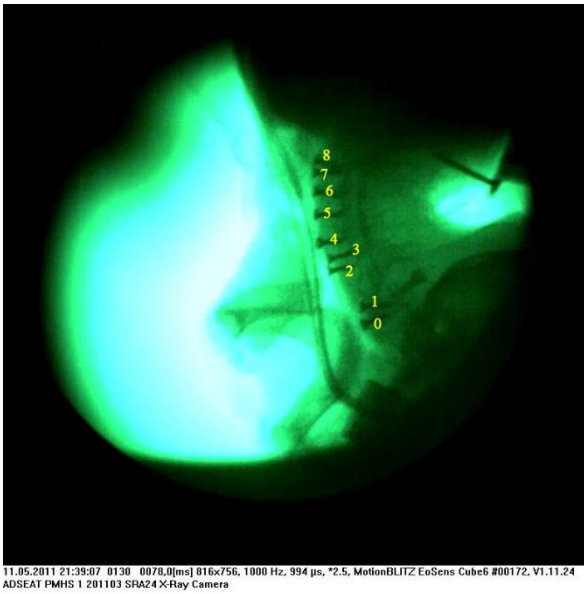


APPENDIX 129 PMHS1_3 X-RAY PICTURE WITH TGT NUMBERS


APPENDIX 130 PMHS1_4 X-RAY PICTURE WITH TGT NUMBERS

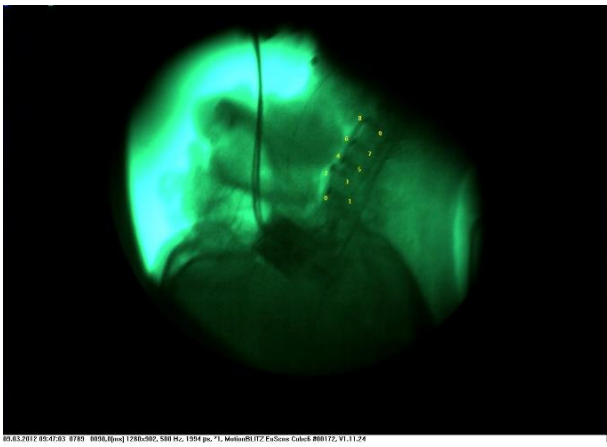

APPENDIX 131 PMHS4_1 X-RAY PICTURE WITH TGT NUMBERS

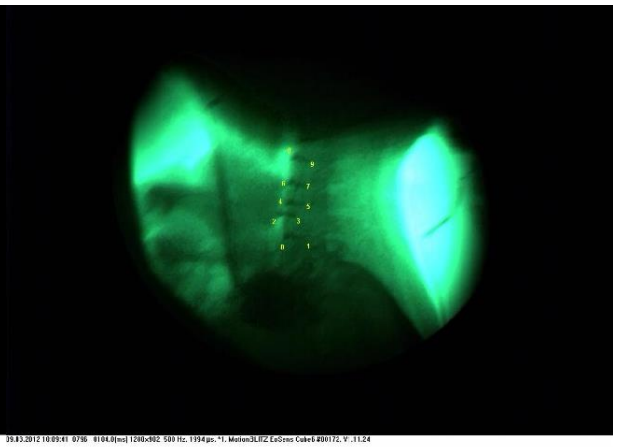

APPENDIX 132 PMHS4_2 X-RAY PICTURE WITH TGT NUMBERS

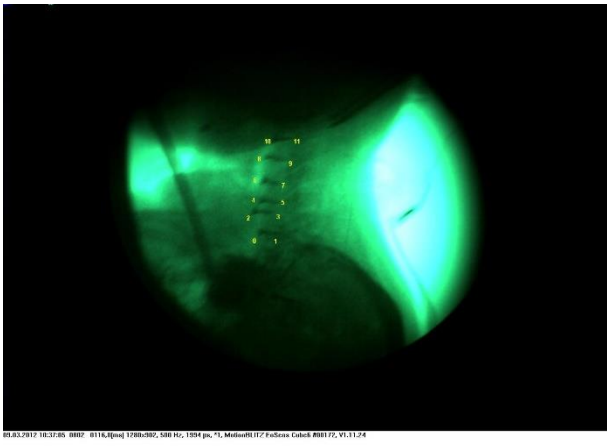

APPENDIX 133 PMHS4_3 X-RAY PICTURE WITH TGT NUMBERS

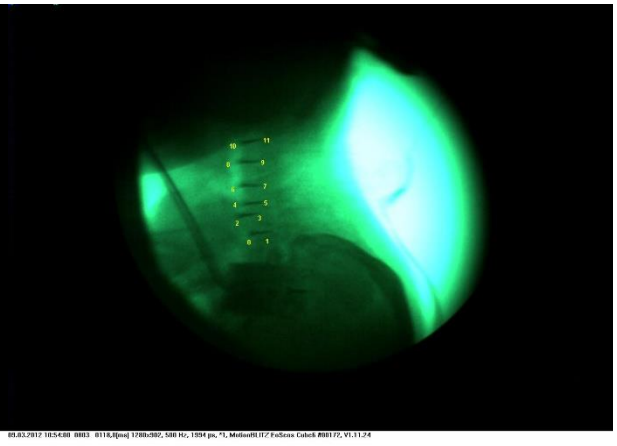

APPENDIX 134 PMHS4_4 X-RAY PICTURE WITH TGT NUMBERS

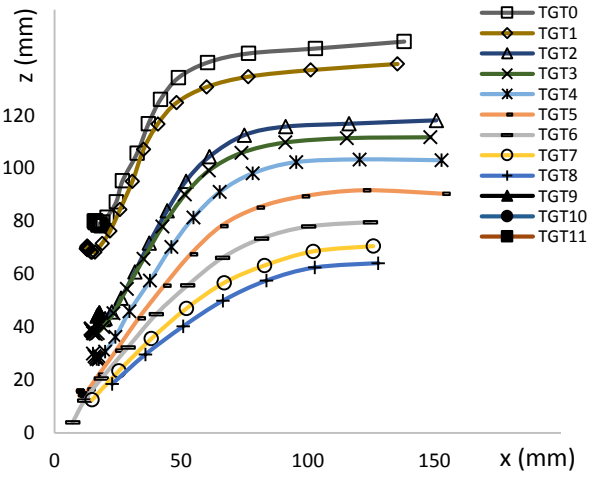


APPENDIX 135 PMHS1_1 ALL TRAJECTORIES TRACKED

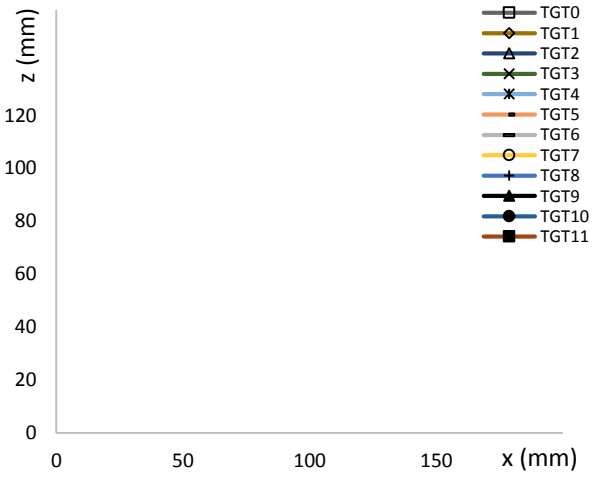


APPENDIX 136 PMHS1_2 ALL TRAJECTORIES TRACKED

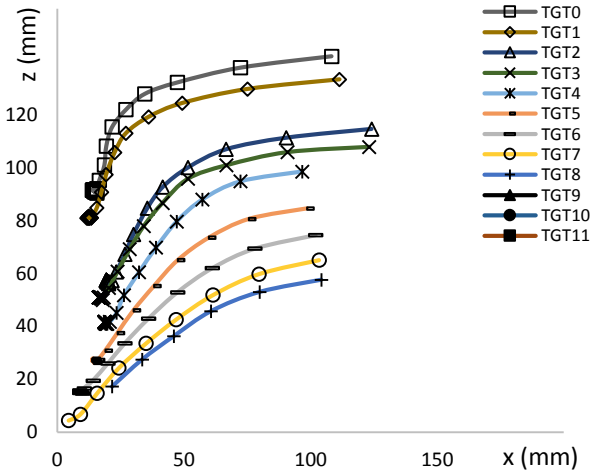


APPENDIX 137 PMHS1_3 ALL TRAJECTORIES TRACKED

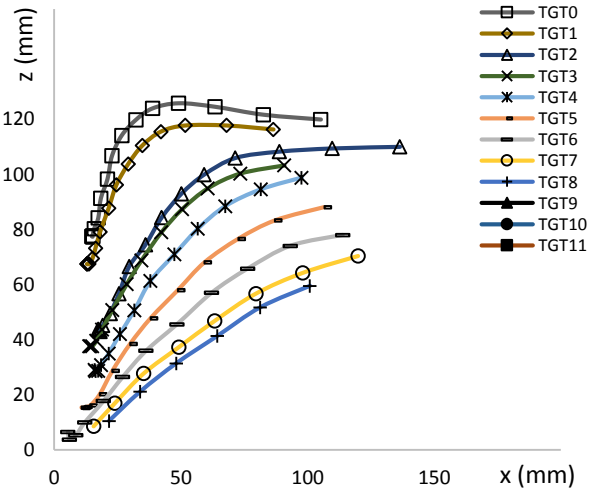


APPENDIX 138 PMHS1_4 ALL TRAJECTORIES TRACKED

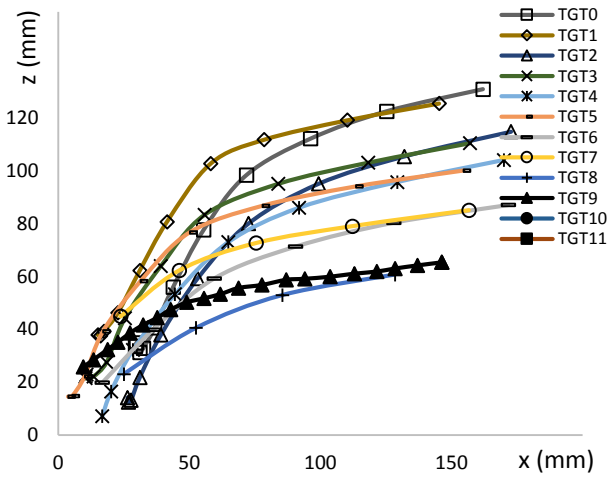


APPENDIX 139 PMHS4_1 ALL TRAJECTORIES TRACKED

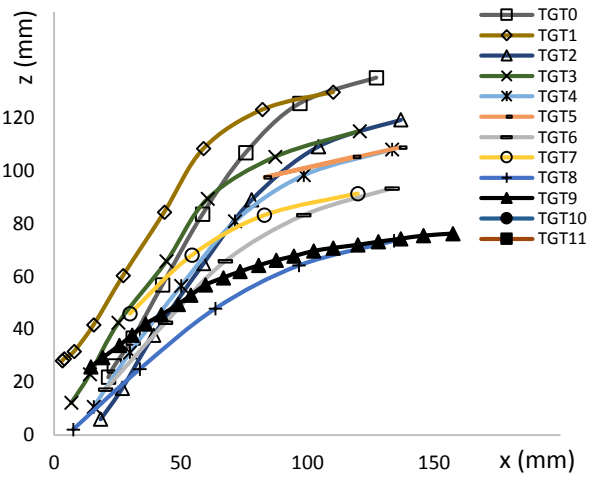


APPENDIX 140 PMHS4_2 ALL TRAJECTORIES TRACKED

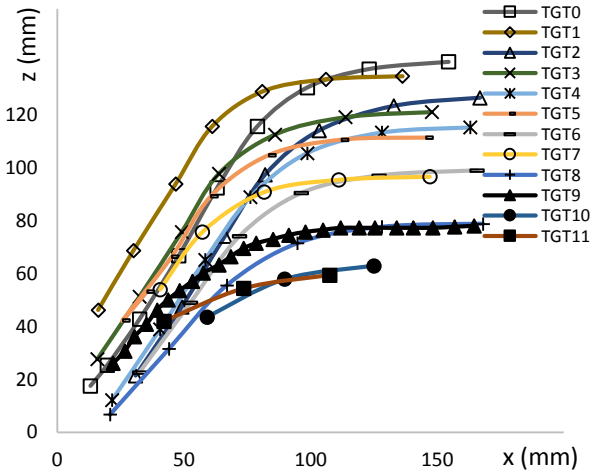


APPENDIX 141 PMHS4_3 ALL TRAJECTORIES TRACKED

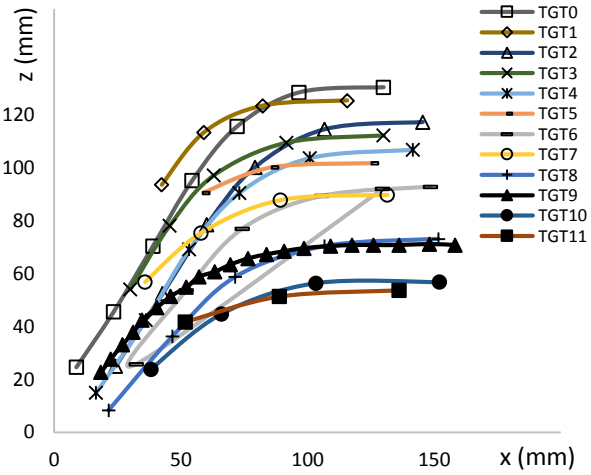


APPENDIX 142 PMHS4_4 ALL TRAJECTORIES TRACKED

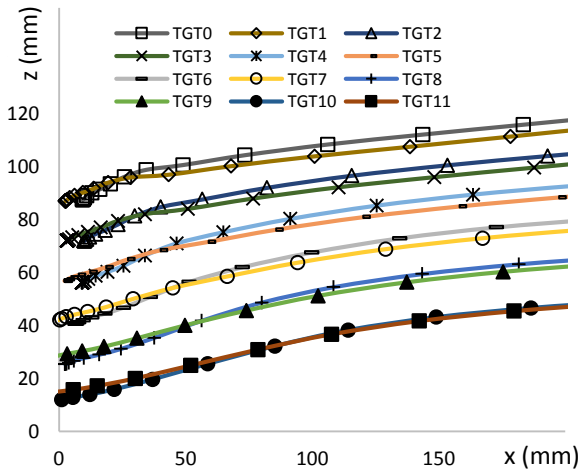


APPENDIX 143 EVA RID IIWPG ALL TRAJECTORIES EXTRACTED

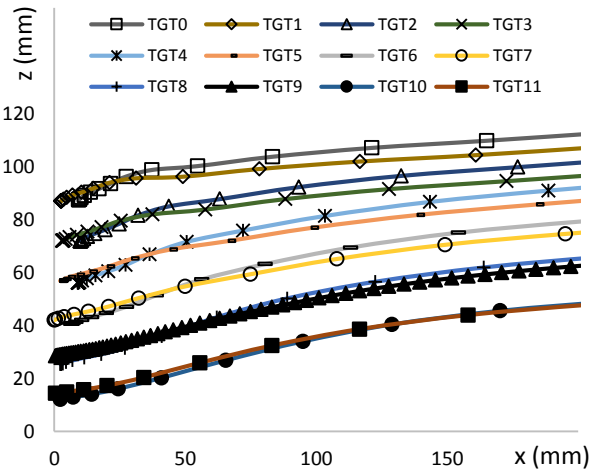


APPENDIX 144 EVA RID SRA 24 ALL TRAJECTORIES EXTRACTED

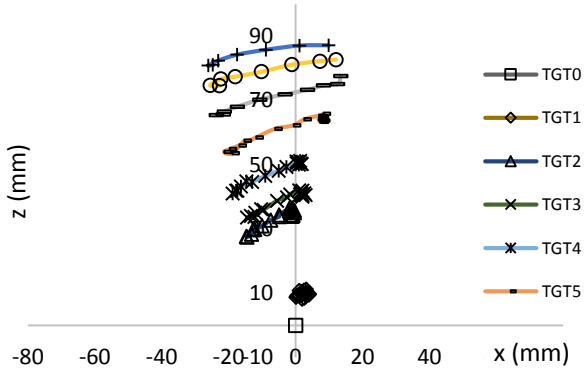


APPENDIX 145 PMHS1_1 MOTION OF TARGETS ABOUT TGT0

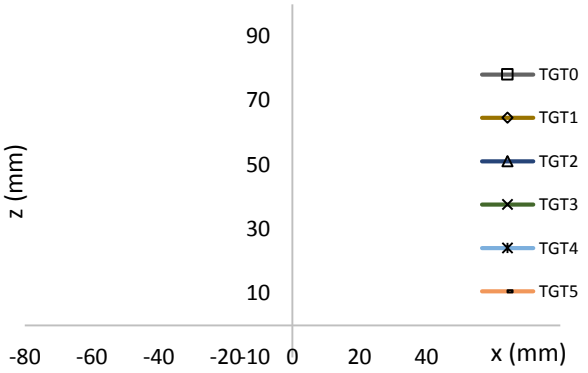


APPENDIX 146 PMHS1_2 MOTION OF TARGETS ABOUT TGT0

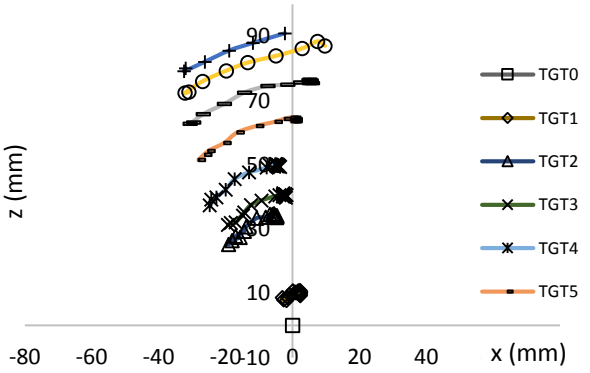


APPENDIX 147 PMHS1_3 MOTION OF TARGETS ABOUT TGT0

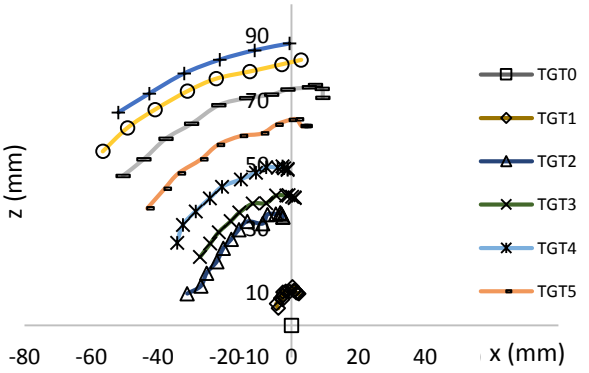


APPENDIX 148 PMHS1_4 MOTION OF TARGETS ABOUT TGT0

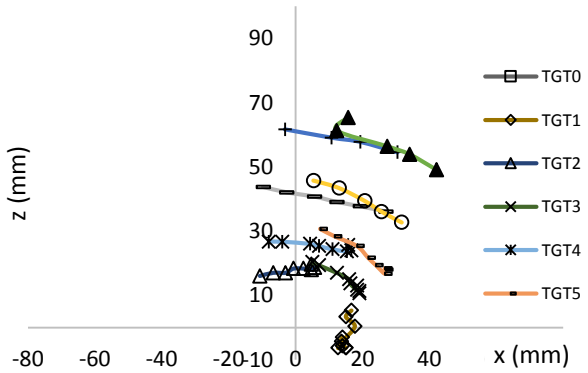


APPENDIX 149 PMHS4_1 MOTION OF TARGETS ABOUT TGT0

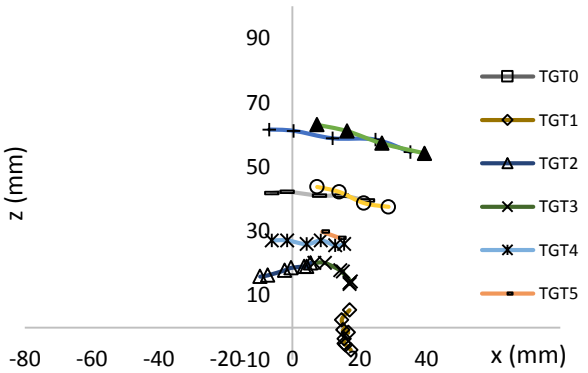


APPENDIX 150 PMHS4_2 MOTION OF TARGETS ABOUT TGT0

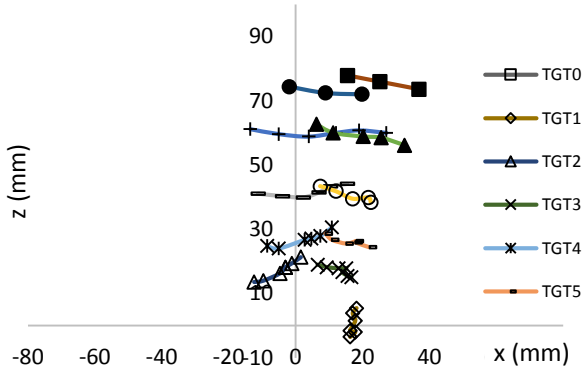


APPENDIX 151 PMHS4_3 MOTION OF TARGETS ABOUT TGT0

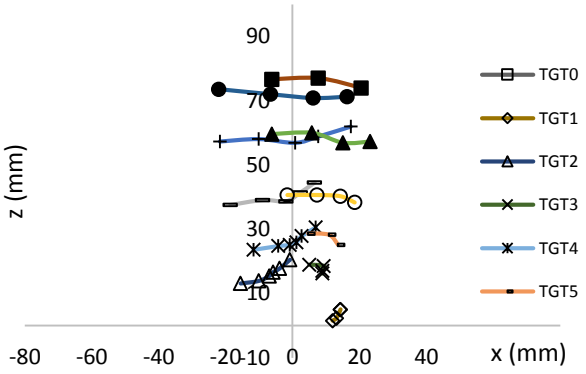


APPENDIX 152 PMHS4_4 MOTION OF TARGETS ABOUT TGT0

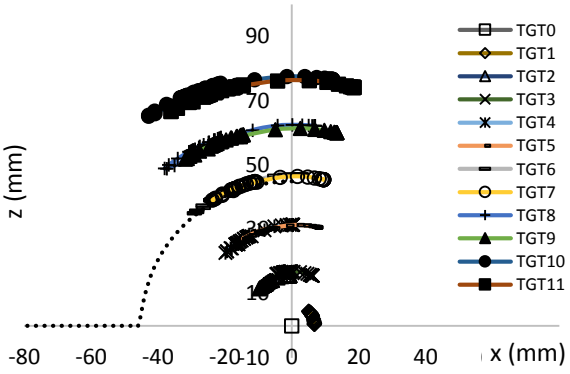


APPENDIX 153 EVA RID IIWPG MOTION OF TARGETS ABOUT TGT0

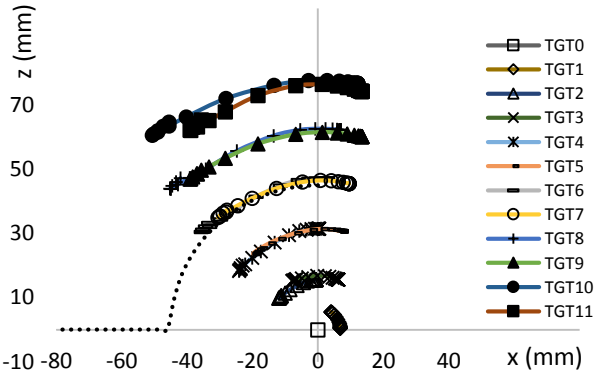


APPENDIX 154 EVA RID SRA 24 MOTION OF TARGETS ABOUT TGT0

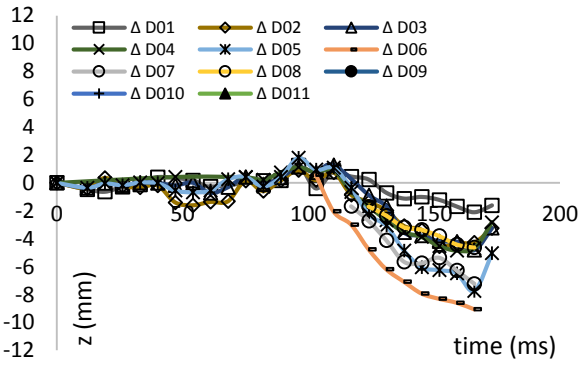


APPENDIX 155 PMHS1_1 RELATIVE ELONGATION IN REFERENCE TO TGT0

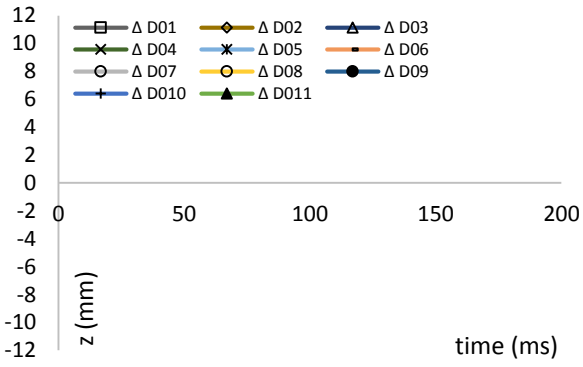


APPENDIX 156 PMHS1_2 RELATIVE ELONGATION IN REFERENCE TO TGT0

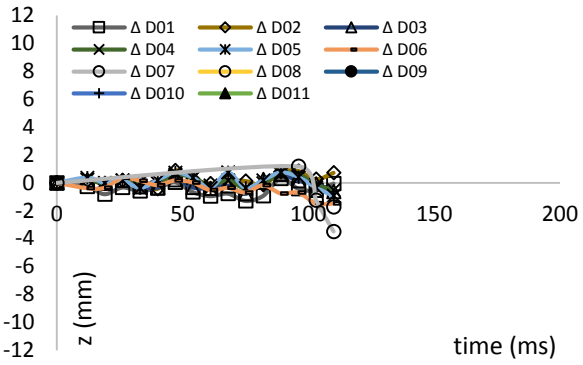


APPENDIX 157 PMHS1_3 RELATIVE ELONGATION IN REFERENCE TO TGT0

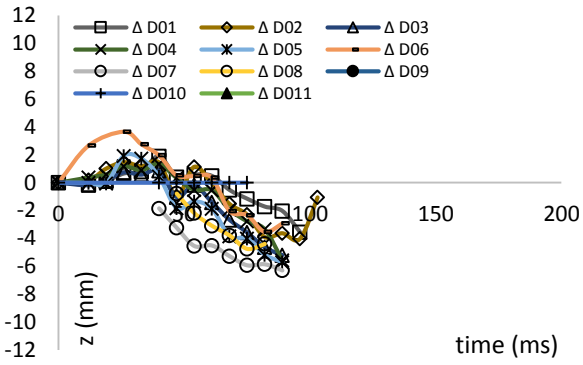


APPENDIX 158 PMHS1_4 RELATIVE ELONGATION IN REFERENCE TO TGT0

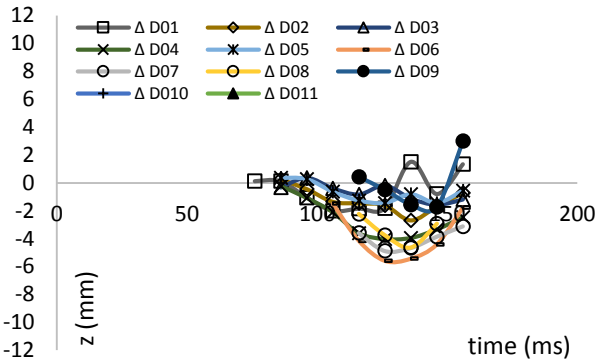


APPENDIX 159 PMHS4_1 RELATIVE ELONGATION IN REFERENCE TO TGT0

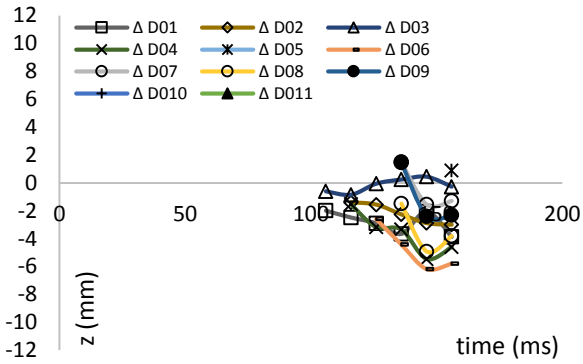


APPENDIX 160 PMHS4_2 RELATIVE ELONGATION IN REFERENCE TO TGT0

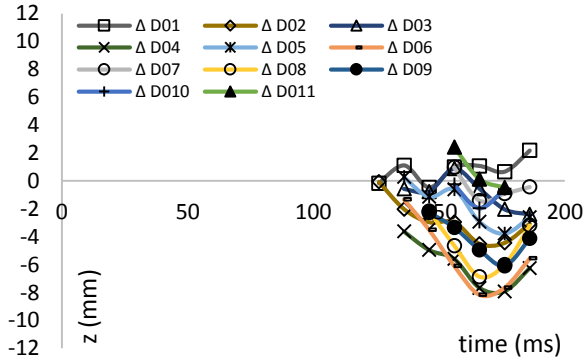


APPENDIX 161 PMHS4_3 RELATIVE ELONGATION IN REFERENCE TO TGT0

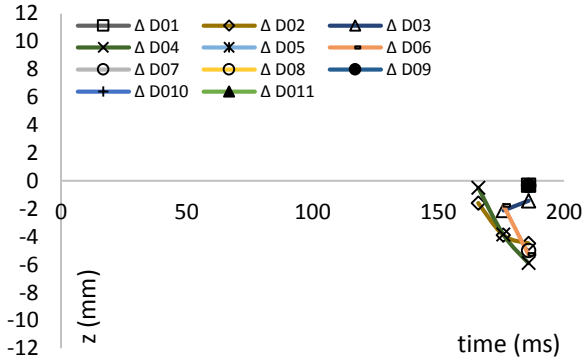


APPENDIX 162 PMHS4_4 RELATIVE ELONGATION IN REFERENCE TO TGT0

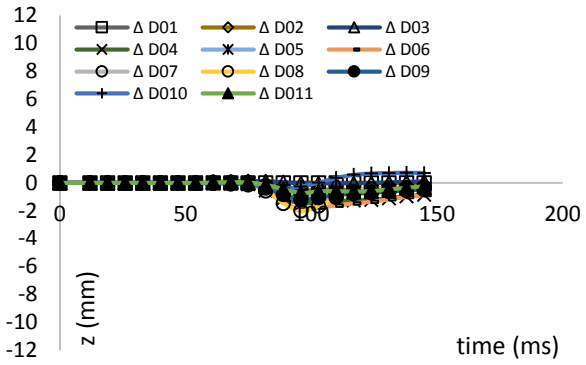


APPENDIX 163 EVA RID IIWPG RELATIVE ELONGATION IN REFERENCE TO TGT0

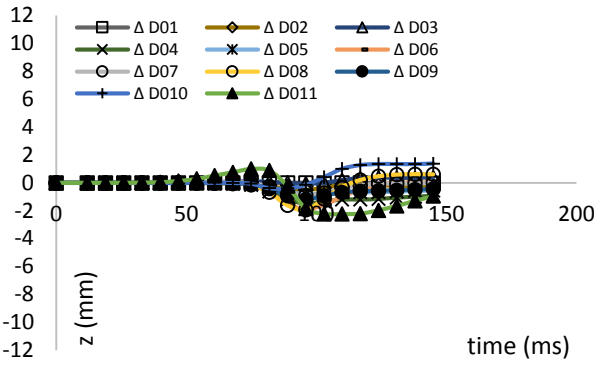


APPENDIX 164 EVA RID SRA 24 RELATIVE ELONGATION IN REFERENCE TO TGT0

## A.6. Bio RID II – generic seat simulations

### A.6.1. Bio RID II – forward backrest – high head restraint 111

#### A.6.1.1. Low Severity Pulse (SRA 16 km/h) L111

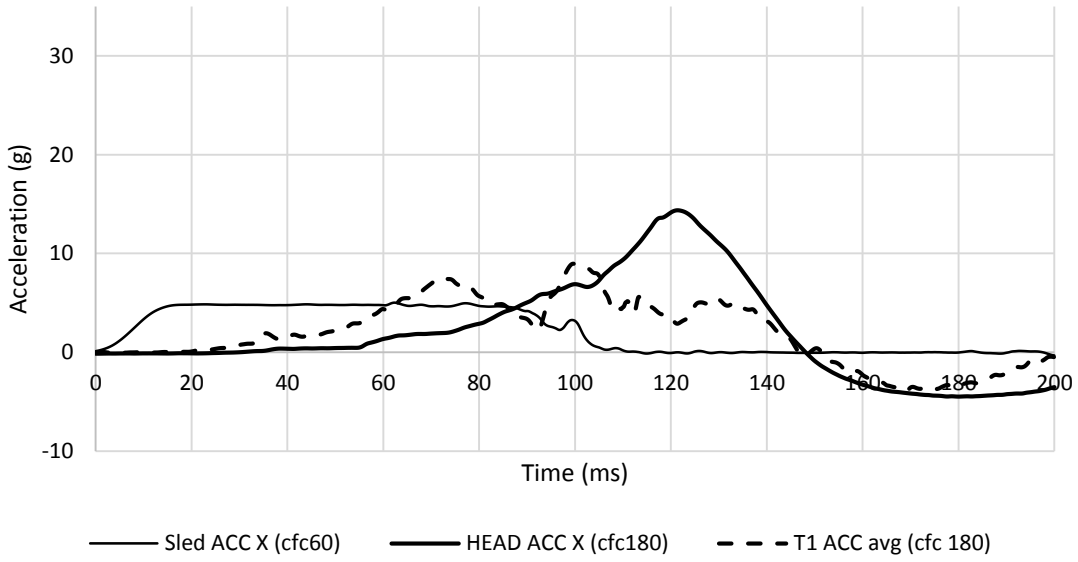


APPENDIX 165 LOADING GRAPHS OF FEA BIO RID CONFIGURATION L111 - ACCELERATION

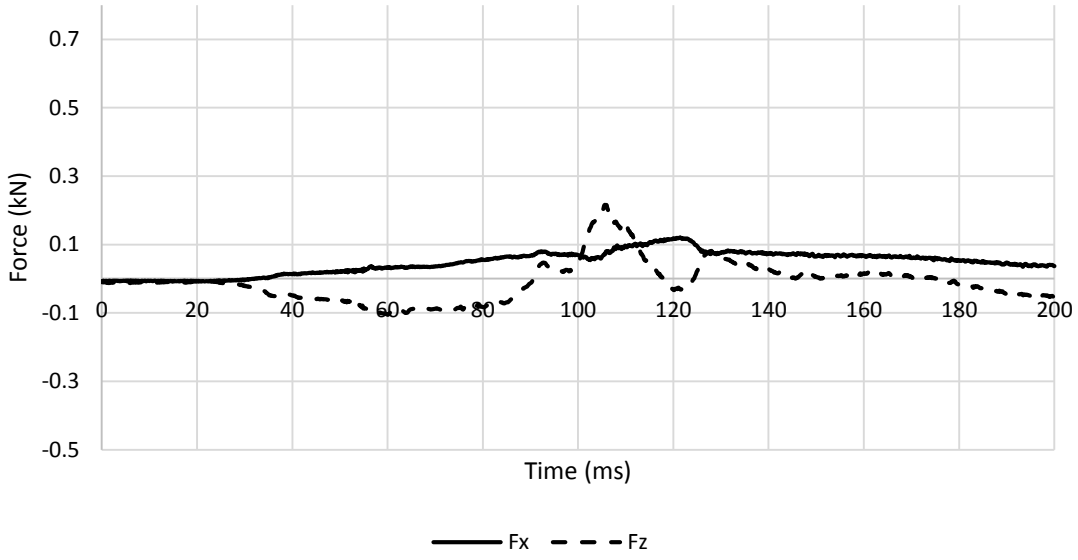


APPENDIX 166 LOADING GRAPHS OF FEA BIO RID CONFIGURATION L111 - FORCE

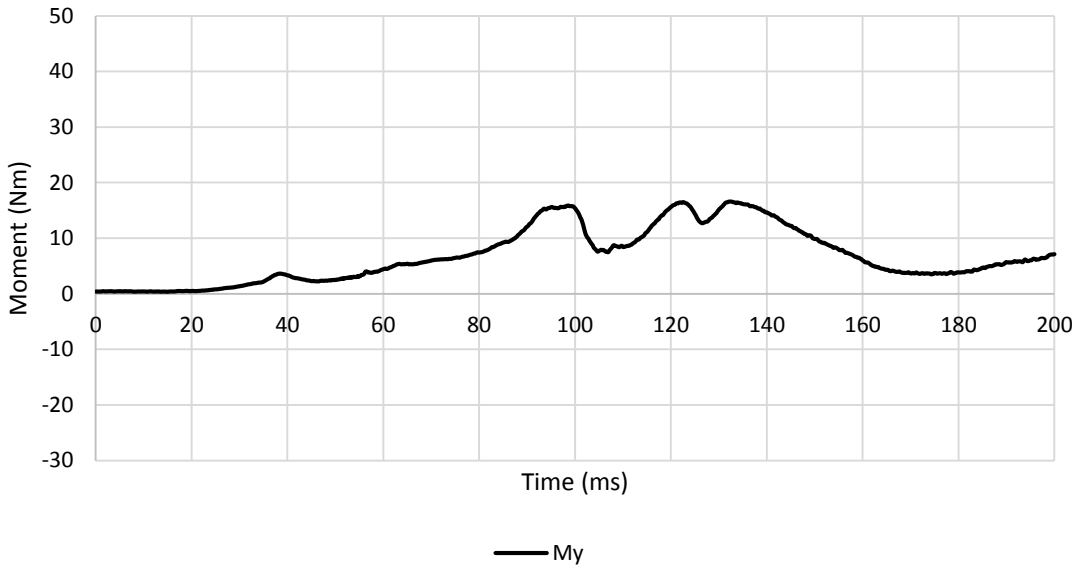


APPENDIX 167 LOADING GRAPHS OF FEA BIO RID CONFIGURATION L111 – MOMENT

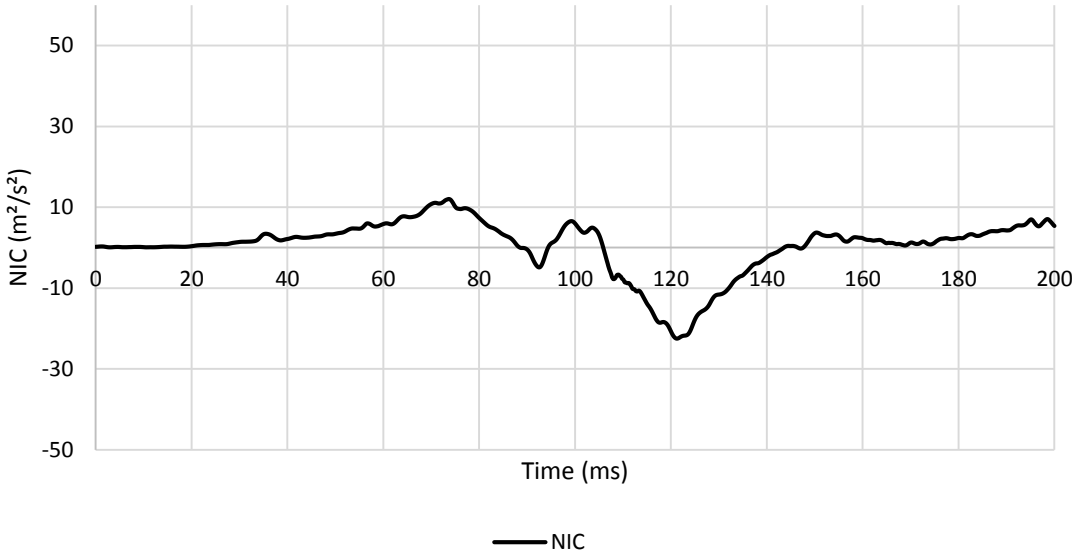


APPENDIX 168 LOADING GRAPHS OF FEA BIO RID CONFIGURATION L111 - NIC

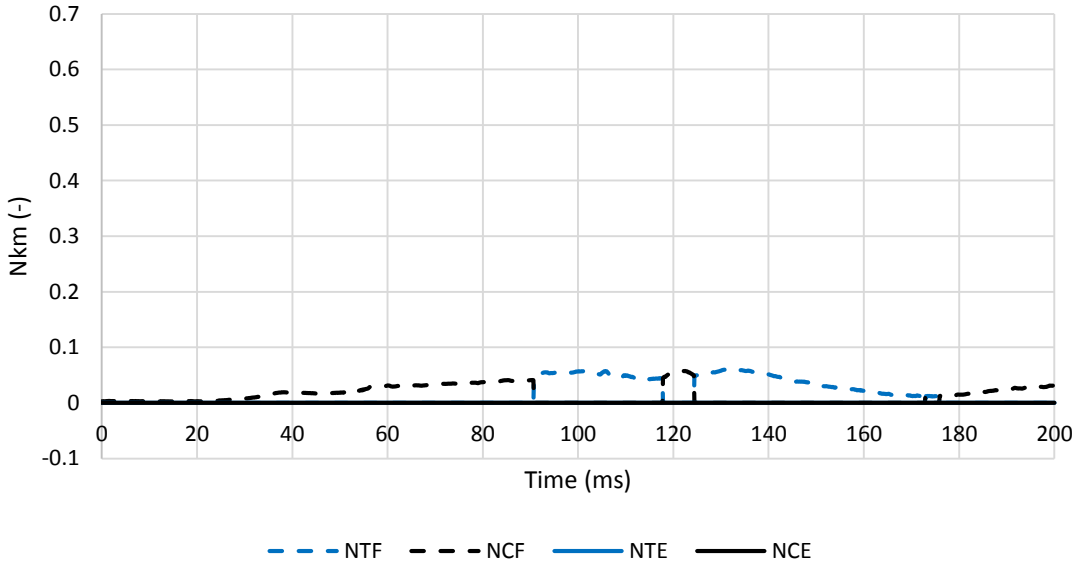


APPENDIX 169 LOADING GRAPHS OF FEA BIO RID CONFIGURATION L111 – NKM

### A.6.1.2. Medium Severity Pulse (IIWPG 16 km/h) M111

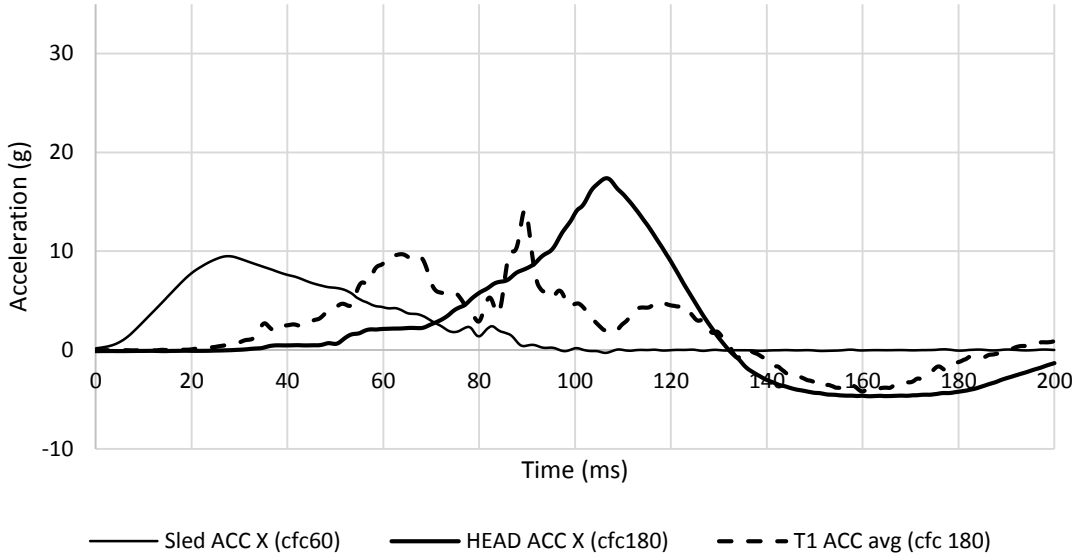


APPENDIX 170 LOADING GRAPHS OF FEA BIO RID CONFIGURATION M111 - ACCELERATION

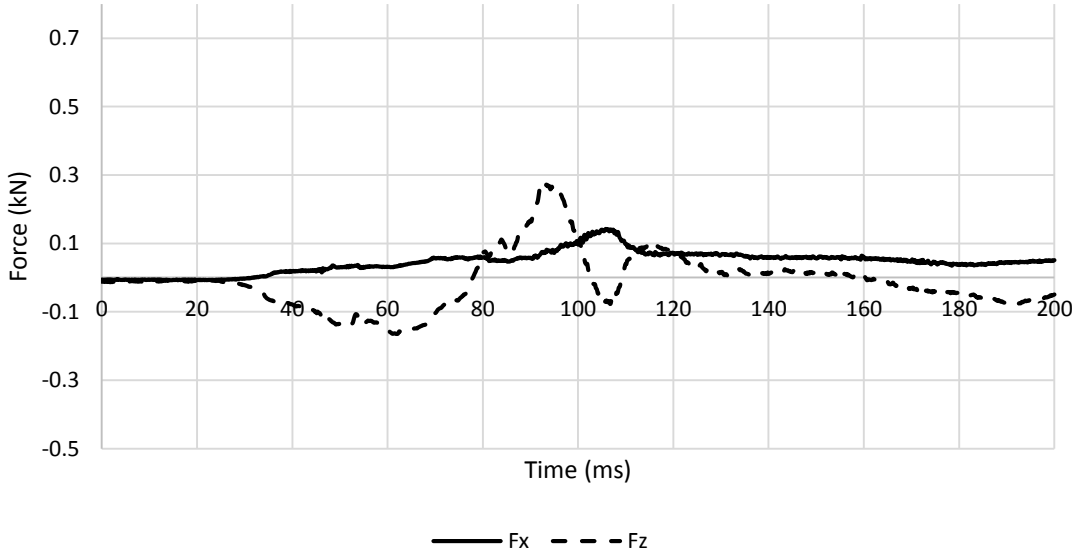


APPENDIX 171 LOADING GRAPHS OF FEA BIO RID CONFIGURATION M111 - FORCE

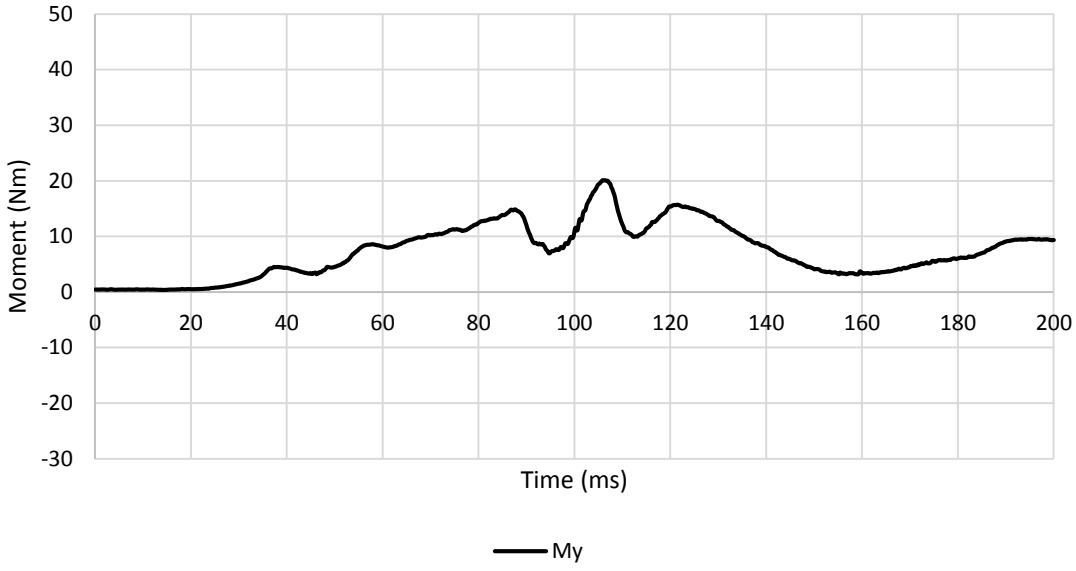


APPENDIX 172 LOADING GRAPHS OF FEA BIO RID CONFIGURATION M111 - MOMENT

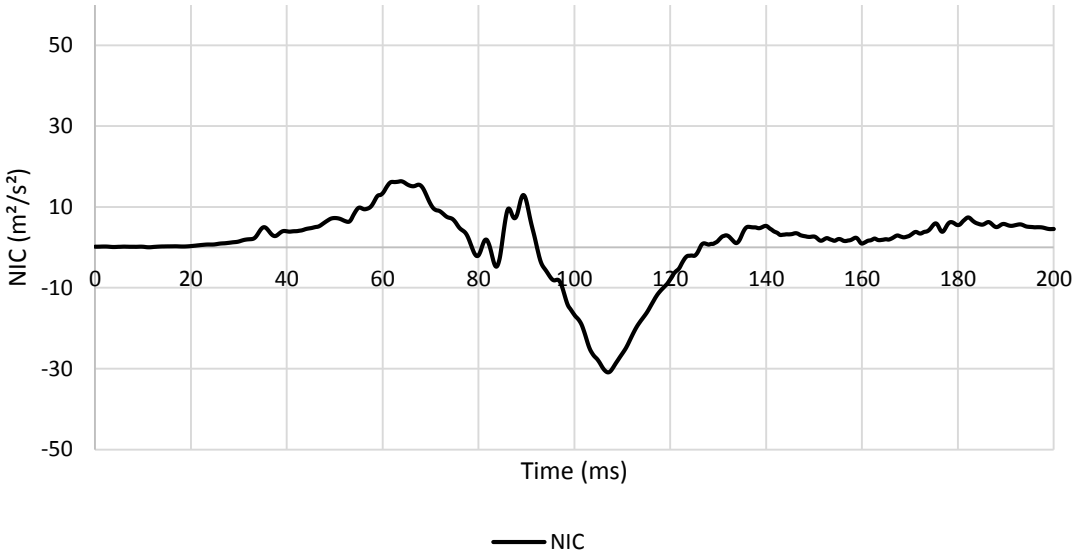


APPENDIX 173 LOADING GRAPHS OF FEA BIO RID CONFIGURATION M111 - NIC

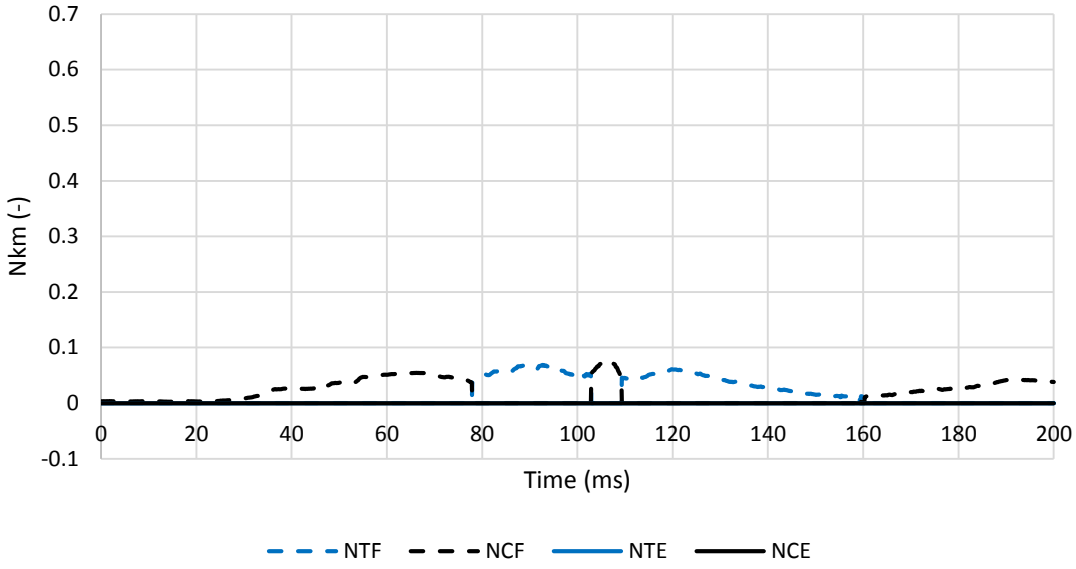


APPENDIX 174 LOADING GRAPHS OF FEA BIO RID CONFIGURATION M111 - NKM

### A.6.1.3. High Severity Pulse (SRA 24 km/h) H111

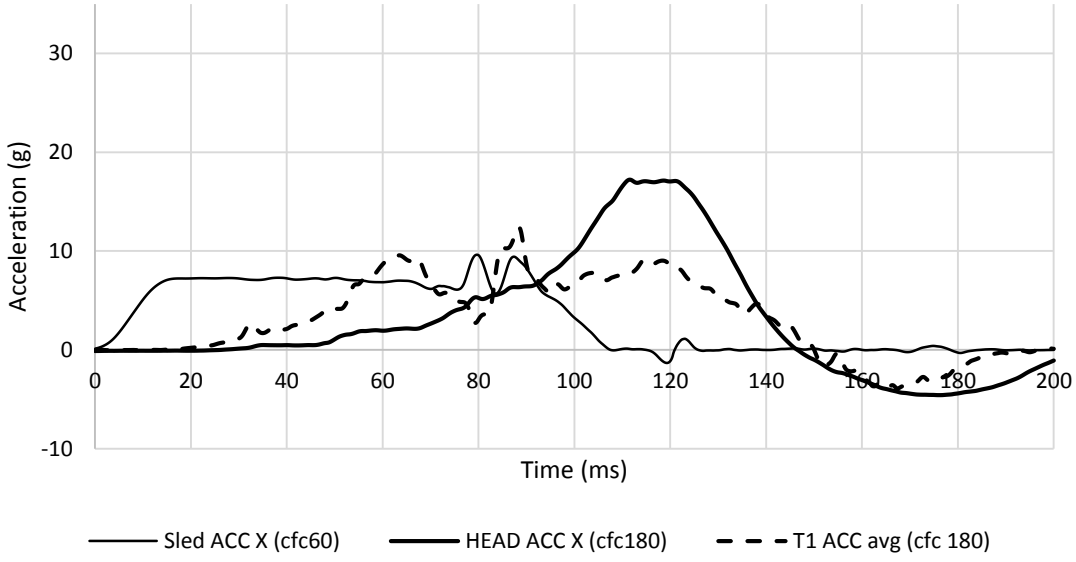


APPENDIX 175 LOADING GRAPHS OF FEA BIO RID CONFIGURATION H111 - ACCELERATION

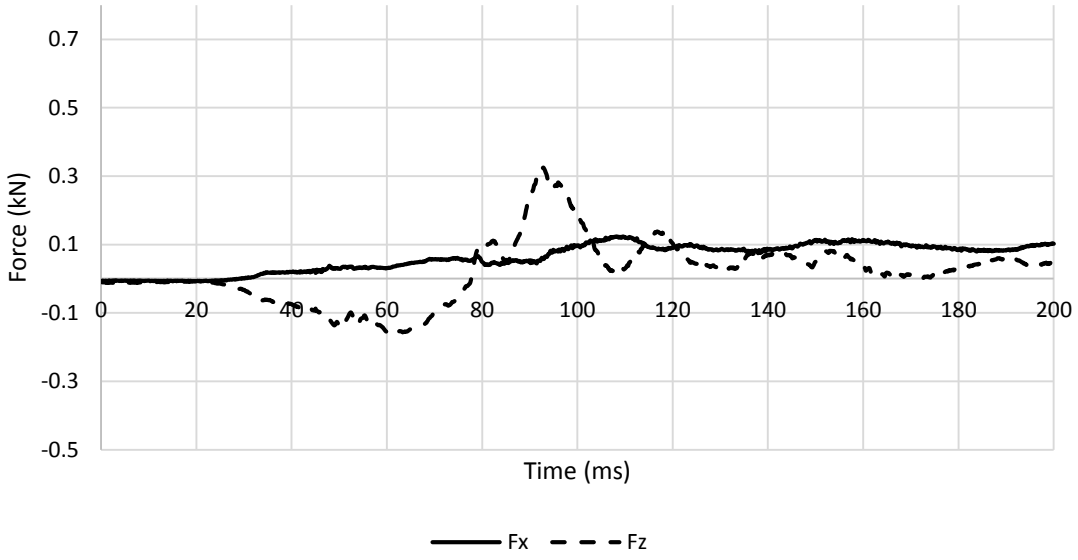


APPENDIX 176 LOADING GRAPHS OF FEA BIO RID CONFIGURATION H111 - FORCE

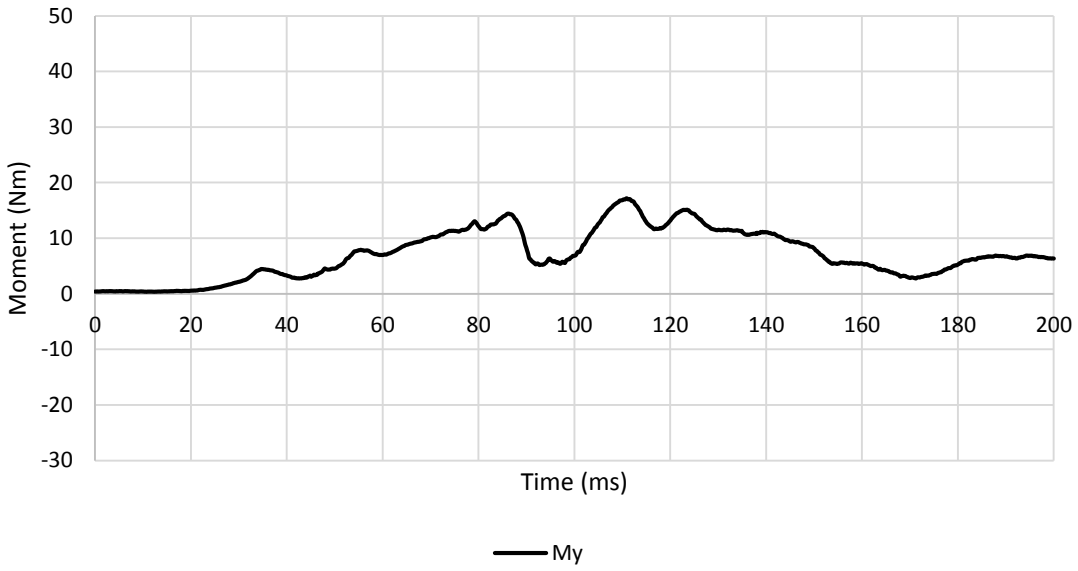


APPENDIX 177 LOADING GRAPHS OF FEA BIO RID CONFIGURATION H111 - MOMENT

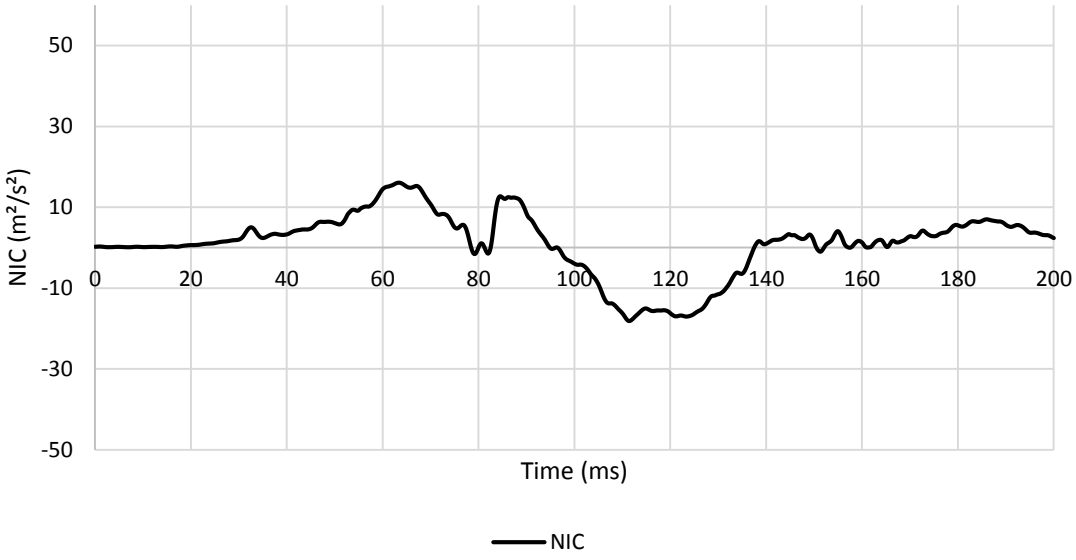


APPENDIX 178 LOADING GRAPHS OF FEA BIO RID CONFIGURATION HL111 - NIC

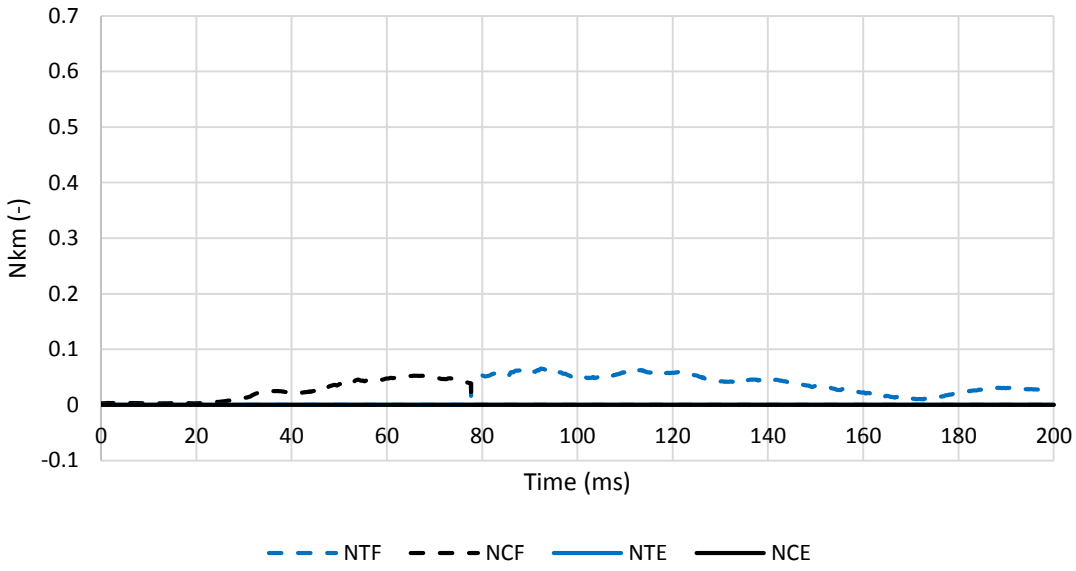


APPENDIX 179 LOADING GRAPHS OF FEA BIO RID CONFIGURATION H111 - NKM

## A.6.2. Bio RID II – forward backrest – middle head restraint 112

### A.6.2.1. Low Severity Pulse (SRA 16 km/h) L112

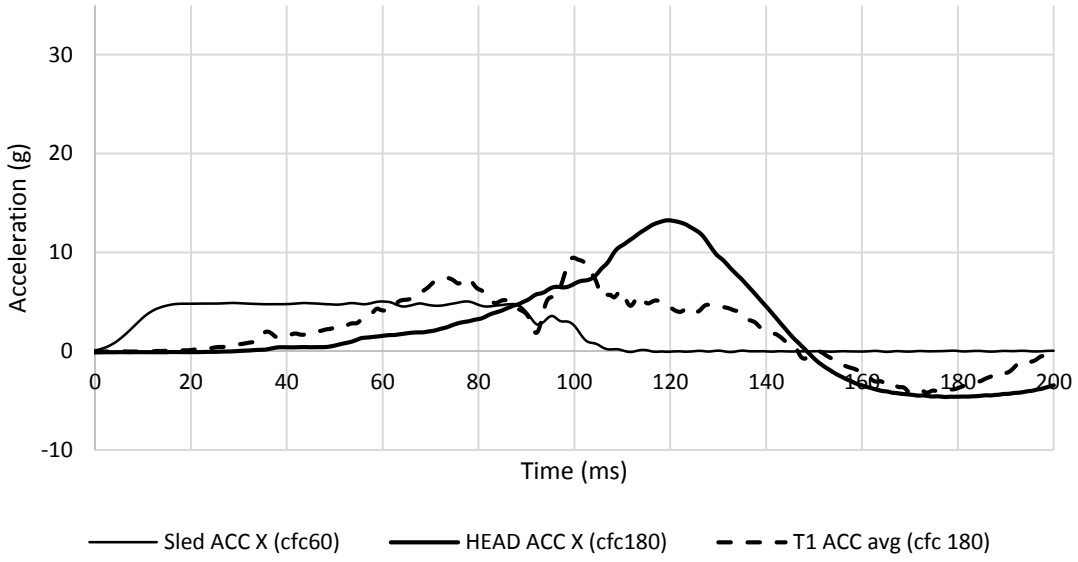


APPENDIX 180 LOADING GRAPHS OF FEA BIO RID CONFIGURATION L112 - ACCELERATION

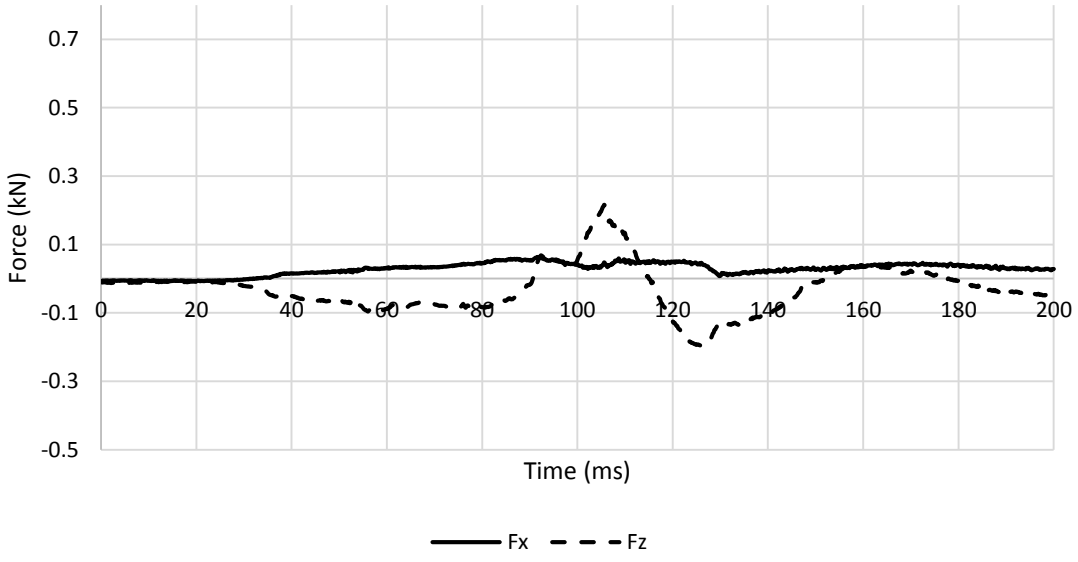


APPENDIX 181 LOADING GRAPHS OF FEA BIO RID CONFIGURATION L112 - FORCE

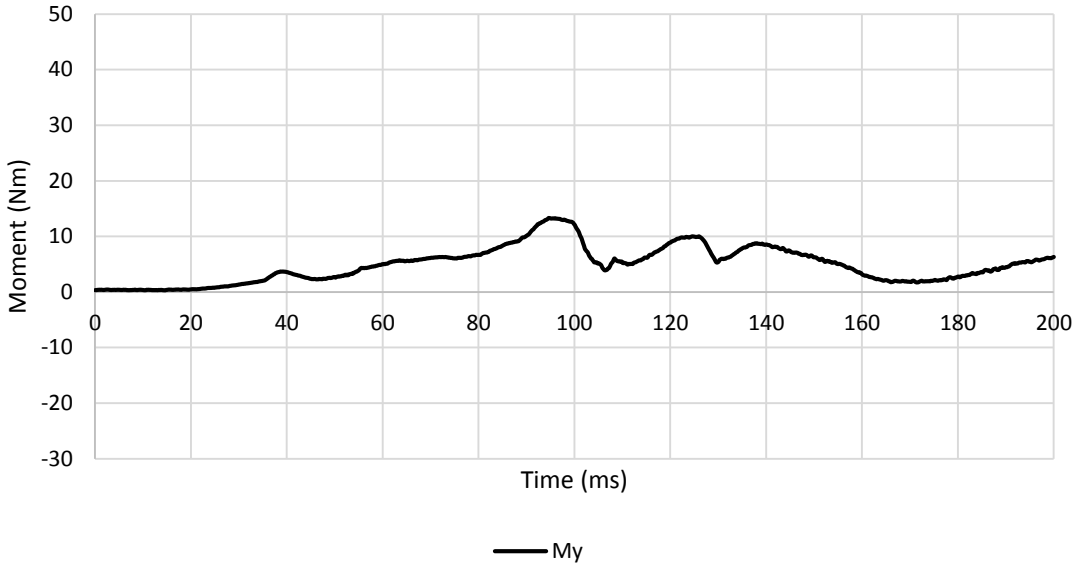


APPENDIX 182 LOADING GRAPHS OF FEA BIO RID CONFIGURATION L112 - MOMENT

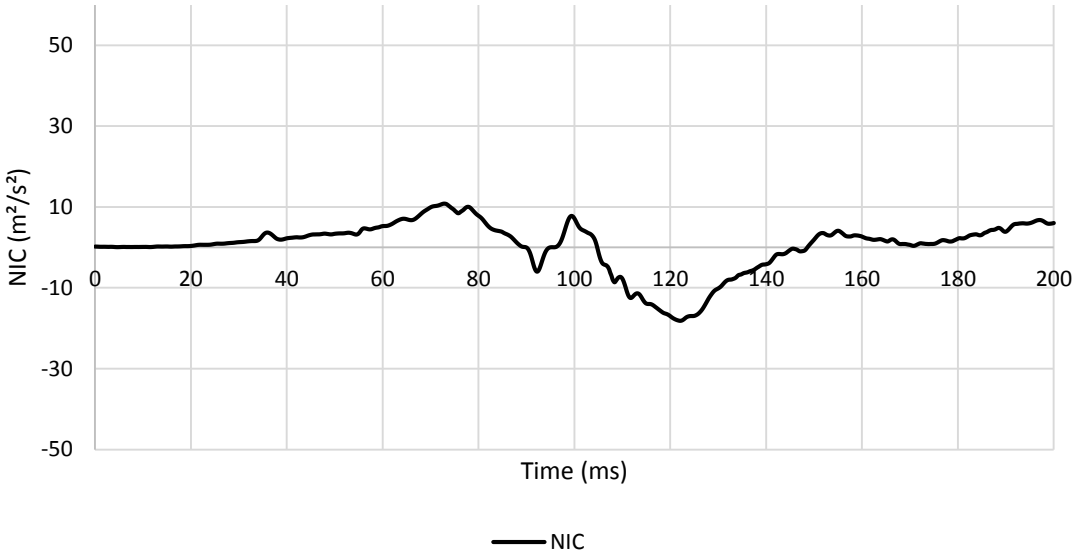


APPENDIX 183 LOADING GRAPHS OF FEA BIO RID CONFIGURATION L112 - NIC

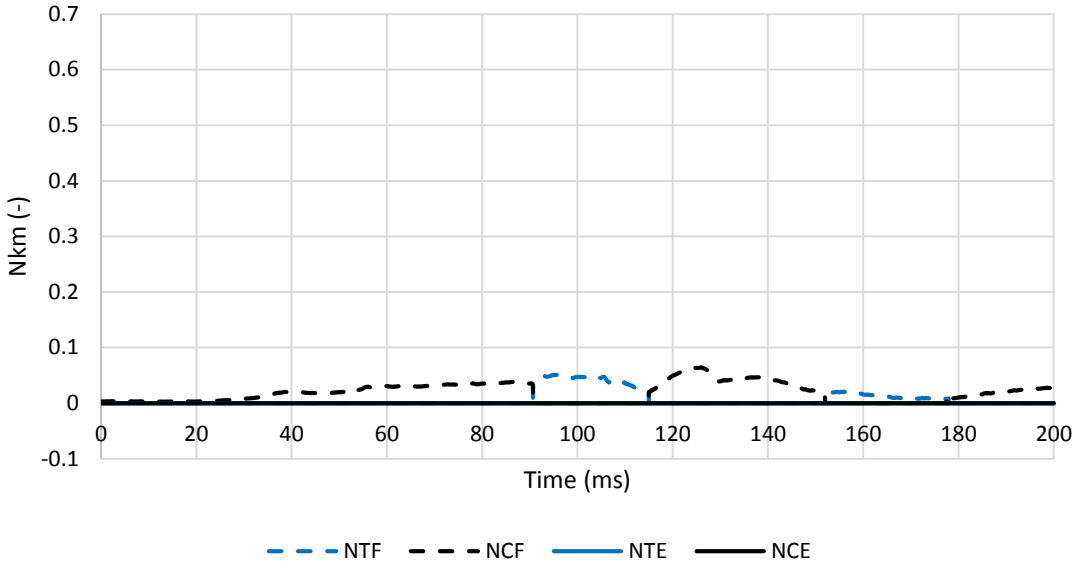


APPENDIX 184 LOADING GRAPHS OF FEA BIO RID CONFIGURATION L112 – NKM

### A.6.2.2. Medium Severity Pulse (IIWPG 16 km/h) M112

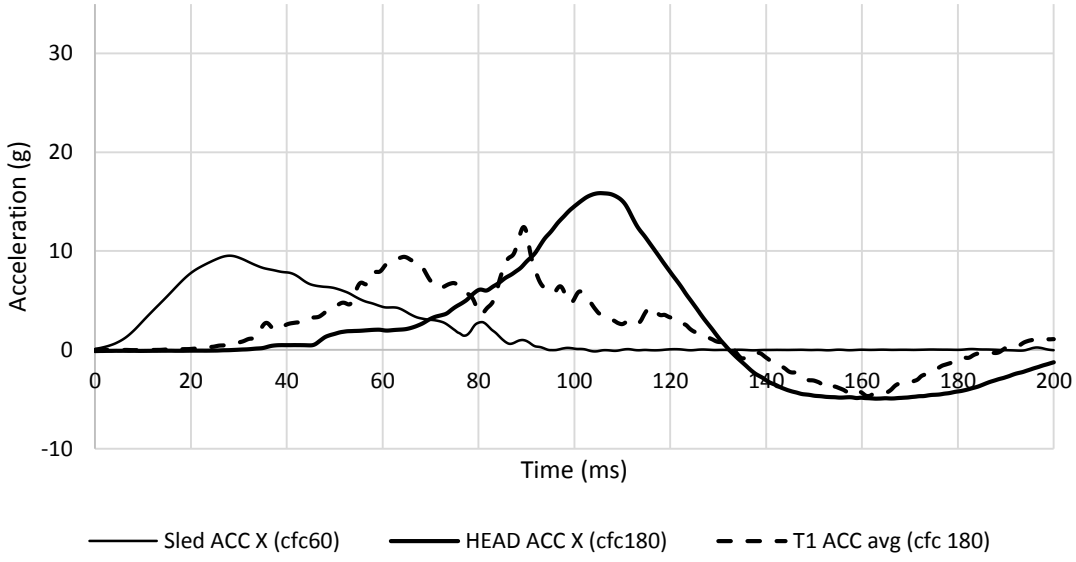


APPENDIX 185 LOADING GRAPHS OF FEA BIO RID CONFIGURATION M112 - ACCELERATION

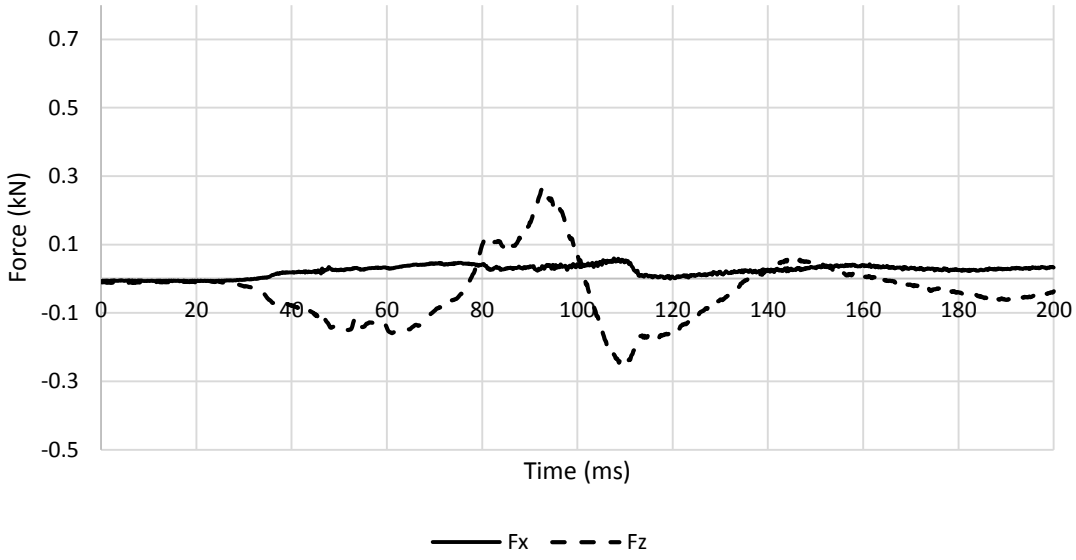


APPENDIX 186 LOADING GRAPHS OF FEA BIO RID CONFIGURATION M112 – FORCE

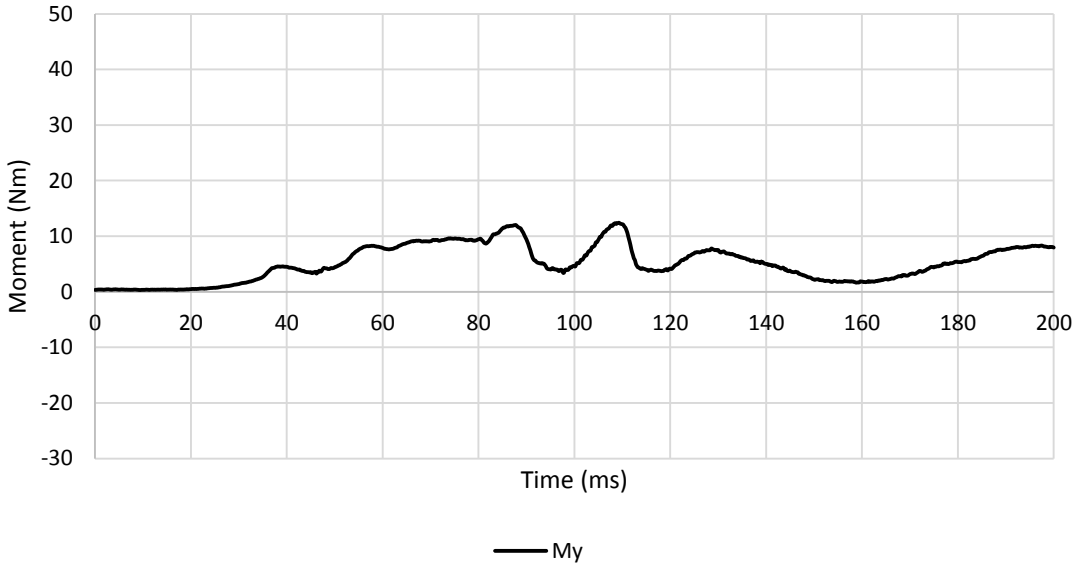


APPENDIX 187 LOADING GRAPHS OF FEA BIO RID CONFIGURATION - M112

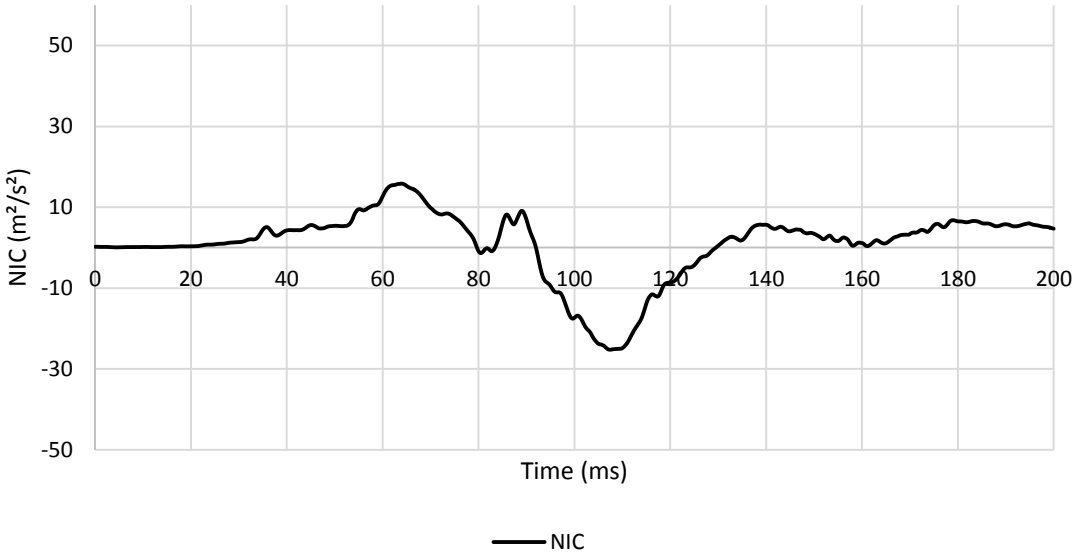


APPENDIX 188 LOADING GRAPHS OF FEA BIO RID CONFIGURATION M112 – NIC

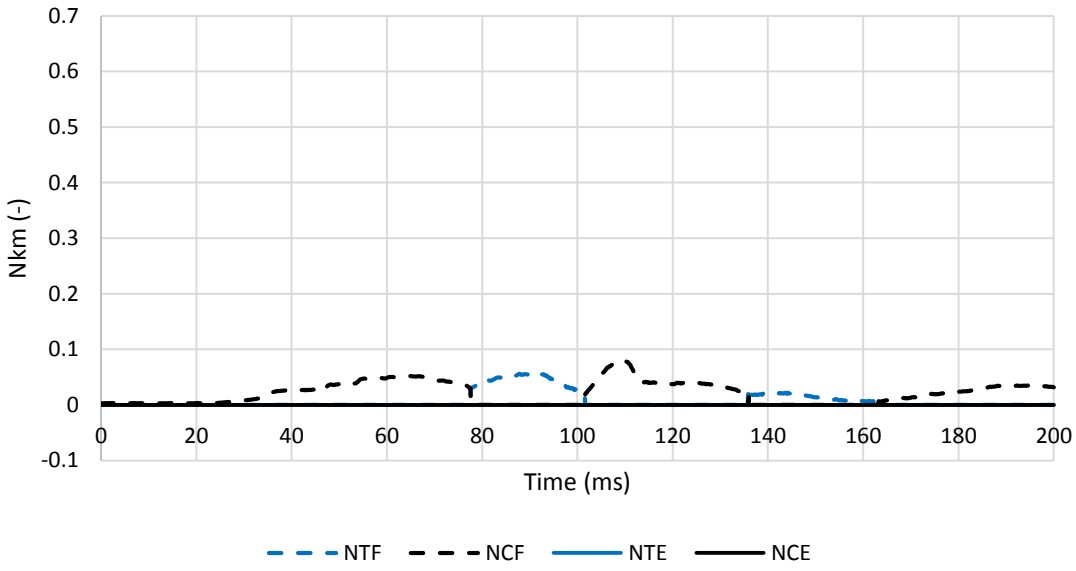


APPENDIX 189 LOADING GRAPHS OF FEA BIO RID CONFIGURATION M112 – NKM

## A.6.2.3. High Severity Pulse (SRA 24 km/h) H112

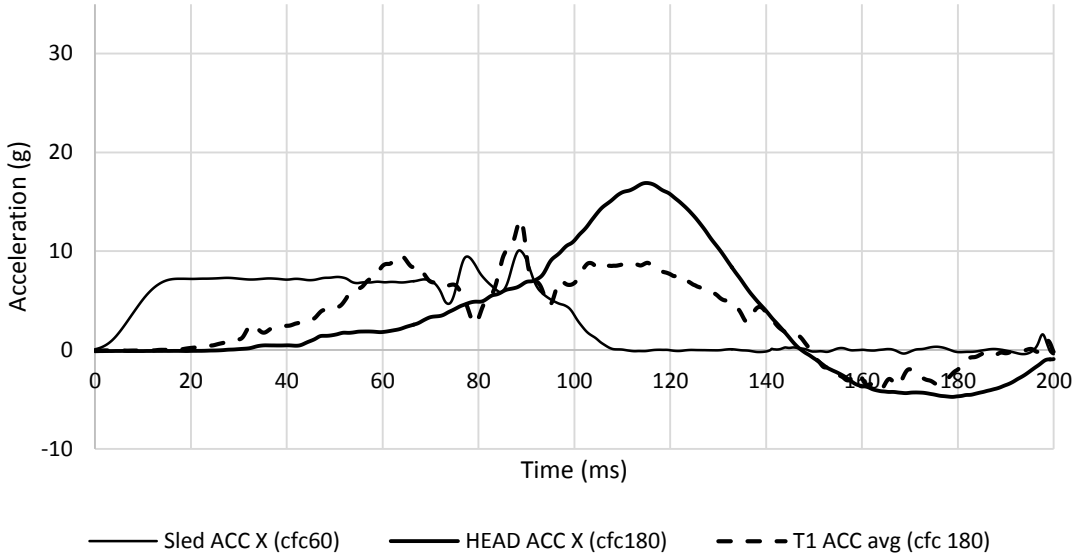


APPENDIX 190 LOADING GRAPHS OF FEA BIO RID CONFIGURATION H112 – ACCELERATION

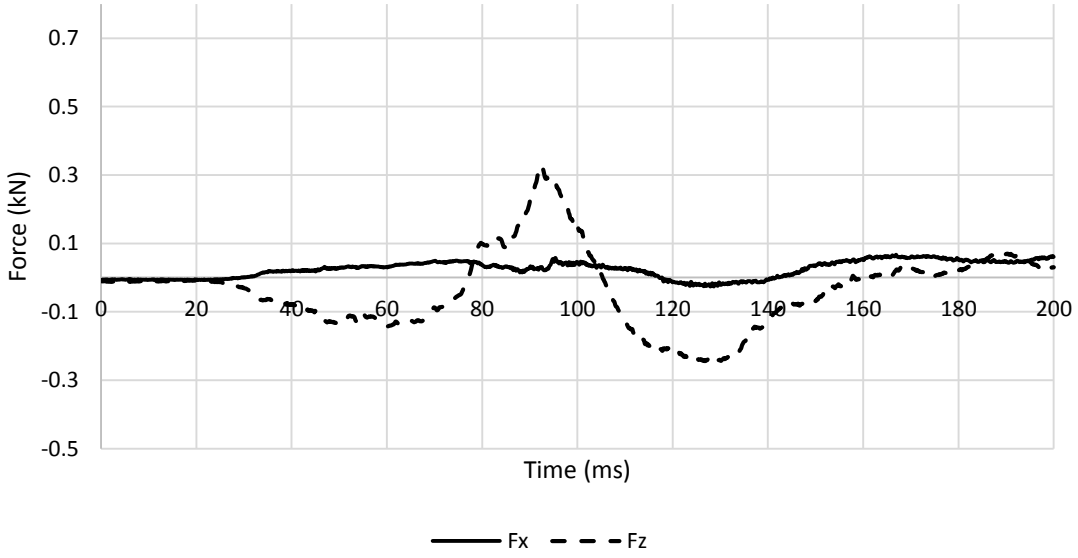


APPENDIX 191 LOADING GRAPHS OF FEA BIO RID CONFIGURATION H112 - FORCE

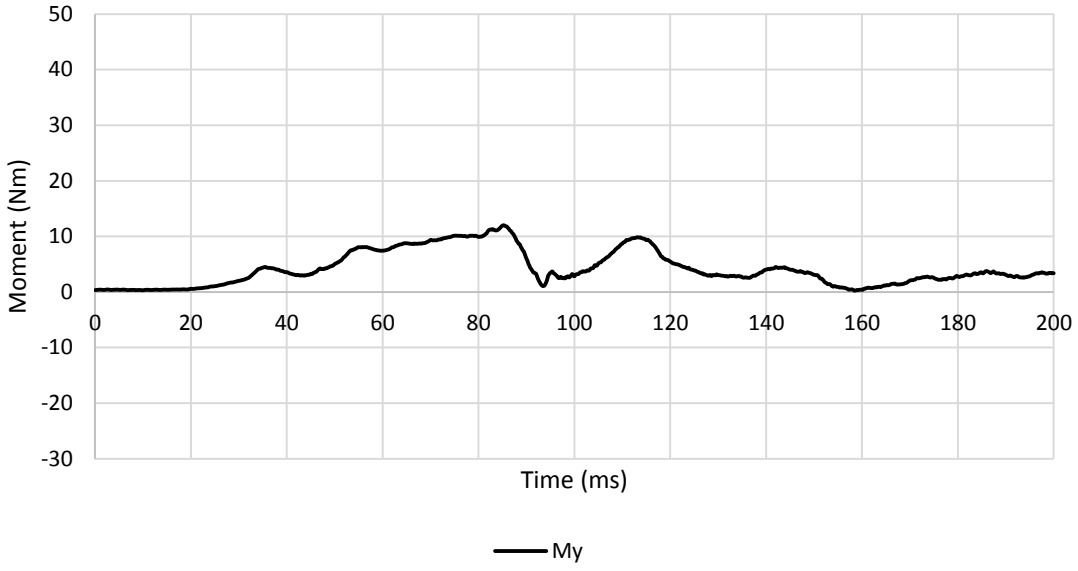


APPENDIX 192 LOADING GRAPHS OF FEA BIO RID CONFIGURATION H112 - MOMENT

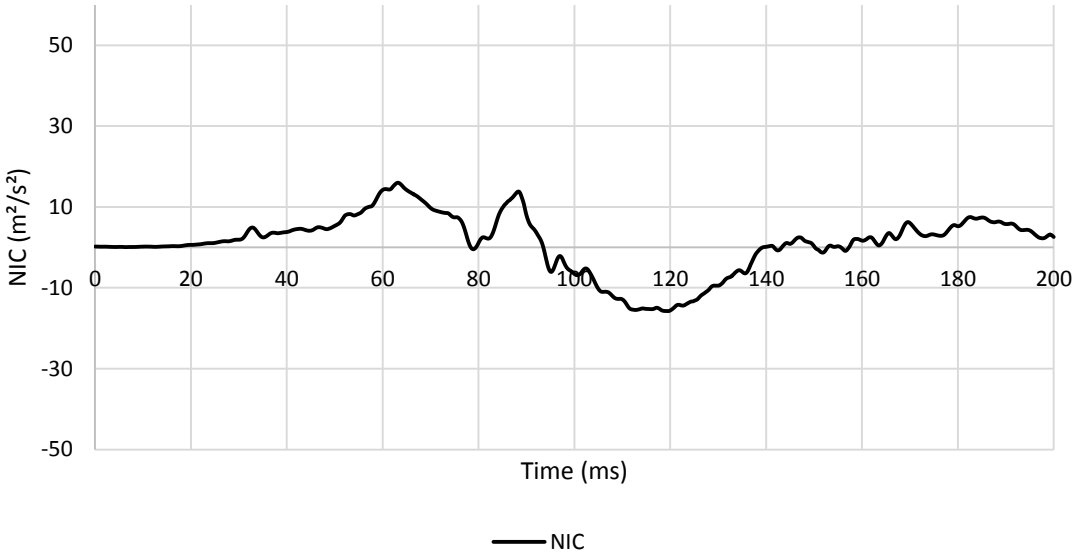


APPENDIX 193 LOADING GRAPHS OF FEA BIO RID CONFIGURATION H112 NIC

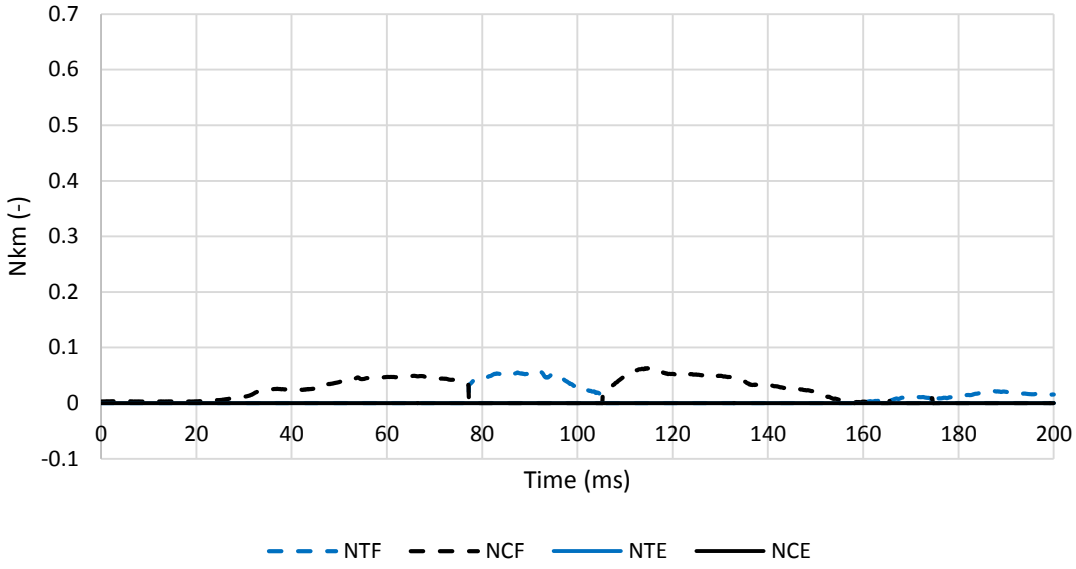


APPENDIX 194 LOADING GRAPHS OF FEA BIO RID CONFIGURATION H112 - NKM

## A.6.3. Bio RID II – forward backrest – low head restraint 113

### A.6.3.1. Low Severity Pulse (SRA 16 km/h) L113

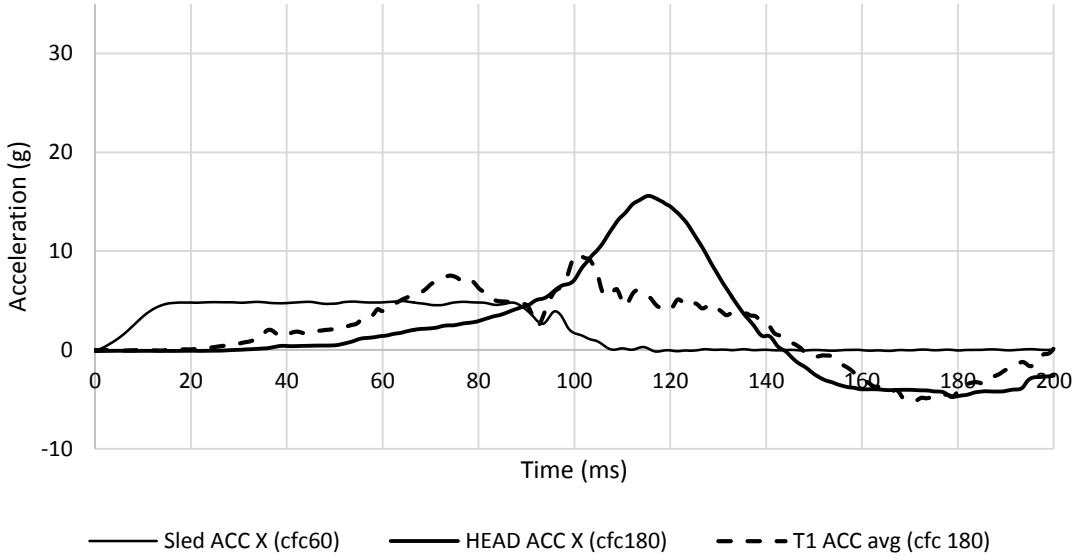


APPENDIX 195 LOADING GRAPHS OF FEA BIO RID CONFIGURATION L113 - ACCELERATION

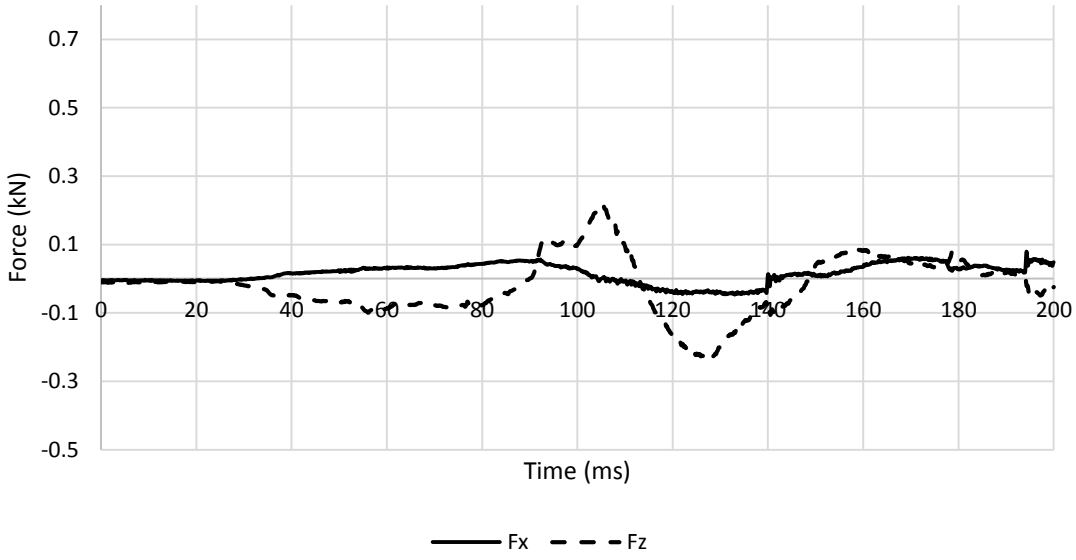


APPENDIX 196 LOADING GRAPHS OF FEA BIO RID CONFIGURATION L113 - FORCE

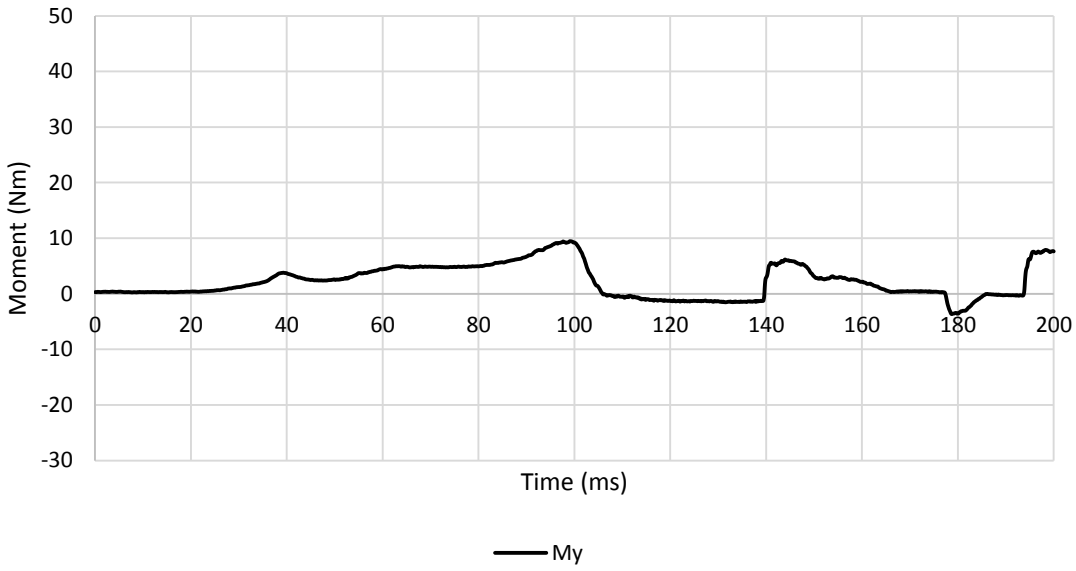


APPENDIX 197 LOADING GRAPHS OF FEA BIO RID CONFIGURATION L113 - MOMENT

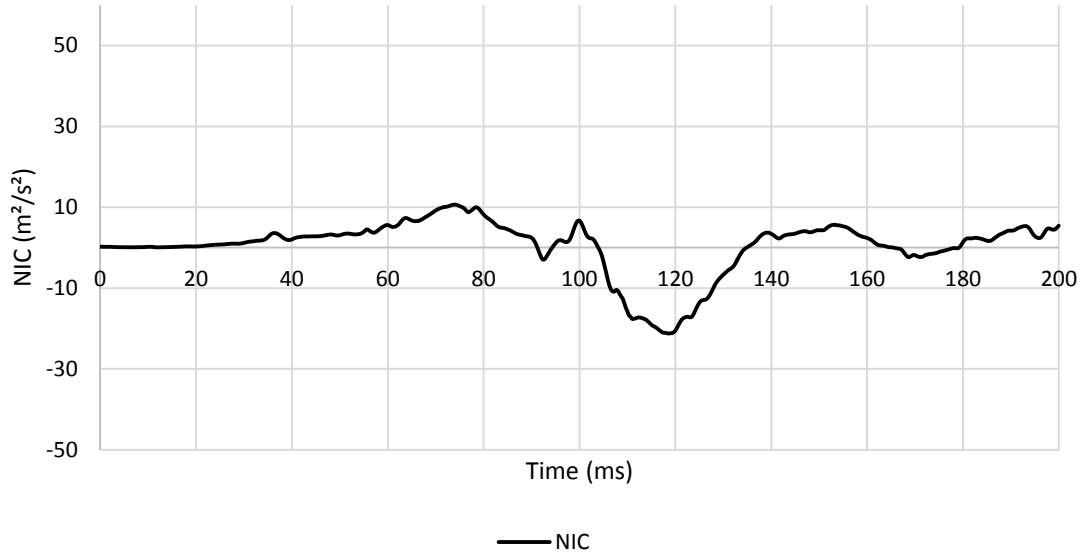


APPENDIX 198 LOADING GRAPHS OF FEA BIO RID CONFIGURATION L113 - NIC

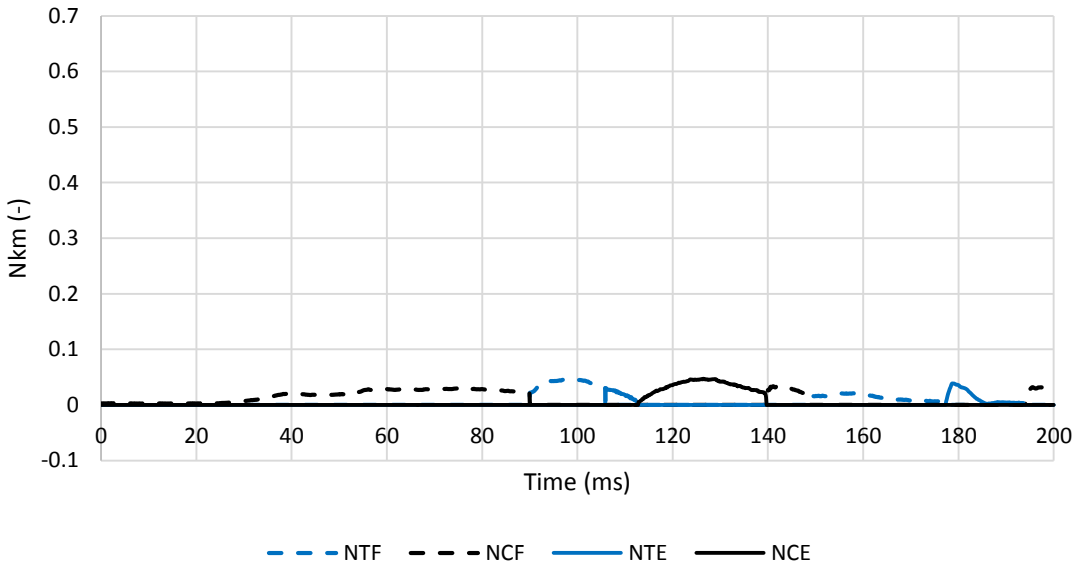


APPENDIX 199 LOADING GRAPHS OF FEA BIO RID CONFIGURATION L113 - NKM

## A.6.3.2. Medium Severity Pulse (IIWPG 16 km/h) M113

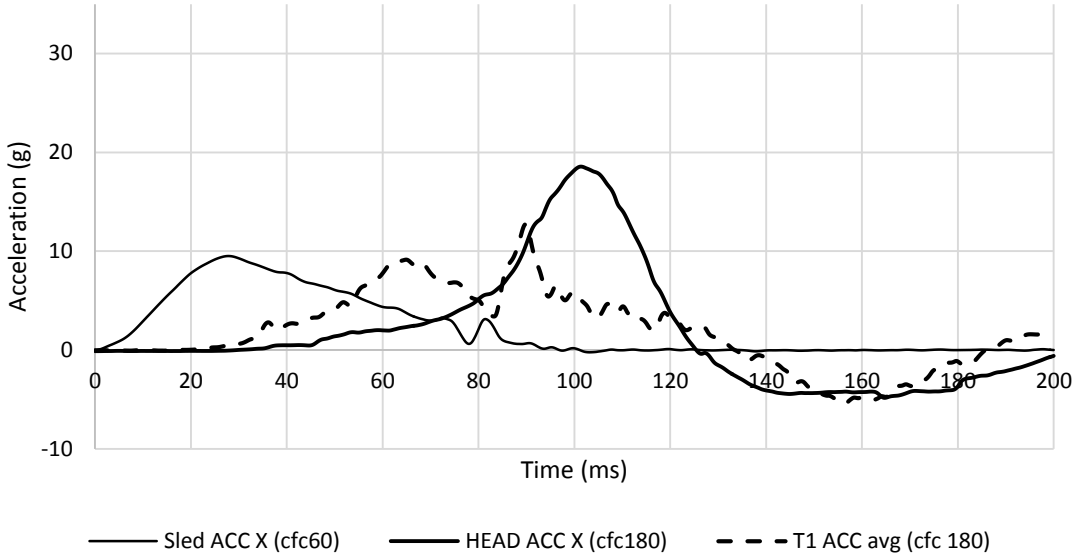


APPENDIX 200 LOADING GRAPHS OF FEA BIO RID CONFIGURATION M113 - ACCELERATION

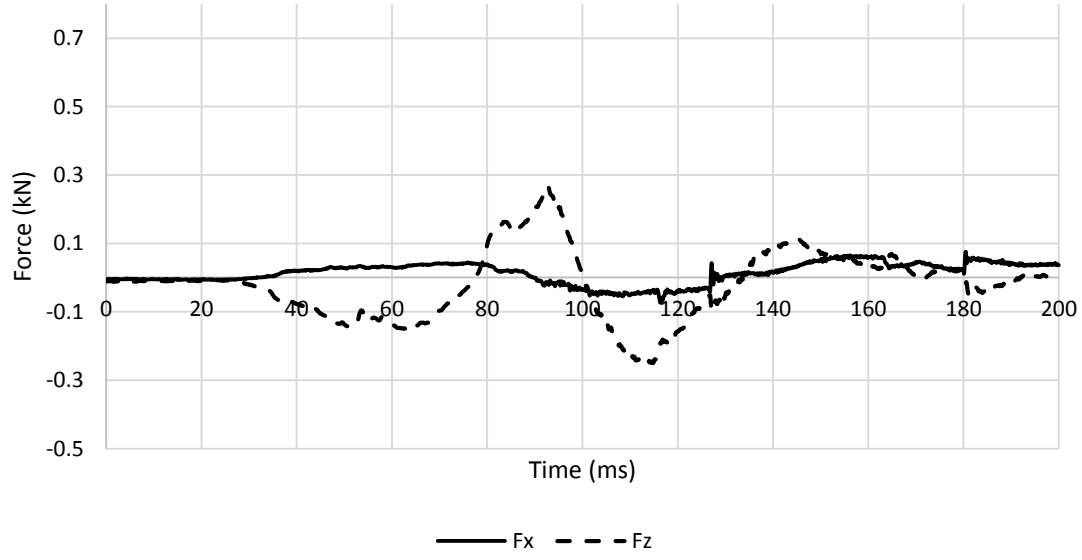


APPENDIX 201 LOADING GRAPHS OF FEA BIO RID CONFIGURATION M113 - FORCE

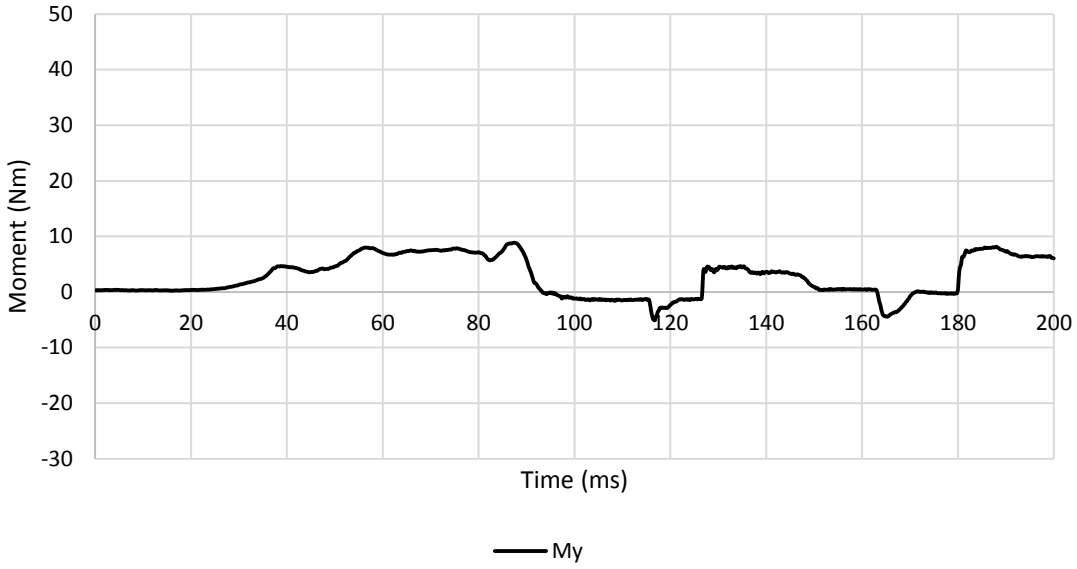


APPENDIX 202 LOADING GRAPHS OF FEA BIO RID CONFIGURATION M113 - MOMENT

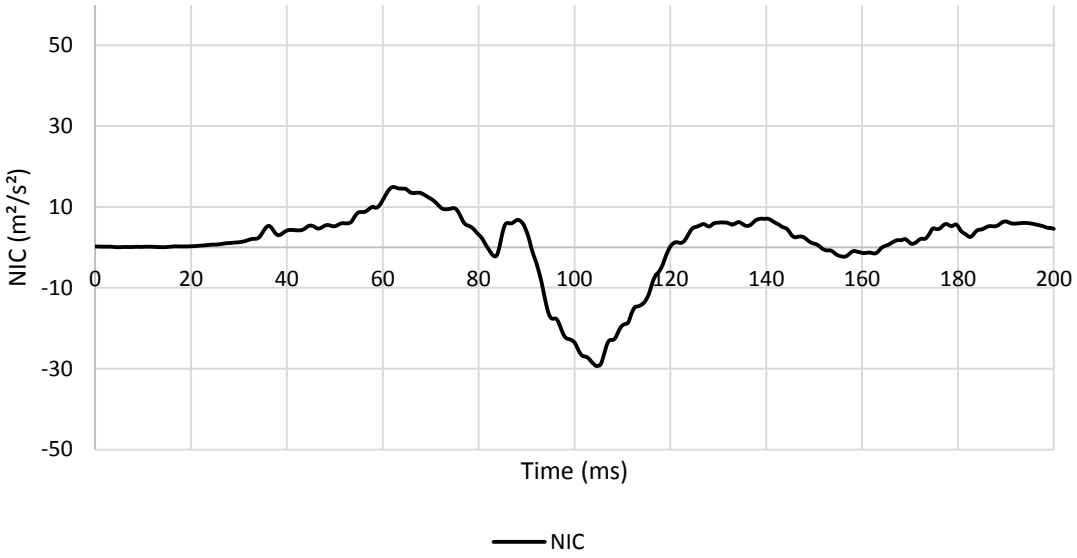


APPENDIX 203 LOADING GRAPHS OF FEA BIO RID CONFIGURATION M113 - NIC

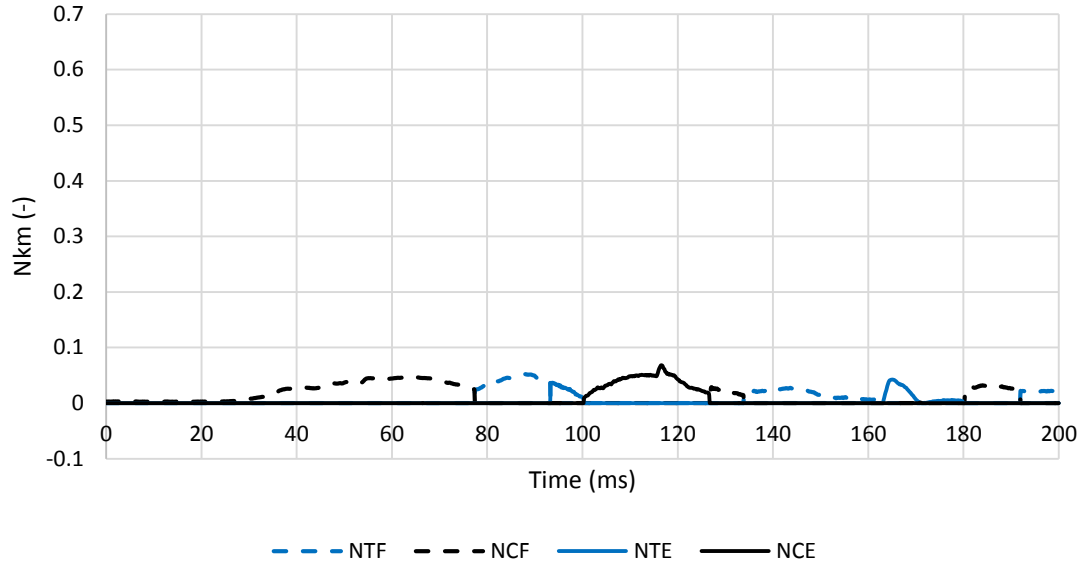


APPENDIX 204 LOADING GRAPHS OF FEA BIO RID CONFIGURATION M113 - NKM

### A.6.3.3. High Severity Pulse (SRA 24 km/h) H113

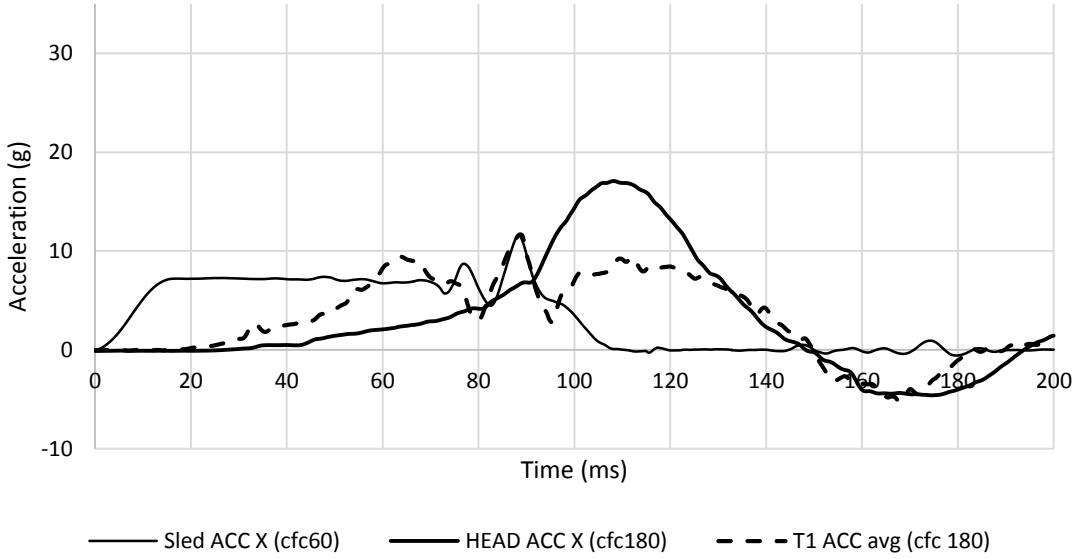


APPENDIX 205 LOADING GRAPHS OF FEA BIO RID CONFIGURATION H113 - ACCELERATION

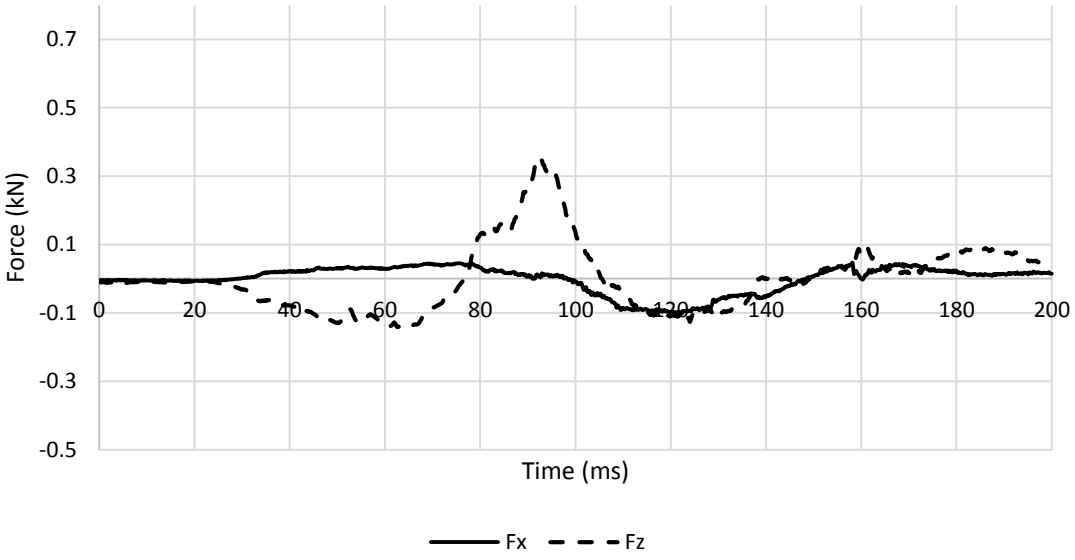


APPENDIX 206 LOADING GRAPHS OF FEA BIO RID CONFIGURATION H113 - FORCE

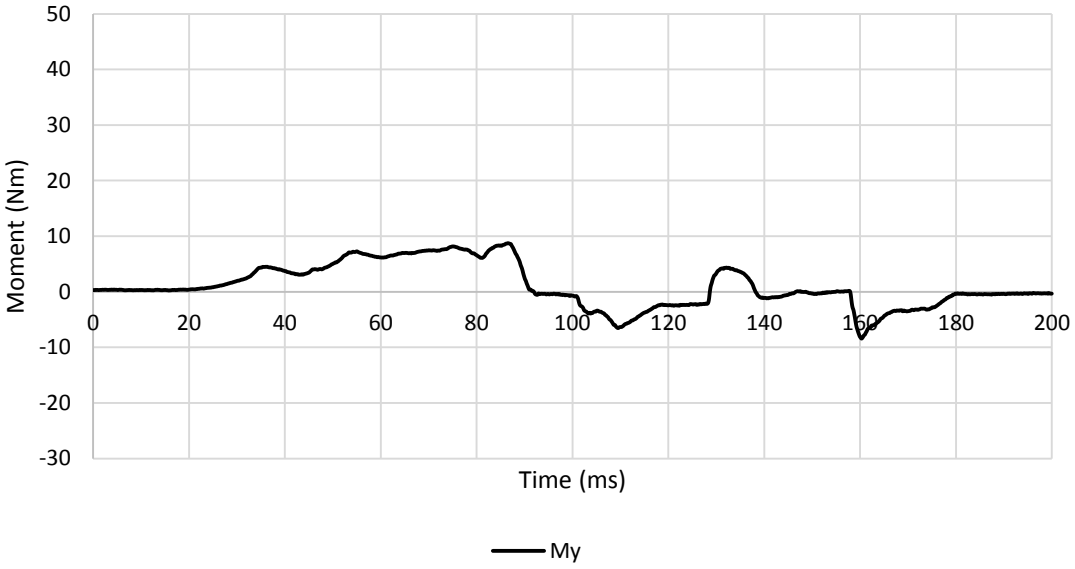


APPENDIX 207 LOADING GRAPHS OF FEA BIO RID CONFIGURATION H113 - MOMENT

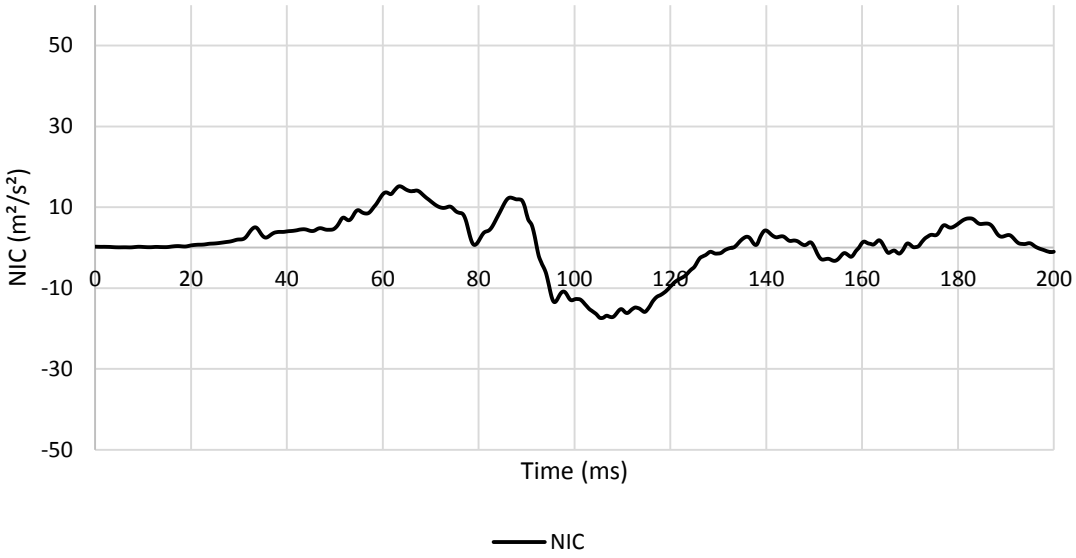


APPENDIX 208 LOADING GRAPHS OF FEA BIO RID CONFIGURATION H113 - NIC

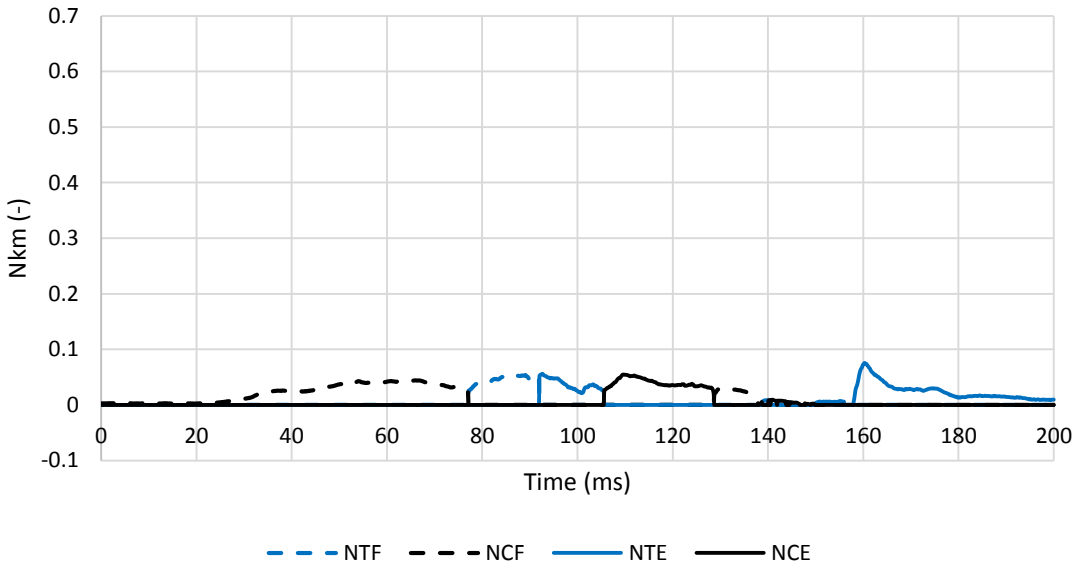


APPENDIX 209 LOADING GRAPHS OF FEA BIO RID CONFIGURATION H113 – NKM

## A.6.4. Bio RID II – centred backrest – high head restraint 121

### A.6.4.1. Low Severity Pulse (SRA 16 km/h) L121

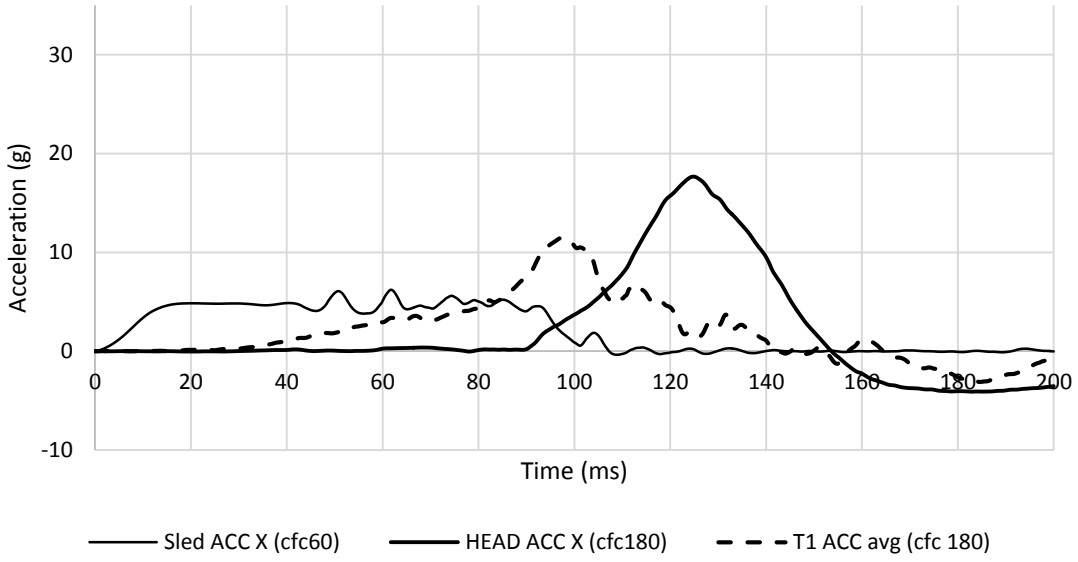


APPENDIX 210 LOADING GRAPHS OF FEA BIO RID CONFIGURATION L121 - ACCELERATION

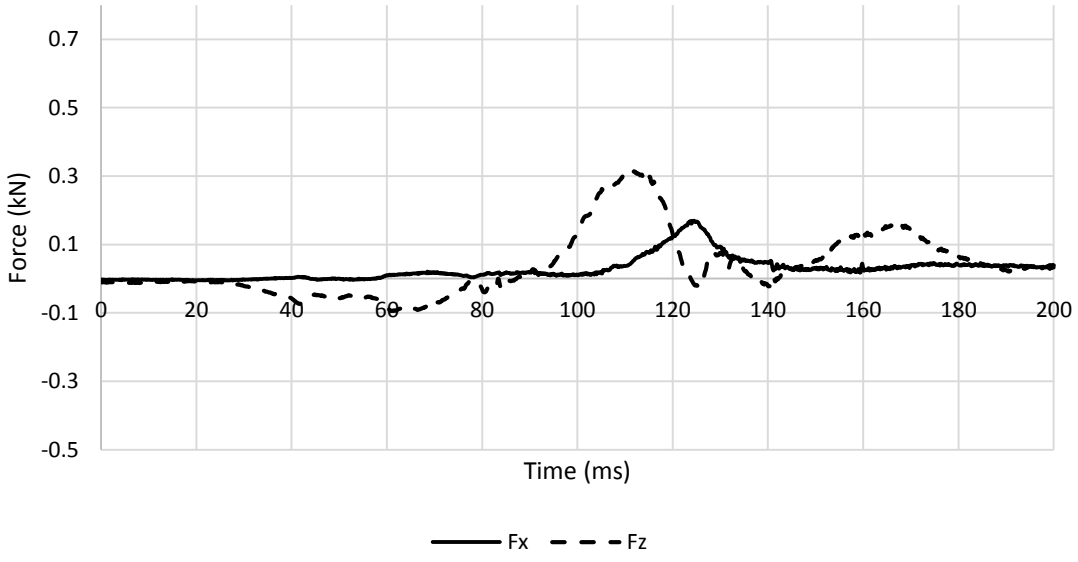


APPENDIX 211 LOADING GRAPHS OF FEA BIO RID CONFIGURATION L121 - FORCE

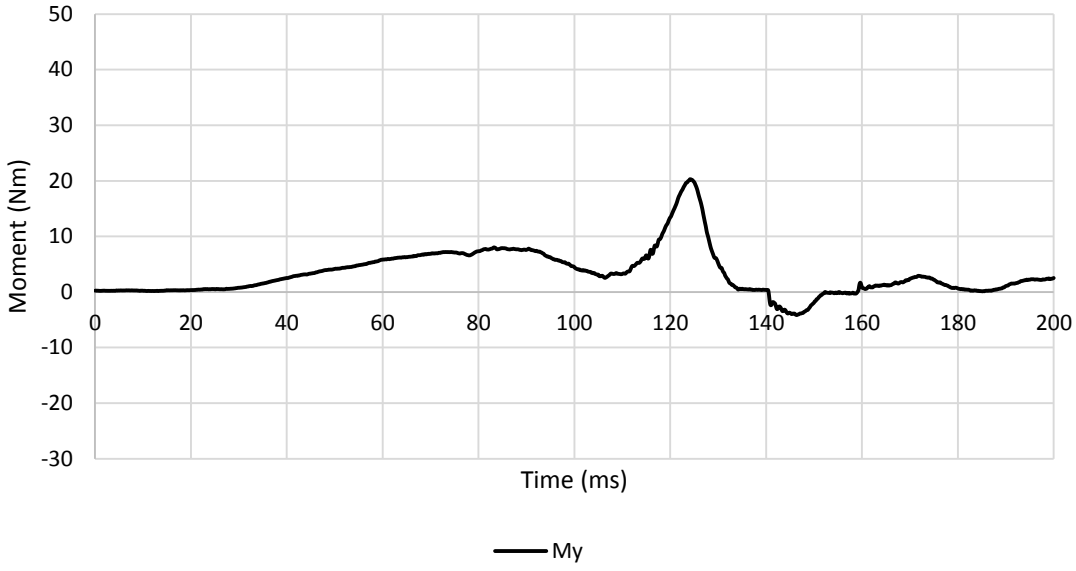


APPENDIX 212 LOADING GRAPHS OF FEA BIO RID CONFIGURATION L121 - MOMENT

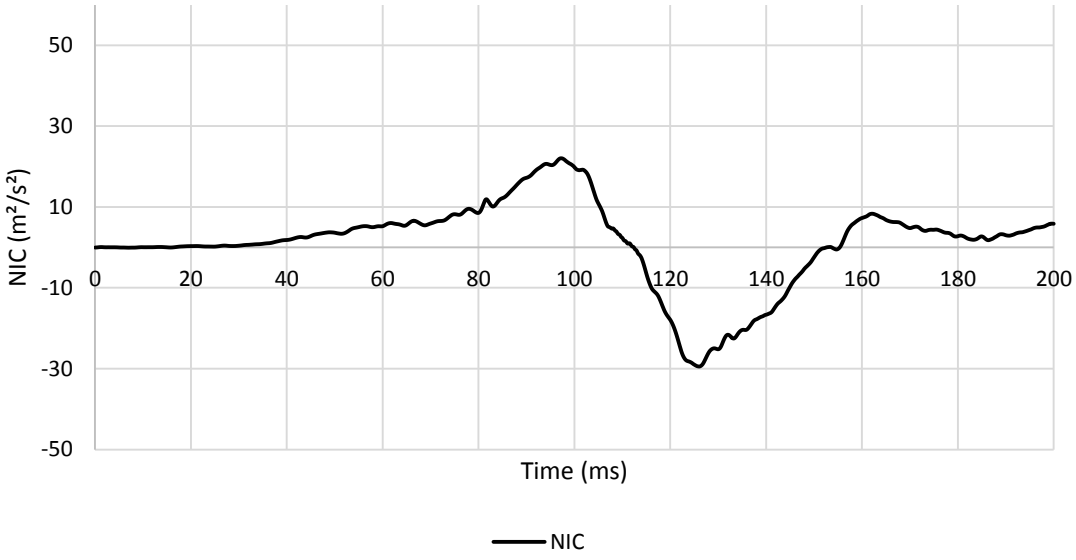


APPENDIX 213 LOADING GRAPHS OF FEA BIO RID CONFIGURATION L121 - NIC

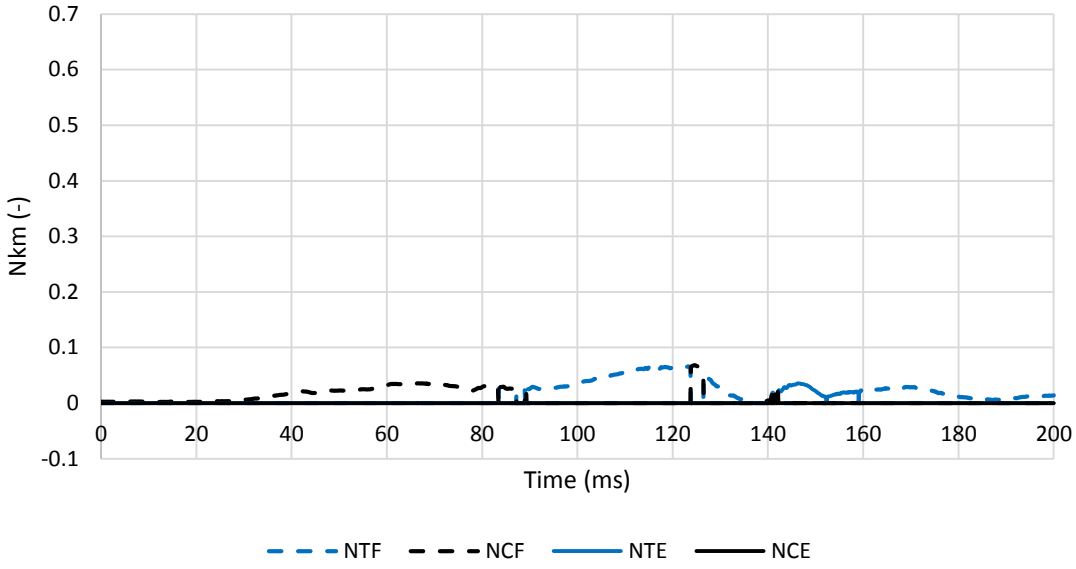


APPENDIX 214 LOADING GRAPHS OF FEA BIO RID CONFIGURATION L121 - NKM

### A.6.4.2. Medium Severity Pulse (IIWPG 16 km/h) M121

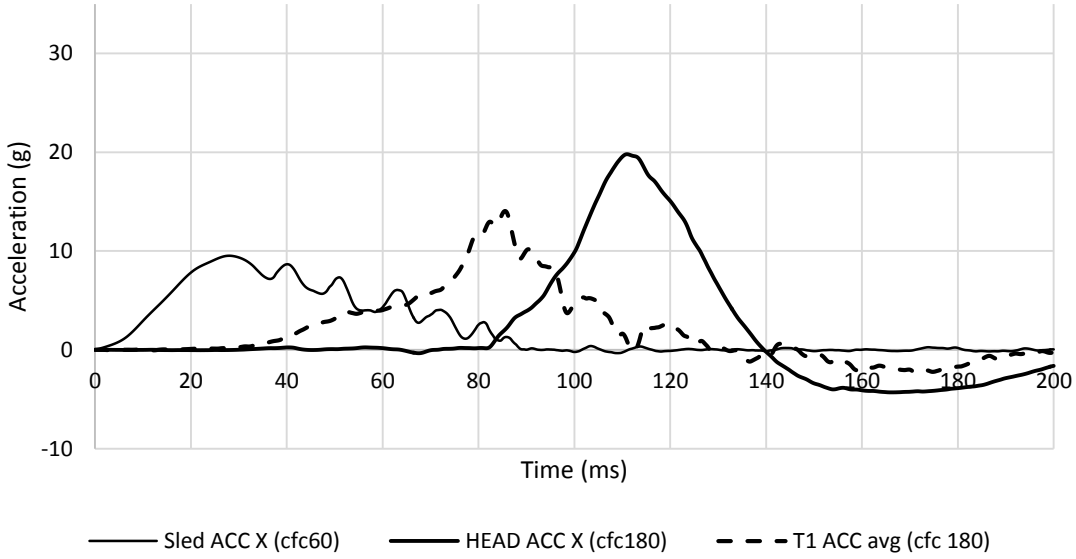


APPENDIX 215 LOADING GRAPHS OF FEA BIO RID CONFIGURATION M121 - ACCELERATION

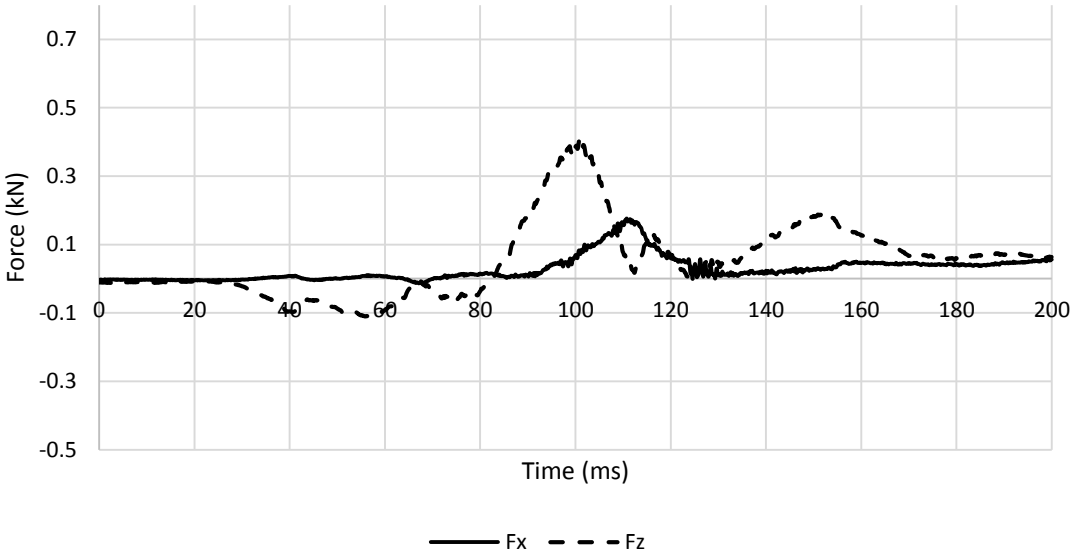


APPENDIX 216 LOADING GRAPHS OF FEA BIO RID CONFIGURATION M121 - FORCE

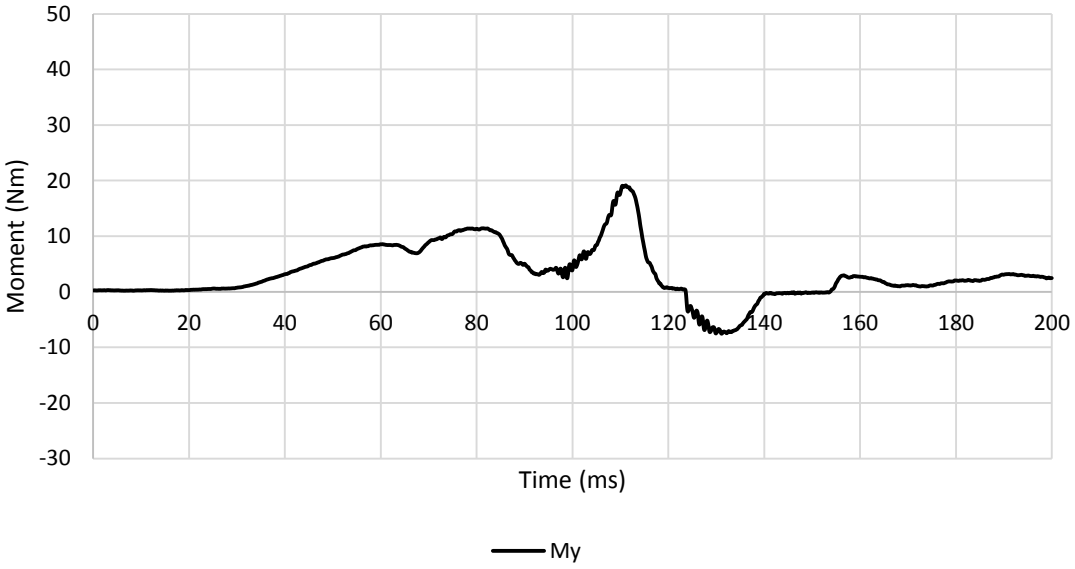


APPENDIX 217 LOADING GRAPHS OF FEA BIO RID CONFIGURATION M121 - MOMENT

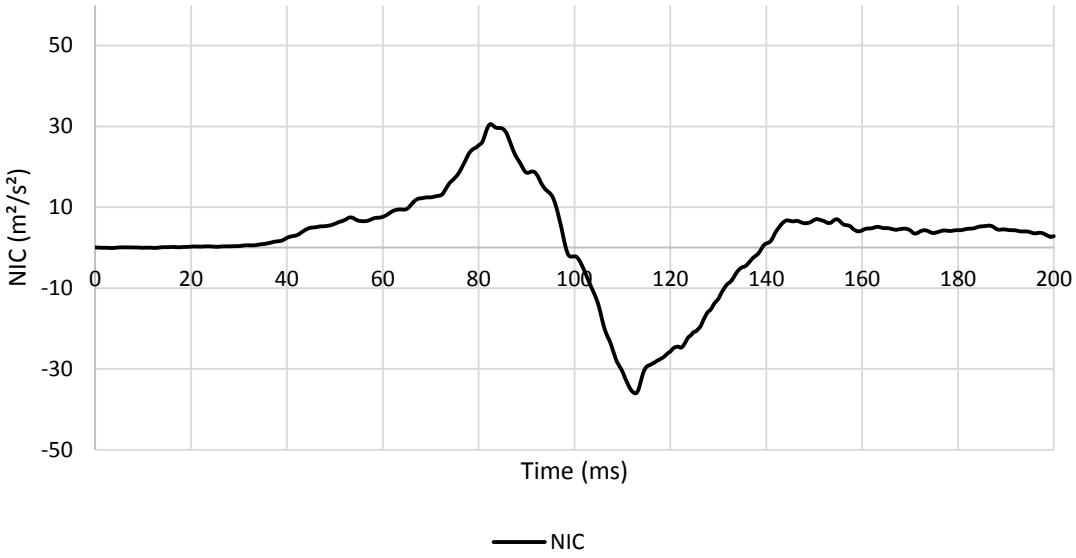


APPENDIX 218 LOADING GRAPHS OF FEA BIO RID CONFIGURATION M121 - NIC

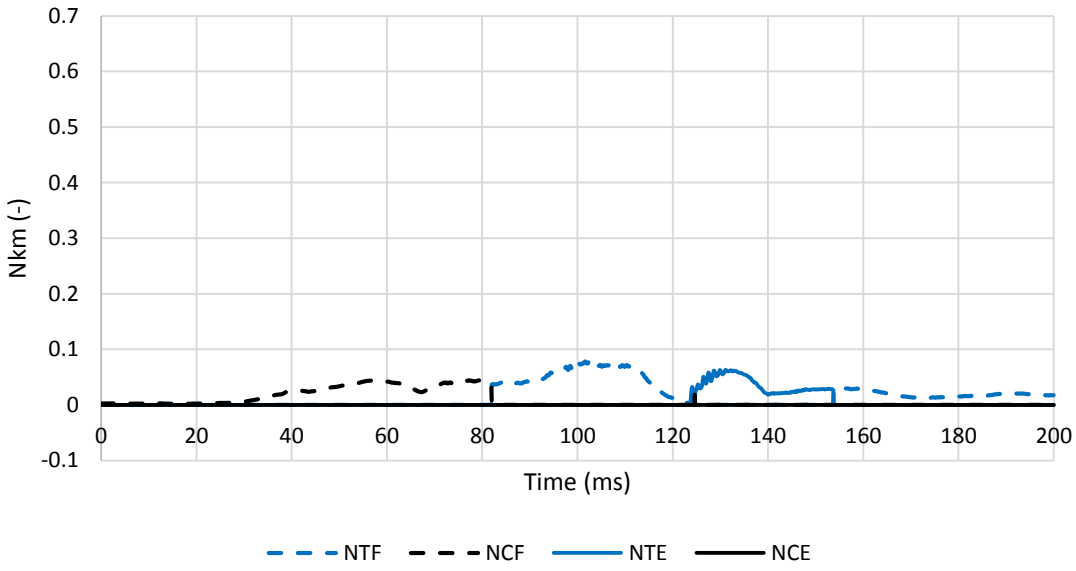


APPENDIX 219 LOADING GRAPHS OF FEA BIO RID CONFIGURATION M121 - NKM

## A.6.4.3. High Severity Pulse (SRA 24 km/h) H121

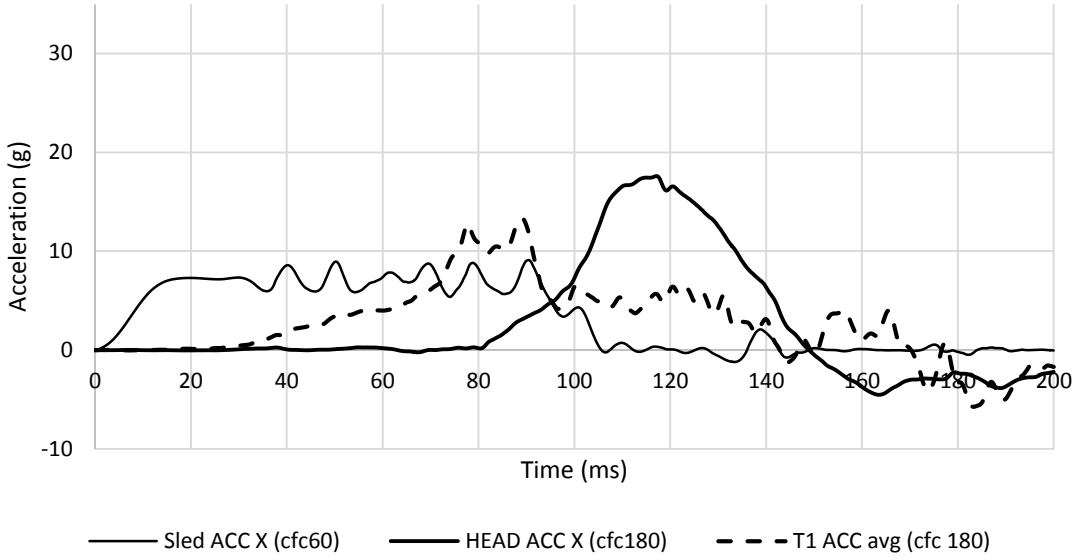


APPENDIX 220 LOADING GRAPHS OF FEA BIO RID CONFIGURATION H121 – ACCELERATION

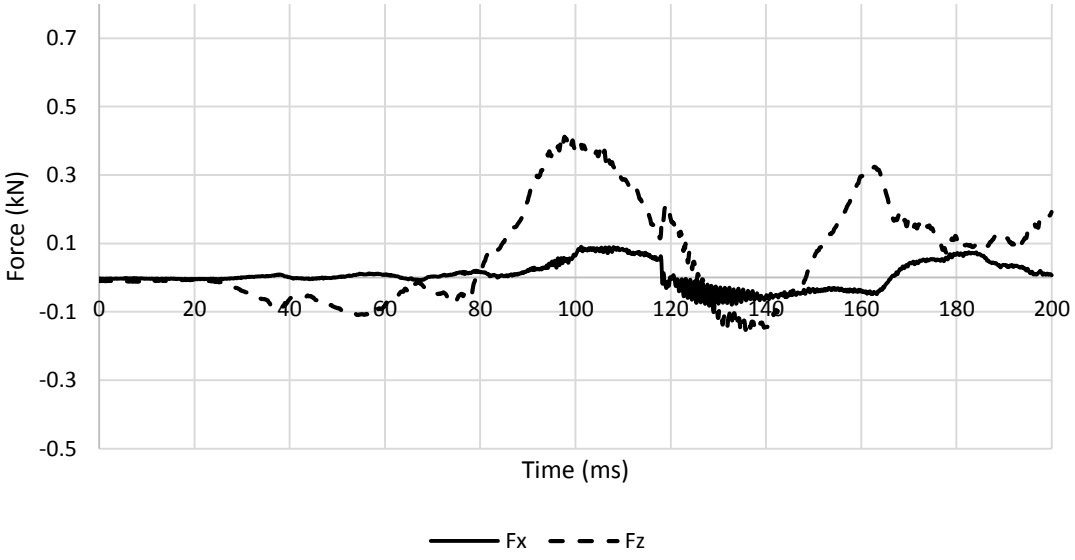


APPENDIX 221 LOADING GRAPHS OF FEA BIO RID CONFIGURATION H121 - FORCE

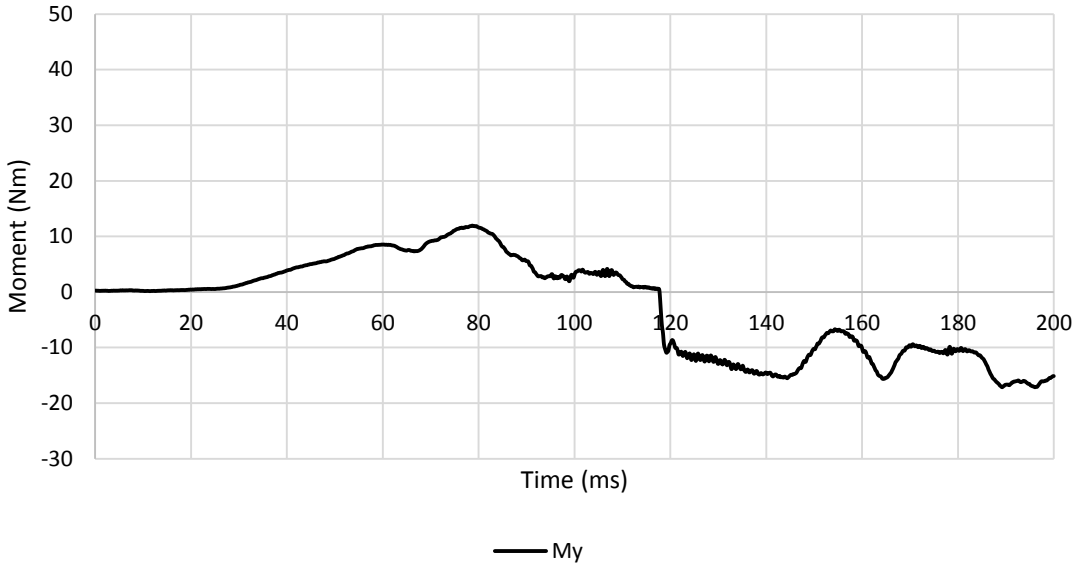


APPENDIX 222 LOADING GRAPHS OF FEA BIO RID CONFIGURATION H121 - MOMENT

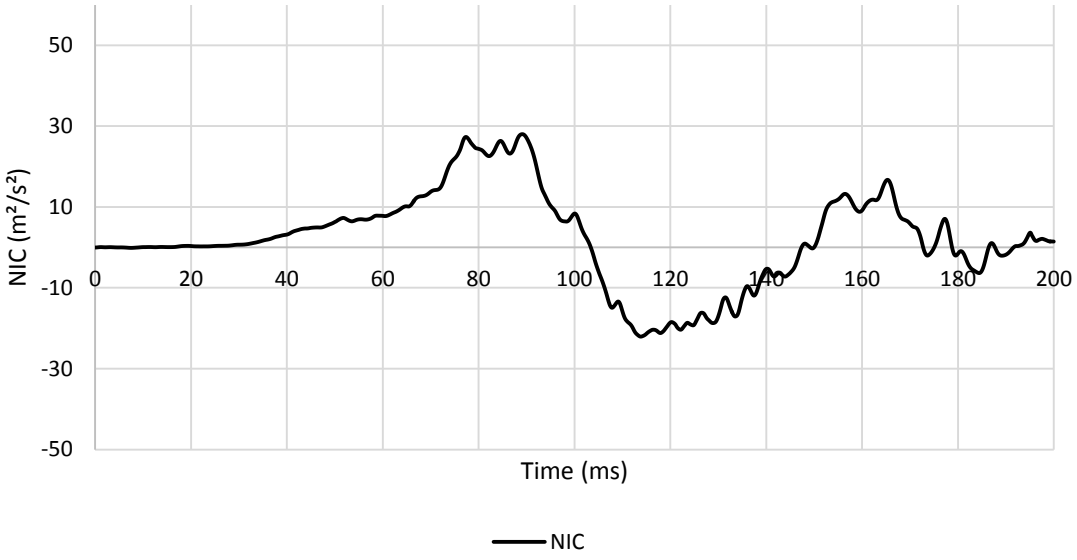


APPENDIX 223 LOADING GRAPHS OF FEA BIO RID CONFIGURATION H121 - NIC

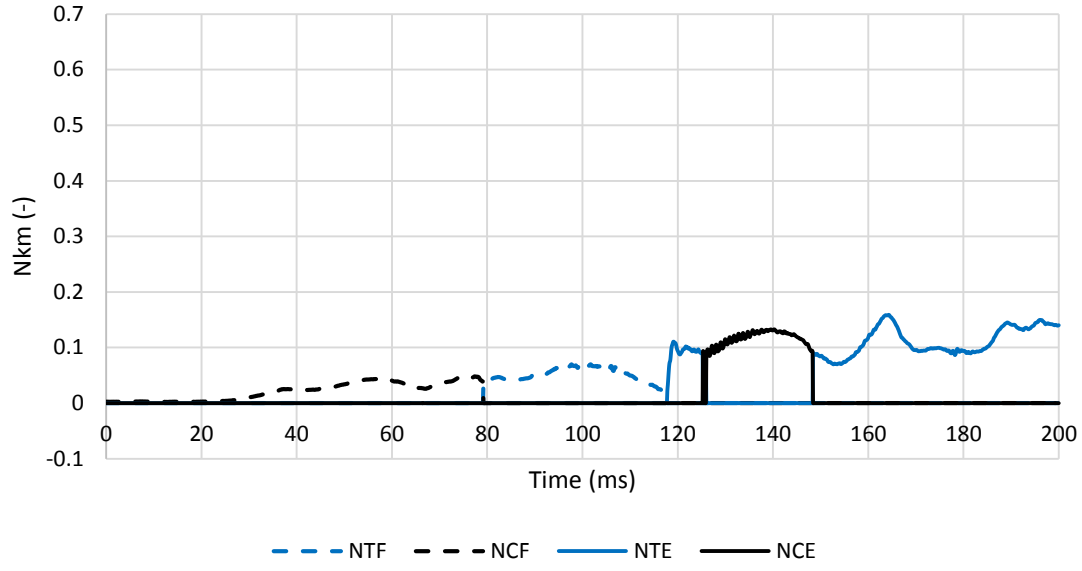


APPENDIX 224 LOADING GRAPHS OF FEA BIO RID CONFIGURATION H121 - NKM

## A.6.5. Bio RID II – centred backrest – middle head restraint 122

### A.6.5.1. Low Severity Pulse (SRA 16 km/h) L122

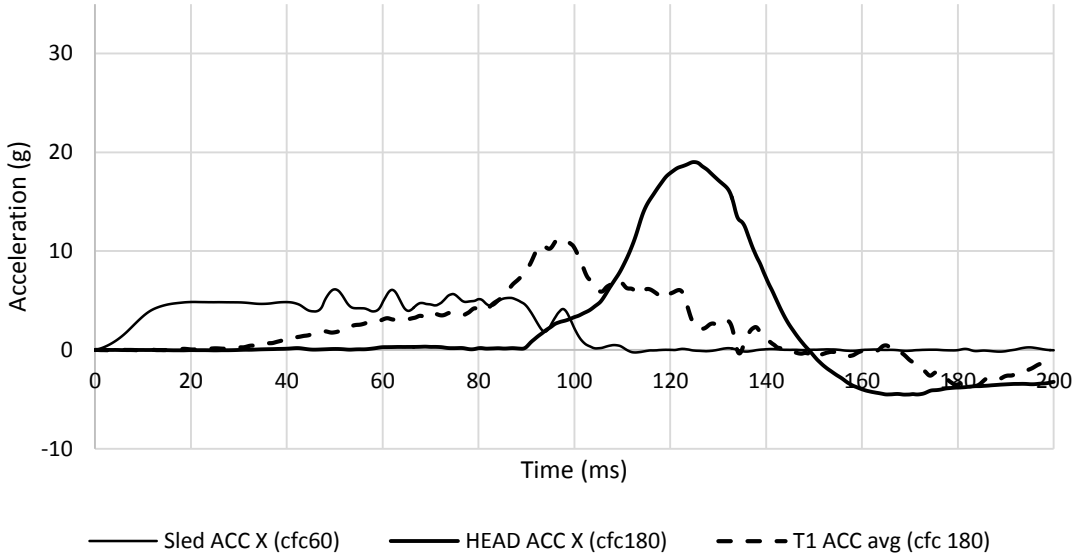


APPENDIX 225 LOADING GRAPHS OF FEA BIO RID CONFIGURATION L122 - ACCELERATION

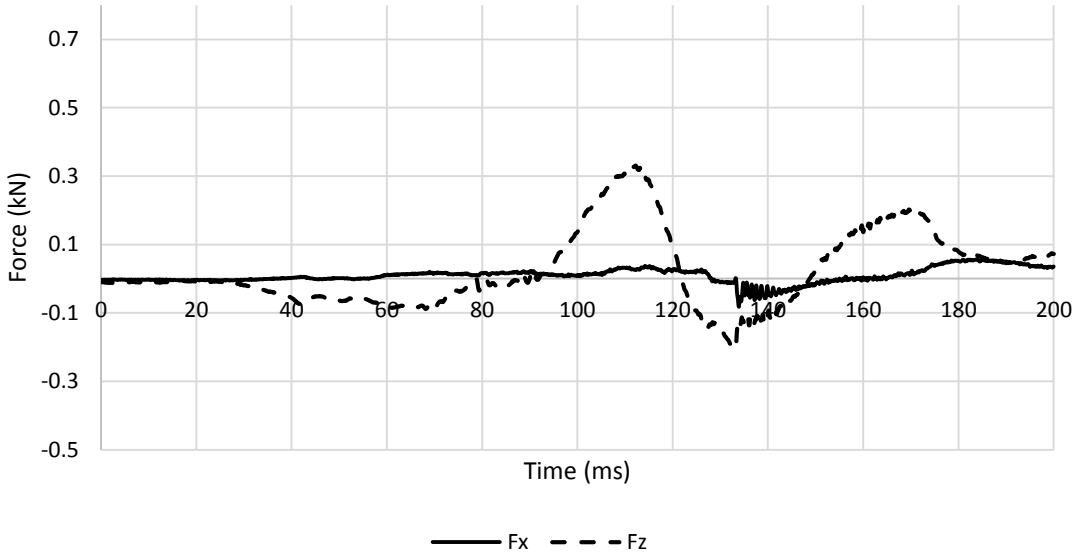


APPENDIX 226 LOADING GRAPHS OF FEA BIO RID CONFIGURATION L122 - FORCE

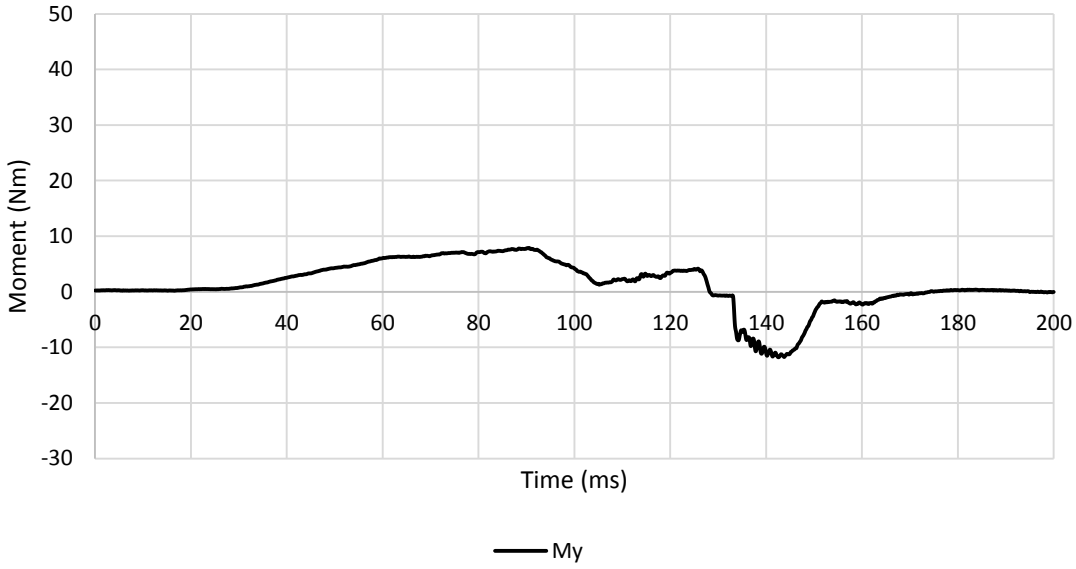


APPENDIX 227 LOADING GRAPHS OF FEA BIO RID CONFIGURATION L122 - MOMENT

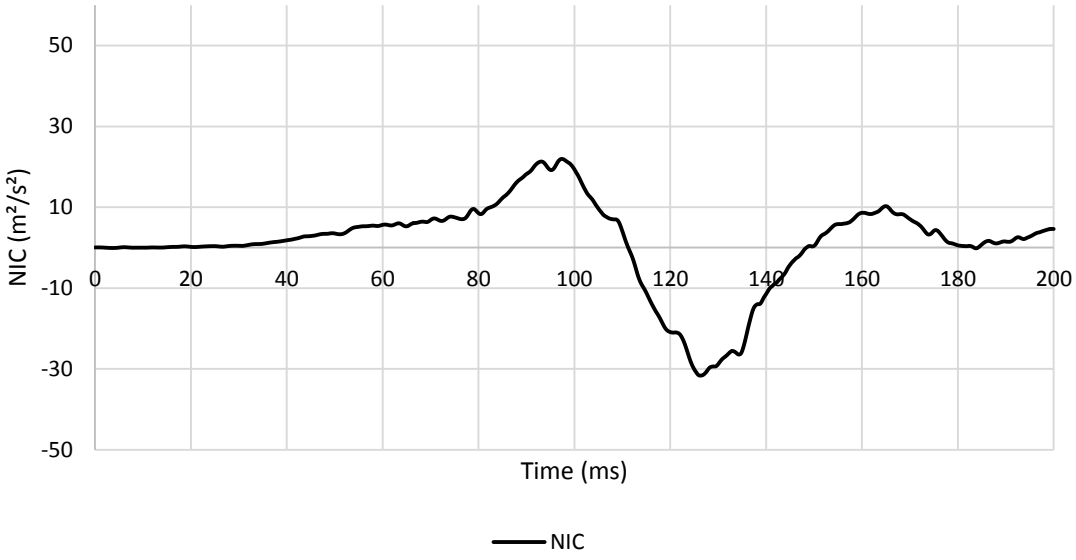


APPENDIX 228 LOADING GRAPHS OF FEA BIO RID CONFIGURATION L122 - NIC

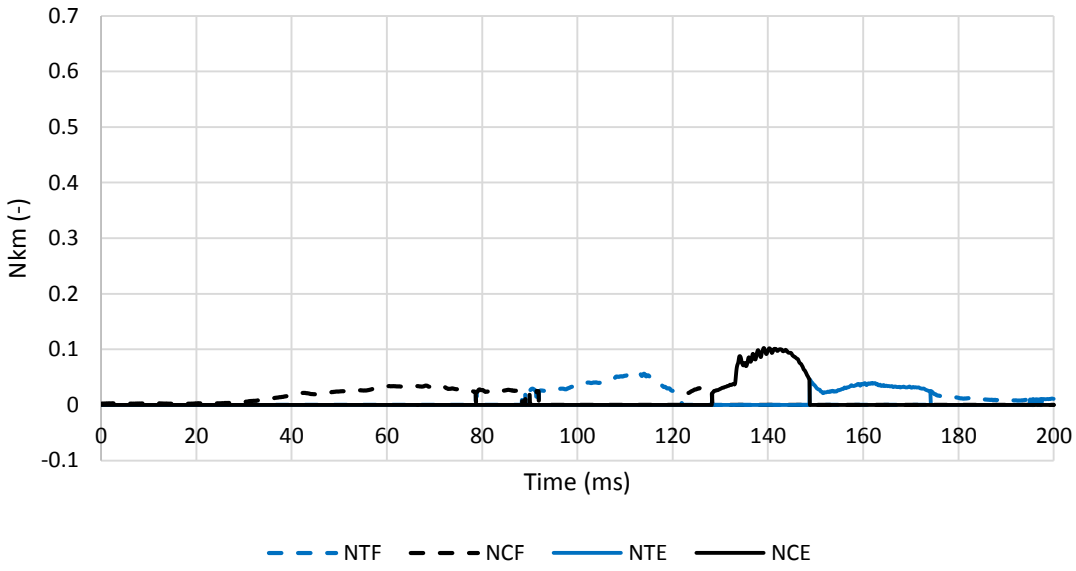


APPENDIX 229 LOADING GRAPHS OF FEA BIO RID CONFIGURATION L122 - NKM

A.6.5.2. Medium Severity Pulse (IIWPG 16 km/h) M122

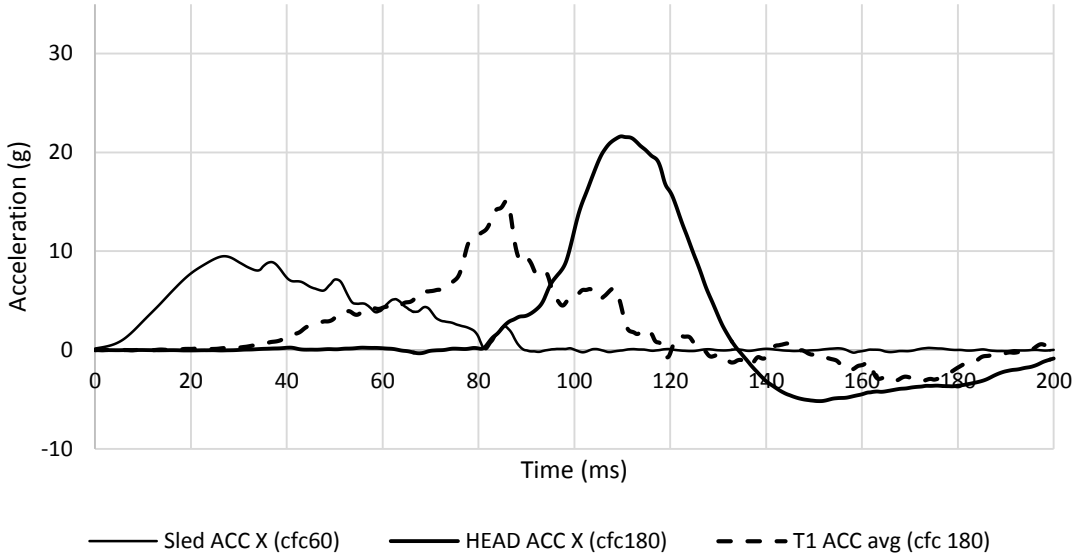


APPENDIX 230 LOADING GRAPHS OF FEA BIO RID CONFIGURATION M122 – ACCELERATION

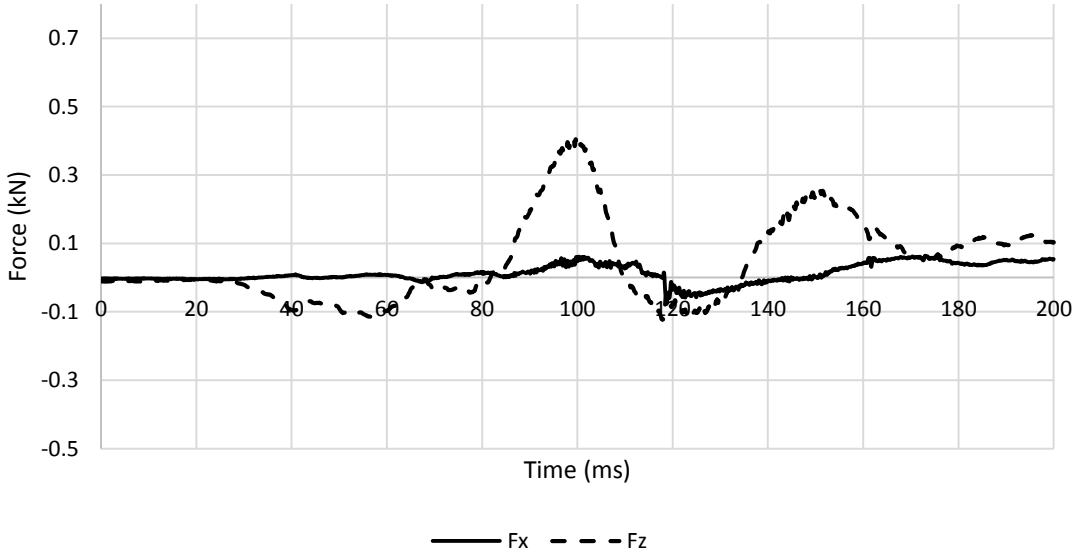


APPENDIX 231 LOADING GRAPHS OF FEA BIO RID CONFIGURATION M112 - FORCE

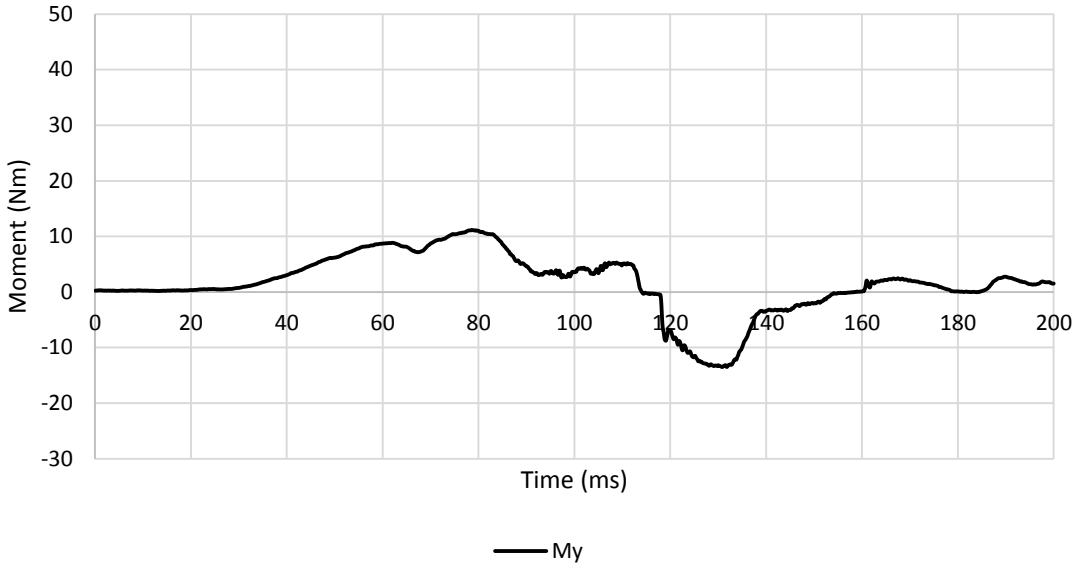


APPENDIX 232 LOADING GRAPHS OF FEA BIO RID CONFIGURATION M112 - MOMENT

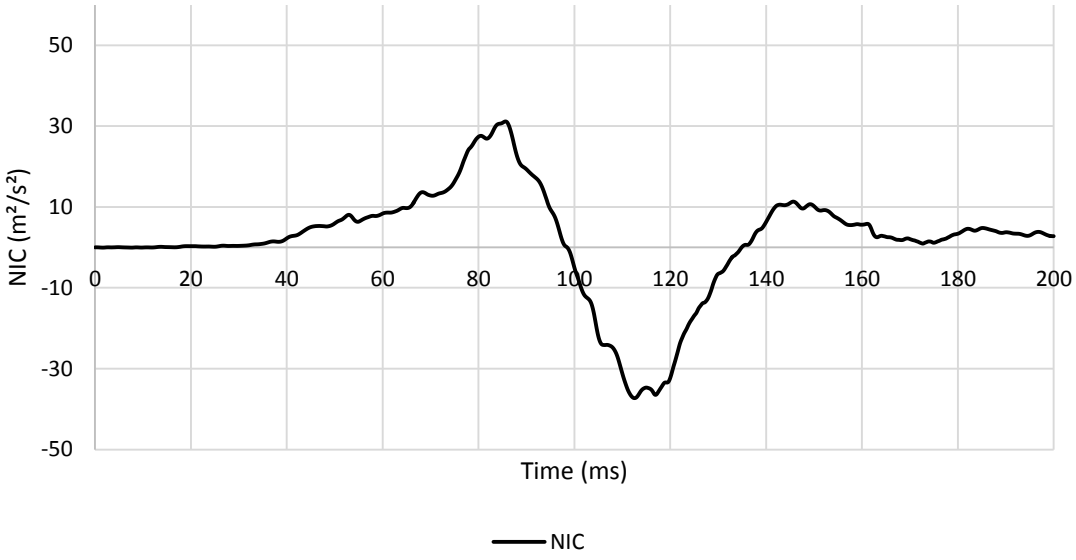


APPENDIX 233 LOADING GRAPHS OF FEA BIO RID CONFIGURATION M122 - NIC

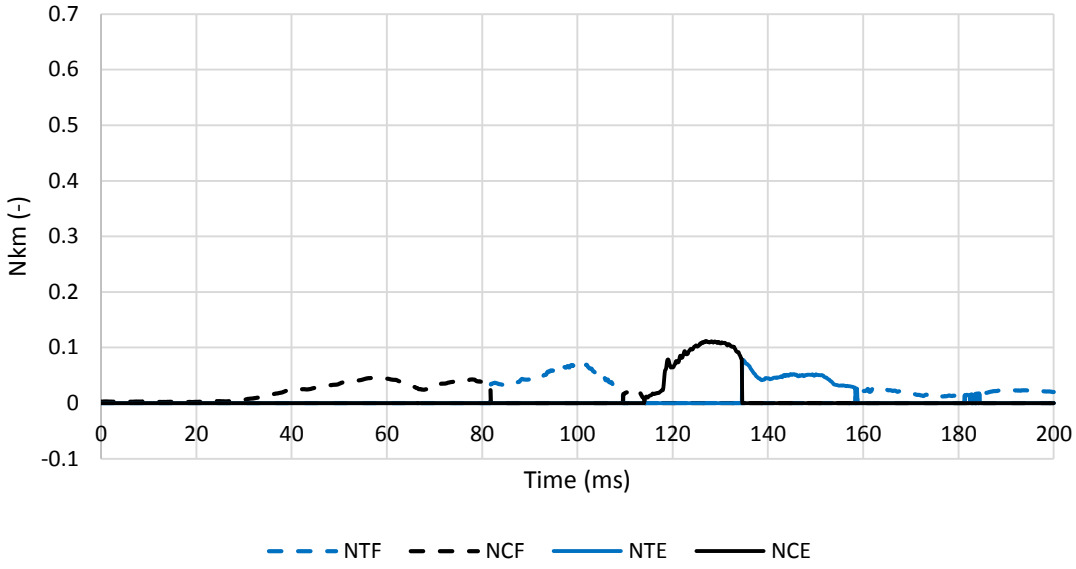


APPENDIX 234 LOADING GRAPHS OF FEA BIO RID CONFIGURATION M122 - NKM

### A.6.5.3. High Severity Pulse (SRA 24 km/h) H122

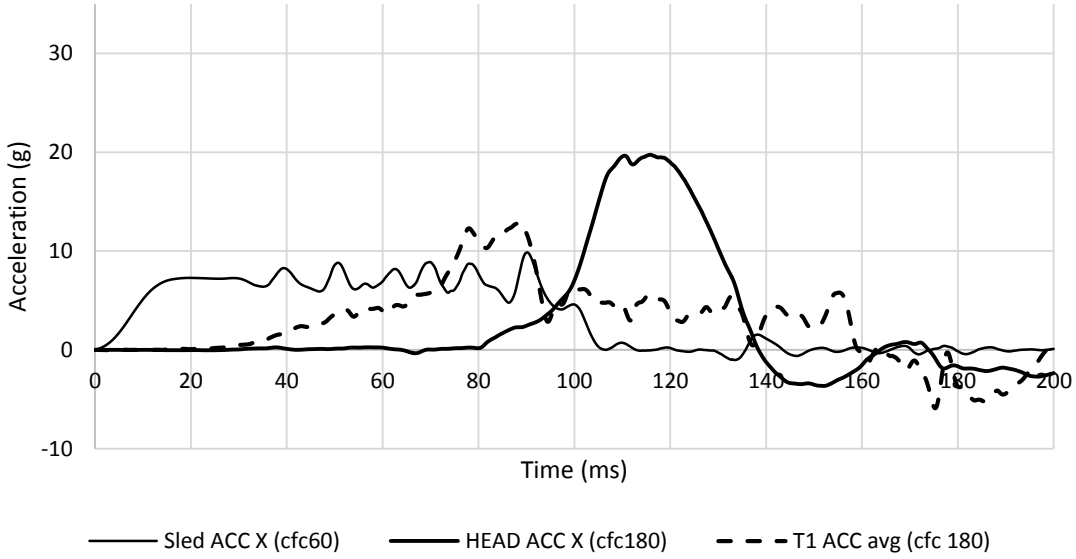


APPENDIX 235 LOADING GRAPHS OF FEA BIO RID CONFIGURATION H122 - ACCELERATION

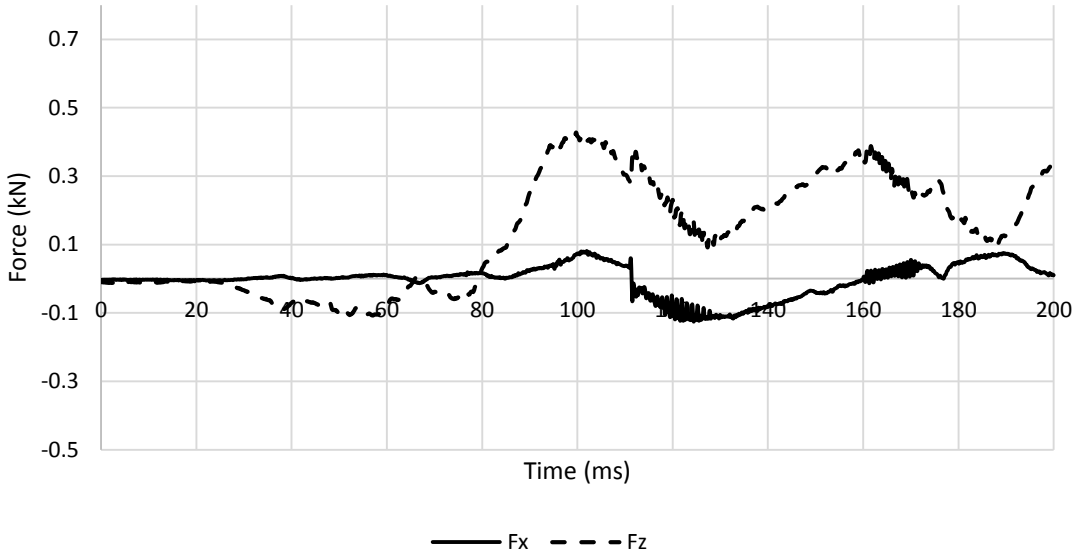


APPENDIX 236 LOADING GRAPHS OF FEA BIO RID CONFIGURATION H122 - FORCE

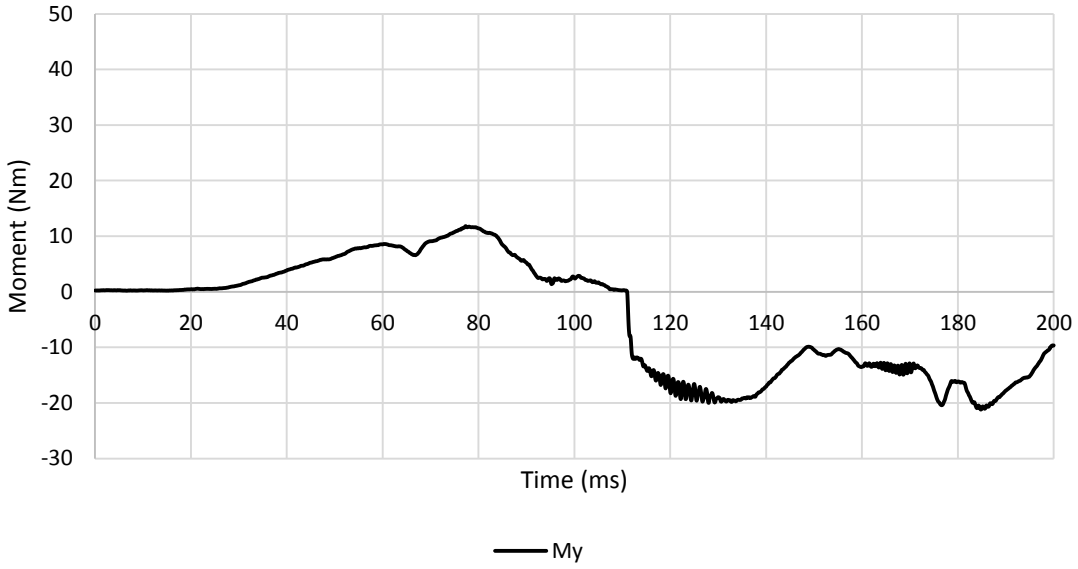


APPENDIX 237 LOADING GRAPHS OF FEA BIO RID CONFIGURATION H122 - MOMENT

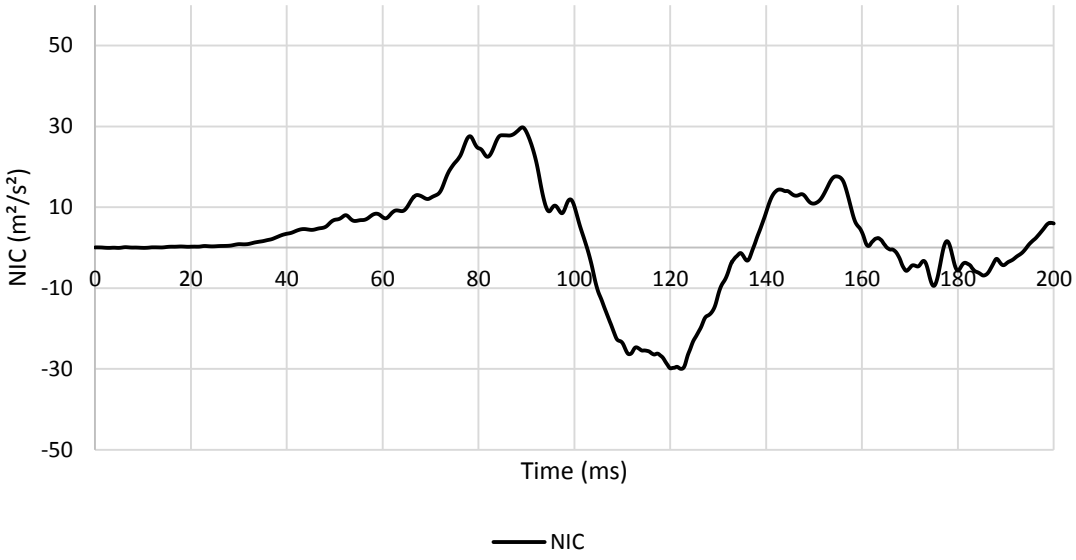


APPENDIX 238 LOADING GRAPHS OF FEA BIO RID CONFIGURATION H122 - NIC

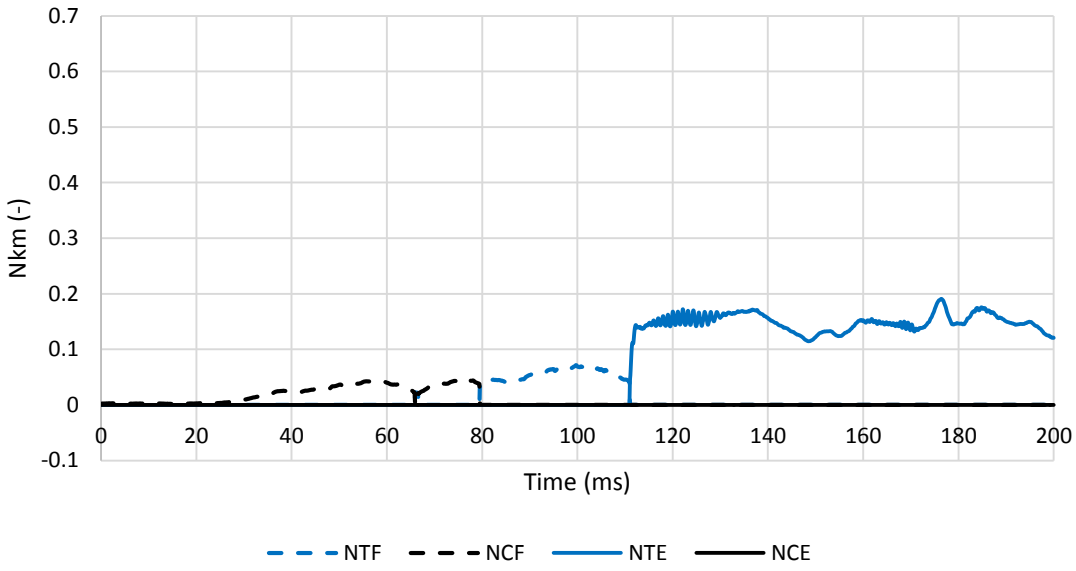


APPENDIX 239 LOADING GRAPHS OF FEA BIO RID CONFIGURATION H122 - NKM

## A.6.6. Bio RID II – centred backrest – low head restraint 123

### A.6.6.1. Low Severity Pulse (SRA 16 km/h) L123

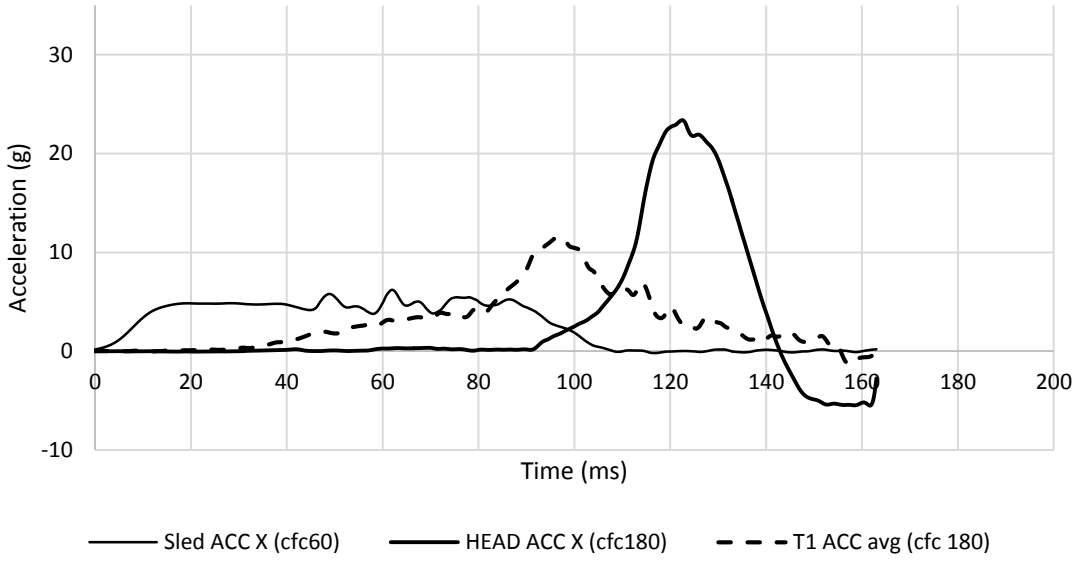


APPENDIX 240 LOADING GRAPHS OF FEA BIO RID CONFIGURATION L123 - ACCELERATION

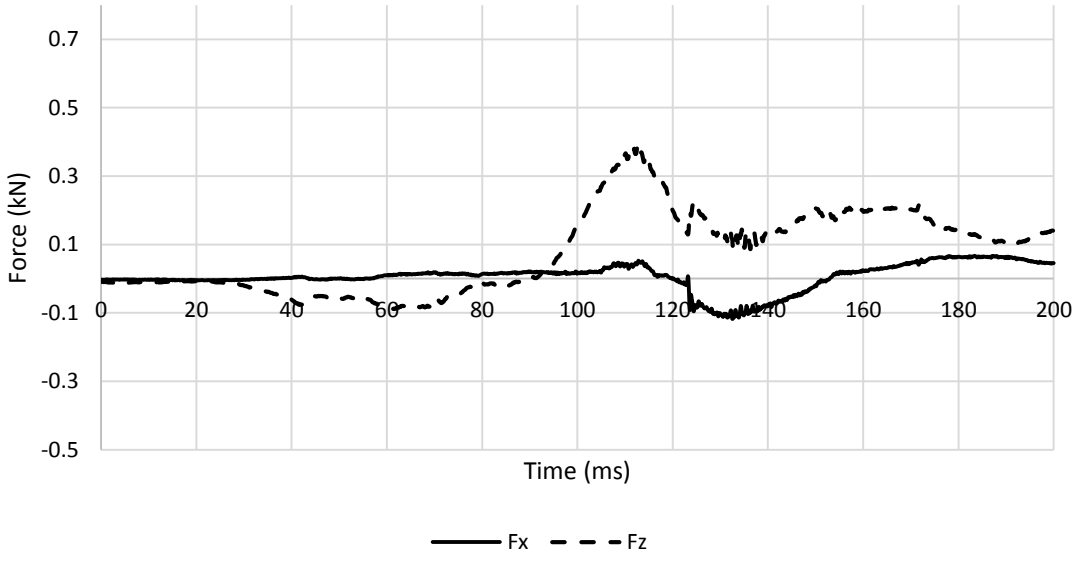


APPENDIX 241 LOADING GRAPHS OF FEA BIO RID CONFIGURATION L123 – FORCE

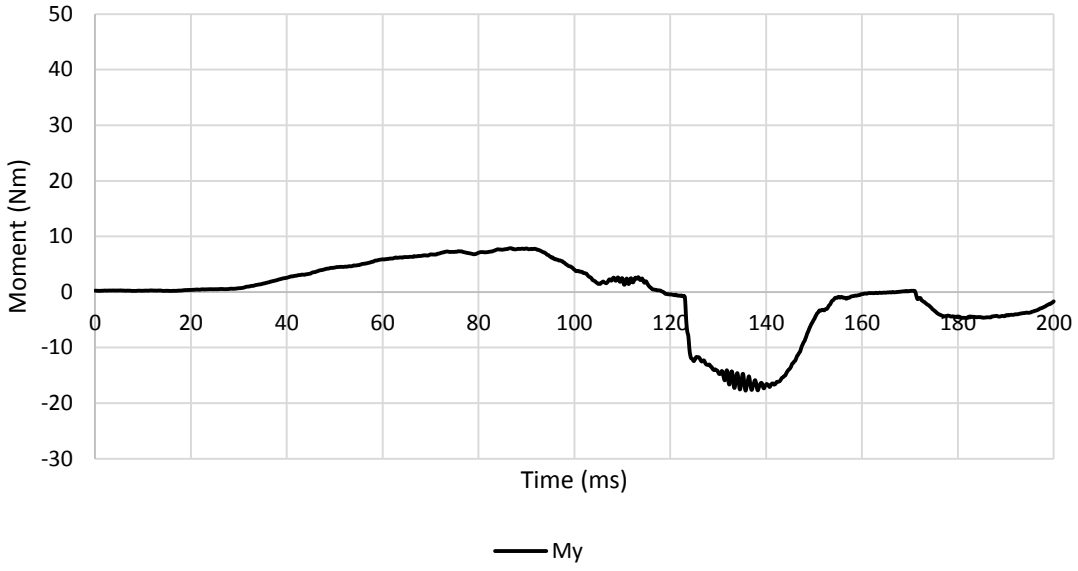


APPENDIX 242 LOADING GRAPHS OF FEA BIO RID CONFIGURATION L123 - MOMENT

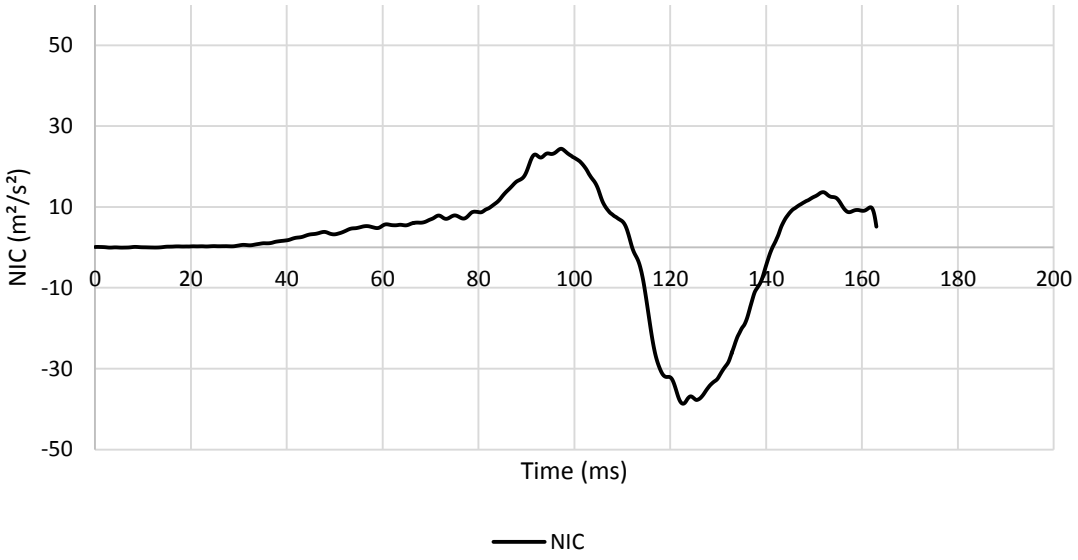


APPENDIX 243 LOADING GRAPHS OF FEA BIO RID CONFIGURATION L123 - NIC

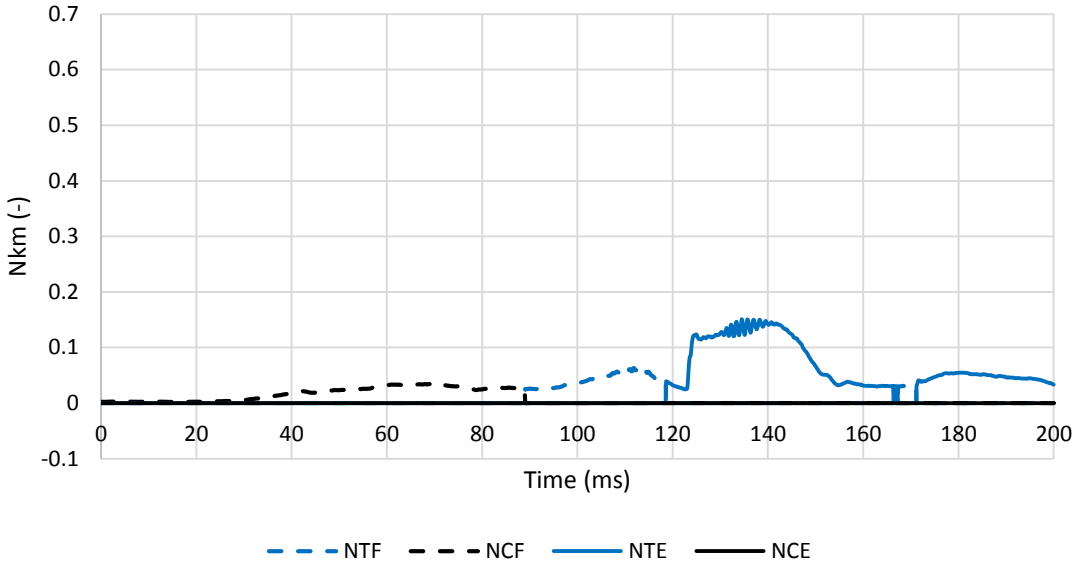


APPENDIX 244 LOADING GRAPHS OF FEA BIO RID CONFIGURATION L123 - NKM

### A.6.6.2. Medium Severity Pulse (IIWPG 16 km/h) M123

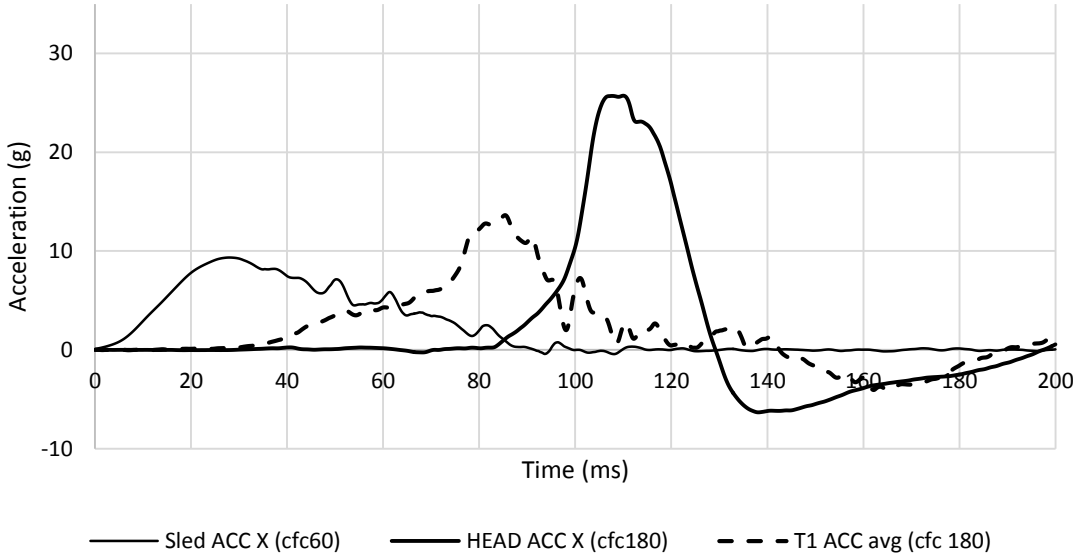


APPENDIX 245 LOADING GRAPHS OF FEA BIO RID CONFIGURATION M123 – ACCELERATION

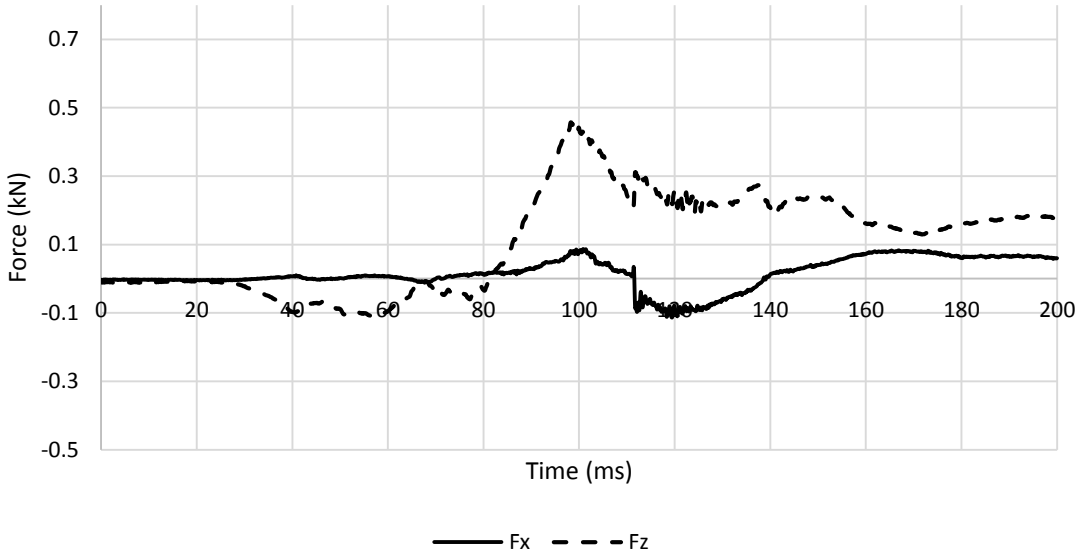


APPENDIX 246 LOADING GRAPHS OF FEA BIO RID CONFIGURATION M123 - FORCE

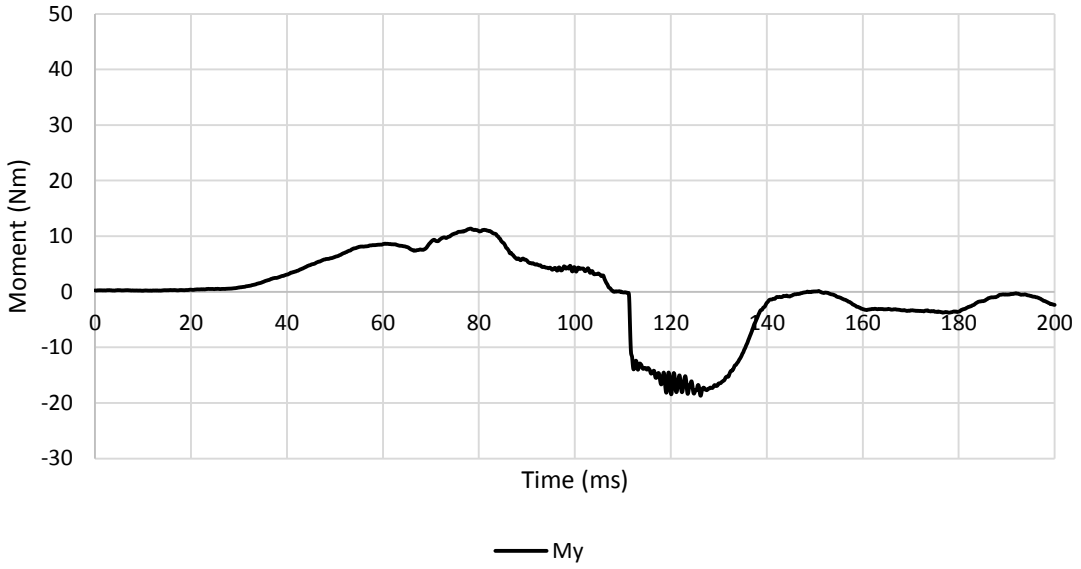


APPENDIX 247 LOADING GRAPHS OF FEA BIO RID CONFIGURATION M123 - MOMENT

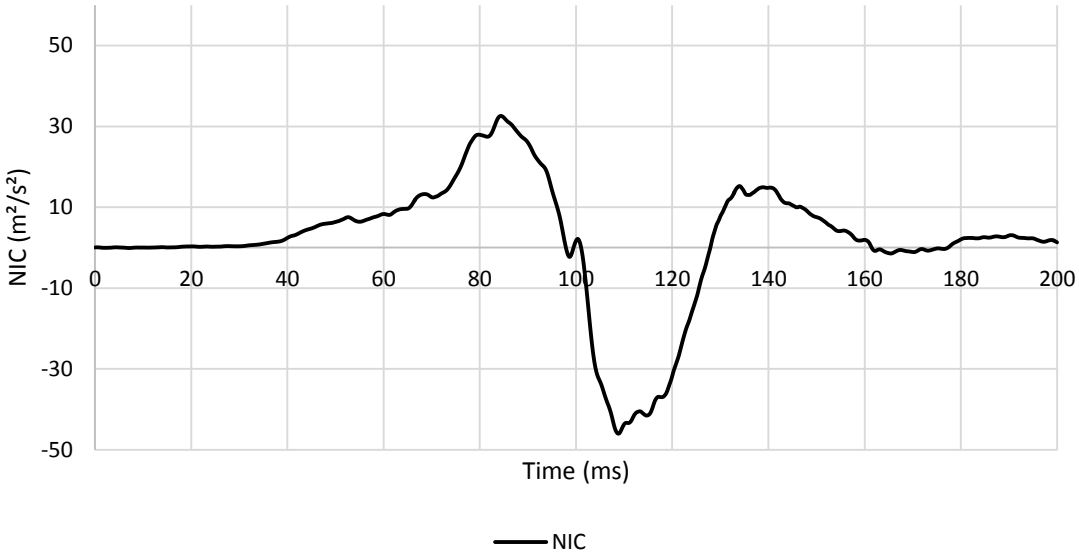


APPENDIX 248 LOADING GRAPHS OF FEA BIO RID CONFIGURATION M123 - NIC

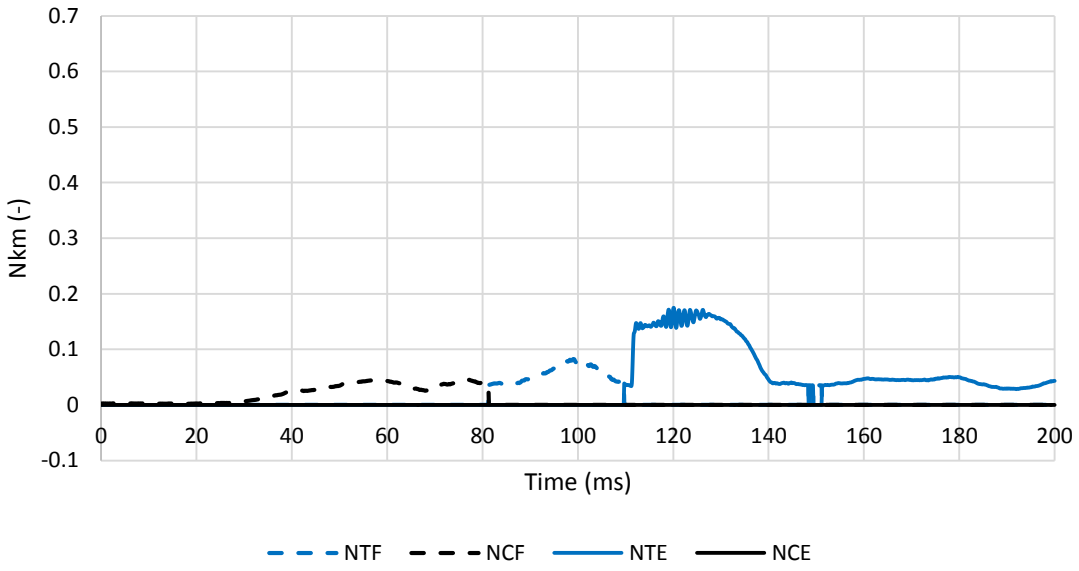


APPENDIX 249 LOADING GRAPHS OF FEA BIO RID CONFIGURATION M123 - NKM

A.6.6.3. High Severity Pulse (SRA 24 km/h) H123

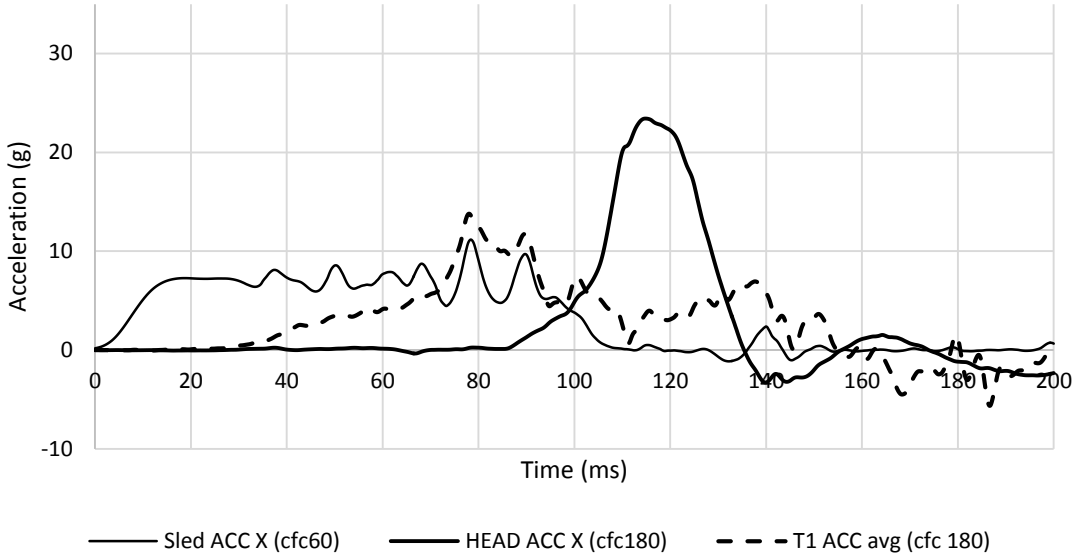


APPENDIX 250 LOADING GRAPHS OF FEA BIO RID CONFIGURATION H123 – ACCELERATION

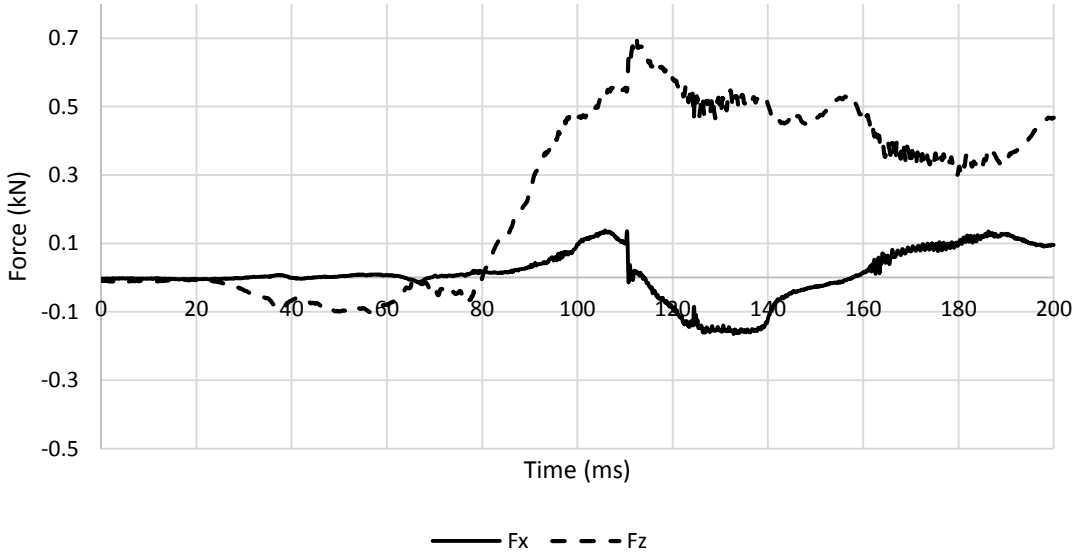


APPENDIX 251 LOADING GRAPHS OF FEA BIO RID CONFIGURATION H123 - FORCE

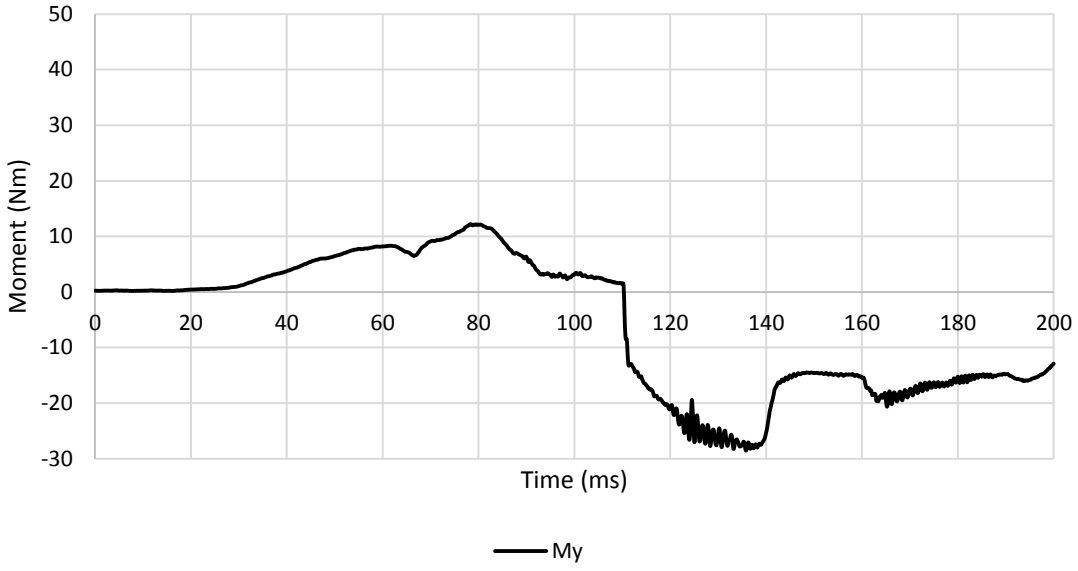


APPENDIX 252 LOADING GRAPHS OF FEA BIO RID CONFIGURATION H123 - MOMENT

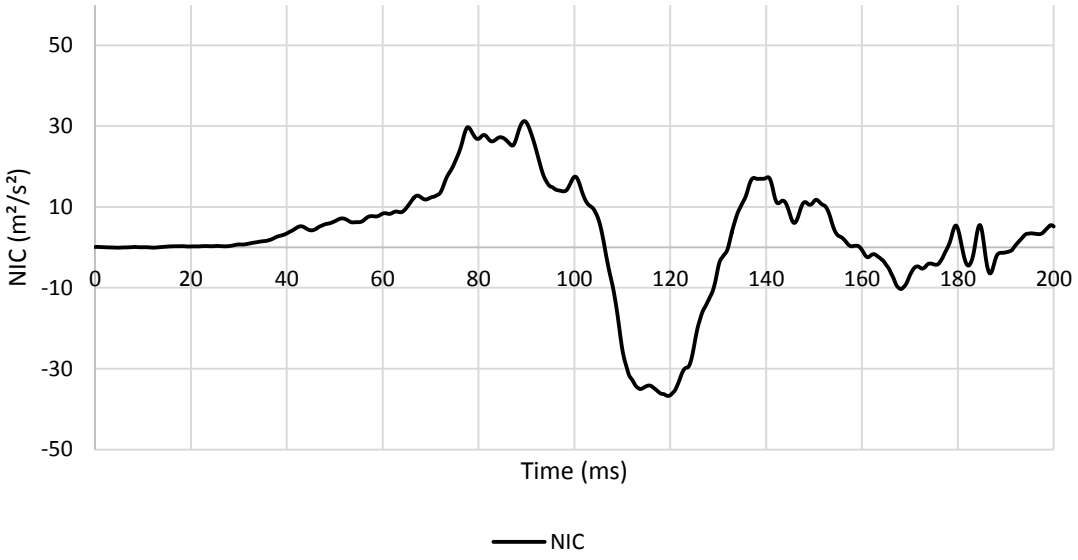


APPENDIX 253 LOADING GRAPHS OF FEA BIO RID CONFIGURATION H123 - NIC

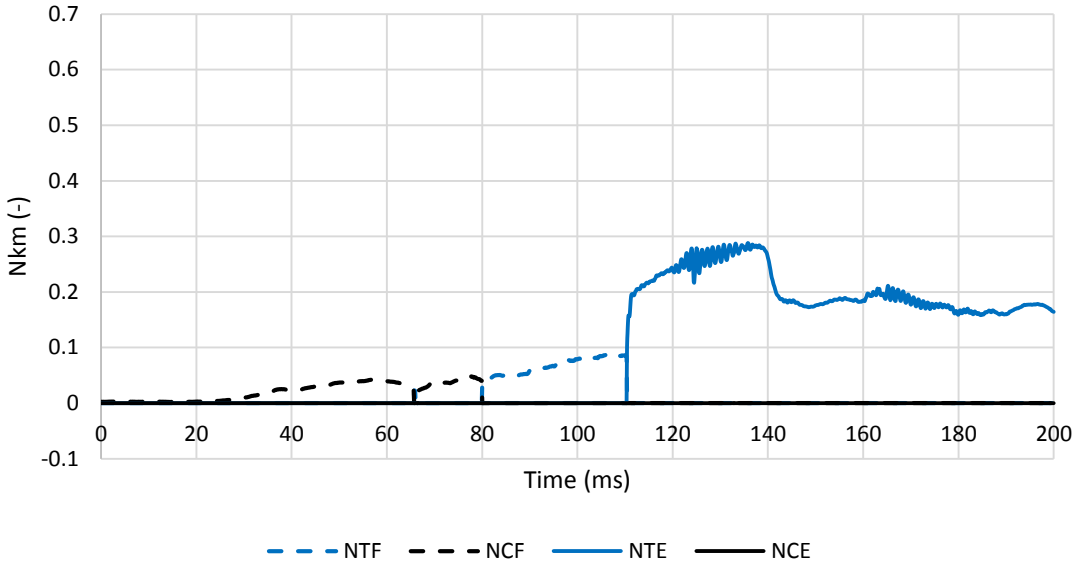


APPENDIX 254 LOADING GRAPHS OF FEA BIO RID CONFIGURATION H123 - NKM

## A.6.7. Bio RID II – backward backrest – high head restraint 131

### A.6.7.1. Low Severity Pulse (SRA 16 km/h) L131

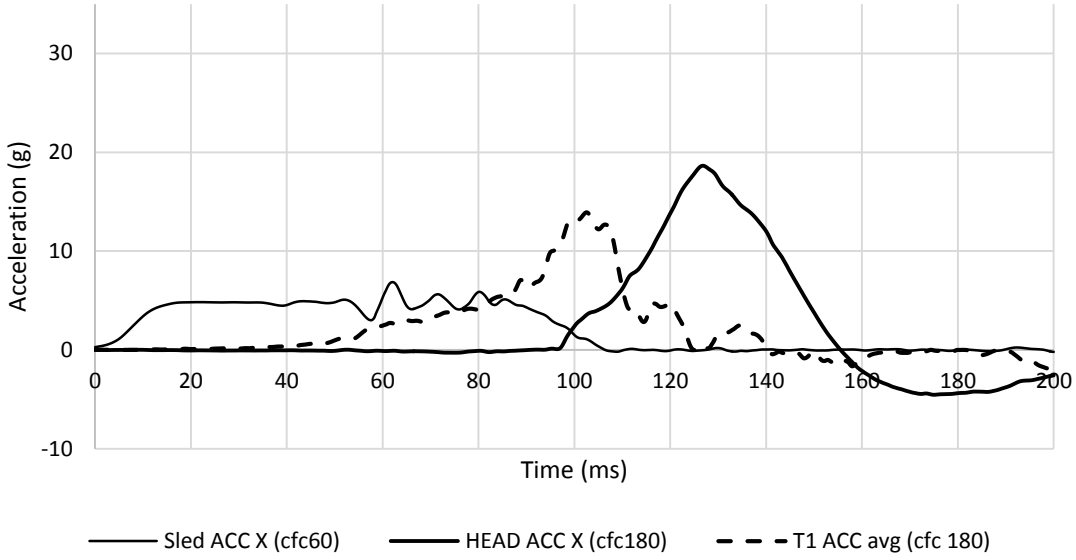


APPENDIX 255 LOADING GRAPHS OF FEA BIO RID CONFIGURATION L131 – ACCELERATION

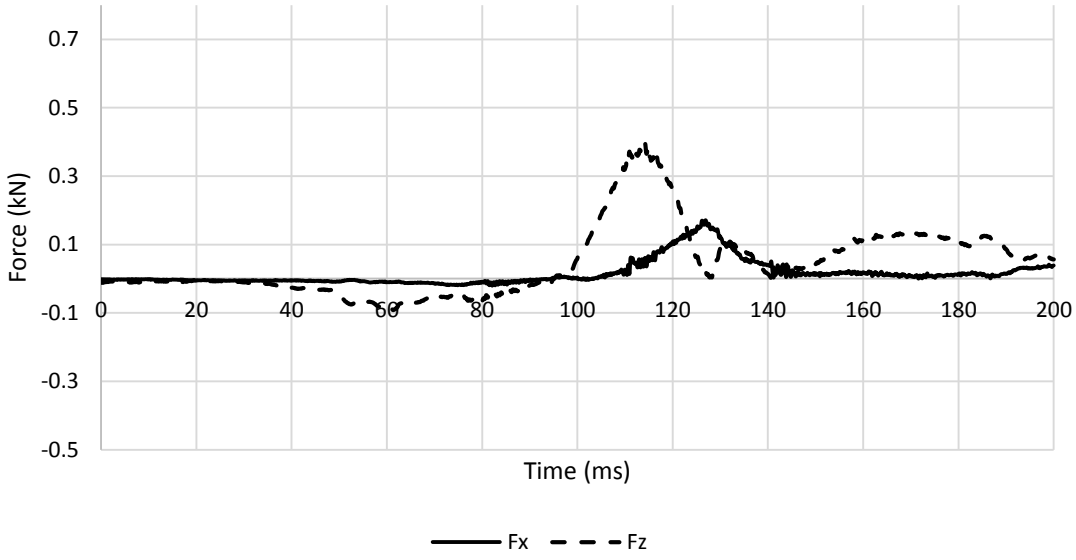


APPENDIX 256 LOADING GRAPHS OF FEA BIO RID CONFIGURATION L131 - FORCE

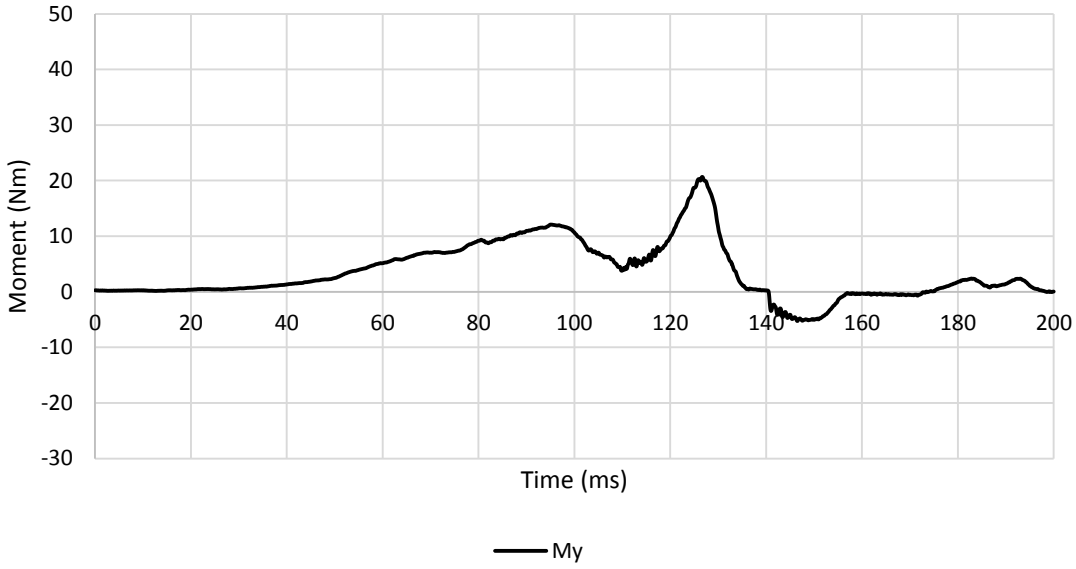


APPENDIX 257 LOADING GRAPHS OF FEA BIO RID CONFIGURATION L131 - MOMENT

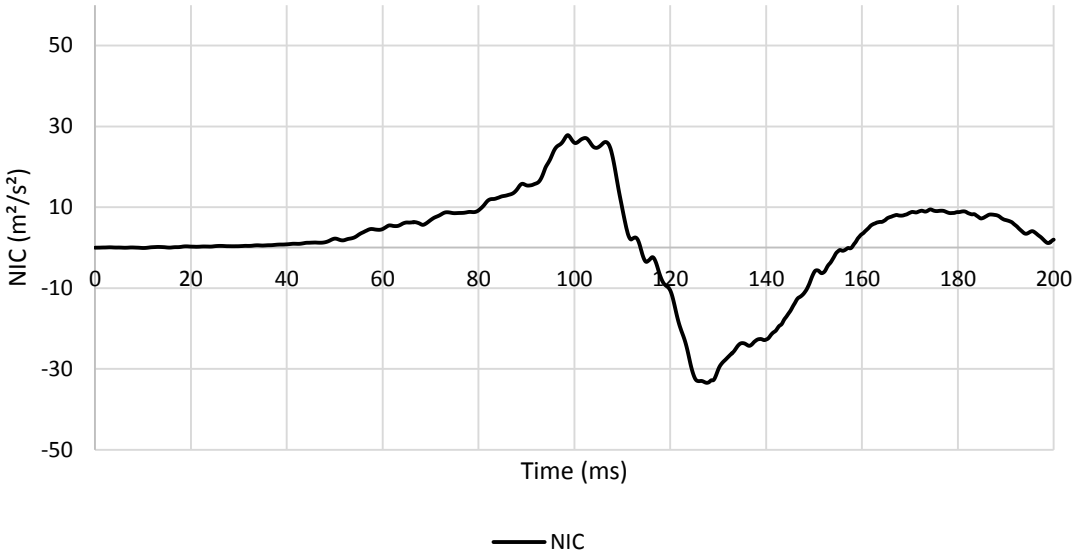


APPENDIX 258 LOADING GRAPHS OF FEA BIO RID CONFIGURATION L131 - NIC

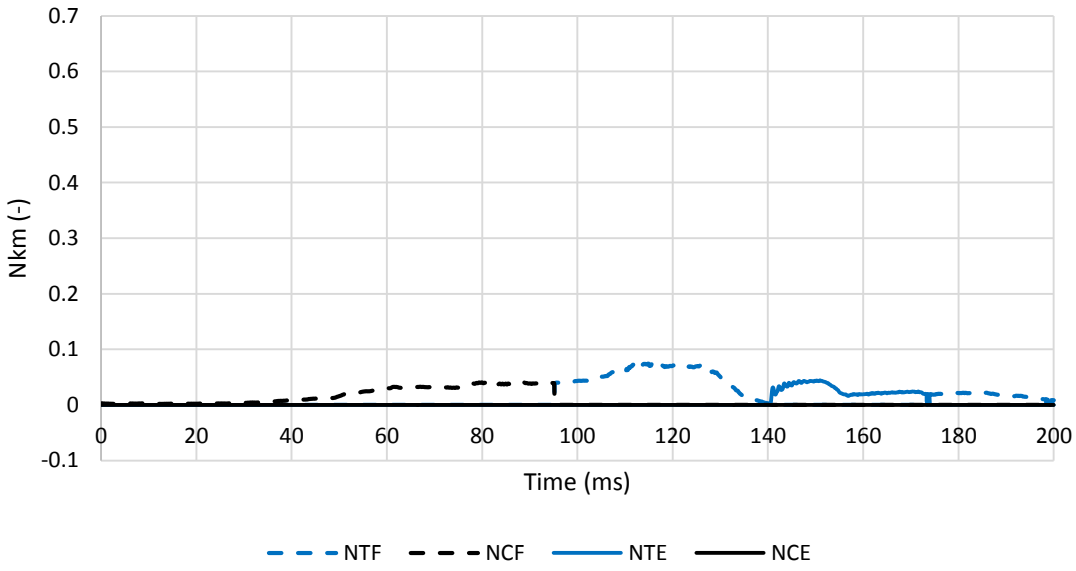


APPENDIX 259 LOADING GRAPHS OF FEA BIO RID CONFIGURATION L131 - NKM

## A.6.7.2. Medium Severity Pulse (IIWPG 16 km/h) M131

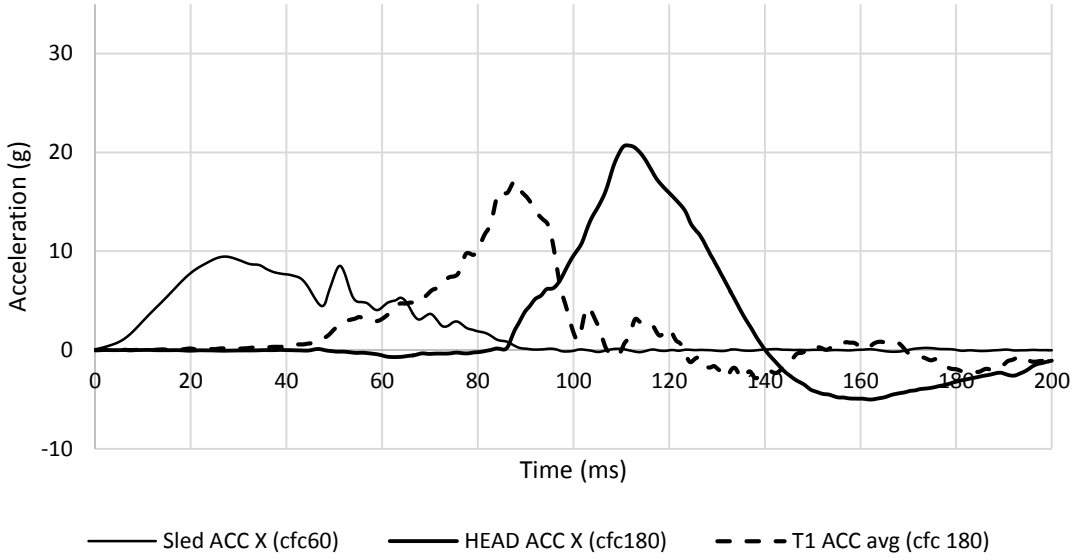


APPENDIX 260 LOADING GRAPHS OF FEA BIO RID CONFIGURATION M131 – ACCELERATION

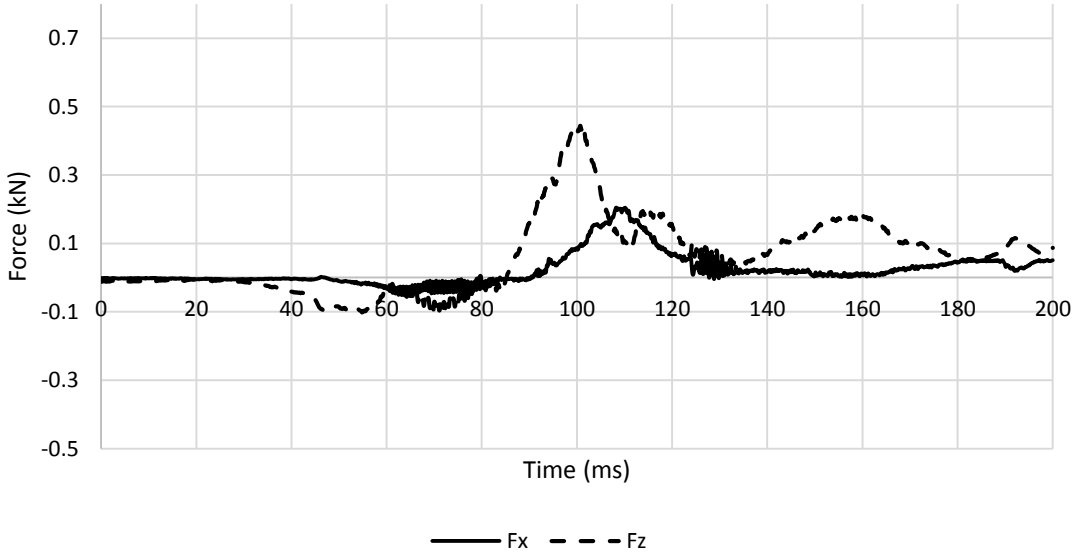


APPENDIX 261 LOADING GRAPHS OF FEA BIO RID CONFIGURATION M131 - FORCE

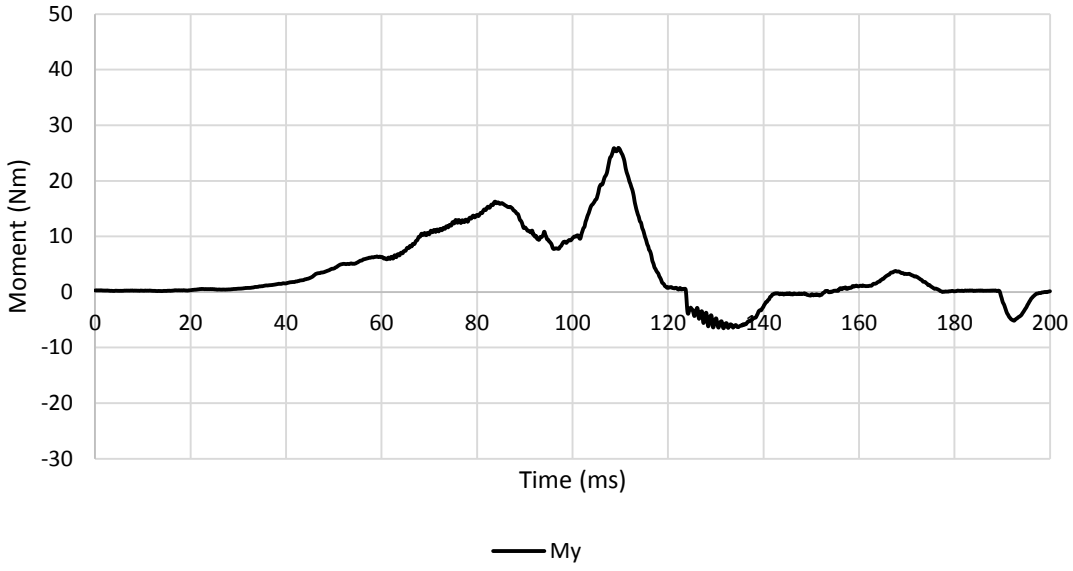


APPENDIX 262 LOADING GRAPHS OF FEA BIO RID CONFIGURATION M131 - MOMENT

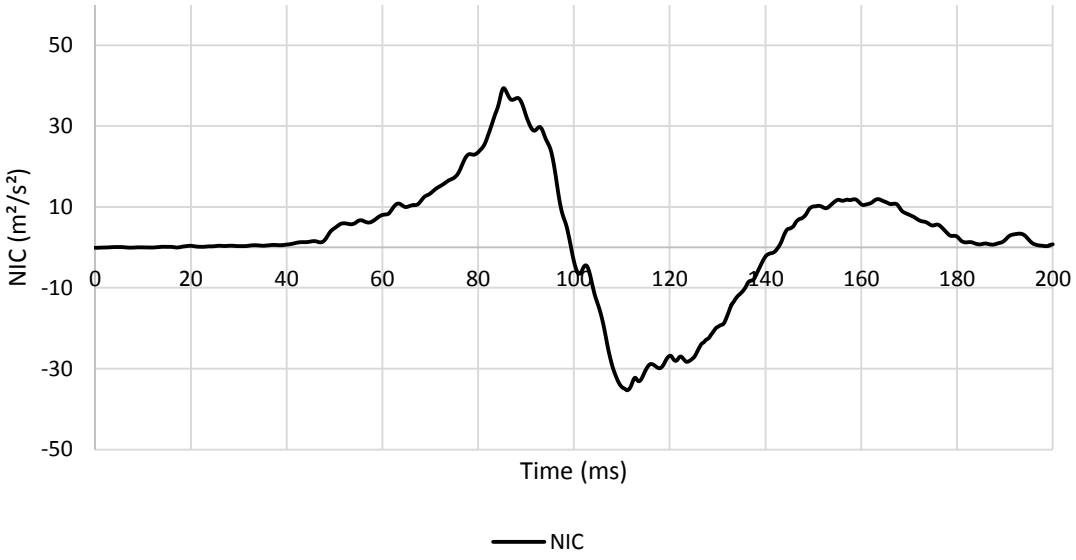


APPENDIX 263 LOADING GRAPHS OF FEA BIO RID CONFIGURATION M131 - NIC

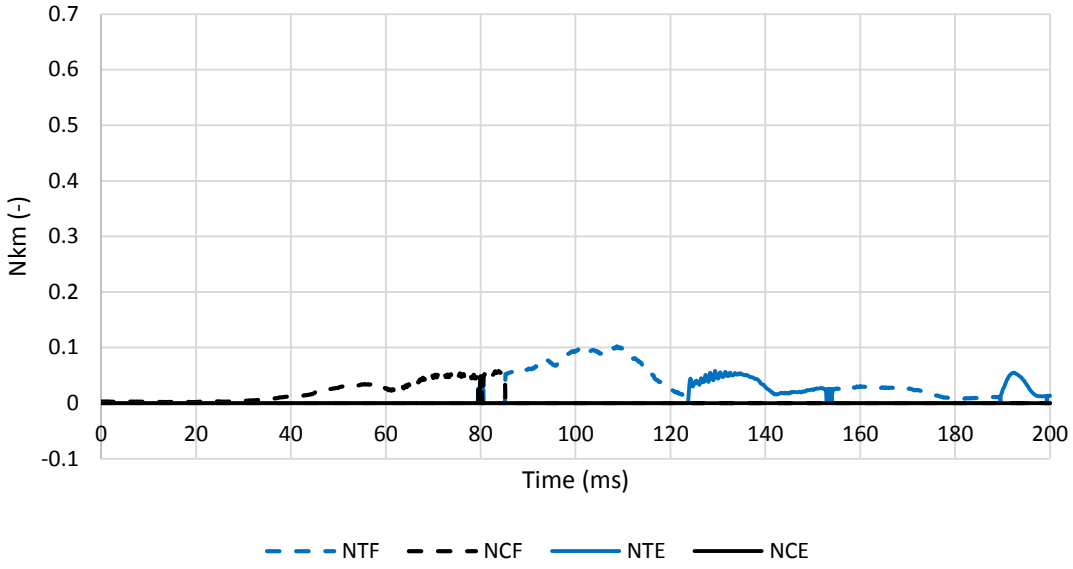


APPENDIX 264 LOADING GRAPHS OF FEA BIO RID CONFIGURATION M131 – NKM

### A.6.7.3. High Severity Pulse (SRA 24 km/h) H131

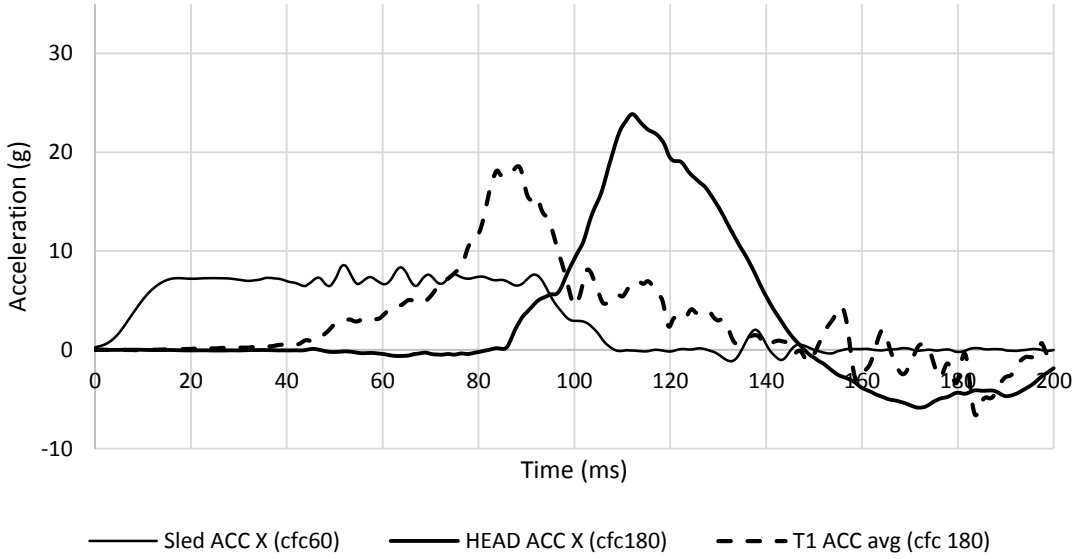


APPENDIX 265 LOADING GRAPHS OF FEA BIO RID CONFIGURATION H131 – ACCELERATION

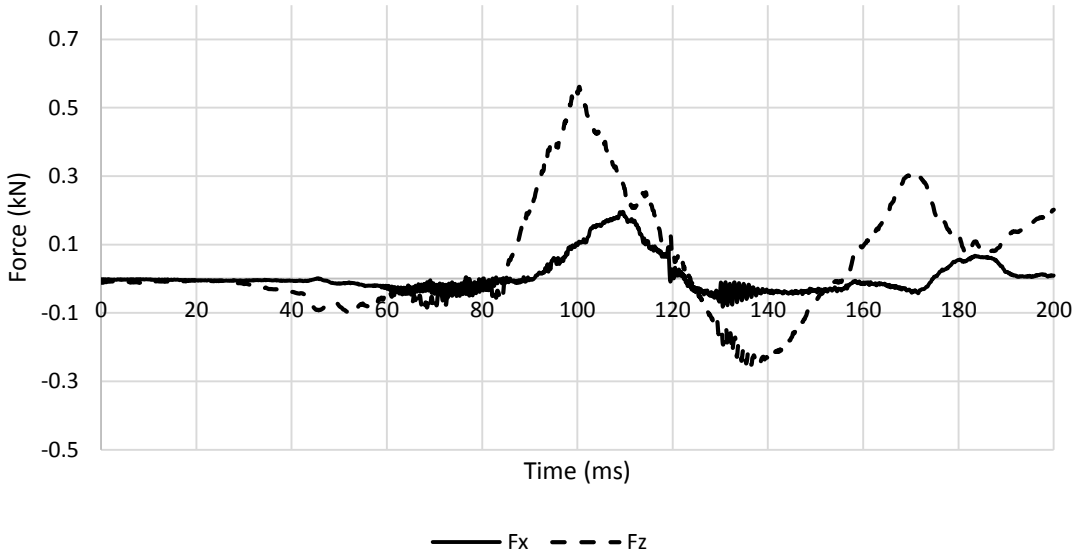


APPENDIX 266 LOADING GRAPHS OF FEA BIO RID CONFIGURATION H131 - FORCE

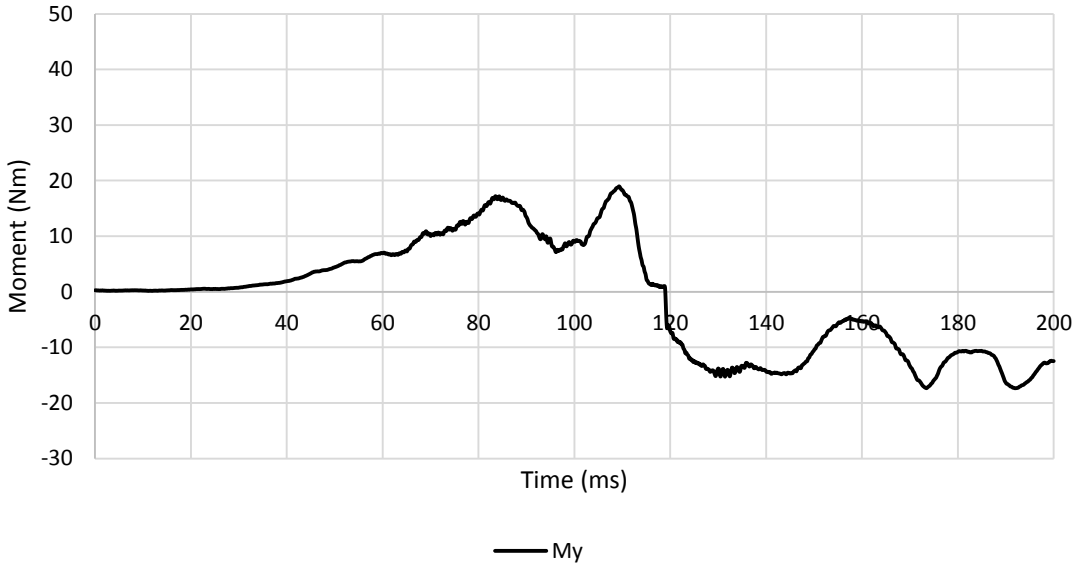


APPENDIX 267 LOADING GRAPHS OF FEA BIO RID CONFIGURATION H131 - MOMENT

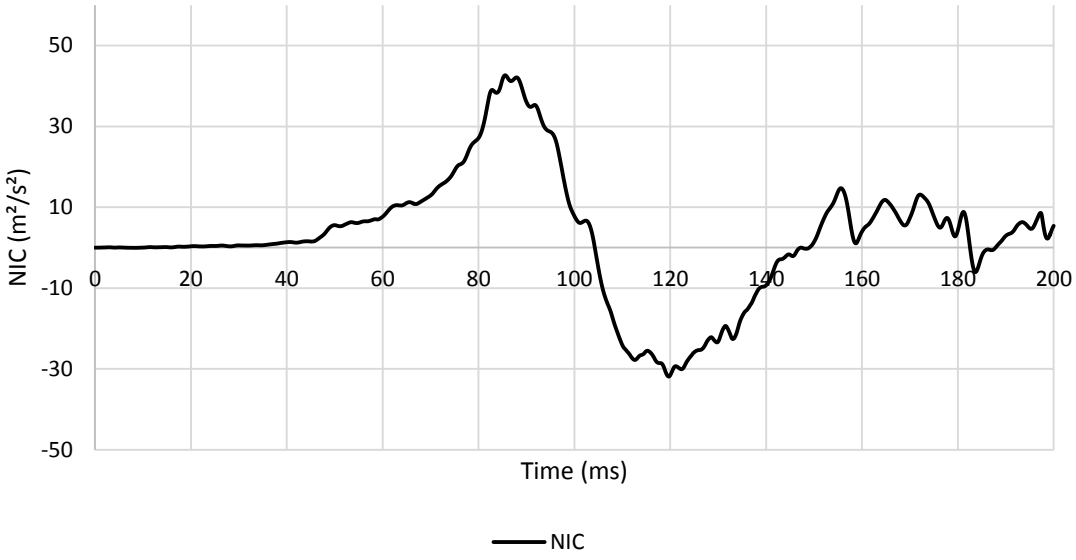


APPENDIX 268 LOADING GRAPHS OF FEA BIO RID CONFIGURATION H131 - NIC

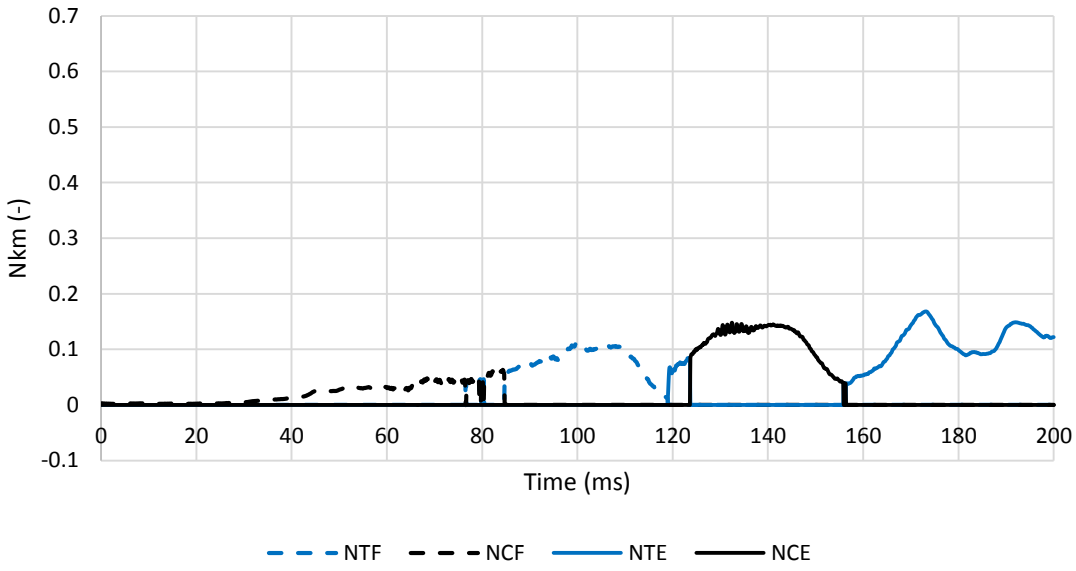


APPENDIX 269 LOADING GRAPHS OF FEA BIO RID CONFIGURATION H131 - NKM

## A.6.8. Bio RID II – backward backrest – middle head restraint 132

### A.6.8.1. Low Severity Pulse (SRA 16 km/h) L132

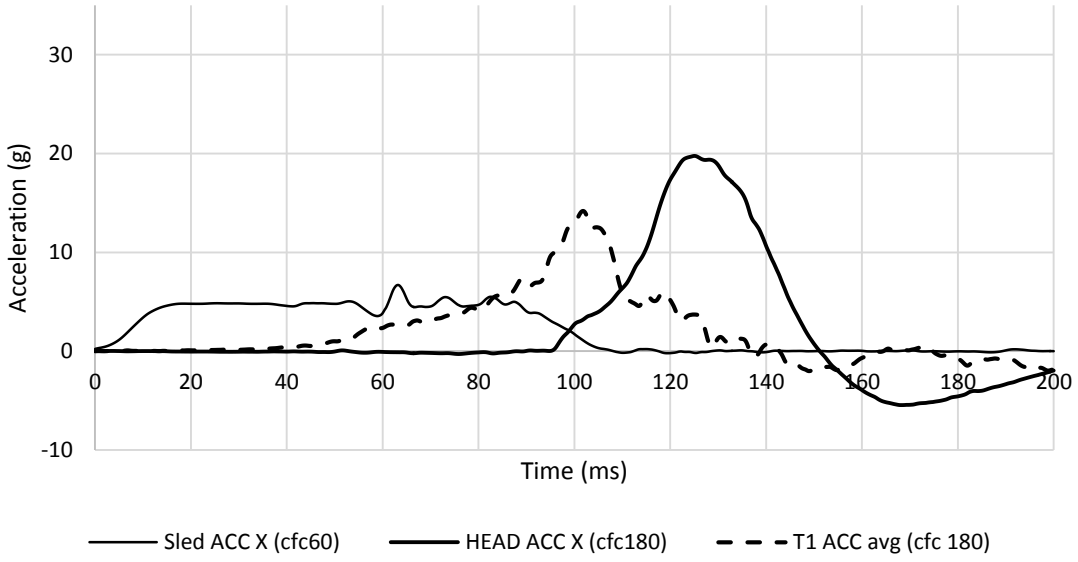


APPENDIX 270 LOADING GRAPHS OF FEA BIO RID CONFIGURATION L132 - ACCELERATION

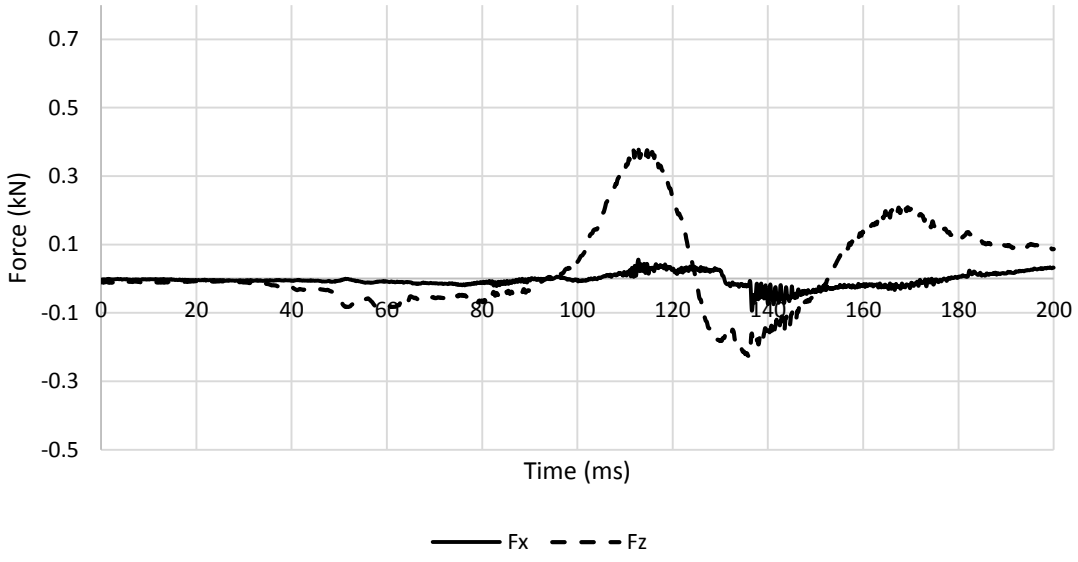


APPENDIX 271 LOADING GRAPHS OF FEA BIO RID CONFIGURATION L132 - FORCE

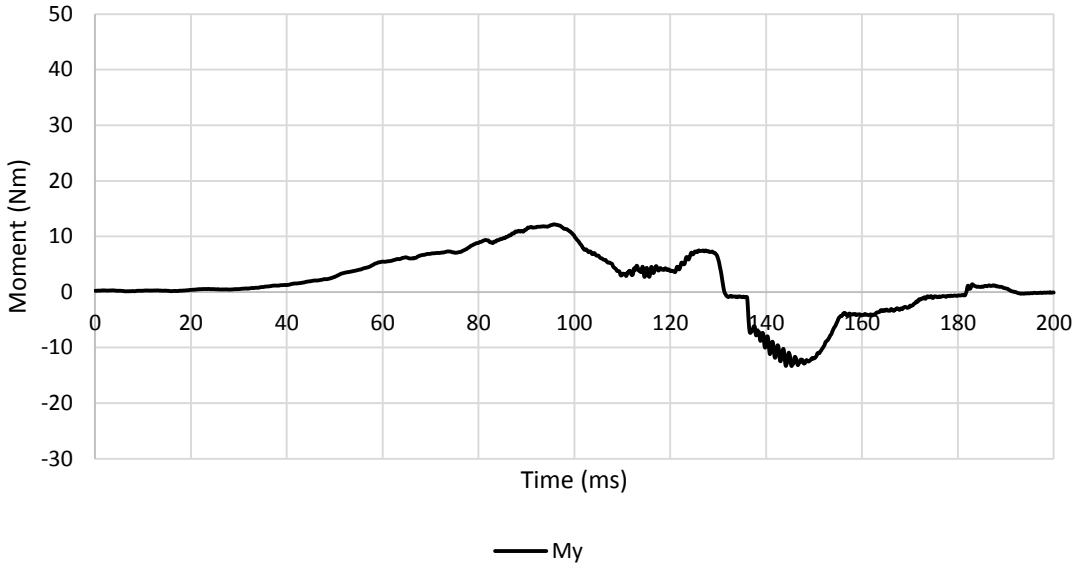


APPENDIX 272 LOADING GRAPHS OF FEA BIO RID CONFIGURATION L132 - MOMENT

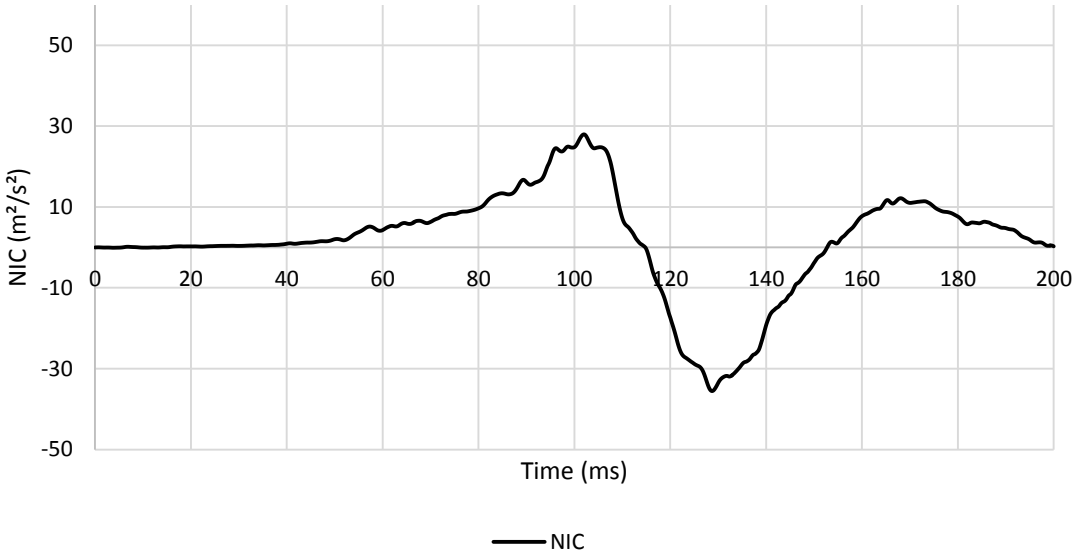


APPENDIX 273 LOADING GRAPHS OF FEA BIO RID CONFIGURATION L132 - NIC

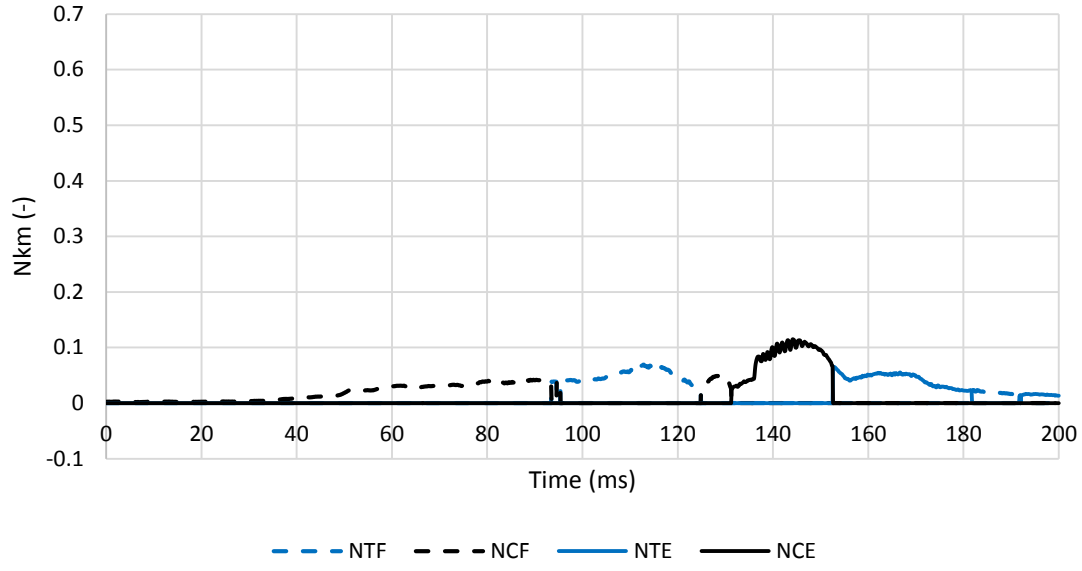


APPENDIX 274 LOADING GRAPHS OF FEA BIO RID CONFIGURATION L132 - NKM

### A.6.8.2. Medium Severity Pulse (IIWPG 16 km/h) M132

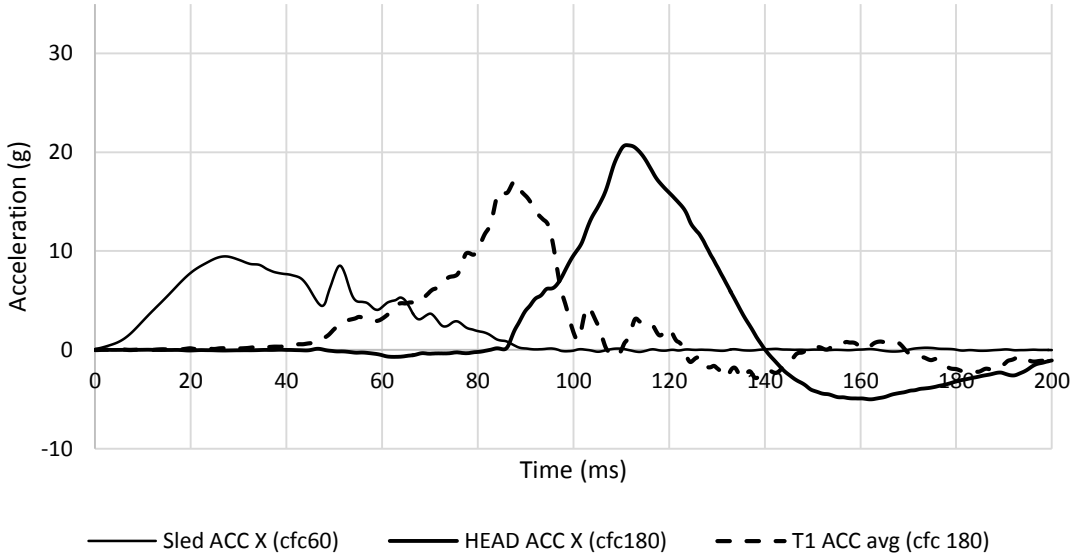


APPENDIX 275 LOADING GRAPHS OF FEA BIO RID CONFIGURATION M132 - ACCELERATION

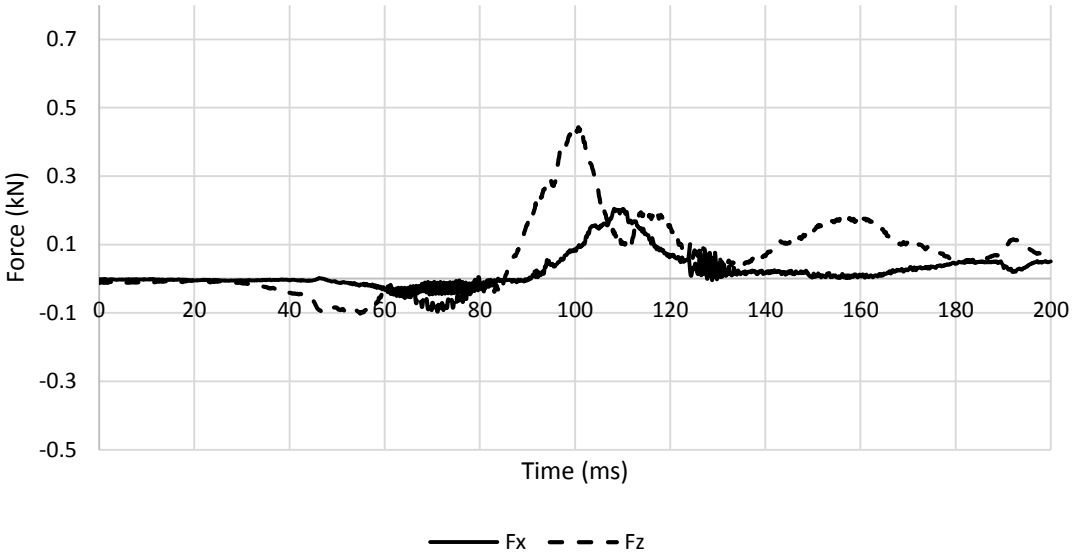


APPENDIX 276 LOADING GRAPHS OF FEA BIO RID CONFIGURATION M132 - FORCE

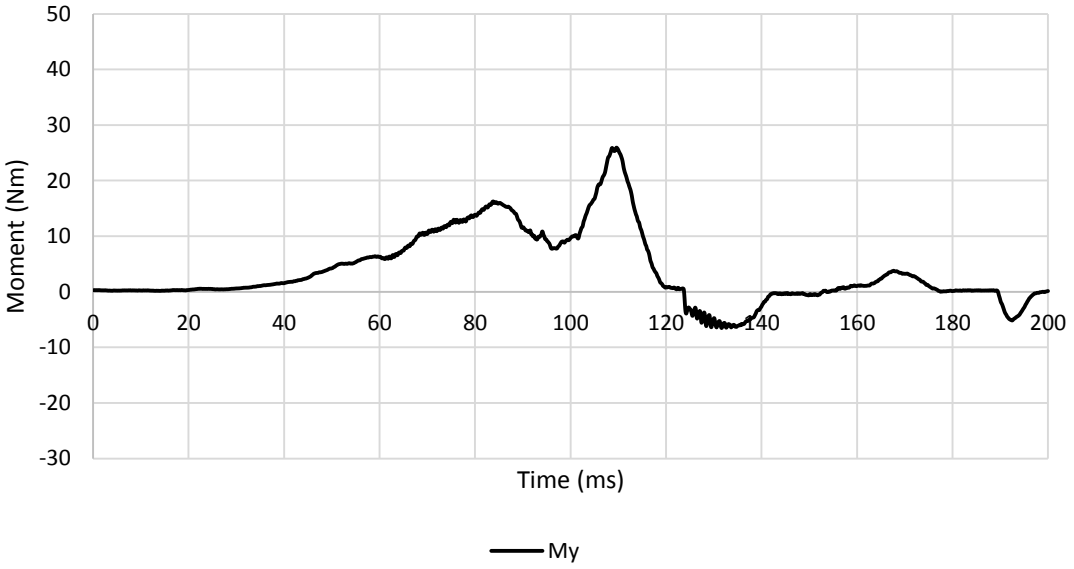


APPENDIX 277 LOADING GRAPHS OF FEA BIO RID CONFIGURATION M132 - MOMENT

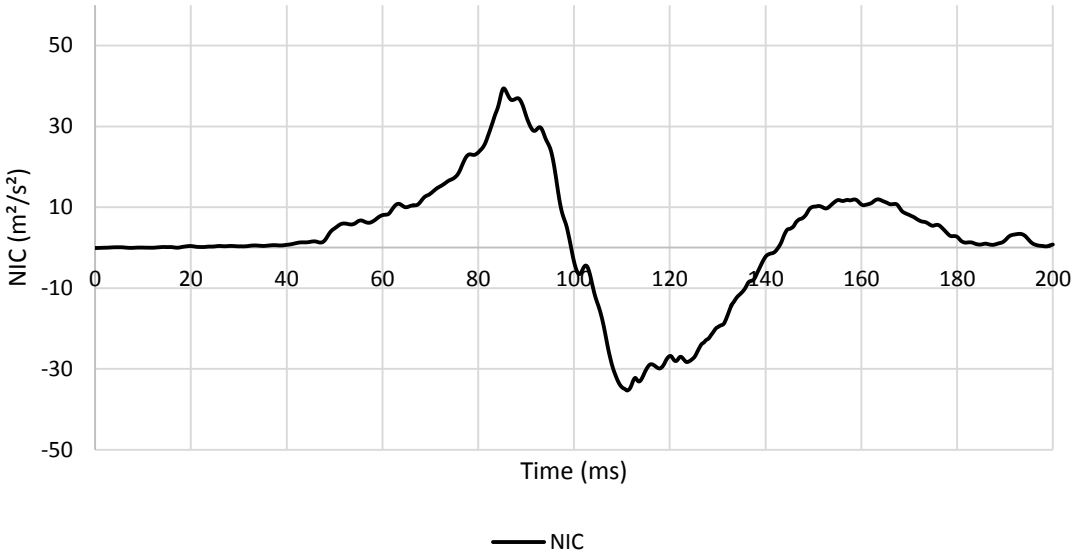


APPENDIX 278 LOADING GRAPHS OF FEA BIO RID CONFIGURATION M132 - NIC

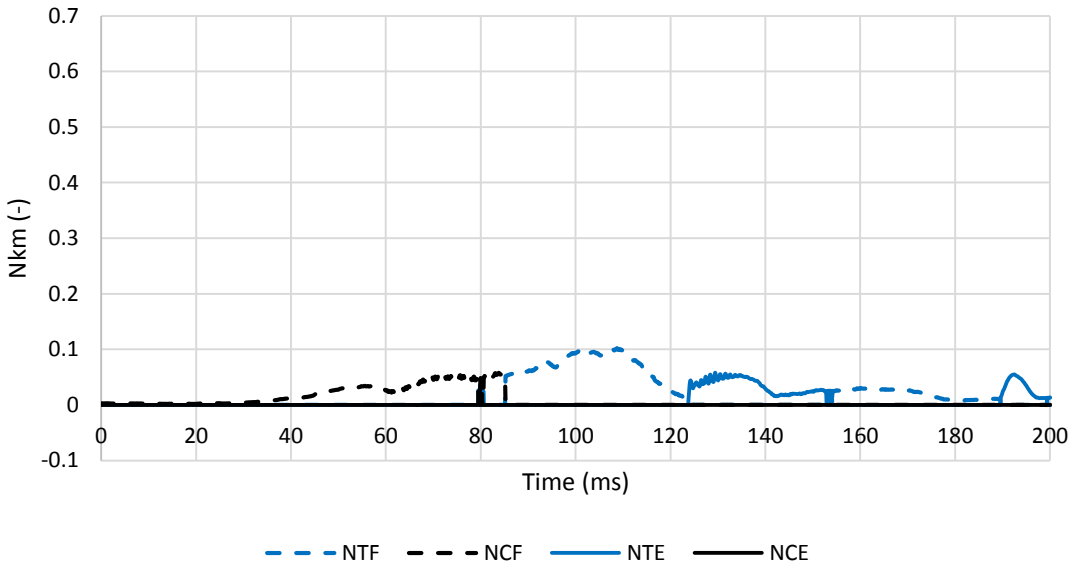


APPENDIX 279 LOADING GRAPHS OF FEA BIO RID CONFIGURATION M132 - NKM

### A.6.8.3. High Severity Pulse (SRA 24 km/h) H132

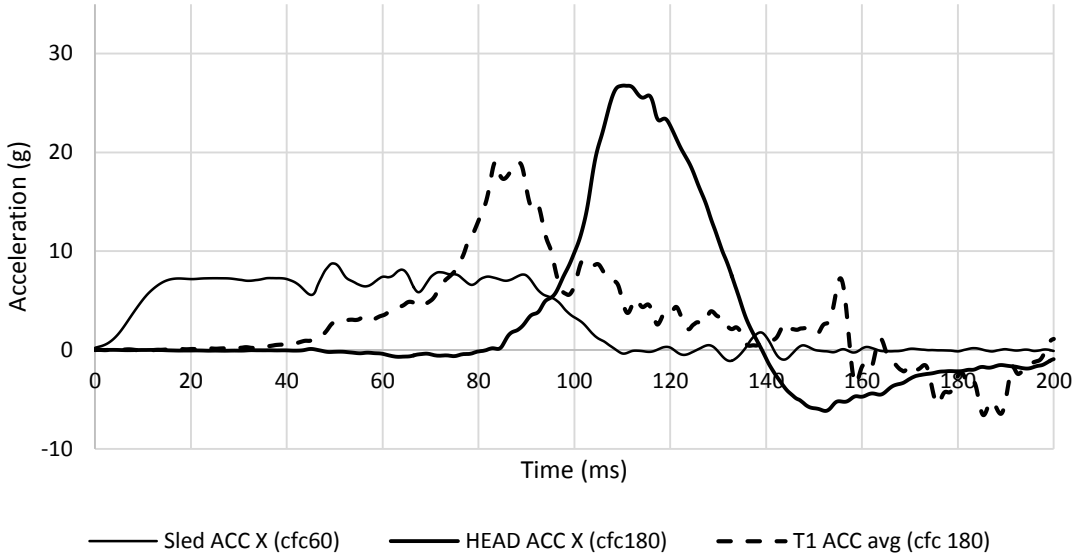


APPENDIX 280 LOADING GRAPHS OF FEA BIO RID CONFIGURATION H132 - ACCELERATION

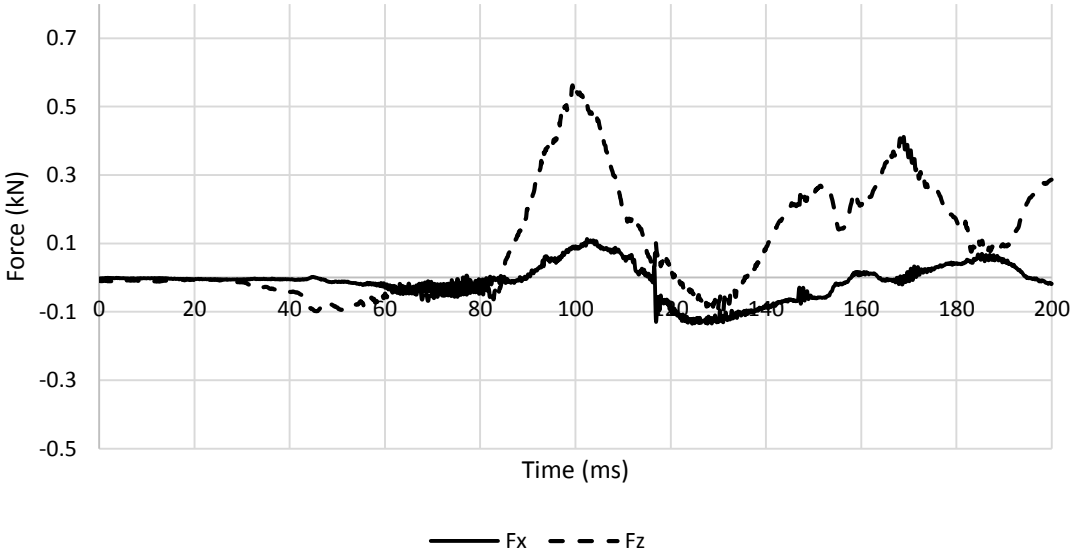


APPENDIX 281 LOADING GRAPHS OF FEA BIO RID CONFIGURATION H132 - FORCE

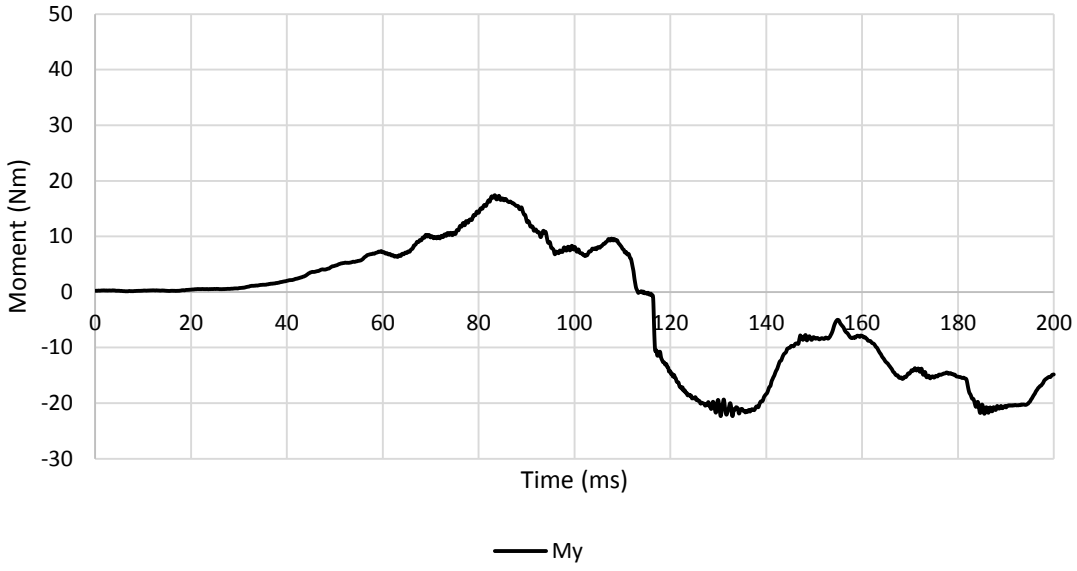


APPENDIX 282 LOADING GRAPHS OF FEA BIO RID CONFIGURATION H132 - MOMENT

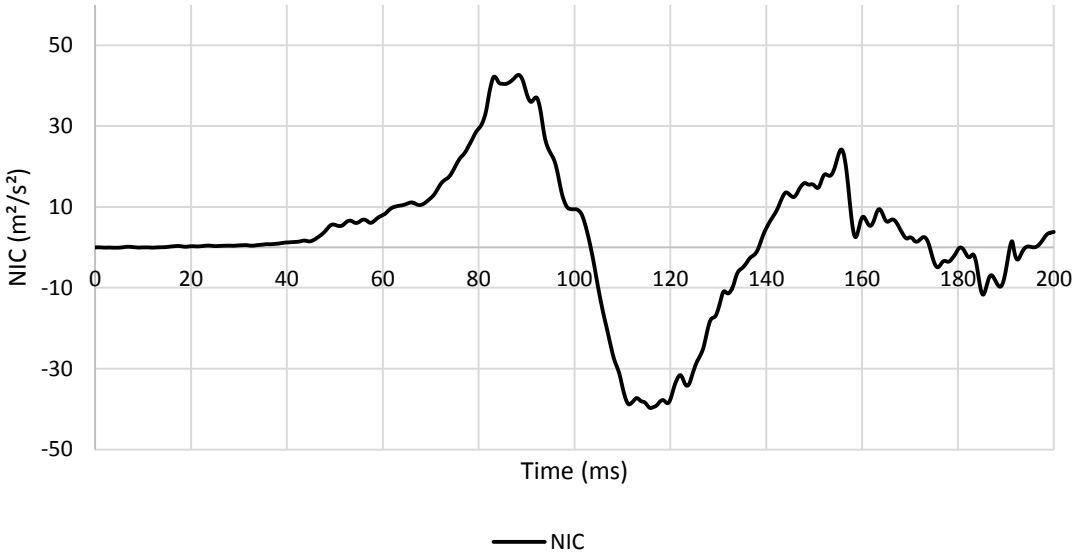


APPENDIX 283 LOADING GRAPHS OF FEA BIO RID CONFIGURATION H132 - NIC

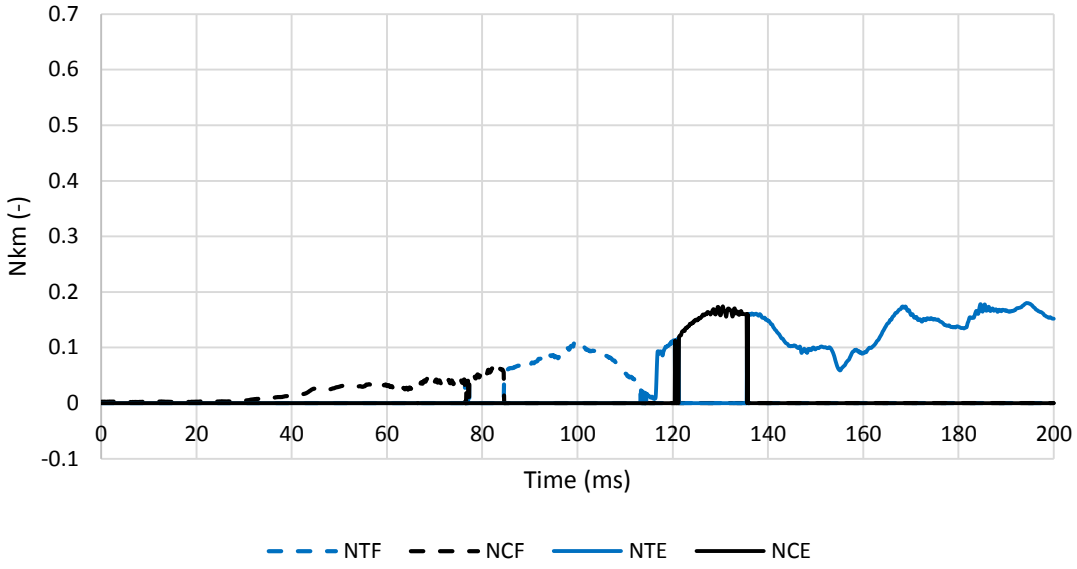


APPENDIX 284 LOADING GRAPHS OF FEA BIO RID CONFIGURATION H132 - NKM

## A.6.9. Bio RID II – backward backrest – low head restraint 133

### A.6.9.1. Low Severity Pulse (SRA 16 km/h) L133

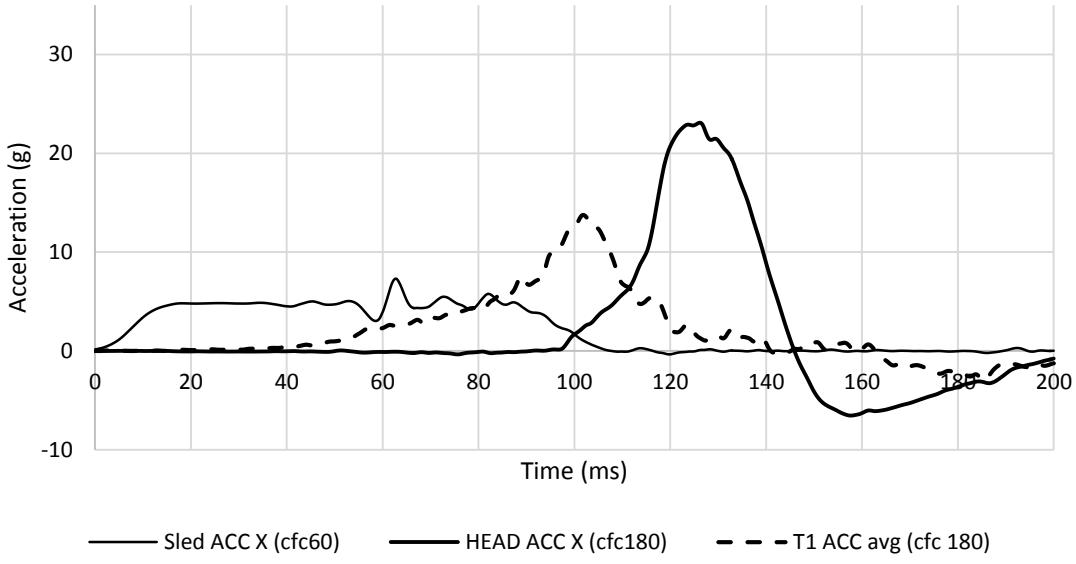


APPENDIX 285 LOADING GRAPHS OF FEA BIO RID CONFIGURATION L133 - ACCELERATION

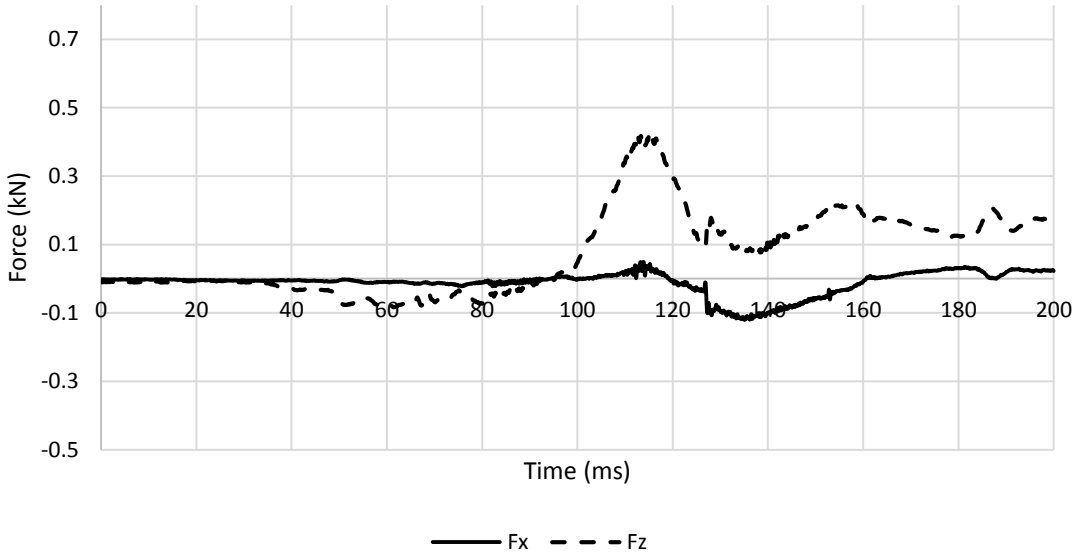


APPENDIX 286 LOADING GRAPHS OF FEA BIO RID CONFIGURATION L133 - FORCE

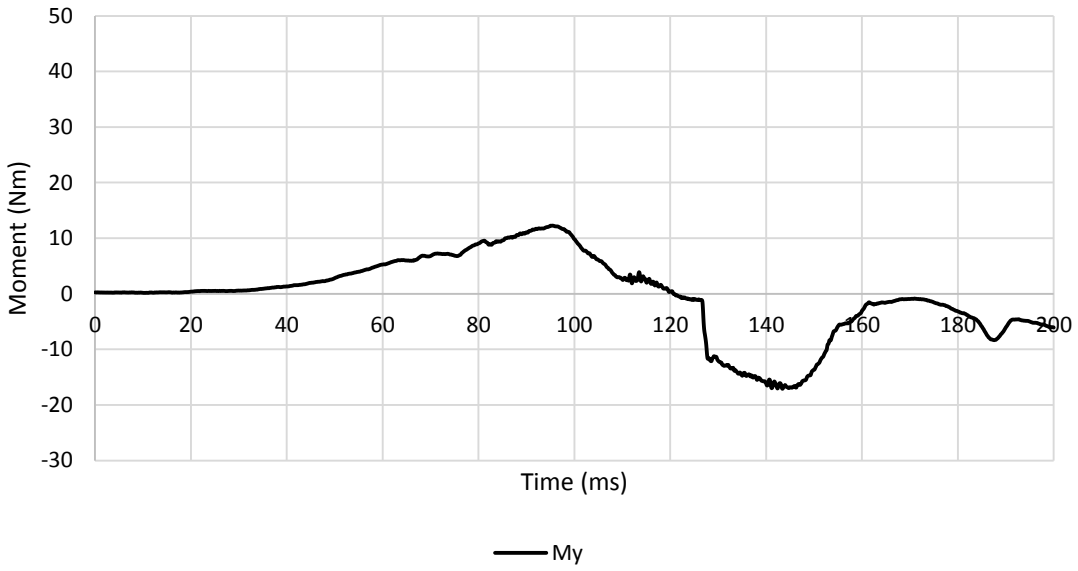


APPENDIX 287 LOADING GRAPHS OF FEA BIO RID CONFIGURATION L133 - MOMENT

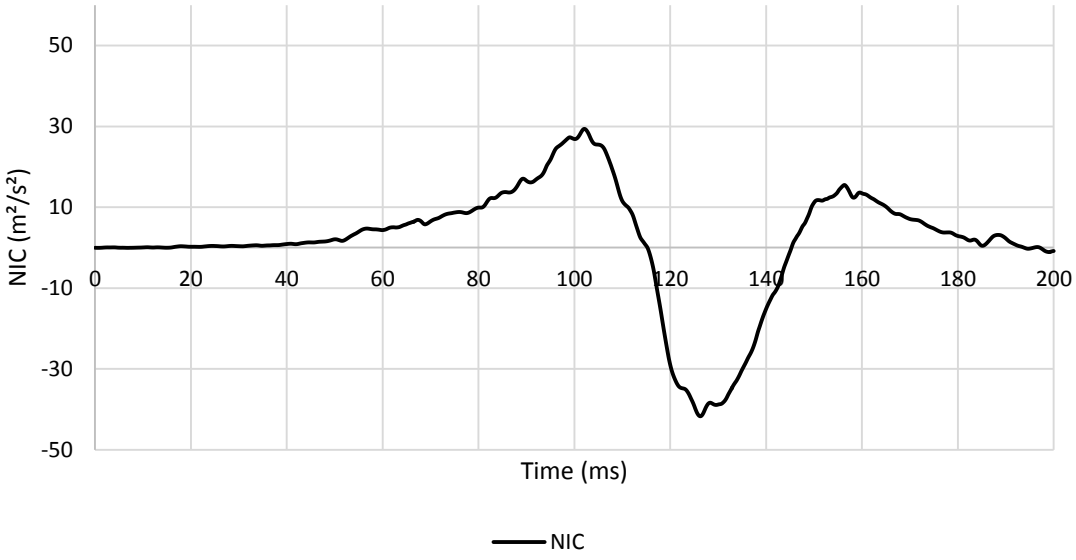


APPENDIX 288 LOADING GRAPHS OF FEA BIO RID CONFIGURATION L133 - NIC

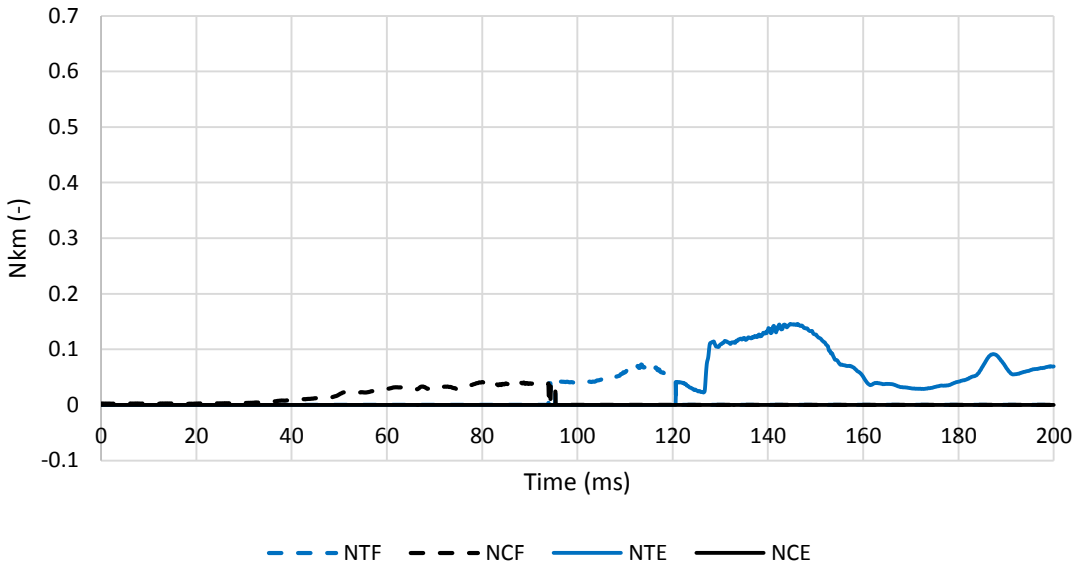


APPENDIX 289 LOADING GRAPHS OF FEA BIO RID CONFIGURATION L133 - NKM

## A.6.9.2. Medium Severity Pulse (IIWPG 16 km/h) M133

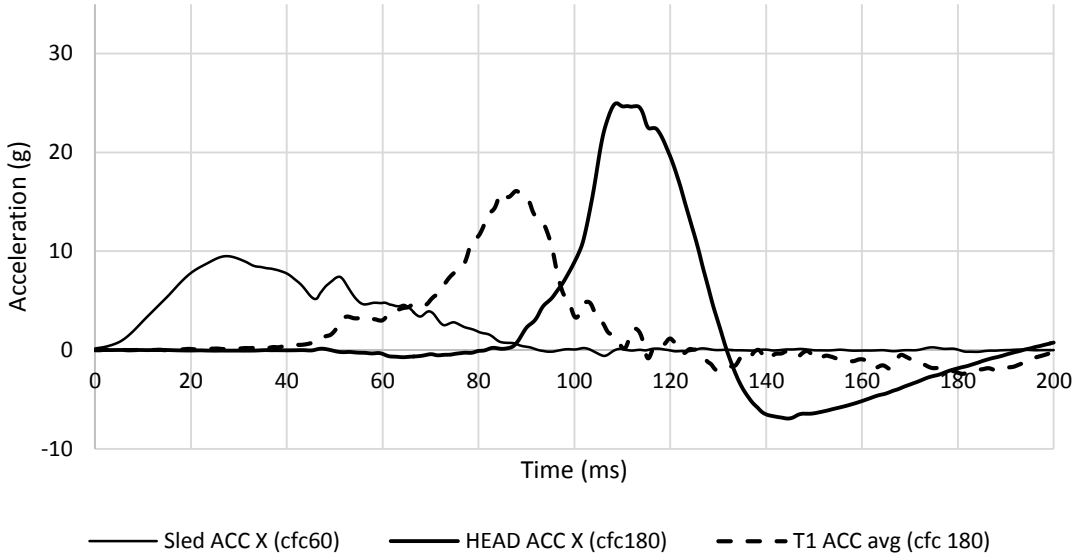


APPENDIX 290 LOADING GRAPHS OF FEA BIO RID CONFIGURATION M133 - ACCELERATION

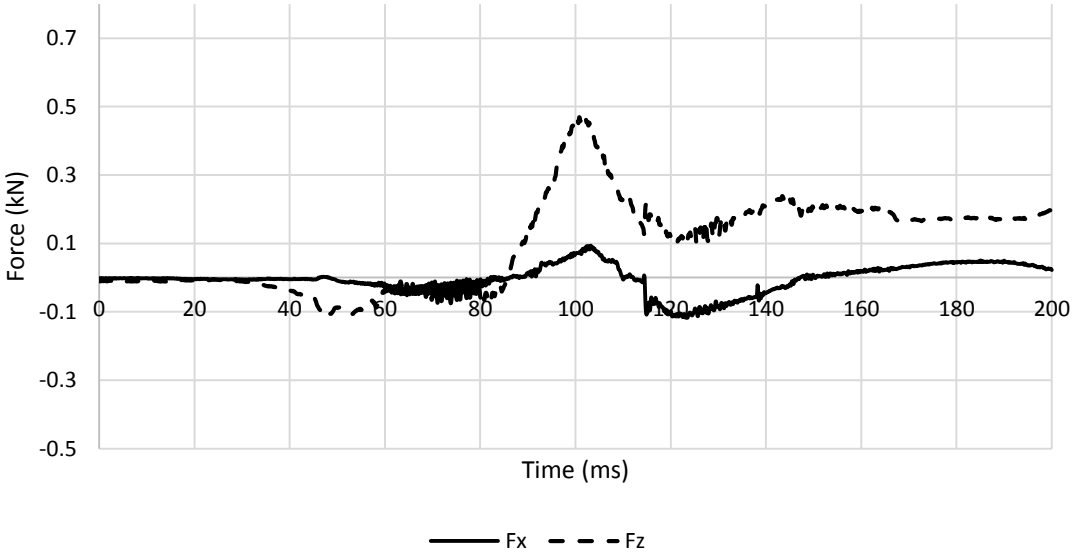


APPENDIX 291 LOADING GRAPHS OF FEA BIO RID CONFIGURATION M133 - FORCE

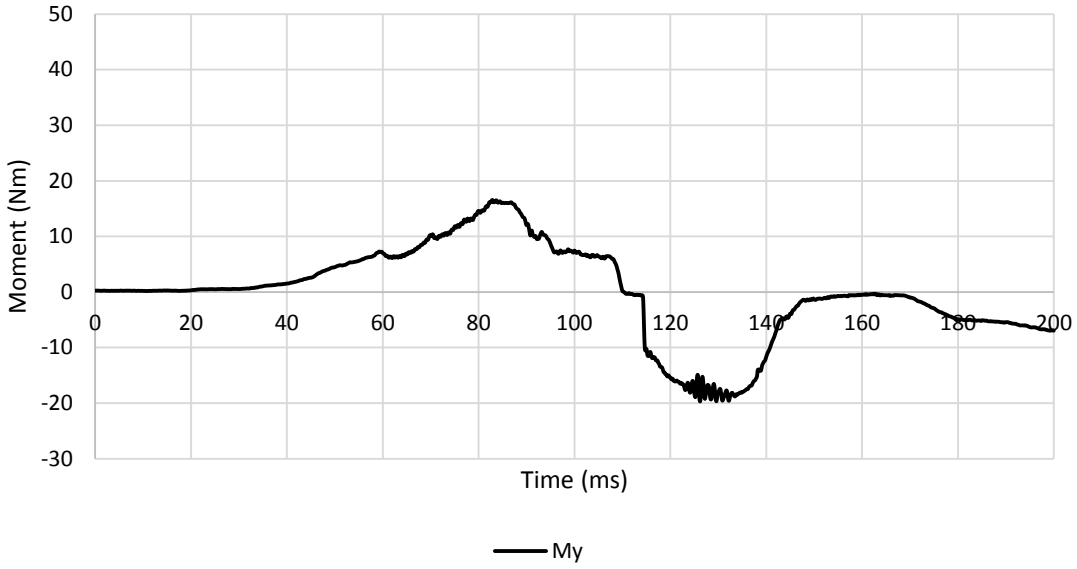


APPENDIX 292 LOADING GRAPHS OF FEA BIO RID CONFIGURATION M133 - MOMENT

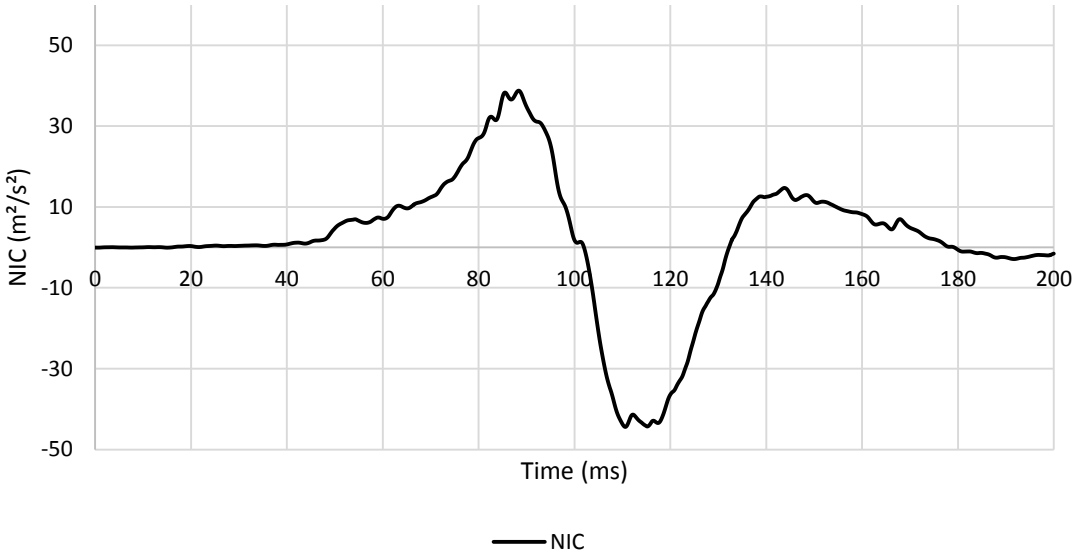


APPENDIX 293 LOADING GRAPHS OF FEA BIO RID CONFIGURATION M133 - NIC

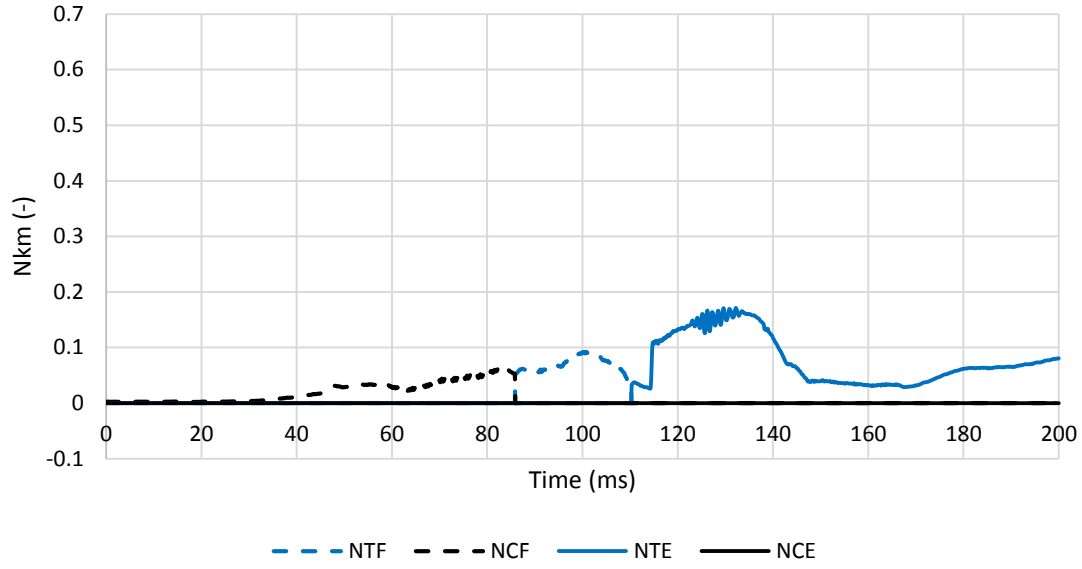


APPENDIX 294 LOADING GRAPHS OF FEA BIO RID CONFIGURATION M133 - NKM

### A.6.9.3. High Severity Pulse (SRA 24 km/h) H133

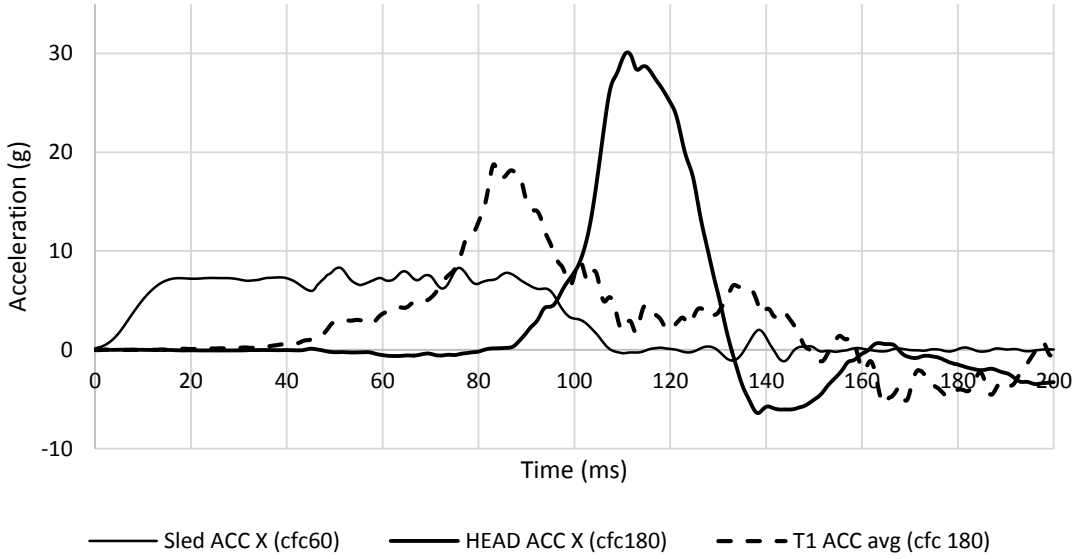


APPENDIX 295 LOADING GRAPHS OF FEA BIO RID CONFIGURATION H133 - ACCELERATION

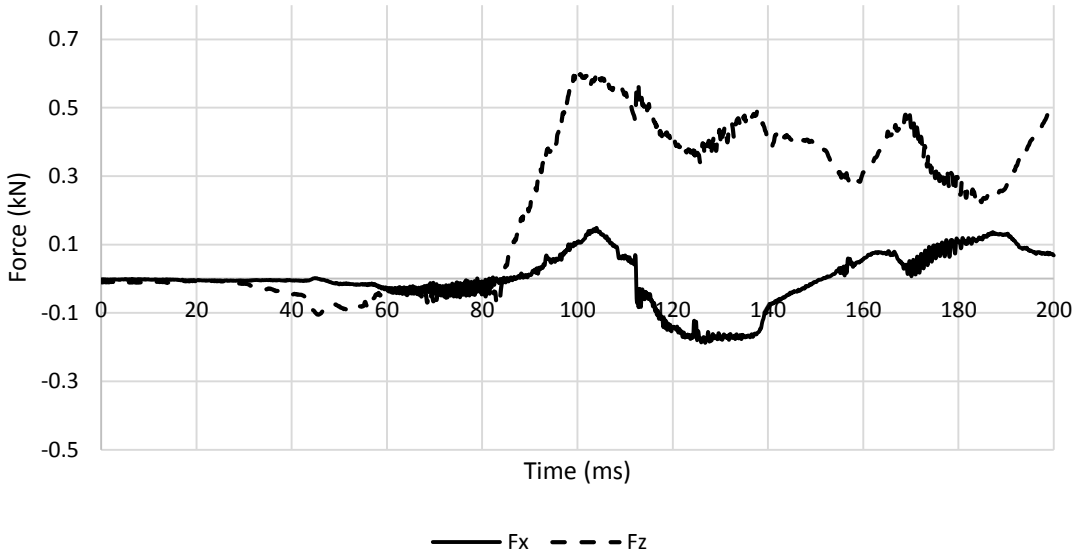


APPENDIX 296 LOADING GRAPHS OF FEA BIO RID CONFIGURATION H133 - FORCE

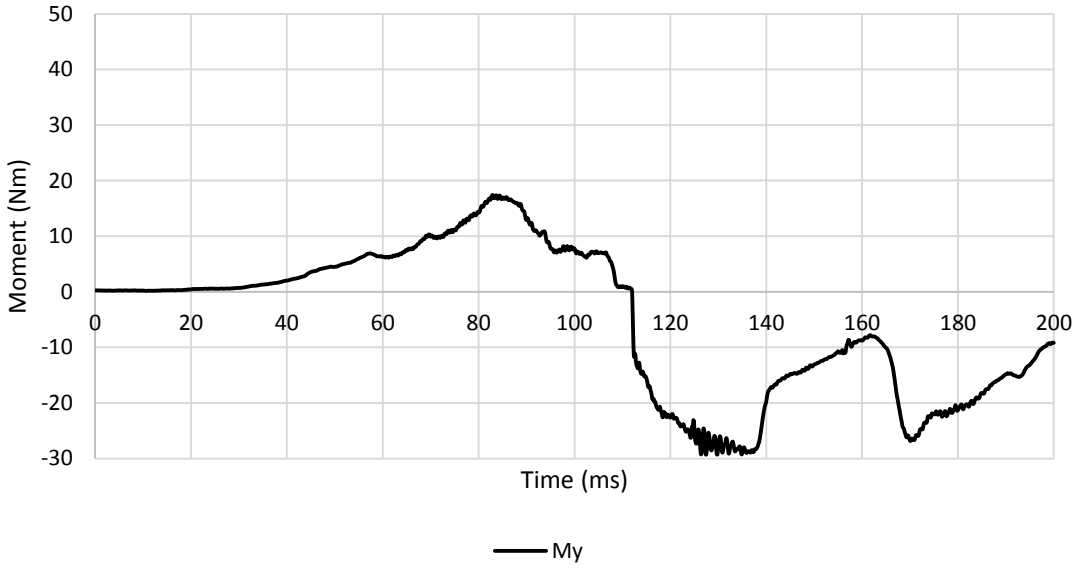


APPENDIX 297 LOADING GRAPHS OF FEA BIO RID CONFIGURATION H133 - MOMENT

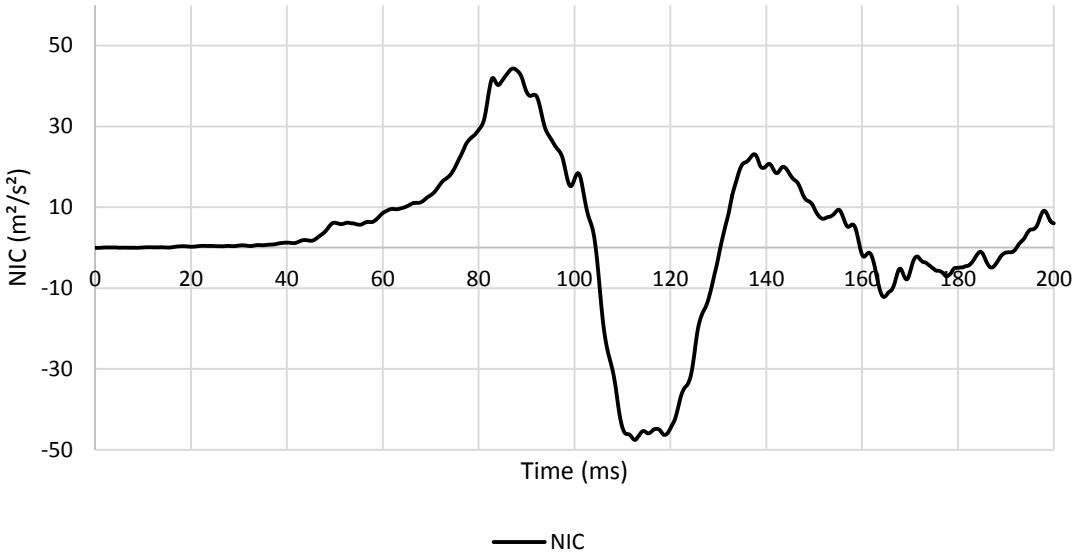


APPENDIX 298 LOADING GRAPHS OF FEA BIO RID CONFIGURATION H133 - NIC

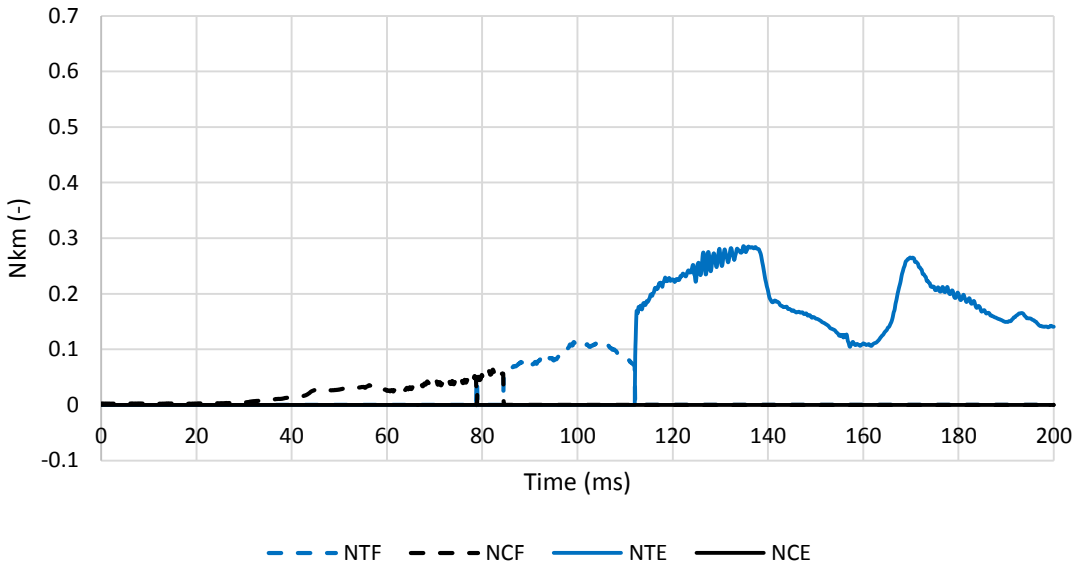


APPENDIX 299 LOADING GRAPHS OF FEA BIO RID CONFIGURATION H133 - NKM

## A.7. Eva RID – generic seat simulations

### A.7.1. Eva RID – forward backrest – high head restraint 211

#### A.7.1.1. Low Severity Pulse (SRA 16 km/h) L211

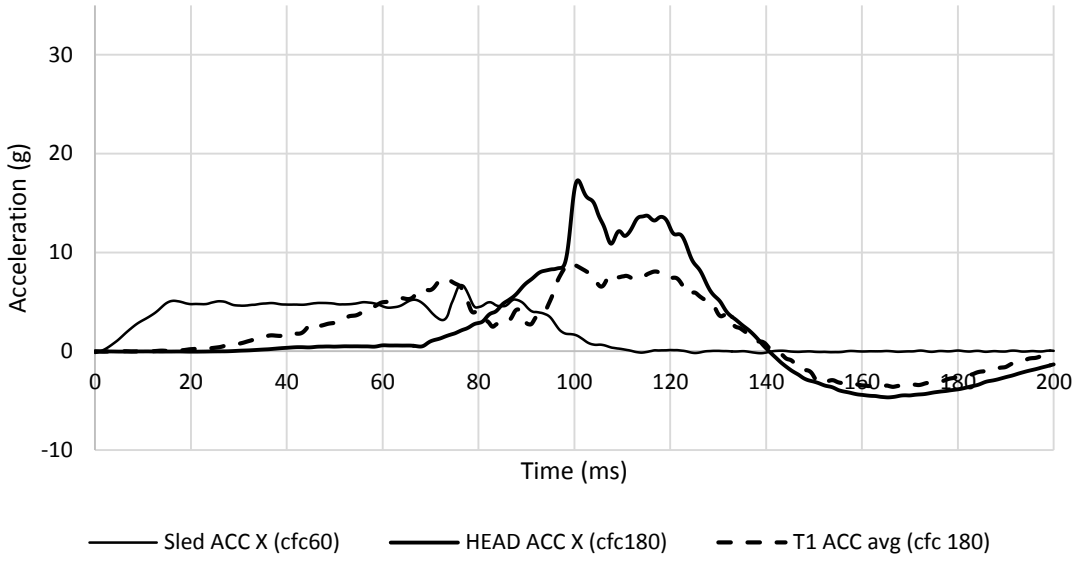


APPENDIX 300 LOADING GRAPHS OF FEA BIO RID CONFIGURATION L211 - ACCELERATION

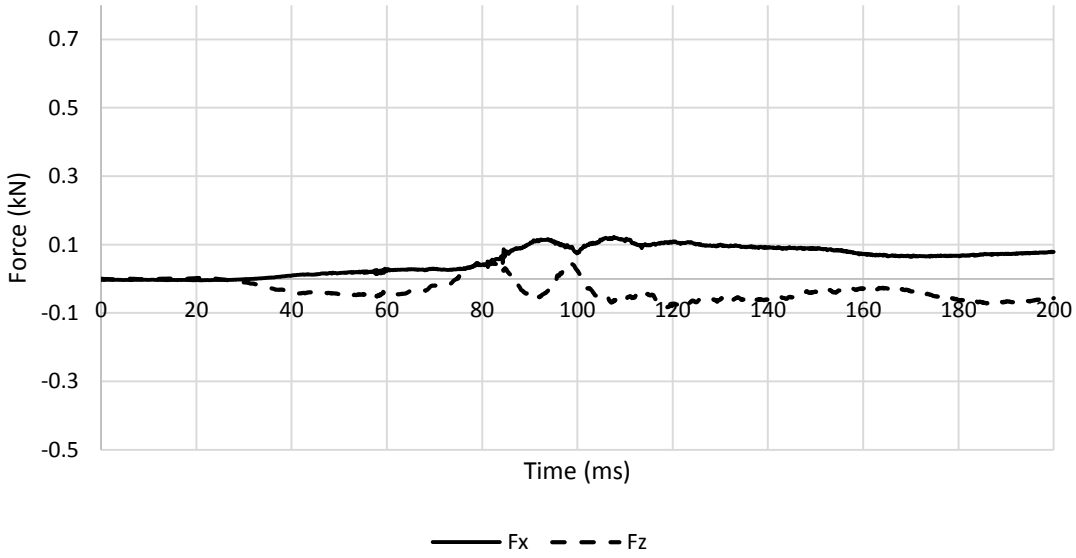


APPENDIX 301 LOADING GRAPHS OF FEA BIO RID CONFIGURATION L211 - FORCE

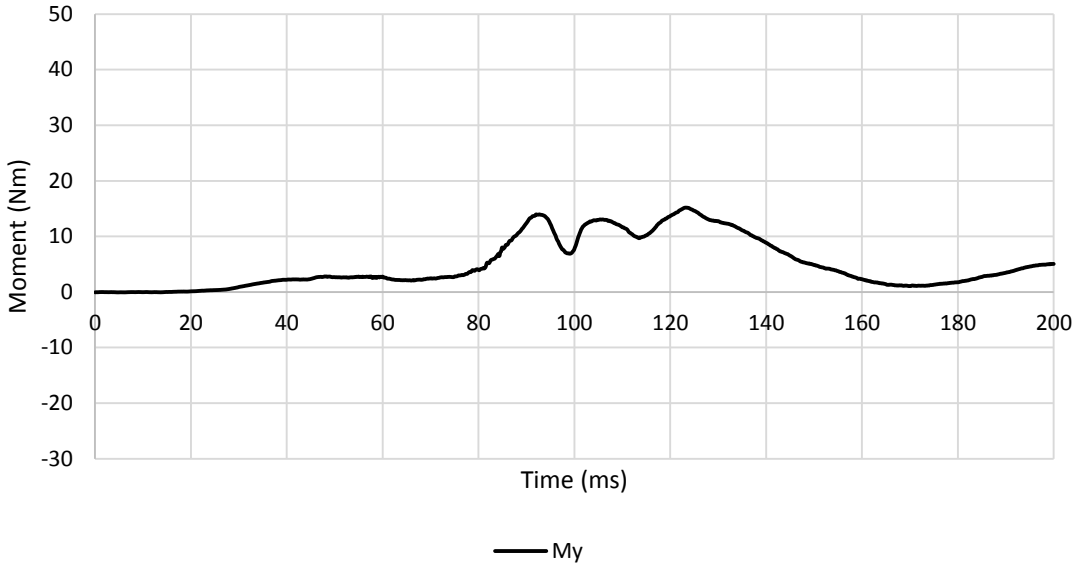


APPENDIX 302 LOADING GRAPHS OF FEA BIO RID CONFIGURATION L211 - MOMENT

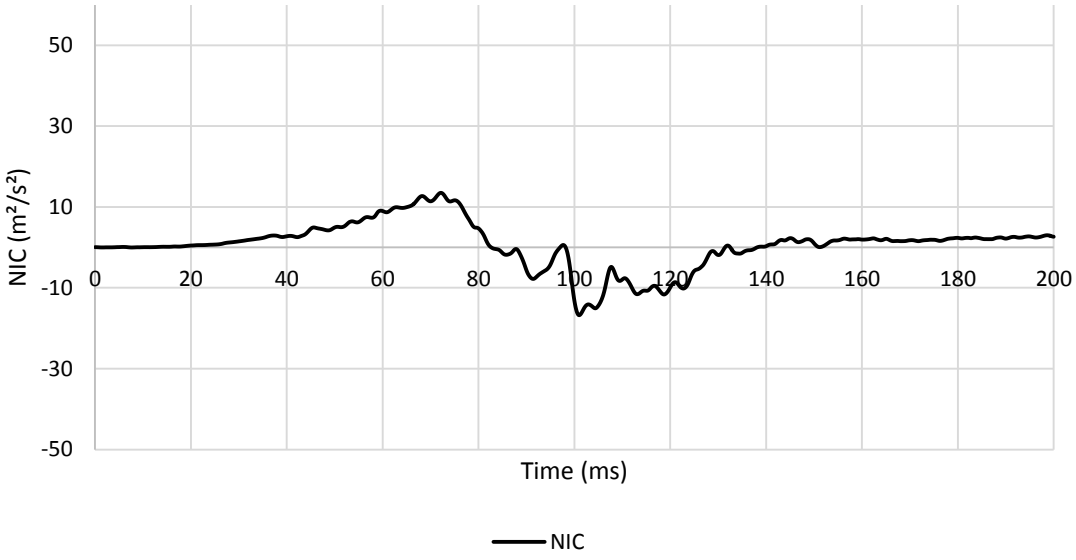


APPENDIX 303 LOADING GRAPHS OF FEA BIO RID CONFIGURATION L211 - NIC

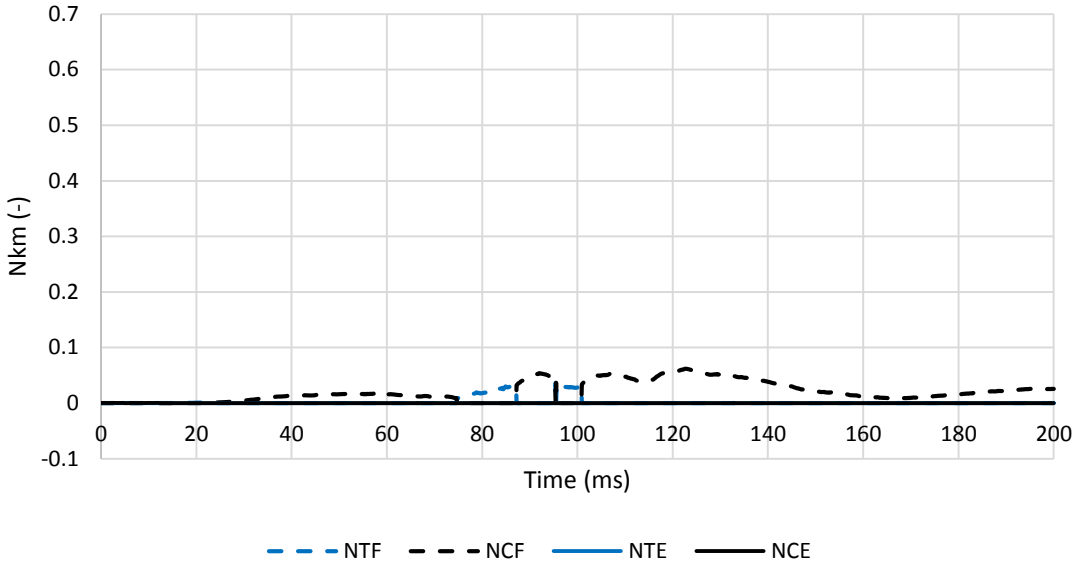


APPENDIX 304 LOADING GRAPHS OF FEA BIO RID CONFIGURATION L211 - NKM

### A.7.1.2. Medium Severity Pulse (IIWPG 16 km/h) M211

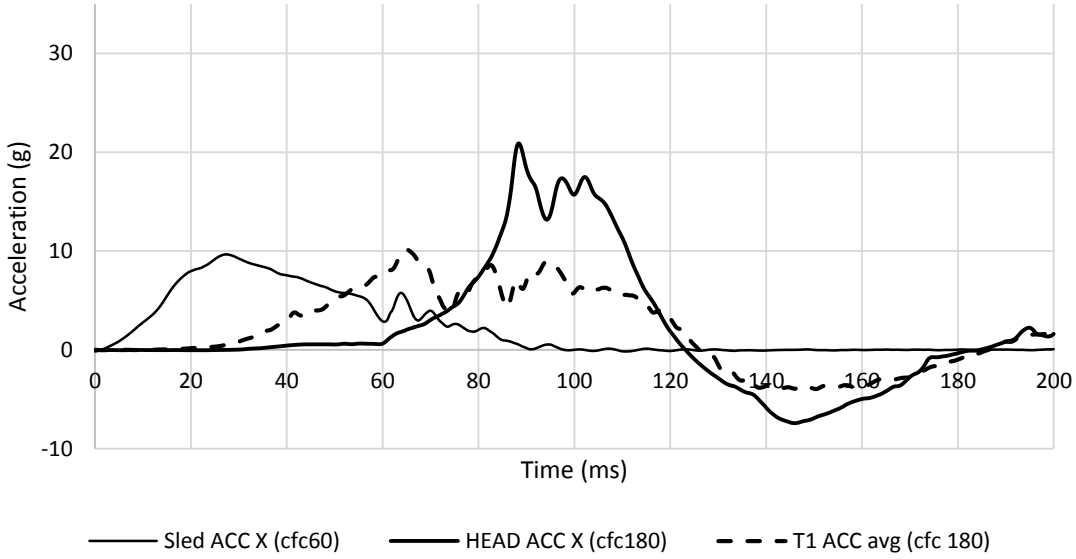


APPENDIX 305 LOADING GRAPHS OF FEA BIO RID CONFIGURATION M211 - ACCELERATION

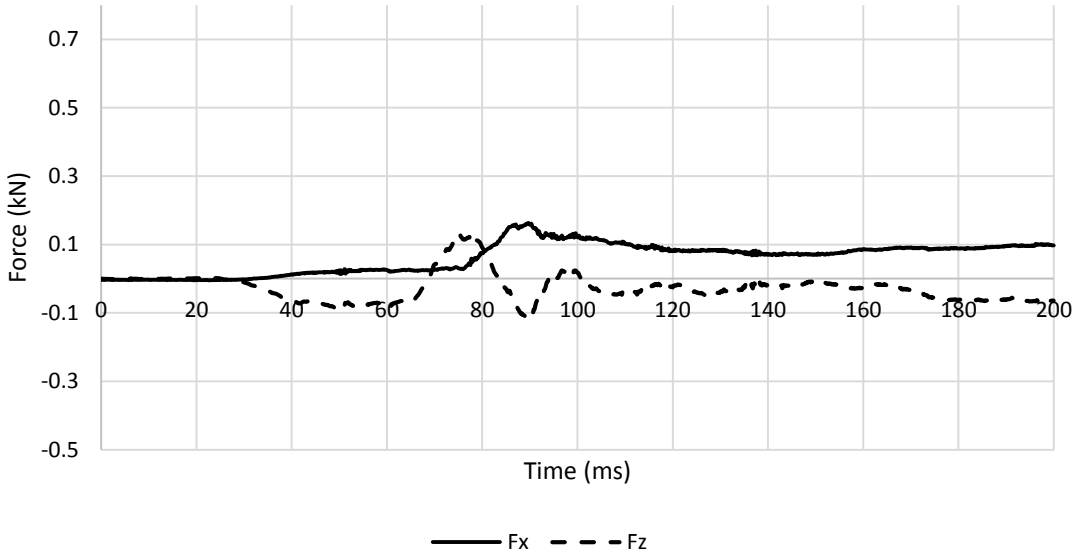


APPENDIX 306 LOADING GRAPHS OF FEA BIO RID CONFIGURATION M211 - FORCE

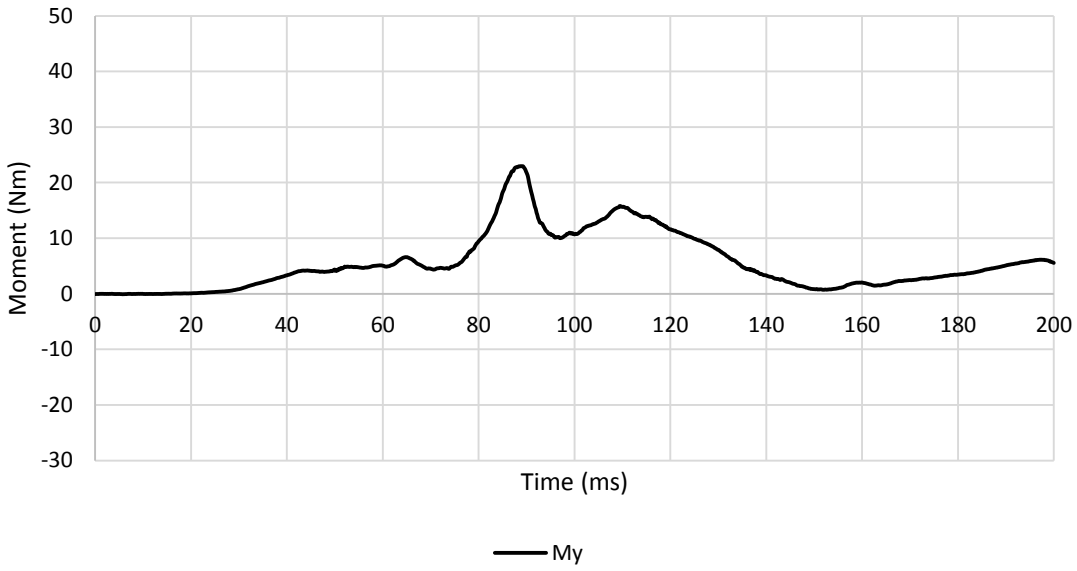


APPENDIX 307 LOADING GRAPHS OF FEA BIO RID CONFIGURATION M211 - MOMENT

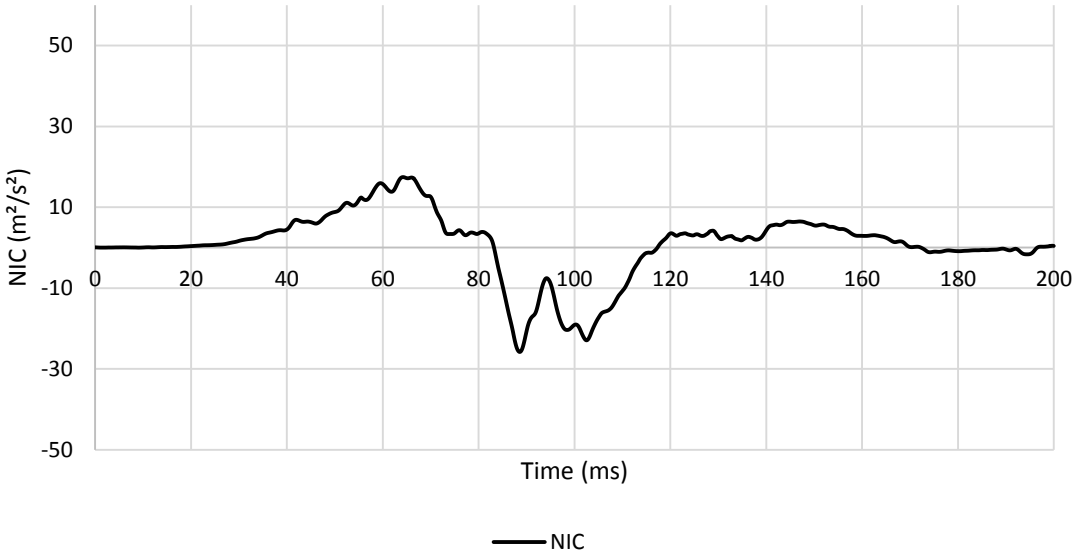


APPENDIX 308 LOADING GRAPHS OF FEA BIO RID CONFIGURATION M211 - NIC

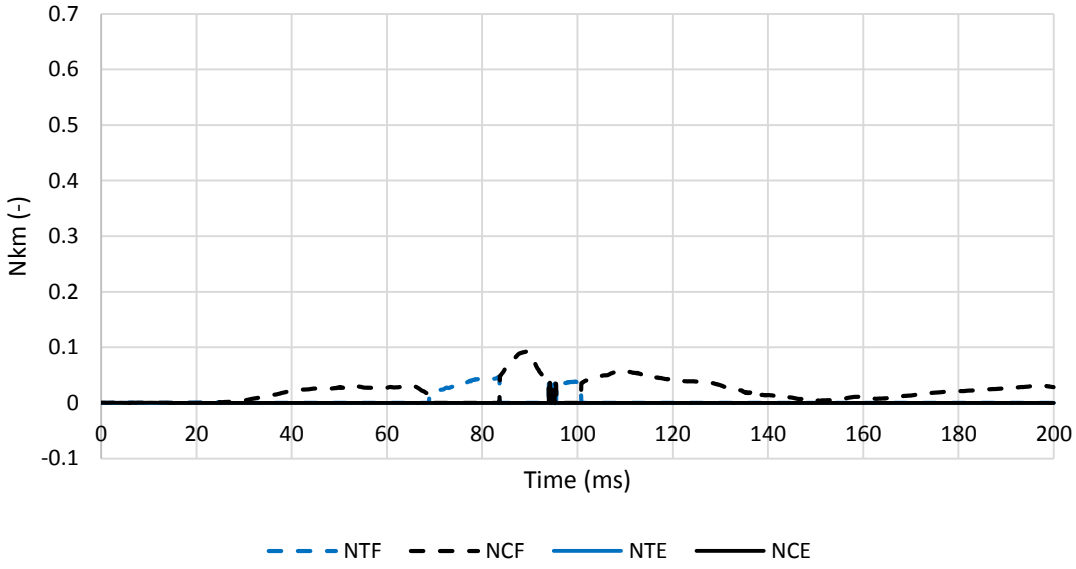


APPENDIX 309 LOADING GRAPHS OF FEA BIO RID CONFIGURATION M211 - NKM

### A.7.1.3. High Severity Pulse (SRA 24 km/h) H211

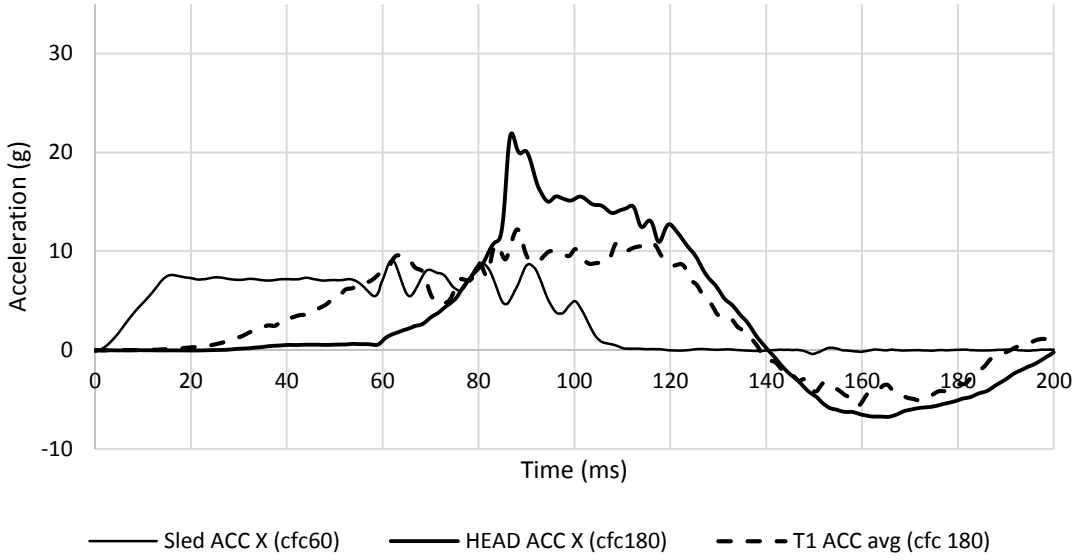


APPENDIX 310 LOADING GRAPHS OF FEA BIO RID CONFIGURATION H211 - ACCELERATION

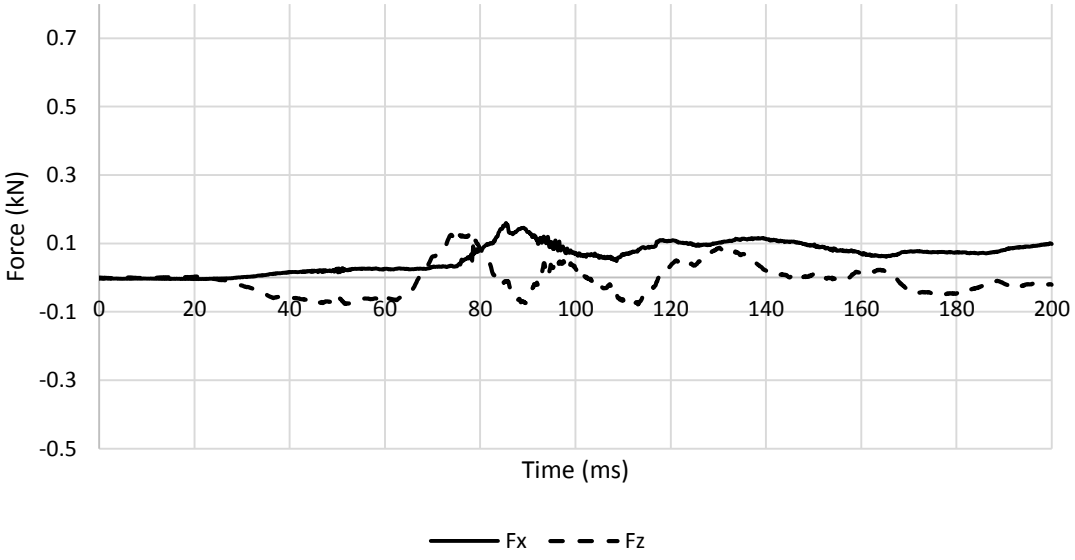


APPENDIX 311 LOADING GRAPHS OF FEA BIO RID CONFIGURATION H211 - FORCE

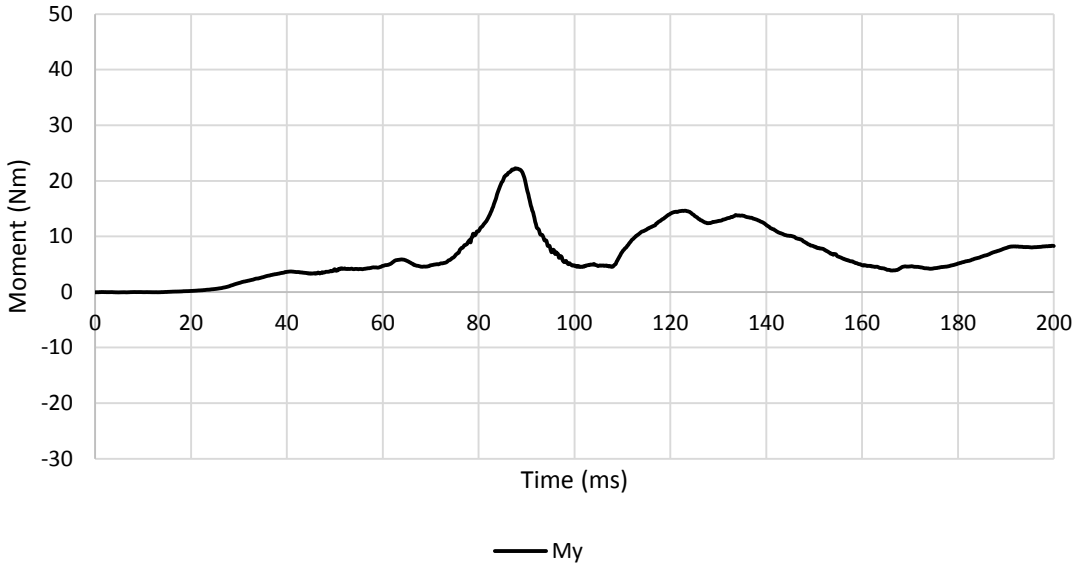


APPENDIX 312 LOADING GRAPHS OF FEA BIO RID CONFIGURATION H211 - MOMENT

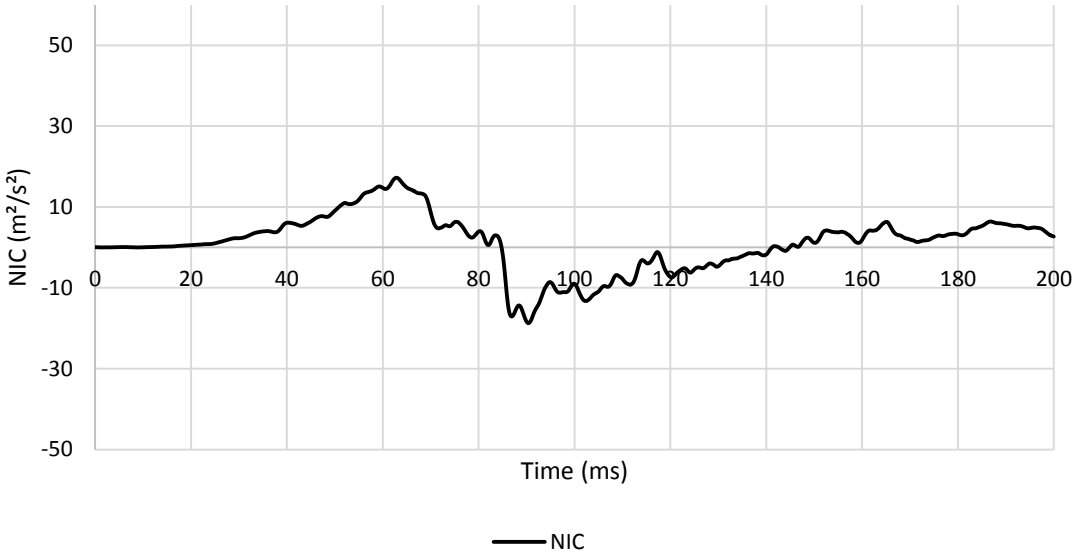


APPENDIX 313 LOADING GRAPHS OF FEA BIO RID CONFIGURATION H211 - NIC

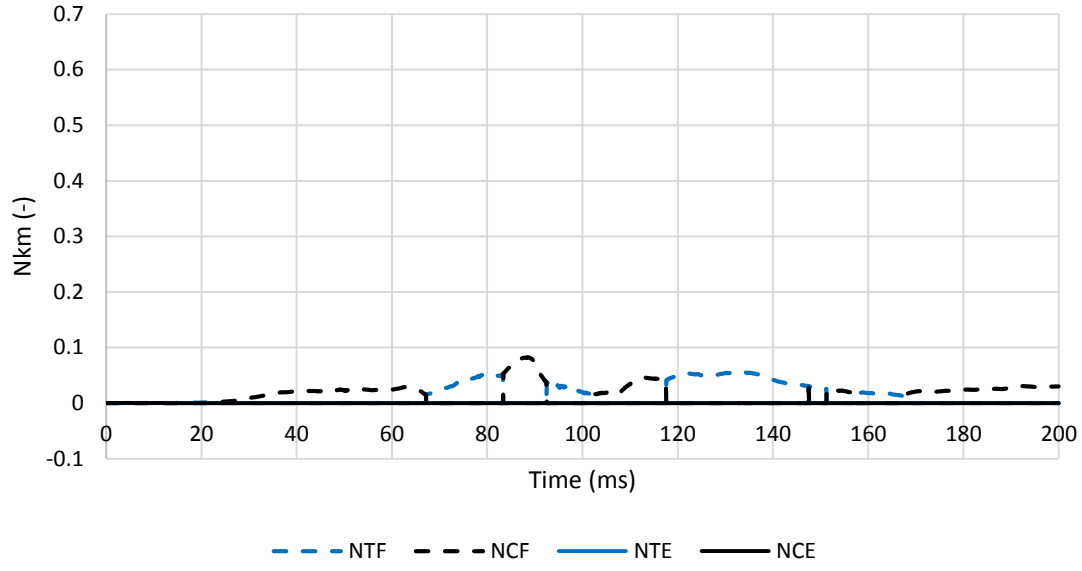


APPENDIX 314 LOADING GRAPHS OF FEA BIO RID CONFIGURATION H211 - NKM

## A.7.2. Eva RID – forward backrest – middle head restraint 212

### A.7.2.1. Low Severity Pulse (SRA 16 km/h) L212

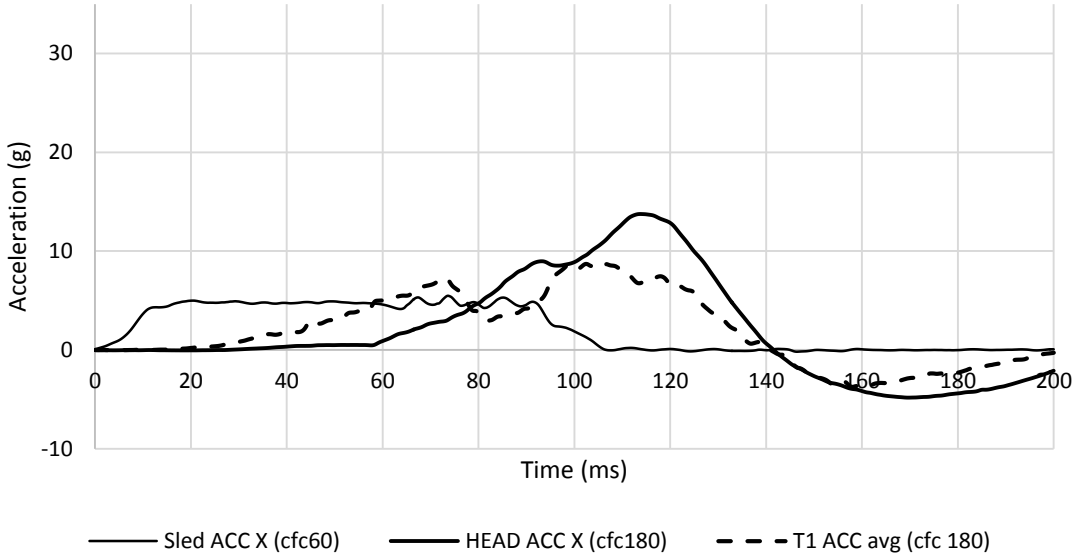


APPENDIX 315 LOADING GRAPHS OF FEA EVA RID CONFIGURATION L212 - ACCELERATION

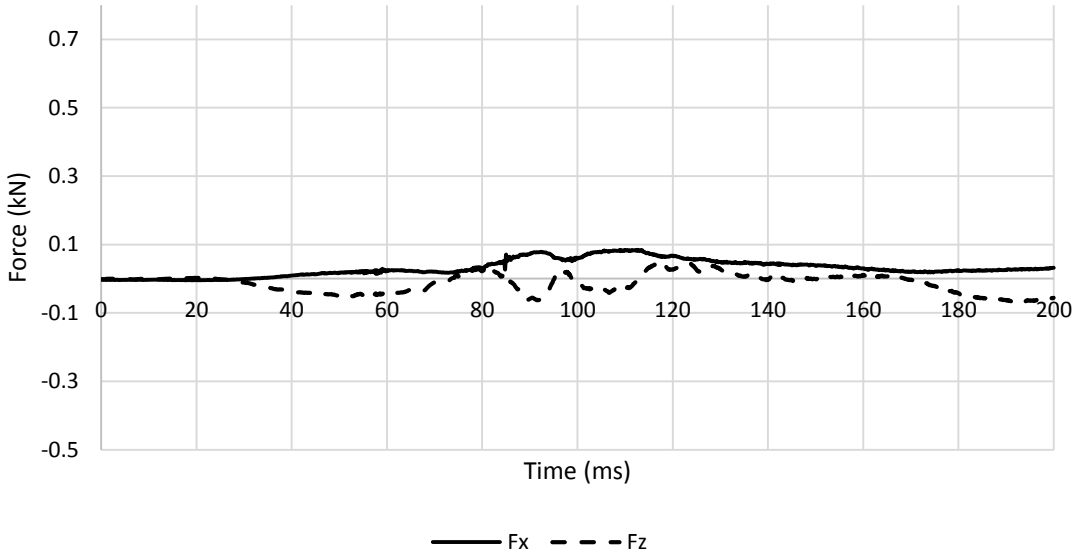


APPENDIX 316 LOADING GRAPHS OF FEA EVA RID CONFIGURATION L212 - FORCE

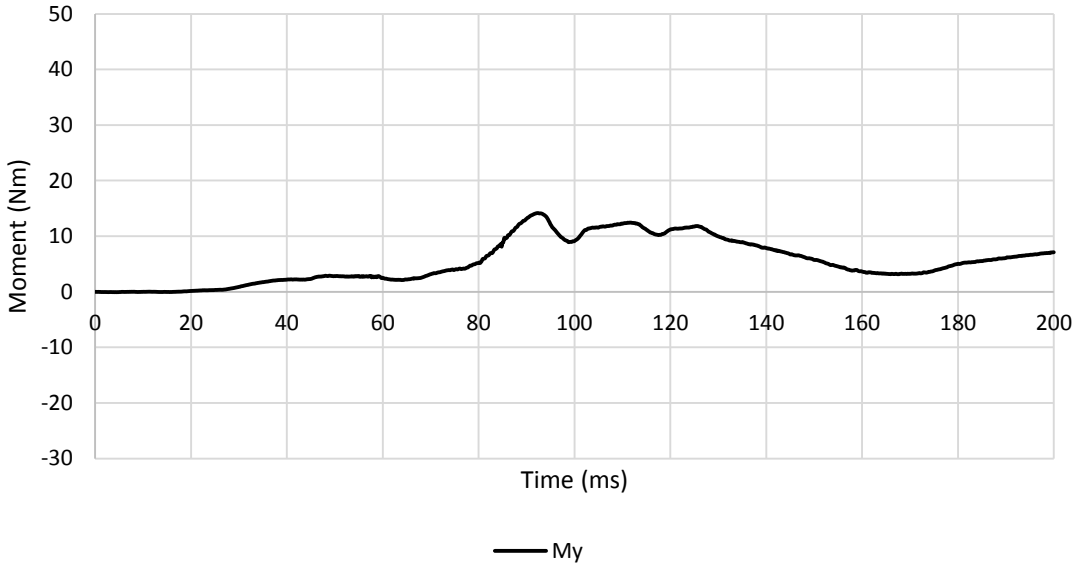


APPENDIX 317 LOADING GRAPHS OF FEA EVA RID CONFIGURATION L212 - MOMENT

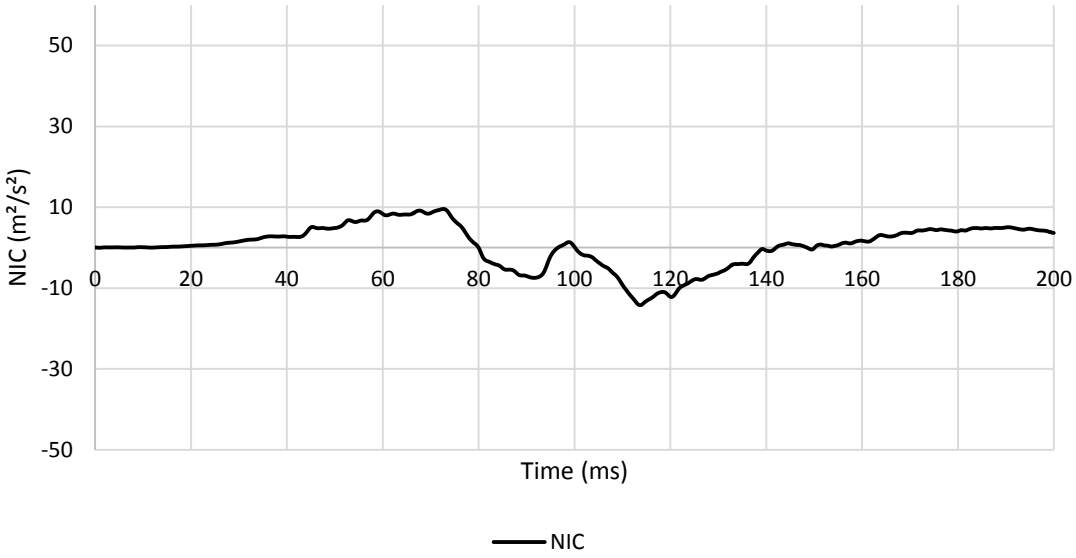


APPENDIX 318 LOADING GRAPHS OF FEA EVA RID CONFIGURATION L212 - NIC

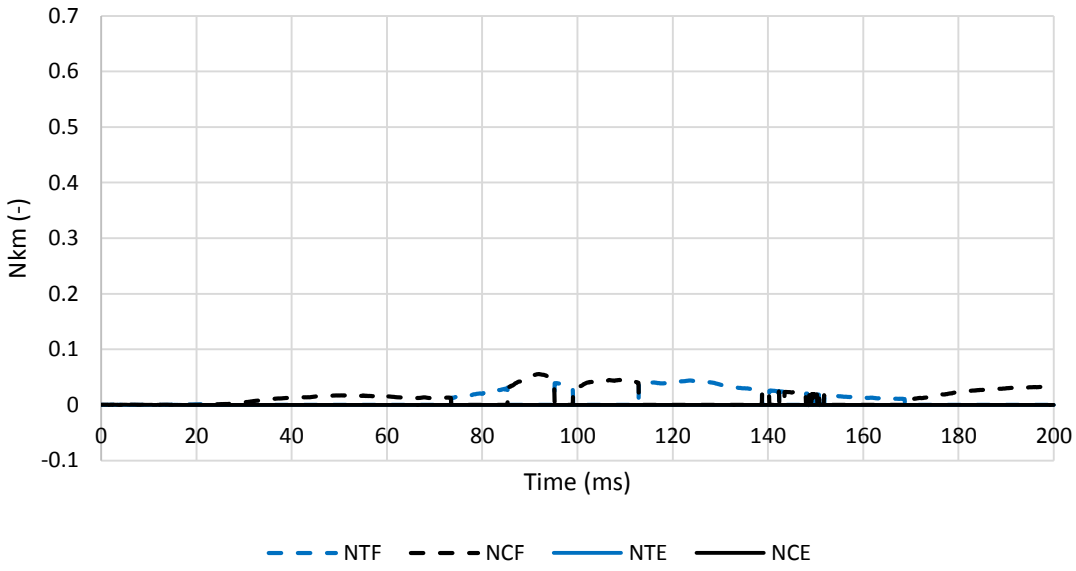


APPENDIX 319 LOADING GRAPHS OF FEA EVA RID CONFIGURATION L212 - NKM

## A.7.2.2. Medium Severity Pulse (IIWPG 16 km/h) M212

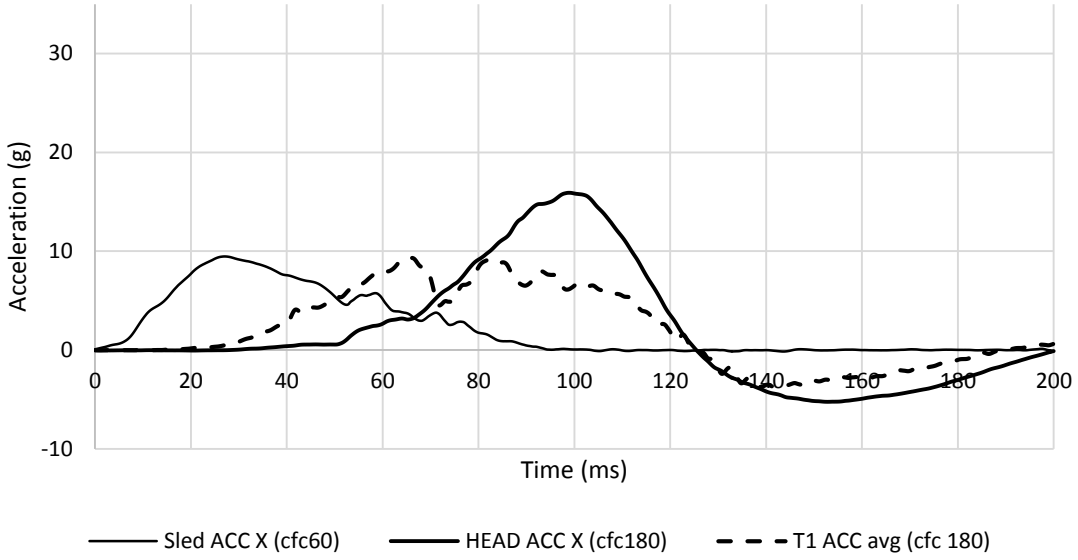


APPENDIX 320 LOADING GRAPHS OF FEA EVA RID CONFIGURATION M212 - ACCELERATION

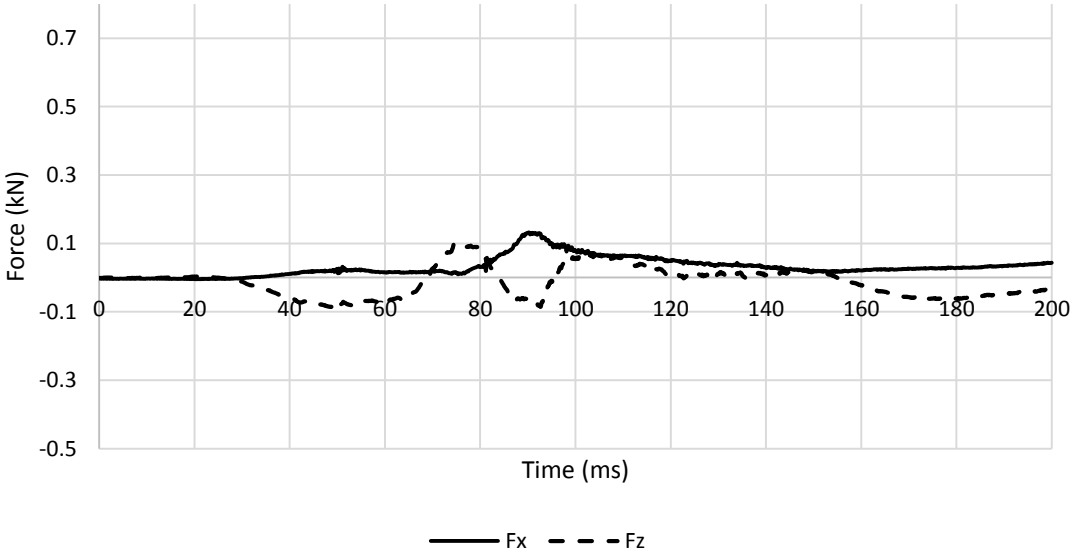


APPENDIX 321 LOADING GRAPHS OF FEA EVA RID CONFIGURATION M212 - FORCE

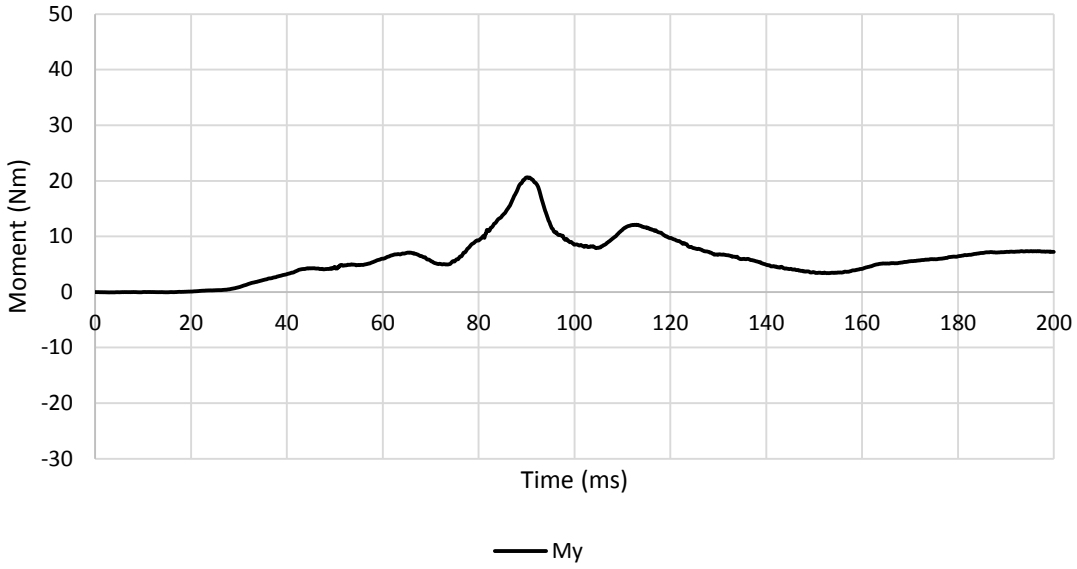


APPENDIX 322 LOADING GRAPHS OF FEA EVA RID CONFIGURATION M212 - MOMENT

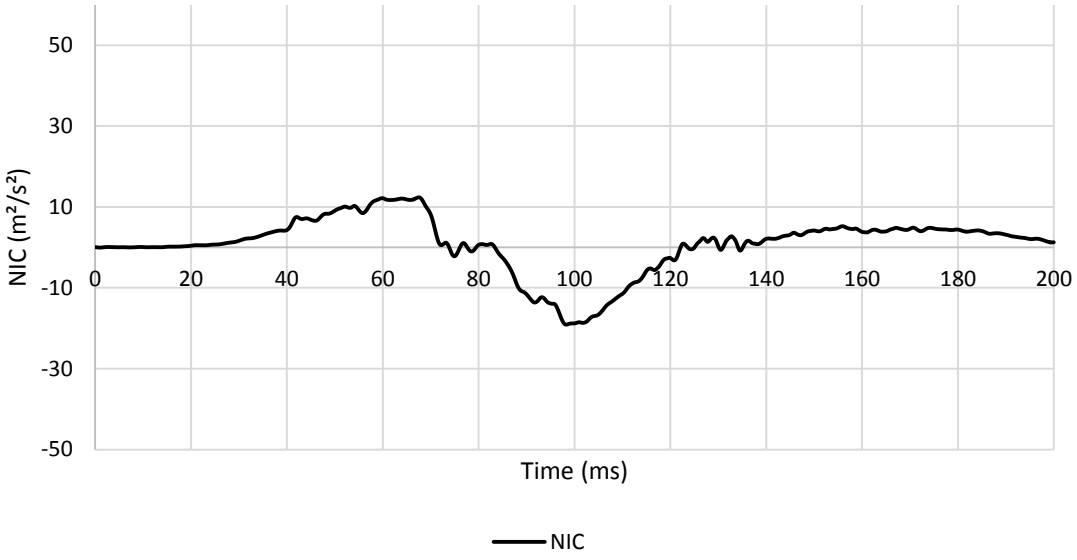


APPENDIX 323 LOADING GRAPHS OF FEA EVA RID CONFIGURATION M212 - NIC

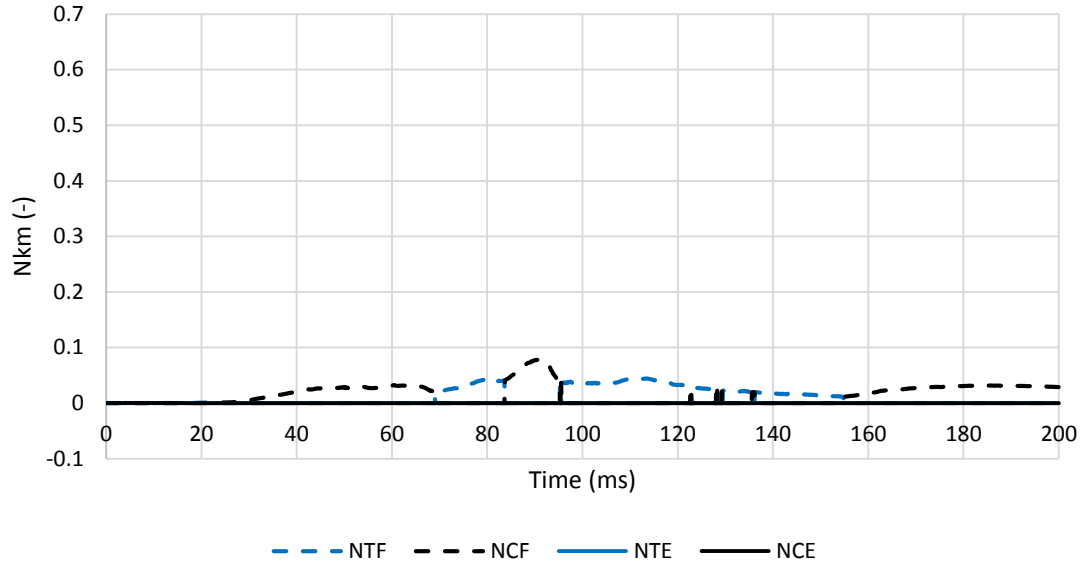


APPENDIX 324 LOADING GRAPHS OF FEA EVA RID CONFIGURATION M212 - NKM

### A.7.2.3. High Severity Pulse (SRA 24 km/h) H212

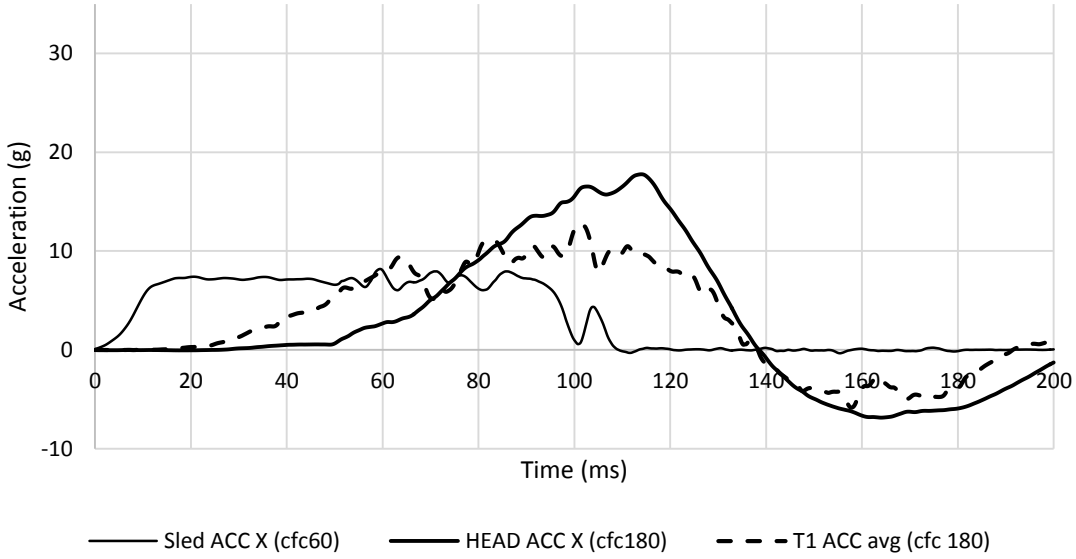


APPENDIX 325 LOADING GRAPHS OF FEA EVA RID CONFIGURATION H212 - ACCELERATION

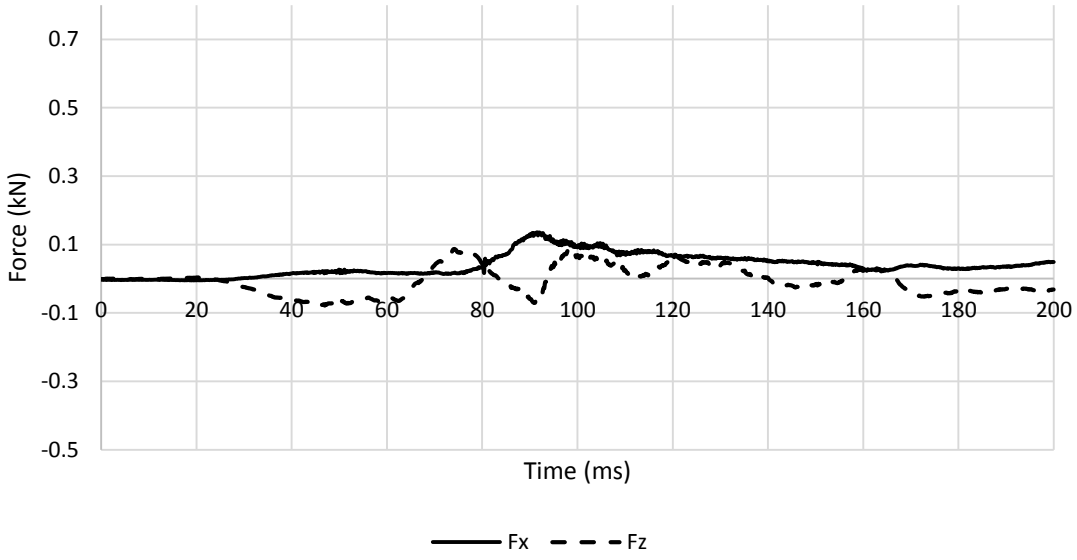


APPENDIX 326 LOADING GRAPHS OF FEA EVA RID CONFIGURATION H212 - FORCE

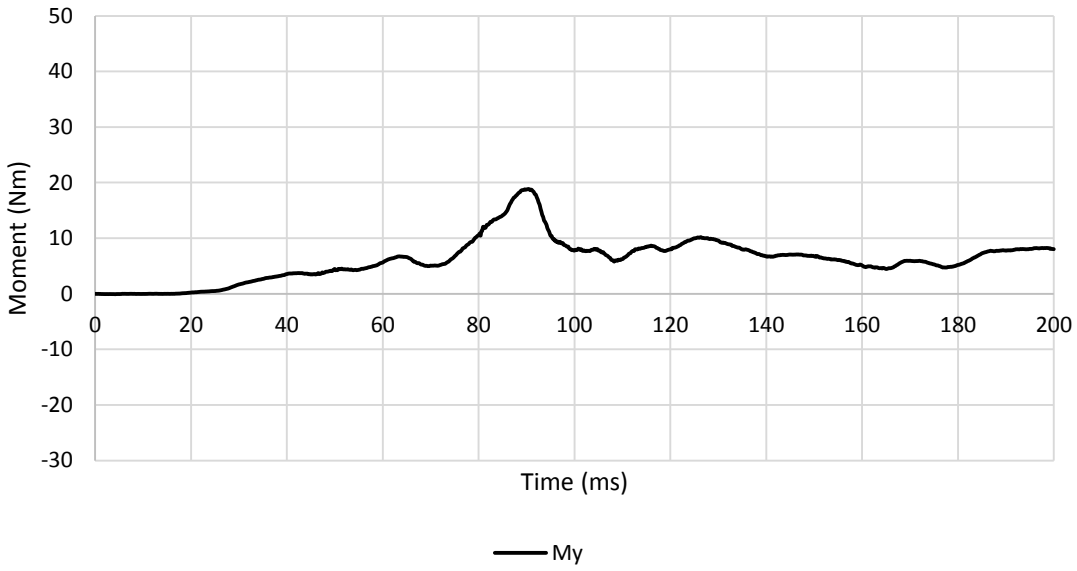


APPENDIX 327 LOADING GRAPHS OF FEA EVA RID CONFIGURATION H212 - MOMENT

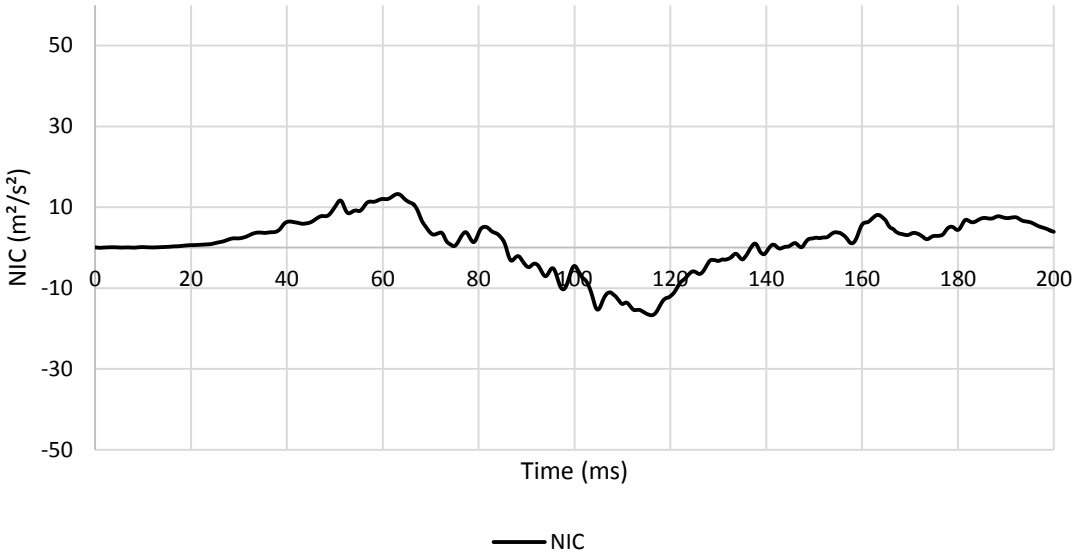


APPENDIX 328 LOADING GRAPHS OF FEA EVA RID CONFIGURATION H212 - NIC

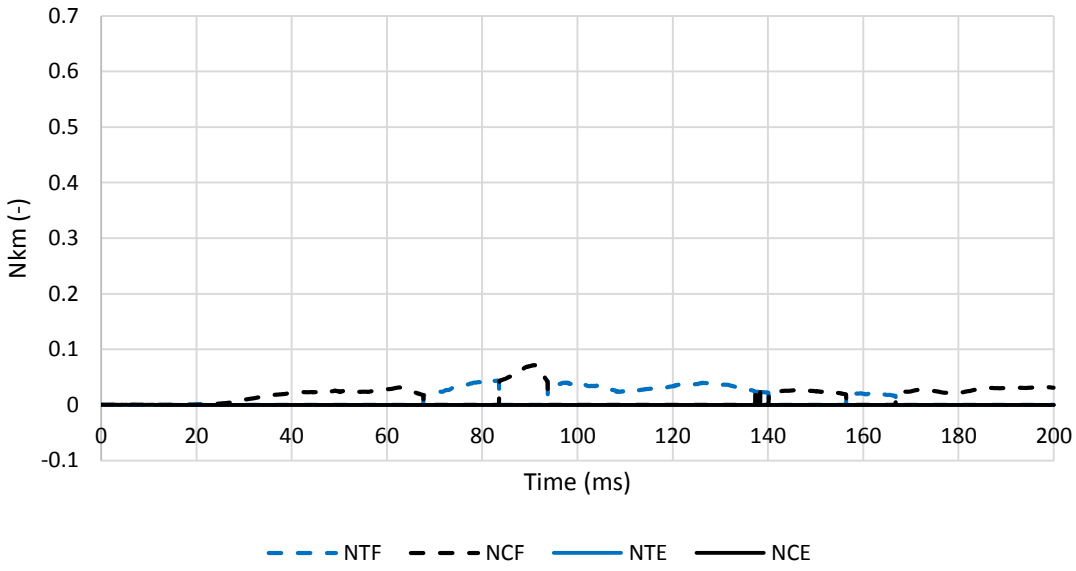


APPENDIX 329 LOADING GRAPHS OF FEA EVA RID CONFIGURATION H212 - NKM

## A.7.3. Eva RID – forward backrest – low head restraint 213

### A.7.3.1. Low Severity Pulse (SRA 16 km/h) L213

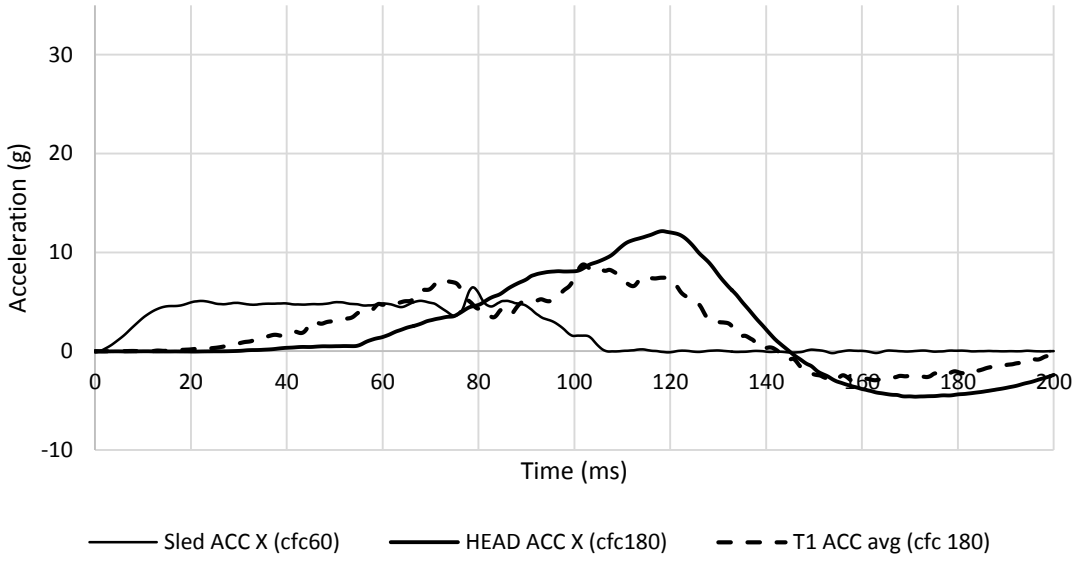


APPENDIX 330 LOADING GRAPHS OF FEA EVA RID CONFIGURATION L213 - ACCELERATION

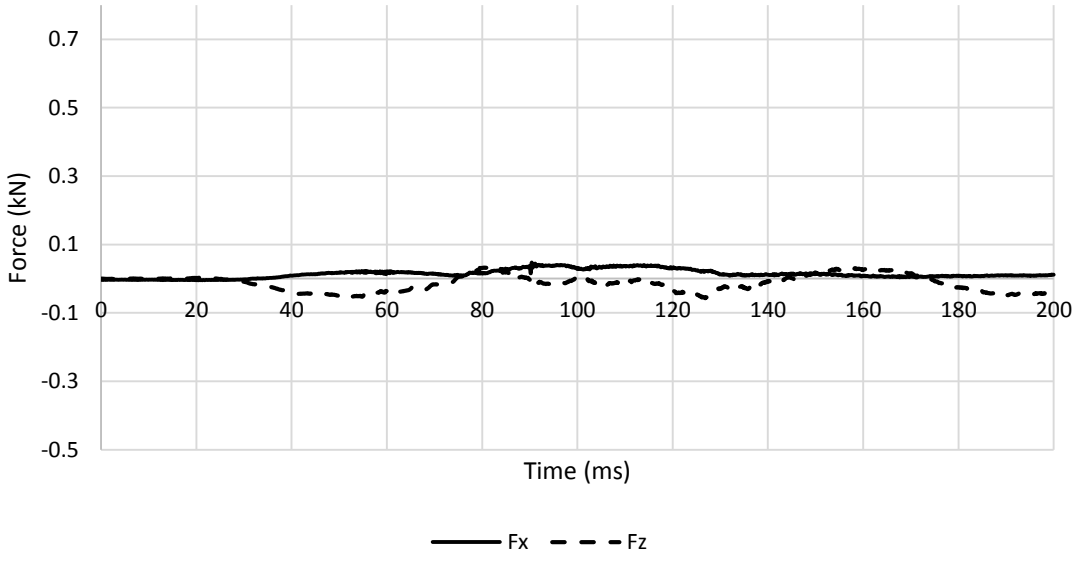


APPENDIX 331 LOADING GRAPHS OF FEA EVA RID CONFIGURATION L213 - FORCE

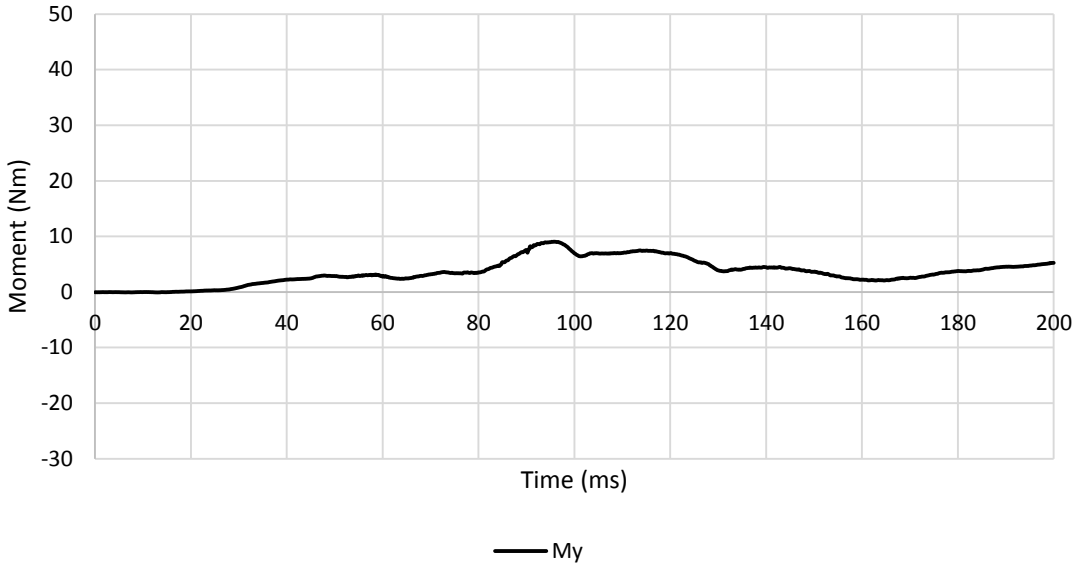


APPENDIX 332 LOADING GRAPHS OF FEA EVA RID CONFIGURATION L213 - MOMENT

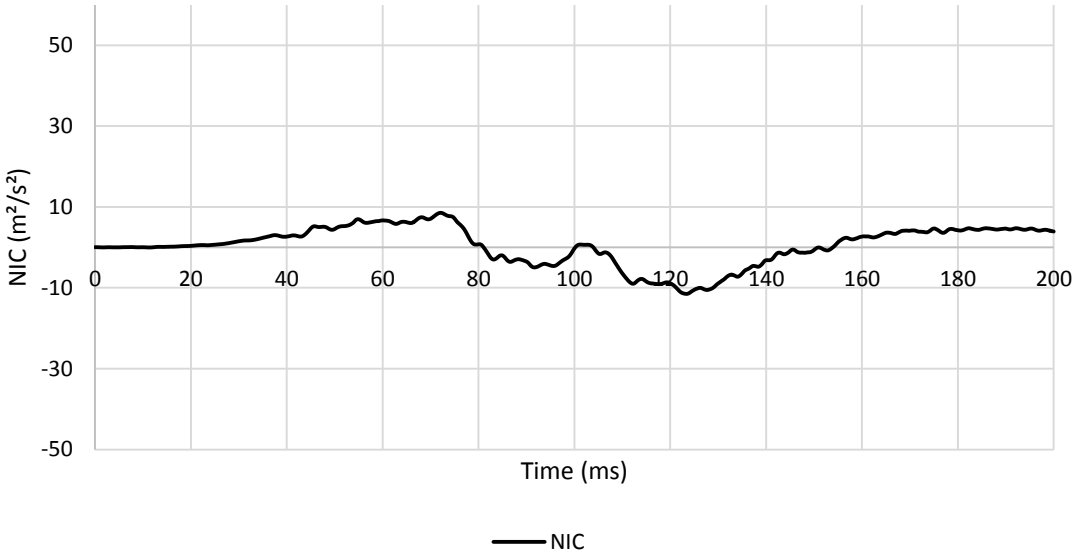


APPENDIX 333 LOADING GRAPHS OF FEA EVA RID CONFIGURATION L213 - NIC

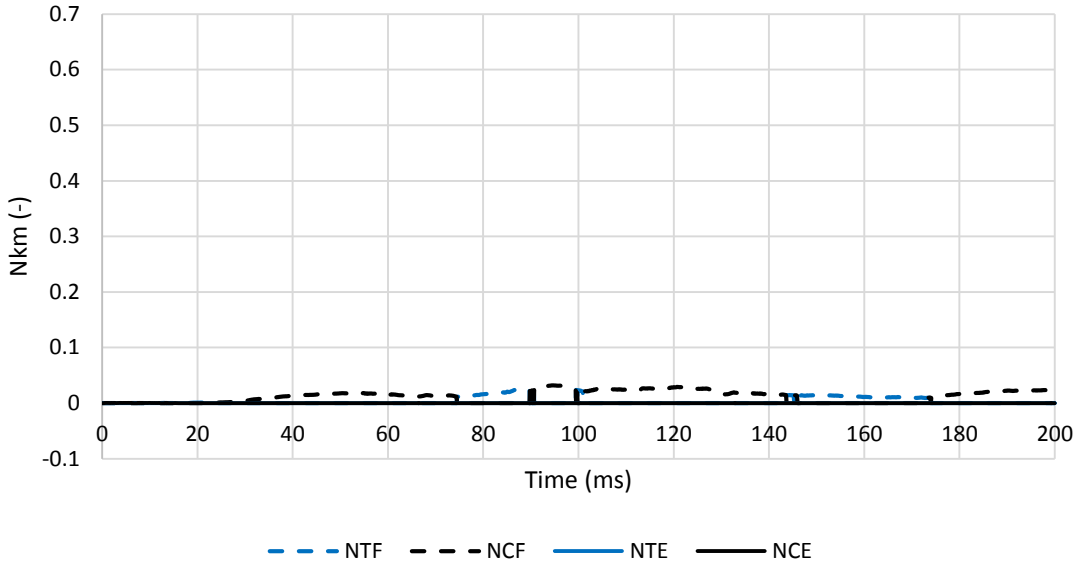


APPENDIX 334 LOADING GRAPHS OF FEA EVA RID CONFIGURATION L213 - NKM

### A.7.3.2. Medium Severity Pulse (IIWPG 16 km/h) M213

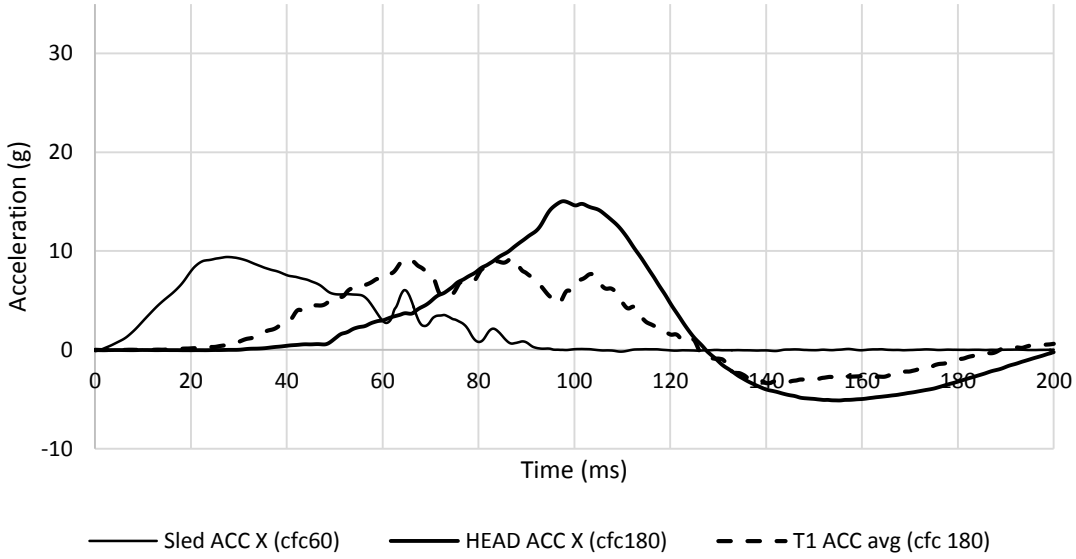


APPENDIX 335 LOADING GRAPHS OF FEA EVA RID CONFIGURATION M213 - ACCELERATION

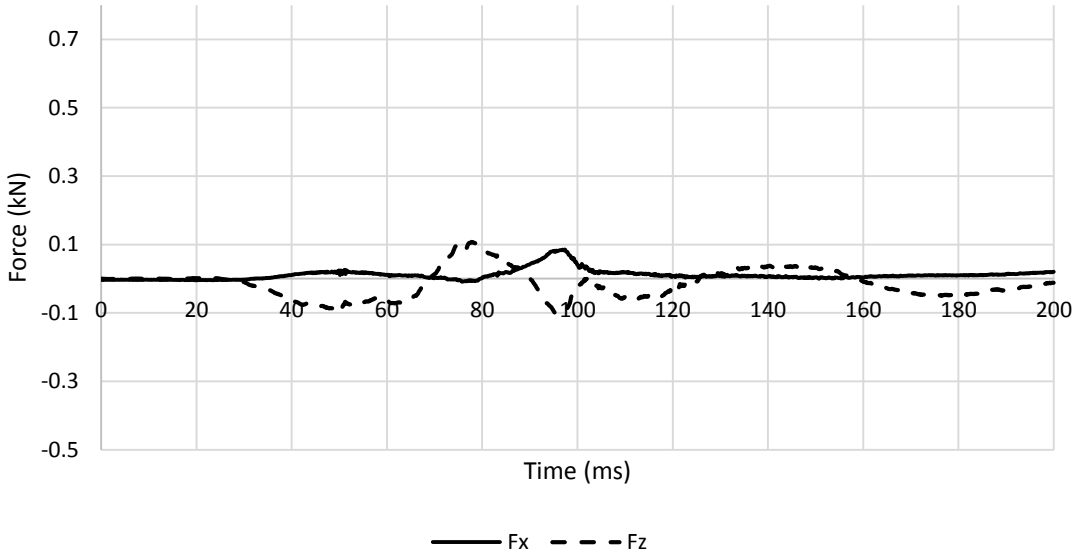


APPENDIX 336 LOADING GRAPHS OF FEA EVA RID CONFIGURATION M213 - FORCE

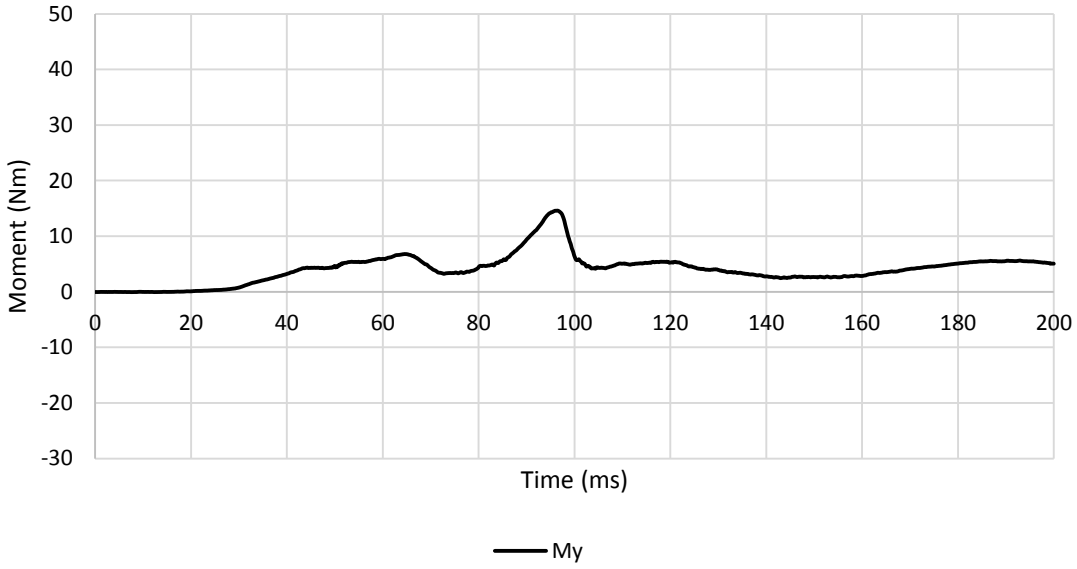


APPENDIX 337 LOADING GRAPHS OF FEA EVA RID CONFIGURATION M213 MOMENT

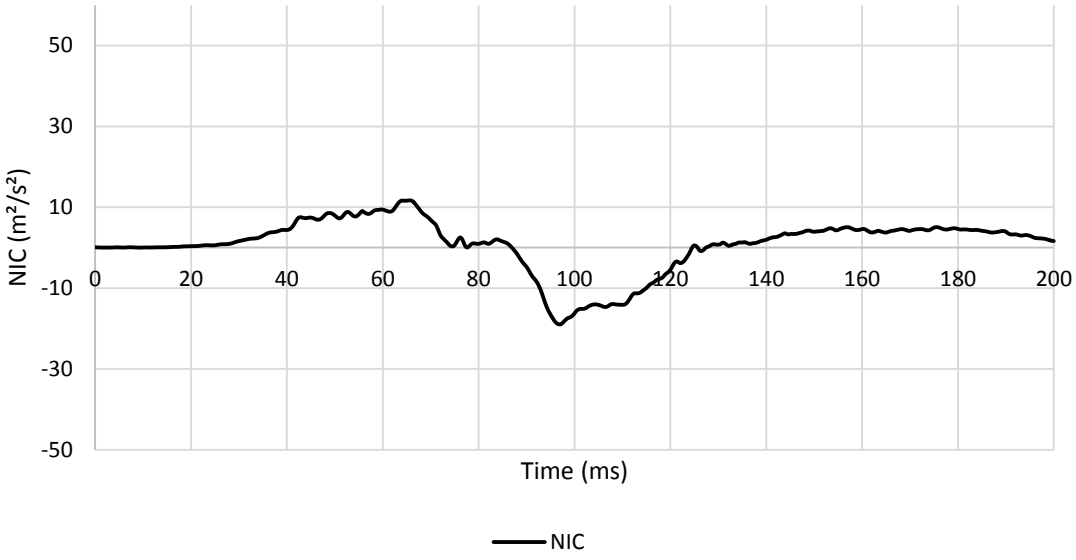


APPENDIX 338 LOADING GRAPHS OF FEA EVA RID CONFIGURATION M213 - NIC

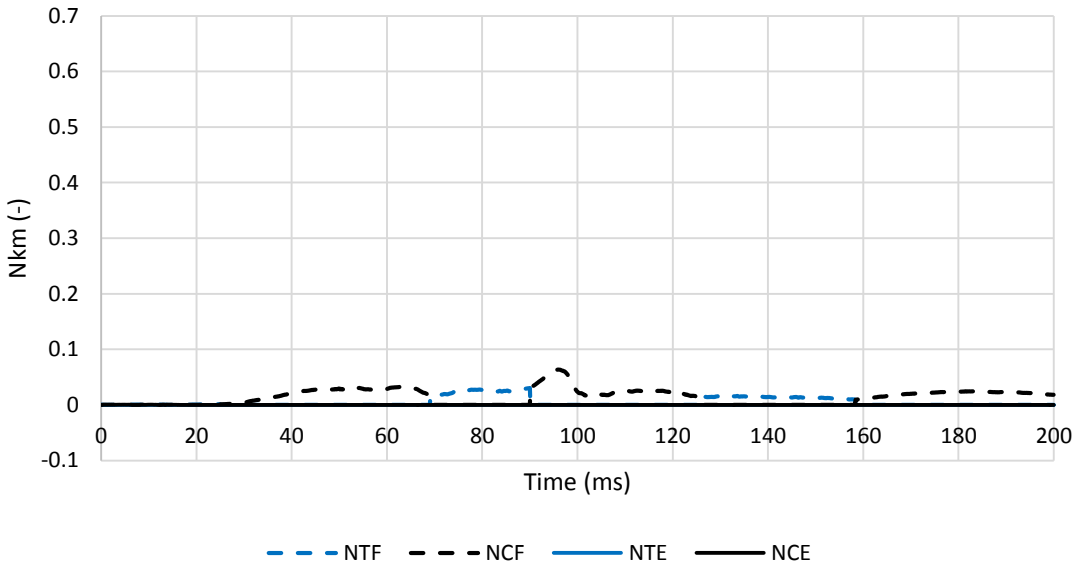


APPENDIX 339 LOADING GRAPHS OF FEA EVA RID CONFIGURATION M213 - NKM

## A.7.3.3. High Severity Pulse (SRA 24 km/h) H213

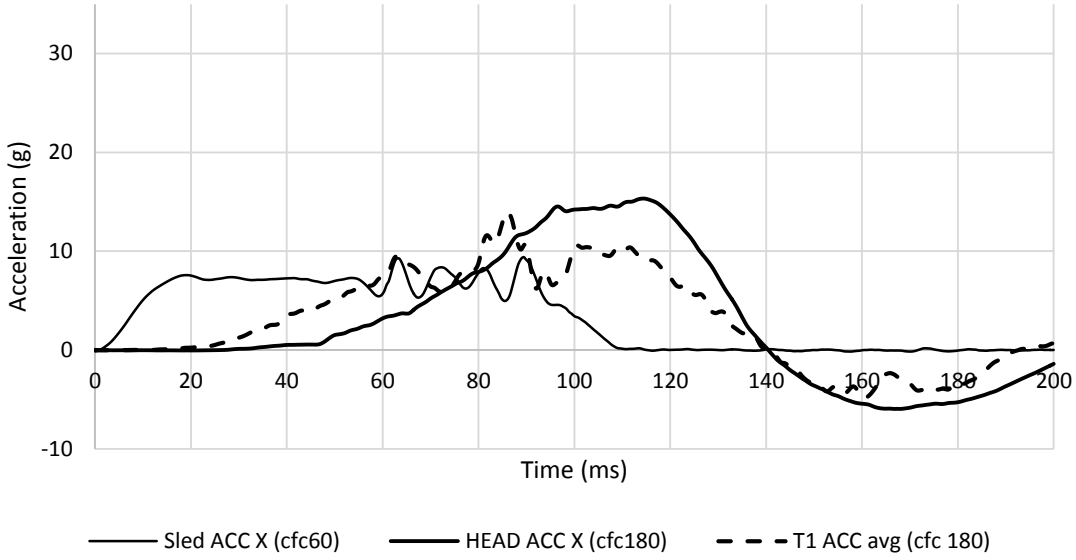


APPENDIX 340 LOADING GRAPHS OF FEA EVA RID CONFIGURATION H213 ACCELERATION

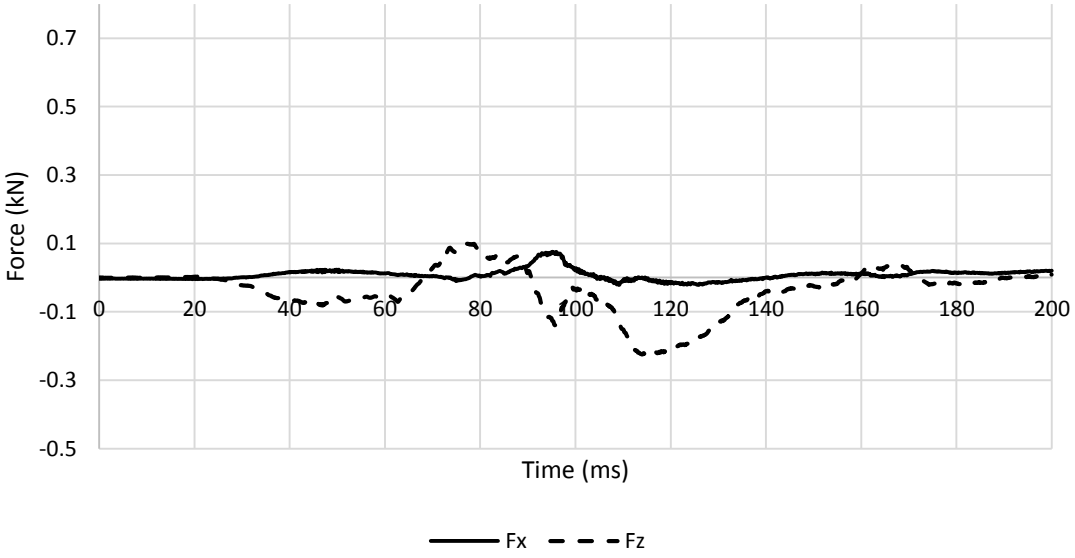


APPENDIX 341 LOADING GRAPHS OF FEA EVA RID CONFIGURATION H213 - FORCE

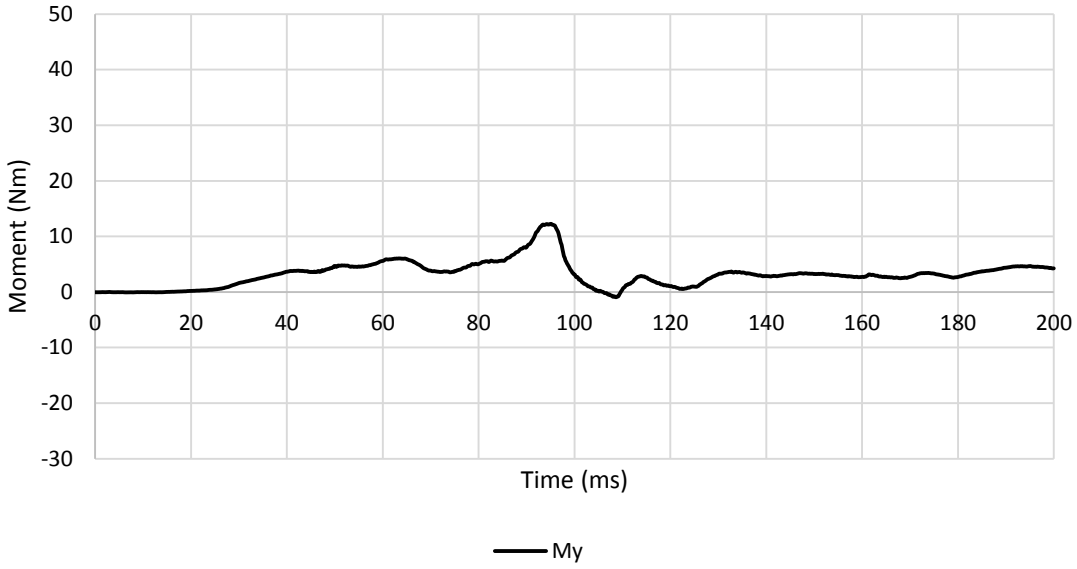


APPENDIX 342 LOADING GRAPHS OF FEA EVA RID CONFIGURATION H213 - MOMENT

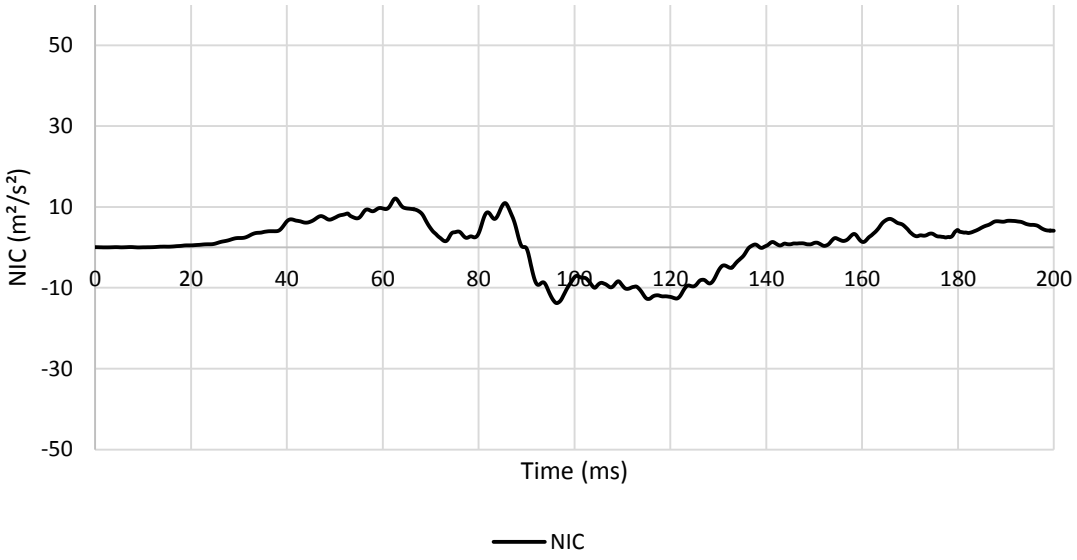


APPENDIX 343 LOADING GRAPHS OF FEA EVA RID CONFIGURATION H213 - NIC

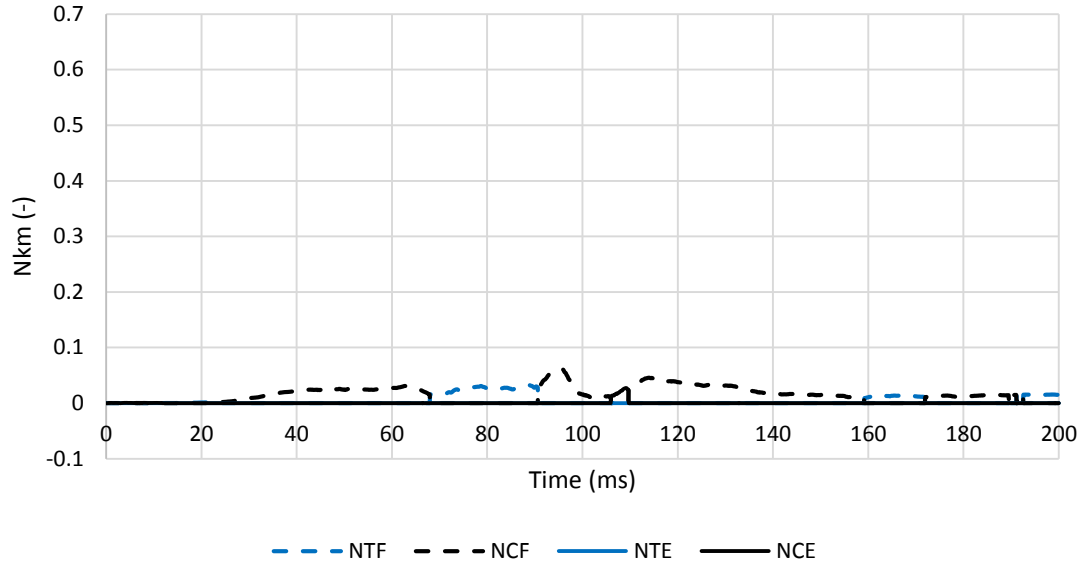


APPENDIX 344 LOADING GRAPHS OF FEA EVA RID CONFIGURATION H213 - NKM

## A.7.4. Eva RID – centred backrest – high head restraint 221

### A.7.4.1. Low Severity Pulse (SRA 16 km/h) L221

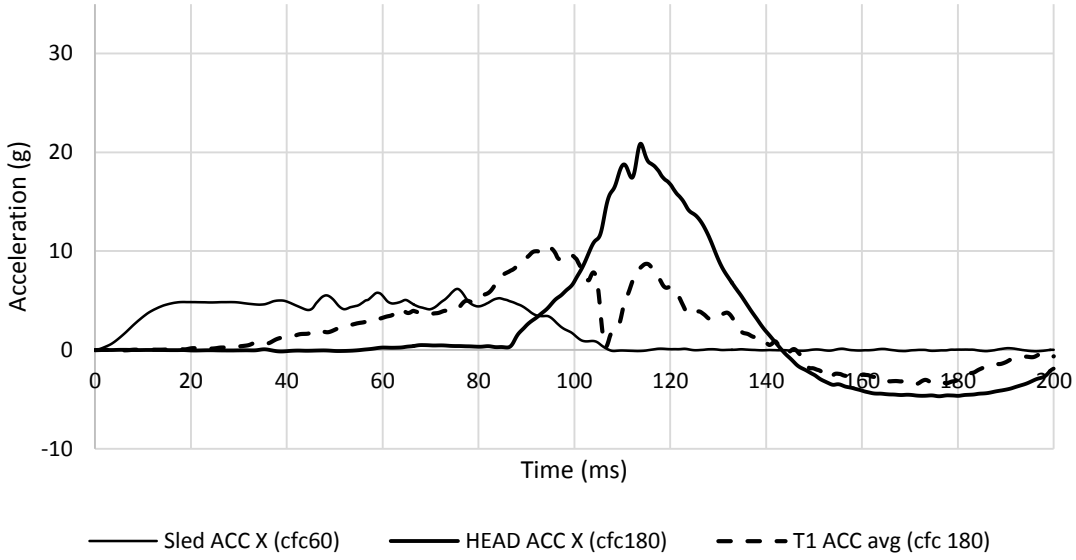


APPENDIX 345 LOADING GRAPHS OF FEA EVA RID CONFIGURATION L221 - ACCELERATION

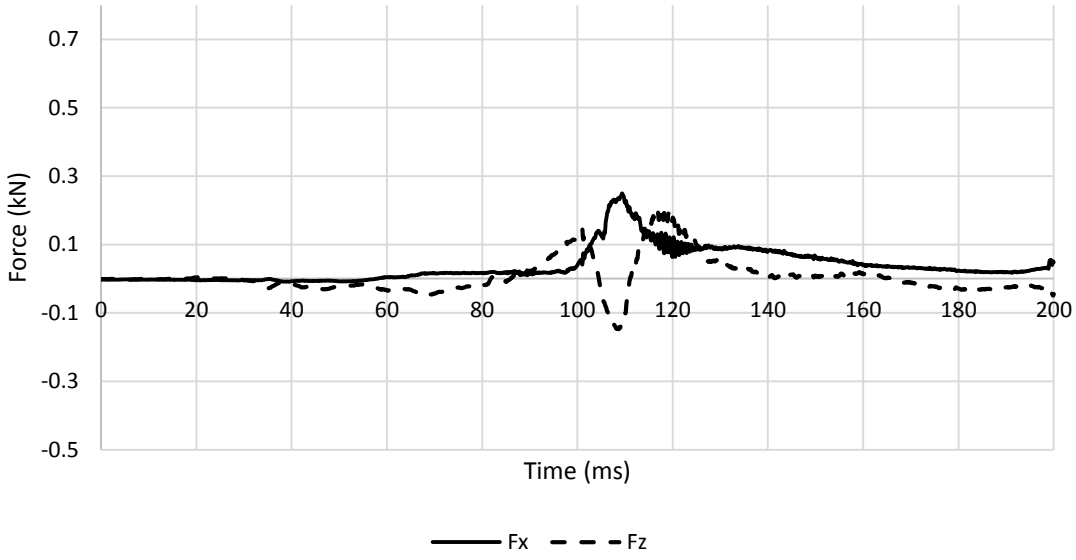


APPENDIX 346 LOADING GRAPHS OF FEA EVA RID CONFIGURATION L221 - FORCE

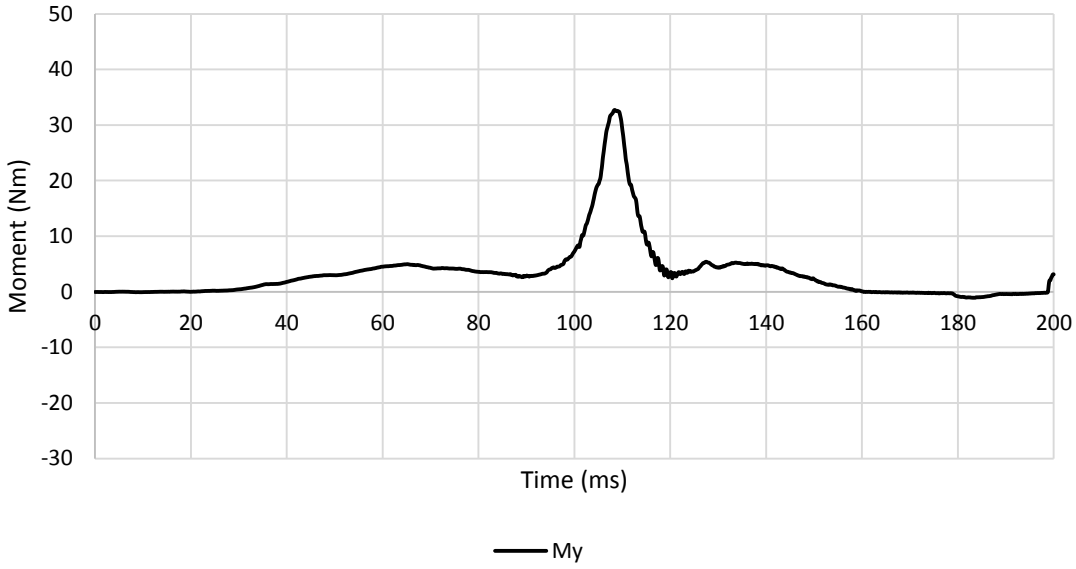


APPENDIX 347 LOADING GRAPHS OF FEA EVA RID CONFIGURATION L221 - MOMENT

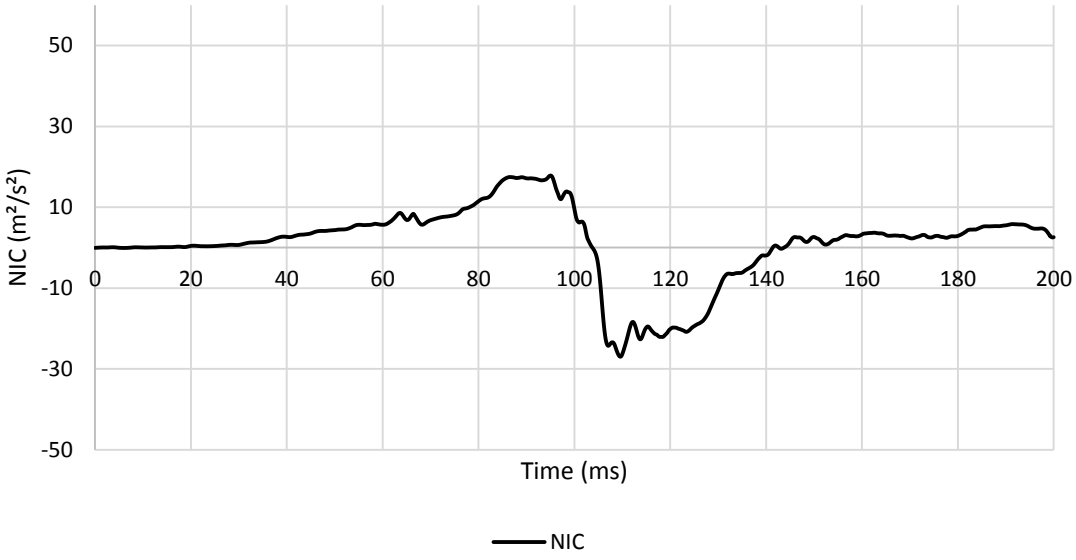


APPENDIX 348 LOADING GRAPHS OF FEA EVA RID CONFIGURATION L221 - NIC

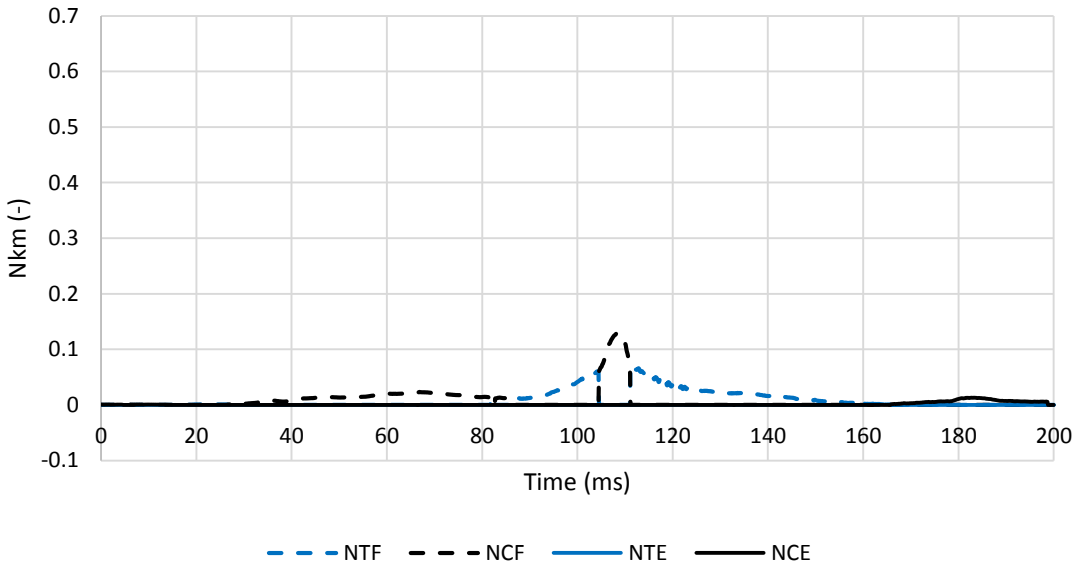


APPENDIX 349 LOADING GRAPHS OF FEA EVA RID CONFIGURATION L221 - NKM

## A.7.4.2. Medium Severity Pulse (IIWPG 16 km/h) M221

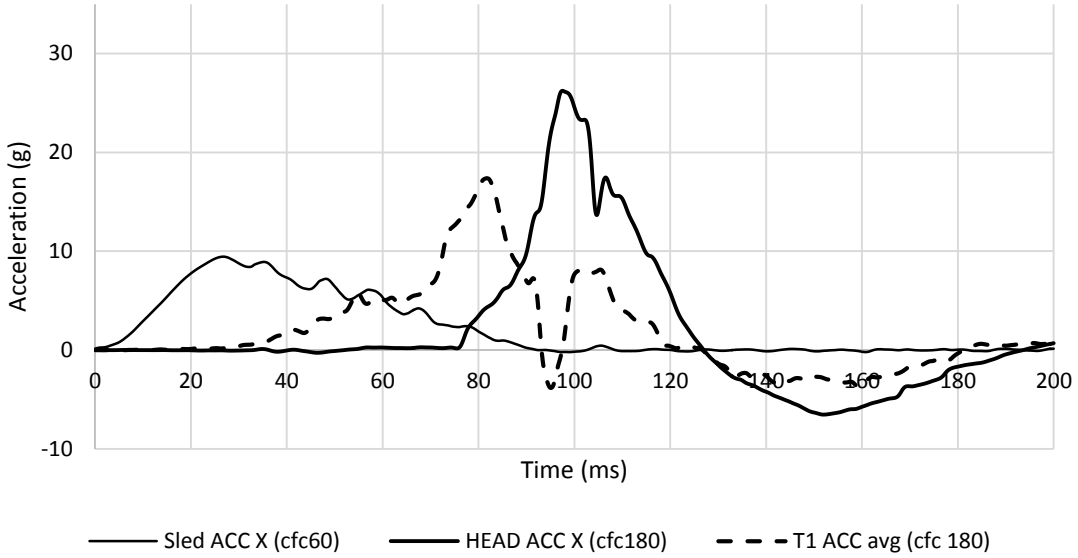


APPENDIX 350 LOADING GRAPHS OF FEA EVA RID CONFIGURATION M221 - ACCELERATION

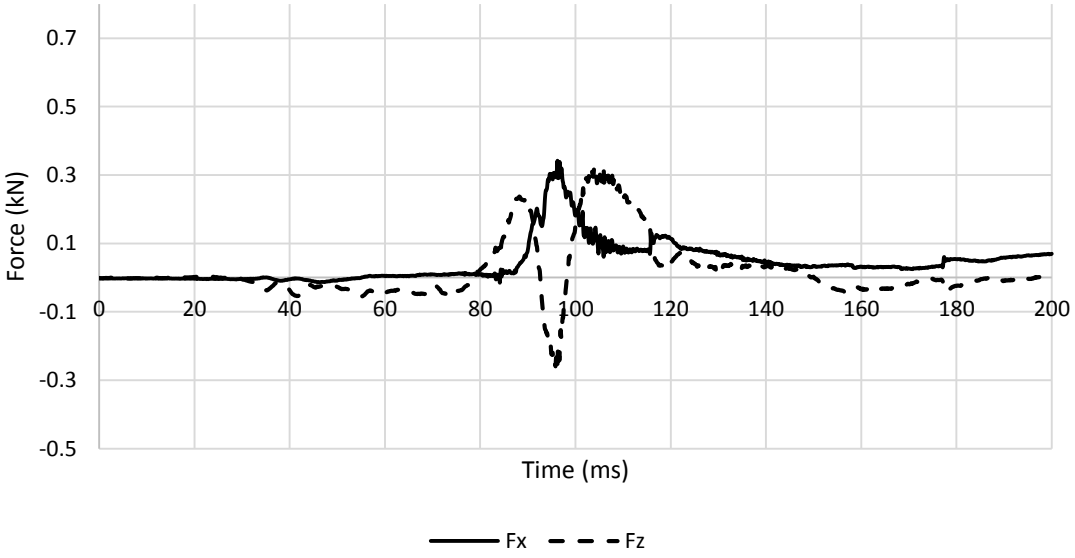


APPENDIX 351 LOADING GRAPHS OF FEA EVA RID CONFIGURATION M221 - FORCE

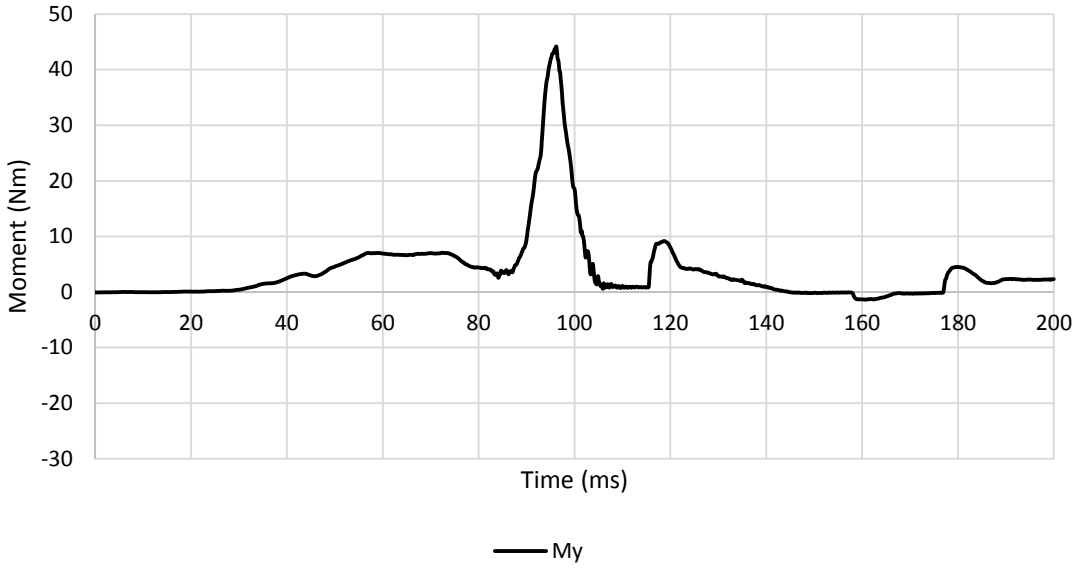


APPENDIX 352 LOADING GRAPHS OF FEA EVA RID CONFIGURATION M221 - MOMENT

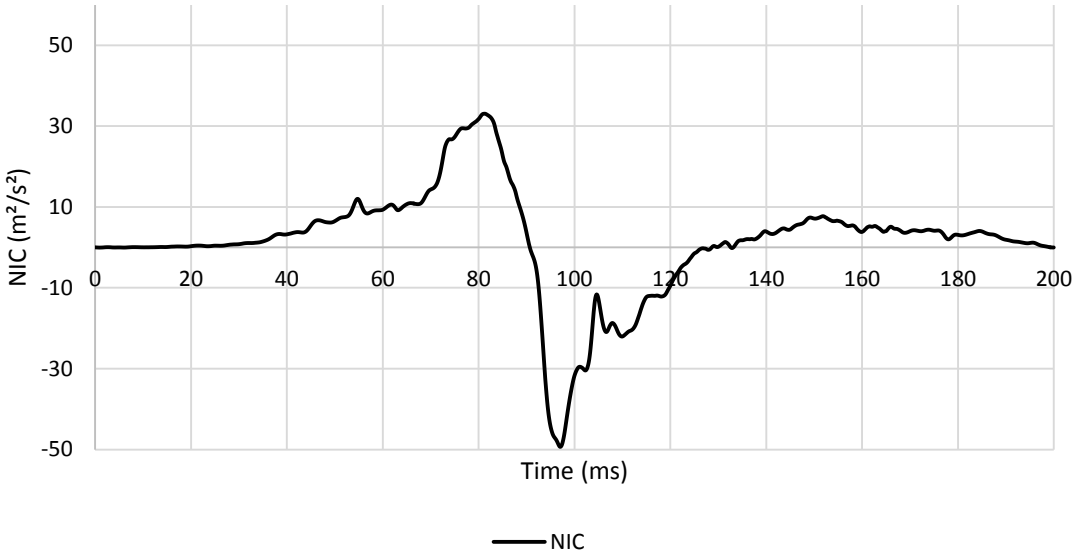


APPENDIX 353 LOADING GRAPHS OF FEA EVA RID CONFIGURATION M221 - NIC

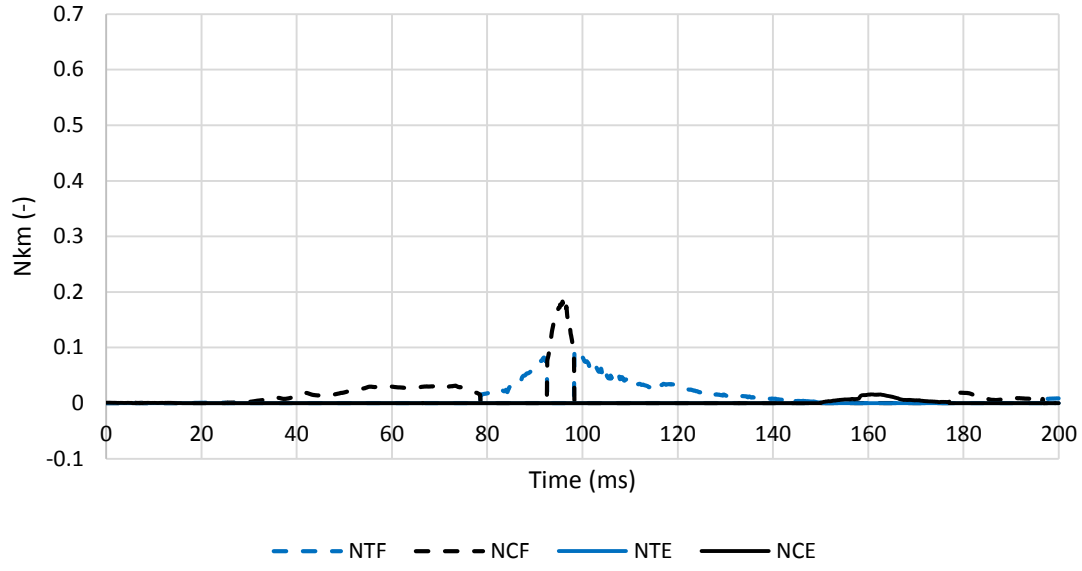


APPENDIX 354 LOADING GRAPHS OF FEA EVA RID CONFIGURATION M221 - NKM

### A.7.4.3. High Severity Pulse (SRA 24 km/h) H221

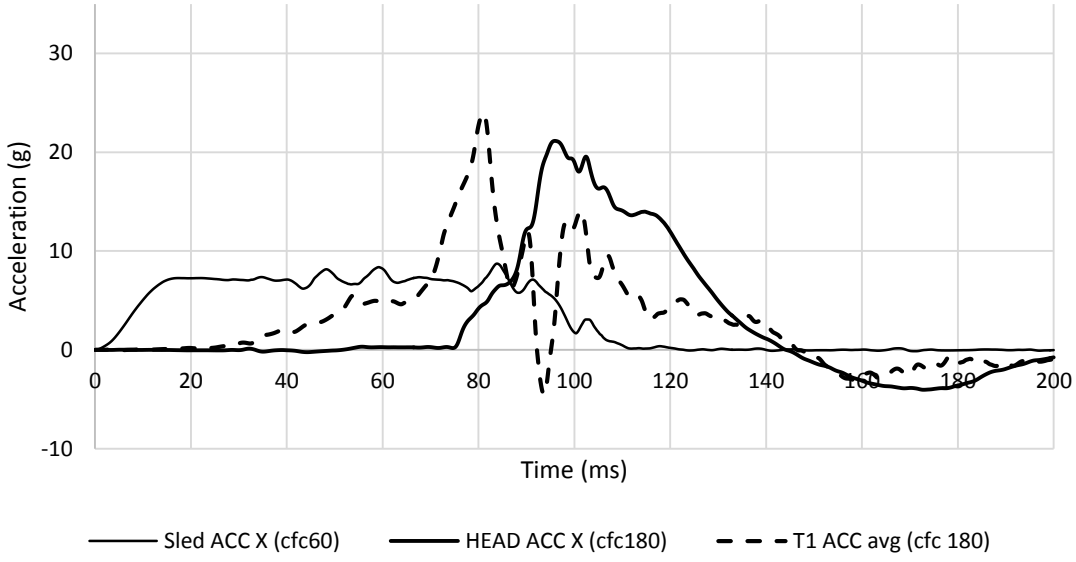


APPENDIX 355 LOADING GRAPHS OF FEA EVA RID CONFIGURATION H221 - ACCELERATION

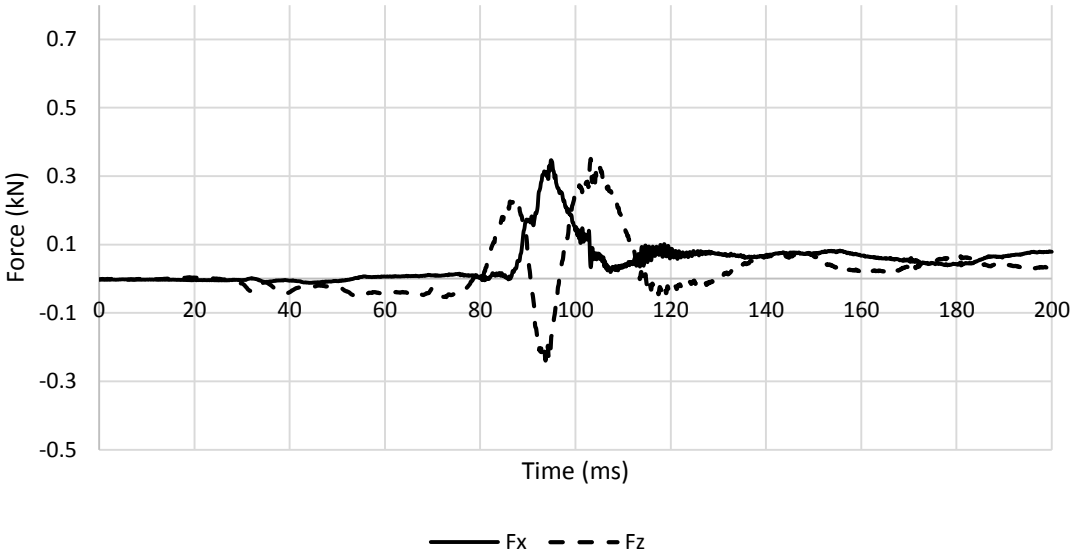


APPENDIX 356 LOADING GRAPHS OF FEA EVA RID CONFIGURATION H221 - FORCE

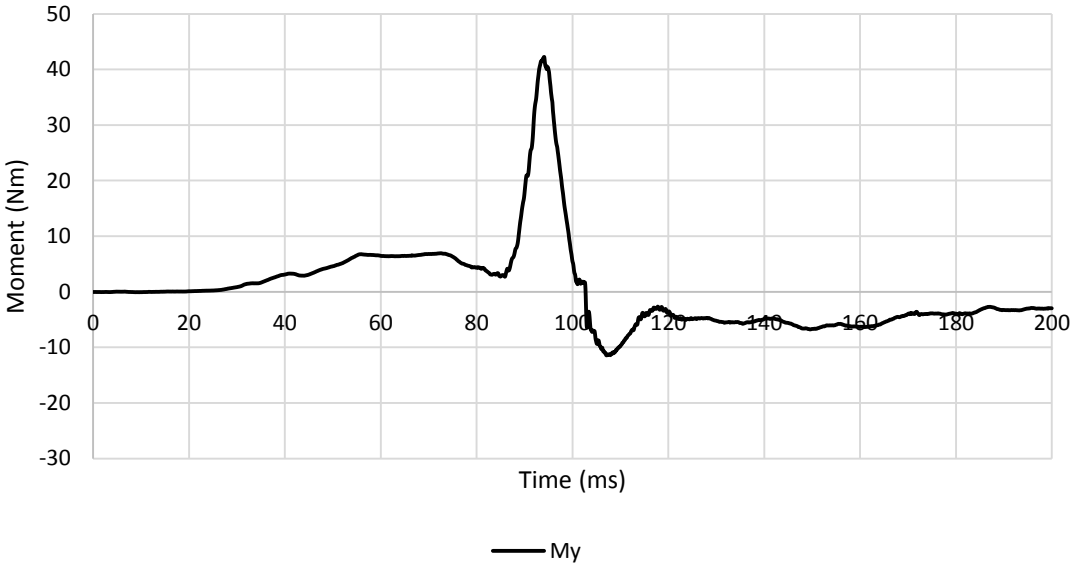


APPENDIX 357 LOADING GRAPHS OF FEA EVA RID CONFIGURATION H221 - MOMENT

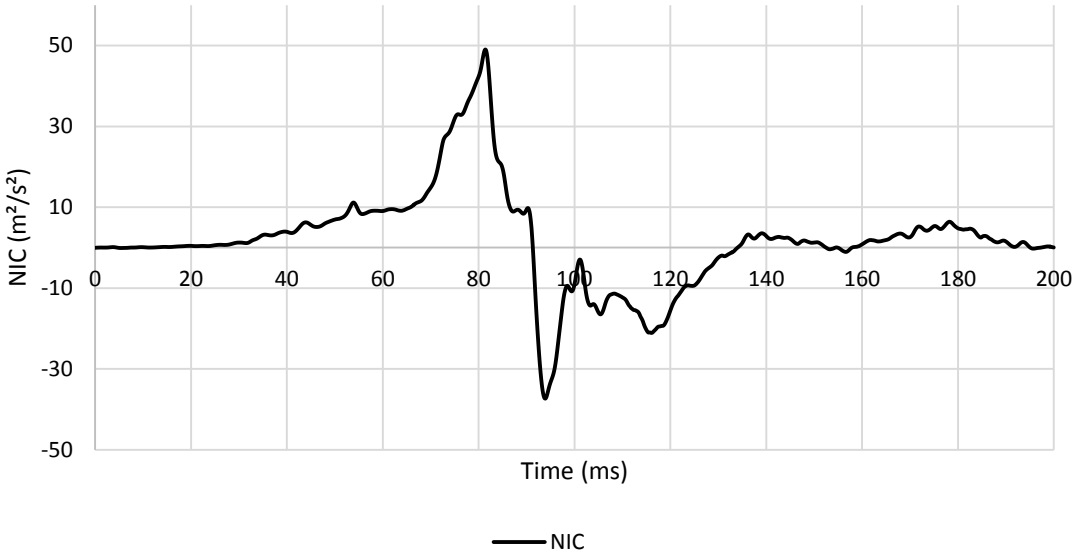


APPENDIX 358 LOADING GRAPHS OF FEA EVA RID CONFIGURATION H221 - NIC

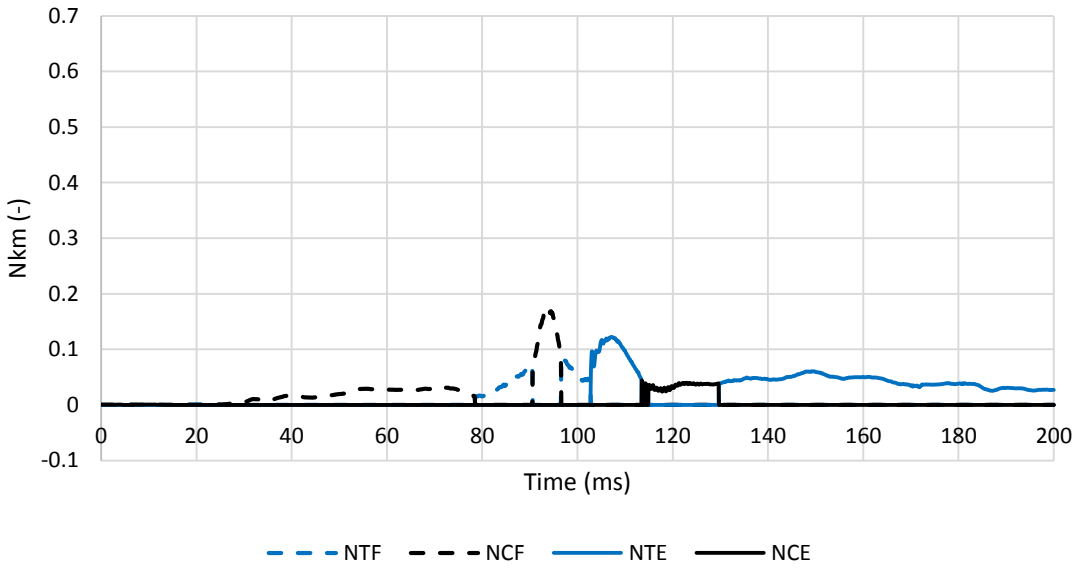


APPENDIX 359 LOADING GRAPHS OF FEA EVA RID CONFIGURATION H221 - NKM

## A.7.5. Eva RID – centred backrest – middle head restraint 222

### A.7.5.1. Low Severity Pulse (SRA 16 km/h) L222

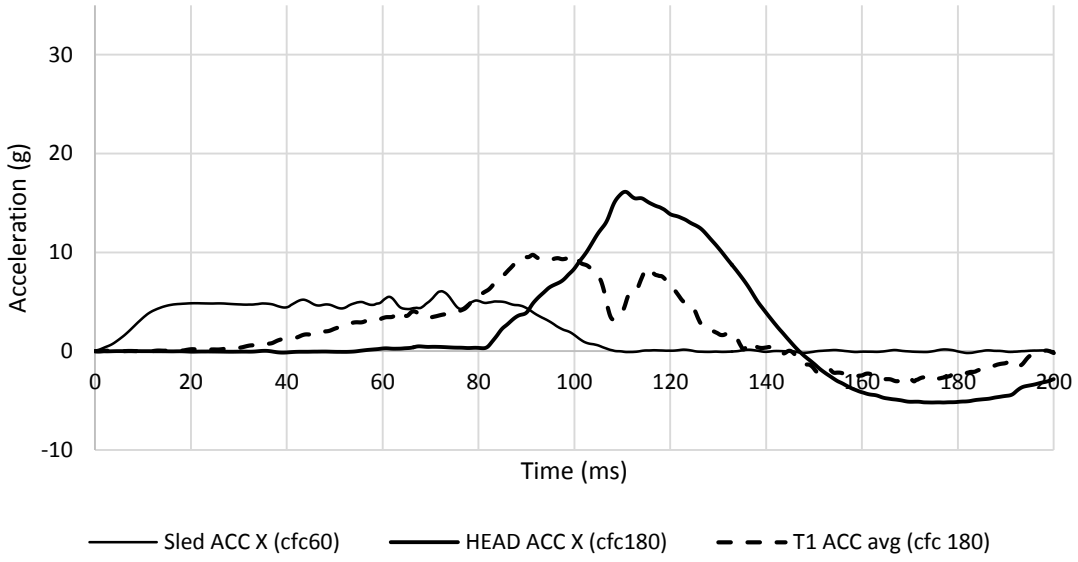


APPENDIX 360 LOADING GRAPHS OF FEA EVA RID CONFIGURATION L222 - ACCELERATION

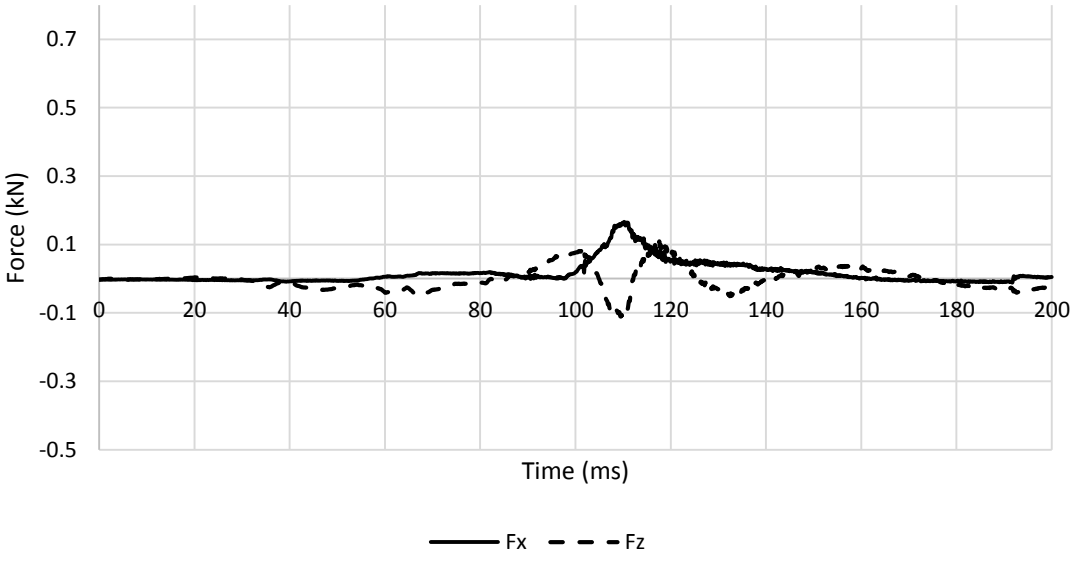


APPENDIX 361 LOADING GRAPHS OF FEA EVA RID CONFIGURATION L222 - FORCE

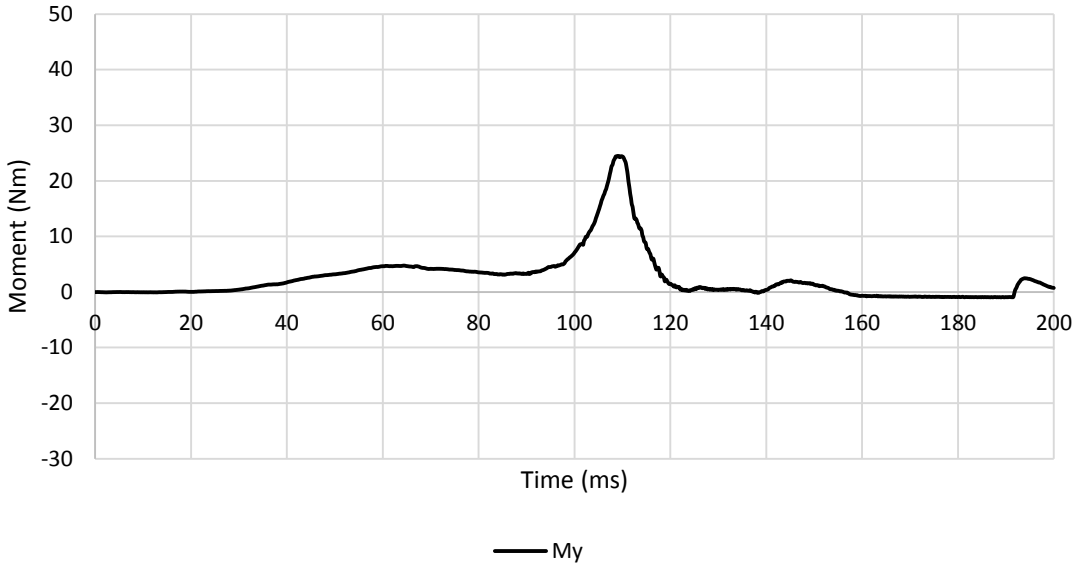


APPENDIX 362 LOADING GRAPHS OF FEA EVA RID CONFIGURATION L222 - MOMENT

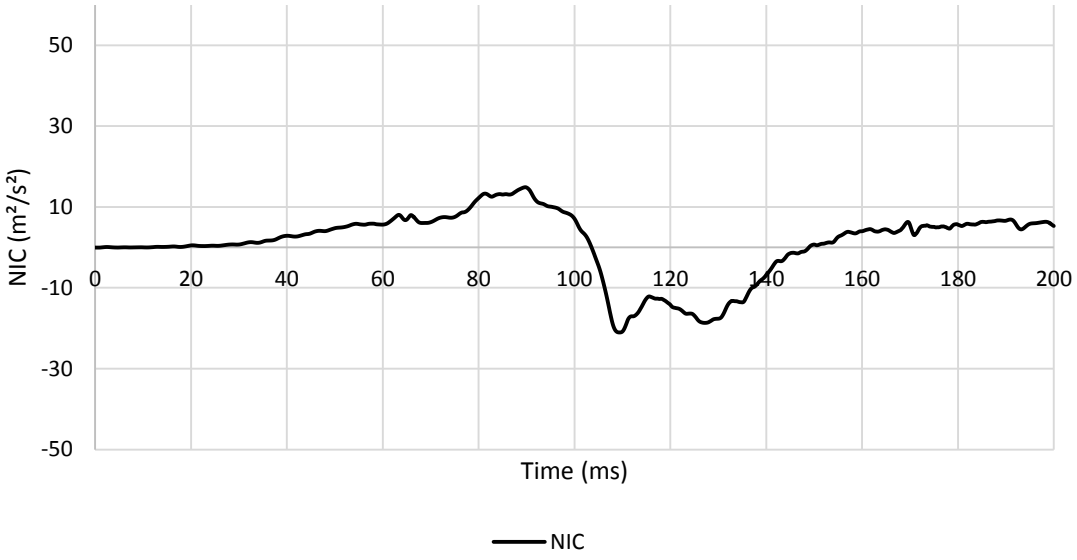


APPENDIX 363 LOADING GRAPHS OF FEA EVA RID CONFIGURATION L222 - NIC

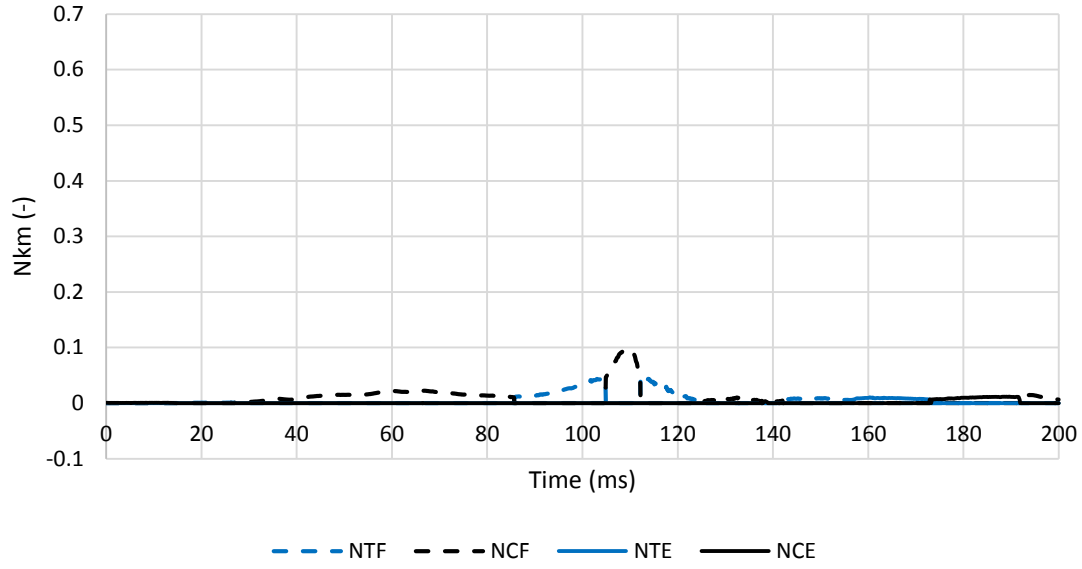


APPENDIX 364 LOADING GRAPHS OF FEA EVA RID CONFIGURATION L222 - NKM

### A.7.5.2. Medium Severity Pulse (IIWPG 16 km/h) M222

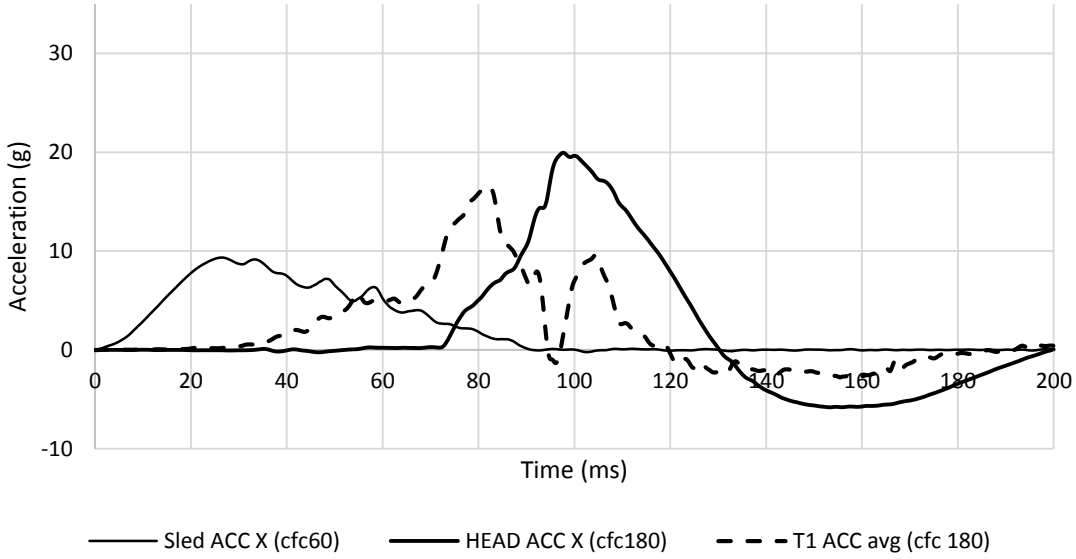


APPENDIX 365 LOADING GRAPHS OF FEA EVA RID CONFIGURATION M222 - ACCELERATION

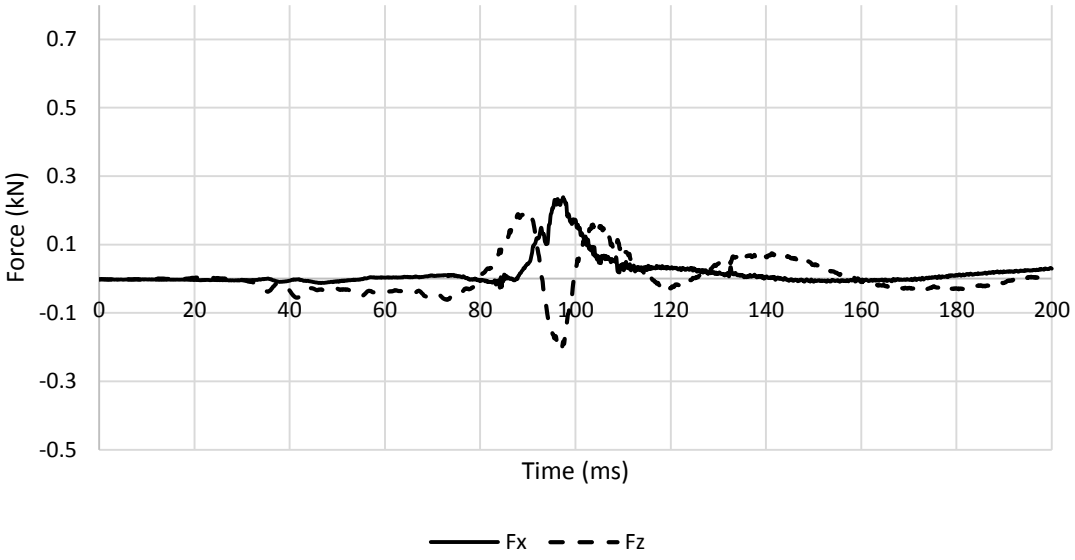


APPENDIX 366 LOADING GRAPHS OF FEA EVA RID CONFIGURATION M222 - FORCE

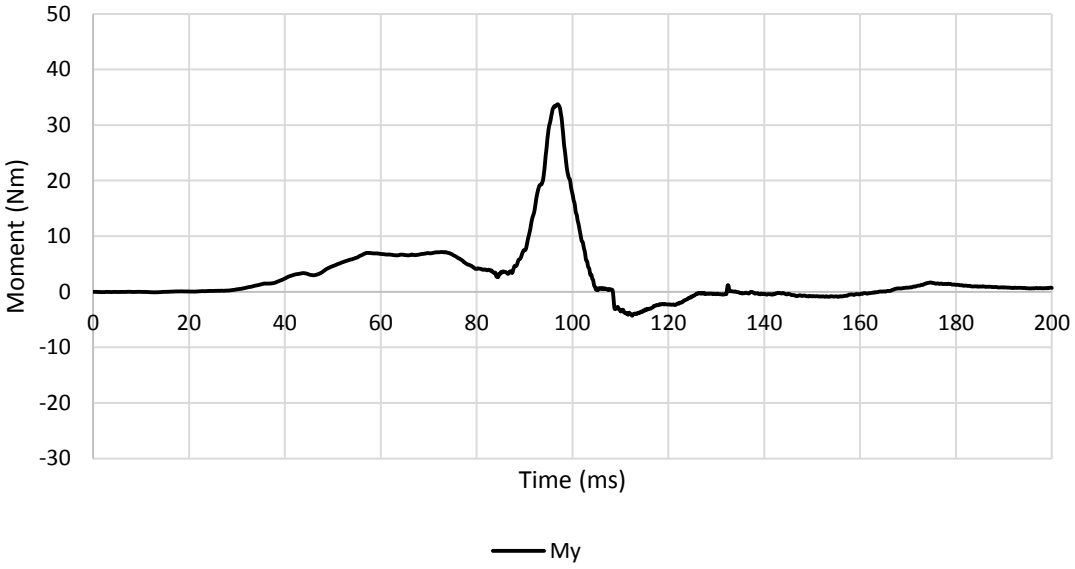


APPENDIX 367 LOADING GRAPHS OF FEA EVA RID CONFIGURATION M222 - MOMENT

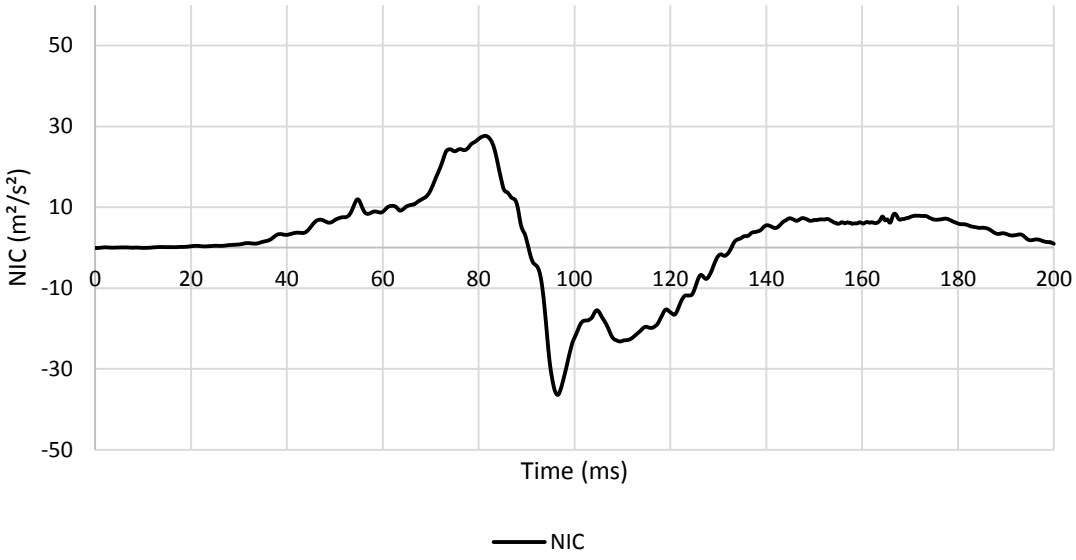


APPENDIX 368 LOADING GRAPHS OF FEA EVA RID CONFIGURATION M222 - NIC

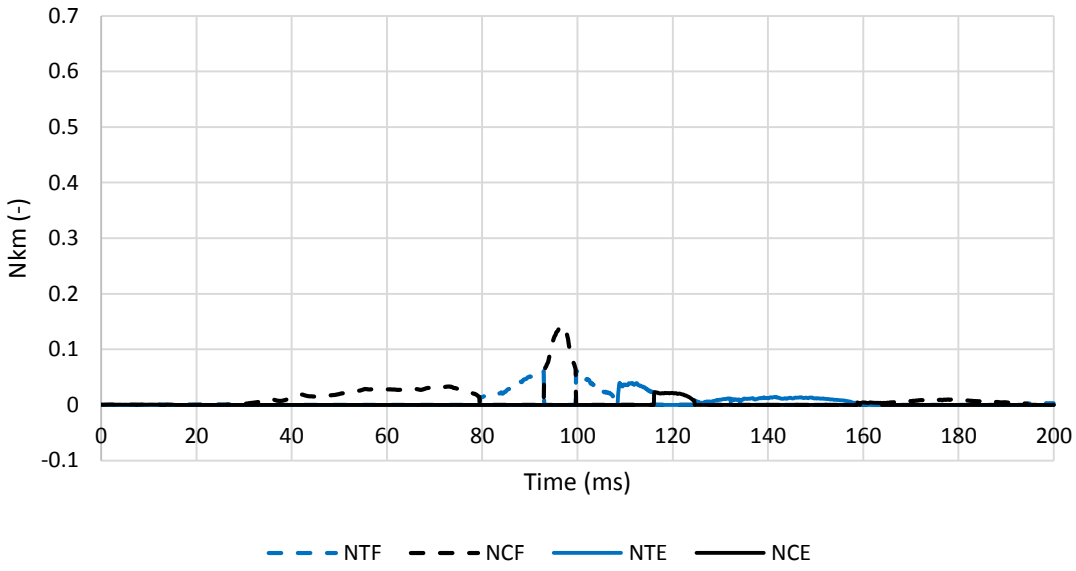


APPENDIX 369 LOADING GRAPHS OF FEA EVA RID CONFIGURATION M222 - NKM

## A.7.5.3. High Severity Pulse (SRA 24 km/h) H222

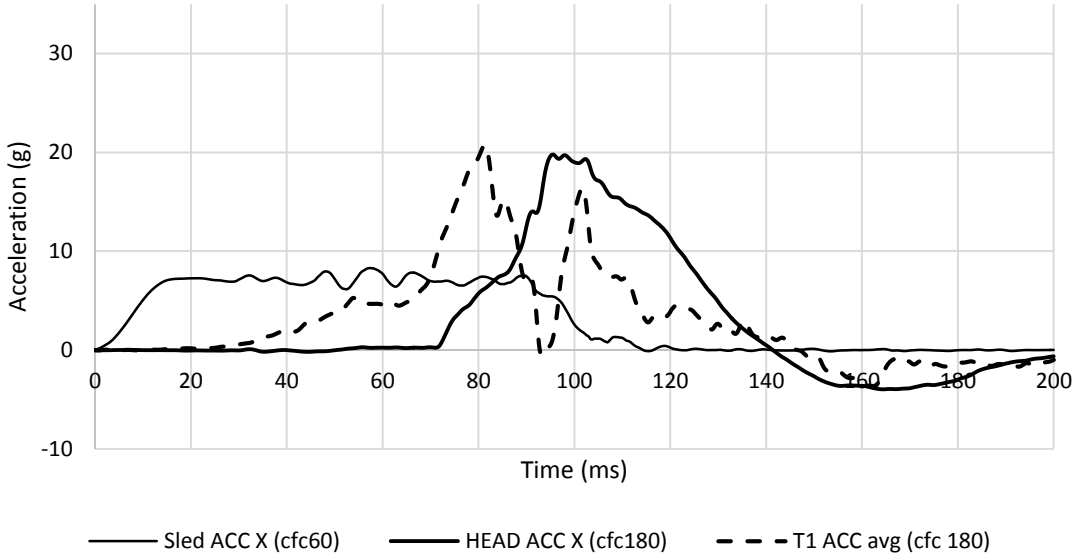


APPENDIX 370 LOADING GRAPHS OF FEA EVA RID CONFIGURATION H222 - ACCELERATION

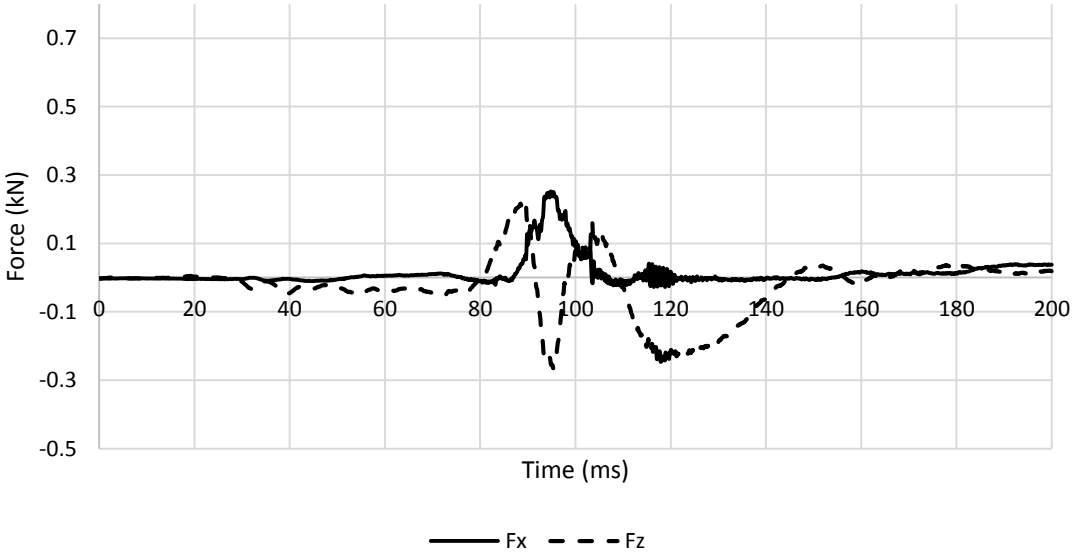


APPENDIX 371 LOADING GRAPHS OF FEA EVA RID CONFIGURATION H222 - FORCE

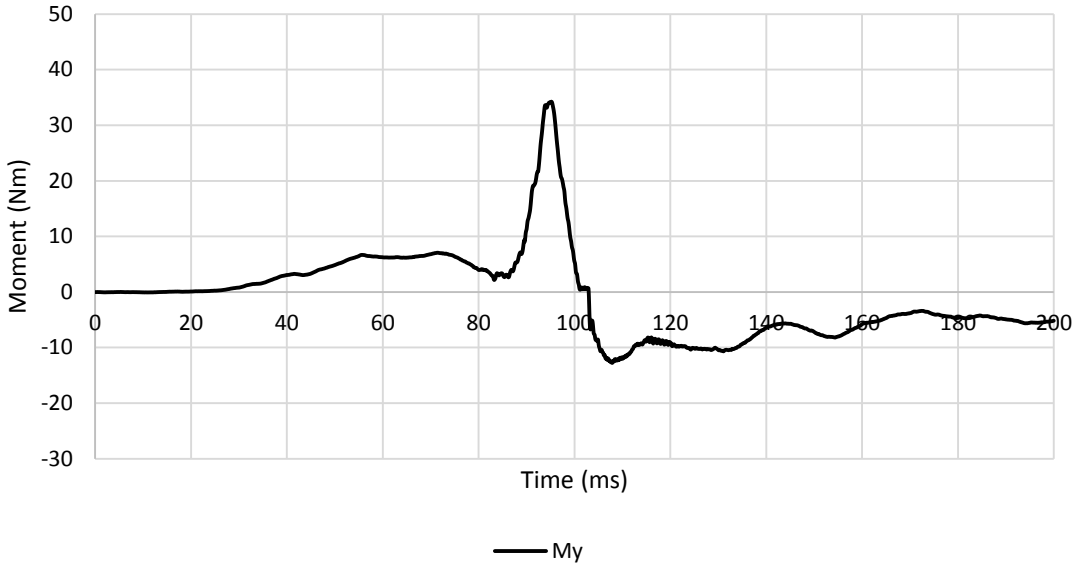


APPENDIX 372 LOADING GRAPHS OF FEA EVA RID CONFIGURATION H222 - MOMENT

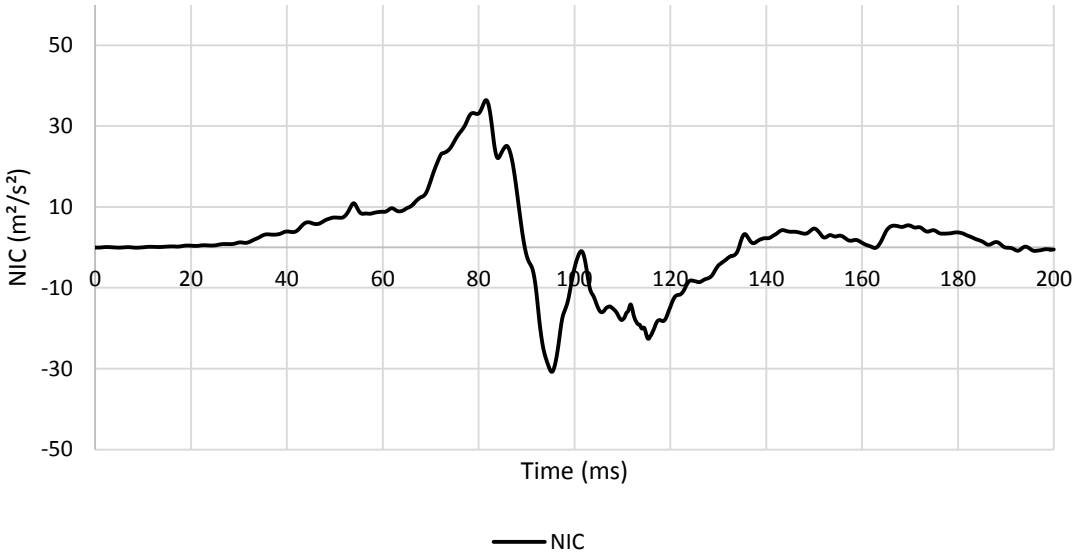


APPENDIX 373 LOADING GRAPHS OF FEA EVA RID CONFIGURATION H222 - NIC

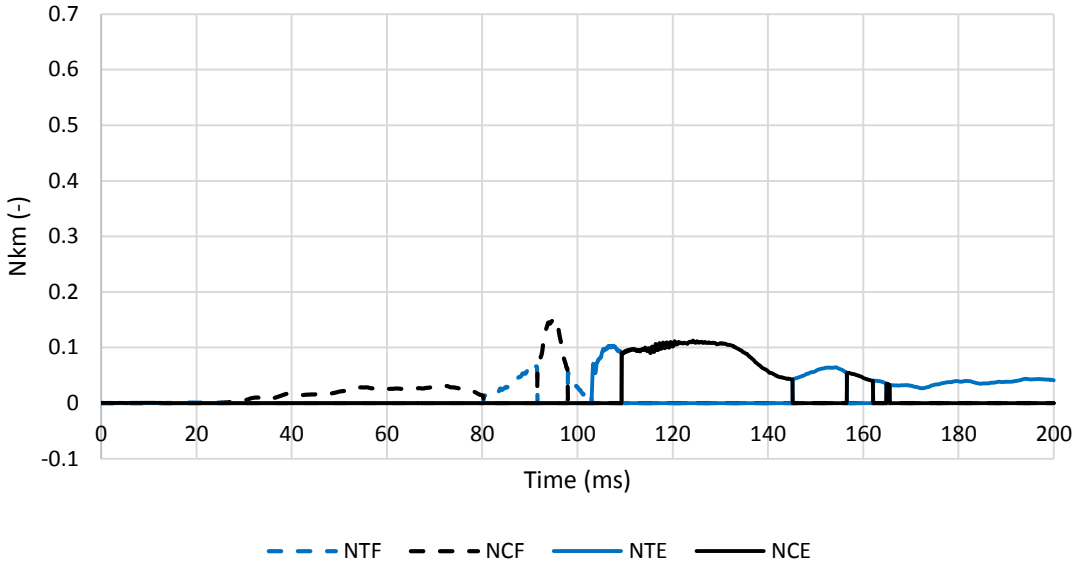


APPENDIX 374 LOADING GRAPHS OF FEA EVA RID CONFIGURATION H222 - NKM

## A.7.6. Eva RID – centred backrest – low head restraint 223

### A.7.6.1. Low Severity Pulse (SRA 16 km/h) L223

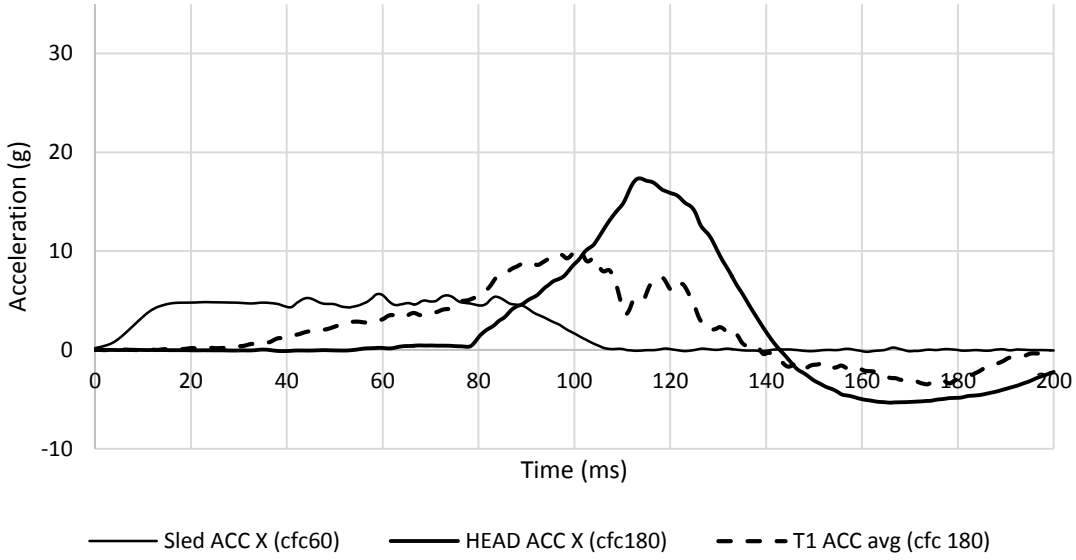


APPENDIX 375 LOADING GRAPHS OF FEA EVA RID CONFIGURATION L223 - ACCELERATION

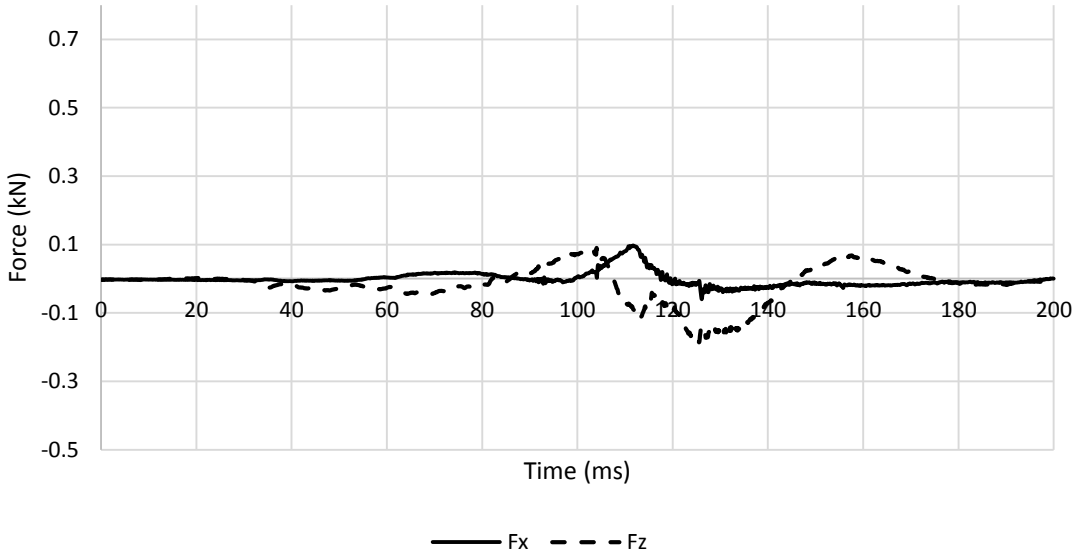


APPENDIX 376 LOADING GRAPHS OF FEA EVA RID CONFIGURATION L223 - FORCE

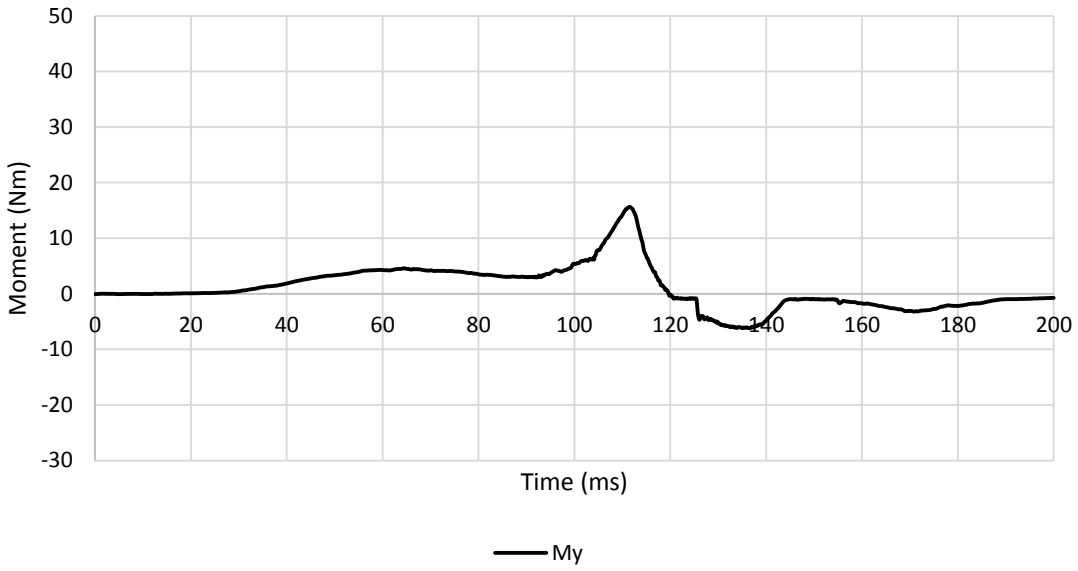


APPENDIX 377 LOADING GRAPHS OF FEA EVA RID CONFIGURATION L223 - MOMENT

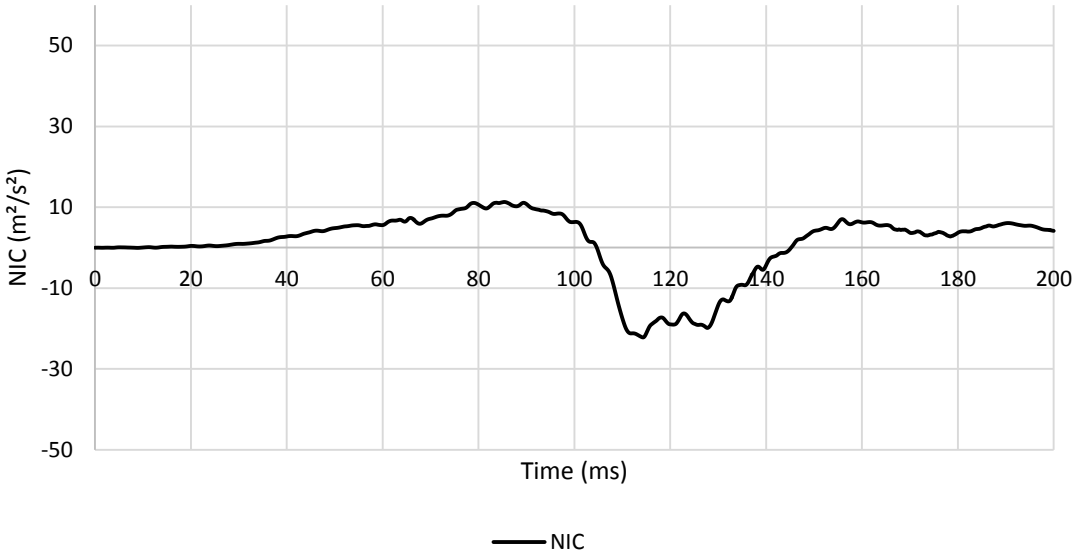


APPENDIX 378 LOADING GRAPHS OF FEA EVA RID CONFIGURATION L223 - NIC

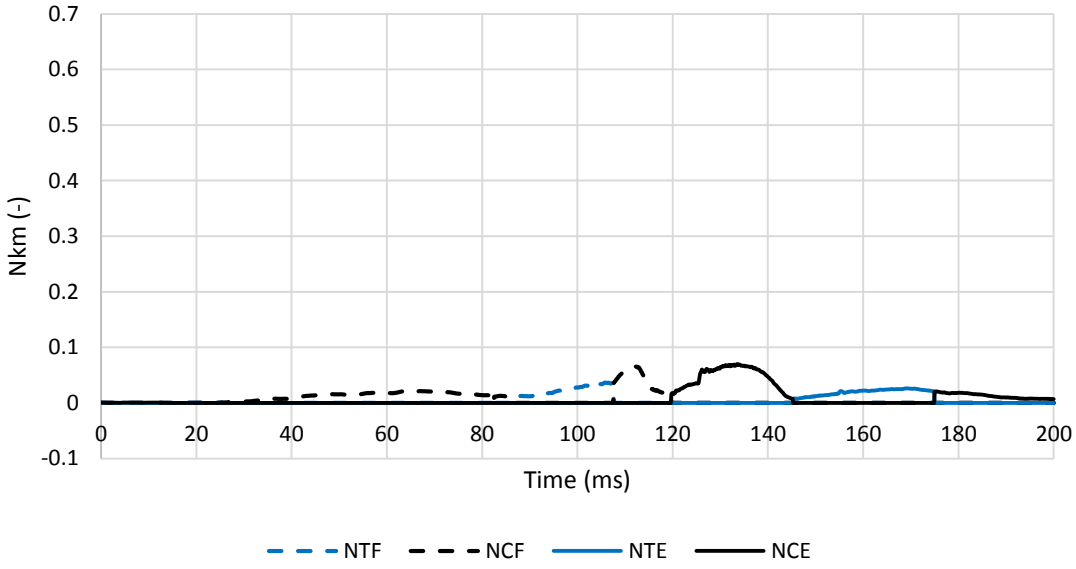


APPENDIX 379 LOADING GRAPHS OF FEA EVA RID CONFIGURATION L223 - NKM

## A.7.6.2. Medium Severity Pulse (IIWPG 16 km/h) M223

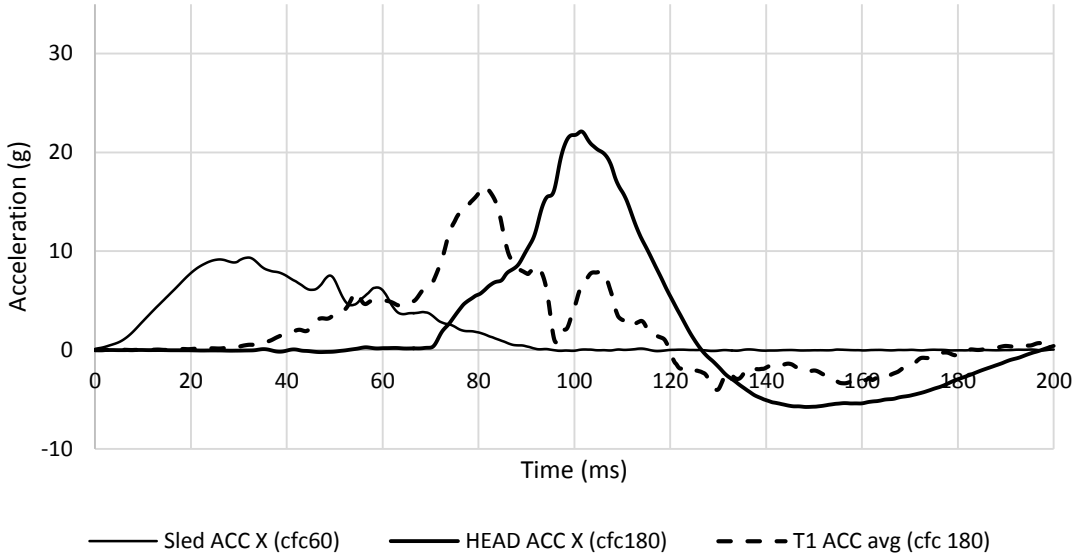


APPENDIX 380 LOADING GRAPHS OF FEA EVA RID CONFIGURATION M223 - ACCELERATION

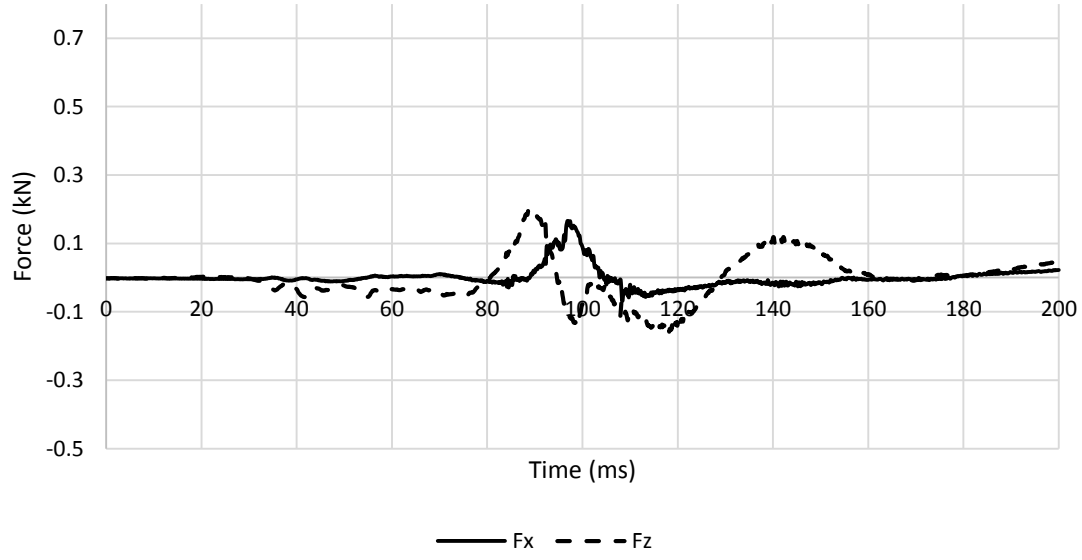


APPENDIX 381 LOADING GRAPHS OF FEA EVA RID CONFIGURATION M223 - FORCE

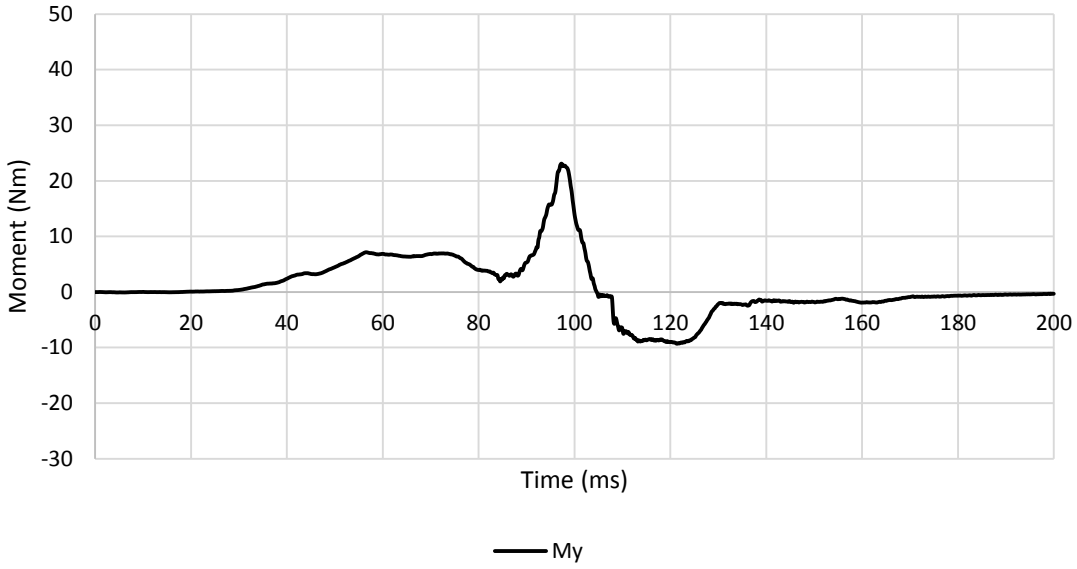


APPENDIX 382 LOADING GRAPHS OF FEA EVA RID CONFIGURATION M223 - MOMENT

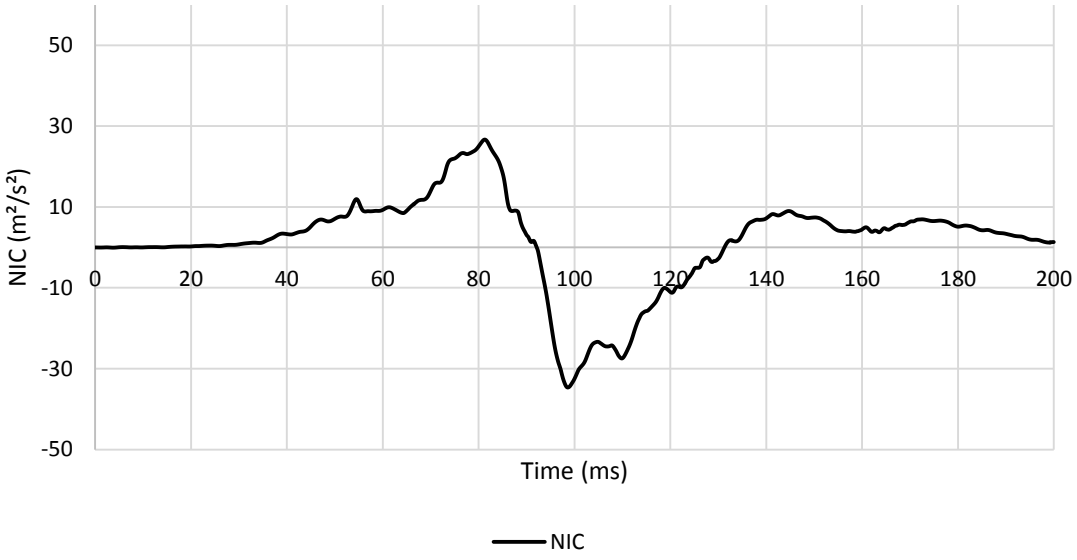


APPENDIX 383 LOADING GRAPHS OF FEA EVA RID CONFIGURATION M223 - NIC

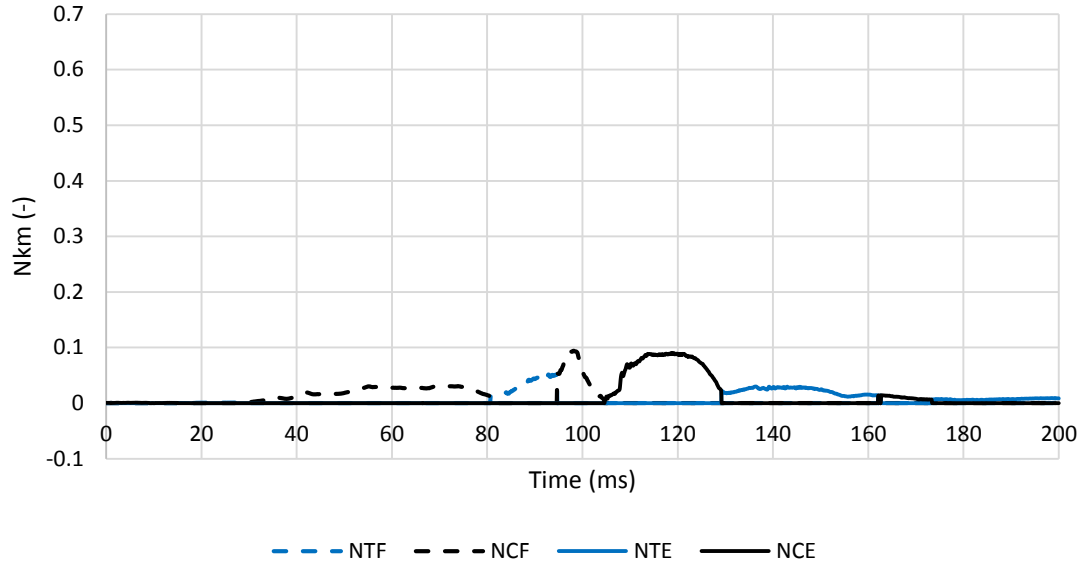


APPENDIX 384 LOADING GRAPHS OF FEA EVA RID CONFIGURATION M223 - NKM

### A.7.6.3. High Severity Pulse (SRA 24 km/h) H223

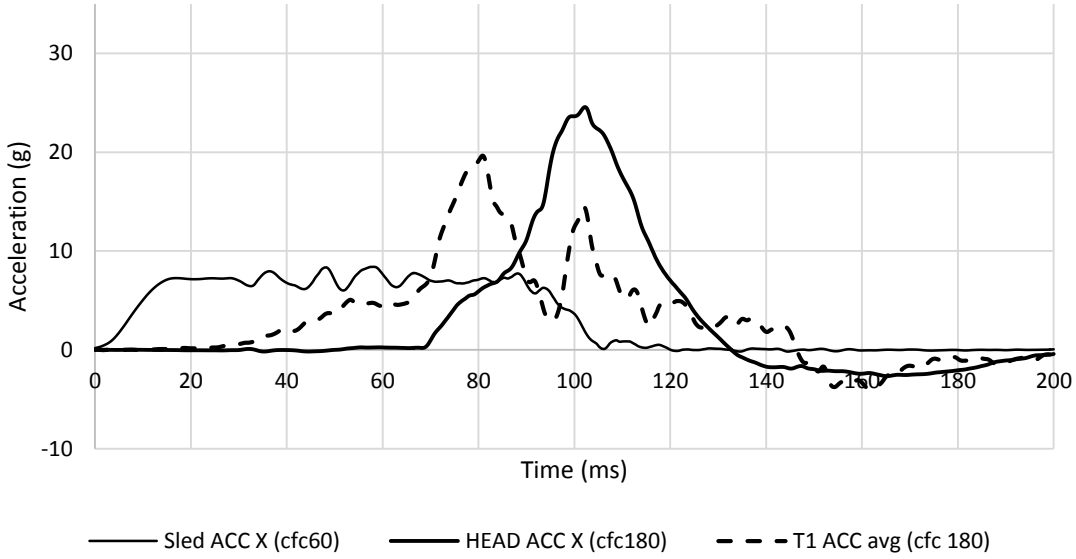


APPENDIX 385 LOADING GRAPHS OF FEA EVA RID CONFIGURATION H223 - ACCELERATION

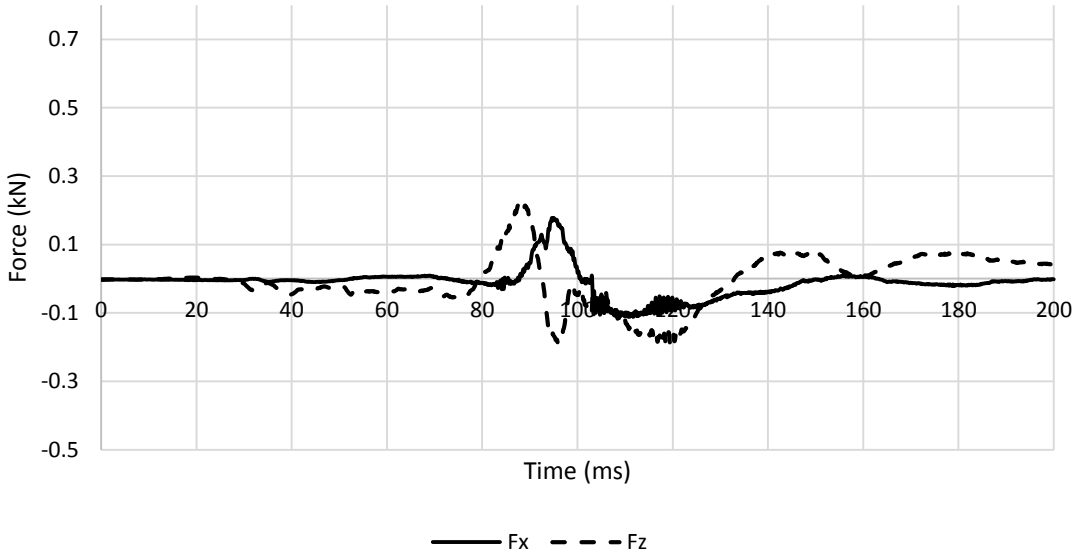


APPENDIX 386 LOADING GRAPHS OF FEA EVA RID CONFIGURATION H223 - FORCE

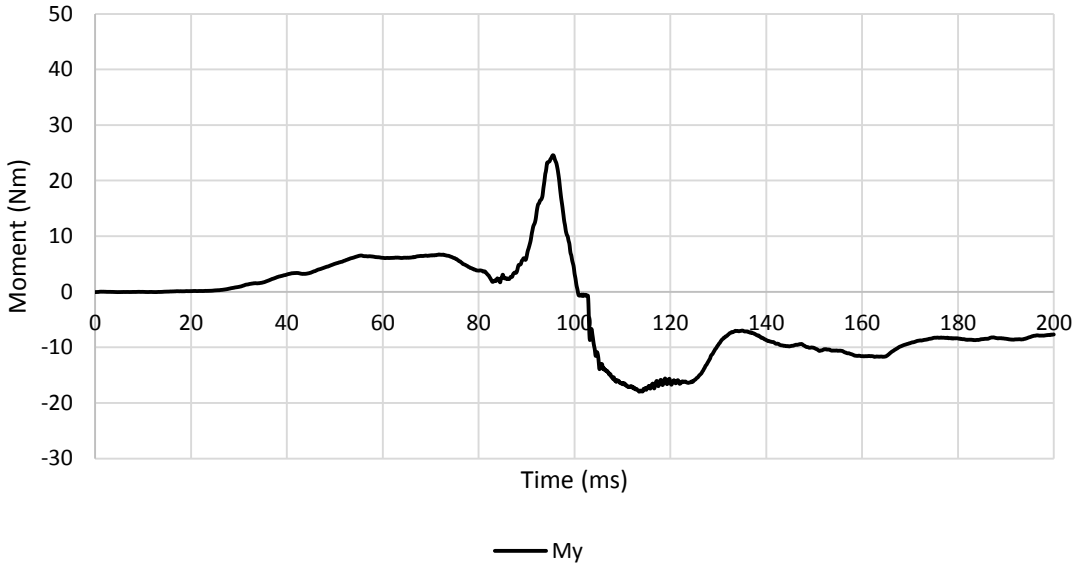


APPENDIX 387 LOADING GRAPHS OF FEA EVA RID CONFIGURATION H223 - MOMENT

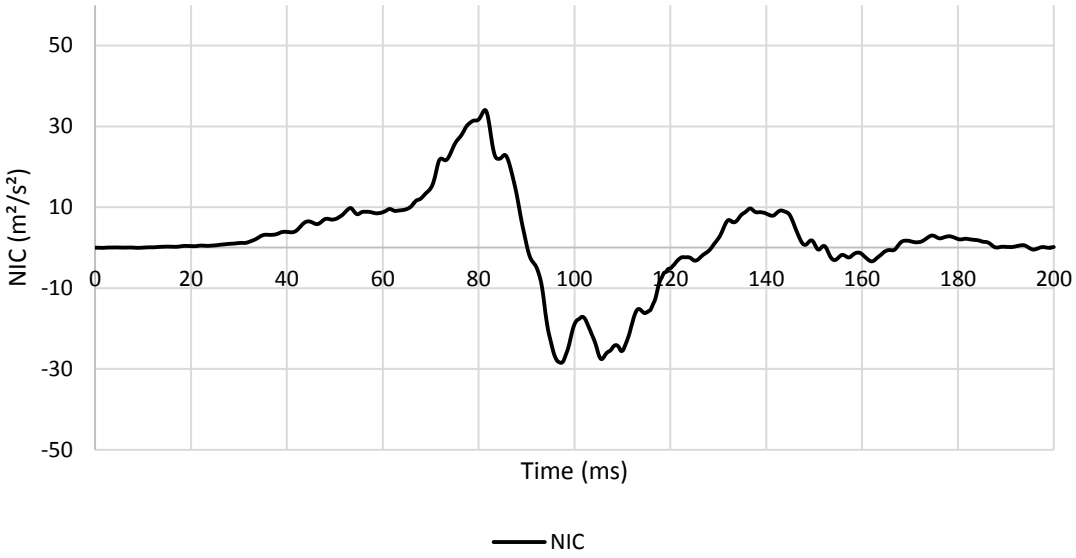


APPENDIX 388 LOADING GRAPHS OF FEA EVA RID CONFIGURATION H223 - NIC

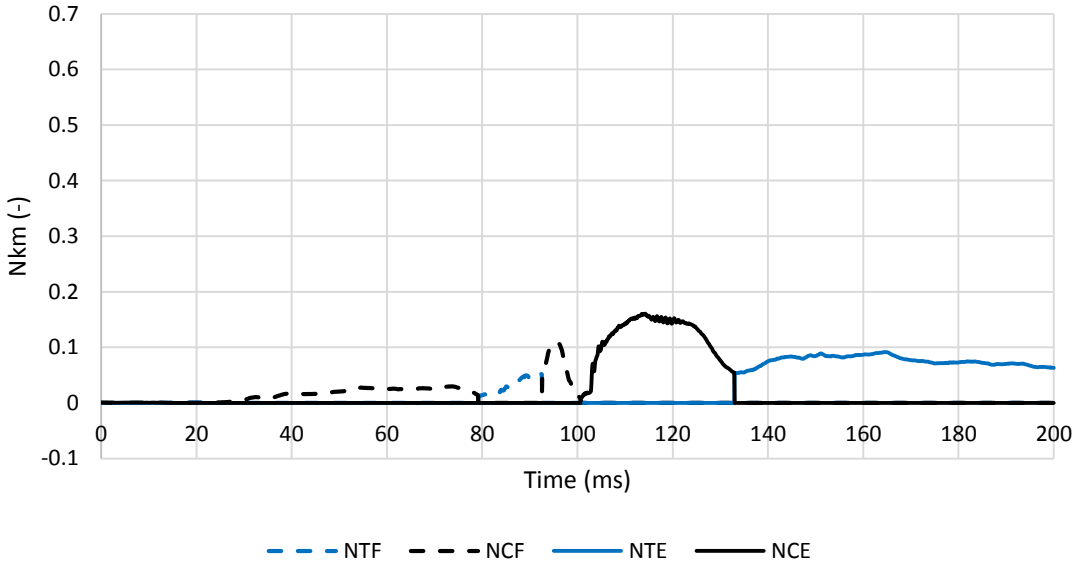


APPENDIX 389 LOADING GRAPHS OF FEA EVA RID CONFIGURATION H223 - NKM

## A.7.7. Eva RID – backward backrest – high head restraint 231

### A.7.7.1. Low Severity Pulse (SRA 16 km/h) L231

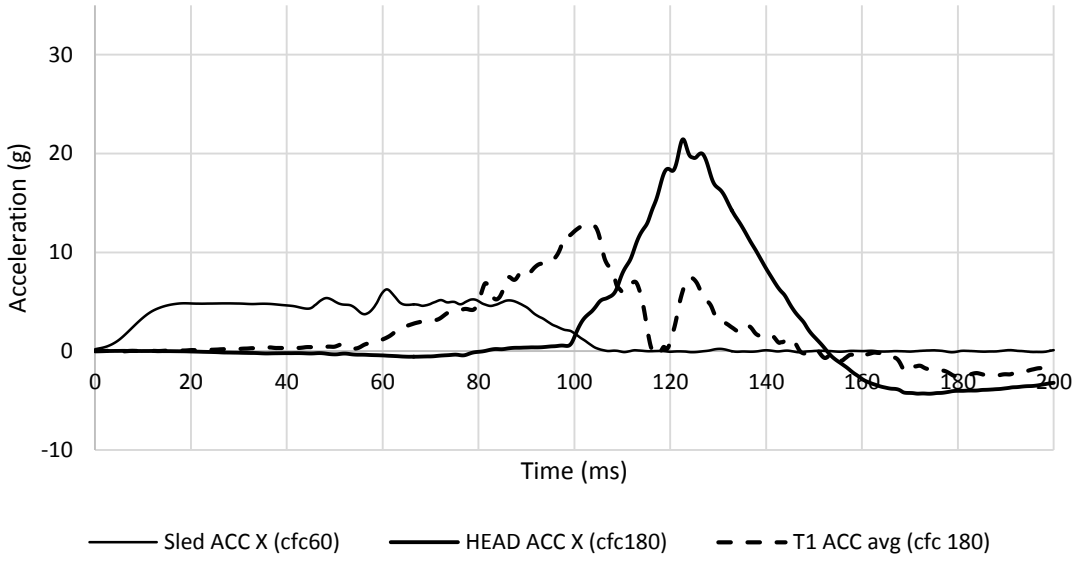


APPENDIX 390 LOADING GRAPHS OF FEA EVA RID CONFIGURATION L231 - ACCELERATION

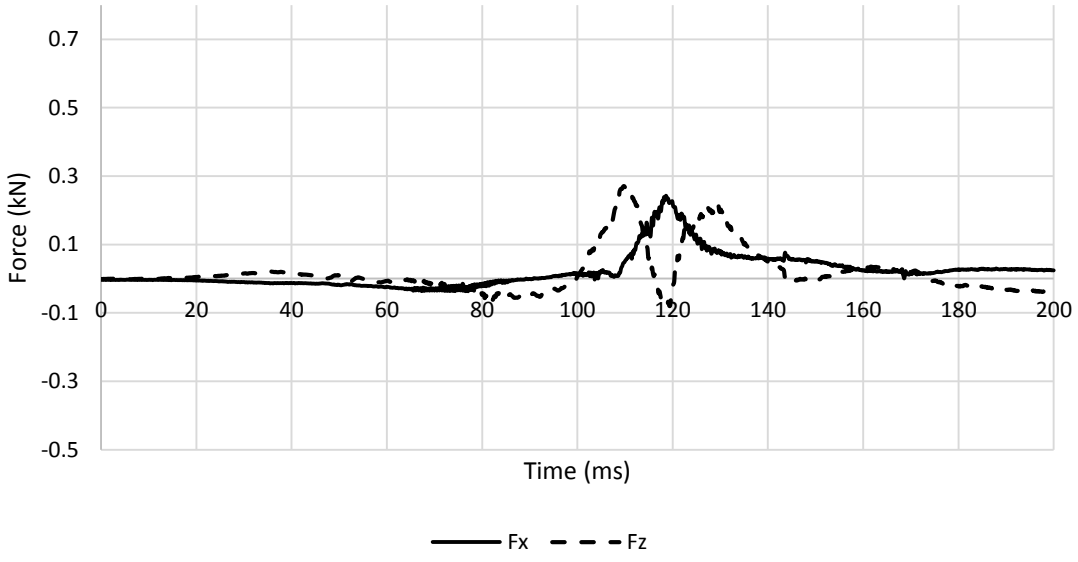


APPENDIX 391 LOADING GRAPHS OF FEA EVA RID CONFIGURATION L231 - FORCE

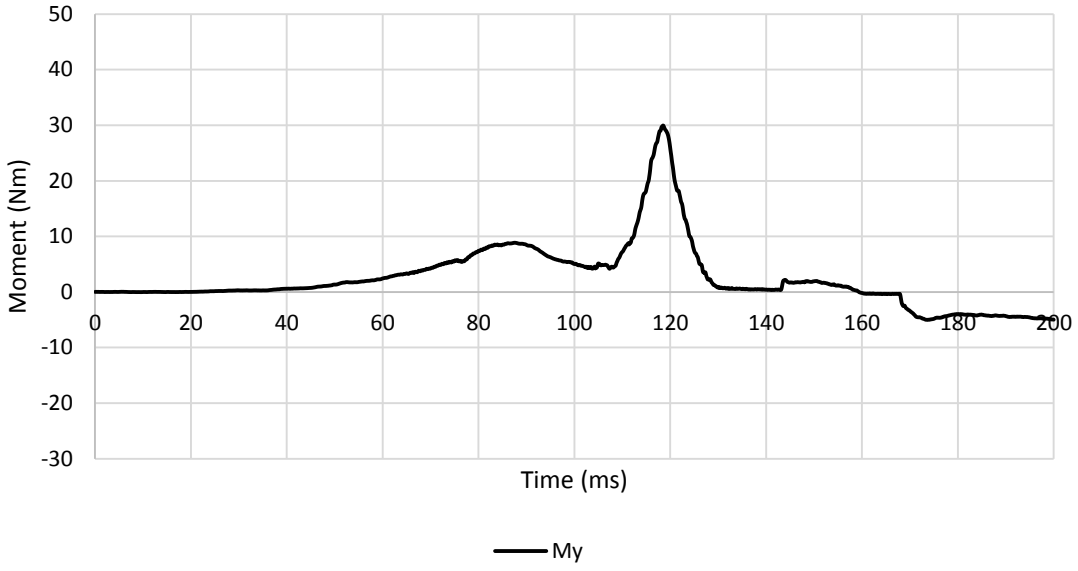


APPENDIX 392 LOADING GRAPHS OF FEA EVA RID CONFIGURATION L231 - MOMENT

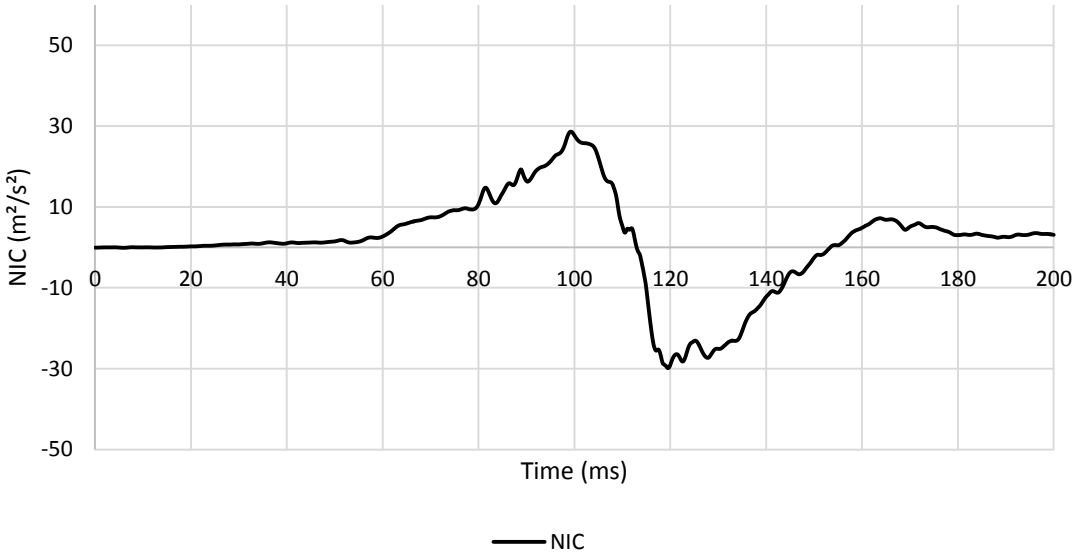


APPENDIX 393 LOADING GRAPHS OF FEA EVA RID CONFIGURATION L231 - NIC

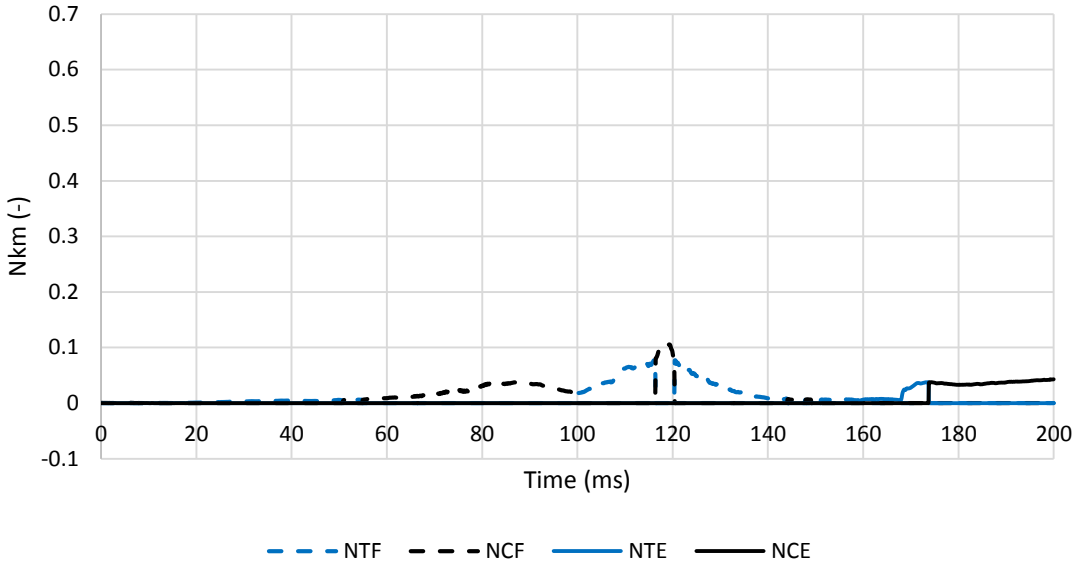


APPENDIX 394 LOADING GRAPHS OF FEA EVA RID CONFIGURATION L231 - NKM

### A.7.7.2. Medium Severity Pulse (IIWPG 16 km/h) M231

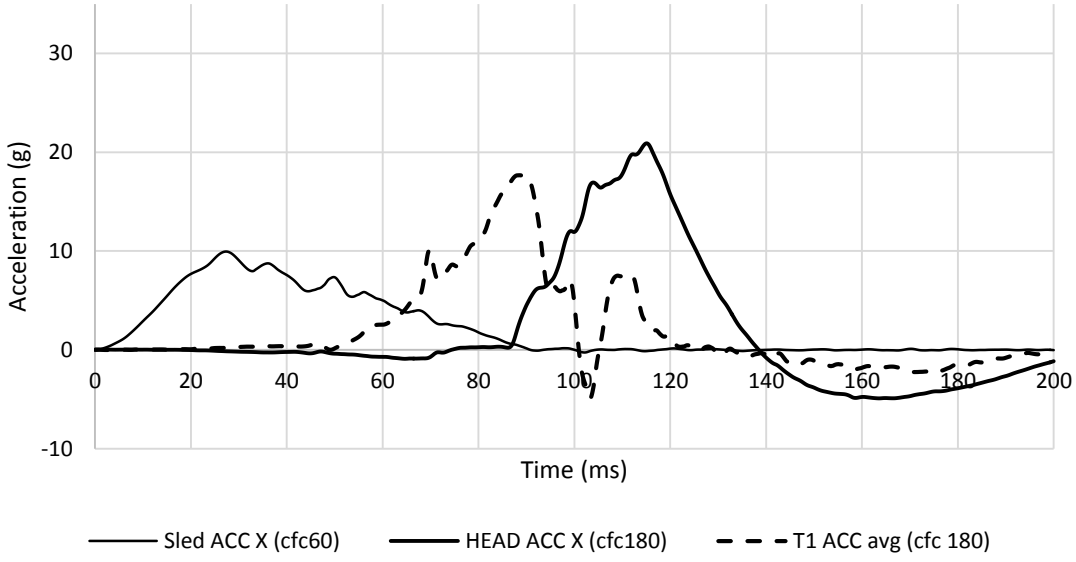


APPENDIX 395 LOADING GRAPHS OF FEA EVA RID CONFIGURATION M231 – ACCELERATION

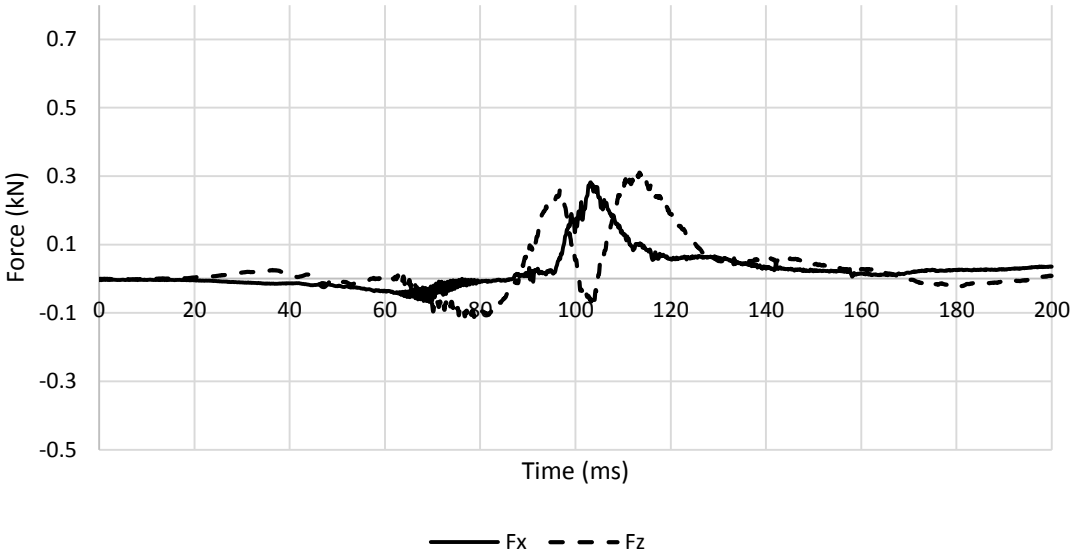


APPENDIX 396 LOADING GRAPHS OF FEA EVA RID CONFIGURATION M231 – FORCE

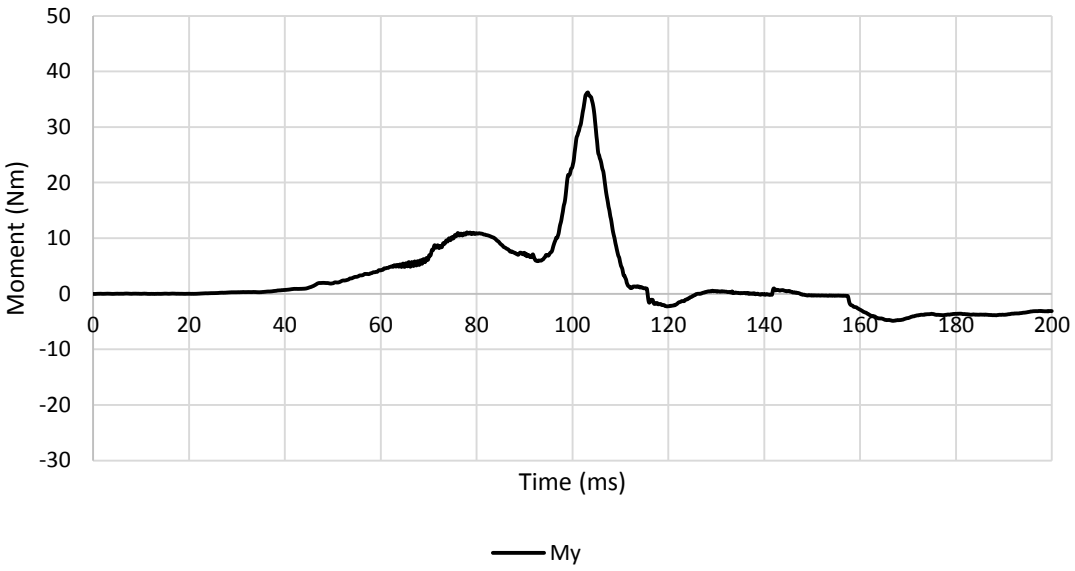


APPENDIX 397 LOADING GRAPHS OF FEA EVA RID CONFIGURATION M231 – MOMENT

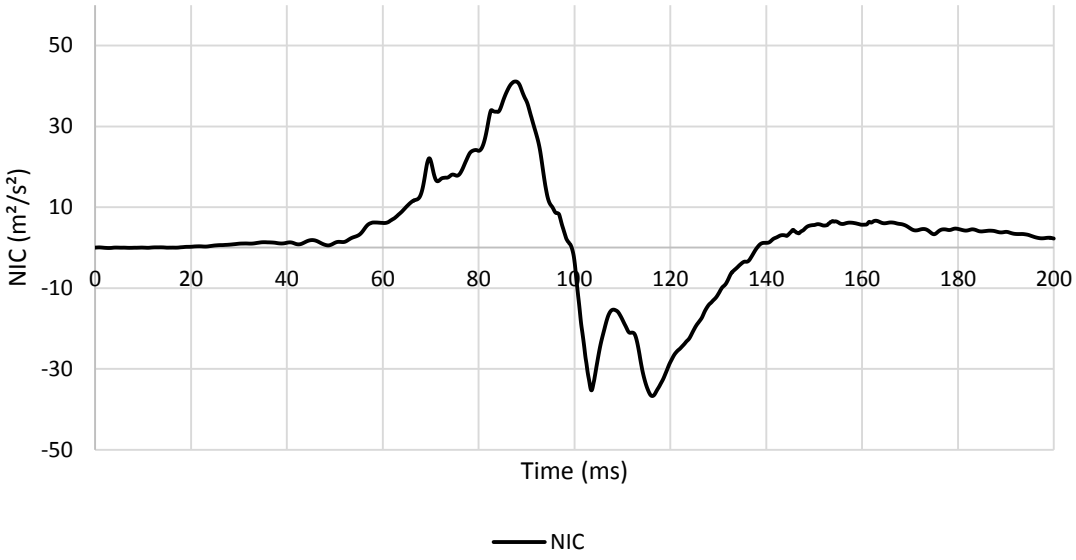


APPENDIX 398 LOADING GRAPHS OF FEA EVA RID CONFIGURATION M231 - NIC

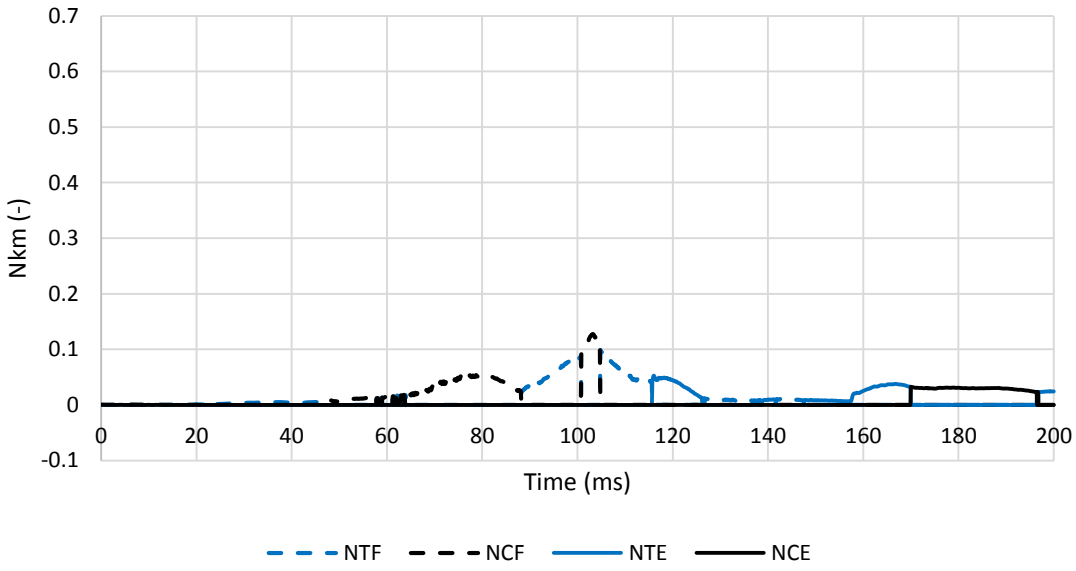


APPENDIX 399 LOADING GRAPHS OF FEA EVA RID CONFIGURATION M231 - NKM

## A.7.7.3. High Severity Pulse (SRA 24 km/h) H231

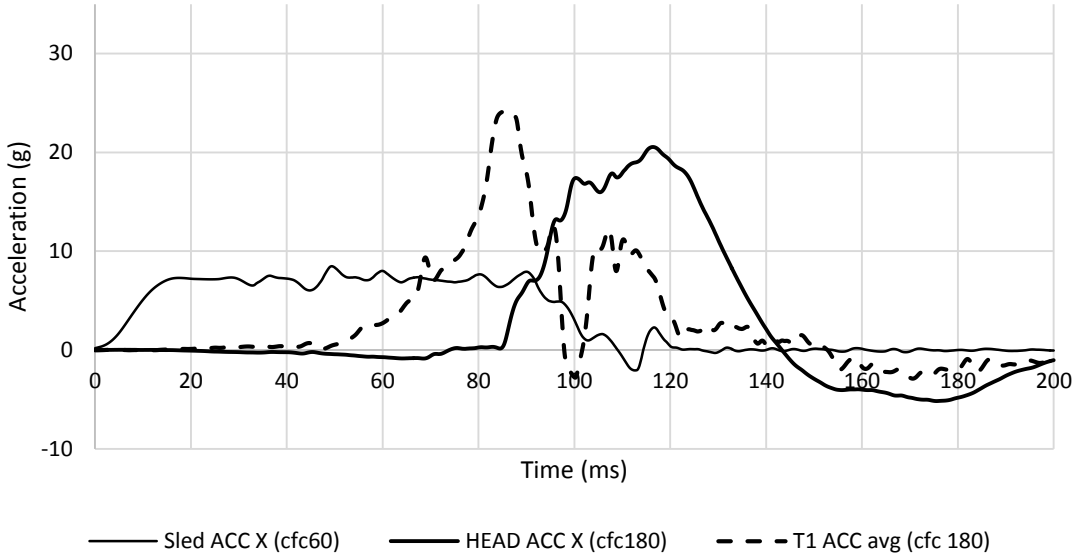


APPENDIX 400 LOADING GRAPHS OF FEA EVA RID CONFIGURATION H231 - ACCELERATION

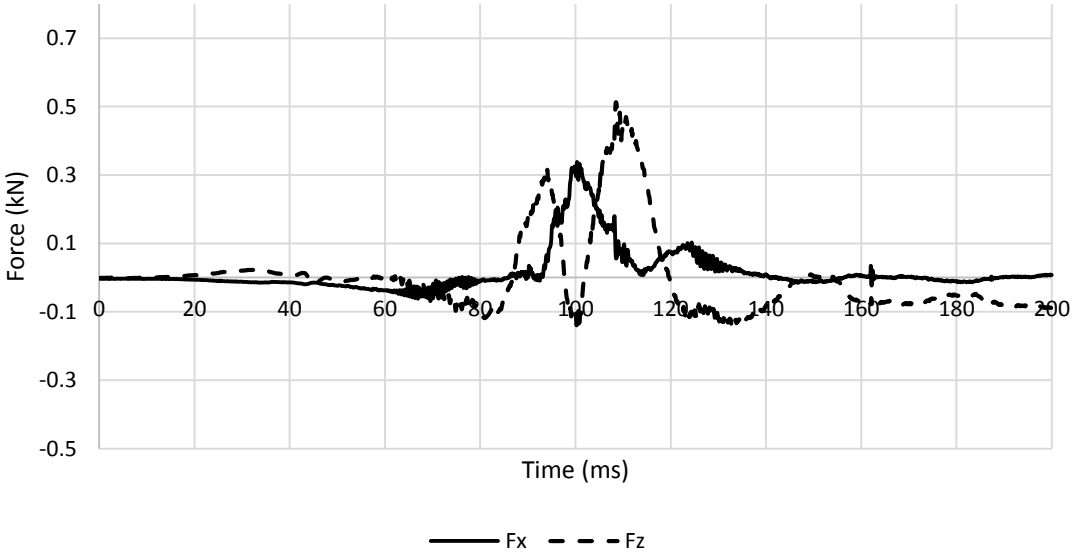


APPENDIX 401 LOADING GRAPHS OF FEA EVA RID CONFIGURATION H231 - FORCE

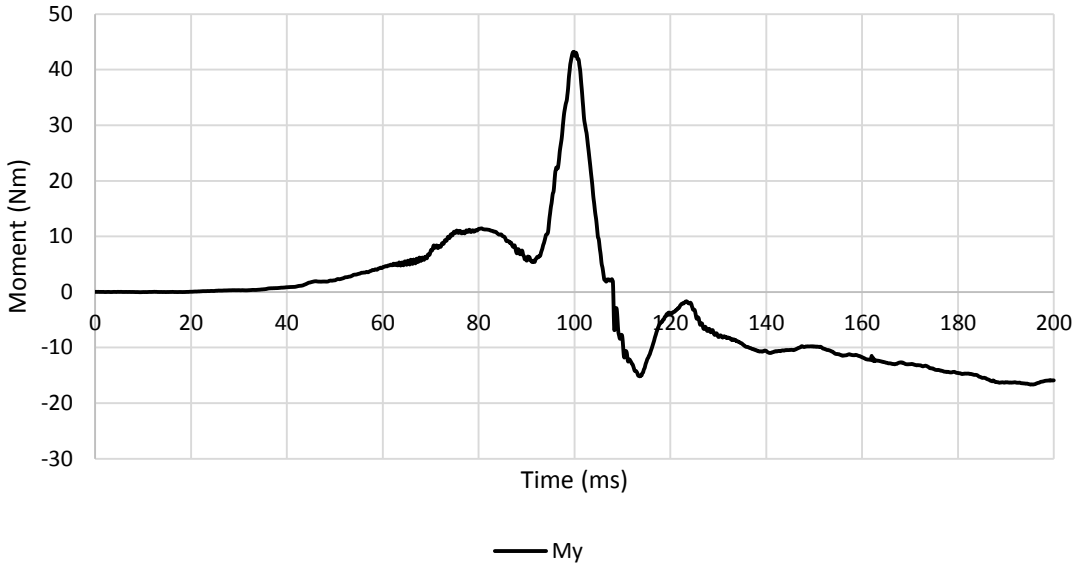


APPENDIX 402 LOADING GRAPHS OF FEA EVA RID CONFIGURATION H231 - MOMENT

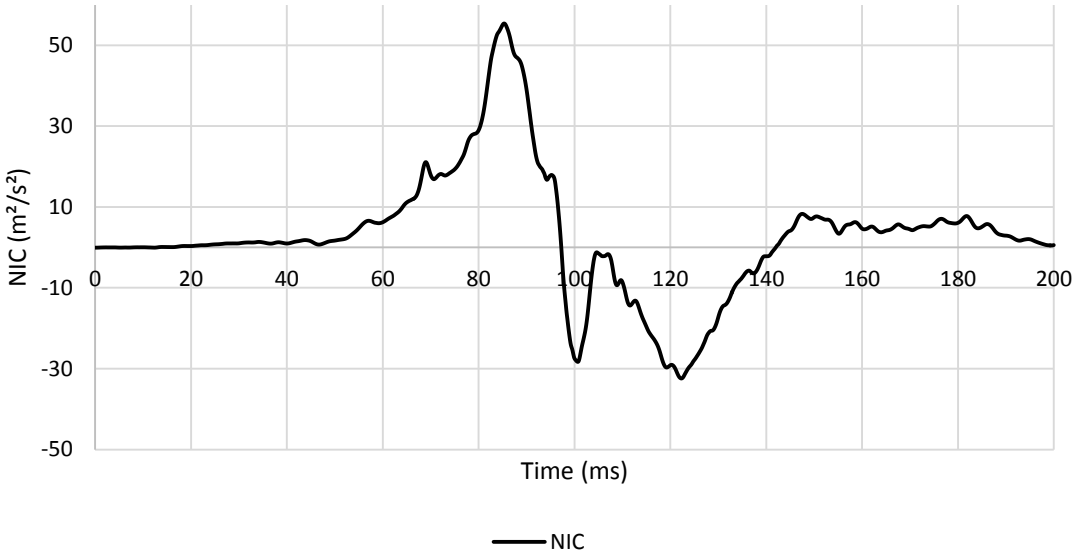


APPENDIX 403 LOADING GRAPHS OF FEA EVA RID CONFIGURATION H231 - NIC

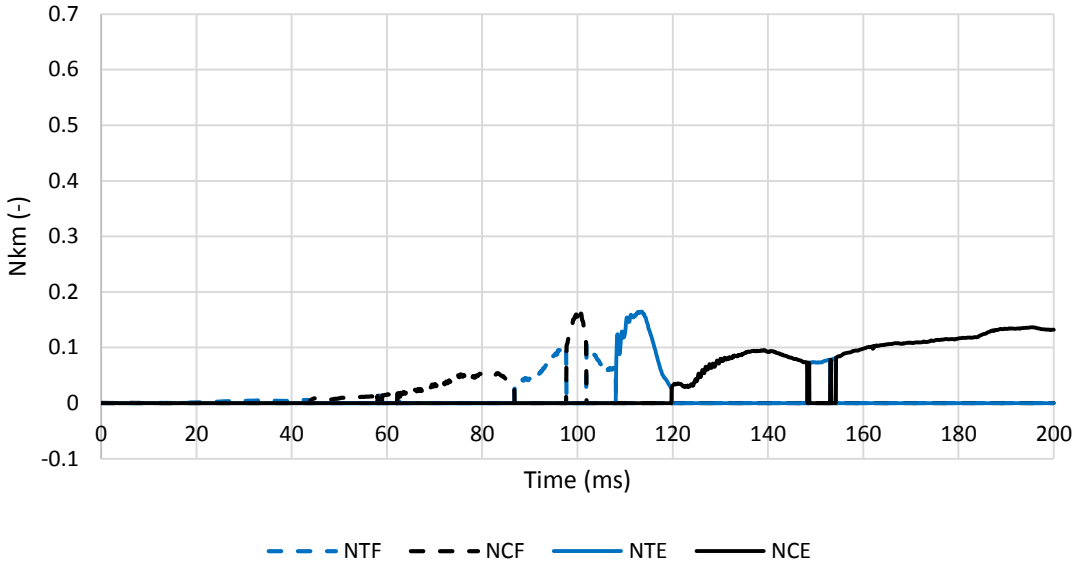


APPENDIX 404 LOADING GRAPHS OF FEA EVA RID CONFIGURATION H231 - NKM

## A.7.8. Eva RID – backward backrest – middle head restraint 232

### A.7.8.1. Low Severity Pulse (SRA 16 km/h) L232

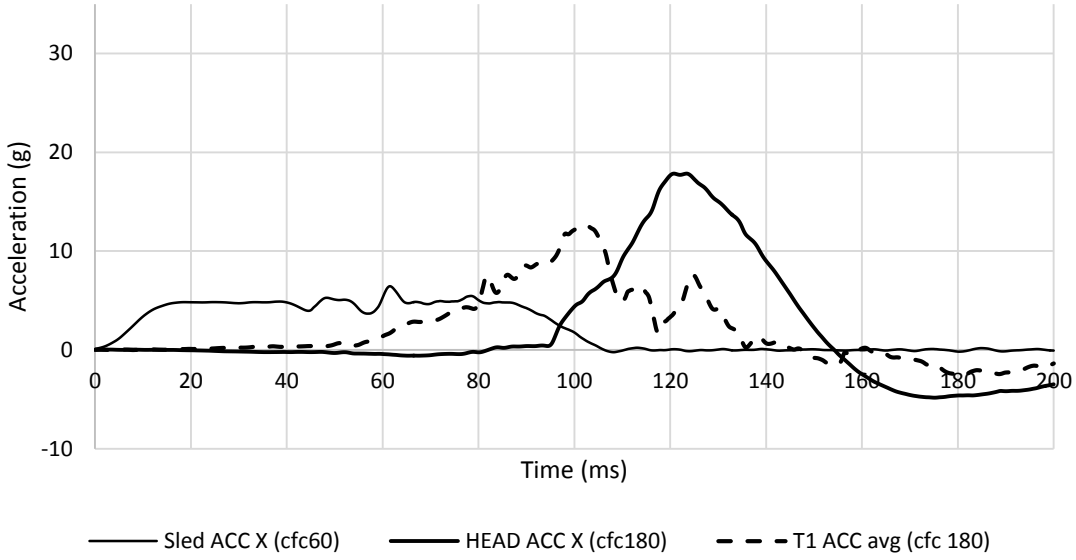


APPENDIX 405 LOADING GRAPHS OF FEA EVA RID CONFIGURATION L232 - ACCELERATION

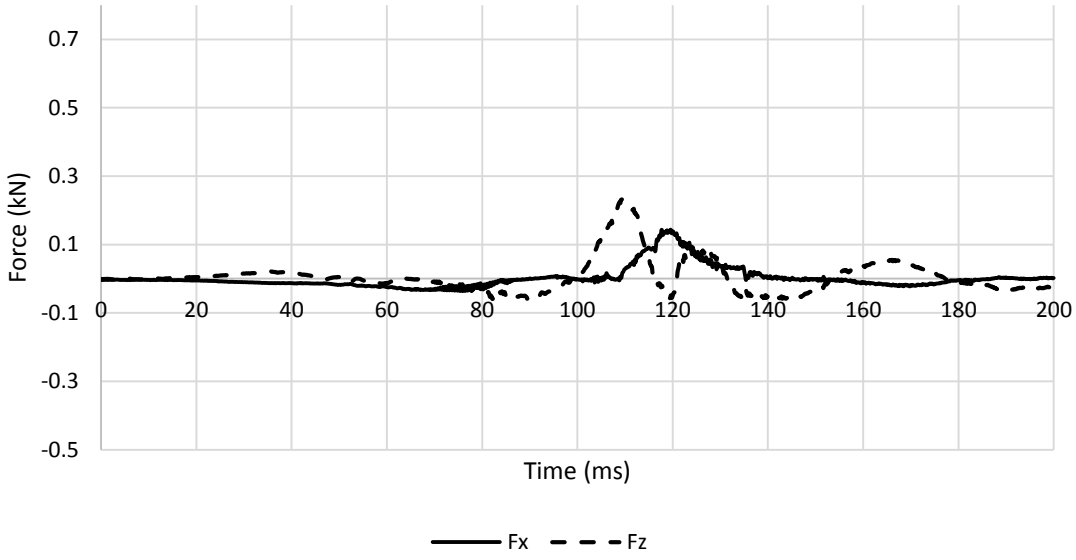


APPENDIX 406 LOADING GRAPHS OF FEA EVA RID CONFIGURATION L232 - FORCE

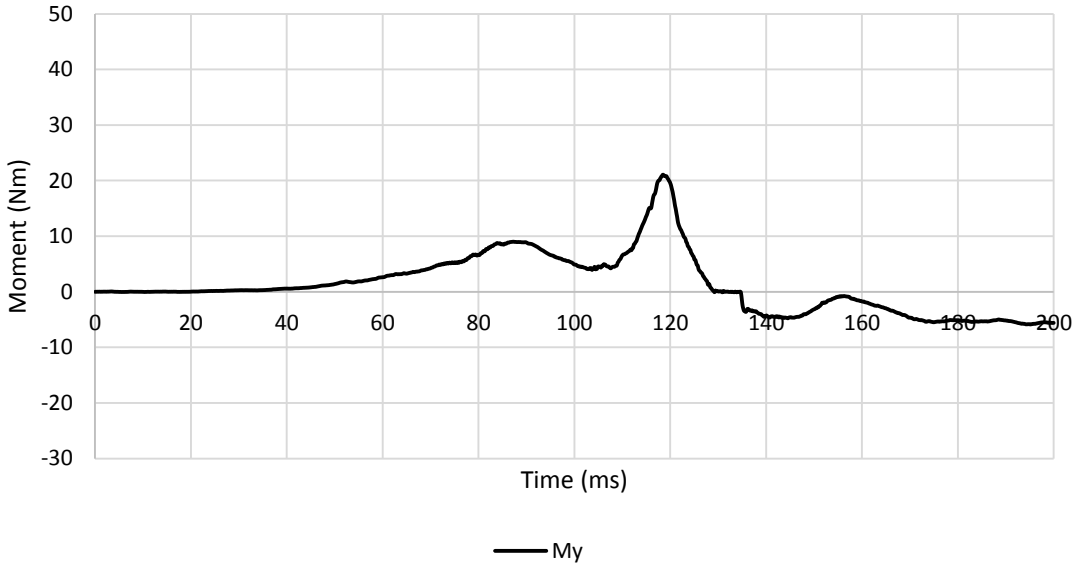


APPENDIX 407 LOADING GRAPHS OF FEA EVA RID CONFIGURATION L232- MOMENT

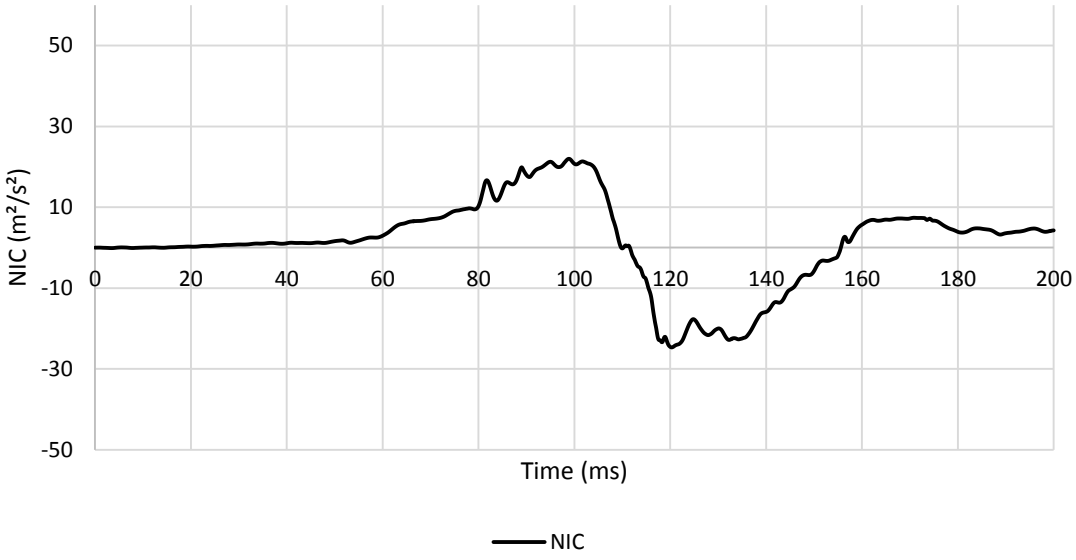


APPENDIX 408 LOADING GRAPHS OF FEA EVA RID CONFIGURATION L232 - NIC

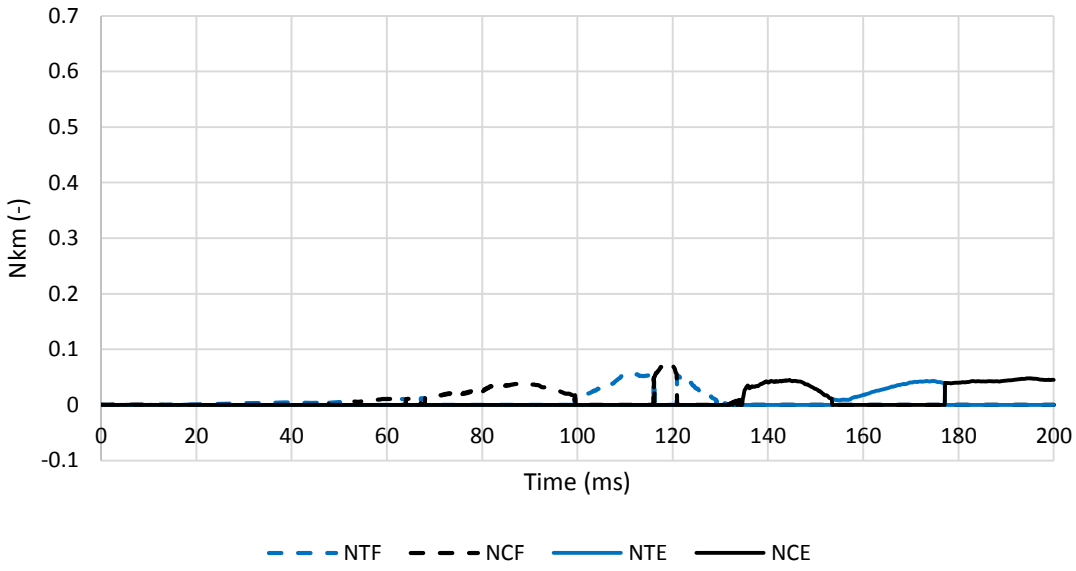


APPENDIX 409 LOADING GRAPHS OF FEA EVA RID CONFIGURATION L232 - NKM

## A.7.8.2. Medium Severity Pulse (IIWPG 16 km/h) M232

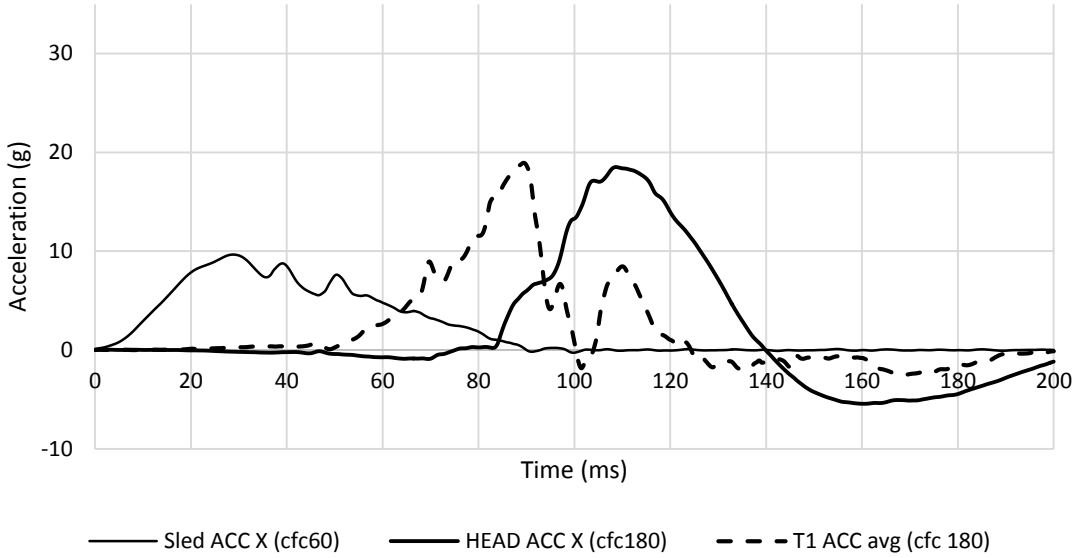


APPENDIX 410 LOADING GRAPHS OF FEA EVA RID CONFIGURATION M232 - ACCELERATION

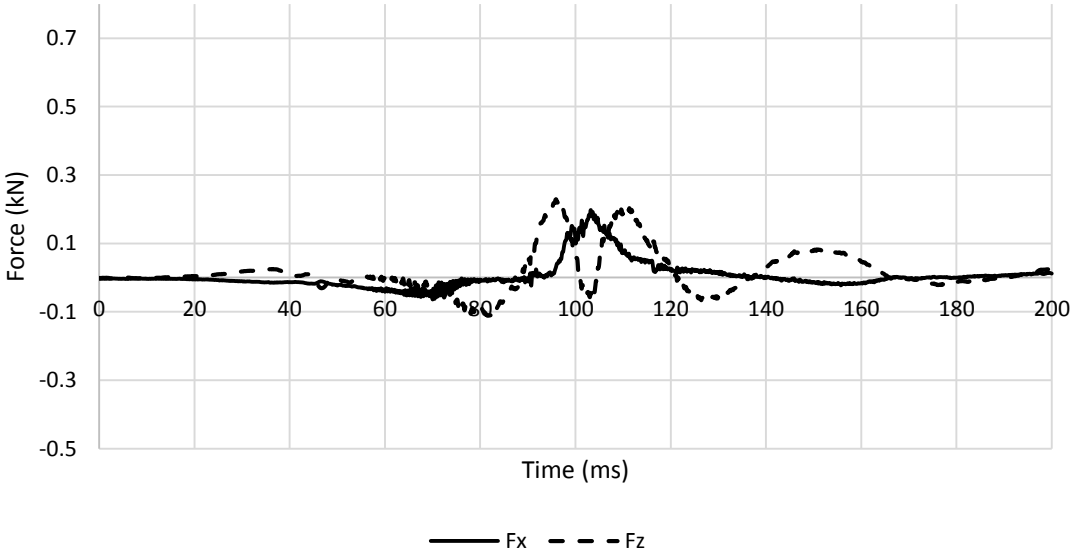


APPENDIX 411 LOADING GRAPHS OF FEA EVA RID CONFIGURATION M232 - FORCE

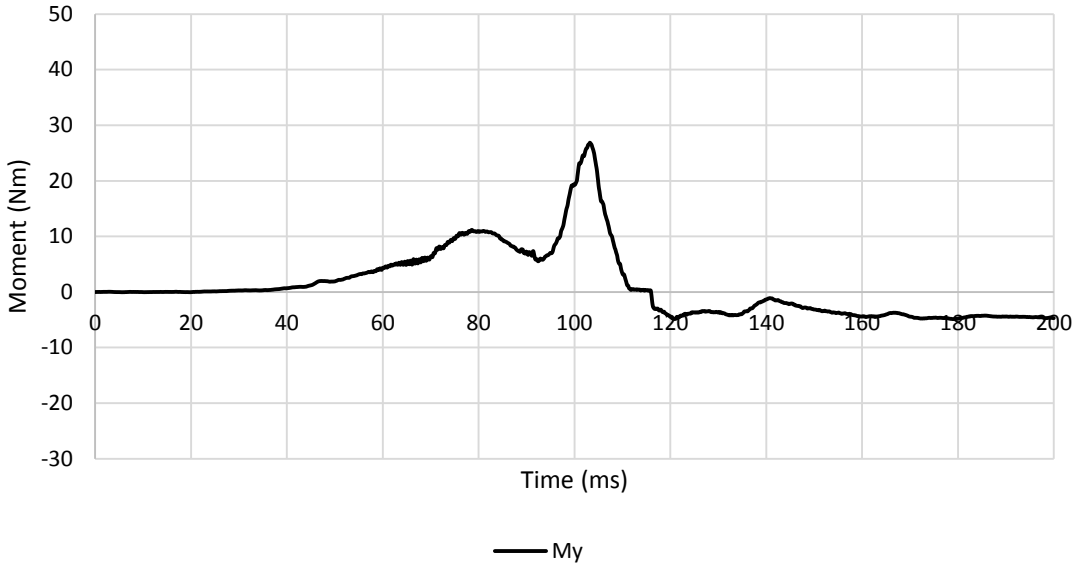


APPENDIX 412 LOADING GRAPHS OF FEA EVA RID CONFIGURATION M232 MOMENT

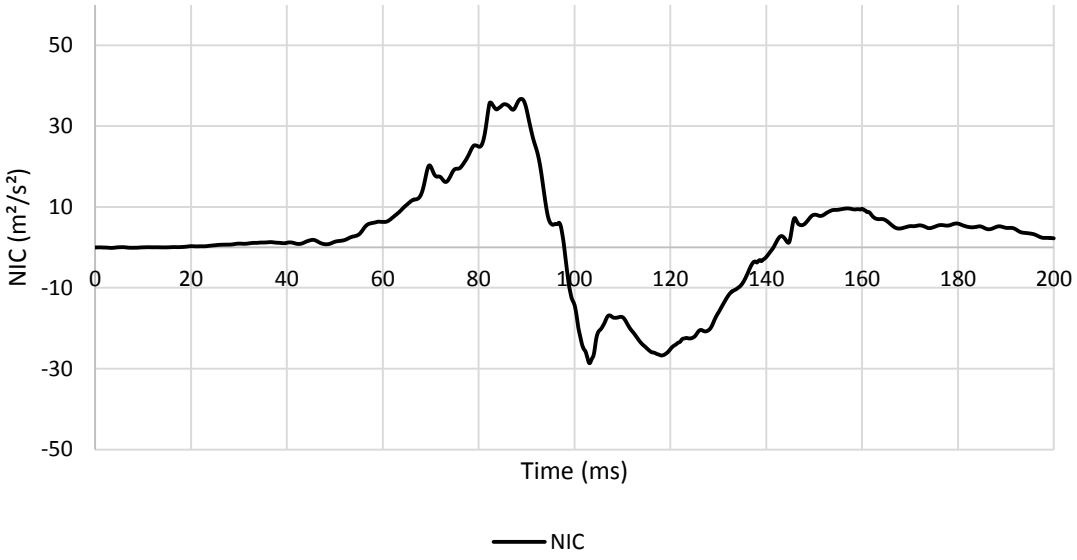


APPENDIX 413 LOADING GRAPHS OF FEA EVA RID CONFIGURATION M232 - NIC

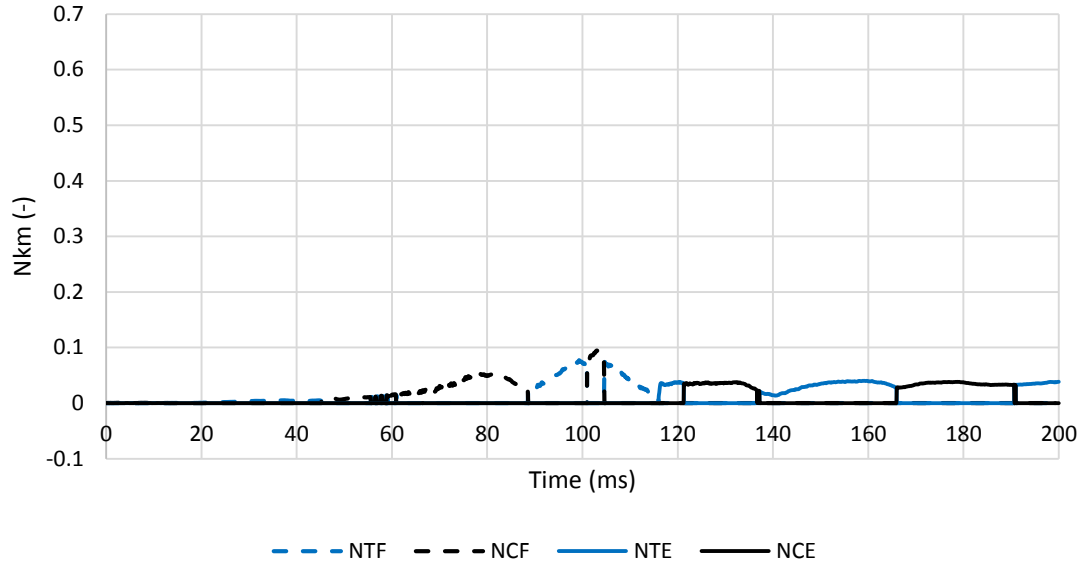


APPENDIX 414 LOADING GRAPHS OF FEA EVA RID CONFIGURATION M232 - NKM

### A.7.8.3. High Severity Pulse (SRA 24 km/h) H232

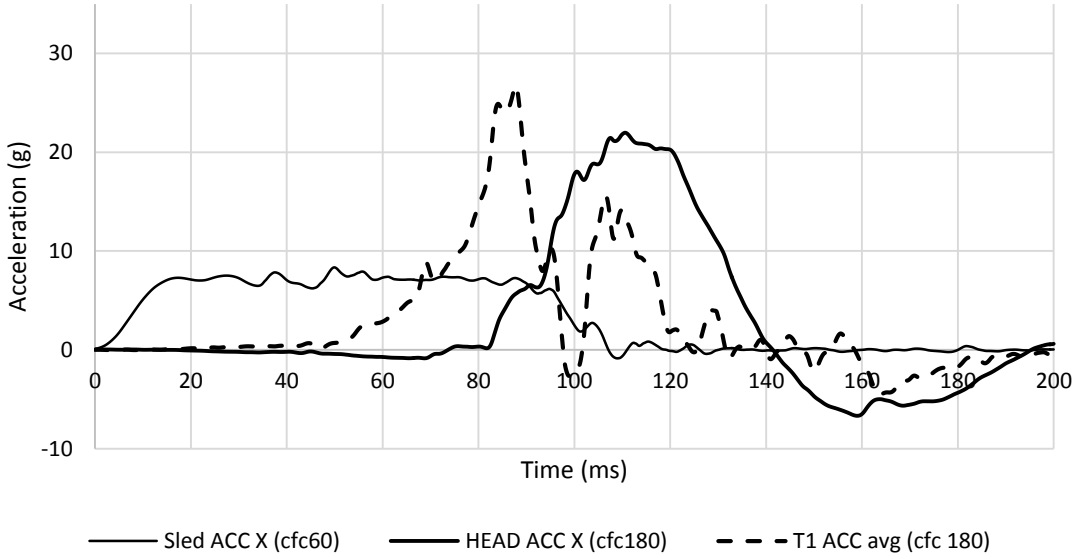


APPENDIX 415 LOADING GRAPHS OF FEA EVA RID CONFIGURATION H232 - ACCELERATION

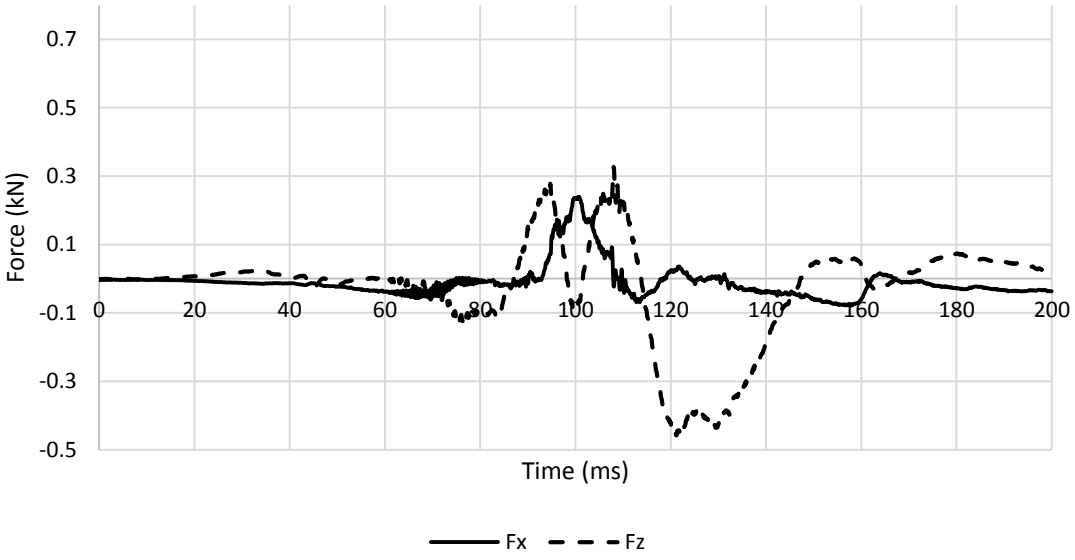


APPENDIX 416 LOADING GRAPHS OF FEA EVA RID CONFIGURATION H232 - FORCE

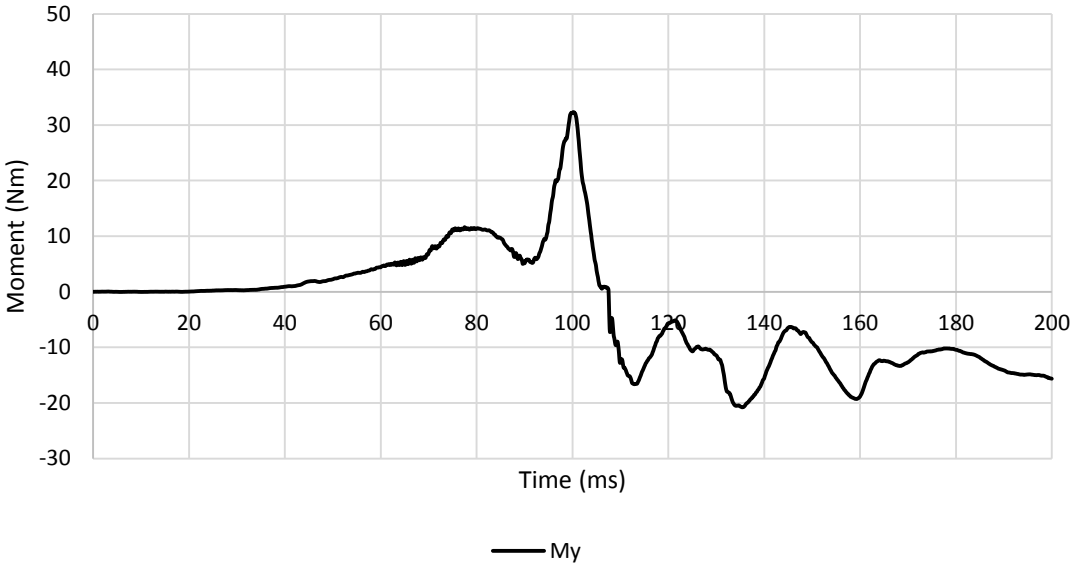


APPENDIX 417 LOADING GRAPHS OF FEA EVA RID CONFIGURATION H232 - MOMENT

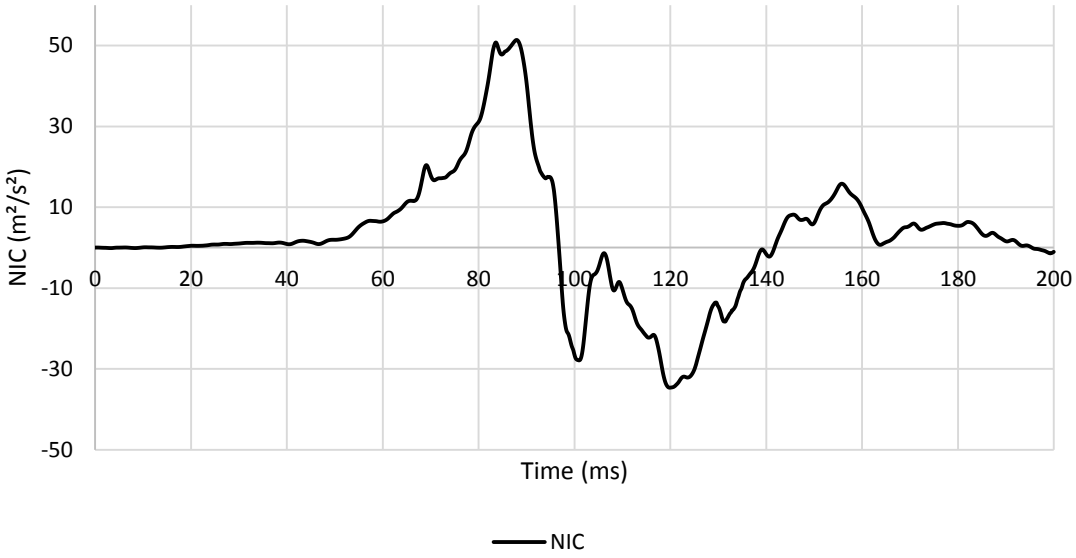


APPENDIX 418 LOADING GRAPHS OF FEA EVA RID CONFIGURATION H232 - NIC

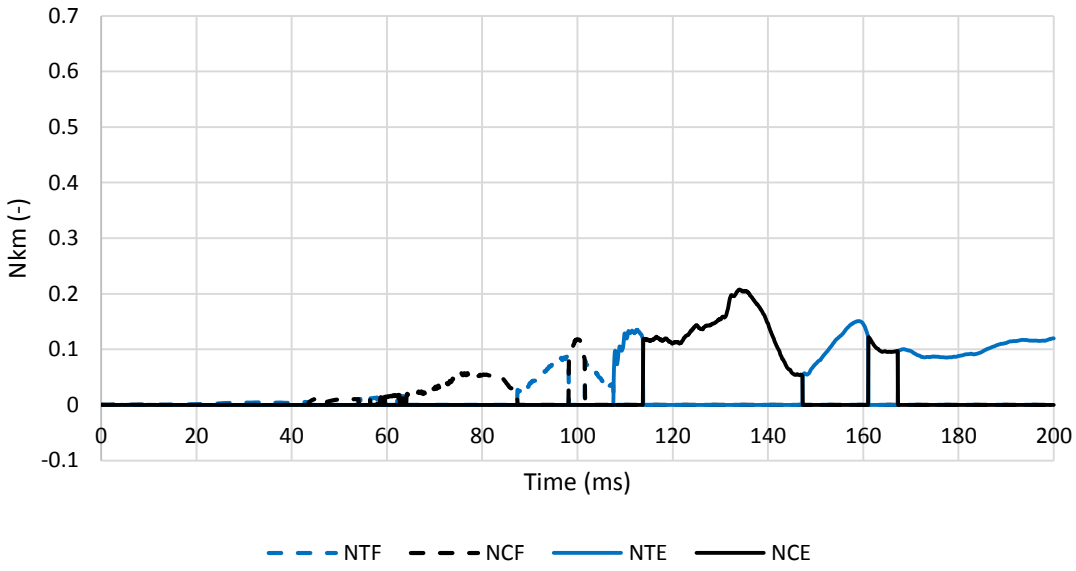


APPENDIX 419 LOADING GRAPHS OF FEA EVA RID CONFIGURATION H232 - NKM

## A.7.9. Eva RID – backward backrest – low head restraint 233

### A.7.9.1. Low Severity Pulse (SRA 16 km/h) L233

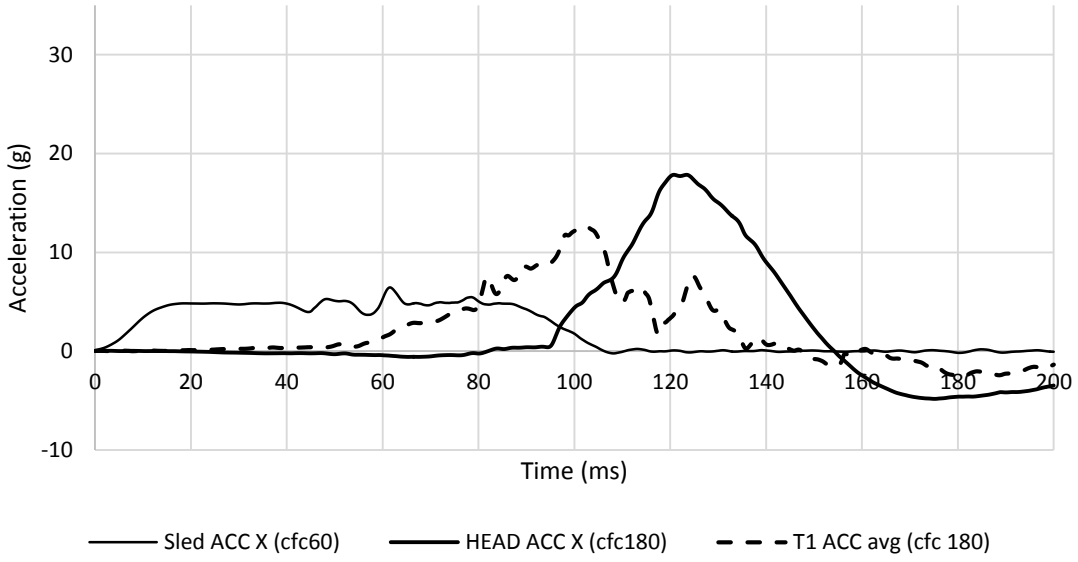


APPENDIX 420 LOADING GRAPHS OF FEA EVA RID CONFIGURATION L233 - ACCELERATION

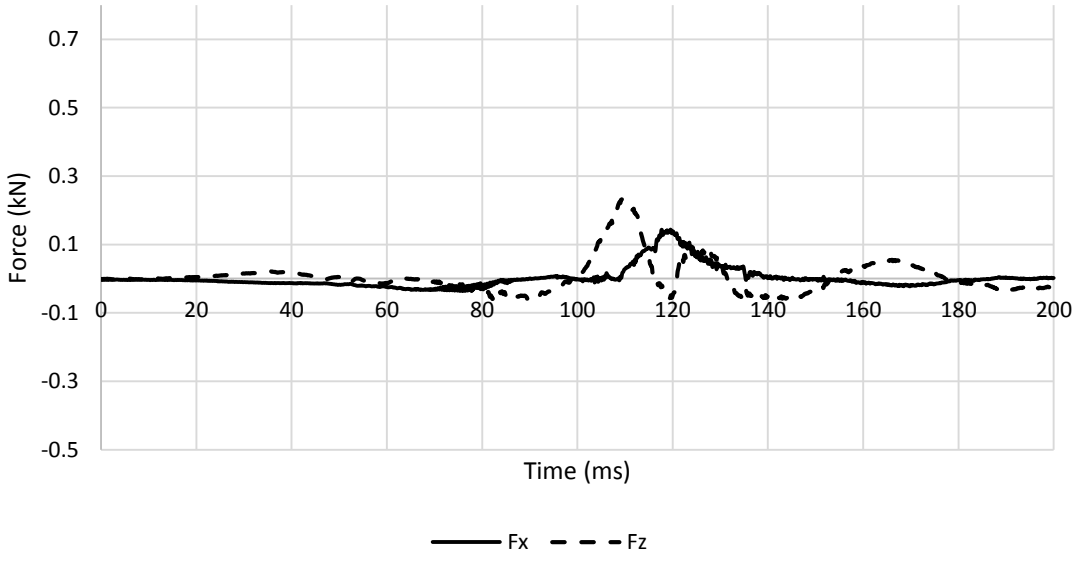


APPENDIX 421 LOADING GRAPHS OF FEA EVA RID CONFIGURATION L233 - FORCE

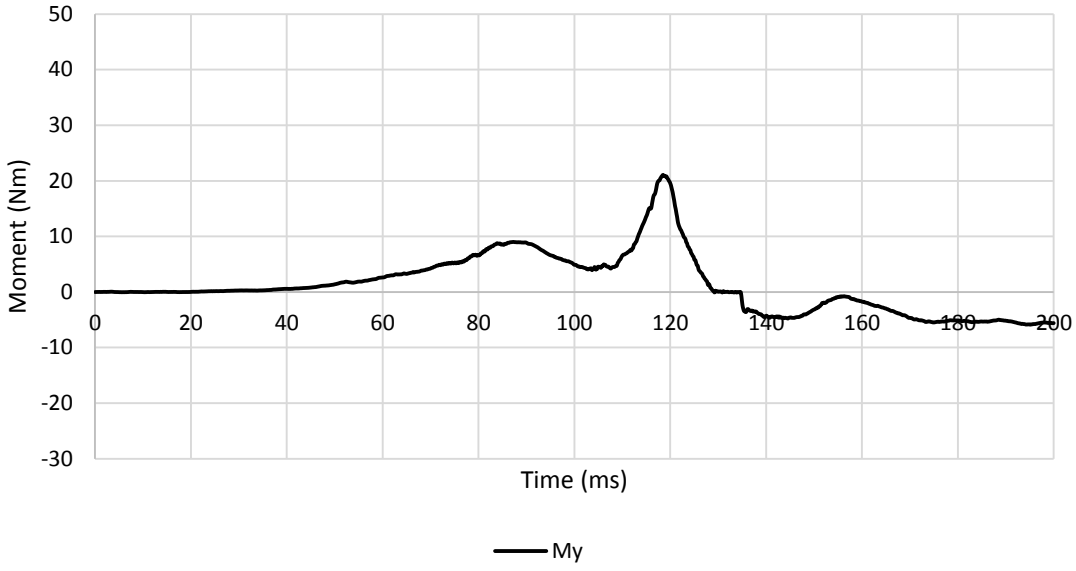


APPENDIX 422 LOADING GRAPHS OF FEA EVA RID CONFIGURATION L233 - MOMENT

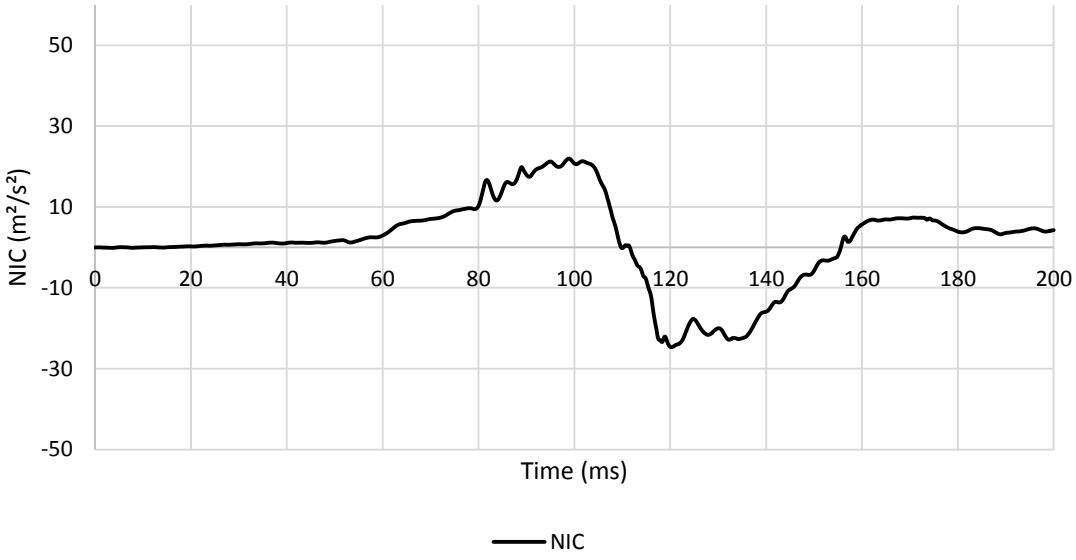


APPENDIX 423 LOADING GRAPHS OF FEA EVA RID CONFIGURATION L233 - NIC

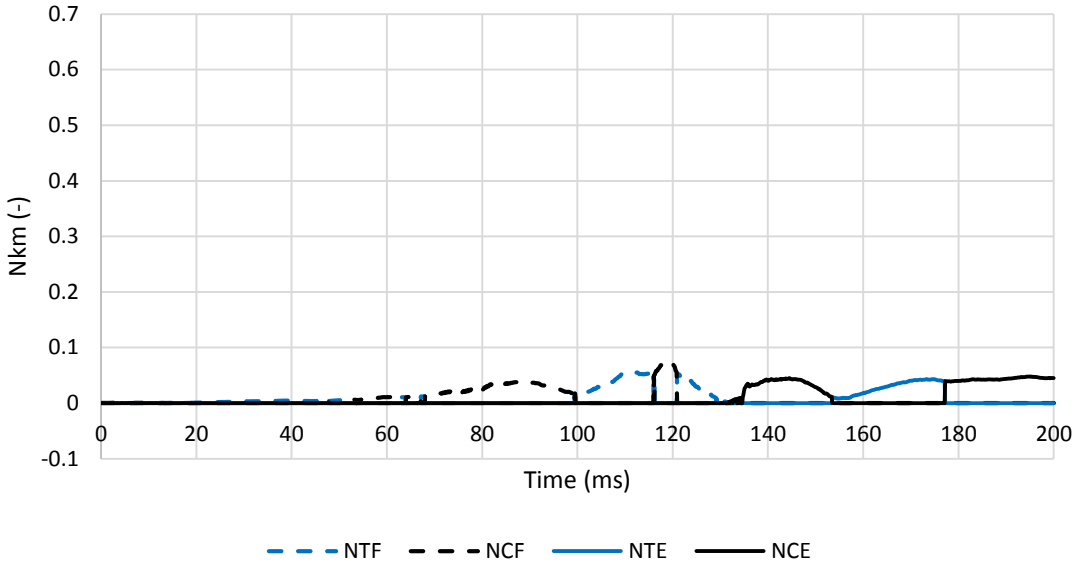


APPENDIX 424 LOADING GRAPHS OF FEA EVA RID CONFIGURATION L233 - NKM

## A.7.9.2. Medium Severity Pulse (IIWPG 16 km/h) M233

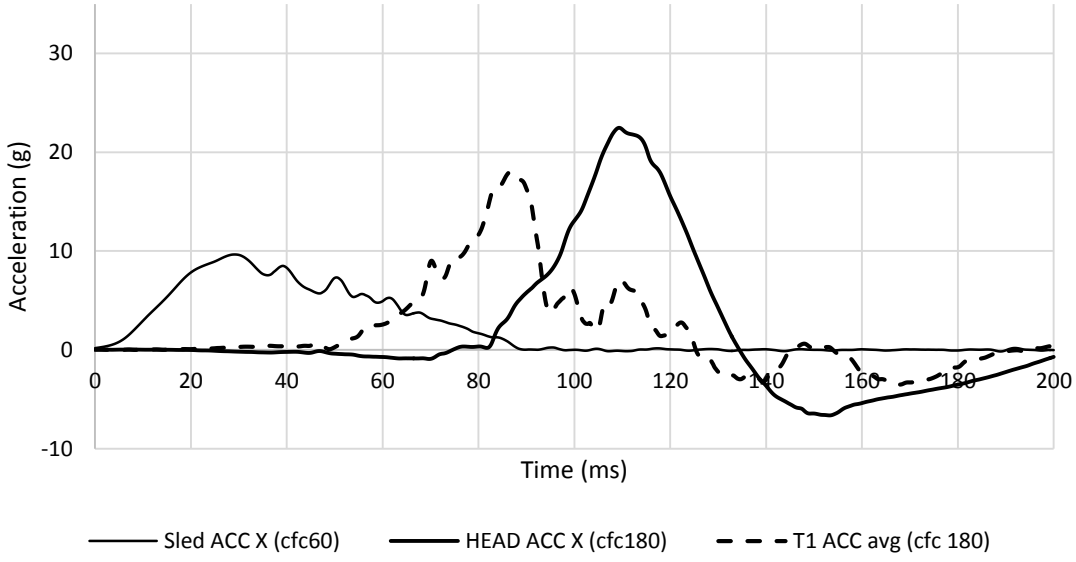


APPENDIX 425 LOADING GRAPHS OF FEA EVA RID CONFIGURATION M233 - ACCELERATION

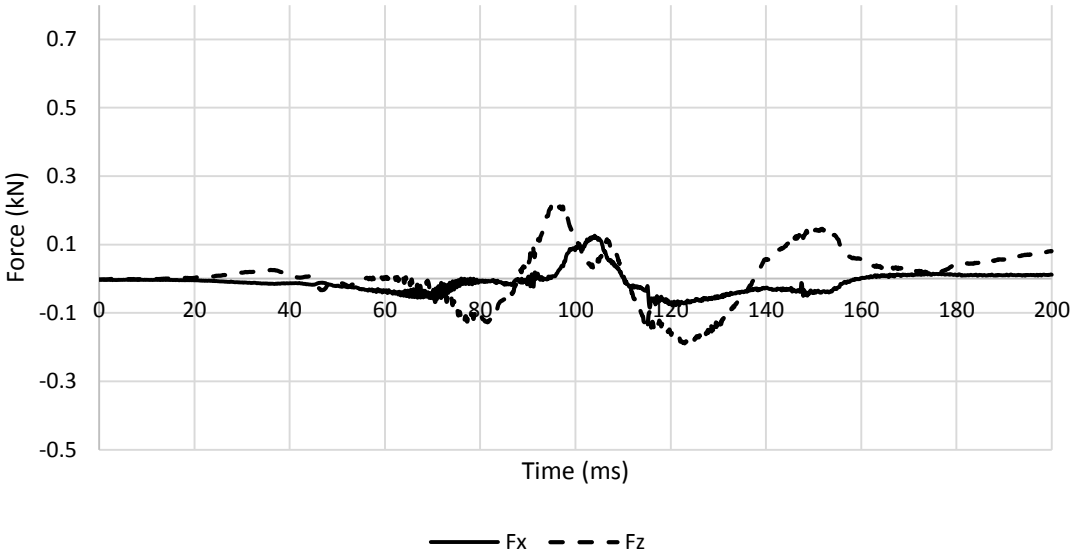


APPENDIX 426 LOADING GRAPHS OF FEA EVA RID CONFIGURATION M233 - FORCE

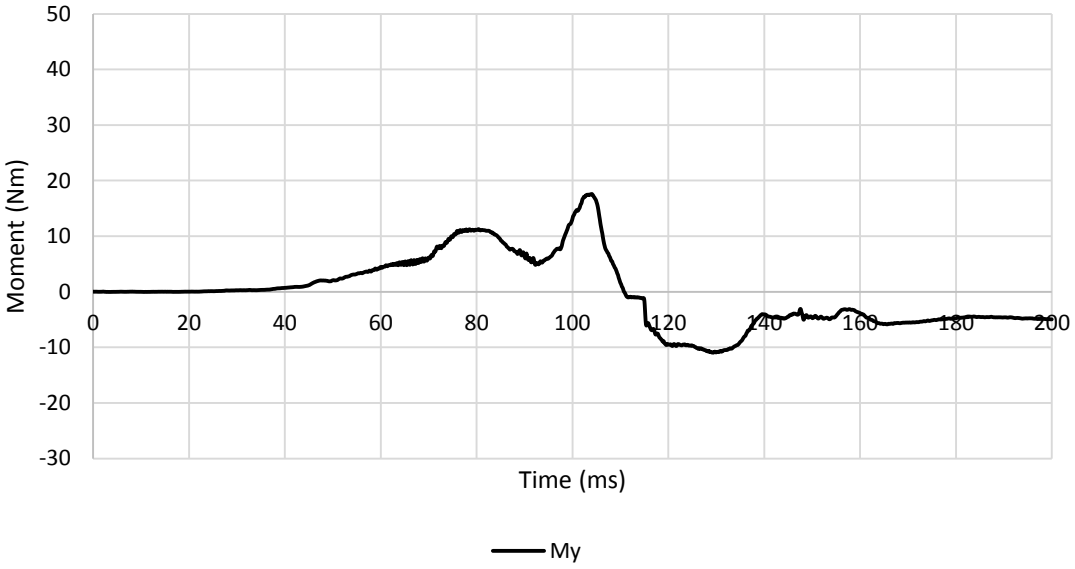


APPENDIX 427 LOADING GRAPHS OF FEA EVA RID CONFIGURATION M233 - MOMENT

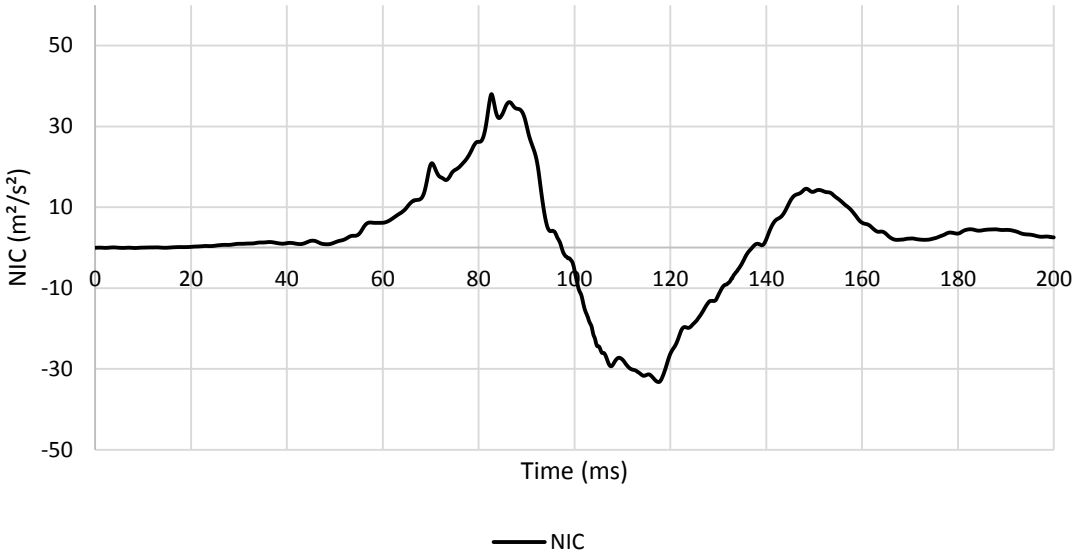


APPENDIX 428 LOADING GRAPHS OF FEA EVA RID CONFIGURATION M233 - NIC

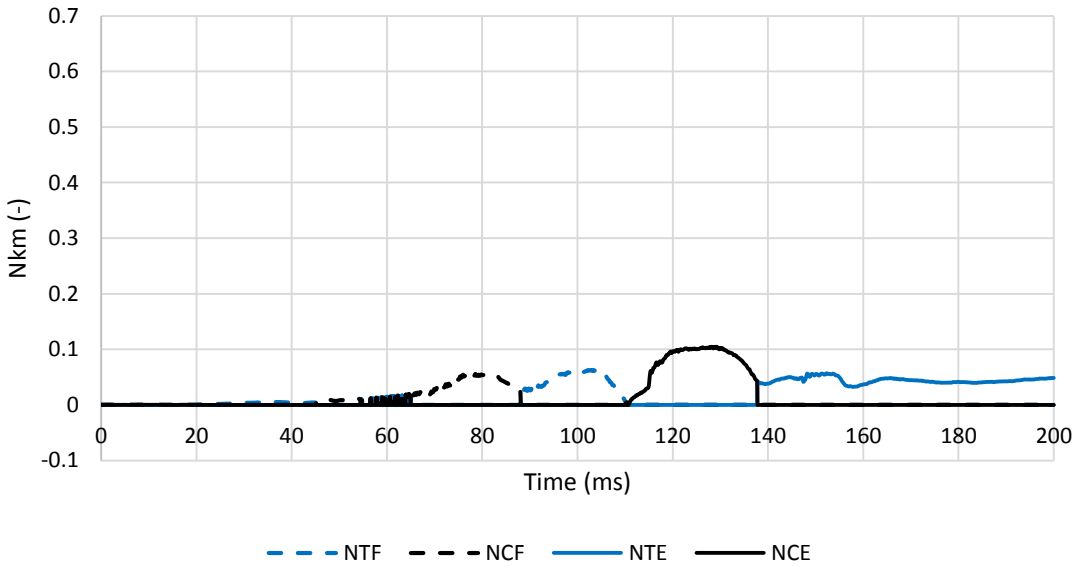


APPENDIX 429 LOADING GRAPHS OF FEA EVA RID CONFIGURATION M233 - NKM

A.7.9.3. High Severity Pulse (SRA 24 km/h) H233

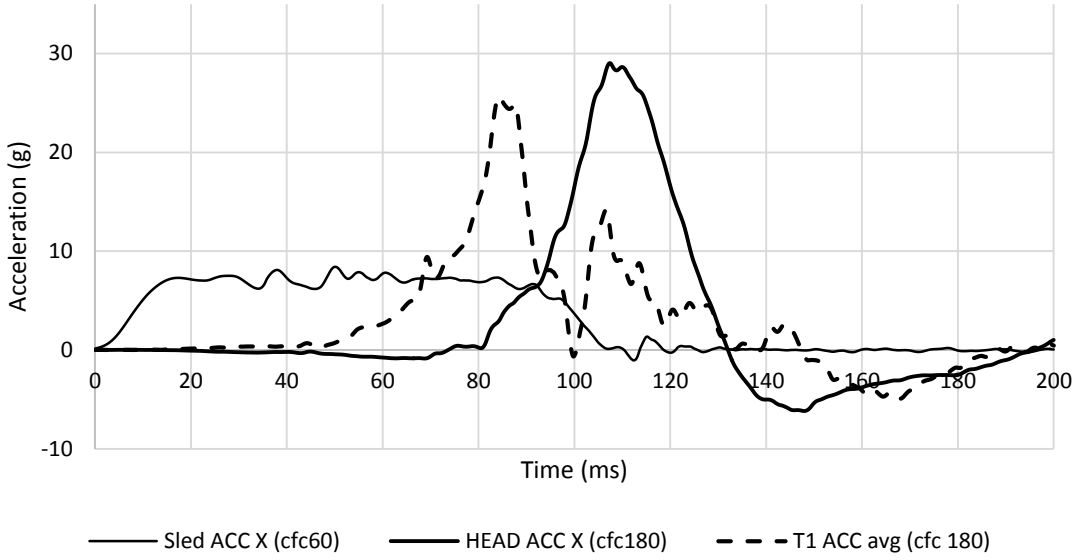


APPENDIX 430 LOADING GRAPHS OF FEA EVA RID CONFIGURATION H233 - ACCELERATION

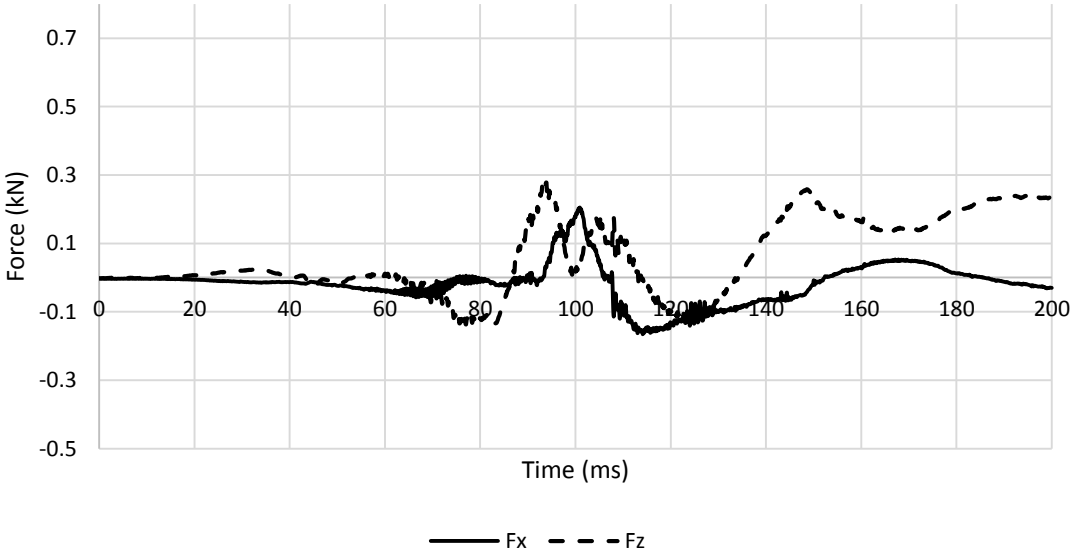


APPENDIX 431 LOADING GRAPHS OF FEA EVA RID CONFIGURATION H233 - FORCE

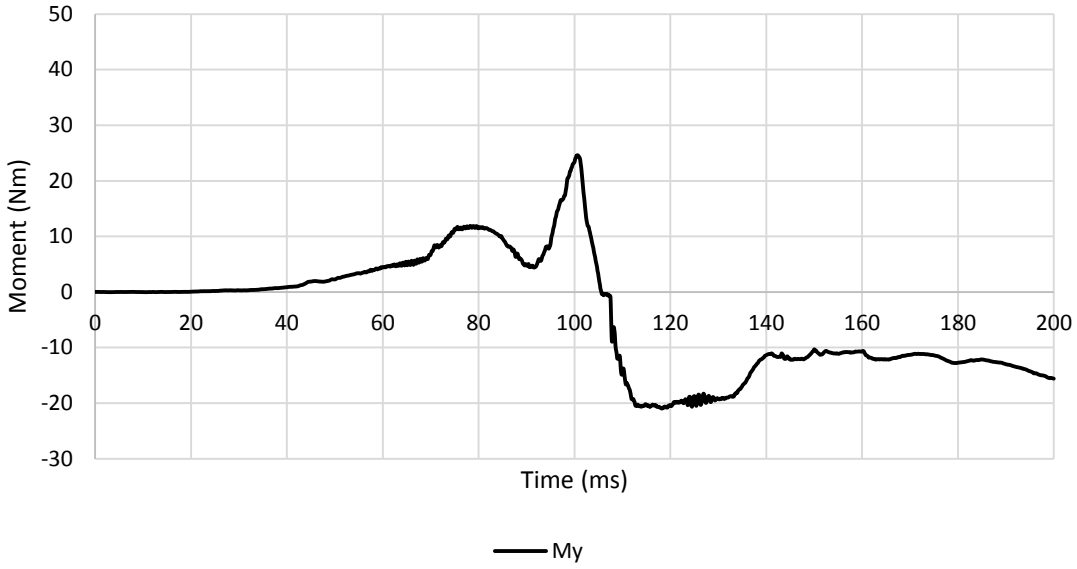


APPENDIX 432 LOADING GRAPHS OF FEA EVA RID CONFIGURATION H233 - MOMENT

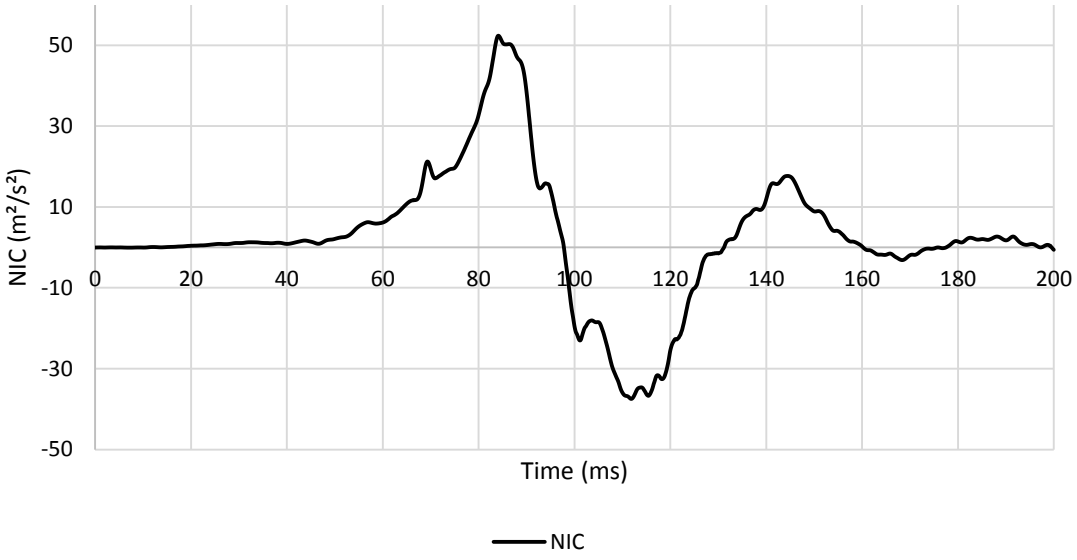


APPENDIX 433 LOADING GRAPHS OF FEA EVA RID CONFIGURATION H233 - NIC

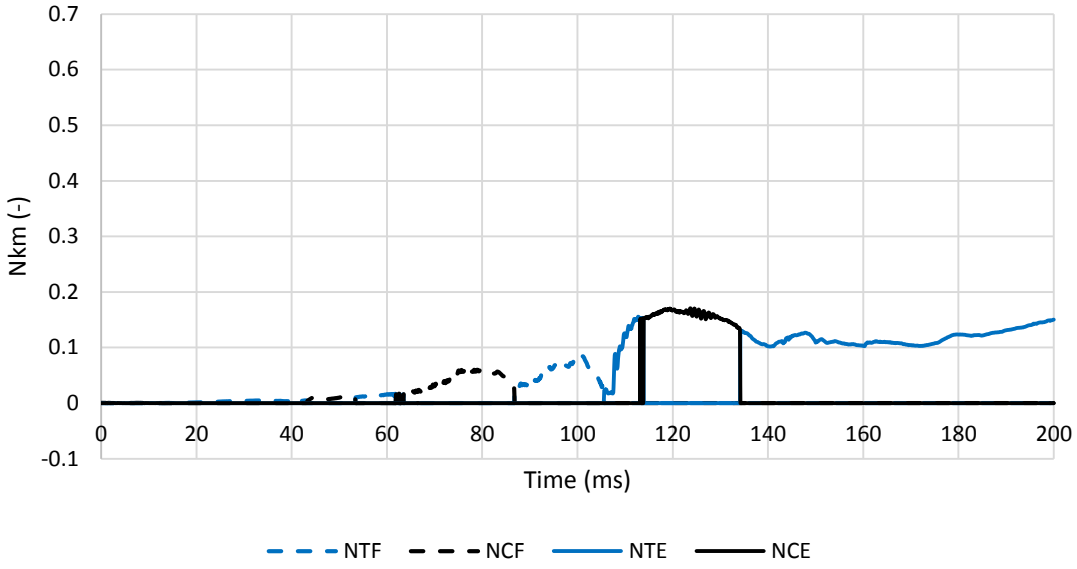


APPENDIX 434 LOADING GRAPHS OF FEA EVA RID CONFIGURATION H233 - NKM

## A.7.10. Eva RID – centred backrest – altered head restraint 22X

### A.7.10.1. Medium Severity Pulse (IIWPG 16 km/h) M22X

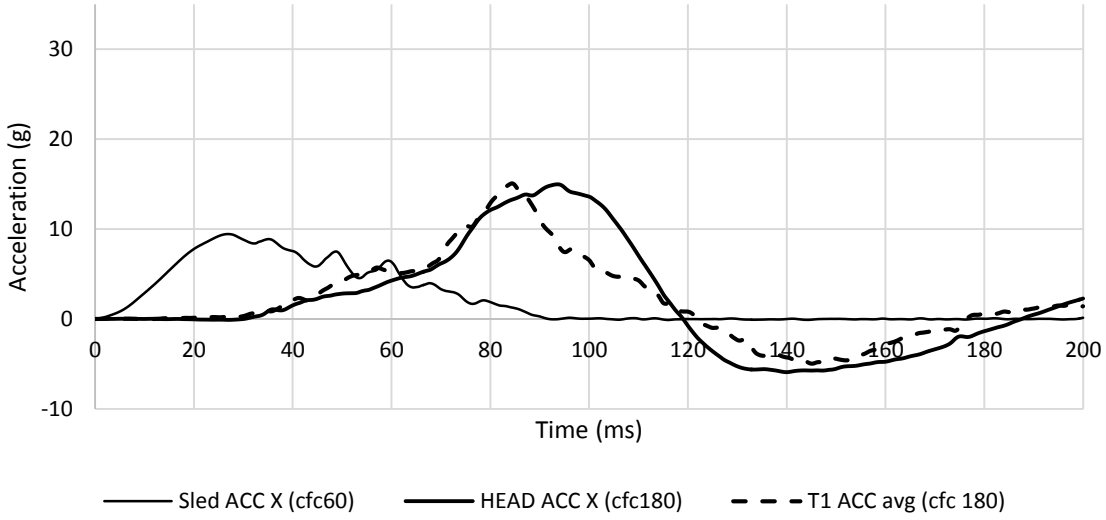


APPENDIX 435 LOADING GRAPHS OF FEA EVA RID CONFIGURATION M22X - ACCELERATION

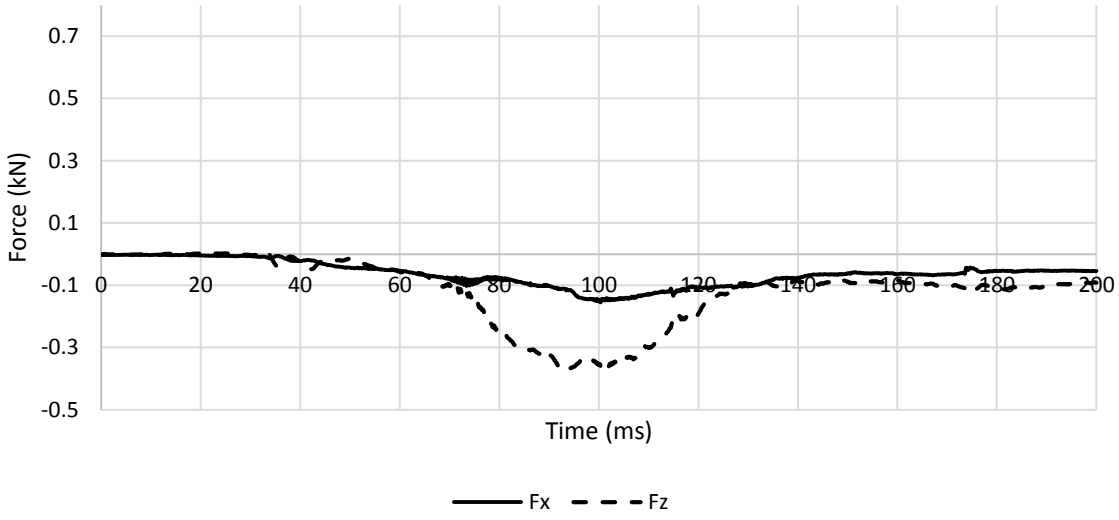


APPENDIX 436 LOADING GRAPHS OF FEA EVA RID CONFIGURATION M22X - FORCE

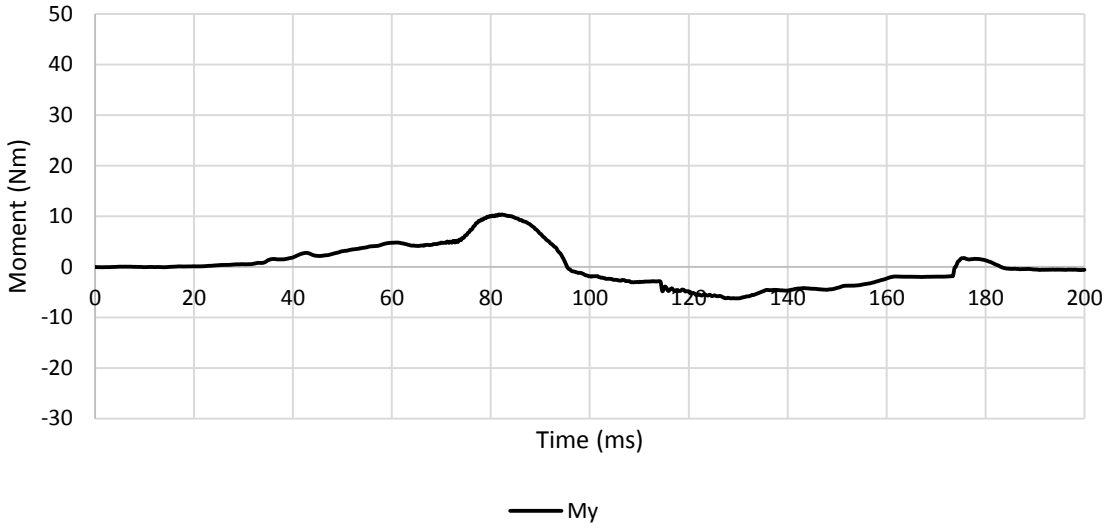


APPENDIX 437 LOADING GRAPHS OF FEA EVA RID CONFIGURATION M22X - MOMENT

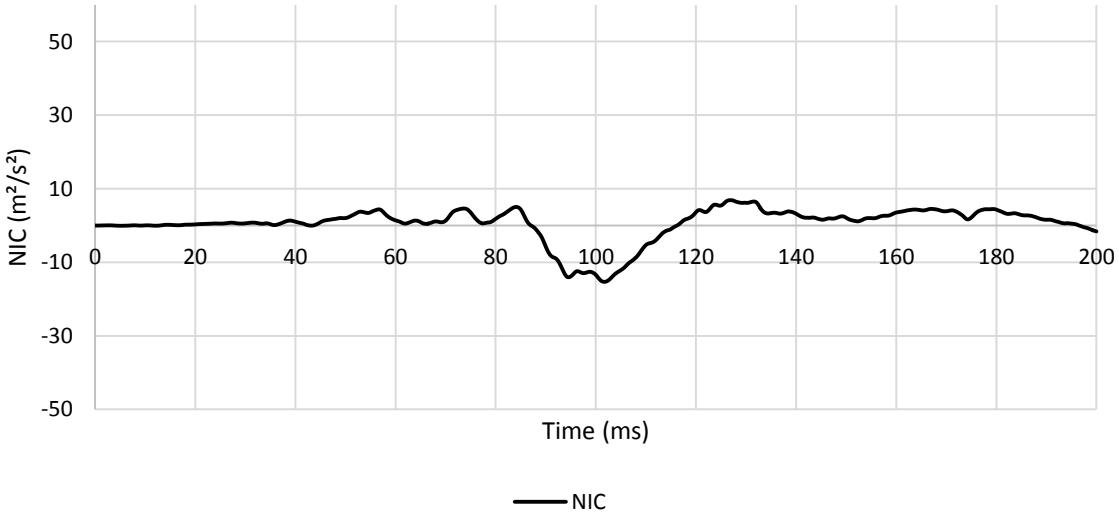


APPENDIX 438 LOADING GRAPHS OF FEA EVA RID CONFIGURATION M22X - NIC

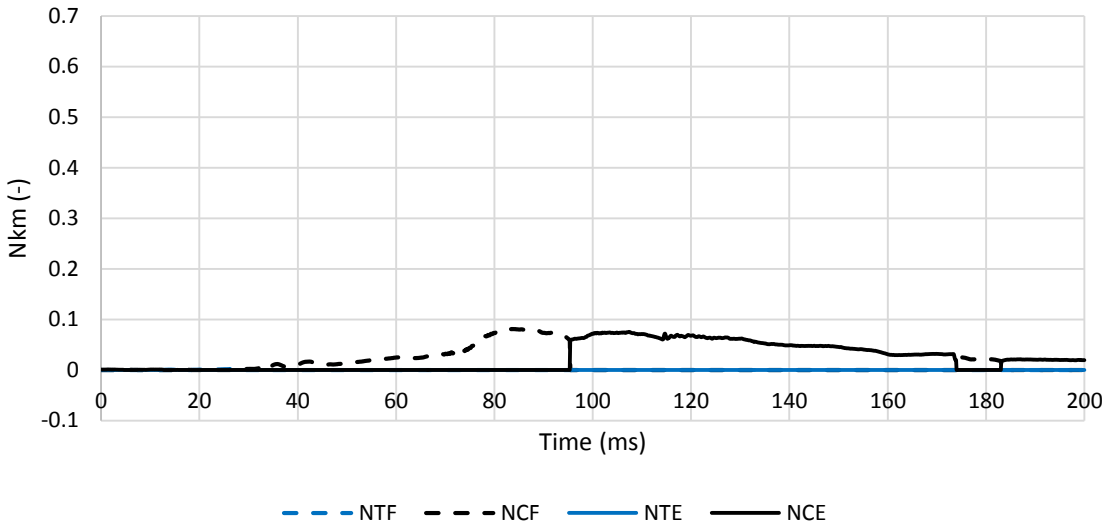


APPENDIX 439 LOADING GRAPHS OF FEA EVA RID CONFIGURATION M22X - NKM